OVERRIDING CISPLATIN RESISTANCE IN LUNG SQUAMOUS CELL CARCINOMA: INSIGHTS FROM COMBINATION WITH HDAC INHIBITOR

KONG LI REN

(*B. Sc. (Hons), NUS*)

A THESIS SUBMITTED

FOR THE DEGREE OF DOCTOR OF PHILOSOPHY

DEPARTMENT OF PHARMACOLOGY

NATIONAL UNIVERSITY OF SINGAPORE

2014

DECLARATION

I hereby declare that this thesis is my original work

and it has been written by me in its entirety.

I have duly acknowledged all the sources of information

which has been used in the thesis.

This thesis has also not been submitted for

any degree in any university previously.

_____

Kong Li Ren

6th January 2013

PRESENTATION AT INTERNATIONAL CONFERENCES

1. **Kong LR**, Chua KN, Wang LZ, Chng WJ, Goh BC.
   "Eludicidating the synergistic action of histone deacetylase inhibitor and cisplatin in lung squamous cell carcinoma."
   AACR Annual Meeting 2013, 6 – 10 April 2013, Washington DC Convention Centre, Washington DC, United States).

2. **Kong LR**, Wang LZ, Thuya WL, Wan SC, Nye PL, Lau JY, Goh BC.
   "The identification of cisplatin resistance pathways in lung squamous cell carcinoma and approaches to overcome resistance."
   Second AACR International Conference on Frontiers in Basic Cancer Research, 14 - 18 Sep 2011, InterContinental San Francisco, San Francisco, United States.

ACKNOWLEDGEMENTS

The journey of pursuing this degree has been challenging and it would not be possible to complete this thesis without the helps and supports from the people around me.

First and foremost, I would like to express my heartfelt gratitude to my supervisor, **Assoc. Prof. Goh Boon Cher**, for his mentorship throughout the duration of my graduate studies. His patience and encouragements have guided me through the hard times, especially towards the end of the dissertation. I have truly benefited from his teaching and guidance that have trained me to be the independent scientist that I am today.

I would like to thank my co-supervisors, **Assoc. Prof. Chng Wee Joo** and **Prof Edmund Lee**, for devoting their time to offer constructive inputs and feedbacks on my project. The project would not have been completed smoothly without their efforts.

I would also like to thank my TAC members, **Prof. Sharzib Pervaiz** and **Assis. Prof Cheok Chit Fang**, and collaborator, **Prof. Sir David Lane**, for their contributions and valuable suggestions on this project.

Special gratitude goes to **Azhar**, who has been a wonderful mate and supportive mentor for the past four years as well as **Kelvin** who has challenged me to strive for excellence in scientific research.

To all my past and present labmates: **Seow Ching**, **Amelia**, **John**, **Pei Ling**, **Serena**, **Huilin**, **Xinyi**, **Peili**, **Joanna**, **Youngjoo**, and **Patrick**, thanks for making lab life fun and cozy! To all gay buddies: **Chee Wai**, **Eddy**, **Meng Kang**, **Rohit**, and **those-who-shall-not-be-named**, thanks for the helps and supports. I know you guys will always be here when needed. To the **Khan's girls** and **APK's girls**, thanks for bringing laughters and joys to the lab.

To **Mum**, **Aunt** and **Onn**, thanks for your unconditional love and understandings. Despite not knowing much about my jobscope, you all have chosen to share my worries and anxieties.

To **Regina**, thanks for your love and support for the past 6 years. It is your unwavering faith in me that gives me the confidence to pursue my dream. It is you who have made this seemingly insurmountable journey possible.

TABLE OF CONTENTS

SUMMARY

Lung cancer remains a leading cause of cancer-related mortality, accounting for an estimated 1.4 million deaths in 2010. In recent years, major advances have been made in the identification of oncogenic driver mutations in lung cancer. Genomic analyses of adenocarcinoma of the lung have yielded significant strategies against pathway activation to improve treatment, but these efforts have been less successful in lung squamous cell carcinoma (SCC). It is generally considered that SCC is associated with few genetic aberrations that are actionable with targeted small molecule compounds or antibodies. Hence, platinum-based chemotherapy remains the standard-of-care treatment for metastatic SCC. However, drug resistance inevitably develops and curtails the efficacy of chemotherapy. Therefore, there is an urgent need to develop novel combinations for the treatment of lung SCC that leverage on understanding the pathways underpinning cisplatin resistance, and to establish predictive biomarkers that could be subjected to therapeutic intervention and facilitate treatment selection.

In this study, Next Generation sequencing technology revealed that aberrant activations in oncogenic pathways by EGFR mutations and ALK fusions were rare in lung SCC. Cell lines with inherent resistance to cisplatin were first identified with cell proliferation assays. To elucidate mechanisms that mediate resistance to cisplatin, drug-induced perturbations to gene and protein expression were compared between cisplatin-sensitive and –resistant SCC cells, and identified MAPK/Erk pathway up-regulation and activation in drug-resistant cells. Erk-induced resistance appeared to be activated by Son of Sevenless (SOS) upstream, and mediated through Bim degradation downstream. Clinically, elevated p-Erk expression was associated with shorter disease-free survival in patients with locally advanced head and neck SCC treated with concurrent chemoradiation. Inhibition of MEK/Erk, but not that of EGFR or RAF, augmented cisplatin sensitivity *in vitro*. Collectively, these findings suggest that up-regulation of the MAPK pathway through SOS-mediated MEK/Erk activation confers resistance to cisplatin treatment, and MEK inhibition may augment patient responses to cisplatin treatment.

Parallel investigations were conducted to identify the potential chemosensitizing mechanism(s) in lung SCC. Belinostat, a pan HDAC inhibitor, was found to exhibit strong synergy with cisplatin in cisplatin-resistant cell lines. Importantly, belinostat treatment suppressed p44/42 MAPK signalling dose-dependently through abrogation of SOS, which led to Bim up-regulation and apoptosis. These observations suggested that

belinostat could attenuate SOS/MAPK-mediated cisplatin resistance. Furthermore, combination of cisplatin together with a clinically tolerable dose of belinostat (0.1μM) significantly induced cell death in several lung SCC cell lines. Using H2170 cell lines as study model, synergistic cytotoxicity of belinostat and cisplatin was correlated with acetylation of mutant p53 (R158G), and was rescued when p53 was silenced. Conversely, ectopic expression of mutant p53 in Calu-1 cells (p53 null, cisplatin-resistant) effectively increased cisplatin sensitivity. The cell death observed in p53 mutant cells after combination treatment of belinostat and cisplatin was further associated with acetylation of p53. Moreover, tenovin-6, a specific acetylator of p53, concomitantly induced p53 acetylation and cellular apoptosis in p53 mutant cells. Taken together, these findings proposed a therapeutic strategy that targets p53 mutant SCC cells through activation of p53-mediated apoptosis.

In summary, this study has described a cisplatin resistance mechanism involving the up-regulation of SOS/MAPK/Erk signalling that is activated under treatment pressure. Such perturbation could be subjected to therapeutic intervention using MEK inhibitors or belinostat. More crucially, this study describes a novel gain-of-function event in p53 mutant cells that is responsible for belinostat/cisplatin-induced cell death. This thesis proposed two promising combination strategies for SCC patients: one targeting tumours with high p-Erk, the other for tumours that harbour mutant p53.

LIST OF TABLES

LIST OF FIGURES

LIST OF ABBREVIATIONS

AA	Amino acid
ABCC2	ATP-binding cassette sub family C2
ADP	Adenosine diphosphate
Akt	Protein kinase B
ALK	Anaplastic lymphoma kinase
ANOVA	One-way-analysis of variance
Apaf-1	Apoptotic protease-activating factor-1
APC	Allophycocyanin
APS	Ammonium persulfate
ARF	Alternative reading frame
ATCC	American Type Culture Collection
ATM	Ataxia telangiectasia-mutated
ATP	Adenosine triphosphate
ATP7B	P-type adenosine triphosphate
ATPase	Adenosine triphosphatase
ATR	Ataxia telangiectasia-mutated and Rad3-related kinase
Bad	Bcl-2 antagonist of cell death
Bak	Bcl-2 homologous antagonist killer
BAX	Bcl-2-associated X
BCA	Bicinchoninic acid
Bcl-2	B-cell lymphoma 2
Bcl-w	Bcl-2-like 2
Bcl-xl	B-cell lymphoma-extra large
BER	Base-excision repair
Bid	BH3 interacting domain death agonist
Bim	Bcl-2 interacting mediator
Bim_{EL}	Bim extra long isoform
Bim_{L}	Bim long isoform
Bim_{S}	Bim short isoform
BLAST	Basic Local Alignment Search Tool
Bok	Bcl-2-related ovarian killer
B-Raf	v-Raf murine sarcoma viral oncogene homolog B1
BRCA1	Breast cancer 1, early onset
BRCA2	Breast cancer 2, early onset
BSA	Bovine serum albumin
C. elegans	*Caenorhabditis elegans*
Caspase	Cysteine-dependent aspartate-specific protease
CBP	Cyclin-AMP-response-element binding protein
CDDP	Cisplatin
CDK	Cyclin-dependent kinase
CDKN1a	p21/cyclin dependent kinase 1a
CDKN2a	p14/cyclin dependent kinase 2a
cDNA	Complementary DNA
CDS	Coding DNA sequence

CED-3	*C. elegans* cell death-3
CI	Combination Index
CK	Casein kinase
CMV	Cytomegalovirus
CO_2	Carbon dioxide
COSMIC	Catalogue of Somatic Mutations in Cancer
CPSS	Computerized Patient Support System
Ct	Threshold cycle
CT	Computed tomography
CTCL	Cutaneous T-cell lymphona
CTR1	Copper transporter 1
DAB	Diaminobenzidine
DAPI	4',6-diamidino-2-phenylindole dye
dATP	Deoxyadenosine triphosphate
dCTP	Deoxycytidine triphosphate
dGTP	Deoxyguanosine triphosphate
DBD	DNA-binding domain
DFS	Disease-free survival
DISC	Death-inducing signalling complex
DMEM	Dulbucco's Modified Eagle's Medium
DMSO	Dimethyl sulfoxide
DNA	Deoxyribonucleic acid
DNA-PK	DNA-dependent protein kinase
DNase	Deoxyribonuclease
dNTP	Deoxyribonucleotide triphosphates
DRI	Dose reduction index
DSRB	Domain-specific Review Board
dTTP	Deoxythymidine triphosphate
E. coli	*Escherichia coli*
ECL	Electrogenerated chemiluminescence
EDTA	Ethylenedinitrilo tetraacetic acid
EGF	Epidermal Growth Factor
EGFR	Epidermal growth factor receptor
ELISA	Enzyme-linked immunosorbent assay
EMEM	Eagle's Minimum Essential Medium
EML4	Microtubule-associated protein-like 4
ERCC1	Excision repair cross-complementing 1
Erk	Extracellular regulated kinase
EV	Empty vector
FACS	Fluorescence-activated cell sorting
FADD	Fas-associated death domain-containing protein
FasL	Fas-ligand
FBS	Fetal bovine serum
FDA	Food and Drug Administration USA
FFPE	Formalin-fixed,
FISH	Fluorescence *in situ* hybridization
g	Gravitational force
G418	Neomycin

GAPDH	Glyceraldehyde 3-phosphate dehydrogenase
GATK	Genome Analysis Toolkit
gDNA	Genomic DNA
GDP	Guanosine diphosphate
GEP	Nucleotide exchange protein
GFP	Green fluorescent protein
GPX	Glutathione peroxidase
GSH	Glutathione
GSK3	Glycogen synthase kinase 3
GST	Glutathione-S-transferase
GTP	Guanosine triphosphate
HA	Hemagglutinin
HAT	Histone acetyl-transferase
HCl	Hydrochloric acid
HDAC	Histone deacetylase
HEPES	4-(2-hydroxyethyl)-1-piperazineethanesulfonic acid
HER2	Human growth factor receptor 2
HIF1α	Hypoxia-inducible factor 1α
HIV	Human immunodeficiency virus
HMG	High-mobility group
HNSCC	Head and neck squamous cell carcinoma
HPV	Human papillomavirus
HR	Homologous recombination
HRP	Horseradish peroxidase
IAP	Inhibitors of apoptosis protein
IC_{50}	Half-maximum inhibitory concentrations
IHC	Immunohistochemistry
IRB	Institutional Review Board
JAK	Janus kinase
JNK	c-Jun N-terminal kinase
KCl	Potassium chloride
KEGG	Kyoto Encyclopedia of Genes and Genomes
KH_2PO_4	Monopotassium phosphate
KIF5B-RET	Kinesin family member 5B-ret proto-oncogene
L	Litre
LB	Luria-Bertani
MAC	Mitochondrial apoptosis-induced channel
MAPK	Mitogen activated protein kinase
MAR	Matrix attachment region
MDM2	Mouse double minute 2
MDR1	Multidrug resistant protein 1
MEF2	Myocyte enhancer factor 2
MEK	Mitogen activated protein kinase kinase
MEKK1	MAP/Erk kinase kinase 1
MET	Mesenchymal-epithelial transition
$MgCl_2$	Magnesium chloride
MGST	Microsomal glutathione S-transferase

mL	Millilitre
mM	Millimolar
MMP	Matrix metalloproteinase
MMR	Mismatch repair
MRI	Magnetic resonance imaging
MRP	Multidrug resistance protein
MSK	Mitogen and stress-activated protein kinase
mTOR	Mammalian target of rapamycin
MTS	3-(4,5-dimethylthiazol-2-yl)-5-(3-carboxymethoxyphenyl)-2-(4-sulfophenyl)-2H-tetrazolium
MTT	3-(4,5-Dimethyl-2-thiazolyl)-2,5-diphenyl-2H-tetrazolium bromide
NaCl	Sodium chloride
NaCl	Sodium chloride
NAD+	Nicotinamide adenine dinucleotide
NaH2PO4	Sodium dihydrogen phosphate
NaOH	Sodium hydroxide
NEB	New England Biolabs
NER	Nucleotide-excision repair
NES	Nuclear export signal
NF-κB	Nuclear factor kappa-light-chain-enhancer of activated B cells
NGS	Next Generation Sequencing
NHEJ	Non-homologous end joining
NHG	National Healthcare Group
NLS	Nuclear localization signal
nm	Nanometer
nM	Nanomolar
NSCLC	Non-small cell lung cancer
NUH	National University Hospital
ORF	Open reading frame
PAGE	Polyacrylamide gel electrophoresis
PARP	Poly(ADP-ribose) polymerase
PBS	Phosphate buffered saline
PBS-T	PBS containing 0.1% (v/v) Tween 20
PCAF	p300/CBP-associated factor
PCR	Polymerase chain reaction
PI	Propidium iodide
PI3K	Phosphatidylinositol-3-kinase
PIK3CA	Phosphatidylinositol-4,5-biphosphate 3-kinase
PIP2	Phosphatidylinositol (4,5)-biphosphate
PIP3	Phosphatidylinositol (3,4,5)-triphosphate
PKC	Protein kinase C
pM	Picomolar
PTCL	Peripheral T-cell lymphoma
PTEN	Phosphatase and tensin homolog
PUMA	p53-upregulated mediator of apoptosis

PVDF	Polyvinylidene difluoride
PXD101	Belinostat
RA	Retinoic acid
Raf	v-Raf murine sarcoma viral oncogene
RARα	Retinoic acid receptor α
Ras	Rat sarcoma
RB	Retinoblastoma protein
RE	Restriction enzyme
RIN	RNA integrity number
RNA	Ribonucleic acid
RNase	Ribonuclease
RNR	Ribonucleotide reductase
ROS	Reactive oxygen species
rpm	Revolutions per minute
RSK	Ribosomal s6 kinase
RT-PCR	Reverse-transcriptase PCR
RTK	Receptor tyrosine kinase
Runx	Runt-related transcription factor
S.O.C	Super Optimal broth with Catabolite repression
SAHA	Suberanilohydroxamic acid; vorinostat
SD	Standard deviation
SDS	Sodium dodecyl sulphate
Sec	Second
SH2	Src-homology 2 domain
SHC	Src homology 2 domain containing transforming protein
shRNA	Short hairpin RNA
siRNA	Small interfering RNA
SirT	Sirtuin
Smac/DIABLO	Small-mitochondria-derived activator of caspases/ direct inhibitor of apoptosis-binding protein with low pI
SNP	Single nucleotide polymorphism
SOS	Son-of-Sevenless
STAT	Signal transducer and activator of transcription
STK11	Serine/threonine kinase 11
TAE	Tris-acetate-EDTA
tBid	Truncated Bid
TBP	TATA box-binding protein
TBP-2	Thioredoxin-binding protein-2
TBS	Tris-buffered saline
TBS-T	TBS containing 0.1% (v/v) Tween 20
TCGA	The Cancer Genome Atlas
TE	Tris-EDTA
TEMED	Tetramethylethylenediamine
TFIID	Transcription factor II D
TFIIH	Transcriptional factor II Human
TGF-α	Transforming growth factor α
TGF-β	Transforming growth factor beta

TKI	Tyrosine kinase inhibitor
TNF	Tumour necrosis factor
TNV	Tenovin
TP53	Tumour suppressor protein 53
TP73	Tumour suppressor protein 73
TRAIL	TNF-related apoptosis inducing ligand
TSA	Trichostatin-A
UTR	Untranslated region
UV	Ultra violet
V	Voltage
v/v	Volume/volume
VEGF	Vascular endothelial growth factor
W	Watt
w/v	Weight/volume
WT	Wild-type
XIAP	X-linked IAP
XPC/XPE/XPF	Xeroderma pigmentosum complementation group C/E/F
β-ME	β-mercaptoethanol
γ-GCS	Gamma-glutamyl cysteine synthetase
µL	Microlitre
µm	Micrometer
µM	Micromolar

CHAPTER 1 INTRODUCTION

1.1 Lung Squamous Cell Carcinoma

1.1.1 The Disease and its Prevalence

Lung cancer is the leading cause of cancer-related death worldwide, and is accounted for an estimated 1.4 million deaths in 2010, thus exceeding the combined mortality of breast, colorectal and prostate carcinomas (World Health Organisation 2013). In Singapore, the incidence and mortality rates for lung cancer have been on the increasing trend through most of last century and it is now among the most frequently diagnosed cancer in both male and female population with a five-year overall survival rate of less that 15% (Teo and Soo 2013).

Lung cancer comprises of tumours that arise from cells lining the airway of the respiratory system. It is generally classified into 2 main types: small cell lung cancer and non-small cell lung cancer (NSCLC) based on clinicopathological features. NSCLC constitutes 85-90% of all lung cancer cases with squamous cell carcinoma (SCC) and adenocarcinoma being two of the major subtypes (30% and 40%) (TCGA 2008). Lung SCC is clinically and histopathologically distinct from adenocarcinoma, as two subtypes are varied in shape, size, site-of-origin and even therapeutic options. Although adenocarcinoma has replaced lung SCC as the most common histology subtype for all lung cancer cases (Travis, Cancer, 1995), lung SCC prevails as a major public health concern worldwide due to its low 5-year overall survival rate (Sato, Shames et al. 2007).

In general, symptoms of lung SCC include but not limited to, persistent cough, coughing out blood, chest pain, wheezing, hoarseness, pneumonia and haemoptysis (A.D.A.M., 2011). Since lung SCC tends to develop near to the larger air passages, its symptoms tend to surface earlier than other form of lung cancer. However, despite the continual development of diagnosis platforms, majority of the lung cancer patients are only diagnosed at advanced stages. The initial detection of lung cancer involves chest X-ray and bronchoscopy. In cases whereby a mass in the lungs or swollen chest lymph nodes were identified, further tests that include computed tomography (CT), magnetic resonance imaging (MRI) and needle biopsy are conducted to determine the nature of the mass by pathologists. As lung SCC often arises in the central bronchi, while its carcinoma *in situ* is asymptomatic and generally undetectable on X-ray, the diagnosis for this disease is made difficult. More importantly, the poor diagnosis of lung SCC directly attributes to the poor prognosis. Upon detection, the stages of the lung tumours will be classified based on the TNM [size of the primary tumour (T), presence of regional lymph node (N) and distant metastasis (M)] staging system (Goldstraw, Crowley et al. 2007), which will determine the treatment options.

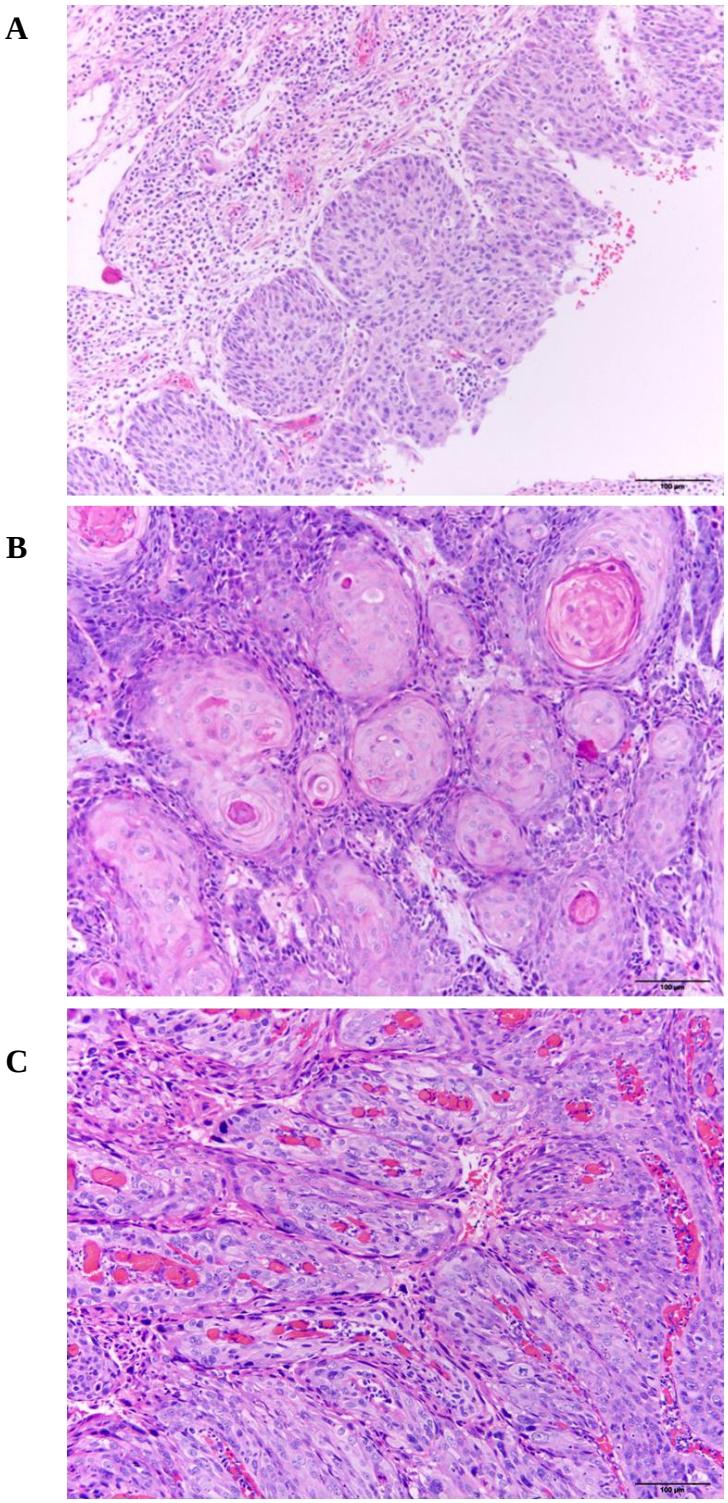

Figure 1.1: Histology tissue section from samples of squamous cell carcinoma stained with Mayer's haematoxylin and eosin.

A, Photomicrograph revealed carcinoma *in situ* (CIS) of SCC. B, Photomicrograph revealed early stage SCC, with keratin pearls surrounded by tumour cells. C, Photomicrograph of poorly differentiated late stage SCC. All photomicrographs where taken in 200x magnification. Scale bars in A – C, 100μm.

1.1.2 Clinicopathology of lung SCC

NSCLC originates from lung epithelial cells of the central bronchi to terminal alveoli. The histological classification of NSCLC is very much dependent on the site-of-origin. Unlike lung adenocarcinoma that is usually located at outer part of the lung, SCC usually arises from central bronchus, where it originates from the squamous tissue along the airway of the lung and lines bronchi that link up the trachea to the lung. This tumour is slow-growing, and requires years to develop from confined metaplasia and dysplasia to carcinoma *in situ* (Saccomanno, Archer et al. 1974) (Figure 1.1 A), before eventually developed into invasive cancer. The hallmark of SCC is the presence of keratinisation, which leads to either the formation of keratin pearls that are surrounded by tumour cells (Figure 1.1 B), or intercellular bridges that link adjacent cells. At early stages, lung SCC are well-differentiated and keratin pearls are usually found; while at late stages, these tumours are poorly differentiated with minimal squamous cell features (Saccomanno, Archer et al. 1974) (Figure 1.1 C).

Lung SCC is inherently heterogeneous and this variability often leads to differential prognosis. Based on their histopathological appearances, lung SCC is further divided into 4 variants: papillary, small cell, clear cell and basaloid. Several reports have demonstrated the variability in drug response among these variants, with high-grade basaloid variants being demonstrated to have poorer prognoses that the overall population of lung SCC (Wang, Wang et al. 2011). More recently, lung SCC are stratified into 4 genetic subtypes (primitive, classical, secretary and basal) based on their mRNA expression profile (Wilkerson, Yin et al. 2010). These subtypes are further shown to have differential survival outcomes, biological processes, and could predict drug response to various therapy (Wu, Pang et al. 2013).

1.1.3 Etiology of lung SCC

Cigarettes smoking is the primary risk factor for lung cancer as patterns of disease occurrence are, to a large extent, determined by tobacco exposure (Molina, Yang et al. 2008). However, other studies have reported 10 - 40% of NSCLC cases occur in patients with no history of smoking (Subramanian and Govindan 2007). Inherent genetic susceptibility and environmental exposure, that include tobacco smoke, radon gas, asbestos, toxic chemical entities, air pollution and ionising radiation, have also been shown to increase risk of NSCLC (Govindan, Ding et al. 2012). Among these factors, the habit of tobacco smoking is most strongly associated with lung SCC. Thus, the incidence of lung SCC decreases in recent years as consequence of changes in smoking habit and construction of new formulation for cigarette content.

Similar to other types of cancer, development and progression of NSCLC is a multi-stage process (Wistuba, Behrens et al. 1999, Yokota and Kohno 2004). It has been shown that the molecular pathways leading to the pathogenesis are relatively different across lung adenocarcinoma and lung SCC. While Kras and β-catenin mutations are common in adenocarcinoma (Yokota and Kohno 2004), loss-of-heterozygosity of chromosome 3p is frequently detected (>80%) in lung SCC (Wistuba, Behrens et al. 1999, Zabarovsky, Lerman et al. 2002). The deletion of chromosome 3p is also accompanied by the p16 abnormalities and alterations of p53 pathways during the development of squamous dysplasia from normal lung epithelium (Shiseki, Kohno et al. 1996). Furthermore, sub-classification of a group of SCC based on their bronchial sites (central, intermediate and peripheral bronchi) reveals certain trends for p53 mutational spectra of these tumours in specific location (Shimmyo, Hashimoto et al. 2006). This study proposed that investigation of the link between p53 mutational status and smoking history may provide insights to etiological factors of lung SCCs. In addition, the progression of confined tumours to metastatic SCC requires sequential aberrations that include allelic loss of chromosome 2q, 9p, 18q and 22q (Shiseki, Kohno et al. 1994, Nishioka, Kohno et al. 2002).

1.1.4 Staging of lung SCC

Defining the stage classification is an important process in patients with cancer, as it often affects the treatment options. Similar to most cancers, the classification of NSCLC is based on the TNM system (Detterbeck, Boffa et al. 2009). The T descriptor defines the extent of the primary tumour; N descriptor the involvement of regional lymph node; and the M descriptor the presence of distant metastasis (Goldstraw, Crowley et al. 2007). The various type of staging could be assessed by clinical staging, which could be determined with magnetic resonance imaging (MRI), computed tomography (CT) scan, positron emission tomography (PET) scan, or endoscopic ultrasound; and pathological stagining, which is usually determined after a resection has been performed (Detterbeck, Boffa et al. 2009). Based on the T, N and M descriptors, NSCLC can be staged as follow: stage 0 is the formation of carcinoma *in situ*; in stage I, cancer has formed but has not spread to lymph nodes; in stage II, tumour has expanded (5 – 7 cm) and spread to nearby lymph nodes; in stage IIIA, cancer has spread to regional lymph nodes on the same side of the chest as the tumour; in stage IIIB, cancer has spread to regional lymph nodes above the collarbone or on the opposite side of the chest as the tumour; and in stage IV, cancer has spread to both side of the lungs, to fluids around the lung, or to other organ of the body (Goldstraw, Crowley et al. 2007).

1.2 Conventional chemotherapies in lung SCC

Treatment of lung cancer is dependent on the stage of the disease upon diagnosed, which are generally assessed by CT, MRI and needle-biopsy. At early stages, surgical resection is usually performed with options of adjuvant chemotherapy. However, as discussed in the previous chapter, early diagnosis of lung tumours is limited by current diagnostic techniques. For many years, treatment of advanced lung cancer has been highly-dependent on chemotherapy as the first-line therapy. Chemotherapies are non-targeting cytotoxic or genotoxic agents that either kill or inhibit proliferation of tumour cells. Cancer cells are characterized by their aberrant proliferation. Thus, most chemotherapies are designed to target rapidly dividing cells by impairing mitosis, a crucial cell division mechanism, of cancer cells. However, healthy cells that divide rapidly, such as hair follicles, bone marrow and digestive tract, are also affected by chemotherapeutic agents. These non-specific targeting of chemotherapies on non-malignant cells give rise to common side effects such as alopecia, mucositis and myelosuppression (Peters 1994, Wong and Giandomenico 1999).

Chemotherapy may be used as a single agent or in combinations with other agents. Several meta-analysis studies have reported the slight advantage of chemotherapy in advanced NSCLC (Grilli, Oxman et al. 1993, Marino, Pampallona et al. 1994). Commonly used chemotherapies for NSCLC include DNA damaging agents, anti-metabolites, and mitotic inhibitors. In a randomized study, four chemotherapeutic regimens (cisplatin and paclitaxel, cisplatin and gemcitabine, cisplatin and docetaxel, carboplatin and paclitaxel) offered comparable treatment outcomes in advanced NSCLC patient with no significant advantages over one another (Schiller, Harrington et al. 2002).

1.2.1 DNA-damaging agents: platinum-containing compounds

Despite the rapid development of anti-neoplastic agents, platinum-based compounds remain as one of the most commonly used and effective treatment options for cancer patients. It has displayed broad spectrum efficacy in a wide range of malignancies such as lung, ovarian, testicular, bladder and head and neck carcinomas (Lebwohl and Canetta 1998, Wang and Lippard 2005). Cisplatin, also known as cis-diamminedichloridoplatinum(II) (CDDP), is the first platinum-based drug that was discovered back in the 1960s when it showed inhibitory effect of DNA synthesis in *Escherichia coli* (Rosenberg, Van Camp et al. 1967). Due to its efficacy as an anti-cancer agent, newer generation of platinum-containing compounds with lower toxicity have been developed that include carboplatin, oxaliplatin, picoplatin, satraplatin and more recently aroplatin and AP5346 (Kelland 2007, Eckardt, Bentsion et al. 2009) (Figure 1.2). Interestingly, some of these analogues display differential sensitivities

among cancer cells. For instant, carboplatin has been shown to exhibit cross-resistance to cisplatin (Rixe, Ortuzar et al. 1996, Johnson, Laub et al. 1997), but oxaliplatin is found to be effective in cancer cells with acquired resistance to cisplatin (Raymond, Faivre et al. 2002) while picoplatin induces cytotoxicity in cisplatin/carboplatin-resistant NSCLC (Tang, Parham et al. 2011).

Platinum drugs are a class of alkylating agents that are capable of forming DNA adducts and leading to cellular cytotoxicity. The interaction with DNA requires intracellular activation of platinum drug under aqueous condition, whereby the chlorine ligands are replaced with hydroxyl group to form the positively charged aquated species that covalently bind to DNA, thus forming intrastrand cross-link adducts (Huang, Zhu et al. 1995, Jamieson and Lippard 1999). These adducts result in distortions within the DNA, and impede cellular processes which require separation of DNA, such as DNA replication and transcription (Siddik 2003). This induces genotoxic stress within the cellular body that triggers the activation of DNA repair pathways (Zamble, Mu et al. 1996). Importantly, the eventual cellular outcome of platinum-based compounds is generally apoptotic cell death (Eastman 1990). Cisplatin and carboplatin are widely used in the treatment of ovarian, cervical, head and neck and NSCLC (Jamieson and Lippard 1999). Particularly in testicular cancer, cisplatin has an overall cure rate exceeding 90% (Raghavan 2003).

1.2.2 Microtubule targeting agents: taxanes

Taxanes are mitotic inhibitors that inhibit the process of cell division by disruption of microtubule function (Abal, Andreu et al. 2003). Microtubules are highly dynamic cellular polymers that are essential for cell division by facilitating the arrangement of dividing spindle and integrity of segregated DNA (Sharp, Rogers et al. 2000). Taxanes stabilize the GDP-bound tubulin and prevent it from disassembly. This inhibits the configuration of metaphase spindle, thus blocks progression of mitosis, induces cell cycle arrest and triggers apoptosis (Abal, Andreu et al. 2003, Mollinedo and Gajate 2003).

Paclitaxel (Taxol) is the first isolated taxanes and is seen as the prototype of the anti-cancer taxane family drugs (Wani, Taylor et al. 1971). The anti-neoplastic effects of taxanes were illustrated by the tumour-suppressive effects in leukemic and xenograft models (Wani, Taylor et al. 1971). Initial therapeutic responses were first observed in melanoma and refractory ovarian cancer patients (McGuire, Rowinsky et al. 1989, Wiernik and Einzig 1993). Currently, paclitaxel is among the first-line chemotherapies for melanoma, breast, prostate and NSCLC patients (Perez 1998, Obasaju and Hudes 2001, Hodi, Soiffer et al. 2002, Ramalingam and Belani 2004).

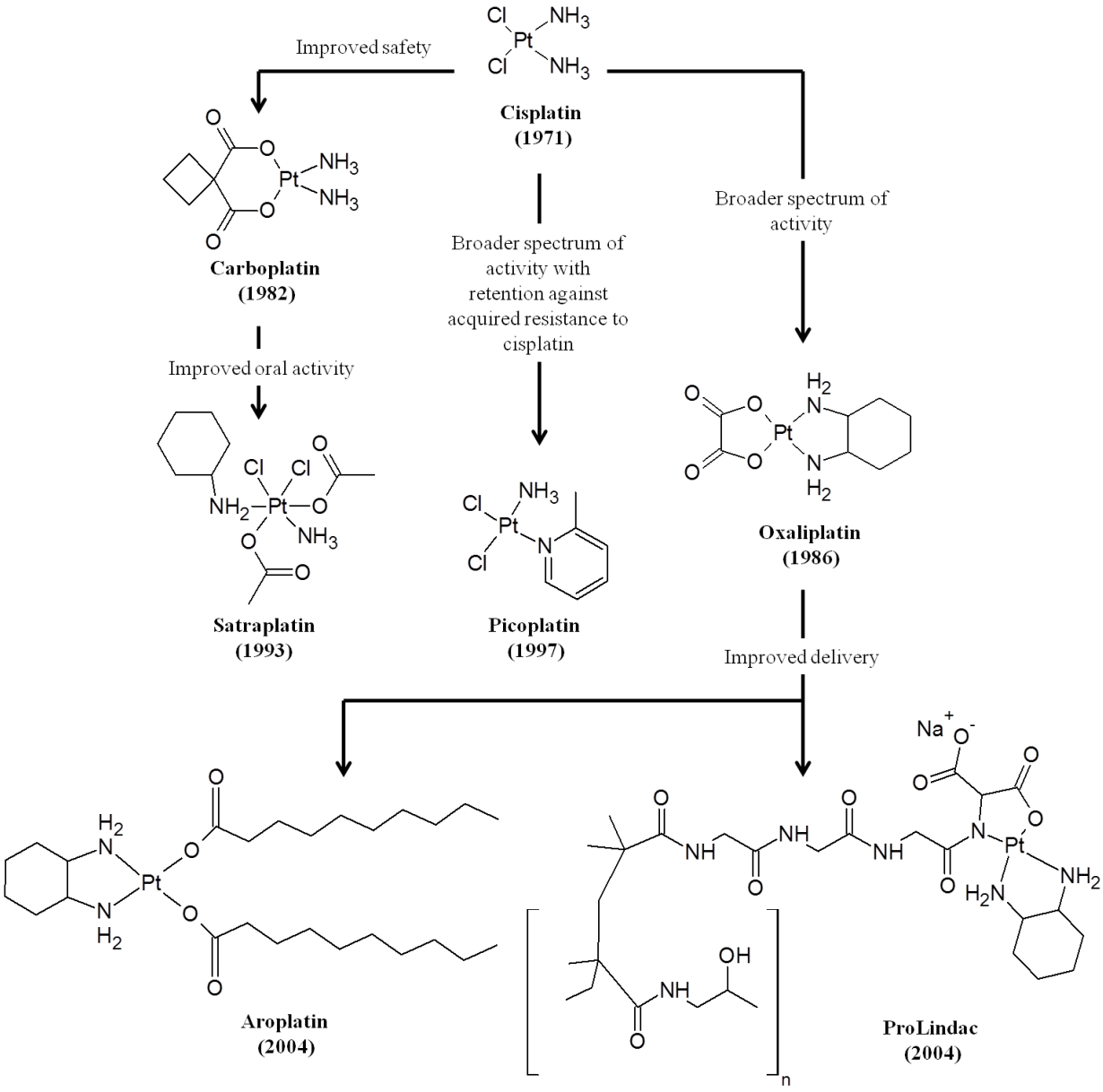

Figure 1.2: The structures of several platinum-based chemotherapies with the history and rationale behind their development.

The dates indicate the time when each agent was first administered to patients. Improvement made on each generation of platinum-containing compound is demonstrated. [Adapted from (Kelland 2007)]

1.2.3 Anti-metabolites: Gemcitabine

Anti-metabolite drugs are among the first effective chemotherapeutic agents identified. The structure of this class of compounds mimics the naturally found molecules that are essential in nucleic acid synthesis (ELION, HITCHINGS et al. 1951). The main representatives of

these drugs are purine analogues, pyrimidine analogues and folic acid. These analogues are structurally similar to naturally occurring purines and pyrimidines (Montgomery, Elliott et al. 1978). During DNA replication, the incorporation of anti-metabolites into DNA or RNA of tumour cells lead to growth arrest and apoptosis (Plunkett, Huang et al. 1995). A key factor that affects the efficacy of anti-metabolite drugs is the rate of facilitated diffusion of both normal and analogue nucleosides in and out of the cells. A wide range of cancer cell lines have been reported to contain transport systems that promote active removal of anti-metabolites (Paterson, Kolassa et al. 1981).

Gemcitabine (dFdC) is a pyrimidine analogue that is a first-line treatment of NSCLC. This compound was first synthesized in 1986 as an antiviral agent. Its subsequent demonstration of anti-neoplastic activities in murine xenograft models led to its evaluation as a chemotherapeutic agent (Hertel, Boder et al. 1990, Lund, Kristjansen et al. 1993). Apart from forming building blocks in nucleic acids, gemcitabine also targets the ribonucleotide reductase (RNR). Irreversible inactivation of RNR inhibits the synthesis of deoxyribonucleotides that are essential for DNA replication and thus induces cell death (Cerqueira, Fernandes et al. 2007). Gemcitabine has been shown to achieve 20 - 26% response rate in NSCLC patients (Abratt, Bezwoda et al. 1994, Anderson, Lund et al. 1994), while co-administration with cisplatin generated response rate as high as 50% (Abratt, Bezwoda et al. 1997, Crinò, Scagliotti et al. 1997).

1.2.4 Programmed cell death by conventional chemotherapies

1.2.4.1 Autophagy, necrosis and apoptosis

The eventual goal of chemotherapy is the killing of tumour cells. Death of tumour cells via programmed cell death can be mediated by extensive regulation of intracellular signalling (Lockshin and Beaulaton 1974). Years of research have identified various types of cell death which are classified based on their distinct molecular characteristics. Among them, apoptosis, necrosis and autophagy are commonly related to cancer therapeutics (Galluzzi, Vitale et al. 2012). Briefly, autophagy is a homeostatic process in which cellular degradation of cytoplasmic organelles within the same cell is carried out through lyzosomal activities (Levine and Klionsky 2004). However, the role of autophagy as a protective adaptation response that promotes cell survival (Lum, DeBerardinis et al. 2005), or as a programmed cell death mechanism remains debatable (Levine and Yuan 2005). Increasing evidences have been demonstrated in support of autophagic cell death as response to chemotherapies (Kanzawa, Kondo et al. 2003, Notte, Leclere et al. 2011). Necrosis is a cell death mechanisms that is morphologically characterized by cell swelling, rupture of plasma

membrane and release of cellular components into extracellular matrix (Majno and Joris 1995). Although being initially believed to be unregulated and accidental, necrotic cell death has been recently found to be actively regulated by several factors, which include exposure to DNA alkylating agents (Vandenabeele, Galluzzi et al. 2010, Baritaud, Cabon et al. 2012).

Despite the improved understandings of autophagy and necroptosis in drug-induced cell death, apoptosis remains as the most extensively characterized form of programmed cell death. Apoptosis was first described in 1972 as a form of cell death that is distinguishable by cell shrinkage, blebbing of plasma membrane, condensation and fragmentation of DNA (Kerr, Wyllie et al. 1972). Apoptotic cell death has since been demonstrated as an important check-point for maintenance of homeostasis and cellular development, with its dysregulation often leads to neurodegenerative disease, autoimmunity and tumourigenesis (Fuchs and Steller 2011). In general, apoptosis is a universal outcome of chemotherapy.

1.2.4.2 Molecular mechanisms of apoptosis

Earlier studies on *Caenorhabditis elegans* (*C. elegans*) have provided insights into the key molecular processes that are involved in apoptosis (Ellis and Horvitz 1986, Horvitz 1999). The identification of CED-3, and subsequently caspases, paves the direction for further understanding on the cellular components of apoptosis (Yuan, Shaham et al. 1993).

Apoptosis have been distinctly classified into two main types: the mitochondria-mediated intrinsic pathway and the death receptor-mediated extrinsic pathway (Nagata 1997, Shi 2001). Briefly, extrinsic apoptosis is controlled by extracellular signals such as hormones, growth factors and cytokines, while intrinsic apoptosis is modulated by intracellular stress responses, such as nutrient deprivations, viral infection and radiation (Nagata 1997, Shi 2001). Caspases are the main effectors that drive apoptosis and 14 isoforms have been identified (Alnemri 1997). Caspases are being synthesized as zymogens (pro-caspases). Apoptotic stimuli trigger the proteolytic cleavage and heterodimerization of pro-caspases. Subsequently, functional tetramers were formed by two heterodimers (Earnshaw, Martins et al. 1999). Caspases are classified into initiator caspases (caspase 2, 8, 9, 10) and effector caspases (caspase 3, 6, 7) based on their respective functions in apoptosis (Alnemri, Livingston et al. 1996, Alnemri 1997). The catalytic activities of caspases are crucial in the induction of apoptosis when initiator caspases trigger the activation of effector caspases, which then lead to the cleavage of vital cellular substrates that include poly(ADP-ribose) polymerase (PARP), a DNA repair enzyme (Fesik 2000).

Although both intrinsic and extrinsic pathways eventually cleave PARP and caspase 3/7, there are different in terms of initiation and execution. Extrinsic apoptotic pathway is directly initiated through binding of tumour necrosis factor (TNF), Fas ligand (FasL) and TNF-related apoptosis-inducing ligand (TRAIL) to death receptors known as the TNF receptor superfamily (Wajant 2002). Binding of ligands triggers the recruitment of adaptor proteins such as Fas-associated death domain (FADD) as well as pro-caspase 8 to form death-inducing signalling complex (DISC) (Muzio, Stockwell et al. 1998, Wajant 2002). As pro-caspase 8 molecules are brought to close proximity by DISC, this promotes its auto-activation through proteolytic cleavage (Muzio, Stockwell et al. 1998).

Intrinsic apoptotic pathway is primarily regulated by mitochondria (Li, Nijhawan et al. 2004). Disruption of mitochondria membrane potential as a result of the formation of mitochondrial apoptosis-induced channel (MAC) is regulated by the pro-apoptotic and anti-apoptotic B-cell lymphoma 2 (Bcl-2) family proteins (Dejean, Martinez-Caballero et al. 2006). Anti-apoptotic Bcl-2 family members (Bcl-2, Bcl-xl, Bcl-w) maintain the integrity of mitotochondria outer membrane by directly inhibiting the pro-apoptotic Bcl-2 proteins (Chipuk and Green 2008). The pro-apoptotic Bcl-2 family members can be further divided into two subgroups: the effector proteins (BAX, Bak, Bok) and the BH3-only proteins (Bid, BAD, Bim, PUMA, Noxa). Briefly, BH3-only proteins function as sensors of death signals and facilitate apoptosis by activating Bcl-2-associated X (BAX)/Bcl-2 homologous antagonist killer (Bak) as well as neutralizing the anti-apoptotic Bcl-2 proteins (Luo, Budihardjo et al. 1998, Wei, Lindsten et al. 2000, Kim, Tu et al. 2009). The oligomerization of BAX/Bak complex forms pores on the mitochondria outer membrane. Thus, the balance between pro-apoptotic and anti-apoptotic Bcl-2 proteins determines the assembly of MAC (Dejean, Martinez-Caballero et al. 2006). This leads to the loss of mitochondria membrane potential and increase in membrane permeability, thus the sequential release of mitochondria-bound Smac/DIABLO (small-mitochondria-derived activator of caspases/ direct inhibitor of apoptosis-binding protein with low pI) and cytochrome c into the cytosol (Zhou, Zhou et al. 2005). Smac/DIABLO functions by deactivating inhibitor of apoptosis proteins (IAPs), such as X-linked IAP (XIAP), that are known to block apoptosis by binding to caspases (Vucic, Deshayes et al. 2002, Eckelman, Salvesen et al. 2006). Cytochrome c functions differently by initiating the formation of apoptosome, a complex comprises of apoptotic protease activating factor-1 (Apaf-1) and pro-caspase 9, that results in the auto-activation of caspase 9 (Srinivasula, Ahmad et al. 1998, Jiang and Wang 2000).

Both intrinsic and extrinsic apoptotic pathways leads to activation of caspase 3 and 7 (Hammerman, Sos et al. 2011), and eventually cell death (Porter and Jänicke 1999). In

addition, convincing evidences have suggested that these two pathways are not mutually exclusive, as the activation of tBid by extrinsic pathway has been shown to trigger intrinsic pathway (Li, Zhu et al. 1998, Shi and Shen 2008). Figure 1.3 illustrates the key regulators of both intrinsic and extrinsic apoptotic pathways.

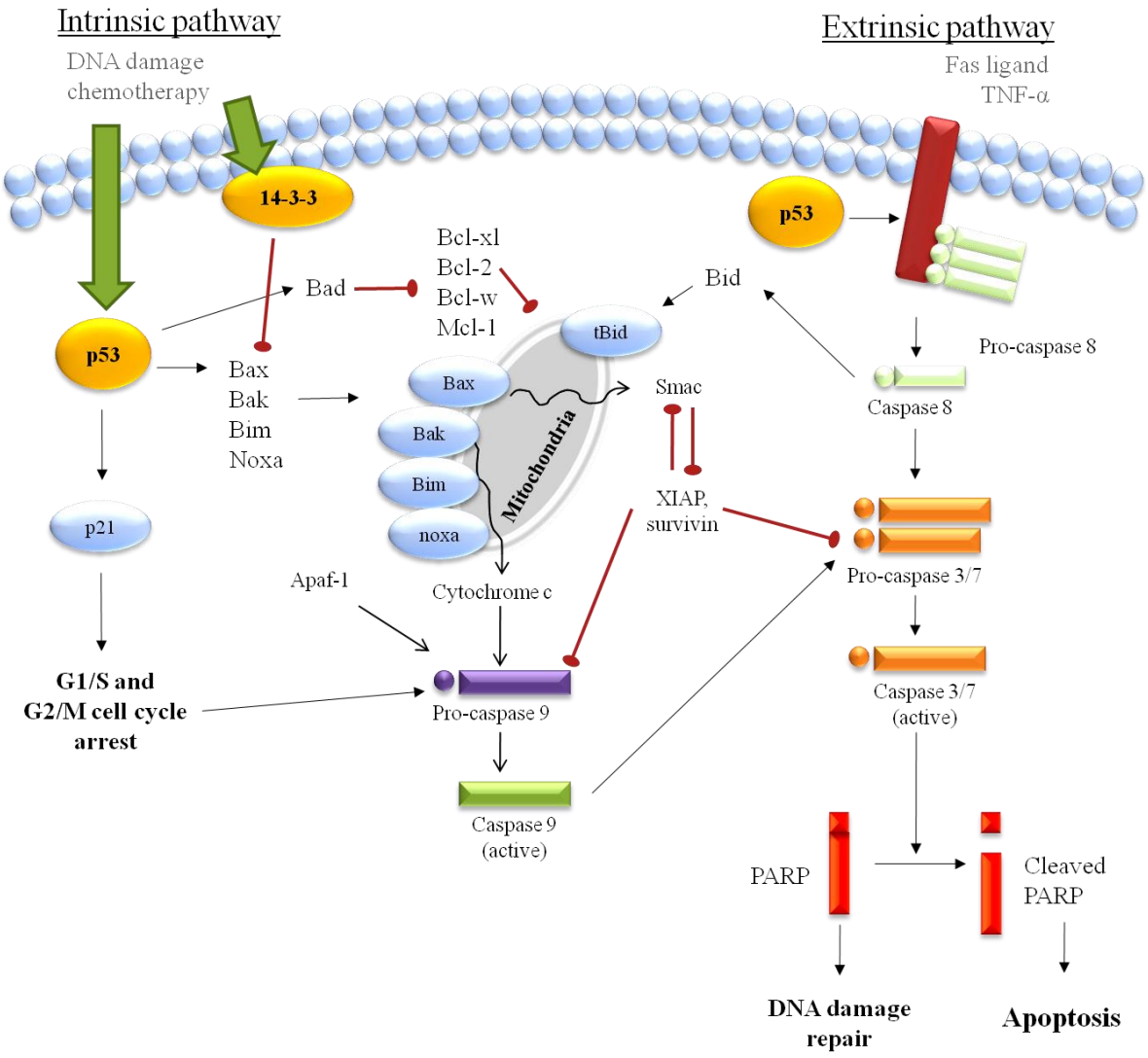

Figure 1 3: Overview of both intrinsic and extrinsic pathways of apoptosis.

Two major apoptotic pathways (intrinsic and extrinsic) leading to apoptosis are illustrated. Both pathways eventually lead to activation of caspases to execute cell death.

1.3 Cisplatin: Standard-of-care treatment for NSCLC

The clinical outcomes of the above mentioned chemotherapies have initially been reported to be comparable and undifferentiated (Schiller, Harrington et al. 2002). Thus, treatment decision is generally dependent on previous treatment history and clinicopathological parameters. In the case of NSCLC, adjuvant chemotherapies have been suggested to yield significant survival benefit over surgery alone (Johnson 2000, Hotta, Matsuo et al. 2004). Furthermore, increasing evidence suggests that platinum-based regimens provide significantly higher responses when compared to non-platinum-based chemotherapies in NSCLC (D'Addario, Pintilie et al. 2005, Jiang, Liang et al. 2007). Some studies have even suggested that cisplatin-based singlet and doublet chemotherapies are associated with improved survival advantage over carboplatin-containing regimens (Go and Adjei 1999, Hotta, Matsuo et al. 2004, Rajeswaran, Trojan et al. 2008). Over the years, cisplatin has been established as the standard of care treatment for NSCLC patients (Schiller 2001).

1.3.1 Cellular processing of cisplatin

DNA damage induced by platinum compounds activates several signalling pathways. Cellular responses to platinum compounds are different in individual tumour cells (Chu 1994). In general, treatment of platinum-based chemotherapy induces cell cycle arrest, cell survival or cell death depending on the activated molecular mechanisms (Wang and Lippard 2005). Understanding the mechanisms by which tumour cells retain and process cisplatin reveals important insights on the regulation of cell death or cell survival. In this chapter, the transport mechanisms and biotransformation of cisplatin, as well as the signal transduction and cellular responses to cisplatin will be discussed.

1.3.1.1 Cellular transportation and biotransformation of cisplatin

The uptake of cisplatin is regulated both passively and actively. Early studies suggested that entry of cisplatin into cells is mainly dependent on passive diffusion as cellular accumulation of cisplatin increases linearly over time until it reaches a saturated point. Furthermore, the transport of cisplatin occurred independently of molecular structure of various analogues (Hromas, North et al. 1987, Binks and Dobrota 1990). However, recent studies have revealed a direct relation between active transporter and cellular accumulation of cisplatin. For instance, deletion or mutation of the *CTR1* gene, which encodes for the copper transporter 1, reduced intracellular platinum levels in yeast and mouse cells; while overexpressing *CTR1* increased influx of cisplatin (Ishida, Lee et al. 2002, Holzer, Samimi et al. 2004). In addition, several efflux transporters, such as copper-transporting P-type

adenosine triphosphate (ATP7B) and ATP-binding cassette sub family C2 (ABCC2), were found to enhance cisplatin removal from tumour cells (Cui, König et al. 1999, Payen, Sparfel et al. 2002, Miyashita, Nitta et al. 2003).

As cytoplasmic concentration of chloride ions is low, cisplatin is activated spontaneously upon entering the cells through aquation of the chloride leaving groups to form form *cis*-$[Pt(NH_3)_2Cl(OH_2)]^+$ and *cis*-$[Pt(NH_3)_2(OH_2)]^{2+}$. The aquated cisplatin molecules are highly reactive and thus susceptible to interaction with several cytoprotective proteins (Eastman 1987, el-Khateeb, Appleton et al. 1999). Despite being highly reactive to the cellular components, these aquated platinums are reportedly more selective towards DNA (Eastman 1987, Jamieson and Lippard 1999). The activated cisplatin covalently binds to the N7 position of purine bases and results in the formation of intra-strand and inter-strand crosslinks (Huang, Zhu et al. 1995) (Figure 1.4). These crosslinkings modify the structure of the double-helix DNA and expose a minor groove region that attracts that binding of high-mobility group (HMG) box-proteins, DNA repair proteins, histone H1, and transcription factors (Pil and Lippard 1992, Farid, Bianchi et al. 1996, Vaisman, Lim et al. 1999, Kartalou and Essigmann 2001, Zdraveski, Mello et al. 2002, Yaneva, Paneva et al. 2007) (Figure 1.4). Binding of these cellular proteins to DNA facilitates the initiation of DNA repair mechanisms, gene expression and gene repression.

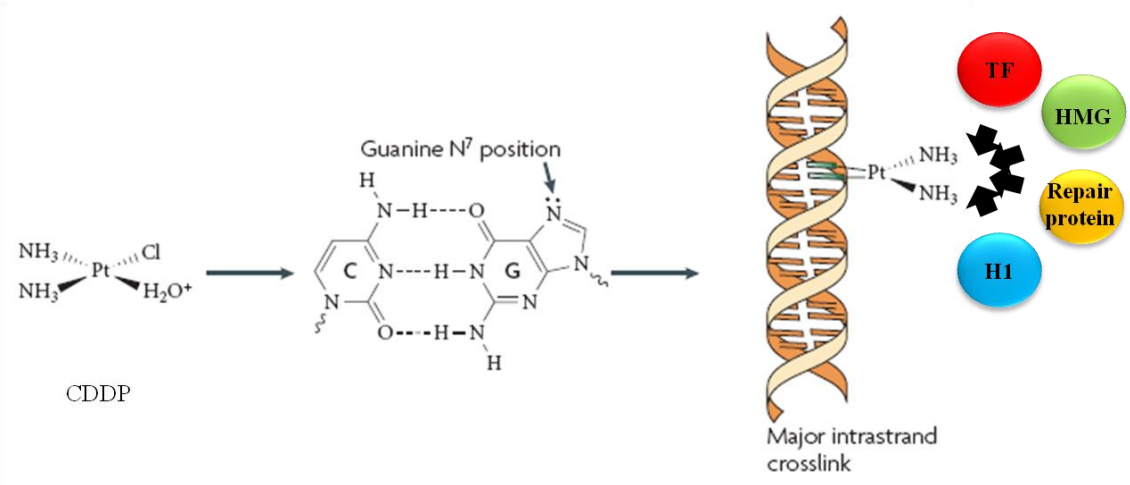

Figure 1.4: Cisplatin crosslinks DNA at N7 position of purine bases and attracts the binding of cellular proteins.

TF: transcription factors; HMG: high-mobility group box-proteins; Repair protein: DNA repair proteins; and H1: histone H1. [Adapted from (Kelland 2007)]

1.3.1.2 Cisplatin and cell cycle arrest

The crosslinking of DNA distorts DNA structure and induces genotoxic stress to the cells. Damage sensor proteins such as ATM (Ataxia telangiectasia mutated) and ATR (Ataxia telangiectasia and Rad3-ralated) identify this improper order of event and arrest cell cycle to allow for DNA repair to occur (Harper and Elledge 2007, Ashwell and Zabludoff 2008). Cisplatin induces both G1/S and G2 arrest via different mechanisms. G1/S checkpoint ensures that the damaged DNA is not replicated through DNA amplification (Bartek and Lukas 2001). Induction of G1/S arrest is initiated by ATM, which then recruits Chk2 and activates p53 (Banin, Moyal et al. 1998, Matsuoka, Huang et al. 1998). G2/M checkpoint prevents cells carrying DNA lesions to progress into mitosis. On the contrary, G2 arrest is mediated by ATR-Chk1 cascades. Activated Chk1 prevents dephosphorylation and activation of cyclin-dependent kinase 1 (CDK1) through inhibition of a protein phosphatase, cdc25 (Peng, Graves et al. 1997, Yang, Winkler et al. 1999) and activation of p53 (Tibbetts, Brumbaugh et al. 1999).

The fate of the cisplatin-treated cells is determined during the period when the cell cycle is arrested (Figure 1.5). It has been previously described that cell cycle arrest at G2 phase is an important event in cisplatin-induced cell death (Dasika, Lin et al. 1999). The dose of the administered cisplatin and the activity of signal transduction directly influence the cell response to cisplatin (Wang and Lippard 2005).

1.3.1.3 Cisplatin and DNA damage repair

The perturbations of cell cycle allow for the activation of DNA repair mechanisms to remove the crosslinks. Among the four major DNA-repair mechanisms [nucleotide-excision repair (NER), base-excision repair (BER), mismatch repair (MMR), double-strand homologous recombination (HR)], NER is recognized to be the primary mechanism that removes cisplatin lesions from DNA (Zamble, Mu et al. 1996, Wang, Hara et al. 2003). DNA repair mechanism of NER is hugely dependent on the excision repair cross-complementing 1 (ERCC1), which stabilizes the endonuclease activity of xeroderma pigmentosum complementation group F (XPF) (Ferry, Hamilton et al. 2000). The heterodimer of ERCC1 and XPF incises the 5' and 3' sides of the DNA respectively and removes the DNA lesion, while the repair is completed by DNA synthesis to reconstitute genetic integrity (Hanawalt 2002, Gillet and Schärer 2006). However, it has been well documented that the recruitment of HMG proteins, which binds to the DNA crosslinks, shields them from the repair machinery and inhibits the repair mechanisms (Huang, Zamble et al. 1994, Zamble, Mu et al. 1996, Zamble, Mikata et al. 2002). Furthermore, MMR repair

machinery has been shown to participate in the recognition but not repair of cisplatin-induced DNA lesions (Vaisman, Varchenko et al. 1998, Lin and Howell 2006), while HR machinery is responsible for the resolution of cisplatin-induced double-strand break (Smith, Tho et al. 2010).

1.3.1.4 Cisplatin and cell death

Cell death is triggered when attempts to repair DNA failed. Cisplatin induces both apoptosis and necrosis, while the mode of cisplatin-induced cell death is dependent on the dose of cisplatin exposure (Gonzalez, Fuertes et al. 2001). Cisplatin has been reported to activate necrotic cell death *in vitro* when used at high concentrations; whereas apoptosis is induced progressively over time at low cisplatin concentration (Lieberthal, Triaca et al. 1996). Furthermore, excessive DNA damage was shown to cause increased activation of PARP, which depletes NAD+ and ATP, and subsequently induces necrotic cell death (Herceg and Wang 2001). However, the induction of apoptosis by cisplatin is a more complicated process. It was first revealed that cisplatin-induced apoptosis is mitochondria-dependent as both the release of cytochrome c and activation of caspase 9 are essential to trigger cell death (Kojima, Endo et al. 1998, Blanc, Deveraux et al. 2000). Subsequently, other reports have demonstrated that cisplatin activates death receptor-mediated cell death via-up-regulation of Fas and FasL, as well as activation of caspase 8 (Fulda, Los et al. 1998, Seki, Yoshikawa et al. 2000). Cisplatin thus regulates cell death through both intrinsic and extrinsic apoptotic pathways. On the contrary, some studies have shown that cisplatin mediates apoptosis in ovarian and renal cancer cell lines via caspase 3-independent mechanisms (Henkels and Turchi 1999, Cummings and Schnellmann 2002), suggesting the broad spectrum of cytotoxicity effects of cisplatin.

1.3.1.5 Cisplatin and signal transduction of PI3K and MAPKs

Generally, cells that manage to repair the cisplatin-induced DNA lesions are released from the state of arrest and progressed into mitosis. Activation of key signalling pathways could determine the fate of tumours cells. Years of research have revealed that cisplatin treatment regulates multiple signal transduction mechanisms. In this chapter, on two major signalling cascades were investigated: phosphoinositide 3-kinase (PI3K) and mitogen-activated protein kinase (MAPK) pathways.

Activation of PI3K pathway is well characterized to promote cell survival and inhibit apoptosis through modulation of a key downstream effector, Akt (Datta, Brunet et al. 1999).

Phosphorylations of Akt are shown to protect cells from cisplatin-induced apoptosis (Datta, Brunet et al. 1999), because of its abilities to inhibit the degradation of X-linked inhibitor of apoptosis (XIAP) (Fraser, Leung et al. 2003, Dan, Sun et al. 2004), activated pro-survival nuclear factor kappa-light-chain-enhancer of activated B cells (NF-κB) signalling (Mabuchi, Ohmichi et al. 2004), and regulate expression of apoptotic modulators (Guinea Viniegra, Hernández Losa et al. 2002).

Members of the MAPK signalling pathways are important cellular modulators that mediate the balance between cell proliferation, cell survival, cell metabolism, and cell death (Chang and Karin 2001). The MAPK family members comprise of kinases that induce sequential phosphorylation of respective target substrates and regulate cellular activities (Chang and Karin 2001, Johnson and Lapadat 2002). There are three well-characterized MAPK sub-families: extracellular-signal regulated kinases (Erks), c-Jun N-terminal kinases (JNKs) and p38 mitogen-activated protein kinases (p38 MAPKs). Although all three MAPK families are responsive to extracellular stimuli, Erks are highly inducible by growth stimuli, while activation of JNKs and p38 MAPKs are more dependent on stress signals, such as UV irradiation and TNF (Olson and Hallahan 2004, Wada and Penninger 2004). Growing evidences have suggested that cisplatin triggers the activation of Erk, JNK and p38 MAPK kinases in tumour cell lines in a dose-dependent and time-dependent manner (Wang, Martindale et al. 2000, Hernández Losa, Parada Cobo et al. 2003).

Unlike the PI3K/Akt signalling, regulation of cellular responses to cisplatin by MAPK pathway(s) is less direct. Sustained activation of p38 MAPKs is reported to be responsible for cisplatin cytotoxicity in tumour cells, while abrogation of p38 function attributes to cisplatin resistance (Hernández Losa, Parada Cobo et al. 2003, Mansouri, Ridgway et al. 2003). However, there are conflicting reports on the nature of Erks and JNKs in influencing cell survival of cisplatin-treated cells. Some studies have associated Erk and JNK activation with improved survival after cisplatin treatment (Potapova, Haghighi et al. 1997, Hayakawa, Ohmichi et al. 1999, Persons, Yazlovitskaya et al. 1999). On the contrary, several studies have provided compelling evidences that both Erk and JNK contribute to cisplatin-induced apoptosis in various cancer types, and the abrogation of these MAPKs resulted in cisplatin-resistant phenotype (Potapova, Haghighi et al. 1997, Levresse, Marek et al. 2002, Yeh, Chuang et al. 2002). Therefore, the relative contribution of MAPK activation to cellular cytotoxicity of cisplatin-treated cells is likely cell type-dependent (Figure 1.5).

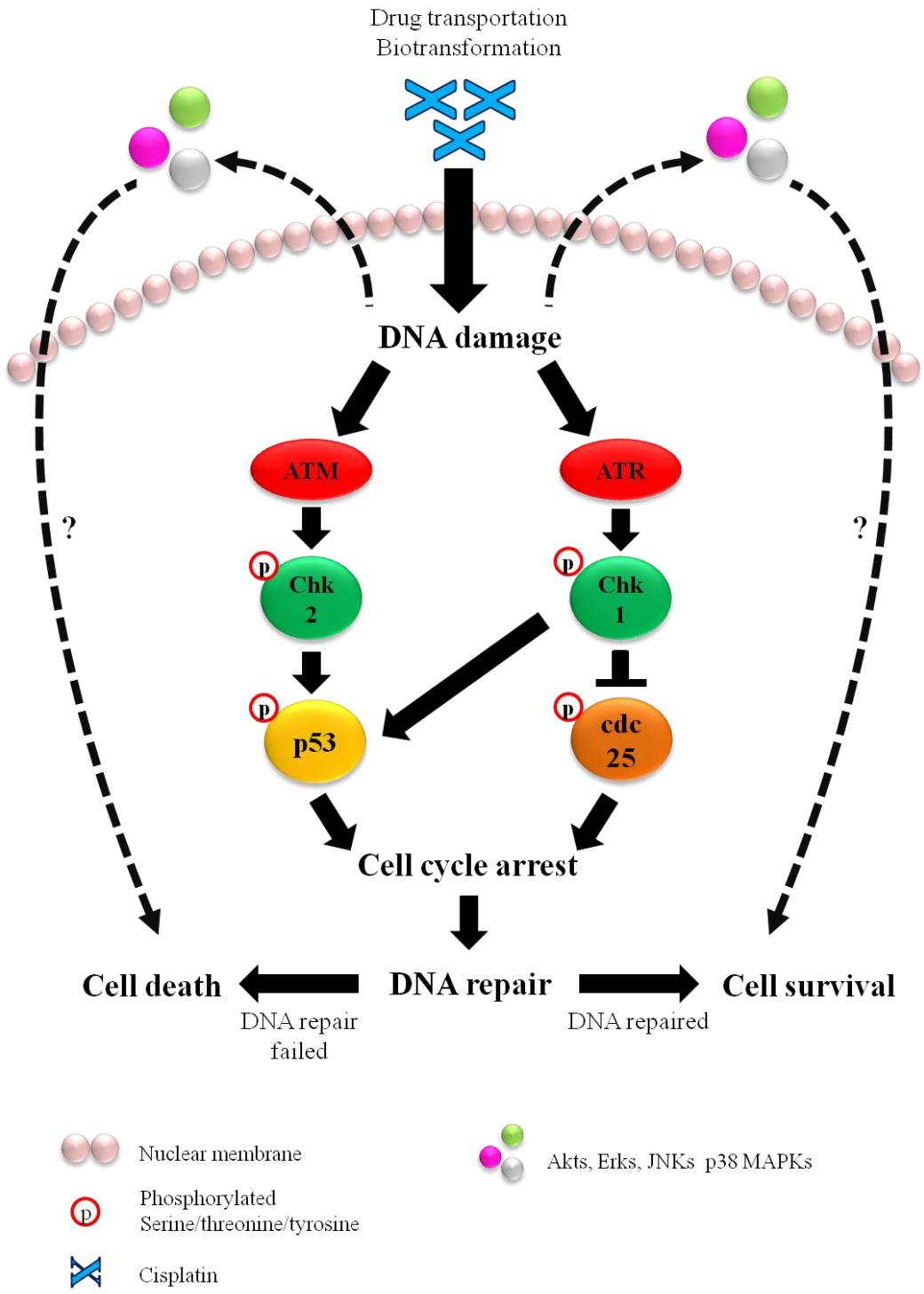

Figure 1.5: Cellular processing of cisplatin.

The efficacy of cisplatin is dependent on its cellular uptake and biotransformation. Cell cycle is arrested when DNA damage is detected through ATM/Chk2 and ATR/Chk1 machinery. Excessive DNA damage will not be repaired, but apoptosis or necrosis will be triggered. Cisplatin also activates PI3K and MAPK pathways. Dotted lines indicate mechanisms with conflicting findings being reported.

1.3.2 Cisplatin and the p53 network

1.3.2.1 Overview of p53: the shift from oncogene to tumour suppressor

The p53 protein was first discovered in 1979 by the culmination of two different studies: firstly, a 55 kDa peptide was found to be a target of simian virus 40 (SV40), a strain that is related to tumour development (Lane and Crawford 1979, Linzer and Levine 1979); secondly, this SV40-related protein was detected in the serum of the mouse infected with tumourigenic cell lines (DeLeo, Jay et al. 1979, Kress, May et al. 1979). After human *TP53* gene was successfully cloned (Zakut-Houri, Bienz-Tadmor et al. 1985), several other studies have proceeded to further characterize the role of p53 in tumourigenesis. At that time where limited details were available regarding the mutational status of *TP53* gene, p53 was initially presumed to be an oncogene due to its high expression in tumours, but not in normal tissue (DeLeo, Jay et al. 1979, Rotter 1983). Furthermore, antibodies against p53 were detected in sera of breast cancer patients (Crawford, Pim et al. 1982). Works by several groups have demonstrated that introducing either p53 antibodies or antisense inhibited cellular growth in tumour cells, suggesting p53 as a positive regulator of cell proliferation (Mercer, Avignolo et al. 1984, Reich and Levine 1984, Shohat, Greenberg et al. 1987, Deppert, Buschhausen-Denker et al. 1990). This notion was strengthened when *in vitro* insertion of cloned p53 cDNAs was shown to transform primary cells in the presence of oncogenic Ras (Eliyahu, Raz et al. 1984). Therefore, p53 protein was considered as a proto-oncogene during the early stages of investigation after its discovery.

However, the notion that p53 is an oncogene was challenged when several contradictory findings were reported. Conflicting reports were published regarding the capability of p53 to transform primary cells, and the genetic differences among the cloned p53 cDNAs were soon revealed (Levine and Oren 2009). Detailed investigations on the *TP53* gene were conducted by infection with Friend virus, whereby p53 was reported to be rearranged at one allele, and lost in the second allele through loss of chromosome or gene deletion (Mowat, Cheng et al. 1985, Munroe, Rovinski et al. 1988). These genetic aberrations resulted in the absence of protein expression or synthesis of a mutated or truncated protein. Interestingly, it was further shown that differences in codon sequences of murine p53 cDNA occurred at a particular region that is highly conserved (Soussi, Caron de Fromentel et al. 1987, Soussi, Caron de Fromentel et al. 1990). Subsequently, it was revealed that the early experiments were performed on cloned p53 cDNAs isolated from tumourigenic cells, which are likely mutant p53 (Levine and Oren 2009). Moreover, overexpression of wild-type p53 suppressed the malignant transformation of mutant p53 and oncogenic Ras in rat embryonic fibroblast cells (Eliyahu, Michalovitz et al. 1989, Finlay, Hinds et al. 1989). These observations somewhat overturned the then-believed notion that p53 is an oncogene.

The p53 protein was first described as a tumour suppressor gene in 1989 by Baker and Fearon by demonstrating the loss of heterozygosity in colorectal carcinoma (Baker, Fearon et al. 1989). In addition to the fact that wild-type p53 inhibited Ras-induced cellular transformation (Eliyahu, Michalovitz et al. 1989, Finlay, Hinds et al. 1989), p53-deficient mice convincingly demonstrated the tumour suppressive effect of p53. Genetically modified p53 null (p53-/-) mice developed malignant tumours shortly after birth (4-6 months), while heterozygous p53+/- mice developed spontaneous tumours with a longer latency period (Donehower, Harvey et al. 1992, Harvey, McArthur et al. 1993, Purdie, Harrison et al. 1994). These findings conclusively indicated that p53 is a tumour suppressor, and this protein is now considered by many as the "guardian of the genome" (Lane 1992).

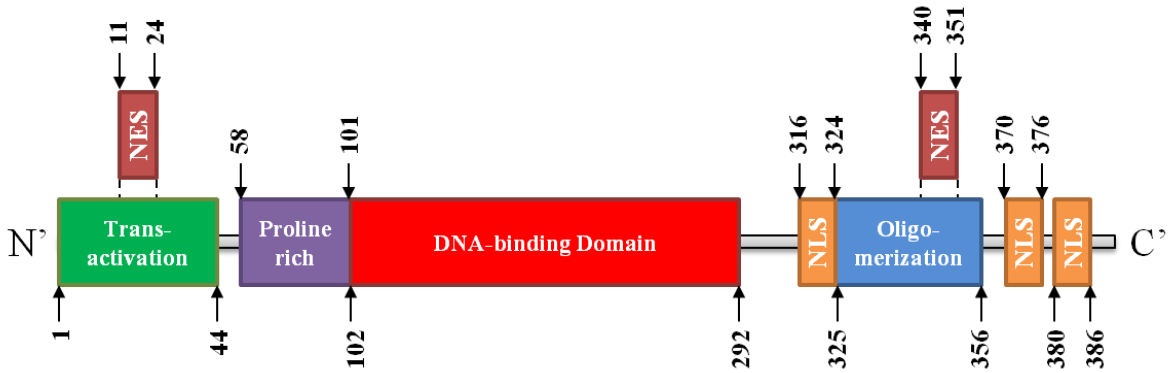

Figure 1.6: The main domains of the p53 protein.

The p53 molecule comprises of 393 amino acid residues and usually forms tetramer. The key domains of p53 include: the transactivation domain, proline-rich domain, DNA-binding domain, oligomerization domain, and the C-terminal regulatory domain. Several regions containing the nuclear localization signal (NLS) and nuclear export signal (NES) are identified. [Adapted and modified from p53 Knowledgebase (URL:http://p53.bii.a-star.edu.sg/aboutp53); assessed on December 2013].

The p53 protein contains 393 amino acid residues that comprises of several domains that contribute to protein stability and specific tumour-suppressive activity. These domains include: the N-terminal transactivation domain, a proline-rich domain, the core DNA-binding domain (DBD), and the C-terminal domain that contains an oligomerization domain and a regulatory domain (Joerger and Fersht 2008, Joerger and Fersht 2010). The transactivation domain is responsible for the stability of p53 protein and activation of downstream target genes (Lees-Miller, Sakaguchi et al. 1992, Kussie, Gorina et al. 1996). The prolife-rich region is found to mediate p53-induced apoptosis in response to DNA

damage (Venot, Maratrat et al. 1998). The DNA binding domain is highly conserved region that allows for recognition and interaction with specific response elements (Pavletich, Chambers et al. 1993, Wang, Schwedes et al. 1995). The oligomerization domain at the C-terminus allows for tetramerization of p53 (Chène 2001, Veprintsev, Freund et al. 2006), thus promotes binding affinity to DNA. Furthermore, three putative nuclear localization signals (NLS) and a nuclear export signal (NES) have been identified at the C-terminal regulatory domain that regulate p53 nuclear translocation (Liang and Clarke 1999, Stommel, Marchenko et al. 1999). However, in most cases, the conformational structure of p53 masks the exposure of the NES, thus retains the p53 in the cell nuclei (Stommel, Marchenko et al. 1999). Furthermore, a second DNA-binding region has been found within the C-terminal region that recognizes and repairs damaged DNA (Jayaraman and Prives 1995, Zotchev, Protopopova et al. 2000).

1.3.2.2 Activation of p53 signalling by cisplatin

In healthy cells, p53 activity is kept at bay by its negative regulator, mouse double minute 2 homolog (MDM2). The MDM2 molecule is an E3 ubiquitin-protein ligase that binds to the transactivation domain of p53 (Momand, Zambetti et al. 1992, Kussie, Gorina et al. 1996). The MDM2-p53 interaction induces p53 ubiquitination, inhibits the nuclear-cytoplasmic shuttling of p53 and signals for the its proteosomal degradation (Haupt, Maya et al. 1997). Interestingly, expression of MDM2 is primarily controlled by transactivation of p53 (Barak, Juven et al. 1993). Furthermore, Akt has been shown to phosphorylate MDM2 at Ser166 and Ser186, which then enhance MDM2-induced unbiquitination and degradation of p53 (Zhou, Liao et al. 2001, Ogawara, Kishishita et al. 2002). The basal p53 activity and regulation of signal transduction will constitutively trigger the activation of MDM2, which then suppress p53 expression. Thus, under unstressed conditions, p53 protein is detected at low level and its pathway is kept inactivated.

Cisplatin causes DNA lesions by binding to the N7 position of purine bases (Huang, Zhu et al. 1995). As described in Chapter 1.3.1.1, the intra-strand crosslinks invite binding of HMG proteins (Farid, Bianchi et al. 1996). The interaction of HMG proteins with DNA alters the chromosomal structure of DNA (Pil and Lippard 1992). It was then discovered that HMG1 is a co-activator of p53, with the interaction of p53-DNA being stimulated by HMG-1 and vice versa (Jayaraman, Moorthy et al. 1998, Imamura, Izumi et al. 2001). The binding of HMG-1 is able to bend the DNA further, thus causes structural changes in the target DNA and promotes the binding of various transcription factors that include p53 (Stros 1998).

Furthermore, apart from recruiting p53, HMG-1 also promotes the assembly of p53 tetramer at the DNA and modulates its interaction with DNA (Jayaraman, Moorthy et al. 1998).

Post-translational modifications that take place in both the N- and C-terminus of p53 molecules are deemed responsible for the activation of p53 signalling (Sakaguchi, Herrera et al. 1998). The primary signalling cascade that links up cisplatin-induced DNA damage with p53-mediated responses involves both ATM/ATR and Chk1/2. The initiation of ATM/Chk2 and ATR/Chk1 signalling cascades constitutively phosphorylates p53 at the N-terminal transactivation domain (Banin, Moyal et al. 1998, Lakin, Hann et al. 1999, Tibbetts, Brumbaugh et al. 1999) (Figure 1.7). In addition, DNA-dependent protein kinase (DNA-PK) is shown to induce p53 phosphorylation at Ser15 and Ser37 (Lees-Miller, Sakaguchi et al. 1992) (Figure 1.7). Phosphorylation of p53 abrogates the MDM2-mediated degradation, thus enhances p53 activity (Shieh, Ikeda et al. 1997, Siliciano, Canman et al. 1997). Furthermore, phosphorylation of MDM2 on Ser395 residue by ATM reduces the degradation of p53 by MDM2 (Maya, Balass et al. 2001). These findings suggest that activation of p53 by DNA damage is achieved partly through attenuation of the inhibitory effect of MDM2.

While phosphorylation at N-terminal transactivation domain inhibits binding on MDM2, post-translational modification at the C-terminus is associated with cytoplasmic to nuclear shutting and sequence-specific binding potential of p53. Phosphorylations of p53 at the oligomerization domain and regulatory domain are induced by cyclin dependent kinases (CDKs), casein kinases (CKs), and protein kinase C (PKC). These phosphorylated p53 proteins are shown to activate *in vitro* sequence specific DNA binding ability (Price, Hughes-Davies et al. 1995, Takenaka, Morin et al. 1995, Wang and Prives 1995, Hall, Campbell et al. 1996, Blaydes and Hupp 1998, Pospísilová, Brázda et al. 2004). In addition to these findings, acetylation of p53 is a critical modulation of p53-mediated transactivation (Sakaguchi, Herrera et al. 1998, Tang, Zhao et al. 2008). The histone acetyl-transferases (HATs) p300, p300/CBP-associated factor (PCAF) and Tip60 are responsible for the *in vivo* acetylation of p53 at various lysine residues upon DNA damage (Liu, Scolnick et al. 1999, Tang, Luo et al. 2006) (Figure 1.7). Acetylation of p53 at the N-terminus is shown to affect its transcriptional activity by activating the sequence-specific binding to DNA (Gu and Roeder 1997, Lill, Grossman et al. 1997, Liu, Scolnick et al. 1999); whereas acetylation at the DBD, in particular K120 residues, is related to p53-dependent apoptosis (Tang, Luo et al. 2006). Furthermore, p300 and PCAF acetylates p53 at Lys320 and Lys382 respectively, and both these resides are located within the NLS of p53, thus suggesting that acetylation is essential for nuclear translocalization of p53 (Sakaguchi, Herrera et al. 1998). In addition, p53 is believed to be the downstream target for several members of the histone deacetylase

(HDAC) family, which include the HDAC1, HDAC3 and sirtuin 1 (Luo, Su et al. 2000, Vaziri, Dessain et al. 2001, Ito, Kawaguchi et al. 2002, Karagianni and Wong 2007). These HDACs are able to cause p53 deacetylation and reduce its transcriptional activity. Thus, inhibition of HDACs is believed to be a probable mechanism of p53 acetylation. However, a link between DNA damage and inhibition of HDAC activity has yet to be established.

1.3.2.3 Regulation of cellular responses by p53 pathway

Activation of p53 is associated with the increase in protein levels and ability to induce multiple downstream effects that include DNA damage repair, cell cycle arrest and cell death (Lakin and Jackson 1999). The broad spectrum of p53 functions thus regulates the response to cisplatin-induced DNA damage. It is interesting to note that the mutational status of p53 and its activity is positively correlated with sensitivity towards cisplatin across a panel of tumour-derived cell lines (O'Connor, Jackman et al. 1997).

The binding of p53 to the DNA and its subsequent activation through post-translational modifications first initiates the DNA repair mechanisms. While other repair mechanisms have been linked with p53, lesions caused by DNA-damaging chemotherapeutic agents are usually fixed by p53-regulated NER (Levine 1997, Smith and Seo 2002). First evidence of the involvement of p53 in NER repair mechanisms was shown in UV-irradiated cells, as wild-type p53 efficiently repair pyrimidine dimers but the transcription-coupled repair (TCR) is lacking (Ford and Hanawalt 1997, Zhu, Wani et al. 2000). Subsequently, it was shown that p53 facilitates NER mechanisms through binding to components of the NER complex, such as transcriptional factor II Human (TFIIH) (Smith, Chen et al. 1995, Léveillard, Andera et al. 1996). Moreover, several NER components are regulated by transactivation of p53: two xeroderma pigmentosum proteins (p48XPE and XPC) and Gadd45 (Carrier, Georgel et al. 1999, Hwang, Ford et al. 1999, Adimoolam and Ford 2002). These proteins are involved in the early recognition of bulky DNA adduct during the process of NER.

Upon detection of DNA damage, transient cell cycle arrests occur in the G1, S, and G2 phases of the cell cycle (O'Connor, Ferris et al. 1992, Agarwal, Agarwal et al. 1995). These perturbations presumably delay the DNA replication process to allow for repair mechanisms to take place, thus preventing the transfer of heritable genetic alterations to the daughter cells (Little 1968). It is now known that p53 regulates both the reversible G1 and G2/M growth arrests through stimulating the synthesis of various inhibitors of CDKs (Kuerbitz, Plunkett et al. 1992, Agarwal, Agarwal et al. 1995). The cyclin-dependent kinase inhibitor 1 ($p21^{WAF1/CIP1}$) is encoded by the *CDKN1A* gene, a downstream transcription target of p53. p21 protein is an universal cyclin kinase inhibitor and has been shown to be an effector of

G1 arrest (Di Leonardo, Linke et al. 1994, Waldman, Kinzler et al. 1995). The cyclin D/CDK4 complex is strongly implicated as the regulator of G1 progression (Sherr 1993), whereas p21 is able to form a multi-protein complex with both cyclin D and CDK4 (Xiong, Zhang et al. 1992, Xiong, Zhang et al. 1993, LaBaer, Garrett et al. 1997). When accumulated at high level, p21 blocks the cell cycle progression through inhibition of CDK4, thus induces G1 arrest (Harper, Adami et al. 1993). Furthermore, p21 induces the activation of the retinoblastoma (RB) protein by inhibiting CDKs that phosphorylate and inhibit RB activity (Slebos, Lee et al. 1994). Activated RB binds and inhibits the transcription factor E2F (Narita, Nũnez et al. 2003), thus represses proteins that are cell cycle facilitator (c-Fos, cyclin A, cyclin B), and results in abrogation of cell cycle progression at G1 phase (Seshadri and Campisi 1990, Stein, Drullinger et al. 1991, Campisi and d'Adda di Fagagna 2007, Garner and Raj 2008). The mechanism of p53 in blocking cells at the G2/M phase involves the inhibition of CDK1, the crucial modulator of mitosis (Zhan, Antinore et al. 1999, Taylor and Stark 2001). Binding of CDK1 to cyclin B1 is required for its function. The p53 protein represses the *cdc2* gene (that encodes for CDK1 protein), and induces the expression of Gadd45 that further inhibit CDK1/cyclin B1 kinase activity (Wang, Zhan et al. 1999, Zhan, Antinore et al. 1999, Jin, Tong et al. 2002). Furthermore, deficiency in either p53 or Gadd45 impaired G2/M checkpoint arrest (Wang, Zhan et al. 1999, Jin, Tong et al. 2002).

Among the various functions of p53, the most prominent downstream activity of p53 signalling is the activation of apoptosis. When DNA damage is deemed to be beyond repair, the stressed cells are released from cell cycle arrest and progressed into cellular senescence, and subsequently apoptosis. As demonstrated in Chapter 1.2.4.2, apoptosis could be regulated either by extrinsic pathway that involves the formation of DISC and activation of caspase 8, or intrinsic pathway that mainly depends on the release of mitochondria cytochrome c and the apoptosome complex (Figure 1.3). It is now certain that DNA damage-induced apoptosis is highly regulated by p53, and the lethal functions of p53 could be regulated via both transcriptional-dependent and –independent mechanisms. It was earlier shown that p53 plays an essential role in mediating death receptor signalling. Firstly, transcriptomic expression and activation of Fas reportedly regulated by wild type p53 (Owen-Schaub, Zhang et al. 1995, Müller, Strand et al. 1997, Bouvard, Zaitchouk et al. 2000). Then, p53 protein is also associated with the transient cell surface trafficking of Fas from Golgi complex and the binding of Fas to FADD (Bennett, Macdonald et al. 1998). Concurrently, p53 response elements were identified in the promoters of Bcl-2 protein BAX and the BH3-only proteins p53-up-regulated modulator of apoptosis (PUMA) and Noxa (Miyashita and Reed 1995, Oda, Ohki et al. 2000, Nakano and Vousden 2001, Thornborrow, Patel et al. 2002). These pro-apoptotic proteins are able to inhibit the pro-survival Bcl-2

proteins, form MAC on mitochondria surface, induce the release of cytochrome c and trigger apoptosis. Moreover, it was first reported in 1994 that p53 could mediate apoptosis without initiating transcription of apoptotic genes (Caelles, Helmberg et al. 1994). The direct binding of p53 to BAX and caspases, and therefore the induction of mitochondria-mediated apoptosis, is well-characterized now (Ding, Lin et al. 2000, Chipuk, Kuwana et al. 2004). A schematic diagram that summarizes these p53-mediated cellular responses is shown in Figure 1.7.

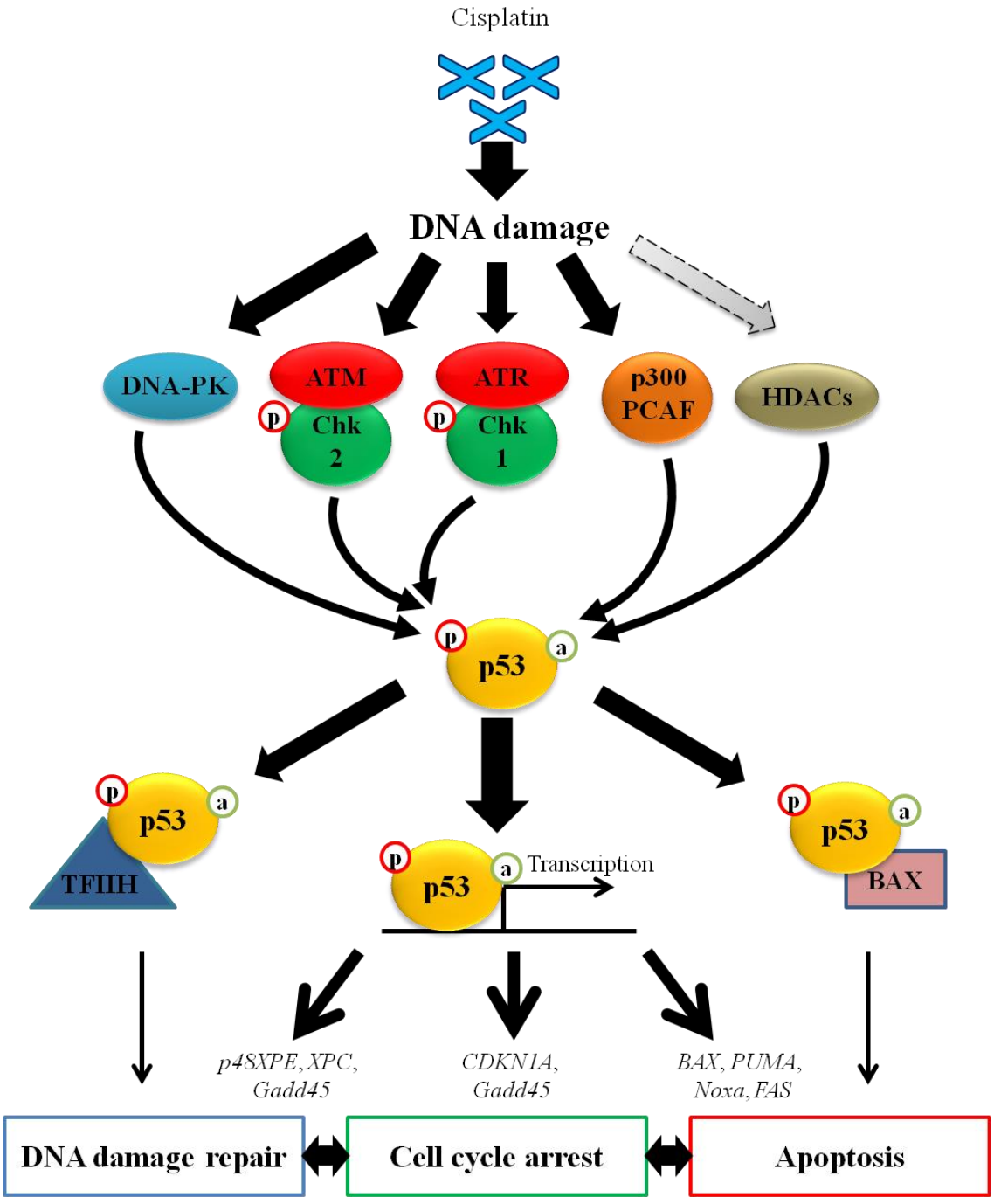

Figure 1.7: p53-mediated cellular response to DNA damage induced by cisplatin.

The DNA lesions induced by cisplatin initiate binding of p53 (by HMG proteins) and activation of p53 through post-translational modifications (by DNA-PK, ATM, ATR, HATs and HDACs). Several cellular responses to the activated p53, both transcription-dependent and –independent, have been described. Doted line indicates pathway that has not been comprehensively established.

1.3.3 Clinical limitations of cisplatin: Adverse side effects and drug resistance

Since its approval for clinical use in 1978, the advancement and clinical efficacy of cisplatin is severely limited by two factors: adverse side effects and cisplatin resistance (Lebwohl and Canetta 1998). The common side effects of cisplatin include nephrotoxicity (kidney injury), neurotoxicity (damage to peripheral nerve), ototoxicity (hearing loss), nausea and vomiting (Kelland 2007, Macciò and Madeddu 2013). As kidney is the major excretory organ of cisplatin, nephrotoxicity is a major concern for patients treated with cisplatin. As cisplatin also causes renal vasculature injury, a culmination of these events can result in acute renal failure (Pabla and Dong 2008). In addition, common neurological adverse effects of cisplatin include hearing and visual disorders, as well as numbness in the four limbs (Kedar, Cohen et al. 1978). Signs of neuronal injury are observable as soon as the first administration of cisplatin (Milosavljevic, Duranton et al. 2010, Pace, Giannarelli et al. 2010). As these adverse effects of cisplatin are dose-dependent, this thus limits the dosage of administrated cisplatin and restricts its therapeutic efficacy.

Another factor that restricts the clinical usage of cisplatin is the development of resistance. At the initial phase of clinical usage, cisplatin often provides favourable therapeutic response and disease stabilization (Lebwohl and Canetta 1998). However, a subset of patients, in particular those with colorectal, prostate or lung cancer, are intrinsically less responsive to cisplatin-based chemotherapies (Giaccone 2000, Köberle, Tomicic et al. 2010). Moreover, patients with initial response to cisplatin eventually relapse with more aggressive tumours that are resistant to cisplatin (Giaccone 2000). Intensive researches for over 30 years have provided detailed insights on the cellular activities of cisplatin, thus allowing for better understanding on the molecular mechanisms that account for resistance in tumour cells. Several inherently detected or acquired genetic aberrations are associated to intrinsic and extrinsic resistance to cisplatin will be discussed in the next chapters. Molecular mechanisms of cisplatin resistance can be classified into four main classes: reduction of cisplatin accumulation, increase in DNA repair pathways, attenuation of cell death mechanisms, and alteration of signal transduction.

1.3.3.1 Cisplatin resistance: Reduced cellular accumulation of cisplatin

The first class of mechanisms that induces cisplatin resistance is the reduction of cisplatin accumulation in the cells. This can be achieved by reducing influx, increasing efflux and increasing inactivation of cisplatin. It has been reported that a transmembrane copper transporter, CTR1, is involved in the active uptake of cisplatin (Ishida, Lee et al. 2002, Holzer, Samimi et al. 2004). Several findings have demonstrated that inhibition of CTR1 activity led to decrease cisplatin accumulation (Ishida, Lee et al. 2002, Katano, Kondo et al. 2002, Holzer, Samimi et al. 2004). Furthermore, increased competitive binding of copper protects cells from cisplatin toxicity (More, Akil et al. 2010), whereas chelating copper increases cisplatin accumulation and toxicity (Ishida, McCormick et al. 2010). More importantly, high *CTR1* expression was associated with better clinical response to platinum-based chemotherapy in ovarian cancer (Lee, Choi et al. 2011). Interestingly, continuous exposure to cisplatin reportedly suppress CTR1 by inducing its internalization and degradation (Holzer and Howell 2006). This mechanism may partially account for the development of acquired cisplatin resistance.

Despite so, cisplatin is still capable to enter cells via passive diffusion across plasma membrane. Accompanying the discovery on the correlation of CTR1 and cisplatin resistance, its copper-exporting counterpart, ATP7B, was shown to be up-regulated in cisplatin-resistant cell lines (Miyashita, Nitta et al. 2003, Safaei, Holzer et al. 2004). Earlier studies have suggested the role of ATPase-like multidrug resistance protein (MRP) family, in particular MRP2, in mediating cisplatin efflux (Koike, Kawabe et al. 1997, Cui, König et al. 1999, Borst, Evers et al. 2000). The expression of MRP2 in tumours is recently been reported as a prognostic marker for platinum-based chemotherapies (Cui, König et al. 1999, Korita, Wakai et al. 2010, Yamasaki, Makino et al. 2011).

As discussed in Chapter 1.3.1.1, aquated cisplatin has high reactivity with cytoplasmic nucleophilic proteins, which include glutathione (GSH) and metallothioneins (Eastman 1987, el-Khateeb, Appleton et al. 1999). Both GSH and metallothioneins are cytoplasmic scavengers that bind to aquated platinum and promote cisplatin efflux or inactivation, leading to cisplatin resistance (Hamilton, Winker et al. 1985, Kelley, Basu et al. 1988, Lewis, Hayes et al. 1988, Kasahara, Fujiwara et al. 1991, Ishikawa 1992). Furthermore, two GSH-related proteins, gamma-glutamyl cysteine synthetase (γ-GCS), that catalyzes GSH synthesis, and glutathione-S-transferse (GST), that conjugate cisplatin and GSH, are positively correlated to cisplatin-resistant cell lines and tumours (Lewis, Hayes et al. 1988, Kigawa, Minagawa et al. 1998, Shiga, Heath et al. 1999, Cullen, Newkirk et al. 2003, Pasello, Michelacci et al. 2008).

1.3.3.2 Cisplatin resistance: Activation of DNA repair machinery

The distortions in DNA caused by cisplatin-induced lesions are repaired predominantly by NER machinery, with MMR and HR playing a lesser role (Zamble, Mu et al. 1996, Vaisman, Varchenko et al. 1998, Smith, Tho et al. 2010). Since the persistent formation of DNA adducts leads to induction of apoptosis, the ability of the cell to repair these crosslinks will result in development of cisplatin resistance. In most cases, damaged nucleotides are excised from the DNA through incision on both sides of the lesions by ERCC1 and XPF (Hanawalt 2002). The endonuclease pair of ERCC1-XPF has been characterized as one of the rate-limiting factors for NER machinery (Ahmad, Robinson et al. 2008). Several *in vitro* studies have shown the influences of ERCC1 proficiency on cisplatin resistance (Li, Gardner et al. 1998, Ferry, Hamilton et al. 2000, Li, Yu et al. 2000), with ERCC1 expression negatively correlating with treatment outcome in various cancer types (Metzger, Leichman et al. 1998, Olaussen, Dunant et al. 2006, Bellmunt, Paz-Ares et al. 2007, Handra-Luca, Hernandez et al. 2007). Thus, the expression of ERCC1 could possibly indicate the functionality of NER machinery in cisplatin-treated patients, although an effective way to measure DNA repair activity in these tumours is by far lacking. Nonetheless, the potential of ERCC1 as a biomarker candidate has been considered for the selection of NSCLC patients in cisplatin-containing trials (Olaussen 2009).

In some cases, inter-strand crosslinking by cisplatin induces double-strand break. This lesion is commonly resolved by HR mechanisms (Dudás and Chovanec 2004). Breast cancer 1, early onset (BRCA1) and breast cancer 2, early onset (BRCA2) proteins are two key components of the HR machinery that mediate strand invasion, a crucial step in HR repair (Venkitaraman 2002). Both *BRCA1* and *BRCA2* genes are considered as tumour-suppressor genes, as loss-of-function mutations are often detected along these genes in multiple tumour types, especially breast and ovarian cancers (Ford, Easton et al. 1998, Welcsh and King 2001, Yoshida and Miki 2004). Deficiencies of BRCA1 and BRCA2 impair DNA repair mechanism, thus increase risk of genetic aberrations and tumourigenesis (Venkitaraman 2002, Evers and Jonkers 2006). However, in line with general viewpoint, lack of BRCA-dependent DNA-repair machinery due to inherent mutations leads to better prognosis in cisplatin-treated tumours (Ben David, Chetrit et al. 2002, Farmer, McCabe et al. 2005, Chetrit, Hirsh-Yechezkel et al. 2008). More recently, it is reported that a secondary mutation of *BRCA1/2*, that restores wild-type *BRCA1/2* reading frame and their DNA repair functions, induces acquired resistance to cisplatin in tumour cells (Sakai, Swisher et al. 2008, Wang and Figg 2008, Dhillon, Swisher et al. 2011). Taken together, these findings suggest that HR machinery has clinical potential as prognostic biomarker in the context of *BRCA1/2*.

1.3.3.3 Cisplatin resistance: Interruption of cell death machinery

Interruption of cell death machinery is another class of mechanisms that leads to cisplatin resistance. Abnormal regulations of key components along the cell death pathway allow the tumour cells to elude the cytotoxic potential of chemotherapy and gain survival advantage (Lowe and Lin 2000). In the case of cisplatin resistance, DNA damage beyond repair leads to activation of pro-apoptotic signalling (Gonzalez, Fuertes et al. 2001). Several genetic and epigenetic alterations within the apoptotic pathway have been associated with cisplatin resistance. One of the most established alterations involves the inactivation of p53 function (Vousden and Lane 2007). It has been documented that somatic mutation of *TP53* is detected in approximately 50% of all human cancers (Olivier, Hollstein et al. 2010), while in other tumours p53 pathway is commonly inactivated by alternative mechanisms (Leach, Tokino et al. 1993, Liggett and Sidransky 1998, Esteller, Tortola et al. 2000, Esteller, Cordon-Cardo et al. 2001, Manfredi 2010). The role of p53 in the apoptotic pathway is described in Chapter 1.3.2.3. Deactivation of p53 pathway impairs the transactivation of apoptotic genes, which include *BAX*, thus prevent the inhibition of pro-survival Bcl-2 by BAX in resistant phenotypes (Perego, Giarola et al. 1996). Several *in vitro* studies have highlighted the role of p53 in determining response to cisplatin, with defects in p53 signalling consistently induce cisplatin resistance (Fan, el-Deiry et al. 1994, Perego, Giarola et al. 1996, O'Connor, Jackman et al. 1997, Branch, Masson et al. 2000). Clinical data have also suggested that *TP53* mutational status negatively correlates with treatment outcome of cisplatin-based regimes in breast, ovarian, and head and neck cancers (Righetti, Della Torre et al. 1996, Shiga, Heath et al. 1999, Gadducci, Cosio et al. 2002, Perrone, Bossi et al. 2010). Furthermore, the pro-apoptotic activity of wild-type p53 in cervical cancer is shown to be abrogated by human papillomavirus (HPV) and thus causes platinum resistance (Kessis, Slebos et al. 1993). Interestingly, p53 function is rarely impaired in testicular germ cell tumours that are extremely sensitive to cisplatin (Peng, Hogg et al. 1993, Raghavan 2003), suggesting a strong implication of p53 activity in predicting cisplatin resistance.

The induction of cellular apoptosis can be regulated by p53-dependent and –independent mechanisms (Zamble, Jacks et al. 1998). Various component of the apoptotic pathway, as illustrated in Figure 1.3, are commonly dysregulated in cisplatin-resistant phenotypes. To begin, activations of critical caspases that mediate apoptosis, caspase 3, 8 and 9, are found to be attenuated in cisplatin-resistant cells (Henkels and Turchi 1999, Blanc, Deveraux et al. 2000). This abrogation of apoptosis in the resistant phenotypes could be regulated via mutations or altered expression of the pro-survival Bcl-2 family members and XIAP (Reed 1995, Beale, Rogers et al. 2000, Asselin, Mills et al. 2001). In line with this concept, overexpression of *Bcl-2*, together with the increase in GSH, has been shown to result in

resistance to cisplatin (Hockenbery, Oltvai et al. 1993, Chiao, Carothers et al. 1995). Similarly, increased expression of Bcl-xl and reduced levels of Bad are observed in resistant tumour cells (Minn, Rudin et al. 1995, Hayakawa, Ohmichi et al. 2000). Lastly, the inhibition of caspase 3 and 8 may be partially related to the down-regulation of *FAS* in ovarian cancer cells (Mansouri, Zhang et al. 2003), whereas up-regulation of Fas re-sensitizes small cell lung cancer cells to cisplatin (Wu, Wang et al. 2010).

1.3.3.4 Cisplatin resistance: Alteration of signal transduction machinery

Till date, the regulation of signalling pathways by cisplatin is yet to be fully deciphered. Furthermore, contrasting findings have been reported on the relative contribution of these signalling cascades on the cytotoxicity of cisplatin. The amplification of a transmembrane receptor tyrosine kinase, human growth factor receptor 2 (HER2), is associated with poor response of breast and ovarian tumours to cisplatin treatment (Slamon, Godolphin et al. 1989, Hengstler, Lange et al. 1999). Under *in vitro* conditions, overexpressing HER2 reduces cisplatin potency (Tsai, Yu et al. 1995), while suppressing this receptor increases cisplatin cytotoxicity (Pietras, Fendly et al. 1994).

The HER2 protein is extensively similar to the human epidermal growth factor receptor (EGFR), which will be discussed later in Chapter 1.4 (Bargmann, Hung et al. 1986, Yamamoto, Ikawa et al. 1986). The activation of HER2/EGFR in cisplatin-resistant cells propagates the activation of SHC/Grb2/SOS/Ras/MAPK and PI3K/Akt pathways (Hung and Lau 1999). The PI3K/Akt signalling is widely considered as a pro-survival pathway (Datta, Brunet et al. 1999). Some of these Akt-induced pro-survival signals involve the inactivation of Bad (Hayakawa, Ohmichi et al. 2000), stabilization of XIAP (Fraser, Leung et al. 2003, Dan, Sun et al. 2004), and induction of Smac release from mitochondria (Fraser, Leung et al. 2003). These events lead to the attenuation of cisplatin-mediated anti-proliferative effects. Furthermore, Akt is shown to promote MDM2 phosphorylation and nuclear translocation, which then lead to degradation of p53 and abrogation of its activities (Mayo and Donner 2001, Mayo and Donner 2002, Ogawara, Kishishita et al. 2002). Taken together, these findings provide possible insights to how Akt attenuate the cell death pathway, but the precise mechanism by which Akt mediates cisplatin resistance remains unclear.

As discussed in Chapter 1.3.1.5, members of the MAPK sub-families (Erk, JNK, p38) are closely associated with the mode of action of cisplatin. Early studies have demonstrated that tumours with *RAS* mutation or amplification are more resistant to cisplatin (van 't Veer, Hermens et al. 1988, Fan, Banerjee et al. 1997, Dempke, Voigt et al. 2000). Subsequently, cisplatin-induced activations of Erk and JNK signal for cellular protection in cisplatin-

resistant cells (Potapova, Haghighi et al. 1997, Persons, Yazlovitskaya et al. 1999, Cui, Yazlovitskaya et al. 2000, Levresse, Marek et al. 2002). Cross-talk between MAPK signalling with other pathways could also regulate cisplatin resistance. In a study on melanoma cell lines, Li and Melton showed that activation of MAPK pathway by cisplatin up-regulates ERCC1 expression and induces chemoresistance (Li and Melton 2012). Moreover, MAPK activation induces up-regulation of several transcription factors, such as c-Myc, c-Fos and c-Jun (Deng and Karin 1994, Robinson and Cobb 1997), which are believed to be responsible for reduced sensitivity to cisplatin. For instance, both c-Fos and c-Jun induce ERCC1 (Li, Gardner et al. 1998, Li, Zhang et al. 1999), a key component of DNA repair mechanism. Furthermore, antisense silencing of c-Jun reverses cisplatin resistance in ovarian cancer cell lines (Pan, Yao et al. 2002). These exemplify some mechanisms of cisplatin resistance that are regulated by MAPK signalling.

However, it is important to note that the cytotoxic effects of HER2, PI3K and MAPK pathways remain controversial due to contradicting findings. Firstly, introduction of HER2 increased cisplatin cytotoxicity in breast cancer cell lines (Arteaga, Winnier et al. 1994). Next, the cisplatin-induced p38 MAPK activity has been linked to cisplatin sensitivity (Hernández Losa, Parada Cobo et al. 2003, Mansouri, Ridgway et al. 2003). Furthermore, inhibition of Erk signalling reduces cisplatin sensitivity in melanoma and ovarian cell lines (Mandic, Viktorsson et al. 2001, Yeh, Chuang et al. 2002), whereas JNK activation contributes to cisplatin-induced cell death (Zanke, Boudreau et al. 1996, Sánchez-Perez, Murguía et al. 1998, Mansouri, Ridgway et al. 2003). Lastly, JNK and its upstream kinase, MAP/Erk kinase kinase 1 (MEKK1), stabilizes and activates p53 through phosphosrylation of p53 (Fuchs, Adler et al. 1998). The loss-of-function defect in MEKK1 could lead to failure in p53 activation and thus contributes to cisplatin resistance in ovarian adenocarcinoma cell lines (Gebauer, Mirakhur et al. 2000). Thus far, the understanding of signal transduction pathways could only provide partial explanation for their influence on the modulation of cisplatin resistance. Studies on the molecular cross-talk involving PI3K, MAPK, p53 and other relevant proteins could provide better insights on the key regulators of cisplatin resistance and the development of more efficient chemosensitization strategies.

1.4 Molecular targeted therapies in lung cancer

At present, much effort has been focused on the development of personalized therapy by defining the biology and molecular features of respective tumour cells. These strategies aim to achieve promotion of apoptosis, inhibition of cell cycle, anti-angiogenesis, inhibition of cell proliferation, and inhibition of multi-drug resistance in tumours cells (Abidin, Garassino et al. 2010). Several molecular targeting therapies have been proposed in NSCLC, which include histone deacetylase (HDAC) inhibitors (Neal and Sequist 2012), matrix metalloproteinase (MMP) inhibitors (Bissett, O'Byrne et al. 2005, Leighl, Paz-Ares et al. 2005), vascular endothelial growth factor receptor (VEGFR) antibody (Sandler, Gray et al. 2006), proteosome inhibitors (Fanucchi, Fossella et al. 2006, Davies, Lara et al. 2007), and immunoconjugates (Elias, Hirschowitz et al. 1990, Goodman, Hellström et al. 1990, Ross, Hart et al. 2006). The mode-of-actions of these therapeutic agents have been explicitly studied by with promising results in trials involving these inhibitors.

Over the past decade, the concept of oncogene addiction has been proposed. It is now well-understood that tumourigenesis is a multi-step process in which mutations in key cellular genes lead to alteration in cellular processes that equip the tumour cells for malignant transformation. These biological processes, which include sustained proliferation, evasion of growth suppression, inhibition of cell death, unrestrictive replication, activation of angiogenesis, induction of invasion and metastasis, occurrence of genomic instability, acquisition of tumour-promoting inflammation, reconstruction of cellular metabolism, and evasion of immune surveillance, are now regarded as the hallmarks of cancer (Hanahan and Weinberg 2000, Hanahan and Weinberg 2011). These features of cancer cells are initiated by the progressive accumulation of genetic aberrations and epigenetic abnormalities within the tumour cells. Oncogenes and tumour suppressor genes that carry highly diverse biochemical functions are commonly mutated and abnormally regulated in many cancer cell types. Characterization of these mutations has led to the observations that specific abrogation of biochemical functions of particular mutated genes is sufficient to improve treatment outcome (Colomer, Lupu et al. 1994, Chin, Tam et al. 1999, Jackson, Willis et al. 2001, Moody, Sarkisian et al. 2002, Moody, Perez et al. 2005). The apparent dependency of certain cancer subsets on one or few genes for the maintenance of tumour malignancy is termed “oncogene addiction” (Weinstein 2002).

Intensive studies have revealed that malignant carcinoma of the lung displayed prominent mutations in multiple oncogenes, which then resulted in aberrant induction of pro-survival signals. Several driver mutations, which include *EGFR* mutation, *KRAS* mutation, *EML4-ALK* fusion, *HER2* mutation, *BRAF* mutation, *PIK3CA* mutation, *AKT1* mutation, *MAP2K1* mutation and *ROS1* fusions, are commonly detected in lung adenocarcinoma (Pao and

Hutchinson 2012) (Figure1.8). Targeted therapies involving kinase inhibitors customized to the genetic mutations of individual tumours have led to superior treatment outcome compared to conventional chemotherapy. Several molecular targeting agents that have yielded clinical successes in NSCLC patients will be discussed in the following chapters.

A

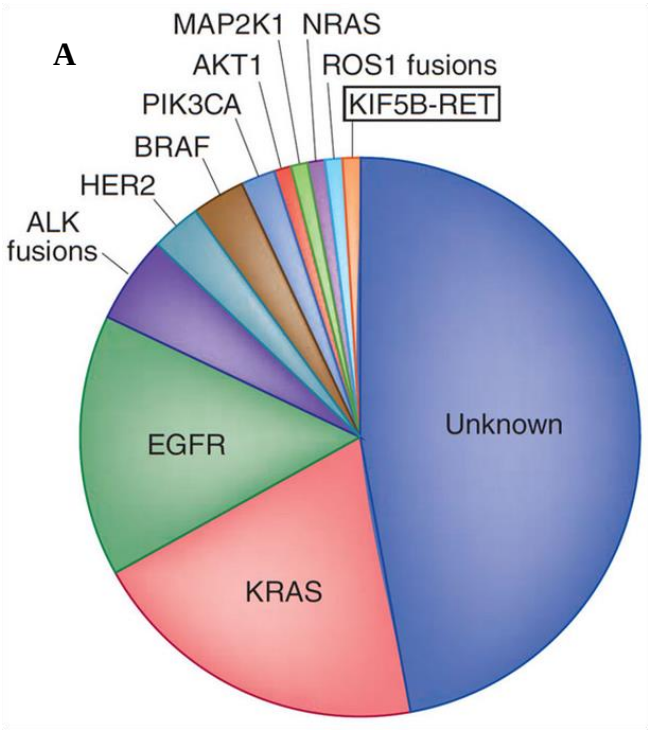

B

Driver mutations	Clinically tested targeted therapies
EGFR	Gefitinib, erlotinib, afatinib Cetuximab
EML4-ALK	Crizotinib
HER2	Lapatinib, trastuzumab
MAP2K	PD0325901, selumetinib, trametinib
B-Raf	Vemurafenib
PIK3CA	GDC0941, BKM120
AKT1	MK2206
ROS1	Crizotinib
KIF5B-RET	Carbozantinib, vandetanib

Figure 1.8: Distribution of clinically relevant driver mutations in lung adenocarcinoma and several clinically available targeted therapies.

In recent years, lung cancer has established as a model for investigation on the "oncogene addiction" concept due to the high frequency of genetic mutations being identified. These mutations include: *EGFR*, *HER2*, *KRAS*, *ALK*, *BRAF*, *PIK3CA*, *AKT1*, *ROS1*, *NRAS* and *MAP2K1* (A). The recently identified kinesin family member 5B-ret proto-oncogene (KIF5B-RET) is boxed (Kohno, Ichikawa et al. 2012, Takeuchi, Soda et al. 2012). Some of the clinically tested targeted therapies that inhibit the aberration activation of oncogenic pathways are shown (B). [Adapted from (Pao and Hutchinson 2012)].

1.4.1 *EGFR* and *HER2* mutations

The EGFR is a transmembrane receptor tyrosine kinase (RTK) that belongs to the HER/ErbB protein family. The EGFR pathway is a crucial cellular signalling mechanism that regulates growth, survival proliferation as well as differentiation in human cells (Hackel, Zwick et al. 1999). It has been well-established that the EGFR network is triggered following the binding to EGF-like growth factors, such as EGF and transforming growth factor α (TGF-α), which leads to dimerization and autophosphorylation of the receptor (Yarden and Sliwkowski 2001). Multiple tyrosine residues found on the cytoplasmic-bound C-terminal domain of EGFR have been identified as autophosphorylation sites. The autophosphorylation of EGFR trigger the downstream pathways through activation of the signalling cascade (Burgess, Cho et al. 2003, Garrett, McKern et al. 2003). The main signalling transduction cascades of EGFR include the MAPK/Ras/Raf/Erk, PI3K/Akt and Janus kinase/signal transducer and activator of transcription (JAK/STAT) pathways (Figure 1.9).

Mutation of EGFR is a common aberration in lung cancer and is detected in almost a quarter of all diagnosed patients (Cheng, Alexander et al. 2012, Pao and Hutchinson 2012). When EGFR is mutated, it often leads to ligand independent receptor homodimerization or ligand-dependent signal amplification, and subsequently enhances downstream signalling of EGFR (Irmer, Funk et al. 2007). It was soon discovered that tumour cells with mutated EGFR are susceptible to tyrosine kinase inhibitors (TKIs), thus these tumours are deemed as oncogene-addicted (Heymach, Nilsson et al. 2006, Irmer, Funk et al. 2007). TKIs, such as gefitinib and erlotinib that targets the cytoplasmic autophosphorylation sites of EGFR, have achieved clinical successes in treatment of NSCLC patients with improved response and prolonged survival (Paez, Jänne et al. 2004, Tsao, Sakurada et al. 2005). Antibodies that target the ligand-binding region of EGFR, such as Cetuximab, have been tested as well. However, both FLEX (First-Line Erbitux in Lung Cancer) and BMS-099 (Bristol-Myers Squibb 099) studies have shown unsatisfactory clinical benefit for the addition of Cetuximab to conventional chemotherapy (Pirker, Pereira et al. 2009, Lynch, Patel et al. 2010).

HER2 is another member of the HER/ErbB RTK family with similar function as EGFR. Unlike EGFR, *HER2* mutation is detected in less than 5% of NSCLC cases (Stephens, Hunter et al. 2004, Cheng, Alexander et al. 2012). Both the TKI lapatinib and HER2 antibody trastuzumab have been applied on NSCLC patients (Cappuzzo, Bemis et al. 2006, Ross, Blumenschein et al. 2010, Kelly, Carter et al. 2012).

1.4.2 *RAS* and *BRAF* mutations

The mutation of *RAS* gene is the second most commonly detected aberration in lung cancer apart from *TP53*. Approximately 25% of all lung adenocarcinoma cases harbour somatic mutations on the *KRAS* gene, with a further 1% with *NRAS* mutation (Cheng, Alexander et al. 2012, Ohashi, Sequist et al. 2013). The GTPase activation protein, Ras, is a downstream effector of EGFR. Through conversion of guanine triphosphates (GTP) to guanine diphosphate (GDP), the Ras protein recruits and stimulates the Raf/MEK/Erk pathway (Buday and Downward 1993, Huang, Marshall et al. 1993). The serine/threonine kinase, Raf, is the direct target of Ras. Activated Ras switches on the signalling of Raf, which activates mitogen-activated protein kinase kinases (MAP2K or MEK) that phosphorylate both extracellular signal-regulated kinases 1 and 2 (Erk1/2) (Figure 1.9).

Ras is inactivated upon binding of GDP, but mutations in Ras prevent the GDP-mediated inhibition, thus lead to the constitutive activation of the MAPK signalling (Bos 1989, Watanabe, Nobuta et al. 1996). Due to the frequency of *RAS* mutation in all human cancers, much effort has been invested on the development of specific inhibitors for the Ras protein. However, this target is by far undruggable as most of the drugs designed have failed to shut down its signalling, probably due to its high affinity to GTP/GDP and the absence of known allosteric sites (Downward 2003). More importantly, as Ras is a downstream effector of EGFR, constitutive activation of mutant Ras induces drug resistance to EGFR inhibitors (O'Byrne, Gatzemeier et al. 2011, Misale, Yaeger et al. 2012). Recently, a research group has synthesized a small molecule that is claimed to inhibit Kras allosterically through reducing GTP affinity and interaction with its effector (Ostrem, Peters et al. 2013). However, the clinical efficacy of this molecule is yet to be determined. Current clinical approach has focused on targeting downstream kinases of Ras for treatment of tumours with mutant Ras (Downward 2003). Thus far, several inhibitors of MEK have shown promising effect in early trials (Chen and Sweet-Cordero 2013, Jänne, Shaw et al. 2013).

Mutation of *BRAF* gene in lung cancer is rare (1-4%) as compared to that of melanoma (Davies, Bignell et al. 2002, Naoki, Chen et al. 2002, Paik, Arcila et al. 2011). Unlike melanoma tumour, *BRAF* mutation in lung cancer does not predominantly occur at valine 600 (V600) residue. In fact, several *BRAF* mutated sites have been identified within the kinase domain (Paik, Arcila et al. 2011). Similar to *RAS* mutation, mutant B-Raf constitutively stimulates the P44/42 MAPK signalling. A B-Raf enzyme inhibitor, vemurafenib, has shown dramatic response in a *BRAF* V600E-mutant lung adenocarcinoma patient (Peters, Michielin et al. 2013).

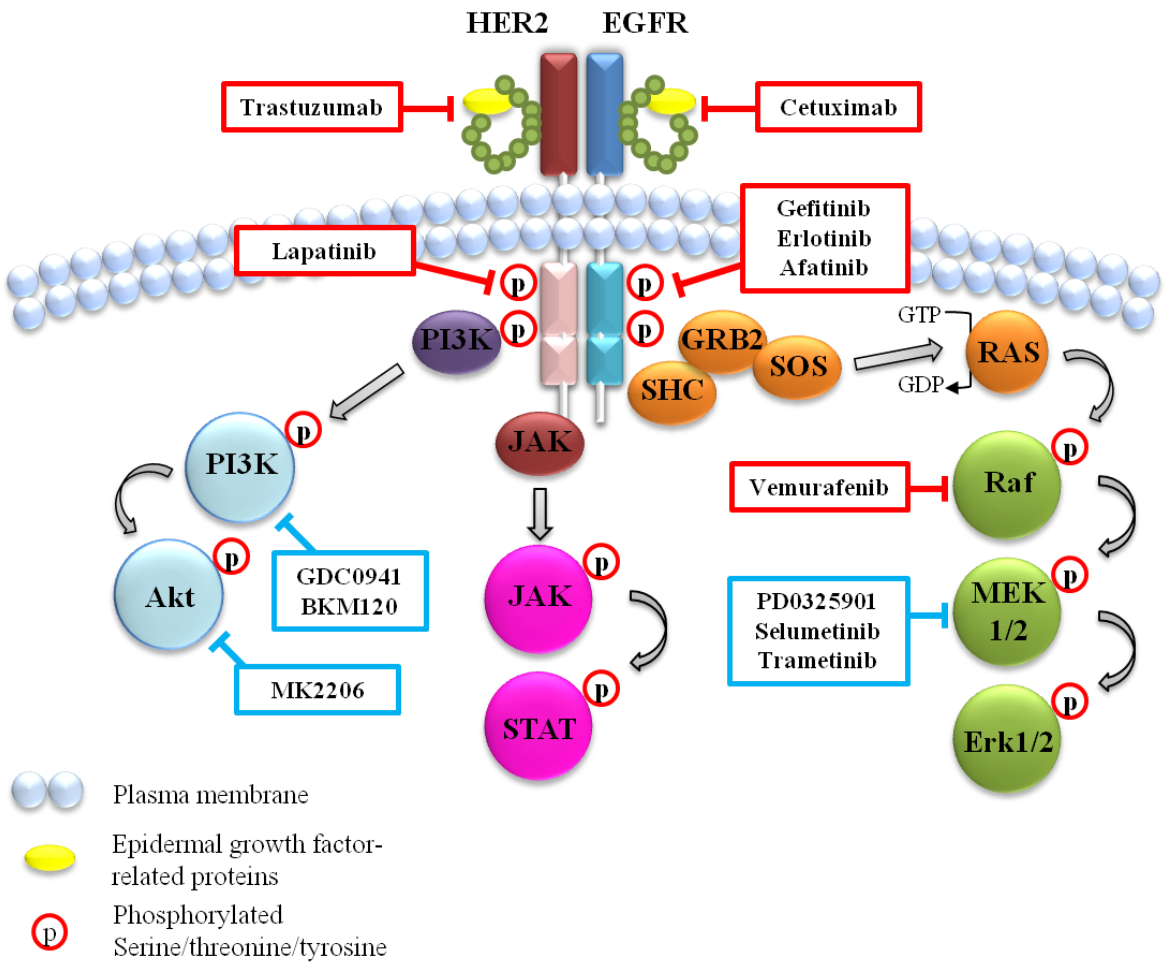

Figure 1.9: Overview of the activation and pharmacologic inhibition of EGFR signalling pathway in lung cancer.

EGFR/HER2 is activated by EGF-like growth factors that results in autophosphorylation of key tyrosine residues. The phosphorylated sites function as docking regions for recruitment of downstream kinases through their Src homology 2 (SH2) domains. Downstream signalling cascades for EGFR/HER2 include MAPK/Ras/Raf/Erk, PI3K/Akt and Janus kinase/signal transducer and activator of transcription 3 (JAK/STAT) pathways. Several clinically tested molecular targeting agents are shown: EGFR inhibitors (gefitinib, erlotinib, afatinib, cetuximab), HER2 inhibitors (trastuzumab, lapatinib), B-Raf inhibitor (Vemurafenib), MEK inhibitors (PD0325901, selumetinib, trametinib), PI3K inhibitors (GDC0941, BKM120), and Akt inhibitor (MK2206). **Red indicates FDA-approved agents**. **Blue indicates agents that are tested in clinical trials**.

1.4.3 *PIK3CA* mutation

EGFR signalling also promotes cell survival through the activation of PI3K/Akt pathway (Henson and Gibson 2006). Upon its activation, cytoplasmic tail of EGFR/HER2 recruits PI3K to its SH2 domains. Activated PI3K phosphorylates phosphatidylinositol (4,5)-biphosphate (PIP2) to phosphatidylinositol (3,4,5)-triphosphate (PIP3), which then activates Akt family members (Bos 1995). Akt promotes cell survival through activation of NF-κB, glycogen synthase kinase 3 (GSK3) and mammalian target of rapamycin (mTOR). PI3K is also known to activate Ras, leading to the activation of p44/42 MAPK signalling (Hennessy, Smith et al. 2005) (Figure 1.9).

Somatic mutation in *PIK3CA* has been detected in 1-3% of NSCLC patients (Samuels, Wang et al. 2004, Kawano, Sasaki et al. 2006, Cheng, Alexander et al. 2012). These mutations often occur at two "hotspots" within exon 9 and exon 20 that encode for the helical domain and kinase domain respectively. Tumour cells with mutated *PIK3CA* show aberrant activation of the PI3K/Akt/mTOR signalling and are less sensitive to chemotherapies (Hennessy, Smith et al. 2005). Recently, mutations on PIK3CA have been shown to predict treatment response to PI3K/Akt/mTOR inhibitors (Janku, Wheler et al. 2012). Several trials are in progress to investigate the efficacy of Akt inhibitor (MK2206) and PI3K inhibitors (GDC0941, BKM120) in NSCLC.

1.4.4 *EML4-ALK* fusion

The fusion of echinoderm microtubule-associated protein-like 4 (EML4) and anaplastic lymphoma kinase (ALK) is found in approximately 3-7% of all lung cancer cases (Wong, Leung et al. 2009, Kwak, Bang et al. 2010, Cheng, Alexander et al. 2012). Although multiple variants of EML4-ALK fusions have been described (Choi, Takeuchi et al. 2008), the fusion of EML4 consistently leads to the ligand-independent oligomerization of ALK and constitutive activation of its kinase activity, thus leading to cancer formation (Choi, Takeuchi et al. 2008).

Upon the identification of this aberration, the development of clinically-ready ALK inhibitor, crizotinib, is rapid and has achieved improvement in progress-free survival in some lung cancer patients (Kwak, Bang et al. 2010). The status of *ALK* fusion is detected by fluorescence *in situ* hybridization (FISH) or immunohistochemistry (IHC) (Paik, Choe et al. 2011, Yi, Boland et al. 2011). Currently, FDA has approved the usage of crizotinib as standard first-line therapy for advanced NSCLC patients harbouring *ALK* rearrangement (Kwak, Bang et al. 2010, Shaw, Yeap et al. 2011)..

1.4.5 Lack of driver mutations in lung SCC

The application and efficacy of molecular targeted therapies in NSCLC patients has been limited to lung adenocarcinoma tumours. Despite being identified as one of the most representative tumour type for investigation of oncogenic dependency, the spread of somatic mutations in NSCLC are unevenly distributed across lung adenocarcinoma and lung SCC (Naoki, Chen et al. 2002). With the exception of *PIK3CA* mutation (Kawano, Sasaki et al. 2006), genetic aberrations in EGFR, Kras, B-Raf and EML4-ALK are more commonly detected in lung adenocarcinoma tumours (Brose, Volpe et al. 2002, Pao, Miller et al. 2004, Boland, Erdogan et al. 2009, Paik, Arcila et al. 2011).

It is now well-established that lung SCC is lacking of clinically relevant oncogenic driver mutations (Rekhtman, Paik et al. 2012). The recently published report by The Cancer Genome Atlas (TCGA) Network has attempted to investigate the alterations of genomic landscape in this disease (Network 2012). Despite the high mutational rate, *EGFR*, *KRAS* mutations and *ALK* fusions are rarely detected among the 178 lung SCC cases. Therefore, the FDA-approved EGFR inhibitors (gefitinib and erlotinib) and ALK inhibitor (Crizotinib) that were developed for lung adenocarcinoma are largely ineffective against lung SCC (Boland, Erdogan et al. 2009, Camidge, Hirsch et al. 2011, Rekhtman, Paik et al. 2012). The more comprehensive platinum-based chemotherapy, used in combination with other chemotherapeutic agents, remains as the first-line treatment for patients diagnosed with lung SCC (Wang and Lippard 2005).

1.5 Histones, HDACs and HDAC inhibitors in cancer

The rapid advancement in understanding of tumourigenesis have revealed the requirements for constitutive activation of oncogenes and functional inactivation of tumour suppressor genes for development of malignancy (Hanahan and Weinberg 2011). The activation or repression of transcription is partly associated with epigenetic regulation and chromatin remodelling. Aberrant acetylation of histone tails has been strongly associated with alteration of chromatin structure and abnormal transcriptomic regulations in tumour cells (Jacobson and Pillus 1999). Subsequently, several mutations that affect activity of HATs are detected in malignant cells, while HDACs are reported to be overexpressed or aberrantly recruited by onco-proteins (Minucci and Pelicci 2006). These lead to inappropriate regulations of a number of well-characterized cellular oncogenes and tumour suppressor genes that favour tumourigenesis (Hess-Stumpp 2005, Glozak and Seto 2007). Understanding the link between histones, HDACs and the transcriptomic expressions has provided opportunities for therapeutic intervention of tumour cells.

1.5.1 Histones

Chromatin is composed of DNA and proteins at ratio of 1:1. Histones are highly alkaline chromosomal proteins that form the building blocks of chromatin. Coiled DNA winds around histones to form nucleosomes, which bundle to form chromatin, and eventually condensed to form the compact chromosome (Ura, Hayes et al. 1995, Kornberg and Lorch 1999). Chromatin architecture can be modified by chromatin remodelling through post-translational modifications of histone tails that relocate nucleosomes and changes nucleosome structure. To date, five major histone families are identified: the linker histones, H1/H5; and the core histones, H2A, H2B, H3 and H4 (Kornberg and Lorch 1999). Two of each of the core histone interact and form the octameric nucleosome core. The superhelical DNA winds around this octameric structure and is stabilized by both protein-protein interactions between the histones as well as the electrostatic attraction of positively-charged lysine residues on histones and the negatively-charged phosphates backbone of DNA (Luger, Mäder et al. 1997, Mizzen and Allis 1998). The linker histone binds the nucleosome at both the entry and exit sites of the DNA, thus increasing the stability of the histone-DNA complex (Pruss, Bartholomew et al. 1996).

The assembly and disassembly of nucleosome is mainly regulated by post-translational modifications of histones. Modifications of histones include acetylation, phosphorylation, methylation, ubiquitination, and sumoylation, which ultimately determine the chromatin structure as the assembly of euchromatin (relaxed chromatin) and heterochromatin

(condensed chromatin) is influenced by the degree of interaction between DNA and histones. The transition between euchromatin and heterochromatin is determined by the extent of acetylation and methylation on histone tails (Casas-Delucchi, van Bemmel et al. 2012). Furthermore, it was reported that certain combinations of modifications are consistently observed, thus postulating the presence of histone codes that directly affect gene transcription through epigenetic regulatory system (Strahl and Allis 2000, Jenuwein and Allis 2001).

Among these modifications, acetylation is probably the most extensively studied mechanism (Ura, Kurumizaka et al. 1997). Histone hyperacetylation leads to unfolding of the nucleosome core complex (Oliva, Bazett-Jones et al. 1990, Struhl 1998, Annunziato and Hansen 2000); whereas histone hypoacetylation strengthens histone tail-DNA interactions (Casas-Delucchi, van Bemmel et al. 2012) (Figure 1.10 A). Histone acetylations modulate transcriptional activity by determining the accessibility of DNA template to the transcription machinery, which begins with the binding of transcription factor II D (TFIID) and TATA box-binding protein (TBP) to core promoter regions (Mizzen and Allis 1998). Taken together, acetylation of histones facilitates the promoter binding of TFIID and TBP, as well as the recruitment of other transcription factors, activators and co-activators, thus initiating transcription.

1.5.2 Histone acetyl-transferases (HATs)

Acetylation of histone tails is regulated in opposing manner by HATs and HDACs. Till date, about 30 HATs that are grouped into 5 different families have been identified (Carrozza, Utley et al. 2003). Tip60, p300, and cyclin-AMP-response-element binding protein (CBP) are among the extensively studied human HATs. These enzymes induce acetylation of the ε-NH_2 group on the lysine residues along the histone tails by utilizing acetyl-Co as a co-factor (Marmorstein and Roth 2001). HATs are also known to bind to transcriptional co-activators, such as p300/CBP-associated factor (PCAF) (Schiltz, Mizzen et al. 1999). Both HATs and PCAF are known to play a critical role in transcriptional control by relieving the repressive effects on chromatin through acetylation of histone tails (Kundu, Palhan et al. 2000, Marmorstein and Roth 2001). The addition of an acetyl-group removes the positive charge on the histones and reduces its interaction with the negatively charged DNA (Figure 1.10 A). This unwinds the coiled DNA and allows access for transcription machinery, and eventually triggers transcriptional activation.

Apart from histones, HATs also acetylate a wide range of non-histone proteins (Glozak, Sengupta et al. 2005). The transactivation of p53 through acetylation by HATs (CBP/p300,

PCAF, Tip60) has been discussed earlier in Chapter 1.3.2.2. Furthermore, HATs regulate the acetylation of HMG proteins (Munshi, Merika et al. 1998), STAT3 (Wang, Cherukuri et al. 2005), c-Myc (Patel, Du et al. 2004), GATA (Boyes, Byfield et al. 1998), and NF-κB (Chen Lf, Fischle et al. 2001). In general, HATs play a significant role in mediating the cellular processes and functions by affecting a wide range of substrates.

1.5.3 Histone deacetylases (HDACs)

HDACs are enzyme complexes that are responsible for the specific deacetylation of histones. This class of enzyme removes the acetyl-group from the lysine residues on histone tails and represses gene transcription by various mechanisms. Firstly, the condensed structure of heterochromatin prevents access of the transcriptional machinery to the DNA strands (Struhl 1998). Secondly, deacetylation of specific lysine residues promotes its recognition by histone methy-transferases (Martin and Zhang 2005). Methylated lysine residues recruit chromodomain proteins that facilitate the assembly of heterochromatin through recognition of trimethylated lysine 9 of histone H3 (Lachner, O'Carroll et al. 2001, Nakayama, Rice et al. 2001). These mechanisms collectively reduce transcriptional activity and increase transcriptional silencing (Figure 1.10 A).

Till date, 17 genes have been identified to encode for four distinct classes of HDACs (Gray and Ekström 2001, de Ruijter, van Gennip et al. 2003). Class I (HDAC1, 2, 3, 8) and class II (HDAC4, 5, 6, 7, 9, 10) are evolutionarily related and universally induced Zn-catalyzed hydrolysis of the acetyl-lysine amide bond. Class IV HDAC (HDAC11) is also Zn-dependent but is phylogenetically different from both class I and II enzymes (de Ruijter, van Gennip et al. 2003). Class III HDAC of the sirtuin (SirT) family is distinctly different from the other classes as it lacks the Zn-dependent enzymatic mechanism and is evolutionarily unrelated (Blander and Guarente 2004, North and Verdin 2004). Instead, lysine deacetylation activity of sirtuins is NAD-dependent. HDAC1, 2, and 3 are mostly nuclear-bound, while the other HDACs are indentified at both nucleus and cytoplasm (Gray and Ekström 2001).

The functions of each HDAC, other than the deacetylation of histone tails, have been comprehensively characterized. Apart from histones, HDACs are found to interact and deacetylate a wide range of non histone proteins (Glozak, Sengupta et al. 2005). The closely related HDAC1 and HDAC2 are found as key components of the transcriptional-repression SIN3-HDAC complex and the nucleosome-remodelling NuRD-Mi2-NRD complex (Khochbin, Verdel et al. 2001, Yang and Seto 2003). The transcriptional repressing effects of class I HDACs are partly regulated by the co-activation of nuclear-receptor corepressor

(NCOR) and silencing mediator for retinoid and thyrold-hormone receptors (SMRT) (Li, Wang et al. 2000, Guenther, Barak et al. 2001, Khochbin, Verdel et al. 2001). Individually, HDAC3 is shown to affect stability and DNA-binding ability of NF-κB by deacetylating its RelA subunit (Kiernan, Brès et al. 2003), while HDAC8 has been reported to protect telomere degradation and play a part in tumourigenesis (Lee, Sengupta et al. 2006). The transcription factor GATA-2 is repressed by both HDAC3 and HDAC5 (Ozawa, Towatari et al. 2001), whereas GATA-1 interacts with HDAC3, 4, and 5 (Watamoto, Towatari et al. 2003). Moreover, several class I HDACs are able to repress transactivation of p53 signalling by deacetylating the p53 protein (Luo, Su et al. 2000, Ito, Kawaguchi et al. 2002, Zeng, Xiao et al. 2006, Karagianni and Wong 2007).

Class II HDACs are characterized by their ability to shuttle between the cytoplasm and nucleus. These HDACs are not involved in the SIN3-HDAC and NuRD-Mi2-NRD complexes (Khochbin, Verdel et al. 2001, Yang and Seto 2003), but mediate transcriptional repression through binding to transcription factors, such as myocyte enhancer factor 2 (MEF2) and members of the Runt-related transcription factor (Runx) family (Lu, McKinsey et al. 2000, Lu, McKinsey et al. 2000, Zhang, McKinsey et al. 2002). Furthermore, several cytoplasmic interactive partners of class II HDACs have been illustrated, which include 14-3-3 (McKinsey, Zhang et al. 2000), tubulin (Hubbert, Guardiola et al. 2002), and Hsp90 (Kovacs, Murphy et al. 2005).

The class III HDACs, commonly referred to as the sirtuins, have been implicated in aging, transcription, apoptosis and inflammation (Donmez and Guarente 2010, Roth and Chen 2013). The knowledge on sirtuins is by far limited. However, it has been reported that sirtuins induce p53 deacetylation at the C-terminus and inhibit p53-mediated functions (Vaziri, Dessain et al. 2001, Haigis and Guarente 2006). Lastly, little is known about the class IV HDAC, despite being reported to be highly expressed in several carcinomas when compared to healthy tissues (Deubzer, Schier et al. 2013).

Abnormal expressions of several HDACs have been reported to be associated with prognosis in various cancers. In NSCLC, low expression of class II HDACs genes, such as HDAC5 and HDAC10, has been correlated with poor prognosis (Osada, Tatematsu et al. 2004). The authors postulate that class II HDACs may repress critical oncogenes, and that low expression of these HDACs may favour the malignant progression of lung tumours. On the contrary, high expression of HDAC1 has been linked with poor prognosis in patients with lung adenocarcinoma (Minamiya, Ono et al. 2011). However, the correlation of HDACs with lung SCC remains contentious.

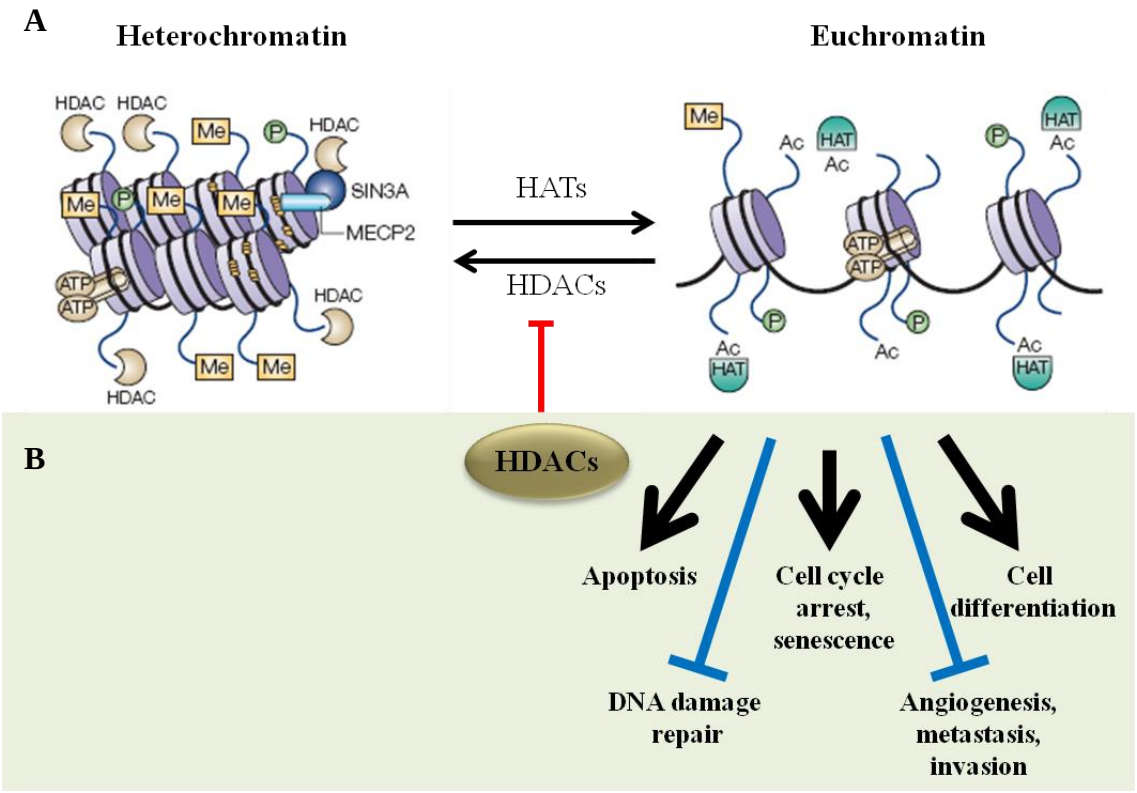

Figure 1.10: Regulation of chromatin structure cellular determines transcriptional activity and cellular processes.

A, Histones is the building block for formation of nucleosome. DNA (black line) winds around the octmeric histones. Condensed heterochromatin recruits methyl-binding proteins (MECP2) and HDACs that maintains its closed-chromatin configuration and transcriptional repression. Post-translational modifications of histone tails by acetylation (Ac), methylation (Me) and phosphorylation (P) alter the nucleosomal architecture. HATs induce histone acetylation that relaxes chromatin and promotes transcriptional activation. B, HDAC inhibitors inhibit enzymatic activity of HDACs, thus causing hyper-acetylation of histones. This represses DNA damage repair, angiogenesis, metastasis and invasion; while increases cell differentiation, cell growth arrest and cell death. [Adapted from (Johnstone 2002)]

1.5.4 Histone deacetylase inhibitors

As summarized in the previous chapter, HATs and HDACs play crucial roles in biological functions through modulation of histones and non-histones proteins. Apart from directly influencing chromatin remodelling, HATs and HDACs modulate cellular processes by affecting the DNA-binding affinity, protein stability and protein-protein interaction of non-histone proteins, thereby indirectly influences transcriptional activity (Glozak, Sengupta et al. 2005). Since imbalanced acetylation of histone and non-histone proteins is common among malignant cells, the therapeutic intervention of epigenetic therapies has been investigated.

These expanding understandings on epigenetic control of gene expression in malignant cells have provided new targets for cancer therapy. For instance, reversing low histone acetylation has been proposed as one possible approach for epigenetic cancer therapy (Dawson and Kouzarides 2012). However, pharmacologic modulators of HATs are limited, with the few available HAT inhibitors and enhancers limited to *in vitro* investigations (Lau, Kundu et al. 2000, Mantelingu, Kishore et al. 2007). On the contrary, HDAC inhibitors discovered at early stages has demonstrated inhibitory effects on HDACs activity (Riggs, Whittaker et al. 1977, Novogrodsky, Dvir et al. 1983, Yoshida, Kijima et al. 1990). Subsequently, pronounced anti-neoplastic effect was observed in trichostatin-A (TSA), a hydroxamic acid class HDAC inhibitor (Vigushin, Ali et al. 2001). This has generated interest in the attempt to identify novel molecules for specific targeting of HDACs. Crystallographic analysis indicates that HDAC inhibitors block the zinc-containing catalytic site of HDACs, thereby inhibiting the enzymatic activity of these compounds (Finnin, Donigian et al. 1999). To date, five classes of HDAC inhibitors with distinctive structures have been developed, which include: short-chain fatty acids like butyric acid, hydroxamic acids, electrophilic ketones, cyclic tetrapeptides, and benzamides (Johnstone 2002).

Over the past 30 years, advances in development of HDAC inhibitors have been made. The short chain fatty acids like butyric acid compounds, such as valproic acid and phenylbutyrate, are among the first HDAC inhibitors to be identified (Riggs, Whittaker et al. 1977, Novogrodsky, Dvir et al. 1983). This class of HDAC is considered as the least potent among all the HDAC inhibitors with short plasma half-life and optimal cytotoxic concentrations at millimolar range (Novogrodsky, Dvir et al. 1983, Phiel, Zhang et al. 2001). Hydroxamic acids, such as TSA and SAHA, were identified in the 1990s. These compounds are now characterized as the most potent class of HDAC inhibitors with improved half-lives, optimal growth inhibition concentration at micromolar range, and specific inhibition of both class I and II HDACs at nanomolar concentrations (Richon, Webb et al. 1996, Kelly and Marks 2005). As the zinc-binding hydroxamic group is deemed responsible for the short half-lives, elextrophilic ketones were developed. However, these HDAC inhibitors only possess modest anti-proliferative effect with poor *in vivo* pharmacokinetic parameters (Frey, Wada et al. 2002, Wada, Frey et al. 2003). The final classes of HDAC inhibitors, benzamides and cyclic tetrapeptides, have shown potent HDAC inhibitory activities (Furumai, Matsuyama et al. 2002, Kraker, Mizzen et al. 2003).

As described, sirtuins are Zn-independent, NAD-dependent class III HDACs (Imai, Armstrong et al. 2000). Thus, pan-HDAC inhibitors that almost certainly target on Zn-dependent catalytic sites are ineffective against sirtuins. Development of sirtuin inhibitors is thus based on inhibition of NAD-catalytic activity (Grozinger, Chao et al. 2001), which

include sirtinol, cambinol, suramin, salermide and tenovin (Villalba and Alcaín 2012). Recently, the potential of sirtuin inhibitors as anti-cancer therapies has been investigated (Ford, Jiang et al. 2005, Lara, Mai et al. 2009). Interestingly, sirtuin inhibitors have been established as a potent activator of p53 functions through acetylating the p53 proteins (Vaziri, Dessain et al. 2001, Lain, Hollick et al. 2008).

1.5.4.1 Mechanism-of-action of HDAC inhibitors

Although HDACs play a crucial role in regulation of gene expression, HDAC inhibitors do not seem to be able to induce global transcriptional regulation. Instead, studies have reported that only about 2 - 10% of genes are affected by treatment of HDAC inhibitors (Van Lint, Emiliani et al. 1996, Mariadason, Corner et al. 2000, Peart, Smyth et al. 2005). It was then observed that HDAC inhibitors trigger the activation of a common set of genes, thus suggesting that these compounds have specific selectivity towards particular loci. Moreover, genes regulating cell proliferation and survival are the most affected by HDAC inhibitors, while many tumour cells display sensitivity to a wide range of HDAC inhibitors (Schrump 2009). More importantly, several HDAC inhibitors have been reported to sensitize both chemotherapy and molecular targeted therapy in drug-resistant cancer cells (Sharma, Lee et al. 2010, Bangert, Häcker et al. 2011, Chen, Chen et al. 2013). These prompted the exploration of the anti-neoplastic mechanisms of HDAC inhibitors in malignant cells. Several mechanisms of HDAC inhibitors have been proposed. These mechanisms often lead to reduced DNA damage repair, increased cell growth arrest and senescence, increased cell death, induction of differentiation, and inhibition of angiogenesis, metastasis and invasion (Figure 1.10 B).

HDAC inhibitors could induce DNA damage as indicated by the accumulation of activated H2AX, especially after exposure to irradiation or cytotoxic agents (Karagiannis, Harikrishnan et al. 2007, Wilson, Holson et al. 2011, Wilson, Lalani et al. 2012). This is achieved through the attenuation of DNA damage repair mechanisms, as HDAC inhibitors have been shown to reduce the expression of genes involved in HR and non-homologous end joining (NHEJ) DNA repair pathways (Munshi, Kurland et al. 2005, Adimoolam, Sirisawad et al. 2007, Chen, Wang et al. 2007, Kachhap, Rosmus et al. 2010). Furthermore, it was reported that DNA damage induces by vorinostat could be effectively repaired by normal cells but not malignant cells (Lee, Choy et al. 2010).

Like other anti-cancer agents, HDAC inhibitors induce both cell senescence and cell death in tumour cells. Several HDAC inhibitors can induce both G1 and G2 cell cycle arrest with depletion of cells progressing into S phase, probably through expression of p21 in both p53-

dependent and –independent manners (Richon, Sandhoff et al. 2000, Ju and Muller 2003, Gui, Ngo et al. 2004). Other potential growth inhibitory mechanisms include up-regulation of *Gadd45* gene and activation of transforming growth factor beta (TGF-β) pathway that induce cell cycle arrest (Chen, Clark et al. 2002, Halder, Cho et al. 2011). Furthermore, HDAC inhibitors trigger both intrinsic and extrinsic apoptotic pathway. Several studies have demonstrated the transcriptional activation of extrinsic apoptosis through up-regulation of death receptors and their ligands, such as Fas, FasL, TRAIL and TNF-α (Imai, Adachi et al. 2003, Nebbioso, Clarke et al. 2005, Sutheesophon, Nishimura et al. 2005, Huang, Scruggs et al. 2013). The induction of mitochondrial death pathway is determined through direct transcriptiomic regulation of Bcl-2 family members and accumulation of intracellular reactive oxygen species (ROS). The expressions of various pro-apoptotic markers, such as Bim, Bak and caspase 9, are increased by HDAC inhibitors (Moore, Barbi et al. 2004, Zhang, Gillespie et al. 2004). On the contrary, HDAC inhibitors attenuate the expression and activity of several anti-apoptotic markers that include Bcl-2, Bcl-xl, Bcl-w, and XIAP (Moore, Barbi et al. 2004, Zhang, Gillespie et al. 2004, Rosato, Maggio et al. 2006). Moreover, elevated levels of ROS are detected in cells treated with HDAC inhibitors (Ruefli, Ausserlechner et al. 2001). As ROS is a negative indicator of mitochondria membrane potential (Jing, Cai et al. 2007), intrinsic apoptosis may be triggered by accumulation of ROS in HDAC inhibitors-treated cells (Ruefli, Ausserlechner et al. 2001, Rosato, Almenara et al. 2003). The detailed mechanism of this phenomenon is still unclear. However, increased expression of thioredoxin-binding protein-2 (*TBP-2*), a positive regulator of oxidative stress, has been reported in vorinostat (suberanilohydroxamic acid; SAHA)-treated cells (Butler, Zhou et al. 2002).

Interestingly, HDAC inhibitors also possess anti-angiogenic and anti-invasive properties both *in vitro* and *in vivo*. HDAC inhibitors block angiogenesis by decreasing the expression of pro-angiogenic genes, such as vascular endothelial growth factor (*VEGF*) and hypoxia-inducible factor 1α (*HIF1α*) (Deroanne, Bonjean et al. 2002, Sasakawa, Naoe et al. 2003). Furthermore, HDAC inhibitors exhibit mesenchymal-epithelial transition (MET) by suppression of MMPs (Kim, Ahn et al. 2004), a mesenchymal marker, and up-regulation of epithelial markers such as E-cadherin and tissue inhibitor of metalloproteinases (TIMPs) (Thelen, Schweyer et al. 2004, Witta, Gemmill et al. 2006, Nasu, Nishida et al. 2008).

Back then in 1990s, vorinostat was first observed to induce differentiation of murine erythroleukemia cells, and subsequently cell cycle arrest and apoptosis (Richon, Webb et al. 1996). It is now clear that different classes of HDAC inhibitors are able to induce cellular differentiation that is characterized by reduced proliferation, alteration of morphology, and accumulation of transcription factors (Werling, Siehler et al. 2001, Svechnikova, Almqvist

et al. 2008). The mechanisms in which cellular differentiation occur have not been fully deciphered, but it could be partly dependent on retinoic acid (RA) and retinoic acid receptor α (RARα) (Côté, Rosenauer et al. 2002). Cell growth arrest induced by low doses of HDAC inhibitors facilitates the occurrence of cell differentiation. In cases whereby high doses of HDAC inhibitors are used, induction of apoptosis usually precedes cell differentiation (Marks, Richon et al. 2000).

1.5.4.2 Clinical limitations of HDAC inhibitors

The promises of HDAC inhibitors both *in vitro* and in xenograft models have allowed this class of agents to progress into clinical settings. The adverse side effects of HDAC inhibitors and the development of resistance mechanisms have been detailed over the years. Despite the differences in chemical structures and specificities, all classes of HDAC inhibitors seemingly produce comparable toxicity profiles that are varied from those observed in conventional chemotherapies (Kelly, O'Connor et al. 2002). The common adverse events include nausea and vomiting (Sandor, Bakke et al. 2002), fatigue (Kummar, Gutierrez et al. 2007), thrombocytopenia, anemia (Giles, Fischer et al. 2006, Ellis, Pan et al. 2008), cardiac toxicity such as CT prolongation (Strevel, Ing et al. 2007), liver toxicities (Garcia-Manero, Assouline et al. 2008), and in some cases neurotoxicity (Ryan, Headlee et al. 2005). These adverse side effects have significantly affected the clinical usage of HDAC inhibitors as a monotherapy.

Similar to other anti-cancer agents, resistance to HDAC inhibitors have been reported. The resistance mechanisms of HDAC inhibitors effectively counteract the mechanism-of-action. In certain cell type, it has been reported that increased activity of Chk1, a component of the G2 checkpoint, is associated with resistance to HDAC inhibitors (Lee, Choy et al. 2011). However, clinical correlation is lacking to support most of these claims. Furthermore, inhibition of apoptotic pathways also leads to resistance to HDAC inhibitors. Increased levels of anti-oxidant genes, such as thioredoxin, superoxide dismutase 2 and glutathione reductase, as well as the anti-apoptotic Bcl-2 are detected in tumours with resistance to HDAC inhibitors (Marks 2006, Garcia-Manero, Yang et al. 2008, Shao, Growney et al. 2010). These changes either inhibit the accumulation of intracellular ROS or inhibit the formation of MAC, thus abrogating the induction of apoptosis. Lastly, several studies have revealed that certain HDAC inhibitors, such as romidepsin, are prone to drug efflux mechanisms that are mediated by P-glycoprotein (Peart, Tainton et al. 2003). Increased expression of *MDR1* gene, which encodes for P-glycoprotein, has been found in peripheral blood mononuclear cells of patients receiving romidepsin treatment (Robey, Zhan et al.

2006). This is postulated as a possible self-induced mechanism of resistance to HDAC inhibitors in certain tumours.

Lastly, it has been discussed earlier that repressive effects of histone deacetylation promotes histone and DNA methylation. The concurrent induction of both acetylation and methylation further facilitates the formation of heterochromatin (Casas-Delucchi, van Bemmel et al. 2012). Importantly, DNA methylation seemingly possesses stronger repressive effects that histone deacetylation (Fuks, Burgers et al. 2000). In these cases, using HDAC inhibitors as a single agent is insufficient to restore gene transcription. The addition of a demethylating agent, such as 5-azacitidine, has successfully increased gene expression significantly in pre-clinical studies (Cameron, Bachman et al. 1999). Clinical evaluation of such drug combinations has yielded tolerable safety profiles (Garcia-Manero, Kantarjian et al. 2006, Gore, Baylin et al. 2006, Soriano, Yang et al. 2007).

Taken together, effects of HDAC inhibitors in the clinical settings have been restricted by the presence of adverse side effect and development of drug resistance. These are presumably due to the usage of high doses of HDAC inhibitors, resulting in cellular toxicity. As reviewed by Azad *et. al.*, induction of cell death may not be the optimal clinical benefit for cancer patients (Azad, Zahnow et al. 2013). Therefore, selecting the right doses of HDAC inhibitors is a crucial determinant for the optimal specificity of these agents.

1.5.4.3 Clinical trials of HDAC inhibitors in lung cancer

Given the above mentioned limitations, HDAC inhibitors could still be potent anti-cancer agents if used with the optimal doses, timing and combinations (Azad, Zahnow et al. 2013). Various candidates from the five classes of HDAC inhibitors have been tested in the clinical setting. Recently, vorinostat and romidepsin have been approved by the FDA for the treatment of cutaneous manifestations in patients with cutaneous T-cell lymphoma (CTCL) (Mann, Johnson et al. 2007, Piekarz, Frye et al. 2009). More recently, romidepsin has gained FDA approval for the treatment of peripheral T-cell lymphoma (PTCL) (Piekarz, Frye et al. 2011). However, the utility of HDAC inhibitors in solid tumours is less established. Trials on HDAC inhibitors have not revealed superior progress in advanced solid malignancies (Bradley, Rathkopf et al. 2009, Ramalingam, Belani et al. 2009, Mackay, Hirte et al. 2010), largely due to the poor bioavailability and potency (Elaut, Rogiers et al. 2007).

The clinical report of HDAC inhibitors as a monotherapy on NSCLC has by far been limited. An initial report by Ramalingam *et. al.* has first investigated the clinical efficacy of

vorinostat, in combination with carboplatin and paclitaxel, in advanced solid tumours. They observed encouraging anti-tumour response among NSCLC patients in this phase I study (Ramalingam, Parise et al. 2007). A follow-up randomized phase II trial on the same combination treatment has shown improved progression-free-survival and overall survival in NSCLC cases (Ramalingam, Maitland et al. 2010). However, a subsequent Phase III trial was discontinued prematurely due to unsatisfactory clinical response and lack of improvement in survival rates (Belani, Ramalingam et al. 2009).

Current therapeutic intervention has attempted to derive the efficacy of HDAC inhibitors with TKIs in lung cancer. A randomized phase II trial on entinostat, a specific inhibitor of class I HDACs, and erlotinib in NSCLC has been completed recently (Witta, Jotte et al. 2012). Disappointingly, this combination regime has again failed to offer additional efficacy as compared to using erlotinib alone. These setbacks in the approach to combine HDAC inhibition with conventional chemotherapy or molecular targeted therapy have restricted the development of HDAC inhibitors in clinical setting for NSCLC patients.

1.5.5 Belinostat

Belinostat (PXD101) is a hydroxamic acid type HDAC inhibitor. Similar to other HDAC inhibitors, belinostat has demonstrated strong anti-neoplastic activity in several cancer types by inhibiting cell proliferation, promoting cellular differentiation, blocking angiogenesis and invasion, and triggering apoptosis in several preclinical studies (Plumb, Finn et al. 2003, Qian, LaRochelle et al. 2006, Lin, Lin et al. 2013). The commonly reported adverse events such as fatigue, diarrhoea, and the more life-threatening cardiac, hematologic and neurologic toxicities are posed to be major obstacles for the progression of HDAC inhibitors in clinic. However, when compared to other HDAC inhibitors, belinostat seemingly produces tolerable adverse effects while haematological toxicity is rare (Gimsing, Hansen et al. 2008, Steele, Plumb et al. 2008, Ramalingam, Belani et al. 2009, Yeo, Chung et al. 2012).

The cytotoxicity of belinostat has been investigated in several tumour cell lines that include hepatocellular carcinoma, leukemia, head and neck SCC (HNSCC), ovarian cancer, colon cancer, thyroid cancer and pancreatic cancer (Qian, LaRochelle et al. 2006, Buckley, Yoon et al. 2007, Duan, Friedman et al. 2007, Dai, Chen et al. 2008, Fazzone, Wilson et al. 2009, Ma, Sung et al. 2010, Chan, Zheng et al. 2013, Chien, Lee et al. 2013). In addition, belinostat has displayed strong anti-neoplastic effects in several drug resistant tumour cells, emphasizing its chemosensitizing properties (Fazzone, Wilson et al. 2009).

Belinostat has progressed to late stage clinical development with multiple haematologic and solid malignancies being investigated. The maximum tolerated dose of belinostat in combination with other chemotherapies has been tested in a recently completed trial (ClinicalTrials.gov Identifier NCT01310244). The efficacy of belinostat has been evaluated in myeloma, lymphoma (Gimsing, Hansen et al. 2008), mesothelioma (Ramalingam, Belani et al. 2009), thymic epithelial carcinoma (Giaccone, Rajan et al. 2011) and ovarian cancer (Mackay, Hirte et al. 2010). Despite the mixed outcome obtained from these clinical evaluations, the well-tolerable adverse effects of belinostat have encouraged the study of combination regimens.

1.6 Objectives

Historically, therapeutic approaches in the field of tumour biology have primarily focused on chemotherapy but recent specific pathway-targeted treatment regimens have proven advantageous. However, treatment options for lung SCC patients have been severely limited to conventional chemotherapies due to lack of oncogenic driver mutations in this disease. Unlike lung adenocarcinoma, whereby *EGFR* and *KRAS* mutations are common, the rarity of genetic aberrations restricts a majority of the targeted therapeutic approaches. The first aim of this thesis is to characterize the mutational landscape of lung SCC and verify representative cell lines as study models for this cancer type through a combination of genomic and proteomic approaches (Chapter 3).

The emergence of chemoresistance in lung SCC patients has led to paucity in treatment regime. While most current efforts have focused on identifying individualized treatment regimes for drug-resistant tumours, it was hypothesized that combination of appropriate chemotherapeutic agents with specific targeting of oncogenic pathways offers a powerful approach to circumvent the drug-resistance mechanisms in treatment of cancer. In the second part of the thesis, the mechanisms of cisplatin resistance in lung SCC cell lines were exploited. In view of the lack of targetable driver oncogenes in this disease, strategies that counteract drug resistance could enhance treatment outcome (Chapter 4).

As outlined in previous chapters, multiple mechanisms-of-action of HDAC inhibitors have been described in pre-clinical studies which include cell death, cell growth arrest, cell differentiation and anti-angiogenesis. However, the genotoxic and cytotoxic stresses exerted on mammalian cells by high doses of HDAC inhibitors often result in immediate induction of cell death and possibly preclude the clinically-important cellular differentiation and reprogramming. Therefore, these cytotoxic effects of HDAC inhibitors at high doses may result to the lack of therapeutic efficacy in most solid tumours as well as adverse side effects. It was postulated that when administered at suitable doses, HDAC inhibitors could effectively alter the tumour biology in clinically-relevant manner. In the next parts of the thesis, the chemosensitizing effect (Chapter 4) and synergistic cytotoxicity (Chapter 5) of belinostat, within tolerable doses, was investigated in lung SCC cells.

CHAPTER 2 MATERIALS AND METHODS

2.1 Materials

2.1.1 General chemicals and reagents

Chemicals/Reagents	Supplier	Place of origin
Acetic acid	Merck	Darmstadt, Germany
β-estradiol	Sigma Aldrich	MO, USA
Bovine serum albumin	Sigma Aldrich	MO, USA
Dimethyl sulfoxide (DMSO)	Sigma Aldrich	MO, USA
Dulbucco's Modified Eagle's Medium (DMEM)	Life Technologies	CA, USA
Eagle's Minimum Essential Medium (EMEM)	Life Technologies	CA, USA
Epidermal Growth Factor (EGF)	Sigma Aldrich	MO, USA
Ethanol	Merck	Darmstadt, Germany
Ethanolamine	Sigma Aldrich	MO, USA
Ethylenedinitrilo tetraacetic acid (EDTA)	Sigma Aldrich	MO, USA
Fetal bovine serum (FBS)	Hyclone Laboratories	Logan, UT
Gene Print® 10 system	Promega	WI, USA
Glycine	Bio-Rad	CA, USA
HEPES	Sigma Aldrich	MO, USA
Hydrochloric acid (HCl)	Merck	Darmstadt, Germany
Hydrocortisone	Sigma Aldrich	MO, USA
Insulin	Sigma Aldrich	MO, USA
Isopropanol	Merck	Darmstadt, Germany
Leibovitz's L-15 medium	Life Technologies	CA, USA
L-glutamine	Life Technologies	CA, USA
McCoy's 5 medium	Life Technologies	CA, USA
Methanol	Merck	Darmstadt, Germany
Penicillin-Streptomycin	Life Technologies	CA, USA
Phosphate buffer saline (PBS)	CSI	Singapore
Phosphorylethanolamine	Sigma Aldrich	MO, USA
RPMI-1640 medium	Life Technologies	CA, USA
Sodium pyruvate	Sigma Aldrich	MO, USA
Sodium selenite	Sigma Aldrich	MO, USA
Transferrin	Sigma Aldrich	MO, USA
Triiodothyronine	Sigma Aldrich	MO, USA
Tris base	Sigma Aldrich	MO, USA
Trypan blue dye	Sigma Aldrich	MO, USA
Trypsin-EDTA	Life Technologies	CA, USA
β-mercaptoethanol (β-ME)	Merck	Darmstadt, Germany

Table 2.1: List of general chemicals and reagents.

2.1.2 Drugs

Drugs	Supplier	Place of origin
Belinostat (PXD101)	Selleck Chemicals	TX, USA
Cetuximab	Merck	Darmstadt, Germany
Cisplatin (CDDP)	Pfizer	NY, USA
GDC0879	Selleck Chemicals	TX, USA
Nutlin-3a	Selleck Chemicals	TX, USA
PD-0325901	Selleck Chemicals	TX, USA
RDEA119	Selleck Chemicals	TX, USA
Tenovin-6	p53Lab	Singapore
Trametinib (GSK1120212)	Selleck Chemicals	TX, USA

Table 2.2: List of drugs.

2.2 Mammalian cell culture

2.2.1 Preparation of media

Medium	Supplements
RPMI 1640	10% FBS, 2mM L-glutamine, 100μg/mL streptomycin and 100U/mL penicillin
EMEM	
McCoy's 5a	
Leibovitz'	
DMEM	10% FBS, 4mM L-glutamine
ACL-4	10% FBS, 2mM L-glutamine, 100μg/mL streptomycin and 100U/mL penicillin, 0.02mg/mL Insulin, 0.01mg/mL transferrin, 25nM sodium selenite, 50nM hydrocortisone, 1ng/mL EGF, 0.01mM ethanolamine, 0.01mM phosphorylethanolamine, 100pM triiodothyronine, 0.5% (w/v) BSA, 10mL HEPES, 0.5mM sodium pyruvate
HITES	5% FBS, 2mM L-glutamine, 100μg/mL streptomycin and 100U/mL penicillin, 0.005mg/mL Insulin, 0.01mg/mL transferrin, 30nM sodium selenite, 10nM hydrocortisone, 10nM beta-estradiol

Table 2.3: Formulation for preparation of tissue culture media.

2.2.2 Mammalian cell lines

All lung squamous cell carcinoma cells (H226, H520, H596, H1869, H2066, H2170, Calu-1, ChaGo-k-1, SK-MES-1, and SW900) and normal fibroblast cells (MRC-5, IMR-90, and WI-38) were purchased from American Type Culture Collection (ATCC; Rockville, MD). HEK293T cells were kindly provided by Prof Jean-Paul Thiery (Cancer Science Institute, Singapore).

2.2.3 Cell culture maintenance

Lung squamous cell carcinoma lines H226, H2170, H520, H596, ChaGo-k-1 were cultured in RMPI 1640, Calu-1 in McCoy's 5a, SK-MES-1 in DMEM, SW900 in Leibovitz', H1869 in ACL-4 and H2066 in HITES medium. Lung normal fibroblast cells MRC-5, IMR-90 and WI-38 were cultured in EMEM medium. HEK293T cells were cultured in DMEM. All medium were enriched with additional supplements as described in Chapter 2.2.1. FBS used was heat-inactivated at 56°C to destroy heat-sensitive complement proteins. All cell lines, except for SW900, were cultured and maintained at 37°C in a humidified incubator of 5% CO_2. SW900 cells were cultured and maintained at 37°C in a humidified incubator without CO_2. All cell lines are adherent in nature. During subculturing, cell lines were rinsed with 1 x PBS (137mM NaCl, 2.7mM KCl, 4.3mM NaH_2PO_4, 1.4mM KH_2PO_4 pH7.4), trypsinized with 0.05% trypsin-EDTA solution and split into new culture flask with an appropriate split ratio. Cell lines were maintained at below 90% confluency.

2.2.4 Cryopreservation of cell lines

Cryopreservation was performed to maintain the primary stocks for individual cell lines. Upon trypsinization with 0.05% trypsin-EDTA solution, cell suspensions were pelleted by centrifugation at 800 rpm for 3 minutes. Cell pellets were resuspended in sterile-filtered freezing medium (90% FBS, 10% DMSO) and placed into sterile cryovials at a maximum density of 1 x 10^6 cells/mL. The cells were allowed to freeze gradually in cryo-freezing containers filled with isopropanol (at a rate of 1°C/min) in -80°C freezers. For long term preservation, frozen cells were stored in liquid nitrogen. Subculturing of cryopreserved cells required quick thawing that was facilitated with 37°C water bath. The thawed cell lines were then mixed in pre-warmed complete medium and centrifuged at 800 rpm for 3 minutes to remove DMSO. The cells were then ready for subculture.

2.2.5 Trypan blue cell counting and seeding density

Upon trypsinization, single cell suspension was obtained from resuspension in complete medium with gentle pipetting. The cell suspension was mixed with equal volume of Trypan blue dye (1:1 ratio) and transferred to a hemocytometer. The viable cells (bright cells, as Trypan blue dye diffuses into dead cells) located at the 4 squares at the corner of the indicated area were counted. As each corner square has a dimension of $0.1mm^3$ (or $0.1\mu L$) (1mm x 1mm x 0.1mm), total cell count in the cell suspension was estimated with the following formula:

$$\text{Cells/mL} = [(\text{counts in 4 corner squares})/4] \times (\text{dilution factor}) \times 10^4$$

Cell lines were seeded in $10cm^2$ dish, 6-well plate, 24-well plate and 96-well plate depending on the nature of the experiment. Seeding density was determined by the growth rate and cell size of each cell line. For a rough estimate, 1×10^6 cells were seeded in $10cm^2$ dish; $1 - 1.5 \times 10^5$ cells for 6-well plate; $2 - 2.5 \times 10^4$ cells for 24-well plate; and $3 - 5 \times 10^3$ cells for 96-well plate.

2.2.6 Cell line authentication

All SCC cell lines were authenticated using *GenePrint*® 10 System according to manufacturer's protocol. The gDNA for the cells lines was extracted as described in Chapter 2.7.3.1. Briefly, 10ng of template DNA was diluted in nuclease-free water to a final volume of 15µL. 5µL each of Master Mix and Primer Pair Mix was added to each sample. A positive amplification control (2800M Control DNA) was added to the list of samples. Thermal cycling was performed on MyCycler PCR thermal cycle (Bio-Rad; CA, USA) according to the manufacturer's protocol for amplification of template DNA. The efficiency of the amplification was determined by agarose gel electrophoresis (Chapter 2.7.7). After PCR amplification, 1µL of each sample was mixed with Internal Lane Standard 600 in Hi-Di™ formamide and subjected to denaturation at 95°C for 3 minutes in a thermal cycler. The denatured samples were placed on ice immediately after heating. Detection of amplified fragments was carried out using the ABI PRISM® 3100 Genetic Analyser (Life Technologies; CA, USA) by Centre for Translational Research and Diagnostics (CTRAD; CSI, Singapore). Data for the *Gene Print*® 10 Panels were imported and analysed with GeneMapper® Software v4.0 (Life Technologies; CA, USA).

2.3 Transient gene silencing

2.3.1 Chemicals and reagents

Chemicals/Reagents	Supplier	Place of origin
JetPRIME buffer	Polyplus Transfection	Illkirch, France
JetPRIME reagent	Polyplus Transfection	Illkirch, France

Table 2.4: List of chemicals and reagents used in siRNA-mediated knockdown.

2.3.2 siRNA sequence

All small-interfering RNAs were obtained from Qiagen (Hilden, Germany).

siRNA	Sequence
Allstar Negative control	NA
MAP2K1I (MEK1)	5'-GUGAAUAAAUGCUUAAUAATT-3'
MAP2K2 (MEK2)	5'-GCAUUUGCAUGGAACACAUTT-3'
MAPK1 (Erk1)	5'-CGUCUAAUAUAUAAAUAUATT-3'
MAPK2 (Erk2)	5'-GUUCGAGUAGCUAUCAAGATT-3'
SOS1	5'-GGAGGUCCUAGGUUAUAAATT-3'
SOS2	5'-UCAUUAUCGUAGUACUCUATT-3'
TP53	5'-GGAAAUUUGCGUGUGGAGUTT-3'

Table 2.5: List siRNA sequences used in siRNA-mediated knockdown.

2.3.3 siRNA transfection

Respective cell lines were seeded at the optimized density in 6-well plate. Transfection was conducted when cells reached 30-50% confluency. Both target and scrambled siRNA (50nM for each siRNA) was diluted in 200µL JetPRIME buffer and mixed thoroughly by vortexing. 4µL of JetPRIME reagent was added to the siRNA mixture for each reaction well, mixed thoroughly by vortexing, and incubated for 15 minutes at room temperature. The siRNA-JetPRIME complexes were then added to the cells for gene delivery. The complexes were removed from the cells after 24 hours of siRNA delivery and fresh complete media were added to each well. Knockdown efficiency was determined 48 hours after transfection by Western blotting. In particular experiments, the transfected cells were re-plated for cell viability assay or Western blotting,

2.4 Stable gene silencing

2.4.1 Reagents and kits

Chemicals/Reagents/Kits	Supplier	Place of origin
FuGENE HD	Promega	WI, USA
MISSION® lentiviral packaging mix	Sigma Aldrich	MO, USA
OptiMEM	Invitrogen	CA,USA
HIV p24 Antigen ELISA kit	ZeptoMetrix Corporation	NY, USA
Polybrene	Sigma Aldrich	MO, USA
Puromycin	Sigma Aldrich	MO, USA

Table 2.6: List of chemicals and reagents used in lentiviral packaging and tranduction.

2.4.2 Plasmids and lentiviral strains

All vectors used in this study contained the pLKO.1-puro backbone. Luciferase shRNA plasmid was kindly provided by Prof Jean-Paul Thiery (Cancer Science Institute, Singapore). Lentiviral particles for transduction of GFP (pLKO.1-puro-CMV-TurboGFP; 2.7 X 10^7 TU/mL) and non-targeting shRNA (pLKO.1-puro-CMV-shNT; 2.7 x 10^7 TU/mL) were obtained from Sigma Aldrich (MO, USA). Two lentiviral strains transducing *TP53* shRNAs (sh55 and sh56) were kindly provided by Sir Prof David P. Lane and Dr Cheok Chit Fang (p53Lab, A*Star, Singapore). All viral work was conducted within the viral facilities provided by Cancer Science Institute of Singapore.

2.4.3 Lentiviral packaging

HEK293T cells were seeded at 1 x 10^6 cells in each $10cm^2$ dish and cultured over night in DMEM media. On day of transfection, the packaging cells should reach 70% confluency. Briefly, 18µl of Fugene HD was mixed in 582µL of serum-free OptiMEM media and incubated for 5 minutes at room temperature. 3µg of shRNA transfer vector and 30µL (3µg of plasmids) of Lentiviral Packaging Mix was then added to the diluted FuGENE HD solution (1µg DNA: 3µL FuGENE). The Lentiviral Packaging Mix contains 2 plasmids: one that encodes for viral packaging genes and one for viral envelope gene. The vector and transfection reagent were then mixed evenly by gentle vortexing, and allowed to incubate for 15 minutes at room temperature. The DNA-FuGENE complexes were then added dropwise to each dish of cells and incubated overnight at 37°C in tissue culture incubator. At 16 hours post-infection, media was removed from the transfected cells gently without disturbing the cells. 5µL of pre-warmed DMEM media was added to each dish. Cells were

incubated for an additional 24 hours at 37°C in tissue culture incubator. The medium supernatant, which contained virus, was removed gently and placed in sterile 15mL Falcon tube. Again, 5mL of pre-warmed DMEM media was added to each dish and incubated overnight at 37°C in tissue culture incubator. The collection procedure was repeated to collect a second set of supernatant. Both sets of viral-containing supernatant were filtered with 0.45μm filter, aliquoted into eppendorf tube, tightly sealed and kept at -80°C. Viral titer was determined by ZeptoMetrix HIV p24 Antigen ELISA kit according to manufacturer's protocol.

2.4.4 Determining the multiplicity of infection (MOI)

Infection efficiency of each cell line was first determined by lentiviral transduction with TurboGFP Control transduction particles, which contains a gene encoding for TurboGFP under the control of Cytomegalovirus (CMV) promoter. Briefly, 3 - 5 x 10^3 cells were seeded into each well in a 96-well plate and cultured overnight at 37°C in tissue culture incubator. Triplicate wells were needed for each lentiviral construct to be used. The next day, media were removed from each well, and each well was added with 50μL of transduction mixture containing a range of serial diluted TurboGFP viral particles and incubated overnight for 20 hours at 37°C in tissue culture incubator. The media containing the lentiviral particles were removed and 200μL of fresh pre-warmed complete media were added to each well. The cells reached 90 - 100% confluency 48 hours after viral transduction. The infection efficiency was estimated by observation of the GFP expressing cells or cell proliferation assay (described in Chapter 2.9.2) with puromycin treatment.

2.4.5 Transduction of target shRNA

Cells were seeded at 1 - 1.5 x 10^5 cells per well of 6-well plate and cultured overnight at 37°C in tissue culture incubator. On day of transduction, the packaging cell should reach 30% confluency. Briefly, each well was added with 1mL of transduction mixture diluted viral particles. The desired amount of viral particles was determined with the following formula:

(No. of cells/well) x (estimated MOI) = Amount of viral particles needed (TU)

The cells were incubated for 20 hours at 37°C in tissue culture incubator. The media containing the lentiviral particles were removed and 2mL of fresh pre-warmed complete media were added to each well for overnight incubation. A pool of cells containing both infected and non-infected populations was obtained.

2.4.6 Selection, maintenance and expansion of infected clones

Lethal doses of Puromycin to each cell line were determined prior to selection of infected clones. The infected cells should reach 80 - 100% confluency at 48 hours post-infection. The supernatants in each well were aspirated and replaced with 2mL of pre-warmed complete media with 5µg/mL (~100% cytotoxic dose for non-infected cells) of Puromycin and incubated overnight at 37°C in tissue culture incubator. The cells were selected 24 hours after antibiotic selection and were maintained under selection pressure until 100% confluency. The knockdown cells were expanded, validated with Real time polymerase chain reaction and Western blotting, and cryopreserved.

2.5 Overexpressing gene-of-interest

2.5.1 Chemicals and reagents

Chemicals/Reagents	Supplier	Place of origin
FuGENE HD	Promega	WI, USA
Neomycin (G418)	Sigma Aldrich	MO, USA
OptiMEM	Invitrogen	CA,USA

Table 2.7: Chemicals and reagents used in plasmid transfection and clonal selection.

2.5.2 Plasmids

Both p53 mutant wild-type overexpression plasmids were generated in this study using pcDNA3.1 vector with Geneticin resistant (*neo*) (Described in detail in Chapter 2.6), namely the pcDNA-*p53wt* and pcDNA-*p53R158G* plasmids. (The first letter of R158G represents the amino acid residues present in the wild-type molecule, while the last letter represents the modified amino acid in the mutated molecule. The number represents the position of the amino acid residue counting from the N terminus. This nomenclature will be used throughout this thesis.)

2.5.3 Plasmids transfection

Cells were seeded in 24 well plate and 6-well plate and cultured overnight at 37°C in complete media. On day of transfection, the cells should reach 30% confluency. Conditions of transfection complexes were listed in Table 2.8. Briefly, Fugene HD was mixed with serum-free OptiMEM media and incubated for 5 minutes at room temperature. Plasmids containing the gene-of-interest were added to the diluted FuGENE HD solution (1µg DNA:

3μL FuGENE), mixed evenly by gentle vortexing, and allowed to incubate for 15 minutes at room temperature. The DNA-FuGENE complex was then added dropwise to each well of cells and incubated overnight at 37°C in tissue culture incubator. At 16 hours post-infection, media was removed from the transfected cells gently. Pre-warmed fresh media were added to each well. Cells were ready for analysis 48 hours post-transfection.

	24-well plate	**6-well plate**
Medium (mL/well)	0.5	2
No. of cells/well	2.5×10^4	1×10^6
OptiMEM (mL/well)	0.1	0.5
FuGENE HD (μL/well)	0.75	3
DNA construct (μL/well)	0.25	1

Table 2.8: Preparation of master mix for plasmid transfection in 24- and 6-well plates.

2.5.4 Selection of transformants

Lethal doses of neomycin (G418) to each cell line were determined prior to selection of stable clones. The transfected cells should reach 80 - 100% confluency at 48 hours post-infection. The cells were trypsinized, resuspended in complete media and re-plated in $10cm^2$ dish. Neomycin at 250μg/mL (~100% cytotoxic for non-infected cells) was added to each dish and cell lines were culture at at 37°C in tissue culture incubator. Culture supernatants were replaced with fresh media containing neomycin every 3 days until 100% confluency. The selected clones were expanded, validated with Western blotting, and cryopreserved.

2.5.5 Generation of single cell colony

The validated cells with overexpression of target proteins were serial diluted with complete media and neomycin (250μg/mL) to 10 cells/mL. 100μL of cells were seeded into each well of 96-well plate and culture at at 37°C in tissue culture incubator. Formation of single cell colonies was monitored over time. Culture supernatants in each well were replaced with fresh media containing neomycin every 3 days until obvious colonies were observed. The colonies were trypsinized, resuspended and re-plated in 24 well plates, followed by 6 well plates and 10 cm2 dishes. The overexpressing clones were validated with Real time polymerase chain reaction and Western blotting. Validated clones were expanded and cryopreserved.

2.6 Molecular cloning

2.6.1 Chemical, reagents and kits

Chemicals/Reagents/Kits	Supplier	Place of origin
Ampicillin	Sigma Aldrich	MO, USA
Luria-Bertani (LB) agar	CSI	Singapore
Luria-Bertani (LB) broth	CSI	Singapore
OneShot® TOP10 competent cells	Life Technologies	CA, USA
QIAquick Plasmid Midi Preps kit	Qiagen	Hilden, Germany
S.O.C medium	Life Technologies	CA, USA

Table 2.9: List of chemicals and reagents used in DNA cloning.

2.6.2 Competent cells and plasmids

One Shot® TOP10 *E. coli* competent cells that allowed for high-efficiency cloning of high-copy number plasmids were obtained from Invitrogen (CA, USA). The backbone plasmid, pcDNA3.1 vector, was kindly provided by Dr John Low and Dr Hsieh Wen-Son.

2.6.3 Primer design

Primers were designed to include the length of the coding region of the gene-of-interest, *TP53*, by beginning at the start codon (ATG) and ending at the stop codon (TGA). A sequence encoding for hemagglutinin (HA)-tag was included at the 5'-end right next to the start codon. A Kozak consensus sequence (GCCGCCCC) was included to facilitate the initiation of translation (Kozak 1987). A HindIII restriction site was added to the 5' end and an EcoRI restriction site was added to the 3' end. The primer designs are listed below:

5' Primer: (5'→3'):

CCAAGCTTGCCGCCACCATGTACCCATACGATGTTCCAGATTACGCTATGGAGGAGCCGCAGTCAGATCCTA

HindIII Kozak HA Tag *TP53* Specific

3' Primer: (5'→3'):

CCGAATTCTCAGTCTGAGTCAGGCCCTTCTGTC

EcoRI *TP53* Specific

2.6.4 Cloning of pcDNA-*TP53R158G* and pcDNA-*TP53wt* plasmids

The primers mentioned in Chapter 2.6.3 were specifically designed for amplification of the open-reading frame (ORF) of *TP53* gene, and was flanked with two restriction digestion sites with a HA-tag sequence at the 5' primer. The mutant (R158G) and wild-type sequences were cloned from H2170 and MRC5 cells respectively by polymerase chain reaction (PCR) using the cDNA extracted from these two cell lines. Restriction digestion was performed on pcDNA3.1 empty vector (EV) and the amplified inserts to expose the ligation site. Both digested vectors and inserts were purified from gel electrophoresis as described in Chapter 2.7.7, and ligated to form expression vectors as described in 2.7.6.

2.6.5 Transformation of chemically competent cells

Chemically competent One Shot® TOP10 cells were transformed based on the manufacturer's protocol with slight modifications. Briefly, One Shot competent cells were thawed on ice (one vial of One Shot® cells was used for each transformation). Immediately upon thawing, all the ligation mix from Chapter 2.6.4 was added into the competent cells, mixed by gentle tapping and incubated on ice for 30 minutes. Subsequently, the competent cells were heat-shocked in a 37°C water bath for 45 seconds without shaking. Immediately after heat-shock, removed the cells from the water bath and placed on ice for 2 minutes. 250µL of pre-warmed S.O.C. medium was added into each vial of competent cells. Competent cells were allowed to recover at 37°C for 2 hours with shaking at 200 rpm in Thermo Twister Orbital Shaker (Quantifoil Instruments; Jena, Germany). During this incubation, the selection plates (10mL of LB agar in each petri dish, supplemented with 100µg/mL ampicillin) were warmed in 37°C incubator. The transformed competent cells (300µL) were streaked on two individual selection plates with different volumes to increase chances of obtaining single colonies (100 and 200µL). The plates were allowed to dry and incubated at 37°C overnight in an inverted position.

2.6.6 Expansion of *E. coli* culture

20 hours after transformation, successfully transformed cells formed colonies on selection plates. Well-spaced single colonies were picked and placed into 2mL of starter culture (LB broth supplemented with 100µg/mL ampicillin). The selected colonies were grown in starter culture for 16 hours at 37°C with shaking at 200 rpm. The competent cells were collected after 16 hours, and further expanded in 50mL of selective LB broth at 37°C with shaking at 200 rpm.

2.6.7 Plasmid extraction

Plasmid DNA was extracted and purified from the expanded *E. coli* culture in Chapter 2.6.6 using the QIAquick Plasmid Midi Preps kit according to manufacturer's protocol. Briefly, the competent cells were harvest by centrifugation at 6000 g for 15 minutes at 4°C. The bacteria pellet was resuspended in Buffer P1 and incubated with same volume of Buffer P2 at room temperature for 5 minutes. Next, same volume of pre-chilled Buffer P3 was added and the suspension was mixed thoroughly before incubation at 4°C for 15 minutes. The mixed suspension was then centrifuged at 20,000 g at 4°C for 30 minutes. The supernatant was collected and again centrifuged at 20,000 g at 4°C for 15 minutes to clear all bacteria debris. The supernatant (containing the plasmid DNA) was allowed to pass through the QIAGEN-tip 100 that has been equilibrated with Buffer QBT by gravity flow. The plasmid DNA was captured by the resin in the QIAGEN-tip, and the resin was washed twice with Buffer QC by gravity flow. The plasmid was eluted with Buffer QF and precipitated by addition of isopropanol (at 0.7 x volume of the eluted DNA). The plasmid DNA was pelleted at 15,000 g at 4°C for 30 minutes. The supernatant was decanted carefully and the pellet was washed at room temperature with 70% ethanol. The DNA pellet was pelleted again by centrifugation at 15,000 g at 4°C for 10 minutes. Ethanol was removed completely and the pellet was air-dried for 10 minutes at room temperature. Plasmid DNA was dissolved in TE buffer (10mM Tris-Cl, 1mM EDTA, pH 7.5). Concentration and purity of the purified plasmid were determined by NanoDrop as described in 2.7.3.3. Integrity of the extracted plasmid was determined by DNA sequencing as described in Chapter 2.7.10.

2.7 Molecular biology

2.7.1 Chemical, reagents and kits

Chemicals/Reagents/Kits	Supplier	Place of origin
100bp DNA ladder	Thermo Fisher	MA, USA
10x PCR Buffer II	Life Technologies	CA, USA
1kb DNA ladder	Thermo Fisher	MA, USA
Agarose powder	Bio-Rad	CA,USA
Applause™ WT-Amp ST RNA Amplification System	NuGEN Technologies	CA, USA
Blue/Orange 6x loading dye	Thermo Fisher	MA, USA
DNase I kit	Qiagen	Hilden, Germany
dNTPs (2.5mM each of dATP, dGTP, dCTP, dTTP)	Life Technologies	CA, USA
EcoRI Rescticion Enzyme	New England Biolabs	MA, USA
Ethidium bromide (EtBr)	Bio-Rad	CA,USA
GoTaq® DNA polymerase	Promega	WI, USA
HindIII Restriction Enzyme	New England Biolabs	MA, USA
Human GeneChip Gene 1.0ST array	Affymetrix	CA, USA
$MgCl_2$	Life Technologies	CA, USA
MiniElute Reaction Cleanup Kit	Qiagen	Hilden, Germany
NEB Buffer II	New England Biolabs	MA, USA
QIAquick Gel Extraction kit	Qiagen	Hilden, Germany
QIAquick PCR Purifiction kit	Qiagen	Hilden, Germany
QIAshredder homogenizer	Qiagen	Hilden, Germany
Random Hexamer primer	Life Technologies	CA, USA
Reverse transcriptase MuLV	Life Technologies	CA, USA
RNase Inhibitor	Life Technologies	CA, USA
RNeasy Mini kit	Qiagen	Hilden, Germany
Takara DNA Ligation kit	Takara Bio Inc.	Shiga, Japan
Wizard® SV Genomic DNA Purification System	Promega	WI, USA

Table 2.10: List of chemicals and reagents used in RT-PCR, qPCR, agarose gel electrophoresis, purification and extraction of PCR product.

2.7.2 List of primers and probes

Target gene	Sequence (5'→3')	Annealing temperature (°C)	No. of cycles
GAPDH	Forward: ATCTCTGCCCCCTCTGCTGA	64	25
	Reverse: GATGACCTTGCCCACAGCCT		
TP53 ORF	Forward: AGTCTAGAGCCACCGTCCA	60	35
	Reverse: TCTGACGCACACCTATTGCAAGC		
TP53-HA	Forward: CCAAGCTTGCCGCCACCATGTACC CATACGATGTTCCAGATTACGCTA TGGAGGAGCCGCAGTCAGATCCTA	61	35
	Reverse: CCGAATTCTCAGTCTGAGTCAGGC CCTTCTGTC		

Table 2.11: List of primers used in RT-PCR. The annealing temperature and cycle number used for each primer pair were shown.

Target gene	Taqman Gene Expression Array ID
BAD	Hs00188930_m1
BAK1	Hs00832876_g1
BAX	Hs00180269_m1
Bcl-2	Hs99999018_m1
BIM	Hs00197982_m1
CDKN1A	Hs00355782_m1
DRAM1	Hs00218049_m1
FAS	Hs00531110_m1
GAPDH	Hs02758991_g1
GPX2	Hs01591589_m1
MDM2	Hs00234753_m1
MGST1	Hs00220393_m1
NOXA	Hs00560402_m1
PARP14	Hs00393814_m1
PARP9	Hs00967084_m1
PUMA	Hs00248075_m1
TP53	Hs01034249_m1
TP73	Hs01056230_m1
XAF1	Hs00213882_m1

Table 2.12: List of Taqman probes used in real time qPCR.

2.7.3 Extraction of nucleic acid

2.7.3.1 Genomic DNA extraction

Extraction of genomic DNA (gDNA) from mammalian cell lines was conducted using Wizard® SV Genomic DNA Purification System according to manufacturer's protocol. Briefly, a maximum of 5 x 10^6 cells was disrupted in Wizard® SV Lysis Buffer. The suspensions containing the lysed cells were transferred to individual Wizard® SV Minicolumn Assembly and centrifuged at 14,000 rpm for 3 minutes until all liquid flowed through. Discard the liquid in the collection tube and washed the column 4 x 650µL with Column Wash Solution (diluted with 95% ethanol). After washing, the collection tubes were emptied and the columns were centrifuged at 14,000 rpm for another 2 minutes to dry the binding matrix. 250µL of nuclease-free water was added to each column and allowed to incubate at room temperature for 2 minutes. The columns were centrifuged at 14,000 rpm for 1 minute in clean eppendorf tubes to elute the DNA. The extracted gDNAs were stored at -80°C. Concentration and purity of the purified RNAs were determined by NanoDrop as described in Chapter 2.7.3.3.

2.7.3.2 RNA extraction

Extraction of total RNA from mammalian cell lines was conducted using RNeasy® Mini kit according to manufacturer's protocol. Briefly, a maximum of 1 x 10^7 cells was disrupted in lysis buffer RLT (containing 1% β-ME) by homogenization using needle and syringe or QIAshredder homogenizer. Equal volume of 70% ethanol was added to the homogenized lysate, mixed well and transferred to RNeasy Mini Spin columns for binding of RNA to the RNeasy membrane through centrifugation at full speed. The membrane of each column was washed once with RW1 buffer, treated with DNase I for 30 minutes for removal of DNA, and washed twice with buffer RPE. Purified RNA was eluted with 30 - 50µL of nuclease-free water. Concentration and purity of the purified RNAs were determined by NanoDrop as described in Chapter 2.7.3.3.

2.7.3.3 Nanodrop quantification

The concentration of total DNA and RNA were quantified by the NanoDrop™ Spectrophotometer (Thermo Scientific). The absorbance range was from 220nm to 750nm. To begin with, 1.5µL of total RNA/DNA was aspirated and placed onto the measurement pedestal. Ratios of absorbance measured at 260nm and 280nm (A260/280) were determined to assess purity of RNA/DNA. RNA with A260/A280 ratio within 1.8 to 2 is considered as

satisfactory quality; whereas DNA with A260/A280 ratio above 2 is considered as satisfactory quality. The concentrations (ng/µL) of DNA/RNA were estimated.

2.7.4 Reverse-transcription polymerase chain reaction (RT-PCR)

2.7.4.1 Reverse transcription

Total RNA extracted was reverse transcribed to complementary DNA (cDNA) strands by RT-PCR. For each RNA sample, 1µg of RNA was diluted to a final volume of 3µL with nuclease-free water. Diluted RNA was denatured at 90°C for 5 minutes to expose the secondary and tertiary structures for proper binding of reverse transcriptase. Heated RNA was cooled on ice immediately. 17µL of RT master mix (Table 2.13) was added to each sample (total reaction volume per 1µg RNA = 20µL). Reverse transcriptase was activated at 23°C for 10 minutes, cDNA synthesis was performed at 42°C for 1 hour, and reverse transcriptase was inactivated at 99°C for 5 minutes. The synthesized cDNA was stored at -20°C.

Reagents	Volume for 1 reaction
RNA + nuclease-free water (µL)	3
dNTPs (µL)	8
10x PCR Buffer II (µL)	2
$MgCl^2$ (µL)	4
Random Hexamer primer (µL)	1
RNase Inhibitor (20U/µL) (µL)	1
Reverse transcriptase MuLV (50U/µL) (µL)	1
Total volume (µL)	20

Table 2.13: Preparation of master mix for reverse transcription.

2.7.4.2 Polymerase chain reaction (PCR)

All PCR reactions in this study were carried out with GoTaq® DNA polymerase and respective primers (Table 2.11) unless specified otherwise. PCR was performed using MyCycler PCR thermal cycle (Bio-Rad; CA, USA). In most cases, 50µL reaction mix [100ng cDNA template, 1.5nM $MgCl_2$, 0.2mM each of dNTPs (dATP, dGTP, dCTP, dTTP), 1.25 unit of GoTaq® polymerase, 0.6µM of each primers, and 1 x reaction buffer] was prepared for each PCR amplification. The setup configuration for PCR: initial denaturation step of 95°C for 10 minutes; followed by 25 - 35 cycles of DNA denaturation at 94°C for 30 sec, primer annealing at indicated temperature for 30 sec, and DNA elongation at 72°C for

30 sec – 2 minutes (depending on size of PCR product, approximately 1 min/kb); and ended with DNA extension step at 72°C for 10 minutes. The PCR products could then be stored at 4°C. The efficacy of the PCR was determined by agarose gel electrophoresis as described in 2.7.7.1. In cases whereby the PCR products were subjected to DNA sequencing or cloning, PCR purification was performed using QIAquick PCR Purification kit according to manufacturer's protocol. Concentration and purity of the purified PCR were determined by NanoDrop as described in Chapter 2.7.3.3.

2.7.5 Restriction enzyme (RE) digestion and DNA ligation

DNA digestion was performed with appropriate REs in their corresponding buffers according to the manufacturer's protocol. As both HindIII and EcoRI REs share the same working buffer (NEB Buffer II), the one-step digestion was performed. The PCR products and pcDNA3.1 vector were subjected to restriction digestion by incubating the DNA-enzyme mixtures at 37°C in a heat block for 2 hours. The restriction profile was analysed by DNA gel electrophoresis (Chapter 2.7.7.1). The bands indicating the linearized vectors and the digested inserts were excised and purified by gel extraction (Chapter 2.7.7.2). After purification, the open-end pcDNA3.1 vectors and inserts were mixed with Takara DNA ligase master mix for 15 minutes at room temperature. Ligation was completed at the end of incubation.

2.7.6 Agarose gel electrophoresis

2.7.6.1 Gel migration

Agarose gel electrophoresis was performed to analyse PCR product/digested DNA/ligated DNA. In most cases, 1 - 2% (w/v) agarose gel was prepared in 100mL of TAE buffer (40mM Tris, 20mM acetate acid, 1mM EDTA, pH7.8) and stained with EtBr at 1: 50 dilution. The product-of-interest was aliquoted and mixed with blue/orange 6x loading dye to a maximum volume of 25µL per well. 6µL of 1kb or 100bp DNA ladder was used as indicator for estimation of band sizes. Electrophoresis was carried out by gel migration in 1 x TAE buffer at 100 V for 30 minutes. DNA bands were visualized under a ultra-violet (UV) transilluminator Gel-Doc System (Bio-Rad; CA, USA)

.

2.7.6.2 Gel extraction

After gel electrophoresis, DNA fragments of interest (for DNA sequencing or DNA ligation) were excised carefully from agarose gel using clean scalpels. Low UV light (366nm) was used to facilitate the visualization of DNA fragments. High UV wavelength and prolonged exposure to UV were avoided to prevent fragmentation of the desired DNA. The excised agarose gels were subjected to DNA extraction using the QIAquick Gel Extraction kit as described in the manufacturer's protocol. Briefly, the excised gel was mixed with 3 volumes of Buffer QX1 and incubated at 50°C until the gel was completely dissolved. Next, 1 gel volume of isopropanol was added to the sample, mixed by inverting the tube, and all sample was loaded to the QIAquick spin column. The DNA fragment was bound to the resin by centrifugation at 14,000 rpm for 1 minute. The flow-through was discarded from the collection tube, and the resin was washed once each with Buffer QX1and Buffer PE. The resin was cleared by centrifugation at 14,000 rpm for 1 minute. The purified DNA was eluted with 20 - 30μL of Elution Buffer.

2.7.7 Real-time quantitative polymerase chain reaction (qPCR)

2.7.7.1 qPCR setup

Real time qPCR was conducted by using the Taqman® Gene Expression Assay System (Applied Biosystem; CA, USA). 10ng of cDNA template was used per reaction. qPCR reaction mix was prepared as shown in Table 2.14. 11μL of reaction mix and 9μL of diluted cDNA template were added into each of the assigned wells in the MicroAmp® Optical 96-well Reaction Plate (Applied Biosystem; CA, USA). Each reaction was performed in triplicates. Nuclease-free water was added instead of the cDNA template as no-template control. Passive reference ROX dye present in the Taqman® master mix serves as an internal fluorescence reference by which the reporter dye signal was normalized against during data analysis. Real-time qPCR was performed using ABI Prism 7500 Real time PCR System (Applied Biosystem; CA, USA). The amplification begins with an initial denaturation step at 95°C for 10 minutes, followed by PCR cycling for 40 cycles comprising of DNA denaturation at 94°C for 15 sec and primer annealing at 60°C for 1 minute, and a final template extension step at 60°C for 10 minutes.

Reagents	Volume for 1 reaction	
cDNA template (µL)	0.2	Sample mix
Nuclease free water (µL)	8.8	
2 x Tagman® Universal PCR master mix (µL)	10	Reaction mix
20 x primer mix (µL)	1	
Total volume (µL)	20	

Table 2.14: Preparation of master mix for real time qPCR.

2.7.7.2 Configuration of qPCR data analysis

The real time qPCR data on gene expression quantification was exported from the Applied Biosystem Standard 7500 software and was interpreted as relative quantification (RQ). The amplification was expressed as fluorescence intensity that was depicted by the amplification curve generated by the system. Baseline value was set at initial cycle where amplification of signal was first detected. The threshold cycle (Ct) values for each sample on respective target gene were determined as the point of intersection between the amplified curve and the indicated threshold. The average Ct values for the triplicates were normalized against the endogenous reference gene (*GAPDH*), which was represented by δCt. The δCt values from each sample were compared against a calibrator, usually the control group, to obtain δδCt values. The RQ values for the changes in gene expression were calculated based on the δδCt values. The formula for the above mentioned calculation was shown:

$$\delta Ct_{sample} = Ct_{sample} - Ct_{GAPDH}$$

$$\delta\delta Ct = \delta Ct_{target} - \delta Ct_{calibrator}$$

$$RQ = 2^{-\delta\delta Ct}$$

2.7.8 Gene expression profiling by Microaary

2.7.8.1 Microarray

Cells were seeded in 10cm^2 dishes and cultured overnight at 37°C in a tissue culture incubator. Drug treatment was performed the subsequent day. Cells were harvested for total RNA purification after 8 hours drug treatment with RNeasy Mini Kit as described in Chapter 2.7.3.2. The RNA purity was checked with NanoDrop (Chapter 2.7.3.3) while the RNA integrity was determined with the RNA 6000 Nano LabChip Bioanalyser (Agilent; CA, USA). The RNA Integrity Number (RIN) for each sample was ensured to be above 9.2 (Good quality). The RNAs that passed quality control tests were subjected to reverse transcription and amplification using Applause^{TM} WT-Amp ST RNA Amplification System according to manufacturer's protocol. 150ng of RNA was required for each sample in duplicates. As an overview, first strand cDNA was generated based on the RNA, which was followed by generation of DNA/RNA heteroduplex double-strand cDNA, SPIA amplification, and post-amplification modification. SPIA amplication is a linear isothermal DNA amplification procedure developed by NuGEN that generates multiple single strands cDNA. The post-SPIA modification allows for annealing of random priers onto the single strand cDNA and extension of second strand cDNA. The amplified cDNAs were purified using Qiagen's MiniElute Reaction Cleanup Kit according to manufacturer's protocol. Briefly, each cDNA sample was mixed well with 300µL of ERC buffer and bound to MiniElute spin column by centrifugation for 1 minute at 14,000 rpm. The columns were washed once with Buffer PE, centrifuged at full speed to remove residual buffer, and eluted with 15µL of nuclease-free water with centrifugation for 1 minute at 14,000 rpm. Yield and purity of each cDNA sample were determined with Nanodrop (Chapter 2.7.3.3). Each sample was then labelled with biotin in preparation for hybridization on microarray GeneChip according to WT-Amp ST Targeting Labeling Protocol. Briefly, 2.5µg of purified SPIA cDNA was diluted in nuclease-free water, fragmented with the provided Fragmentation enzymes and labelled with Encore Biotin Module. The purified and labelled cDNAs were then processed and hybridized onto Human GeneChip Gene 1.0ST array for gene expression profiling. In brief, each cDNA sample was mixed at room temperature with the hybridization cocktail. The mixture was denatured at 99°C for 2 minutes and heated for 45°C in a heat block for 5 minutes. Prior to loading, all samples were centrifuged at 14,000 rpm speed for 1 minute. 90µL of each hybridization mixture was loaded into single array chip and hybridized for 18 hours at 60 rpm in a GeneChip Hybridization Oven 640 (Affymetrix; CA, USA). The arrays were washed using GeneChip Fluidics station 450 (Affymetrix; CA, USA) using fluidic protocol FS450_0001 and scanned using GeneChip Scanner 3000 7G (Affymetrix; CA, USA) according to manufacturer's instructions.

2.7.8.2 Transcriptomic analysis

Thirty-two microarray data, including duplicates for both treated and untreated samples, were obtained in .CEL format. The CEL files were imported into GeneSpring Software V12 (Agilent; CA, USA) for data normalization and identification of differentially expressed mRNAs of interest. The gene sets with absolute fold change > 1.5 across the comparison groups were denoted as commonly altered genes (Appendix 1 and 2). Pathway analysis was conducted with the publicly available Database for Annotation, Visualisation and Integrated Discovery (DAVID) Bioinformatics Resources 6.7 Software (Huang, Sherman et al. 2009) and mapped to the Kyoto Encyclopedia of Genes and Genomes (KEGG) database for pathway analysis.

2.7.9 DNA sequencing

Purified plasmids or PCR products were sent to Integrated DNA Technologies (IDT; Singapore) for Sanger sequencing with the indicated primers. The FASTA file was analysed for nucleotide changes. The obtained sequence was aligned and search in the human genome database by using NCBI BLAST program (http://blast.ncbi.nlm.nih.gov/).

2.8 Protein expression analysis

2.8.1 Chemicals reagents and kits

Chemicals/Reagents/Kits	Supplier	Place of origin
30% Acrylamide-Bis Solution	Bio-Rad	CA, USA
Amersham ECL Prime Chemiluminescent reagent	GE Healthcare	Little Chalfont, UK
Ammonium Persulfate (APS)	Bio-Rad	CA, USA
Bicinchoninic Acid (BCA) Protein Assay kit	Pierce Biotech	IL, USA
Blocking-grade Skim milk powder	Bio-Rad	CA, USA
Bromophenol blue	Bio-Rad	CA, USA
Cell Lytic™ Buffer	Sigma Aldrich	MO, USA
Glycerol	Sigma Aldrich	MO, USA
Nuclear extraction kit	Active Motif	CA, USA
PhosSTOP phosphatase inhibitor cocktail	Roche	Penzberg, Germany
Pre-stained protein ladder	Thermo Fisher	MA, USA
Protease inhibitor cocktail	Roche	Penzberg, Germany
Proteome Profiler MAPK-array	R&D System	MN, USA
PVDF Membrane	Bio-Rad	CA, USA
Tetramethylethylenediamine (TEMED)	Bio-Rad	CA, USA
Tween-20	Sigma Aldrich	MO, USA
Western blot stripping buffer	Thermo Fisher	MA, USA
X-Ray film	AGFA Healthcare	Mortsel, Belgium

Table 2.15: List of chemicals, reagents and kits for protein studies.

2.8.2 Antibodies for Western blotting

Antibody Target		Supplier	Dilution
Acetyl-CBP (Lys1535)/p300	Rabbit	Cell Signalling	1:2000
Acetyl-Histone H3 (Lys23)	Rabbit	Cell Signalling	1:10000
Acetyl-Histone H3 (Lys9/Lys14)	Rabbit	Cell Signalling	1:10000
Acetyl-Histone H4	Rabbit	Millipore	1:10000
Acetyl-p53 (Lys379)	Rabbit	Cell Signalling	1:1000
acetyl-p53 (Lys382)	Rabbit	Cell Signalling	1:2000
BAD	Rabbit	Cell Signalling	1:2000
BAK	Rabbit	Cell Signalling	1:2000
BAX	Rabbit	Cell Signalling	1:5000
Bcl-2	Rabbit	Cell Signalling	1:2000
Bcl-w	Rabbit	Cell Signalling	1:2000
Bcl-xl	Rabbit	Cell Signalling	1:2000
Bid	Rabbit	Cell Signalling	1:2000
Bim	Rabbit	Cell Signalling	1:2000
Caspase-3	Rabbit	Cell Signalling	1:1000
Caspase-4	Rabbit	Cell Signalling	1:2000
Caspase-7	Rabbit	Cell Signalling	1:2000

Caspase-8	Mouse	Cell Signalling	1:2000
Caspase-9	Rabbit	Cell Signalling	1:2000
EGFR	Rabbit	Cell Signalling	1:2000
HA-tag	Rabbit	Cell Signalling	1:2000
HDAC1	Mouse	Cell Signalling	1:2000
HDAC2	Mouse	Cell Signalling	1:2000
HDAC3	Mouse	Cell Signalling	1:2000
HDAC4 (D15C3)	Rabbit	Cell Signalling	1:2000
HDAC6 (D2E5)	Rabbit	Cell Signalling	1:2000
HRP-conjugated β-actin	-	Cell Signalling	1:5000
p21 Waf/Cip 1	Rabbit	Cell Signalling	1:2000
PARP	Rabbit	Cell Signalling	1:2000
Phospho-B-Raf (Ser445)	Rabbit	Cell Signalling	1:2000
Phospho-Erk 1/2 (T202/Y204)	Rabbit	Cell Signalling	1:2000
Phospho-HDAC3 (Ser424)	Rabbit	Cell Signalling	1:2000
Phospho-MDM2 (Ser166)	Rabbit	Cell Signalling	1:2000
Phospho-MEK1/2 (Ser217/221)	Rabbit	Cell Signalling	1:2000
Phospho-MSK1 (Ser360)	Rabbit	Cell Signalling	1:2000
Phospho-p38 (T180/Y182)	Rabbit	Cell Signalling	1:2000
Phospho-p53 (ser15)	Mouse	Cell Signalling	1:2000
Phospho-Sirt1 (Ser27)	Rabbit	Cell Signalling	1:2000
PUMA	Rabbit	Cell Signalling	1:2000
SOS1	Rabbit	Cell Signalling	1:1000
SOS2	Rabbit	abcam	1:1000
Survivin	Rabbit	Cell Signalling	1:2000
TATA box binding protein (TBP)	Mouse	Abcam	1:3000
Total Erk	Rabbit	Cell Signalling	1:5000
Total H4	Rabbit	Cell Signalling	1:5000
Total Histone H3	Rabbit	Cell Signalling	1:10000
Total MEK1/2	Rabbit	Cell Signalling	1:1000
Total MSK1	Rabbit	Cell Signalling	1:1000
Total p38	Rabbit	Cell Signalling	1:2000
Total p53	Rabbit	Cell Signalling	1:2000
Total p53	Mouse	Santa Cruz	1:5000
Total Sirt1	Rabbit	Cell Signalling	1:2000
XIAP	Rabbit	Cell Signalling	1:2000
α-tubulin	Mouse	Santa Cruz	1:5000
HRP-conjugated Anti-Mouse IgG	Secondary	Cell Signalling	1:2000
HRP-conjugated Anti-Rabbit IgG	Secondary	Cell Signalling	1:2000

Table 2.16: List of antibodies used for Western blotting.

2.8.3 Total protein extraction

For preparation of protein lysates, all cells (from treated/untreated groups) were collected. The culture supernatant from each treatment group was aspirated and placed in collection tubes. The attached cells were washed once with 1 x PBS (PBS was collected as well), trypsinized from their respective culture plates and placed in the same collection tubes as their culture supernatant. Cells were centrifuged at 1000 rpm for 5 minutes at room temperature. The obtained pellets were rinsed once with ice-cold 1 x PBS and pelleted again by centrifugation at 1000 rpm for 5 minutes at room temperature. The supernatant was removed, and appropriate amount (dependent on the size of the pellet) of lysis buffer [Cell Lytic™ Buffer (50mM NaCl, 0.41% bicine, 2% EDTA) supplemented with complete protease inhibitor cocktail and PhosSTOP phosphatase inhibitor cocktail] was added. Cell lysis was completed with sonication on ice at 5W for 10 sec twice. Lysates were then centrifuged for 20 minutes at 14,000 rpm to remove cell debris. Protein concentration was determined by BCA protein assay as described in Chapter 2.8.5. The supernatants were collected and aliquoted for storage at -80°C.

2.8.4 Nuclear and cytosolic extraction

Separation of cuclear and cytosolic fractions was perfoemd using Active Motif Nuclear Extraction kit according to the manufacturer's protocol with minor modifications. All cells were collected as described in Chapter 2.8.3. Cells were centrifuged at 1000 rpm for 5 minutes at room temperature. The obtained pellets were rinsed once with ice-cold PBS/phosphatase inhibitor mix provided by manufacturer and centrifuged at 1000 rpm for 5 minutes at room temperature. The cell pellets were then resuspended in 1 x Hypotonic Buffer and incubated on ice for 10 minutes. Next, detergent was added to each sample and the suspension was vortexed for 10 seconds. The cell suspensions were then centrifuged at 14,000 rpm for 30 seconds at 4°C. After this step, the nuclei were pelleted while the supernatants (cytoplasmic fractions) were collected. The cell pellets (nuclear fractions) were resuspended in Complete Lysis Buffer, vortexed for 10 sec at maximum speed, and incubated on ice for 30 minutes on a rocking platform at 150 rpm. After incubation, the cell suspensions were vortexed for 30 sec at maximum speed and centrifuged at 14,000 rpm for 10 minutes at 4°C. The supernatants (nuclear fractions) were collected. Both nuclear and cytoplasmic fractions were sonicated on ice at 5W for 10 seconds twice. Protein concentration was determined by BCA protein assay as described in Chapter 2.8.5. The supernatants were aliquoted for storage at -80°C.

2.8.5 Quantification and preparation of protein lysates

BCA protein assay was performed to determine the concentration of the obtained protein lysates according to manufacturer's protocol. 5µL of each sample was used for quantification. A range of BSA concentration (2mg/mL, 1.5mg/mL, 1mg/mL, 0.75mg/mL, 0.5mg/mL, 0.25mg/mL and 0.125mg/mL) was used as reference standards. All samples and standards were placed in 96-well plates. 200µL of BCA working reagent (1: 50 dilution for buffer A: buffer B) was added to each sample and standard. The mixture was incubated at 37°C for 30 minutes and absorbance was measured at 562nm with Infinite200 Pro 96-well plate reader (Tecan; Switzerland). Preparation of samples for SDS-PAGE Western blotting was completed by heat denaturation and β-ME reduction. The quantified lysates were mixed with SDS loading buffer [final concentration: 62.5mM Tris-HCl (pH7.4), 10% glycerol, 2.5% SDS, 0.01% bromophenol blue, 5% β-ME]. Lysates were then denatured at 95°C for 5 minutes. The samples were stored at -20°C.

2.8.6 Sodium dodecyl sulphate-Polyacrylamide gel electrophoresis (SDS-PAGE)

The prepared protein lysates in Chapter 2.8.7 were resolved in acrylamide gels using the SDS-PAGE Mini-Protein II system (Bio-Rad; CA, USA). Acrylamide gels were casted in two layers (stacking and resolving layers) at various percentage of acrylamide (Table 2.17) for separation of various protein sizes. The gels were assembled into the Mini-Protein II gel tank. The tank was filled up with SDS-PAGE running buffer (25mM Tris, 192mM glycine, 0.1% SDS). Protein samples and pre-stained protein ladder were then loaded into respective wells. Gel electrophoresis was conducted at a constant voltage of 80V (for the first 20 minutes while proteins were at stacking gel) and subsequently increased to 100V for protein separation in resolving gel for approximately 2 hours.

	Resolving Gel (%)					**Stacking Gel (%)**
Component	**6%**	**8%**	**10%**	**12%**	**15%**	**5%**
Water (mL)	5.3	4.65	4	3.3	2.3	5.7
30% Acrylamide/Bis (mL)	2	2.65	3.3	4	5	1.7
1.5 M Tris-HCl, pH 8.8 (mL)	2.5	2.5	2.5	2.5	2.5	-
0.5 M Tris-HCl, pH 6.8 (mL)	-	-	-	-	-	2.5
10% SDS (µL)	100	100	100	100	100	100
10% APS (µL)	100	100	100	100	100	50
TEMED (µL)	8	6	4	4	4	10
Total volume (mL)	10	10	10	10	10	10

Table 2.17: Preparation of stacking and resolving gels for SDS-PAGE.

2.8.7 Western blotting

After SDS-PAGE, the resolved proteins were transferred onto methanol-activated 6cm x 8cm PVDF membrane using Bio-Rad wet transfer system. The resolved gels were assembled with the PVDF membrane and filter papers. Prior to eletro-transfer, the gels, PVDF membranes and filter papers were pre-wet with Towbin transfer buffer [25mM Tris, 192mM glycine, 20% (v/v) methanol) for 15 minutes. Wet transfer was performed at 80V for 2 hours. After completion of electro-transfer, the PVDF membranes were blocked with 5% skim milk diluted in 1 x PBS/TBS with 0.1% Tween-20 (PBS-T/TBS-T) at room temperature for 1 hour. Primary antibodies (Table 2.16) were then probed on the PVDF membrane for 1 hour at room temperature or overnight at 4°C depending on the optimal incubation time for individual antibodies. Tris-buffered saline (TBS) (50mM Tris-Cl, 150mM NaCl, pH7.4) was used when probing for protein targets containing phosphate group. After primary antibody incubation, membranes were washed 5 x 10 minutes with PBS-T/TBS-T and probed with secondary antibodies (Table 2.16) in 5% milk/PBS-T/TBS-T for 1 - 2 hours at room temperature. After secondary antibody incubation, membranes were again washed 5 x 10 minutes with PBS-T/TBS-T. Chemiluminescence detection of immunoblotted proteins was carried out with Amersham ECL Prime Western Blotting Chemiluminescent reagents and exposed with X-Ray film. After immuno-detection, membranes were stripped gently in Stripping Buffer for 10 minutes with mild shaking. The stripped membranes were washed with PBS-T/TBS-T, blocked with 5% milk/PBS-T/TBS-T and reprobed with primary antibodies if necessary.

2.8.8 Phospho-kinase array analysis

2.8.8.1 Target capturing and chemiluminescence detection

The Proteome Profiler MAPK-array was obtained from R&D Systems and the experiment was performed according to the manufacturer's instructions. Briefly, whole cell lysate from cells treated with cisplatin or untreated control were collected after 48 hours of drug incubation and quantified using BCA protein assay as described in Chapter 2.8.3. Briefly, the Proteome Profiler Phospho-MAPK membranes that are spotted with capture and control antibodies in duplicate were blocked with Array Buffer 1 for 1 hour. 250µg of protein lysates were then diluted in Array Buffer 1 to a final volume of 2mL and incubated on the blocked Proteome Profiler Phospho-MAPK membranes overnight at 4°C. Subsequent day, the membranes were washed 3 x 10 minutes with washing buffer provided. Next, the membranes were probed with 1mL of Detection Antibody Cocktail diluted in Array Buffer 2 for 2 hours at room temperature on a rocking platform. After incubation, the membranes

were washed 3 x 10 minutes with washing buffer provided. After washing, residual buffers were carefully removed for the membranes. The membranes were then incubated with 1mL of Streptavidin-HRP diluted in Array Buffer 2 for 30 minutes at room temperature on a rocking platform. Washed the membranes 3 x 10 minutes with washing buffer and removed the residual buffers before immuno-detection was carried out with Amersham ECL Prime Western Blotting Chemiluminescent reagents and exposed with X-Ray film. Multiple films with varied exposure time were developed to obtain the optimal signals of phosphorylated protein on each antibody spot.

2.8.8.2 Densitometric analysis

ImageJ Software (http://rsb.info.nih.gov.libproxy1.nus.edu.sg/ij/; v.1.45s, NIH) was utilised for densitometric analysis. Briefly, the developed films were scanned and the images were imported into ImageJ. Pixel density of each spot was measured using the <Analyse→ Gel → lane> function. Background signal (in pixels) was obtained from the negative control spot. Signals generated from the positive control spots were used for normalization. In summary, densitometric analysis of each spot was performed by subtraction of background density signal and normalization with corresponding positive controls. Fold change was obtained by comparing the normalized values of the treatment groups against the calibrator (untreated control).

2.9 Cell-based assays

2.9.1 Reagents and kits

Chemicals/Reagents/Kits	Supplier	Place of origin
3-(4,5-dimethylthiazol-2-yl)-2,5-diphenyltetrazolium bromide (MTT)	Roche	Penzberg, Germany
3-(4,5-dimethylthiazol-2-yl)-5-(3-carboxymethoxyphenyl)-2-(4-sulfophenyl)-2H-tetrazolium (MTS)	Promega	WI, USA
4',6-diamidino-2-phenylindole (DAPI) dye	Invitrogen	CA,USA
Annexin-V binding buffer	Life Technologies	CA, USA
Annexin-V-Allophycocyanin (APC) antibody	Life Technologies	CA, USA
Bacto™ agar	Becton Dickinson	NJ, USA
Caspase-Glo® 3/7 kit	Promega	WI, USA
Caspase-Glo® 8 kit	Promega	WI, USA
Caspase-Glo® 9 kit	Promega	WI, USA
Hoechst 33342 dye	Becton Dickinson (BD)	NJ, USA
Paraformaldehyde	Sigma Aldrich	MO,USA
Prolong Gold Antifade Reagent with 4',6-diamidino-2-phenylindole (DAPI)	Invitrogen	CA,USA
Propidium iodide (PI)	Becton Dickinson (BD)	NJ, USA
Triton X-100	Sigma Aldrich	MO,USA

Table 2.18: List of chemicals, reagents and kits used in cell-based assays.

2.9.2 MTS cell proliferation assay

Cell viability was estimated by CellTiter 96® AQ_{ueous} One Solution cell proliferation assay (MTS) that measures mitochondrial dehydrogenase activity according to manufacturer's protocol with minor modifications. Briefly, cell lines in 100µL of complete media were seeded into 96-well plate, co-incubated with 100µL of media containing drugs at various concentrations (0.01 - 100µM), and cultured at 37°C in tissue culture incubator for 72 hours. The cells reached 80 - 100% confluency on day of assay. 20µL of MTS solution was added to each well and incubated at 37°C for 2 - 4 hours at a humidified, 5% CO_2 atmosphere. Absorbance at 490nm was measured with Infinite200 Pro 96-well plate reader (Tecan; Switzerland). The half-maximum inhibitory concentration (IC_{50}) was calculated by GraphPad Prism software (GraphPad Software; CA, USA) based on curve fitting concept.

2.9.3 Anchorange-independent soft agar assay

2.9.3.1 Colony forming assay

Anchorage-independent soft agar assay was performed on 24-well plate. Layers of soft agar (0.6% bottom layer; 0.36% middle layer) were formed by mixing complete culture media with 3% Bacto™ agar. Bacto™ agar was liquefied by heating with microwave oven. Media were pre-warmed to 40°C in a water bath. The mixture of agar and media was equilibrated to 40°C while being monitored to prevent solidification. Briefly, each well of 24-well plates were first layered with 600µL of 0.6% agar layer (3mL of Bacto™ agar in 12mL of complete media per plate) and allowed to solidify for roughly 15 minutes at room temperature. The second layer comprised of an agar mixture and cell mixture. The agar mixture (1.8mL of Bacto™ agar in 11.7mL of complete media per plate) was prepared, equilibrated to 40°C and mixed with 1.5mL of cell mixture. 500µL of the final agar mixture was added onto the bottom layer. Each well contained approximately 5,000 to 10,000 cells depending on the number and size of colony formed. The second layer was allowed to solidify for roughly 30 minutes at room temperature. The top layer comprised of complete media containing drugs at a range of concentrations (0.001 - 10µM). Each treatment group was conducted in duplicates. The colonies were allowed to form for 2 - 4 weeks depending on the growth rate. Colonies were stained by adding 40µL of MTT solutions (5mg/mL in PBS) to each and incubated at 37°C for 4 hours. The extent of anchorage-independent growth was imaged with Epson Perfection V330 Photo scanner.

2.9.3.2 Colony counting and data analysis

The scanned images from Chapter 2.9.3.1 were analysed using ImageJ Software. Individual images were cropped into similar sizes and processed simultaneously. Colonies were identified as particles with the <Find Edges> function. The number of particles for individual image was counted with the <Find Particles> function. Values from duplicates were averaged and IC_{50} was calculated by GraphPad Prism software (GraphPad Software; CA, USA) based on curve fitting concept.

2.9.4 Combination Index (CI) and Dose Reduction Index (DRI)

Combination index (CI) values for multiple drug interactions was determined by CalcuSyn Software (Biosoft, UK) based on the median-effect equation and CI algorithms (Chou and Talalay 1984, Chou 2010). The CI values provide quantitative definition for the nature of drug interaction: synergism (CI < 0.8), additive effect (0.8 < CI < 1.2), and antagonism (CI >

1.2). Dose Reduction Index (DRI) measures the fold reduced of each drug in a synergistic combination when compared with the dose of each individual drug. The reduced DRI implicates for increased effect of individual drugs in the combination: DRI = 1 indicates no dose reduction, DRI > 1 indicates favourable dose-reduction, and DRI < 1 indicates unfavourable dose-reduction.

2.9.5 Imaging

2.9.5.1 Antibodies

Antibody Target		Supplier	Dilution
Acetyl-lysine	Rabbit	Cell Signalling	1:1000
Acetyl-p53 (Lys382)	Rabbit	Cell Signalling	1:500
Phospho-Erk1/2 (T202/Y204)	Rabbit	Cell Signalling	1:1000
Phospho-p53 (Ser15)	Rabbit	Cell Signalling	1:1000
Total p53	Mouse	Santa Cruz	1:1000
Alexa Fluor Chicken Anti-Rabbit 488	Secondary	Invitrogen	CA,USA
Alexa Fluor Chicken Anti-Mouse 488	Secondary	Invitrogen	CA,USA
Alexa Fluor Chicken Anti-Mouse 594	Secondary	Invitrogen	CA,USA

Table 2.19: List of antibodies used in immunofluorescence staining.

2.9.5.2 Immunofluorescence staining

Immunofluorescence staining on cultured cells was performed either on glass coverslips in 6-well plate or directly on Corning® black-walled, clear-bottomed 96-well plates. Briefly, 1 x 10^5 cells (in 6-well plate) or 5 x 10^3 cells (in 96-well plate) were seeded and cultured at 37°C in tissue culture incubator overnight. Media containing drugs were added on the subsequent day and cultured at 37°C in tissue culture incubator for 48 hours. The cells reached 70 - 80% confluency on day of assay. The cells were gently rinsed once with 1 x PBS and fixed with 4% (w/v) paraformaldehyde for 30 minutes in room temperature on a rocking platform. After fixation, the cells were washed 3 x 10 minutes with PBS to completely remove residual paraformaldehyde. Next, fixed cells were blocked with blocking buffer [5% (w/v) BSA in PBS with 0.3% (v/v) Triton X-100] for 1 hour in room temperature on a rocking platform, washed 3 x 10 minutes with PBS, and incubated with primary antibody (Table 2.19) in the dark at 4°C overnight on a rocking platform. The volumes of antibody added have to cover the entire well. After incubation, the cells were again washed 3 x 10 minutes with PBS, and incubated with secondary antibody (Table 2.19) in the dark at 4°C overnight on a rocking platform. At the end of secondary antibody

incubation, Hoechst 33342 or DAPI (to a final dilution of 1:5000) dye was added to counterstain cell nuclei for 15 minutes at room temperature on a rocking platform. The cells were then washed 3 x 10 minutes with PBS. Cells seed on 96-well plate were covered in 200µL of PBS, sealed with sealing mats and were ready for imaging. Cells seeded on coverslips were rinsed once in deionised water to remove salt residues, air dried in the dark, and mounted with 20µL of Prolong Gold anti-fade reagent. The anti-fade reagents were allowed to dry overnight at 4°C before being sealed with nail polish and were now ready for imaging.

2.9.5.3 Fluorescence and confocal microscopy

Fluorescence imaging was conducted with AxioPlan 2 imaging fluorescence microscope (Carl Zeiss; Oberkochen, Germany) at 1000 x magnification. Confocal images were captured with A1R Confocal (Nikon; Tokyo, Japan) at 1000 x magnification. High content imaging was carried out with ImageXpress Unltra confocal system (Molecular Devices; CA, USA) at 400 x magnification.

2.9.5.4 High-content imaging analysis

For high content screening, cells were seeded in black-walled 96-well plates in duplicates. All images for the same experiment were acquired in 4 - 8 adjacent fields. High-content analysis was performed with ImageJ Software for separation of nuclear and cytoplasmic signals as previously described (Chua, Sim et al. 2012). Briefly, the cell nuclei were identified and segmented according to the Hoechst 33342 staining. Nuclear signals were measured by determining the signal intensity within the segmented area. Cytoplasmic signals were measure by subtracting the total signal with the obtained nuclear signal.

2.9.6 Fluorescence-activated cell sorting (FACS) on apoptosis

FACS analysis was performed to detect the extent of apoptosis induced by drug treatment. APC conjugated Annexin-V antibody was stained for identification of the phosphatidylserine (PS) on the outer membrane surface of the apoptotic cells, while PI was stained for detection of dead cells with permeabilized membrane. Annexin-V/PI staining was carried out according to manufacturer's protocol with slight modifications. Briefly, 1 - 1.5 x 10^5 cells were seeded in 6-well plates and drug treated for 48 hours at 37°C in tissue culture incubator. On day of assay, all cells were harvested and cell pellets were obtained

through centrifugation at 1000 rpm for 5 minutes at room temperature. The cell pellets were washed once with 1mL of Annexin-V binding buffer, centrifuged again at 1000 rpm for 5 minutes at room temperature. The supernatants were removed and the cell pellets were resuspended in 100μL 1 x Annexin-V binding buffer. For each sample, 3μL of Annexin-V-APC and 1μL of PI dye were added, mixed well by vortexing, and incubated in the dark for 15 minutes at room temperature. After incubation, 400μL of Annexin-V binding buffer was added into each sample. The staining profile was analysed by flow cytometry using LSR II Flow Cytometer (BD; NJ, USA) within 1 hour after staining.

2.9.7 Caspase activity assay

The activity of caspase 3/7, 8 and 9 was measured with Caspase-Glo® kits according to manufacturer's protocol. Activation of caspases was determined using luminogenic substrates that are synthetic oligopeptides that contain the tetrapeptide sequence DEVD at N-terminus. DEVD are substrates of luciferase. Release of DEVD from the oligopeptides by caspases cleavages results for luciferase activity. Briefly, 3 - 5 x 10^3 cells were seeded in white-walled 96-well plate and cultured at 37°C in tissue culture incubator overnight. Drug treatment was performed 24 hours after seeding and incubated at 37°C in tissue culture incubator for 72 hours. At the end of incubation, 100μL of Caspase-Glo® reagents that contain lysis buffer, luminogenic substrates and luciferase and luciferase were added into each well and incubated at room temperature for 30 minutes at a rocking platform set at 200 rpm. The luminescence signal of each sample was measured at 1 sec interval with Infinite200 Pro 96-well plate reader (Tecan; Switzerland). Caspase activity was normalized against vehicle control and expressed as fold change in relative to vehicle control.

2.10 Luciferase assay

2.10.1 Reagents and kits

Reagents/Kits	Supplier	Place of origin
Cignal p53 reporter (Luc) kit	Qiagen	Hilden, Germany
Dual-Luciferase Reporter Assay System	Promega	WI, USA

Table 2.20: List of reagents and kits used in luciferase reporter assay.

2.10.1 Promoter constructs

The p53-responsive *firefly* luciferase construct, non-inducible firefly luciferase construct (negative control), constitutively expressing CMV-GFP construct, constitutively expressing CMV-*firefly* construct (positive control), and the constitutively expressing CMV-*Renilla* construct were obtained from Qiagen (Hilden, Germany). The CMV-*Renilla* construct was used as normalization construct for each sample.

2.10.2 Luciferase Promoter assay

Cells were seeded in 24-well plate and cultured overnight at 37°C in complete media. On day of transfection, the cells should reach 30% confluency. Transfection procedures were described in Chapter 2.5.3. Drug treatments were performed 24 hours after transfection and cells were incubated at 37°C in incubator for 24, 48 and 72 hours. All cells were collected for the assay. Briefly, the culture supernatant from each treatment group was aspirated and placed in collection tubes. Cells were washed once with 1 x PBS (PBS was collected as well), trypsinized, and collected in the same collection tubes. The cells were centrifuged at 1000 rpm for 5 minutes at room temperature, rinsed once with ice-cold 1 x PBS and pelleted again by centrifugation at 1000 rpm for 5 minutes at room temperature. The supernatant was removed, lysed with 200µL of Passive Lysis Buffer (PLB) and incubated for 15 minutes on a rocking platform. After incubation, the samples were centrifuged at 14,000 rpm for 30 sec at 4°C and supernatants were collected for the assay. *Firefly* and *Renilla* luciferase activities were measured according to manufacturer's protocol. 20µL of each of the sample was added to luminometer tubes that contained 100µL of LARII solution (containing substrates for *firefly* luciferase) and mixed by gentle tapping. The *firefly* luminescence signals were recorded in a luminometer (Berthold Technologies; Bad Wildbad, Germany) with 10 sec interval. Next, 100µL of Stop & Glo® Reagent was added to each sample, tapped to mix, and the *Renilla* luminescence signals were recorded. For data analysis, the *Firefly* luciferase signal from each sample was normalized with corresponding *Renilla* signal.

2.11 Clinicopathological analysis

2.11.1 Clinical samples

Head and neck SCC tissues were obtained from 33 cases diagnosed with the disease. The formalin-fixed, paraffin-embedded (FFPE) tissues were retrieved from the tissue repository of National University Hospital (NUH), Singapore. Tissue sections were provided by Dr Nga Min En from the Department of Pathology, NUH, and stored at 4°C prior to staining.

2.11.2 Ethical approval

The use of these head and neck SCC samples has been approved by the NUHS Institutional Review Board (IRB). The protocol for the study has been drafted by A/P Goh Boon Cher and Kong Li Ren under the title "Evaluation of Platinum-resistance Pathways in Squamous Cell Carcinoma of the Head and Neck", and has been approved by the Domain-specific Review Board (DSRB) of National Healthcare Group (NHG).

2.11.3 Chemicals, reagents and kits

Chemicals/Reagents/Kits	Supplier	Place of origin
Ammonium hydroxide	Merck	Darmstadt, Germany
Canada Balsam	Sigma Aldrich	MO,USA
Dako Antibody Diluent	DakoCytomation	CA, USA
Dako EnVision™+ System-HRP (DAB) Kit (Peroxidase Block, Labelled polymer-HRP anti-Rabbit, DAB+ Substrate Buffer, DAB+ chromogen)	DakoCytomation	CA, USA
Dako Target Retrieval Solution, Citrate pH 6.0	DakoCytomation	CA, USA
Histo-Clear II	Agar Scientific	Essex, UK
Mayer's Haematoxylin	Sigma Aldrich	MO,USA

Table 2.21: List of chemical, reagents and kits used in IHC staining.

2.11.4 Antibodies

Antibody Target		Supplier	Dilution
Phospho-Erk1/2 (T202/Y204)	Rabbit	Cell Signalling	1:1000

Table 2.22: List of antibodies used in IHC staining.

2.11.5 Immunohistochemistry (IHC) staining

IHC staining was performed according to the Dako Cytomation™ IHC Methods that applied diaminobenzidine (DAB) substrate-chromogen system. Prior to staining, tissue slides were warmed at 40°C for 10 minutes on a heat block and deparaffinized in Histo-Clear II solution for 3 x 5 minutes. After complete removal of paraffin, the slides were rehydrated in descending grades of ethanol (twice each of 100%, 90%, and 75%, 3 minutes each) and placed in deionised water for 5 minutes at room temperature. Antigen retrieval was performed on the tissue slides to retrieve epitopes that were cross-linked during formalin fixation by using Dako Target Retrieval Solution according to manufacturer's protocol. Briefly, the rehydrated slides were placed into the processing chamber, which was then located in the assigned Retriever. The Retriever was filled with Target Retrieval Solution until all slides were thoroughly covered. Pressure-induced antigen retrieval was performed at 98°C for 20 minutes. The slides were allowed to cool in the Retriever for 15 minutes under running water before being removed from the chamber and placed into deionised water. Next, the slides were tapped off excess buffer and wiped around the samples with Kimwipe to removed remaining liquid. The samples were treated with 3 - 5 drops of Dako Peroxidase Block (3% hydrogen peroxide) for 10 minutes to remove endogenous peroxidase activity. After blocking, the slides were tapped, wiped as before, washed 3 x 5 minutes with 1 x TBS and incubated with primary antibody (diluted in Antibody Diluent) overnight at 4°C. The next day, the slides were washed 3 x 5 minutes with 1 x TBS, wiped as before and incubated with several drops of Labeled polymer-HRP anti-Rabbit for 30 minutes at room temperature. Subsequently, the slides were washed 3 x 5 minutes with 1 x TBS and wiped as before. Sufficient DAB+ substrate-chromogen solution (20µL chromogen: 1mL buffer) was added to each slide to cover the sample and incubated for 5 – 15 minutes until optimal signal was developed. The reaction was inhibited by dipping the slides into deionised water. Next, the slides were counterstained with Mayer's Hematoxylin dye for 10 sec with mild agitation, rinsed in flowing water immediately and dipped 10 x in 1% ammonium hydroxide solution to blue nuclei. Lastly, the slides were rinsed in deionised water, dehydrated in ascending grades of ethanol (2 minutes each of 75%, 90% and 100%), cleared with 3 x 2 minutes Histo-Clear II solution, and mounted with coverslips with Canada Balsam. The slides were allowed to dry overnight at room temperature in the fume hood.

2.11.6 Scoring

Scoring of the TMAs was performed by a pathologist (Dr Nga Min En) in a blinded manner with respect to the details of clinical data. Here, the German semi-quantification scoring system as reported in previous studies was adopted based on the staining intensity and area

extent (Cheng, Wu et al. 2007, Koo, Kok et al. 2009). Each tissue was scored according to the region stain (nuclear/cytosol), staining intensity (0, negative; 1, weak; 2, moderate; and 3, strong) and the fraction of stained tumour cells (0 - 100%). The final immunoreactive score was determined by multiplying the intensity score with the fraction stained (0 - 300). For clinicopathological analyses, samples were separated based on the immunoreactive score. Survival outcomes were defined by overall progression-free survival.

2.12 Next Generation Sequencing (NGS) of lung SCC samples

2.12.1 Clinical samples

Lung SCC tissues were obtained from 45 cases diagnosed with the disease. The formalin-fixed, paraffin-embedded (FFPE) tissues were retrieved from the tissue repository of National University Hospital (NUH), Singapore. Tissue sections were prepared by Dr Pang Yin-Huei from the Department of Pathology, NUH, and stored at 4°C prior to staining.

2.12.2 Ethical approval

The use of these lung SCC samples has been approved by the NUHS Institutional Review Board (IRB). The protocol for the study has been provided by A/P Ross Soo (NUH).

2.12.3 Reagents

Chemicals/Reagents	Supplier	Place of origin
Agencourt AMPure XP Magnetic Beads	Beckman Coulter	CA, USA
GeneRead Adapter I 1-plex	Qiagen	Hilden, Germany
GeneRead DNA Amplification Kit	Qiagen	Hilden, Germany
GeneRead DNAseq Gene Human Lung Panel	Qiagen	Hilden, Germany
GeneRead DNAseq Library Quant Array	Qiagen	Hilden, Germany
GeneRead Size Selection Kit	Qiagen	Hilden, Germany
QIAamp® DNA FFPE Tissue Kit	Qiagen	Hilden, Germany
QIAquick PCR Purification Kit	Qiagen	Hilden, Germany
Xylene	Merck	Darmstadt, Germany

Table 2.23: List of chemicals, reagents and kits used in library preparation for NGS.

2.12.4 Primers for Indexing

Universal Forward 5' Primer:

AATGATACGGCGACCACCGAGATCTACACTCTTTCCCTACACGACGCTCTTCCGATC*T

Index ID	Index	Index ID	Index	Index ID	Index
MP_01	CGTGAT	**MP_16**	GGACGG	**MP_31**	ATCGTG
MP_02	ACATCG	**MP_17**	CTCTAC	**MP_32**	TGAGTG
MP_03	GCCTAA	**MP_18**	GCGGAC	**MP_33**	CGCCTG
MP_04	TGGTCA	**MP_19**	TTTCAC	**MP_34**	GCCATG
MP_05	CACTGT	**MP_20**	GGCCAC	**MP_35**	AAAATG
MP_06	ATTGGC	**MP_21**	CGAAAC	**MP_36**	TGTTGG
MP_07	GATCTG	**MP_22**	CGTACG	**MP_37**	ATTCCG
MP_08	TCAAGT	**MP_23**	CCACTC	**MP_38**	AGCTAG
MP_09	CTGATC	**MP_24**	GCTACC	**MP_39**	GTATAG
MP_10	AAGCTA	**MP_25**	ATCAGT	**MP_40**	TCTGAG
MP_11	GTAGCC	**MP_26**	GCTCAT	**MP_41**	GTCGTC
MP_12	TACAAG	**MP_27**	AGGAAT	**MP_42**	CGATTA
MP_13	TTGACT	**MP_28**	CTTTTG	**MP_43**	GCTGTA
MP_14	GGAACT	**MP_29**	TAGTTG	**MP_44**	ATTATA
MP_15	TGACAT	**MP_30**	CCGGTG	**MP_45**	GAATGA

Table 2.24: List of indexes used for multiplexing of libraries for NGS.

The reverse primers with unique indexes were provided by Dr Ong Qi Rui (Qiagen; Hilden, Germany).

2.12.5 Genomic DNA (gDNA) extraction from FFPE samples

For better yield, 5 x 10µm of each sample were pooled into 1.5mL eppendorf tube. Extraction of gDNA from tissue sample was carried out using QIAamp® DNA FFPE Tissue Kit according to manufacturer's protocol. Briefly, 1mL of xylene was added to each sample and vortex vigorously for 10 sec to deparaffinize the sample. The xylene solution was centrifuged at 14,000 rpm for 2 minutes at room temperature. The supernatant containing the dissolved paraffin was removed. The pellet (tissue) was resuspended with 1mL of 100% ethanol for extraction of residual xylene from sample. Again, the solution was centrifuged at 14,000 rpm for 2 minutes at room temperature and all liquid are removed carefully. The samples were allowed to air-dry at room temperature for 10 minutes to evaporate all residual ethanol. The dried pellet was resuspended in Buffer ATL containing 20µL of proteinase K and incubated on a heat block at 56°C for 3 hours until the sample was fully dissolved. The

sample was further heated at 90°C for 1 hour to reverse formaldehyde modification of gDNA. The gDNA was precipitated by mixing the sample with Buffer AL and ethanol. All samples were then loaded onto QIAamp MinElute column. The gDNA was bound to the resin through centrifugation at 8000 rpm for 1 minute at room temperarture, washed once each with Buffer AW1 and AW2 with the same centrifugation condition. The column was centrifuged at 14,000 rpm to dry the membrane completely. The gDNA was eluted with 50µL of Buffer ATE. Quality control was conducted on the extracted gDNA. Concentration and purity of the purified PCR were determined by NanoDrop as described in Chapter 2.7.3.3. All samples achieved A_{260}:A_{230} > 1.7, A_{260}:A_{280} > 1.8, and concentration > 4ng/µL and were progressed to library construction.

2.12.6 Library construction

The GeneRead DNAseq Gene Human Lung Panel provides overlapping primer sets across the exonic regions of multiple genes. This allows for wide coverage of the sequencing reads that could align to the target genes. The primer sets were split into 4 groups to ensure for uniform coverage. Targeted exon enrichment and library construction was performed according to manufacturer's protocol. Briefly, each sample was diluted to 4ng/µL and 20ng was mixed with each of the 4 x primer sets. PCR amplification was conducted in the MyCycler thermal cycler. Upon completion of PCR, all 4 sets of PCR products from the same sample were pooled and purified with QIAquick PCR Purification kit according to manufacturer's protocol. Next, library was constructed for each sample by adding both Start and End adaptors (60bp each) to the PCR fragments (~150bp) through end-repair and adaptor ligation steps. Subsequently, two size selection steps were conducted to remove the small and large fragments. The smaller fragments (< 280bp) were removed by GeneRead Size Selection kit by binding of large fragments to the MinElute spin column and allowed the smaller fragments to be washed off. The selected fragments were eluted in 90µL of Elution Buffer. The larger fragments (> 280bp) were then removed by AMPure XP Beads according to manufacturer's protocol. Briefly, 72µL (0.8 x of initial volume) of AMPure XP Beads was added to the eluted solution and incubated for 5 minutes at room temperature. The suspension mix was then placed on a magnetic rack to separate the beads from the supernatant. In the 1st bead selection process, the supernatant was transferred to a fresh tube and the beads that contained the larger fragments were discarded. Next, 27µL (0.3 x of initial volume) of AMPure Beads was added to the supernatant, allowed to incubate for 5 minutes at room temperature, and placed on magnetic rack again. In the 2nd bead selection process, the supernatant was discarded while the beads that contained the DNA targets were collected. Each pellet (with the beads) was rinsed 2 x 200µL freshly-prepared 80% ethanol

in the magnetic stand. The ethanol was carefully removed from each sample without disturbing the pellet. Upon air-dried of residual ethanol, the DNA target was eluted from beads by pipetting with 19μL of nuclease-free water, placed on magnetic rack until solution was clear, and transferred to a new tube. The size-selected libraries were proceeded on with DNA amplification and multiplexing.

2.12.7 Library amplification and multiplexing

Barcoding of the constructed libraries was performed during DNA amplification with slight modifications from GeneRead DNA Amplification Kit to include the designed primers for sample barcoding. Each sample was mixed with a universal forward primer and an individual reverse primer. Each reverse primer contains conservative sequence that is complimentary to the adapter and a short region of unique indexing sequence for the purpose of sample identification (Table 2.24). Briefly, the size-selected libraries (17μL) were mixed with DNA Amplification cocktail containing HiFi HotStar DNA Master Mix, universal forward primer (0.3μM) and index reverse primer (0.3μM). The setup configuration for PCR: initial denaturation step of 98°C for 2 minutes; followed by 9 cycles of DNA denaturation at 98°C for 20 sec, primer annealing 60°C for 30 sec, and DNA elongation at 72°C for 30 sec; and ended with DNA extension step at 72°C for 1 minute. PCR purification was performed using QIAquick PCR Purification kit according to manufacturer's protocol.

2.12.8 Quality controls for libraries and NGS Run

NGS for this study was carried out on HiSeq 2000 System (Illumina; CA, USA). Prior to NGS run, several quality check procedures were conducted on the purified and size-selected samples. The sizes of target gene fragments were determined using Agilent 2100 Bioanalyser (Agilent; CA, USA) and QIAxel Advanced System (Qiagen; Hilden, Germany). A clean fragment of ~276bp was detected for each sample (150bp of amplified fragment; 60bp of Start adaptor; 60bp of End adaptor; and 6bp of barcode). To ensure for highly accurate quantification of the libraries, qPCR was carried out with GeneRead DNAseq Library Quant Array according to manufacturer's protocol. A standard curve was generated using the sequential diluted DNA standards provided and the DNA molecules with adaptors at both ends were specifically were quantified based on the standard curve. The libraries that passed quality check were sent to Macrogen Inc. (Seoul, Korea) for NGS run. Sequencing reads were decoded based on the indexes displayed in Table 2.24.

2.13 Statistical analysis

All experiments were carried out 3 times unless stated otherwise. Results were expressed as mean ± SD. Statistical analysis for comparison between two groups was conducted using unpaired Student's *t*-test; while analysis for comparison of multiple groups was conducted using one-way-analysis of variance (ANOVA) and followed by Post-hoc Bonferroni test. Chi-square test was performed to test the statistical difference of clinical outcomes between groups with different immunoreactive scores (high and low).The confidence intervals were set at 95% for all analyses. All tests were 2-sided and the significance level was set at $P < 0.05$.

CHAPTER 3 Evaluating lung SCC cell lines as tumour models by comparison of genetic aberrations, drug sensitivities and transcriptome profiles

A common challenge to effectively reproduce treatment efficacy of adenocarcinoma in lung SCC is the identification of oncogenic driver mutation. According to TCGA Research Network, lung SCC has an average of 8.1 mutations per megabase, which is higher than rates reported for acute myelogenous leukemia, breast cancer, ovarian cancer, glioblastoma and colorectal cancer (Network 2012). Despite so, no common oncogene driver mutations have been clearly identified in lung SCC to guide therapy. Hence, platinum-based chemotherapy remains as the established standard-of-care treatment for lung SCCs either as a single therapy or in combination with other chemotherapeutic agents or radiotherapy (Wang and Lippard 2005). Despite so, intra-tumour heterogeneity and drug resistance have limited the potency of cisplatin-based chemotherapies.

In this chapter, a panel of tumour-derived lung SCC cell lines was being analysed, using several genomic and proteomic-based technologies, to characterize the molecular profile of this disease. These profiles were validated against a panel of human SCC samples to determine their clinical relevance. Secondly, the *in vitro* sensitivities of cisplatin, one of the most commonly used platinum-based chemotherapy, was determined within this panel of cell lines that may be contributed by the phenotypic and functional heterogeneity in cancer cells. Thirdly, pathways associated with platinum resistance were identified by investigating the transcriptomic profiling of these study models. Lastly, through molecular dissection of the mechanism of synergistic cytotoxicity of cisplatin and belinostat, therapeutic potential of this combination was explored.

3.1 Global mutational landscape of lung SCC

3.1.1 Lack of driver oncogenic mutations in lung SCC

As described in Chapter 1.4, *EGFR* mutation, *RAS* mutation, *EML4-ALK* fusion, *HER2* (*ERBB2*) mutation, *BRAF* mutation, *PIK3CA* mutation, and *AKT1* mutation are common driver mutations in NSCLC (Pao and Hutchinson 2012). Moreover, abnormal activation of mTOR signalling appears to be frequently observed in human cancer (Schmelzle and Hall 2000), whereas *STK11* (serine/threonine kinase 11), negative regulator or mTOR signalling, is often inactivated in lung tumours. Furthermore, loss-of-function mutations in key tumour suppressor genes, such as *TP53*, *PTEN* (Phosphatase and tensin homolog), *RB1* and *CDKN2A*, usually precede malignant transformation of lung cancer (Horowitz, Park et al. 1990, Marsit, Zheng et al. 2005, Andujar, Wang et al. 2010). Somatic mutations in *PTEN*, *CDKN2A* and *RB1* result in aberrant activation of Akt/PKB pathway, inactivation of p53 and dysregulation of cell cycle checkpoint respectively (Murphree and Benedict 1984, Pacifico and Leone 2007, Song, Salmena et al. 2012). Alterations of activities of these genes via mutations are found to often lead to oncogenic processes. NGS was performed on 45 lung SCC specimens obtained from patients presenting at the National University Hospital from 1989 to 2008. The multiplexed PCR-based assay, Human Lung Cancer GeneRead DNAseq Gene Panel, was used for targeted enrichment of the coding and untranslated region (UTR) of several commonly mutated genes in lung cancer.

Detailed processing and barcoding of amplified DNA products were previously described in Chapter 2.12 and NGS was performed using the Illumina platform. Sequencing reads were first analysed with GeneRead Targeted Exon Enrichment Panel Data Analysis. A preliminary alignment was then performed using the entire read set and Quality Filter was subsequently applied to remove sequencing reads with an untrimmed length of less than 45bp. The mean of total number of reads mapped (11,447,300) and median depth of coverage (94.75%) for each sample was generated after Quality Filter (Data not shown). Final sequencing reads were subjected to variant calling by using Genome Analysis Toolkit (GATK; http://www.broadinstitute.org/gatk/) from Broad Institute (MA; USA). The results generated displayed a variety of DNA alterations among the 15 genes tested with a mean of 56.3 SNPs and 8.62 insertions/deletions per tumour for each sample (Data not shown). The list of SNPs/ insertions/deletions was then compared with the Catalogue of Somatic Mutations in Cancer (COSMIC) Database (Wellcome Trust Sanger Institute; http://www.sanger.ac.uk/cosmic). COSMIC mutations identified in the sequencing reads were clustered and aligned with respective samples. Heat maps were generated by first sorting the obtained gene lists according to the number of mutation hits detected across individual samples (highest to lowest from top to bottom) and subsequently by the number

of mutations detected in each gene in all samples (highest to lowest from right to left) (Figure 3.1 A). After filtering, each lung SCC specimen had a mean of 7.87 COSMIC mutations (Taken as average of all samples in Figure 3.1 A; values not shown). Among the 15 genes investigated, *ALK* mutation was detected in all specimens, while high mutational frequencies were observed in *TP53* (71.11%), *CDKN2A* (80%) and *EGFR* (80%) across all samples (Figure 3.1 B). Next, *HRAS* mutation was detected in roughly a quarter of the samples (26.67%), while mutations of *PTEN* (15.56%), *RB1* (15.56%), *STK11* (13.33%), *PIK3CA* (13.33%), *BRAF* (11.11%) and *NRAS* (11.11%) were also detected (Figure 3.1 B).

To investigate the significance of these somatic DNA alterations on the disease, the sum of each mutation in all specimens was determined. Among these 15 genes, *ALK* (76), *TP53* (75), *CDKN2A* (70) and *EGFR* (64) had the highest number of mutational hits across all samples (obtained by summation of mutational hits in all samples for each gene) (Figure 3.1 C). Next, the mutation hits based on the COSMIC ID of each individual mutation were clustered. Among the 76 mutational hits in *ALK* gene, 8 different COSMIC mutations were identified (Figure 3.1 D). Likewise for *CDKN2A* and *EGFR*, 16 and 21 COSMIC mutations were identified respectively (Figure 3.1 D). These results indicate the presence of recurring mutations within each gene across all samples. However, among the 75 mutational hits of *TP53*, a total of 65 individual variants were identified based on their COSMIC IDs. As the weightage of each variant could possibly reflect the significance of a specific mutation in lung SCC, 14 variants that were identified in more than 3 specimens were identified (5% of total samples). The identity and details of each variant is shown in Table 3.1.

Further analysis led to the identification of a *CDKN2A* variant with intronic substitution (COSM14251) in all samples (Table 3.1). However, the impact of this intronic substitution has yet to be characterized. Next, a missense mutation from lysine (K) to arginine (R) was identified at AA position 1491 of *ALK* gene in 40 out of 45 specimens (88.89%) at a mean of 77.3% in each sample harbouring this mutation (Table 3.1). The high frequency of this SNP across all samples suggested that it could be a germ-line polymorphism instead of somatic mutation. However this could not be verified as adjacent normal tissues were not available for the study. Two common mutations were detected in the *EGFR* gene in 18 and 26 specimens, however both were silent mutations and did not affect the phenotype of translated EGFR protein. The remaining COSMIC mutations in *ALK*, *HRAS*, *PTEN* and *RB1* were either found within the untranslated intronic region or silent mutations (Table 3.1); whereas alteration of *TP53* gene were relatively uncommon (< 10%) in all samples (Table 3.1).

The mutational landscape of lung SCC tumors has been previously characterized by The Cancer Genome Atlas (TCGA) group (Network 2012). To look for oncogenic mutations in SCC tumours among Asian patients that would be responsive to molecular targeting, the mutated driver oncogenes that were frequently found in NSCLC were investigated: *EGFR*, *KRAS*, *NRAS*, *HRAS*, *ALK*, *ERBB2*, *BRAF*, *PIK3CA*, and *AKT1*; as well as the commonly altered tumour-suppressor genes: *TP53*, *CDKN2A*, *PTEN* and *RB1* (Figure 3.1 E). Consistent with the findings by TCGA, common mutations to driver oncogenes in lung adenocarcinoma were rarely found in these SCC tumors. Despite observing *EGFR* mutation in 82% of all samples (37/45), these alterations were almost codon silent event exclusively (30/37). All detected *TP53* mutations (31/45 of all samples) were non-synonymous alterations, suggesting loss-of-function. Moreover, non-synonymous mutations in *ERBB2*, *KRAS*, *BRAF*, *AKT1* and *PIK3CA* were rare (< 10%). These observations concluded the lack of oncogenic driver mutations in lung SCC tumours.

Collectively, these observations concluded the lack of oncogenic driver mutations in lung SCC tumours. An ALK A1491R mutation was consistently detected in 88.89% of all samples with a mean coverage depth of 77.3%, which could be a germ-line polymorphism.

A

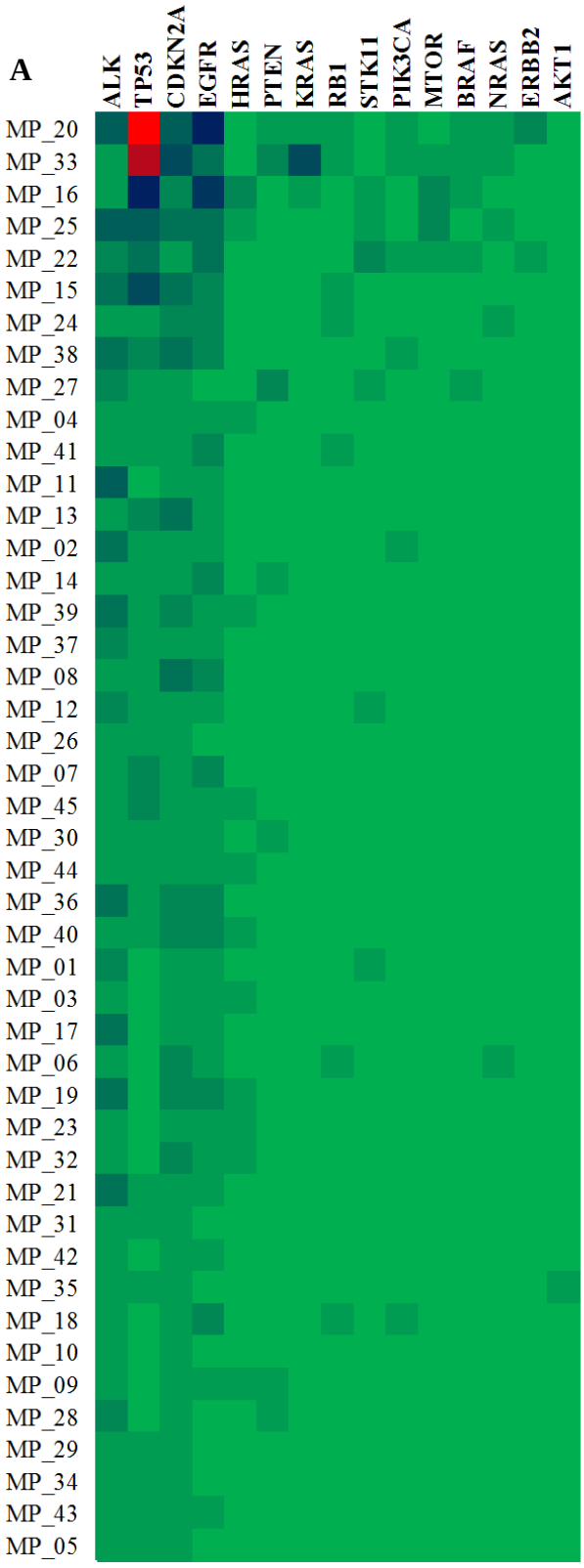

B

Genes	Frequency of gene mutation	Percentage of mutation
ALK	45	100.00
TP53	32	71.11
CDKN2A	36	80.00
EGFR	36	80.00
HRAS	12	26.67
PTEN	7	15.56
KRAS	3	6.67
RB1	7	15.56
STK11	6	13.33
PIK3CA	6	13.33
MTOR	4	8.89
BRAF	5	11.11
NRAS	5	11.11
ERBB2	2	4.44
AKT1	1	2.22

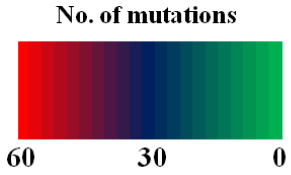

C

	Sum of mutational hits in all samples
ALK	76
TP53	75
CDKN2A	70
EGFR	64
HRAS	13
PTEN	9
KRAS	7
RB1	7
STK11	7
PIK3CA	6
MTOR	6
BRAF	5
NRAS	5
ERBB2	3
AKT1	1

D

	Number of COSMIC mutation
ALK	8
TP53	65
CDKN2A	16
EGFR	21
HRAS	3
PTEN	6
KRAS	7
RB1	2
STK11	4
PIK3CA	6
MTOR	6
BRAF	5
NRAS	4
ERBB2	3
AKT1	1

E

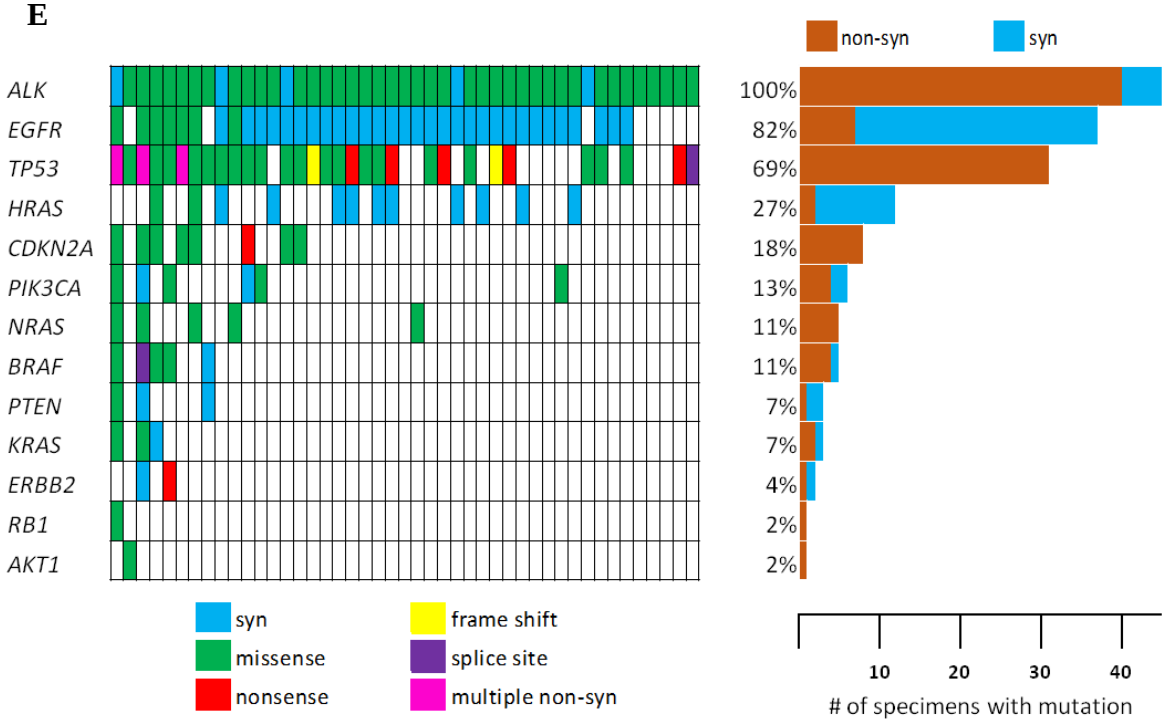

Figure 3.1: Mutated genes in lung SCC.

A, Heat map was generated based on the somatic mutations identified in each tumour specimen. The mutations were determined by variant calling through GATK and comparing the NGS sequencing reads to the COSMIC Database. Genes covered by GeneRead Lung Panel were listed horizontally according to the number of mutational hits detected in each gene (highest to lowest from right to left). Samples were displayed vertically, with the

highest overall number of mutations plotted at the top. B, frequency and percentage of gene mutation in all samples were determined. Sum of the mutational hits (C) and number of somatic variants (D) in each gene were shown. E, Lack of significantly altered genes in lung squamous cell carcinoma (SCC) tumors. Exome sequencing after targeted enrichment identified significant mutations ($P < 0.01$) within a panel of 45 lung SCC specimens. Percentage of samples with mutation(s) detected by automated calling was displayed on the right. Genes were listed vertically according to the percentage of mutation with the highest number at the top. Samples were displayed horizontally according to the number of mutations detected with the highest frequency on the left. Types of mutations were indicated: synonymous (syn), non-synonymous (non-syn), missense, nonsense, frame shift and splice site.

GENE	COSMIC ID	CDS mutation		AA mutation		Frequency of mutation	Percentage of mutation
ALK	COSM1130802	c.4472A>G	Sub	p.K1491R	Sub - Missense	40	88.89
	COSM148825	c.2535T>C	Sub	p.G845G	Sub - CS	18	40.00
	COSM148824	c.3036G>A	Sub	p.T1012T	Sub - CS	11	24.44
	COSM1407683	c.784T>C	Sub	p.Y262H	Sub - Missense	3	6.67
TP53	COSM45292	c.1057G>A	Sub	p.A353T	Sub - Missense	3	6.67
	COSM99602	c.743G>A	Sub	p.R248Q	Sub - Missense	3	6.67
CDKN2A	COSM14251	c.471+29G>C	Sub - intronic	-	Unknown	45	100.00
	COSM14252	c.471+69C>T	Sub - intronic	-	Unknown	11	24.44
EGFR	COSM1451600	c.2361G>A	Sub	p.Q787Q	Sub - CS	18	40.00
	COSM42978	c.474C>T	Sub	p.N158N	Sub - CS	26	57.78
HRAS	COSM249860	c.81T>C	Sub	p.H27H	Sub - CS	11	24.44
PTEN	COSM5915	c.1-9C>G	Sub - intronic	-	Unknown	4	8.89
RB1	COSM147687	c.2664-10T>A	Sub - intronic	-	Unknown	6	13.33
STK11	COSM21360	c.1062C>G	Sub	p.F354L	Sub - Missense	4	8.89

Table 3.1: COSMIC mutations detected in > 5% of lung SCC.

Among the genes investigated using NGS, several specific somatic mutations were frequently detected in more than 5% of the tumours (at least 3 out of the 45 samples): *ALK* (4), *TP53* (2), *CDKN2A* (2), *EGFR* (2), *HRAS* (1), *PTEN* (1), *RB1* (1), and *STK11* (1). The COSMIC IDs, coding sequence (CDS) mutations, amino acid (AA) mutations (Sub – substitution mutation; CS – coding silent mutation) for each mutation were shown. The frequency and percentage of the indicated mutation across 45 lung SCC samples were displayed.

3.1.2 *TP53* mutations in lung SCC occur predominantly within DNA-binding domain

Inactivation of p53 pathway is a commonly observed phenomenon in multiple cancer types (Olivier, Hollstein et al. 2010). Several mechanisms have been previously reported to abrogate p53 function which includes loss-of-function mutations of *TP53* and *CDKN2A* genes (Bates, Phillips et al. 1998, Olivier, Hollstein et al. 2010). From the NGS analysis, both genes were found mutated in 71.11% (*TP53*) and 80% (*CDKN2A*) of all samples (Figure 3.1 B). Majority of the COSMIC mutations on *CDKN2A* was detected at 2 sites (Table 3.1), resulting in intronic substitution and there is no report on their effects on the coding region. On the contrary, 65 different COSMIC mutations were identified from the 75 mutational count of *TP53* gene in all samples. The effects of these somatic mutations on affecting the translated p53 protein were next analysed.

Among the 65 COSMIC mutations, 5 intronic substitutions, 1 frameshift deletion, 6 nonsense mutations, 10 codon silent substitutions, and 43 missense mutations were identified (Table 3.2). Both frameshift deletion and nonsense mutations resulted in premature termination of protein translation. While the effect of the intronic substitutions was unknown, codon silent substitutions did not affect the AA sequence of the translated protein. As p53 functions correspond to the roles of the four main domains (Chapter 1.3.2), the impact of these AA changes was predicted by noting the sites of mutations. Among the 43 somatic variants with missense mutation, majority of the AA alterations were detected within the DBD (31), with several cases in the proline-rich domain (7) and oligomerization domain (4), as well as one mutation that was located outside the four main domains (Table 3.2). To identify the common "hotspot" of p53 mutation, the frequency of these missence mutations in terms of translated AA residues was determined. While most AA alterations were unique to only one case, 4 residues (G152, R158, M246, and R249) were mutated twice while mutations on R248 were detected on 6 occasions (Table 3.2).

Despite the absence of dominant somatic mutation in *TP53*, 31 out of the 65 mutations (47.69%) occurred within the DBD. AA alterations at R248 residue were detected in 6 cases while AA alternations at G152, R158, M246, and R249 were detected twice each (Table 3.2). These suggested that a large proportion of *TP53* mutations occurred along the DBD with residue R248 being a potential "hotspot" in lung SCC.

COSMIC ID	CDS mutation		AA mutation		Domain of mutation	Frequency of mutation	Percentage of mutation
COSM11496	c.476C>A	Sub	p.A159D	Sub - Missense	DBD	1	2.22
COSM116690	c.184G>A	Sub	p.E62K	Sub - Missense	Proline-rich	1	2.22
COSM1189383	c.463C>G	Sub	p.R155G	Sub - Missense	DBD	1	2.22
COSM126981	c.880G>T	Sub	p.E294*	Sub - Nonsense	-	1	2.22
COSM1386800	c.146G>A	Sub	p.R49H	Sub - Missense	-	1	2.22
COSM1610837	c.454G>C	Sub	p.G152R	Sub - Missense	DBD	1	2.22
COSM1645282	c.455C>T	Sub	p.P152L	Sub - Missense	DBD	1	2.22
COSM1649381	c.488A>G	Sub	p.Y163C	Sub - Missense	DBD	1	2.22
COSM18569	c.216delC	Deletion	p.V73fs*50	Deletion - Frameshift	-	2	4.44
COSM216410	c.797G>A	Sub	p.G266E	Sub - Missense	DBD	1	2.22
COSM307329	c.1020G>A	Sub	p.M340I	Sub - Missense	Oligo	1	2.22
COSM308309	c.299A>G	Sub	p.H100R	Sub - Missense	Proline-rich	1	2.22
COSM43555	c.736A>G	Sub	p.M246V	Sub - Missense	DBD	1	2.22
COSM43615	c.473G>C	Sub	p.R158P	Sub - Missense	DBD	1	2.22
COSM43629	c.745A>T	Sub	p.R249W	Sub - Missense	DBD	1	2.22
COSM43632	c.493C>T	Sub	p.Q165*	Sub - Nonsense	DBD	1	2.22
COSM43650	c.638G>T	Sub	p.R213L	Sub - Missense	DBD	1	2.22
COSM43688	c.265C>T	Sub	p.P89S	Sub - Missense	Proline-rich	1	2.22
COSM43702	c.571C>T	Sub	p.P191S	Sub - Missense	DBD	1	2.22
COSM43739	c.467G>A	Sub	p.R156H	Sub - Missense	DBD	1	2.22
COSM437483	c.809T>C	Sub	p.F270S	Sub - Missense	DBD	1	2.22
COSM43871	c.746G>T	Sub	p.R249M	Sub - Missense	DBD	1	2.22
COSM43910	c.245C>T	Sub	p.P82L	Sub - Missense	Proline-rich	1	2.22
COSM43940	c.474C>T	Sub	p.R158R	Sub – CS	DBD	1	2.22
COSM44115	c.350G>A	Sub	p.G117E	Sub - Missense	DBD	1	2.22
COSM44119	c.483C>T	Sub	p.A161A	Sub - Missense	DBD	1	2.22
COSM44192	c.272G>A	Sub	p.W91*	Sub - Nonsense	Proline-rich	1	2.22
COSM44295	c.993+1G>A	Sub - intronic	-	Unknown	-	1	2.22
COSM44300	c.548C>T	Sub	p.S183L	Sub - Missense	DBD	1	2.22
COSM44310	c.738G>A	Sub	p.M246I	Sub - Missense	DBD	1	2.22
COSM44384	c.510G>A	Sub	p.T170T	Sub – CS	DBD	1	2.22
COSM44410	c.559+3G>A	Sub - intronic	-	Unknown	-	1	2.22
COSM44520	c.424C>T	Sub	p.P142S	Sub - Missense	DBD	1	2.22
COSM44524	c.521G>A	Sub	p.R174K	Sub - Missense	DBD	1	2.22
COSM44624	c.399G>A	Sub	p.M133I	Sub - Missense	DBD	1	2.22
COSM44696	c.409C>T	Sub	p.L137L	Sub – CS	DBD	1	2.22
COSM44722	c.630C>T	Sub	p.N210N	Sub – CS	DBD	1	2.22
COSM44739	c.559+24C>T	Sub - intronic	-	Unknown	-	1	2.22
COSM44783	c.744G>T	Sub	p.R248R	Sub - CS	DBD	1	2.22
COSM44787	c.732C>T	Sub	p.G244G	Sub - CS	DBD	1	2.22
COSM44817	c.661G>T	Sub	p.E221*	Sub - Nonsense	DBD	2	4.44
COSM44962	c.774A>T	Sub	p.E258D	Sub - Missense	DBD	1	2.22
COSM45102	c.423C>T	Sub	p.C141C	Sub - CS	DBD	2	4.44
COSM45200	c.233C>T	Sub	p.A78V	Sub - Missense	Proline-rich	1	2.22
COSM45292	c.1057G>A	Sub	p.A353T	Sub - Missense	Oligo	3	6.67
COSM45512	c.252C>T	Sub	p.A84A	Sub - CS	Proline-rich	1	2.22
COSM45622	c.461G>A	Sub	p.G154D	Sub - Missense	DBD	2	4.44
COSM45717	c.1039G>A	Sub	p.A347T	Sub - Missense	Oligo	1	2.22

COSM45796	c.623A>G	Sub	p.D208G	Sub - Missense	DBD	1	2.22
COSM45841	c.559+25G>A	Sub - intronic	-	Unknown	-	1	2.22
COSM45868	c.678C>T	Sub	p.G226G	Sub - CS	DBD	1	2.22
COSM45918	c.253C>T	Sub	p.P85S	Sub - Missense	Proline-rich	1	2.22
COSM46113	c.987C>T	Sub	p.T329T	Sub - CS	Oligo	1	2.22
COSM46116	c.376-10C>T	Sub - intronic	-	Unknown	-	1	2.22
COSM46153	c.1015G>A	Sub	p.E339K	Sub - Missense	Oligo	1	2.22
COSM46281	c.187G>A	Sub	p.A63T	Sub - Missense	Proline-rich	1	2.22
COSM6549	c.743G>T	Sub	p.R248L	Sub - Missense	DBD	2	4.44
COSM99602	c.743G>A	Sub	p.R248Q	Sub - Missense	DBD	3	6.67
COSM99618	c.637C>T	Sub	p.R213*	Sub - Nonsense	DBD	1	2.22
COSM99668	c.586C>T	Sub	p.R196*	Sub - Nonsense	DBD	1	2.22
COSM99678	c.473G>T	Sub	p.R158L	Sub - Missense	DBD	1	2.22
COSM99720	c.659A>G	Sub	p.Y220C	Sub - Missense	DBD	1	2.22
COSM99914	c.524G>A	Sub	p.R175H	Sub - Missense	DBD	2	4.44
COSM99925	c.844C>T	Sub	p.R282W	Sub - Missense	DBD	1	2.22
COSM99950	c.814G>A	Sub	p.V272M	Sub - Missense	DBD	1	2.22

Table 3.2: *TP53* variants detected in lung SCC.

Somatic mutations on *TP53* gene were indicated with the respective COSMIC IDs, coding DNA sequence (CDS) mutations and amino acid (AA) mutations for each mutation were shown (Sub – substitution mutation; CS – coding silent mutation). The region whereby the mutation was detected was identified (DBD – DNA-binding domain; Proline-rich – proline-rich domain; Oligo – oligomerization domain). The frequency and percentage of the indicated mutation across 45 lung SCC samples were displayed.

Summary of findings in Chapter 3.1:

- *KRAS*, *PIK3CA*, *AKT1*, *MTOR* and *RB1* mutations are rare in lung SCC.
- High mutation frequencies in *ALK*, *TP53*, *CDKN2A* and *EGFR* genes across all samples were detected.
- A COMSIC mutation on *ALK* gene that resulted in A1491R was detected in high frequency in lung SCC.
- A common intronic substitution on *CDKN2A* gene was detected with unknown impact on the translated protein.
- Both codon substitutions on *EGFR* gene resulted in silent mutations that do not affect the functions of EGFR.
- Despite the high mutational count on *TP53*, no common COSMIC mutation was detected among all samples.
- ~50% of *TP53* mutations found in lung SCC are located on the region encoding the DNA-binding domain.
- Paucity of targetable driver mutations in lung SCC.

3.2 Transcriptional and translational diversities amongst lung SCC cell lines

3.2.1 Somatic mutations in lung SCC cell lines

Our genomic analyses in Chapter 3.1 had demonstrated a paucity of driver mutation in lung SCC, which tallied with the findings by TCGA Research Network (Network 2012). The presence of somatic mutations in the panel of lung SCC cell lines was investigated. Genomic aberrations of the selected cell lines were curated based on the COSMIC Database. As shown in Table 3.3, 5 of the 10 SCC lines are reported with codon deletions on the *CDKN2A* gene (SW900, H2170, H520, SK-MES-1, H226), 2 have mutated *KRAS* (SW900, Calu-1), while mutated *RB1* and *PIK3CA* are observed in only 1 cell line (H596). All the selected cell lines, except for H2066 where its information is not available on the database, have wild-type *EGFR* and *BRAF* genes.

TP53, an important tumour-suppressor gene, usually determines treatment response to various chemotherapeutic agents. However, based on the COSMIC database, there are conflicting reports on the mutation status of *TP53* gene in 3 of the cell lines (H2170, ChaGo-k-1 and H226). Sanger sequencing was performed to determine the somatic mutations of *TP53* in all cell lines (Table 3.4). The sequencing data confirmed that H226 has wild-type *TP53*; Calu-1 is a p53-null cell; while the remaining 8 cell lines contain substitution mutations along the *TP53* gene. Among those with single-nucleotide substitutions, 5 of them result in missense mutations (in H596, H1869, H2170, H2066 and ChaGo-k-1) that produce altered amino acid along the DNA-binding domain of the p53 molecules (Table 3.4). The remaining 3 lines (H520, SK-MES-1 and SW900) have nonsense mutations that lead to the production of truncated p53 (Table 3.4).

Collectively, it was verified that 9 out of the 10 lung SCC cell lines have aberrations in *TP53* gene, 5 have mutated *CDKN2A* gene, while mutations at *EGFR*, *KRAS*, *RB1* and *PIK3CA* genes are rare. These observations demonstrated the lack of driver oncogenic mutation in these cell lines. Taken together, the genomic characterization of the selected SCC cell lines are comparable to that of the actual SCC, suggesting that these cell lines are suitable study models to represent the disease for further investigations.

	Gene	CDS mutation	AA mutation
SW900	*CDKN2A*	c.1_471del471	p.0?
	CDKN2a(p14)	c.1_522del522	p.0?
	KRAS	c.35G>T	p.G12V
	NF1	c.889_8520del7632	p.?
	TP53	c.499C>T	p.Q167*
	EGFR	- (Wildtype)	- (wildtype)
	BRAF	- (Wildtype)	- (wildtype)
H2170	*CDKN2A*	c.1_471del471	p.0?
	CDKN2a(p14)	c.1_522del522	p.0?
	TP53	c.472C>G	p.R158G
		- (Wildtype)	- (wildtype)
	EGFR	- (Wildtype)	- (wildtype)
	BRAF	- (Wildtype)	- (wildtype)
H520	*CDKN2A*	c.134delG	p.G45fs*8
	TP53	c.438G>A	p.W146*
	EGFR	- (Wildtype)	- (wildtype)
	BRAF	- (Wildtype)	- (wildtype)
SK-MES-1	*CDKN2A*	c.1_471del471	p.0?
	CDKN2a(p14)	c.1_522del522	p.0?
	TP53	c.892G>T	p.E298*
	EGFR	- (Wildtype)	- (wildtype)
	BRAF	- (Wildtype)	- (wildtype)
ChaGo-k-1	*STK11*	c.167G>T	p.G56V
	TP53	c.97-1G>C	p.?
		c.824G>T	p.C275F
	EGFR	- (Wildtype)	- (wildtype)
	BRAF	- (Wildtype)	- (wildtype)
H596	*PIK3CA*	c.1633G>A	p.E545K
	RB1	c.541_542insT	p.S182fs*3
	TP53	c.733G>T	p.G245C
	MET	c.3082+1G>T	p.?
	EGFR	- (Wildtype)	- (wildtype)
	BRAF	- (Wildtype)	- (wildtype)
H1869	*TP53*		p.M237I
	BRAF	- (Wildtype)	- (wildtype)
H226	*CDKN2A*	c.1_150del150	p.?
	TP53	c.998C>G	p.P309A
		- (Wildtype)	- (wildtype)
	EGFR	- (Wildtype)	- (wildtype)
	BRAF	- (Wildtype)	- (wildtype)
Calu-1	*KRAS*	c.34G>T	p.G12C
	EGFR	- (Wildtype)	- (wildtype)
	BRAF	- (Wildtype)	- (wildtype)
H2066	Not Available		

Table 3.3: Somatic mutations of lung SCC cell lines as stated on COSMIC database.

All coding DNA sequence (CDS) mutations and amino acid (AA) mutations curated by the database are displayed, while *EGFR* and *BRAF* are included. **Genes with conflicting reports on mutation status are highlighted in yellow**. **Cell line with no available information on the database is highlighted in green**.

	CDS mutation		AA mutation	
SW900	c.499C>T	Substitution	p.Q167*	Substitution - Nonsense
H2170	c.472C>G	Substitution	p.R158G	Substitution - Missense
H520	c.438G>A	Substitution	p.W146*	Substitution - Nonsense
SK-MES-1	c.892G>T	Substitution	p.E298*	Substitution - Nonsense
ChaGo-k-1	c.824G>T	Substitution	p.C275F	Substitution - Missense
H596	c.733G>T	Substitution	p.G245C	Substitution - Missense
H1869	c.711G>A	Substitution	p.M237I	Substitution - Missense
H2066	c.467G>T	Substitution	p.V157F	Substitution - Missense
H226	Wild-type			
Calu-1	Deletion			

Table 3.4: Mutational status of *TP53* in lung SCC cell lines.

Sanger sequencing was performed to verify the mutations on *TP53* gene through amplication of the ORF region by using both 5' and 3' primers. Both CDS mutations and AA mutations are tabulated.

3.2.2 Comparative analysis on expression of cancer-related proteins in lung SCC cell lines

The high frequencies of *TP53* mutations and the rarity of *EGFR* and *KRAS* aberrations among SCC were shown in Table 3.3 and 3.4. The abundance of p53 and EGFR were examined at the protein level. Three normal lung fibroblast cell lines (MRC5, IMR90, WI-38) were included as controls for comparison between malignant and non-malignant cells. All three normal fibroblast lines and H226, that have wild type p53, expressed low quantity of p53. Cell lines with missense mutation on p53 (H2066, H2170, H1869, ChaGo-k-1, H596) had high expression of p53, while p53-null cell (Calu-1) and p53-nonsense mutation cell (SW900, H520, SK-MES-1) do not express full-length p53 (Figure 3.2). Expression of EGFR was high in H2170 cell, undetected in H2066, SW900 and H1869, and consistent low in other cell lines. Interestingly, none of these cell lines expressed phosphorylated EGFR (Data not shown).

Mutations and altered expressions of HDACs have been related to tumour development through aberrant regulation of cellular functions such as cell proliferation and cell death (Glozak and Seto 2007). Furthermore, several class I and class II HDACs have been associated with prognosis of lung cancer (Osada, Tatematsu et al. 2004, Minamiya, Ono et al. 2011). To better understand the mode-of-action of belinostat, a pan-HDAC inhibitor, the basal expression of HDACs was determined. There are four main classes of HDACs. Here, the expression levels of representative HDAC from class I (HDAC 1, 2, 3), class II (HDAC 4, 6) and class III (Sirtuin-1) were examined. Expression levels of HDACs were consistent in all three normal fibroblast cells (Figure 3.2), while both HDAC 1 and 2 were universally overexpressed in all SCC lines. In relative to normal fibroblast, HDAC 3 had lower expression in SW900, H1869, ChaGo-k-1, H596, and H226; HDAC 4 was highly expressed in H520 and ChaGo-k-1 but lowly expressed in H1869; reduced expression of HDAC 6 was detected in most lung SCC cell lines except for H2170, H520 and SK-MES-1; Class III HDAC, Sirtuin-1, was highly expressed in H520, but found in low abundance in H1869, H596 and H226 (Figure 3.2). H1869 was found to have minimal expression of HDAC 3, 4, 6 and Sirtuin-1.

The results here showed the basal expression of p53, a tumour suppressor protein, EGFR, a commonly altered receptor in NSCLC, and various HDACs. The abundance of p53 molecules corresponded to the mutational status among the lung SCC cell lines, as shown by the accumulation of p53 in cell lines harbouring *TP53* mutation. Basal expression of HDACs, however, was less predictable in these cell lines.

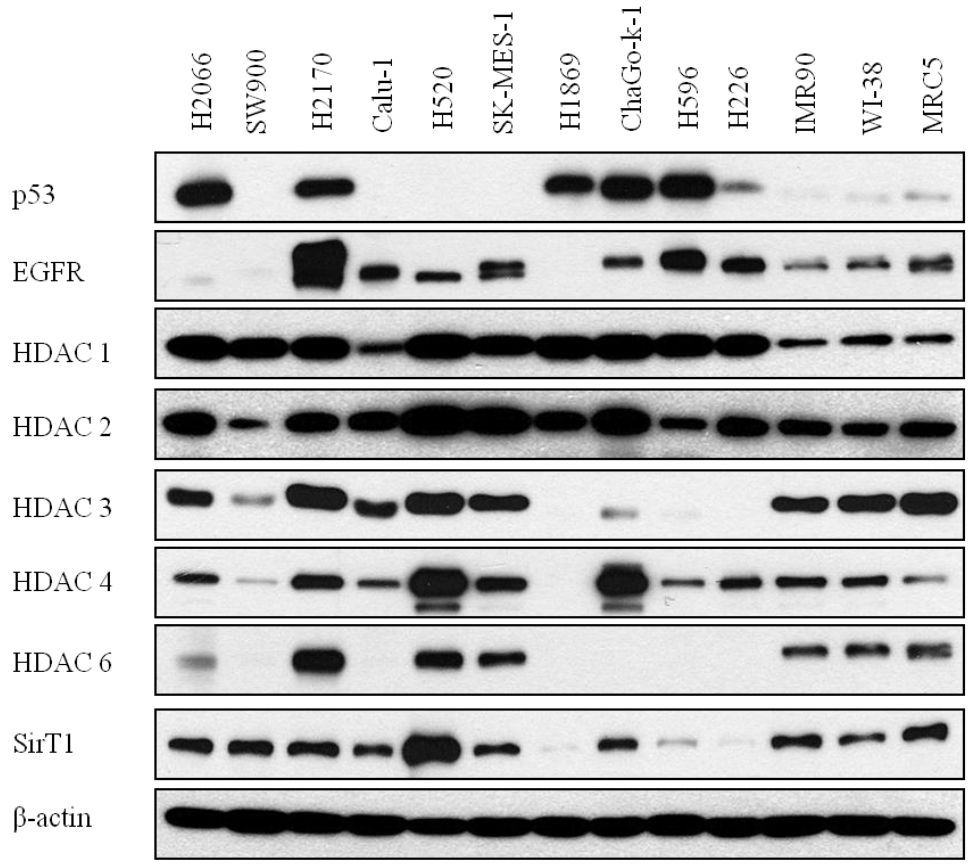

Figure 3.2: Basal expression of p53. EGFR and HDACs in lung SCC and normal lung fibroblast cell lines.

Western blot analyses were performed on protein lysates harvested from all selected cell lines. Western blot data shown are representative of three independent experiments for the indicated targets with β-actin as input control.

Summary of findings in Chapter 3.2:

- *EGFR*, *KRAS*, *RB1* and *PIK3CA* mutations are rare in lung SCC cell lines.
- 5 of the 10 cell lines have *CDKN2A* mutation.
- 1 cell line (Calu-1) is p53-null.
- 8 cell lines have mutations on *TP53* gene: 5 of these mutations encoded for p53 with aberrations on DNA-binding domain.
- The 5 cell lines with missense *TP53* mutation expressed high levels of p53.
- HDAC1 and HDAC2 are highly expressed in all lung SCC cell lines.
- Lung SCC cell lines have differential expression of EGFR, HDAC3, HDAC4, HDAC6 and SirT1.
- Paucity of targetable driver mutations in lung SCC cell lines.
- This panel of cell lines has comparable genomic characteristic to lung SCC.

3.3 Cytotoxicity and synergy of cisplatin and belinostat in lung SCC cell lines

3.3.1 Drug sensitivity under anchorage-dependent condition

The *in vitro* sensitivities of cisplatin, the first line treatment for lung SCC, and belinostat, a pan-HDAC inhibitor, in the selected lung SCC cell lines were next determined. 10-tumour-derived lung SCC and 3 normal lung fibroblast-derived cell lines were utilised as the initial study panel. Within this study panel, the effects of cisplatin and belinostat were quantified by determining the half-maximum inhibitory concentration (IC_{50}) of each drug via cell proliferation assay. It was observed that lung SCC cells have variable sensitivities to both agents. In relation to cisplatin, 4 cell lines (H596, H1869, H226, ChaGo-k-1) have IC_{50} < 10μM (classified as cisplatin-sensitive) and the remaining 6 cell lines have IC_{50} > 10μM (classified as cisplatin-resistant) (Figure 3.3 A). All 3 normal fibroblast lines were more sensitive to cisplatin with IC_{50} < 5μM.

A similar approach was performed to evaluate sensitivity to belinostat with IC_{50} < 2μM designated as belinostat-sensitive and IC_{50} > 3μM as –resistant (Figure 3.3 B). Interestingly, belinostat has stronger repressive effects on the proliferation of cisplatin-resistant cells (H2066, SW900, SK-MES-1, H2170, H520, and Calu-1) as well as the normal fibroblast lines. Cisplatin-sensitive cells responded poorer to belinostat. These data suggested that the lung SCC cell lines exhibit reciprocally inverse sensitivities towards cisplatin and belinostat.

To measure the synergistic effects between cisplatin and belinostat, combination index (CI) was calculated based on Chou and Talalay's method for synergy quantification (Chou and Talalay 1984). The average CI for effective dose in 50% to 80% of the population (ED_{50}-ED_{80}) was determined. CI values lower that ED_{50} will not be optimal for drug efficacy studies, while values higher that ED_{80} will be impractical in term of clinical relevance. The average CI suggested that synergistic combination was achieved in all normal fibroblast lines and most SCC lines (CI < 0.80), with the exception of ChaGo-k-1 and H2066 whereby additivity effects were achieved (CI = 0.88, 1.02 respectively) (Figure 3.3 C)

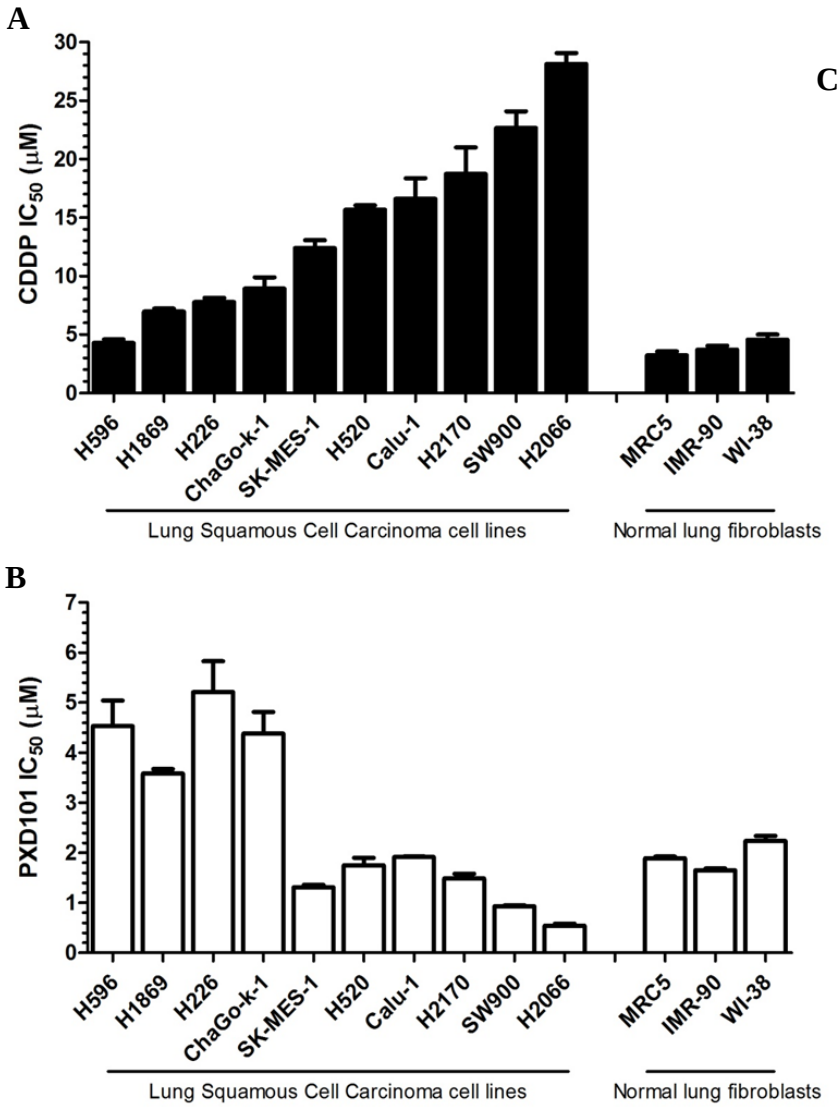

C

	CI (ED_{50}-ED_{80})	
	average	**std. dev.**
SK-MES-1	0.45	0.06
Calu-1	0.54	0.05
H520	0.55	0.07
H2170	0.60	0.04
SW900	0.63	0.01
H596	0.68	0.02
H1869	0.72	0.08
H226	0.74	0.02
ChaGo-k-1	0.88	0.03
H2066	1.02	0.05
MRC5	0.72	0.09
WI-38	0.74	0.12
IMR90	0.82	0.07

Figure 3.3: Lung squamous cell carcinoma cell lines exhibit differential *in vitro* sensitivities to cisplatin and belinostat.

Lung SCC cells and normal lung fibroblast cell lines were drug treated for 72 hours and cell viability assay (MTS) was used to determine the IC_{50} of cisplatin (A) and belinostat (PXD101) (B). Data are presented as mean ± SD (n = 3). C, Combination index (CI) of cisplatin/belinostat for lung SCC cell lines in anchorage-dependent conditions. The nature of drug interaction is defined as synergism (CI < 0.8), additive effect (0.8 < CI < 1.2), and antagonism (CI > 1.2). Data are presented as mean ± SD (n = 3).

3.3.2 Drug sensitivity under anchorage-independent condition

Anchorage-independent cell growth is a marker of the hallmark of oncogenic transformation, as it indicates the ability of the tumour cells to survive and proliferate in the absence of solid substratum, extra-cellular matrix and cell-cell contact (Mori, Chang et al. 2009). It is widely considered as the most accurate and stringent *in vitro* measurement of malignant transformation in tumour cells.

Anchorage-independent growth of lung SCC cells in the presence of drug treatment were performed using soft agar colony forming assay to determine the sensitivities of cisplatin and belinostat in the absence of anchorage. Across the 5 tested cell lines (H226, H520, H2170, Calu-1 and ChaGo-k-1), cisplatin strongly inhibited colony formation of H226 and ChaGo-k-1 cells with IC_{50} < 100nM. The remaining three lines (H2170, ChaGo-k-1) were more resistant to cisplatin (Figure 3.4 A). Inhibitory effects of belinostat in lung SCC cells were determined with the similar approach. H226 and H2170 responded better to belinostat with IC_{50} < 400nM while ChaGo-k-1, Calu-1 and H520 had IC_{50} > 400nM (Figure 3.4 B).

The calculated average CI at ED_{50}-ED_{80} indicated that the combined treatment of cisplatin and belinostat demonstrated additivity in all five lung SCC lines under anchorage-independent condition (Figure 3.4 C). Based on the obtained IC_{50}, the dose reduction index (DRI) was measured to determine the magnitude of dose reduction allowed for each compound when used in dual combination, as opposed to single-drug treatment. Combined treatment (1:1 ratio) showed substantial reduction of cisplatin IC_{50} for H226 (from 70.4nM to 43.9nM; DRI = 1.60), H520 (from 311nM to 204nM; DRI = 1.59) and H2170 (from 213nM to 105.6nM; DRI = 2.42) (Figure 3.4 C, D). Representative images for the dose-dependent inhibition of cisplatin, belinostat and combination treatment in colony forming assay are shown in Figure 3.4 E, F, G, H and I.

Our data indicated that lung SCC cell lines have consistent sensitivities to cisplatin in both anchorage-dependent and –independent conditions (H2170, Calu-1 and H520 as resistant; ChaGo-k-1 and H226 as sensitive). However, in comparison to *in vitro* cell proliferation assay, synergy of belinostat and cisplatin was reduced under anchorage-independent conditions, implying that combinatorial effect of belinostat and cisplatin is more robust under anchorage-dependent condition.

A

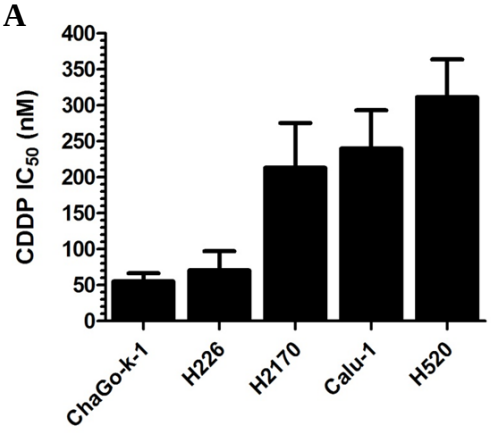

B

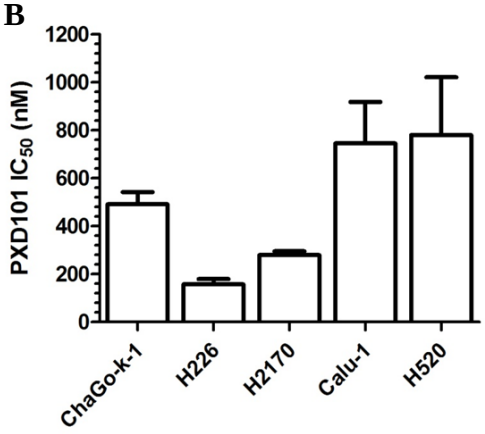

C

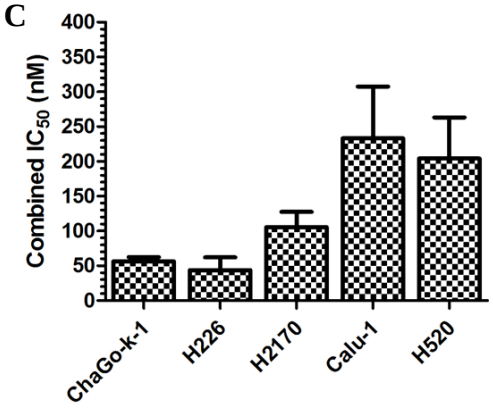

D

	CI (ED50-ED80)		DRI (ED50-ED80)	
	average	std. dev.	average	std. dev.
H2170	0.82	0.18	2.42	0.60
H520	0.91	0.07	1.59	0.19
H226	1.00	0.22	1.60	0.21
ChaGo-k-1	1.05	0.14	1.15	0.24
Calu-1	1.19	0.23	1.31	0.15

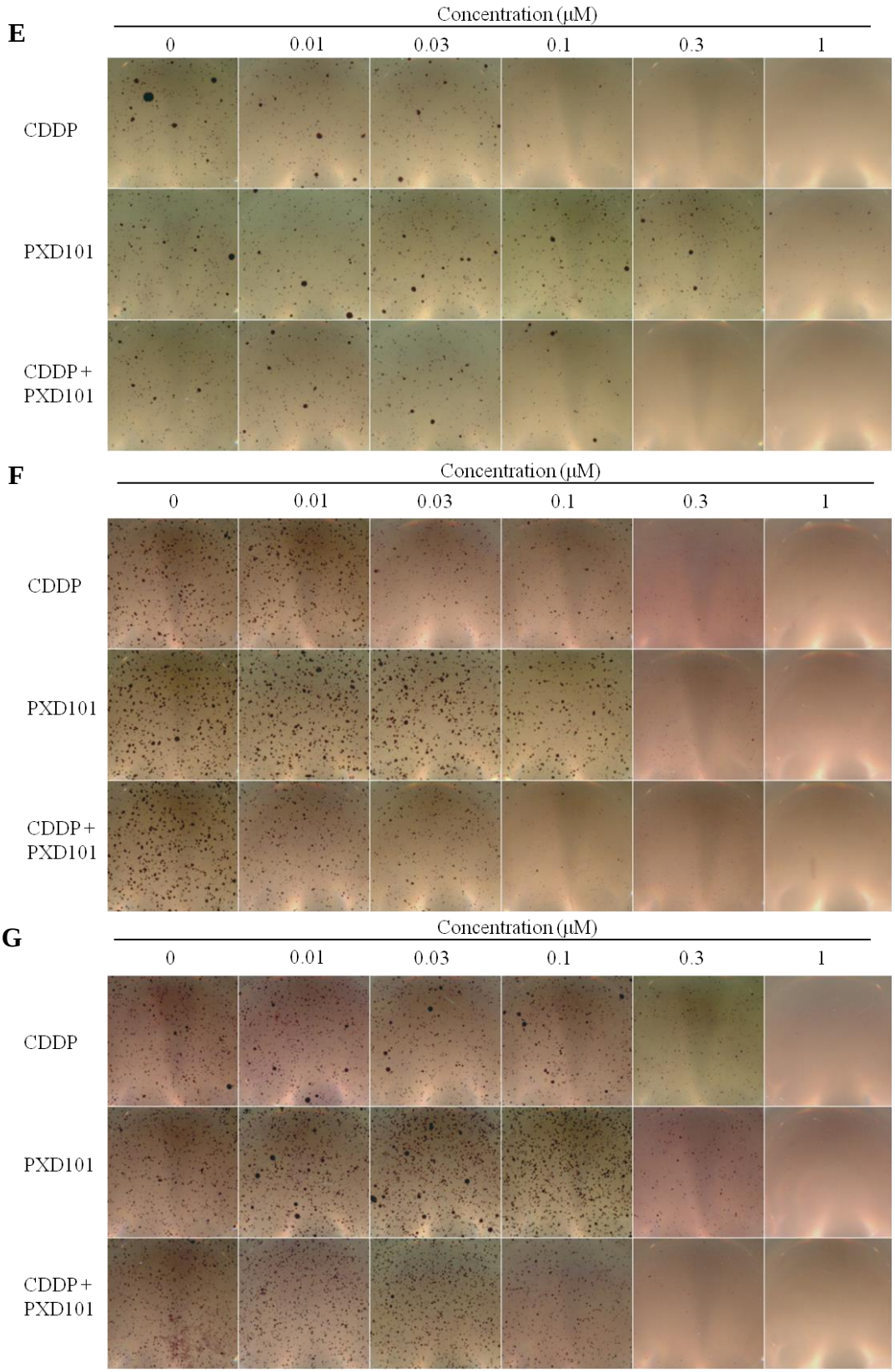
E
Concentration (μM)
0
0.01
0.03
0.1
0.3
1
CDDP
PXD101
CDDP + PXD101
F
Concentration (μM)
0
0.01
0.03
0.1
0.3
1
CDDP
PXD101
CDDP + PXD101
G
Concentration (μM)
0
0.01
0.03
0.1
0.3
1
CDDP
PXD101
CDDP + PXD101

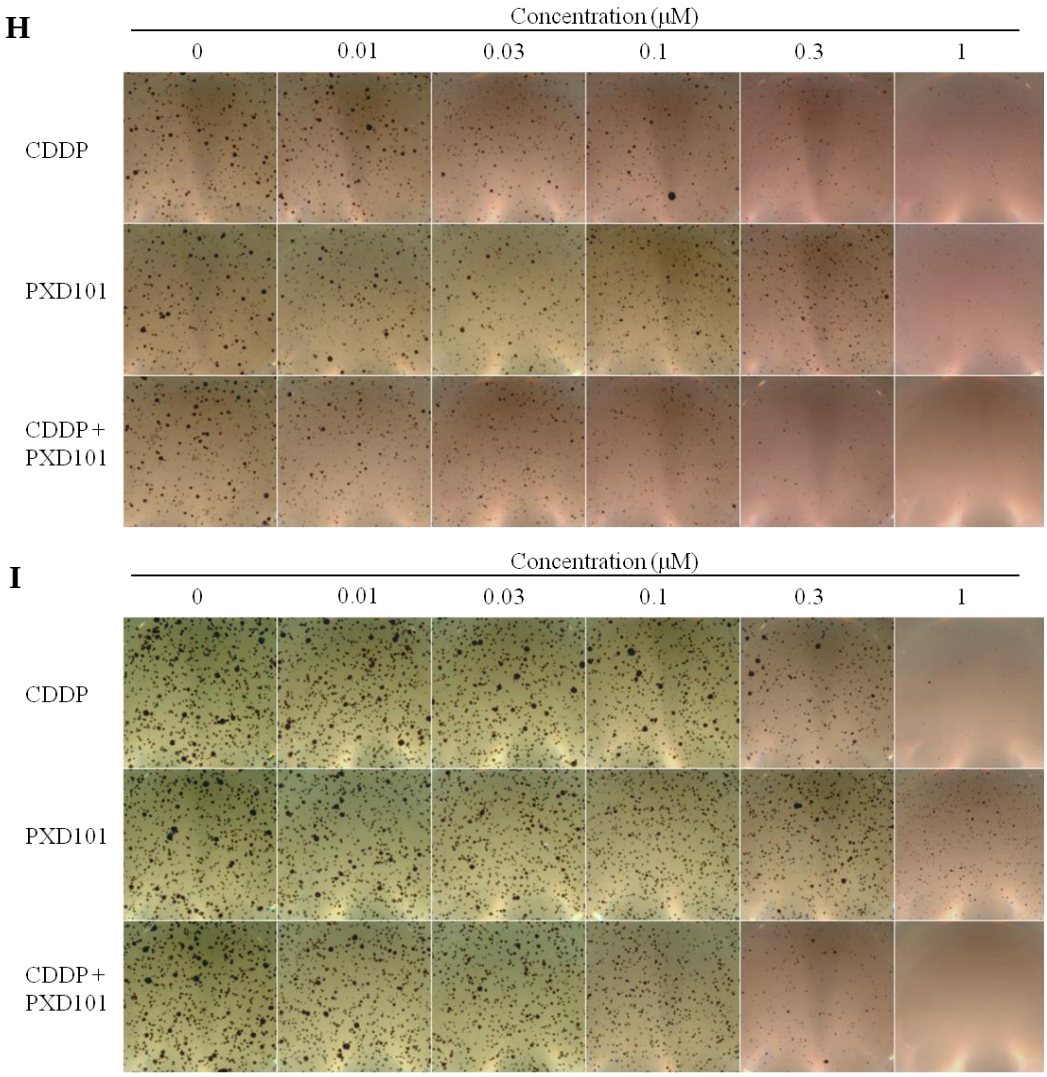

Figure 3.4: Cisplatin and belinostat inhibit malignant transformation in lung SCC cell lines.

Sensitivities of lung SCC cells to cisplatin (A), belinostat (PXD101) (B) and combined treatment (C) in anchorage-independent condition were determined by using soft agar colony forming assay. Belinostat and cisplatin were combined at 1:1 ratio at the indicated doses. Reduction in colony formation was determined by MTT assay. IC_{50} are shown as mean ± SD (n = 3). D, Combination index and dose reduction index of cisplatin for lung SCC cell lines in soft agar assay are assessed. The nature of drug interaction is defined as synergism (CI < 0.8), additive effect (0.8 < CI < 1.2), and antagonism (CI > 1.2). Data are presented as mean ± SD (n = 3). Representative images for colony formations and dose-dependent colony inhibition in ChaGo-k-1 (E), H226 (F), H2170 (G), Calu-1 (H) and H520 (I) cell lines are presented.

3.3.3 Belinostat induces histone acetylation in lung SCC cells

HDAC inhibitors have been reported to promote cytotoxicity via transcriptional and post-translational modifications, but the precise mechanim(s) remain elusive. To understand the mode-of-action of belinostat in lung SCC, the expression of its downstream substrates (HDACs) was determined. Belinostat is a pan-HDAC inhibitor that is known to interfere with HDAC function by inhibiting its catalytic activity. This promotes the acetylation of lysine residues along the histone tails. Core histones such as H3 and H4 form tetrameric nucleosomes, which are essential for the helical structure of DNA (Luger, Mäder et al. 1997). Acetylation of H3 and H4 increases chromatin accessibility, and is associated with active transcription (Jenuwein and Allis 2001).

To prove the efficacy of belinostat in the panel of lung SCC cell lines, Western blotting was performed to verify the acetylation of H3 and H4 after belinostat treatment. H3 and H4 were extracted through acidic purification, as acid could prevent denaturation of histones and provide higher yield. The data showed that belinostat induced acetylation of both H3 (Lys9/Lys14) and H4 in all 4 tested lung SCC lines (H2170, Calu-1, H226, and H596). Low dose of belinostat (0.1μM) was sufficient to acetylate histone tails (Figure 3.5).

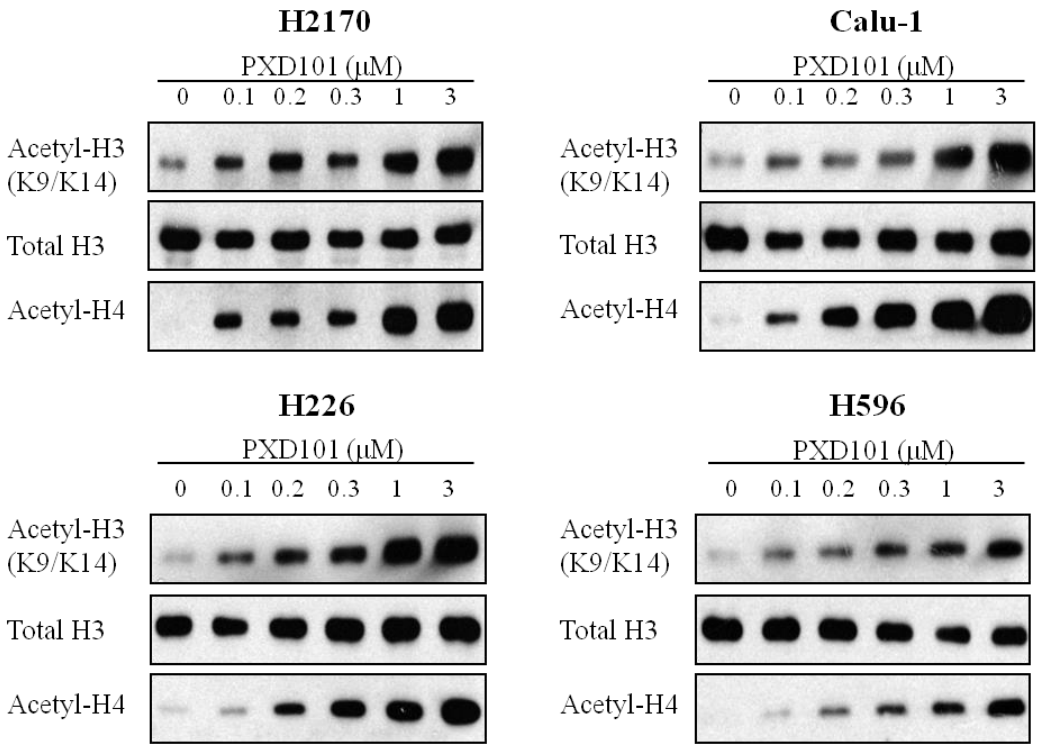

Figure 3.5: Belinostat induces dose-dependent acetylation of H3 and H4 in lung SCC cells.

Western blot analyses were performed on H3 and H4 in H2170, Calu-1, H226 and H596 after belinostat (PXD101) treatment (0.1, 0.2, 0.3, 1, 3μM) with DMSO as vehicle control. Histones were purified through acid extraction. Western blot data shown are representative of three independent experiments for the indicated targets with total H3 as input control.

Summary of findings in Chapter 3.3:

- Lung SCC cell lines displayed differential drug sensitivities to cisplatin and belinostat under both anchorage-dependent and –independent conditions.
- H2066, SW900, SK-MES-1, H2170, H520, and Calu-1 were classified as cisplatin-resistant cells.
- H596, H1869, H226, and ChaGo-k-1 cells were classified as cisplatin-sensitive cells.
- Belinostat had stronger cytotoxic effects on cisplatin-resistant cells.
- Cisplatin and belinostat showed synergistic combination in lung SCC cell lines.
- Most cisplatin-resistant cell lines showed good synergy (CI < 1) when cisplatin and belinostat treatments were combined.
- Belinostat induced H3/H4 acetylation in dose-dependent manner.

3.4 Comparative transcriptomic of cisplatin-sensitive and –resistant lung SCC cells

One key focus of this project was to analyse the transcriptomes of cisplatin-resistant and –sensitive cell lines. Gene expression profiling using the Affymetrix GeneChip 1.0ST microarray was conducted and analysed by GeneSpring Software V12. Basal transcriptome profiles were obtained for each cell lines and clustered into study sets according to their IC_{50} towards cisplatin (H596, H1869, H226, ChaGo-k-1 as sensitive; Calu-1, H2170, SW900, H2066 as resistant). To investigate the possible mechanisms that participate in cisplatin resistance, the gene expressions of the resistant study set was compared to that of the sensitive study set (fold change > 1.5; $P < 0.1$). Within the cisplatin-resistant study set, 756 genes were found to be up-regulated while 804 genes were down-regulated (Appendix 1 and 2). Heat map for all altered genes > 3 fold was shown with cell lines displayed in column and group by cisplatin-response phenotype (Figure 3.6 A). The microarray data was validated by performing qPCR on selected genes. Among the enriched genes, *GPX2* was verified to be highly expressed in two cisplatin-resistant lines (H2170 and H2066), while *MGST1* was barely detected in two cisplatin-sensitive lines (H226, ChaGo-k-1) (Figure 3.7 B). Among the down-regulated genes, *FAS*, *DRAM1*, *PARP9*, *PARP14*, and *XAF1* genes were consistently down-regulated in cisplatin-resistant lines, while *TP53* was highly expressed in H2066 and all cisplatin-sensitive lines (Figure 3.6 C).

Both gene lists were subjected to KEGG pathway mapping via DAVID Bioinformatics Resources 6.7 ($p < 0.1$). This analysis mainly focused on the identification of genomic homogeneity (among cell lines with similar responses to cisplatin) and heterogeneity (across cell lines with different responses to cisplatin). Among the genes that were down-regulated in the resistant study set, several pathways with biological relevance to tumourigenesis were identified by the database: p53 signalling pathway (*TNFRSF10B*, *CCND2*, *SERPINE1*, *CASP8*, *TP53*, *SFN*, *FAS*, *IGFBP3*, *PTENP1*), apoptosis (*TNFRSF1A*, *IL1R1*, *TNFRSF10B*, *IL1RAP*, *CASP8*, *TP53*, *NFKB1*, *BCL2L1*, *FAS*, *BIRC3*), and MAPK signalling pathway (*EGFR*, *FGFR2*, *IL1R1*, *PDGFA*, *FGF9*, *NF1*, *TP53*, *CACNB3*, *NFKB1*, *DAXX*, *FLNB*, *TNFRSF1A*, *BDNF*, *DUSP1*, *MAPK13*, *RASGRP1*, *HSPB1*, *FAS*, *FGF2*, *MAP3K13*, *DUSP7*, *RASA2*) (Table 3.5). Interestingly, among those genes enriched in the resistant cell lines, pathway analysis revealed several biological terms that are related to glutathione metabolism (*GSTM1*, *GSTA1*, *GPX2*, *GSTM2*, *GSR*, *GSTM3*, *GSTA4*, *G6PD*, *GSTO1*, *GCLM*, *MGST1*, *GSTP1*), metabolism of xenobiotics by cytochrome P450 (*GSTM1*, *AKR1C3*, *GSTA1*, *GSTM2*, *AKR1C2*, *GSTM3*, *GSTA4*, *GSTO1*, *MGST1*, *GSTP1*), and drug metabolism (*GSTM1*, *GSTA1*, *GSTM2*, *GSTM3*, *GSTA4*, *AOX1*, *GSTO1*, *MGST1*, *GSTP1*) (Table 3.6). The data implied that cisplatin resistance could be related to suppression of tumour suppression (p53) and apoptotic signals, with increased in drug metabolism.

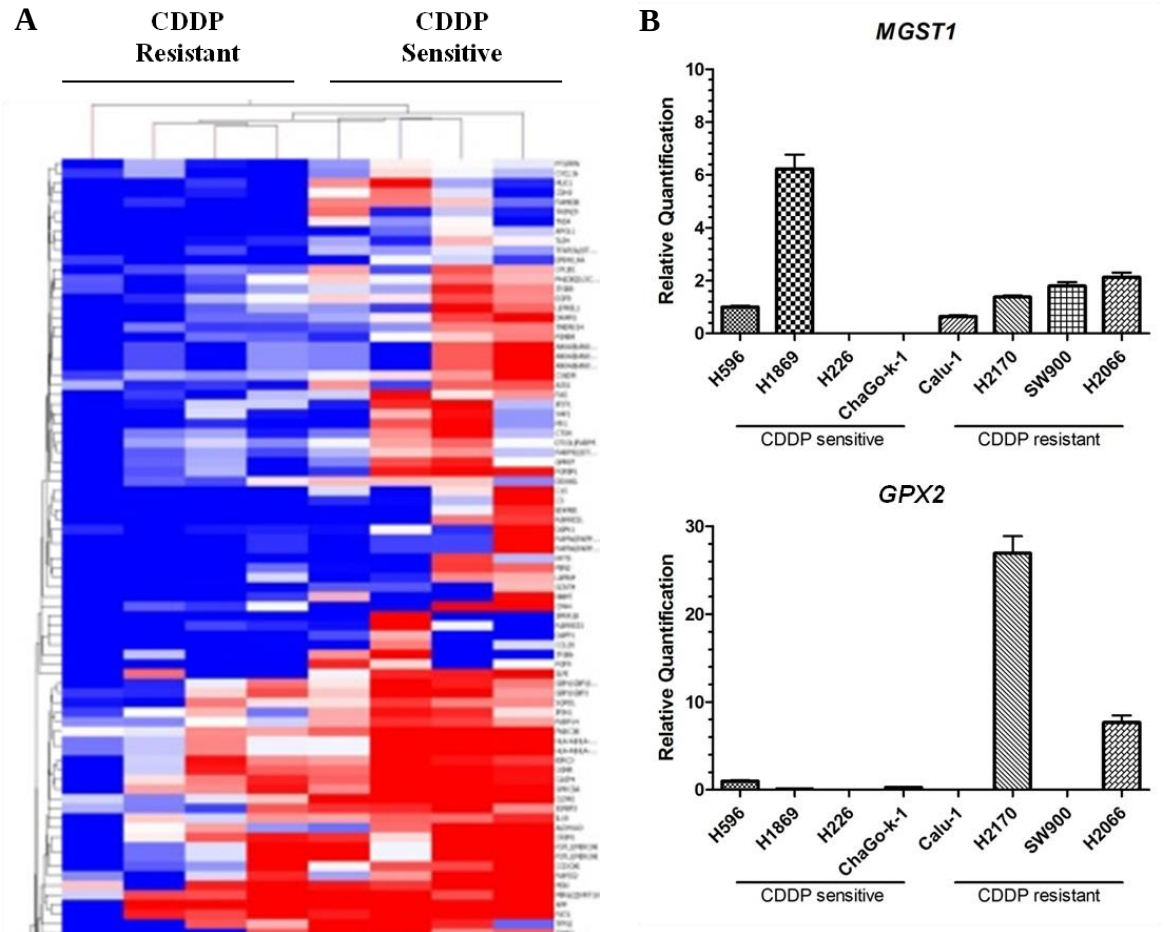
A
CDDP Resistant
CDDP Sensitive
B
MGST1
Relative Quantification
10
8
6
4
2
0
H596
H1869
H226
ChaGo-k-1
Calu-1
H2170
SW900
H2066
CDDP sensitive
CDDP resistant
GPX2
Relative Quantification
30
20
10
0
H596
H1869
H226
ChaGo-k-1
Calu-1
H2170
SW900
H2066
CDDP sensitive
CDDP resistant

C

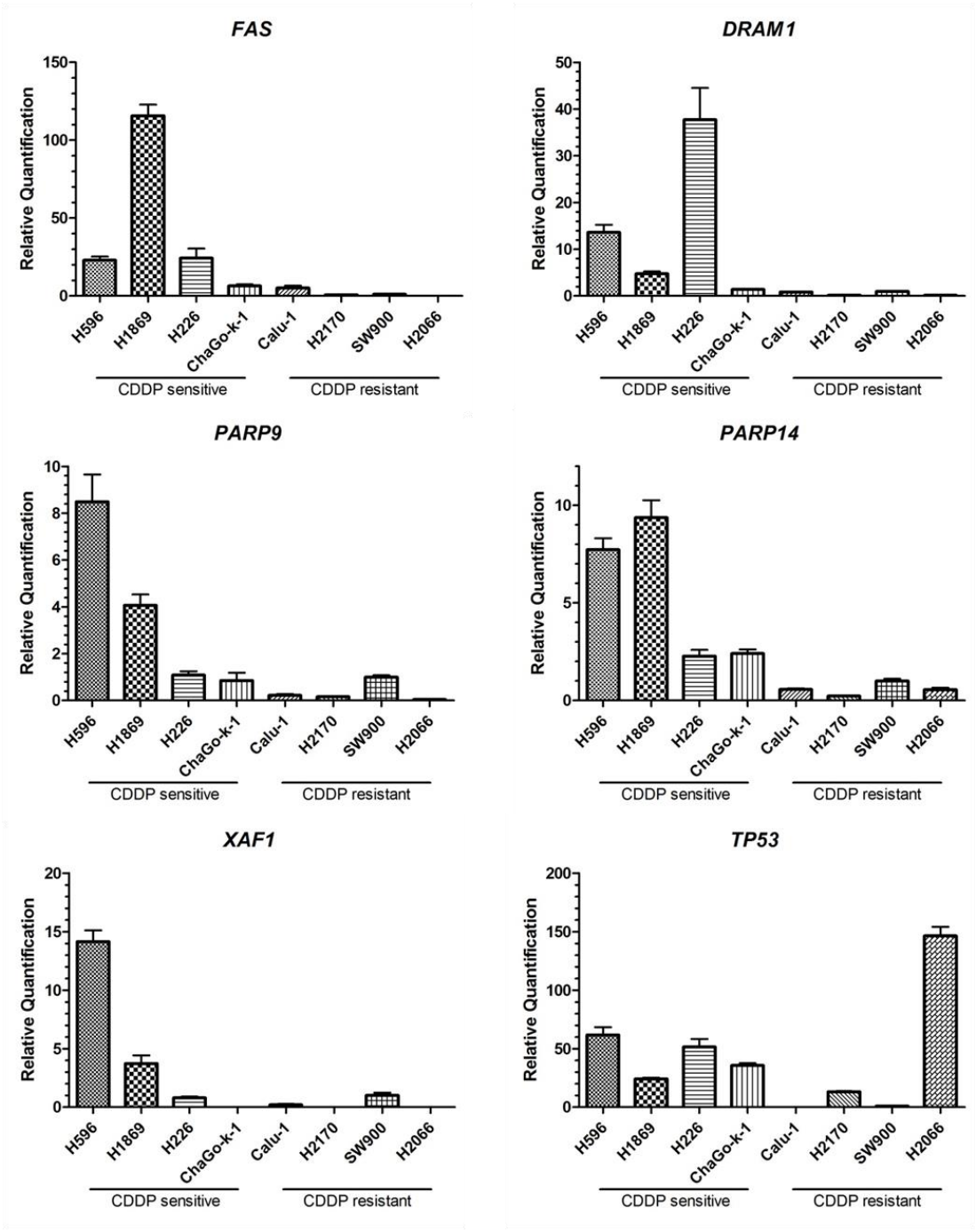

Figure 3.6: Comparative transcriptomic analysis of cisplatin-sensitive and –resistant phenotypes.

Gene expression profiling was performed on cisplatin-sensitive (H596, H1869, H226, ChaGo-k-1) and cisplatin-resistant (Calu-1, H2170, SW900, H2066) cell lines. Affymetrix Microarray analysis was performed in technical duplicates. A, Heat map shows the expression of all differentially expressed genes (fold change > 3; $P < 0.05$). Real time qPCR was performed to validate the (B) enriched and (C) suppressed genes in the cisplatin-resistant phenotypes ($n = 1$). SW900 and H596 were used as references for (B) and (C) respectively. Data are shown as an average of triplicates ± SD.

Terms	Genes
Cytokine-cytokine receptor interaction	CXCL1, TNFRSF21, IL1R1, CCL2, CXCL5, OSMR, PDGFA, TNFRSF12A, IL18, CXCL2, CCL5, CCL28, TNFRSF1A, CCL22, CCL20, IL1RAP, FAS, CSF2RA, EGFR, IL6, IL8, LIFR, EDA2R, KDR, INHBA, TNFRSF9, IFNAR2, TNFRSF10B, IL20RB, PRLR, CXCL16, BMP7, BMPR1A
NOD-like receptor signaling pathway	CXCL1, IL6, CCL2, IL8, IL18, CXCL2, NFKB1, BIRC3, CCL5, MAPK13, CASP8, CASP1, TNFAIP3
Focal adhesion	CAV1, PDGFA, ITGB4, VCL, IGF1R, ITGB8, ITGB6, SHC1, ZYX, THBS2, THBS3, EGFR, COL4A1, ITGA3, BIRC3, FLNB, KDR, LAMA4, ITGA6, FYN, CCND2, LAMC2, LAMC1, PTENP1, PARVA
ECM-receptor interaction	COL4A1, DAG1, ITGB4, ITGA3, SDC4, CD47, LAMA4, ITGA6, ITGB8, ITGB6, LAMC2, LAMC1, THBS2, THBS3
Cell adhesion molecules (CAMs)	F11R, ICAM1, PTPRM, CADM1, PTPRF, HLA-A, CLDN22, CDH1, L1CAM, HLA-B, CDH3, HLA-E, SDC4, HLA-F, NCAM2, ITGA6, ITGB8, CLDN1
Pathways in cancer	FGFR2, PDGFA, FGF9, CDH1, NFKB1, BCL2L1, GLI3, IGF1R, CASP8, RALB, FAS, FGF2, CSF2RA, EGFR, IL6, PLD1, COL4A1, EPAS1, IL8, TP53, ITGA3, STAT1, BIRC3, STAT3, WNT2B, DAPK1, LAMA4, ITGA6, ETS1, JAK1, LAMC2, LAMC1, PTENP1
Viral myocarditis	ICAM1, CAV1, CD55, FYN, CASP8, HLA-A, DAG1, HLA-B, HLA-E, CXADR, HLA-F
Adherens junction	EGFR, PTPRJ, IGF1R, PTPRM, PTPRF, FYN, LY6G5B, CDH1, FER, IQGAP1, VCL
Epithelial cell signaling in Helicobacter pylori infection	EGFR, CXCL1, F11R, IL8, LYN, MAPK13, HBEGF, NFKB1, ATP6V0D1, CCL5
Complement and coagulation cascades	CD55, C3, CFB, CD59, SERPINE1, C1R, BDKRB1, SERPINA1, C1S, PLAUR
Small cell lung cancer	LAMA4, COL4A1, ITGA6, TP53, NFKB1, LAMC2, ITGA3, LAMC1, BCL2L1, BIRC3, PTENP1
p53 signaling pathway	TNFRSF10B, CCND2, SERPINE1, CASP8, TP53, SFN, FAS, IGFBP3, PTENP1
Nicotinate and nicotinamide metabolism	NMNAT2, BST1, ENPP3, NT5C3, NNMT
Pancreatic cancer	EGFR, PLD1, RALB, TP53, JAK1, NFKB1, BCL2L1, STAT1, STAT3
Apoptosis	TNFRSF1A, IL1R1, TNFRSF10B, IL1RAP, CASP8, TP53, NFKB1, BCL2L1, FAS, BIRC3
Chemokine signaling pathway	CXCL1, CCL2, LYN, IL8, CXCL5, ADCY6, CXCL2, NFKB1, STAT1, CCL5, CCL28, STAT3, CCL22, CCL20, PTK2B, CXCL16, SHC1
Axon guidance	PLXNB2, EFNB2, NTN4, L1CAM, EPHA2, SLIT2, EPHA3, SLIT3, SEMA5A, EPHA4, FYN, NFAT5, SEMA3C
MAPK signaling pathway	EGFR, FGFR2, IL1R1, PDGFA, FGF9, NF1, TP53, CACNB3, NFKB1, DAXX, FLNB, TNFRSF1A, BDNF, DUSP1, MAPK13, RASGRP1, HSPB1, FAS, FGF2, MAP3K13, DUSP7, RASA2
Graft-versus-host disease	IL6, HLA-A, HLA-B, FAS, HLA-E, HLA-F
Hypertrophic cardiomyopathy (HCM)	IL6, ITGA6, ITGB8, ITGB6, DAG1, ITGB4, CACNB3, ITGA3, TPM2
Melanoma	EGFR, IGF1R, FGF9, PDGFA, TP53, CDH1, FGF2, PTENP1
Hematopoietic cell lineage	CD9, CD55, IL1R1, IL6, ITGA6, CD59, MME, ITGA3, CSF2RA

Table 3.5: Pathway analysis for differential terms/genes down-regulated in cisplatin resistant lines compared with sensitive lines in KEGG databases ($P < 0.1$).

Terms	Genes
Glutathione metabolism	GSTM1, GSTA1, GPX2, GSTM2, GSR, GSTM3, GSTA4, G6PD, GSTO1, GCLM, MGST1, GSTP1
Metabolism of xenobiotics by cytochrome P450	GSTM1, AKR1C3, GSTA1, GSTM2, AKR1C2, GSTM3, GSTA4, GSTO1, MGST1, GSTP1
Drug metabolism	GSTM1, GSTA1, GSTM2, GSTM3, GSTA4, AOX1, GSTO1, MGST1, GSTP1
Systemic lupus erythematosus	HIST1H2AC, HIST1H2BC, HIST1H2BG, C5, HIST1H2BH, SNRPD1, HIST1H4B, HIST2H2BE, HIST2H2BF, SNRPB, HIST1H3B, HIST1H4C, HIST1H3F, HLA-DRA
Valine, leucine and isoleucine degradation	BCAT1, ACAA2, ACADSB, ALDH7A1, AOX1, ACAT1
Nicotinate and nicotinamide metabolism	NNT, ENPP1, AOX1, NT5E
Pyruvate metabolism	ME1, LDHB, ALDH7A1, ACYP1, ACAT1
Bladder cancer	RPS6KA5, KRAS, ERBB2, RB1, MMP1

Table 3.6: Pathway analysis for differential terms/genes up-regulated in cisplatin resistant lines compared with sensitive lines in KEGG databases ($P < 0.1$).

Summary of findings in Chapter 3.4:

- Comparative transcriptomic were performed on cisplatin-sensitive (H596, H1869, H226, ChaGo-k-1) and –resistant (Calu-1, H2170, SW900, H2066) lung SCC cell lines, and followed by KEGG pathway analysis.
- Genes related to apoptosis, p53 signalling pathway and MAPK signalling pathway were down-regulated in cisplatin-resistant cells.
- Genes related to glutathione metabolism, metabolism of xenobiotics by cytochrome P450 and drug metabolism were up-regulated in cisplatin-resistant cells.

3.5 Discussion

3.5.1 The insights of genetic aberrations in lung SCC and tumour-derived cell lines

A key feature that directly contributed to the success of molecularly targeted therapy in lung cancer is the identification of genetic abnormalities. A recent study conducted by TCGA Research Network has comprehensively characterized the genomic alterations in lung SCC, whereby several genomic assays were performed to dissect the somatic mutations and transcriptome expression profiles in each of the 178 samples (Network 2012). This study confirmed the scarcity of *EGFR* and *KRAS* mutations, two commonly observed oncogenic aberrations in lung adenocarcinoma, within SCC. According to this report, *TP53* mutation is commonly detected in lung SCC, while other common genetic aberrations identified include *HLA-A*, *CDKN2A*, *RB1*, *FGFR*, phosphatidylinositol-3-kinase genes, and receptor tyrosine kinase signalling genes (*EGFR* amplification, *BRAF* mutation or *FGFR* amplification). These findings reveal the window of opportunity for personalized therapy in lung SCC. For instance, Hammerman *et. al*. have proposed the use of dasatinib, a multi-kinase inhibitor that has activity on DDR2, on a small subset of SCC harbouring *DDR2* kinase mutation (Hammerman, Sos et al. 2011). Furthermore, few studies have shown that *FGFR1* is more frequently mutated in lung SCC than adenocarcinoma, while demonstrating the efficacy of FGFR inhibitor in this subset of SCC (Weiss, Sos et al. 2010, Dutt, Ramos et al. 2011). These growing evidences facilitated the personalization of effective therapy for lung SCC patients. Despite so, no common oncogene driver mutations have been clearly identified in lung SCC to guide therapy.

In this study, lung SCC specimens were obtained from 45 locally diagnosed cases. Somatic DNA alterations within 15 lung cancer-related genes were characterized by using NGS. Similar to earlier reports (Pacifico and Leone 2007, Network 2012), mutations of *TP53* and *CDKN2A* are commonly detected in lung SCC; while *KRAS*/*HRAS*/*NRAS*, *PTEN*, and *BRAF* mutations are rare (Figure 3.1B). In the study conducted by TCGA, genes related to phosphatidylinositol-3-kinase pathway were found to be mutated in 47% of tumours (Network 2012). Among these samples, however, only 8 samples (17.78%) were found with mutated *PIK3CA*, *AKT1* or *MTOR* (Figure 3.1 A, B). Furthermore, despite detecting at least a codon substitution on *EGFR* gene in 80% of lung SCC, majority of these mutations was soon identified to be silent mutations. Collectively, these implicated the lack of efficacy of EGFR TKIs in lung SCC. As the NGS run was performed on targeted amplification of specific exons, the presence of ALK fusion proteins could not be identified. Despite so, at least one mutated *ALK* variant was detected in every sample (Figure 3.1 B). More importantly, an ALK protein with altered kinase domain (K1491R) was identified as a common mutation (Table 3.1). Mutations at the kinase domain of ALK had been reported to

cause resistance to ALK kinase inhibitor, such as Crizotinib (Choi, Soda et al. 2010, Sasaki, Koivunen et al. 2011, Katayama, Shaw et al. 2012). This finding suggested that lung SCC patients might not respond to ALK inhibitors.

Taken together, these sequencing analyses confirmed the paucity of driver oncogenes in lung SCC. Therefore, targeted therapies with good clinical efficacy in lung adenocarcinoma, such as EGFR and ALK inhibitors, might not be beneficial to these SCC patients. The genetic aberrations of the panel of lung SCC cell lines were found to be comparable to the genetic characterization of lung SCC specimens (Chapter 3.2). Apart from *TP53* gene, mutations on *EGFR*, *KRAS*, *PIK2CA*, *BRAF*, *RB1* and *STK11* are rare in these cell lines. Based on these informations, the selected cell lines are suitable candidates as representative tumour models for lung SCC.

3.5.2 Tumour heterogeneity, clonal evolution and cisplatin sensitivity in lung SCC

One of the major challenges that hinders the progression of curative treatment in solid tumour is the presence of heterogenous sub-clones that are intrinsically different on a molecular level (Driessens, Beck et al. 2012, Turner and Reis-Filho 2012). The two most established aspects of intra-tumour diversity are the existence of metastatic variants and presence of inherently resistant clones (Dexter and Leith 1986). While metastases are generally seen as the more resilient subpopulation that resulted in acquired resistance to chemotherapy, inherently resistant subsets of tumour often result in expansion of more malignant clones. Under therapy intervention, the selection pressure may favour the evolution and proliferation of tumour sub-clones with survival advantages. Thus it is common that after initial response to chemotherapy, tumours relapsed in more aggressive forms and are less responsive to chemotherapy. The main driver of tumour heterogeneity is believed to be DNA mutation. The high mutation rates in lung SCC thus implied for a significant degree of heterogeneity in this disease.

In this study, lung SCC cell lines were shown to exhibit variable *in vitro* sensitivities towards cisplatin, with 5-fold differences distinguishing the most sensitive cell (H596) from the most resistant cell (H2066) (Chapter 3.3.1). This indicated the presence of inherently resistant clones within the selected panel of cell lines. Comparatively, normal lung fibroblast cell lines were less tolerable to cisplatin treatment than the most sensitive lung SCC cell line. This partly explained the adverse side effects experienced by cancer patients treated with cisplatin.

In addition, the capability to grow in anchorage-independent condition could determine the lung SCC cell lines that are more malignantly transformed (Guadamillas, Cerezo et al. 2011). The close correlation of anchorage-independent growth with tumourigenicity in animal models makes it an important assay for investigation of cellular response to anti-tumour drug (Freedman and Shin 1974, Colburn, Bruegge et al. 1978). In the absence of anchorage, only five cell lines were able to form colonies (Chapter 3.3.2), again indicating the lack of homogeneity in lung SCC. Furthermore, these cell lines displayed differential sensitivity to cisplatin, with a trend concordant with anchorage-dependent cell sensitivities (H520, Calu-1 and H2170 cells as cisplatin-resistant).

Collectively, these findings demonstrated the differences in cellular context of these lung SCC cell lines in term of drug sensitivity. The identification of intrinsically drug-resistant cell lines allowed for selection of study models to investigate the cisplatin resistance mechanisms. An important point to note is that apart from somatic mutations, epigenetic factors might initiate and mediate the formation of drug-resistant subclones (Sharma, Lee et al. 2010). In the same study, the authors suggested that epigenetic regulations might resulted in high tolerance to both traditional chemotherapies and targeted therapies (Sharma, Lee et al. 2010). Therefore, restriction of these epigenetic factors by HDAC inhibitor (belinostat) was being investigated in this study.

3.5.3 The therapeutic conundrum of belinostat: promising *in vitro* sensitivity but modest clinical outcome

HDAC inhibitors have displayed strong *in vitro* anti-neoplastic effects in several tumour types. Several studies have demonstrated the combinatorial effect of HDAC inhibitor with chemo- and radiotherapy in lung cancer (Kim, Kim et al. 2010, Owonikoko, Ramalingam et al. 2010), but this present study was the first to focus on the cytotoxicity of HDAC inhibition in lung SCC cells.

Similar to cisplatin treatment, lung SCC cell lines exhibited variable sensitivities towards belinostat treatment (Chapter 3.3.1). Interestingly, cisplatin and belinostat have reciprocal sensitivities in lung SCC, as cell lines identified as cisplatin-resistance were more susceptible to belinostat treatment. Normal lung fibroblast cells were found to have better tolerability to belinostat in relative to the cisplatin-resistant cell lines. Moreover, the combination of both agents appeared to achieve synergy in most cisplatin-resistant lines (Figure 3.3 C). Taken together, this selectivity of belinostat in targeting cisplatin-resistant cell lines clearly emphasized the chemosensitizing effect as well as synergistic cytotoxicity of this pan-HDAC inhibitor in lung SCC cells.

Although the precise mode-of-action of HDAC inhibitors has remained elusive, the accumulation of acetylated histones and transcription factors is well-accepted to be the universal determinants of cellular response to HDAC inhibition (Minucci and Pelicci 2006). The epigenetic regulations of belinostat in lung SCC cell lines were determind with the dose-dependent acetylation of H3 and H4 (Chapter 3.3.3). Intriguingly, the hyperacetylations of histones in both belinostat-sensitive and resistant groups were found to be regulated in a similar manner, suggesting that the belinostat sensitivity might not be dependent on epigenetic alteration of histones (Figure 3.5). Furthermore, belinostat is a pan-HDAC inhibitor that inhibits the class I, II and IV enzymes. While HDAC 1, 2 and 4 are overexpressed in most lung SCC cells, protein levels of HDAC 3, 6 and Sirtuin-1 were found to be differentially expressed (Figure 3.2). Taken together, it is unlikely that the efficacy of belinostat on SCC cell lines could be predicted by determining the expression of histone proteins.

It has been reported that high doses of HDAC inhibitors used in the clinic could lead to extension of DNA damage and impairment of DNA damage repair (Karagiannis, Harikrishnan et al. 2007, Wilson, Holson et al. 2011, Wilson, Lalani et al. 2012). These often result in rapid induction of cell senescence and cell death that are similar to conventional chemotherapeutic agents, which may not be the optimal effects of HDAC inhibitors (Azad, Zahnow et al. 2013). At lower doses, the epigenetic effects of HDAC inhibitors trigger cellular differentiation and reprogramming, while these effects might be compromised when high doses of HDAC inhibitors are used. In truth, despite being tested in multiple phase I and II clinical trials (Glaser 2007), clinical development of HDAC inhibitors remains challenging from the viewpoint of toxicity and exploiting a therapeutic window for tumour control without intolerable adverse event. The usage of HDAC inhibitors at non-toxic doses could possibly offer treatment advantage by alteration of tumour biology instead of immediate induction of cell death.

In comparison with other HDAC inhibitors, belinostat is well tolerated, thus allowed for combination with chemotherapy without causing bone marrow toxicity. Since its development by Topotarget, clinical studies on belinostat have been conducted in haematological and solid malignancies. Data from these studies have demonstrated beneficial anti-neoplastic effects of belinostat as monotherapy in PTCL, CTCL, liver cancer and thymic carcinoma (Giaccone, Rajan et al. 2011, Jain, Zain et al. 2012, Yeo, Chung et al. 2012, Reimer and Chawla 2013). However, similar to other HDAC inhibitors, belinostat as single or combined therapy has minimal anti-tumour effects in advanced solid malignancies (Ramalingam, Belani et al. 2009, Mackay, Hirte et al. 2010, Giaccone, Rajan et al. 2011). As single agents, HDAC inhibitors are generally limited by clinical toxicity while plasma

concentrations achievable in clinical use would likely not reach the amounts required for anti-neoplastic activity in solid tumours. To overcome this pharmacological barrier, the hypothesis is that reduced concentrations of HDAC inhibitors would be sufficient to demonstrate synergism with chemotherapeutic agents and provide adequate therapeutic window for clinical utility. Furthermore, elucidating the mechanisms of synergistic cytotoxicity between belinostat and cisplatin may reveal treatment strategies that are more precise and less toxic.

3.5.4 Comparative analysis of the genetic heterogeneity among cisplatin-sensitive and –resistant phenotypes

Cisplatin is among the most commonly used alkylating cytotoxic agent with a broad spectrum of anti-cancer activity. Furthermore, certain lung SCC clones are intrinsically more resistant to cisplatin (Figure 3.3). This prompted the investigation on the molecular events that determine susceptibility to cisplatin treatment. In order to make broader generalization on the cisplatin resistance mechanisms, the geneotypic homogeneity within each phenotype was determined (by clustering the transcriptomes of resistant/sensitive cell lines as one group), before the transcriptomic diversity across the resistant and sensitive phenotypes was investigated (by comparing the clustered transcriptomes across the two phenotypes) (Chapter 3.4).

Several mechanisms of cisplatin resistance have been proposed that include regulation of drug influx/efflux, increased drug detoxification, increased DNA repair and inhibition of apoptosis. Furthermore, p53 activity had been negatively correlated with the development of cisplatin resistance, as tumour cells with functional wild-type p53 were shown to be more susceptible to cisplatin (Vekris, Meynard et al. 2004). In addition, cell lines with mutated p53 were more tolerable to cisplatin, but could be sensitized when wild-type p53 is genetically introduced (Wang, Li et al. 2005). As the genome wide pathway analysis revealed that p53 signalling could be repressed in cisplatin-resistant phenotype (Chapter 3.4), it was initially believed that p53 status is an important predictive biomarker for cisplatin sensitivity in lung SCC cells. Expectedly, the normal lung fibroblast cells and a lung SCC cell lines with wild-type p53 (H226) were indeed more sensitive to cisplatin. However, most lung SCC cells harboured mutation on *TP53* gene and yet displayed differential sensitivities to cisplatin, strongly suggestive of the presence of other factors that determine cisplatin resistance.

Transcriptomic analysis on lung SCC cell lines further revealed significantly reduced transcriptional activity of MAPK signalling pathway and apoptosis (Chapter 3.4). Several

preclinical studies have suggested that MAPK/p38 signalling could activate downstream Fas/FasL pathway and trigger apoptosis (Mansouri, Ridgway et al. 2003, Brozovic and Osmak 2007). Moreover, suppressed MAPK/p38 activation and FasL expression was associated with cisplatin resistance (Brozovic, Fritz et al. 2004). In the cisplatin-resistant phenotypes, down-regulation of *FAS* gene (Figure 3.6 C) and genes related to MAPK signalling pathway was observed (Table 3.6). These suggested that the cisplatin-resistant lung SCC cells could have an attenuated MAPK signalling as a mean of limiting Fas-induced extrinsic apoptosis, thus reduced cisplatin sensitivity.

Another key regulator of cisplatin resistance is the intracellular accumulation of cisplatin, which is mediated by the balance in drug uptake/efflux as well as drug inactivation. It is known that binding of cisplatin to cytoplasmic scavenger molecules, such as GSH, will reduced the amount of active cisplatin (Kasahara, Fujiwara et al. 1991). In the study models, genes encoding for GSTs (*GSTM1, GSTA1, GSTM2, GSTM3, GSTA4, GSTO1, MGST1, GSTP1*) were predominantly enriched in the resistant phenotypes. High expressions of GSTs probably catalyze GSH synthesis (Lewis, Hayes et al. 1988) and induce detoxification of cisplatin in resistant cells.

These findings allowed for better understanding on the genetic context that may confer cisplatin resistance in lung SCC cells. Through characterizing the transcriptomes of cisplatin-sensitive and –resistant phenotypes, p53 signalling, MAPK signalling, apoptosis pathway and drug detoxification mechanism could be associated to cisplatin resistance in lung SCC cells.

3.5.5 Conclusions and future directions

The lack of driver oncogenic transformation, the molecular heterogeneity of lung SCC cancer cells, together with the pleiotropic nature of the cellular processes within intrinsically resistant clones, have posed a challenging task in the understanding of tumour biology and chemotherapeutic intervention in lung SCC. By using several genomic technologies, the paucity of oncogene-dependency among lung SCC and cell lines was validated. Moreover, the work here provided evidence on the differential drug sensitivities and degree of malignancy among lung SCC cell lines.

In this chapter, several molecular events that could be accounted for the cisplatin-resistant phenotype in lung SCC was reported. However, as drug resistance is multifactorial and tumour is heterogenic, it is likely that several of these events occur simultaneously within an individual tumour, and inhibition of single pathway will not be sufficient to circumvent

cisplatin resistance. At present, it remains unclear which of these molecular events should be preferentially modulated for optimal sensitization of cisplatin efficacy. Thus, the search for more effective treatment strategies is needed. In view of these considerations, targeting the universal downstream transduction signalling of cisplatin-resistant cells could be a more successful strategy. Accumulating evidence suggests that cisplatin-resistance can be sustained by aberrant regulations of signalling cascade, such as the SHC/Grb2/SOS and PI3K/Akt1 signalling (Citri and Yarden 2006). Further investigation will be conducted in Chapter 4 to identify the possible target(s) that favours cellular proliferation under cisplatin treatment.

HDAC inhibitor is an interesting class of anti-neoplastic compound. In line with current knowledge, this study has demonstrated the strong *in vitro* cytotoxicity of belinostat in lung SCC cells (Komatsu, Kawamata et al. 2006, Mukhopadhyay, Weisberg et al. 2006). Despite so, the combinatorial effect of belinostat with cisplatin was somewhat compromised in anchorage-dependent tumour cell. Furthermore, limited clinical efficacy observed in solid tumours has restricted its potential as a blockbuster chemotherapeutic agent. Despite so, the selectivity, specificity and synergy of belinostat in cisplatin-resistant lung SCC lines should not be overlooked. It was hypothesized that belinostat may alter crucial signal transduction pathways that lead to chemosensitization of cisplatin in tumour cells. As such, the chemosensitizing mechanisms of belinostat were elucidated, and novel druggable target(s) that could circumvent cisplatin resistance in Chapter 4 and 5 were identified.

CHAPTER 4 Cisplatin-mediated activation of MAPK: A mechanism of cisplatin resistance in lung SCC

Platinum agents including cisplatin form the backbone of cancer therapy for NSCLC. However, the effectiveness of chemotherapy for NSCLC is limited by eventual development of resistance. In adenocarcinoma of the lung, advances in care have been improved by the development of small molecular inhibitors targeting specific oncogenic signalling. However, cisplatin remains as the most potent of therapeutic compounds and one of the few curative first-line anti-cancer drugs for lung SCC patients due to the lack of oncogenic driver mutation. The development of platinum resistance has limited its clinical efficacy in lung cancer treatment. Patients with metastatic SCC of the lung, in particular, ultimately relapse despite initial response to platinum containing regimens (Schiller, Harrington et al. 2002, Pignon, Tribodet et al. 2008). Combination chemotherapy consisting of platinum compounds has since been established as standard treatment regime based on superior response and survival over single agent therapy (Souquet, Chauvin et al. 1993, Sandler, Nemunaitis et al. 2000). Despite resulting in symptomatic relief and improvement in overall survival, adverse side effects were often greater than those of molecular targeted therapies due to the non-specificity of chemotherapeutic agents (Group 2008). As such, recent therapeutic approach has focused on developing more effective combination with molecular-targeting therapies. Several clinical studies are currently assessing the therapeutic intervention of Onartuzumab (anti-c-Met monoclonal antibody), Necitumumab (anti-EGFR monoclonal antibody) or Bevacizumab (anti-VEGF monoclonal antibody) plus platinum-based chemotherapy in patients with advanced or recurrent lung SCC (ClinicalTrials.gov Identifier NCT01519804, NCT00981058, and NCT00946712).

In Chapter 3, several predictive molecular events corresponding to cisplatin sensitivity in lung SCC cells were described. These events depict a general cisplatin-resistant model with decrease in apoptosis-related signalling pathways and increase in drug metabolic mechanisms. However, this model only partially explains the inherent factors that give rise to intrinsic cisplatin resistance, while the cisplatin-elicited cellular responses remain elusive. As accumulating evidences have reported the involvement of Akt and MAPK signalling pathways in regulating cellular response to cisplatin in several tumour types (Pommier, Sordet et al. 2004, Wada and Penninger 2004, Citri and Yarden 2006), potential druggable kinase targets that could be involved in cisplatin resistance in lung SCC cell lines were examined.

Undoubtedly, the major limitation to clinical efficacy of cisplatin is the high occurrence of chemoresistance. While the synergistic effects of belinostat on several cisplatin-resistant cell

lines was shown (Chapter 3.3.1 and 3.3.2), the mechanisms leading to sensitization for cisplatin treatment have yet to be established. In this chapter, parallel investigations were conducted to: elucidate the signalling transduction pathways that confer cisplatin resistance in lung SCCs; and dissect the potential chemosensitizing mechanism(s) of belinostat. Exploiting the overlapping mechanisms by which lung SCC cells become refractory to cisplatin while remain susceptible to belinostat could reveal not only superior chemosensitization strategies, but also identify novel prognostic and predictive biomarkers.

4.1 Identification of cisplatin resistance mechanisms in lung SCC cells

4.1.1 Transcriptional diversity in sensitive and resistant lung SCC cell lines upon exposure to cisplatin

To identify putative pathways that are modulated differently in cisplatin-sensitive and -resistant cell lines, gene expression profiling was conducted on the representative cell lines under the pressure of cisplatin exposure. Here, cell lines were treated with cisplatin at their respective IC_{50} concentration for a short duration (8 hours) to avoid the induction of apoptosis-related genes, which may mask the intrinsic genetic responses to cisplatin. Micoarrays were performed and the transcriptomes were compared against the basal gene expression profiles obtained in Chapter 3.4.1.

Across the resistant and sensitive study sets, a total of 150 and 382 genes were found to be altered at a fold change of > 1.5 after cisplatin treatment ($P < 0.05$). Among these genes, 123 were commonly mediated in both study sets (Figure 4.1 A). Distinctive genes that were differentially regulated between the resistant (27) and sensitive (259) phenotypes were selected (Figure 4.1 A). The differentially expressed genes are listed in Appendix 3. Heat maps generated based on hierarchical clustering enable direct visualization of the altered genes in cisplatin-resistant (Figure 4.1 B) and –sensitive (Figure 4.1 C) study sets, with the columns displaying differences after cisplatin treatment and paired according to cell lines.

To identify pathways related to cisplatin resistance, KEGG analysis on the significantly modulated gene list was performed ($P < 0.05$) (Appendix 3) by mapping them on the KEGG Pathways database. The database did not identify any relevant pathway among the genes that were up-regulated after cisplatin treatment in both sensitive and resistant study sets. Among the genes suppressed in the resistant cells, pathway related to systemic lupus erythematosus (*HIST1H2AC*, *HIST1H4B*, *HIST1H3B*) was identified (Table 4.1). Interestingly, among the genes suppressed in the sensitive cells, three signalling pathways that were identified to be closely related to tumour cell survival, cell proliferation and cell death: ErbB pathway (*PRKCA, CBLB, GSK3B, SOS2, AKT3*), MAPK pathway (*PRKCA, MAP4K3, NF1, SOS2, RAPGEF2, STK3, AKT3, MAP2K5*), and phosphatidylinositol pathway (*PRKCA*, *INPP4B*, *PIP4K2A*, *ITPR2*) (Table 4.2).

This study revealed the possible involvement of these functional pathways (ErbB, MAPK and phosphatidylinositol pathways) in determining treatment outcome in lung SCC cell lines. Thus, understanding the activation/inhibition of these pathways may provide insights to the mechanisms of cisplatin resistance in lung SCC cell lines.

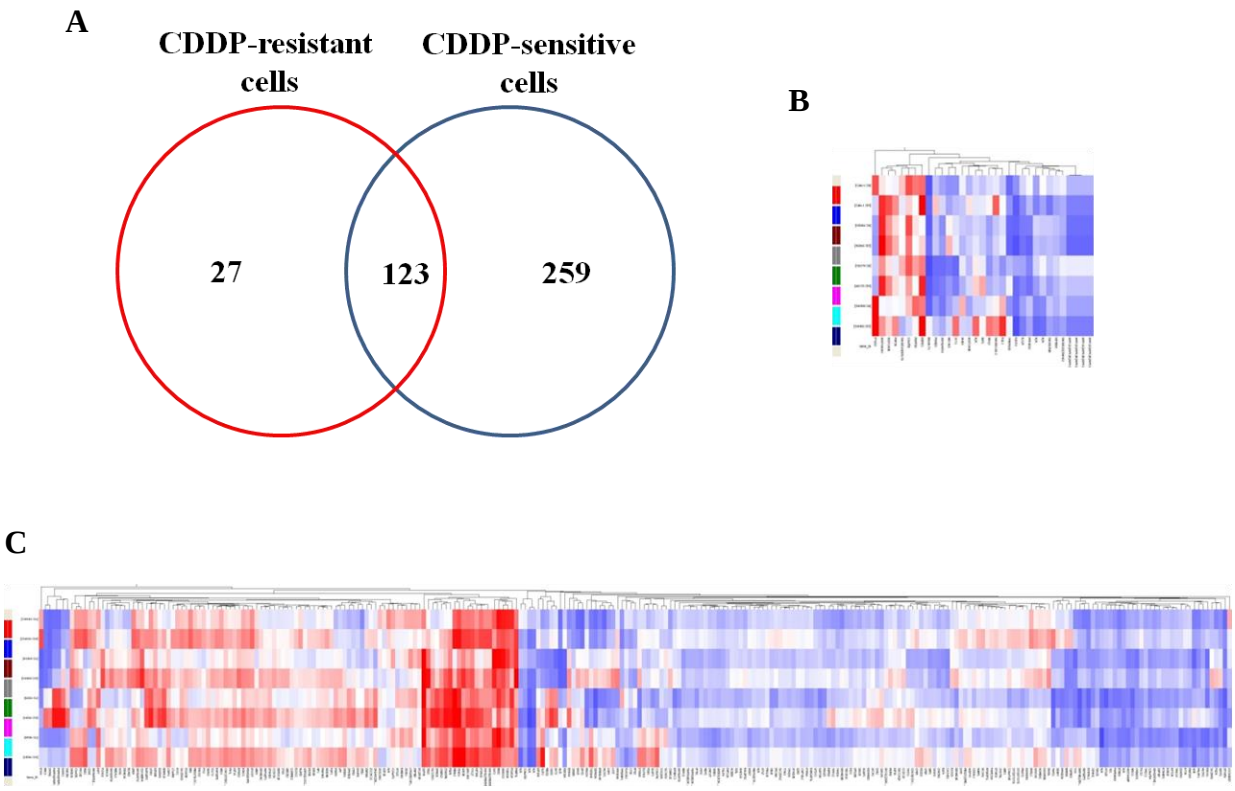

Figure 4.1: Comparative transcriptomic analysis indentifies differentially-regulated pathways in lung SCC cell lines after exposure to cisplatin.

Cisplatin-sensitive (H596, H1869, H226, ChaGo-k-1) and cisplatin-resistant (Calu-1, H2170, SW900, H2066) cell lines were treated with cisplatin at their respective IC_{50}. Affymetrix Microarray analysis was performed in technical duplicates. A, Venn diagram represents the number of genes altered (fold change > 1.5; $P < 0.05$) in each phenotype. Heat map shows the expression of all significantly altered genes in resistant (B) and sensitive (C) cells after cisplatin treatment.

Terms	Genes
Pathways in cancer	PRKCA, PLD1, CBLB, MSH3, GSK3B, SOS2, SMAD3, CDK6, GLI3, AKT3, DAPK1
T cell receptor signaling pathway	CBLB, GSK3B, SOS2, VAV2, AKT3, TEC
Chronic myeloid leukemia	CBLB, SOS2, SMAD3, CDK6, AKT3
Colorectal cancer	MSH3, GSK3B, SOS2, SMAD3, AKT3
Tight junction	PRKCA, MAGI3, INADL, ASH1L, PRKCH, AKT3
ErbB signaling pathway	PRKCA, CBLB, GSK3B, SOS2, AKT3
Non-small cell lung cancer	PRKCA, SOS2, CDK6, AKT3
MAPK signaling pathway	PRKCA, MAP4K3, NF1, SOS2, RAPGEF2, STK3, AKT3, MAP2K5
Glioma	PRKCA, SOS2, CDK6, AKT3
Pancreatic cancer	PLD1, SMAD3, CDK6, AKT3
Phosphatidylinositol signaling system	PRKCA, INPP4B, PIP4K2A, ITPR2
B cell receptor signaling pathway	GSK3B, SOS2, VAV2, AKT3
Axon guidance	EPHA4, GSK3B, SEMA3A, SLIT2, SRGAP2
Fc epsilon RI signaling pathway	PRKCA, SOS2, VAV2, AKT3

Table 4.1: Pathway analysis for differential terms/genes down-regulated in cisplatin-sensitive lines after cisplatin treatment in KEGG databases ($P < 0.05$).

Terms	Genes
Systemic lupus erythematosus	HIST1H2AC, HIST1H4B, HIST1H3B

Table 4.2: Pathway analysis for differential terms/genes down-regulated in cisplatin-resistant lines after cisplatin treatment in KEGG databases ($P < 0.05$).

4.1.2 Phospho-kinase signalling in cisplatin-treated Calu-1 and H596 cells

Next, the association of ErbB, MAPK and phosphatidylinositol signalling pathways with cisplatin sensitivities was explored using phospho-kinase array. H596 was selected to represent the cisplatin-sensitive group as it has the lowest cisplatin IC_{50}. Among the 3 cisplatin-resistant cell lines, Calu-1 was considered more representative. Despite having higher cisplatin IC_{50}, H2066 and SW900 were deemed impractical for further experimentations due to their growth conditions: H2066 cell requires multiple supplements for optimal growth (Table 2.3). SW900 has to be grown in normal air as CO_2 is detrimental to this cell. The varying culture conditions for these two lines could potentially introduce additional confounding factors that may influence the experiment outcomes.

Parallel phospho-MAPK array assays were performed on Calu-1 (resistant) and H596 (sensitive) cells after cisplatin exposure at doses closed to their IC_{50} (10μM and 5μM respective). Intensity of each spot represents the degree of phosphorylation for the indicated target (Figure 4.2 A). The pixel intensity of each pair of duplicate spots was measured with ImageJ as described in Chapter 2.8.8.2. Densitometry analysis was performed by first comparing the absolute pixel intensities of all targets in both resistant and sensitive cell lines (Figure 4.2 B, C) and differences in term of fold change of differently regulated kinases (Figure 4.2 D). The analyses showed that cisplatin treatment had profound effects on kinase phosphorylation in both cell lines. In cisplatin-treated H596, almost all proteins were dephosphorylated, except for p53 (Ser15) (Figure 4.2 B). In Calu-1 cells, however, cisplatin treatment had variable effects on kinase phosphorylation (Figure 4.2 C).

To gain a better understanding of the potential pathway perturbations that reflect resistance to cisplatin treatment, the differences in fold-change of kinase activation after cisplatin treatment were analysed. Fold change is defined as: ratio of post-treatment pixel density to that of untreated control with normalization to positive control. The fold changes for each kinase in Calu-1 were compared with those in H596. Those kinases with highest differences among the two lines were selected and displayed in Figure 4.2 D. By setting a 20% induction/reduction threshold to increase the stringency of the analysis, it was observed that p-Erk2, p-MSK2, p-p38α and p-p38γ were increased by 1.87, 1.22, 1.47 and 1.15-fold respectively in Calu-1 cells following cisplatin treatment. On the other hand, these kinases were reduced by 0.51, 0.49, 0.14 and 0.25-fold in H596 cells (Figure 4.2 E), suggesting that this subset of kinases may be pertinent to the cisplatin-resistant phenotype.

Expression of p-Akt, p-GSK3, p-Hsp27, p-MKK3/6, p-p38β/δ, p-RSK1/2 and p-mTOR were reduced in both Calu-1 and H596 cells after cisplatin treatment, while expressions of Erk1/2, MSK2 and p38α/γ were regulated in opposite manner, suggesting that transduction

of DNA-damage signals might be differently regulated in cisplatin-resistant and –sensitive cells and possibly mediated cellular responses to cisplatin. The detailed expressions of Erk, MSK2 and p38 were investigated among the resistant and sensitive cell lines in the next chapter.

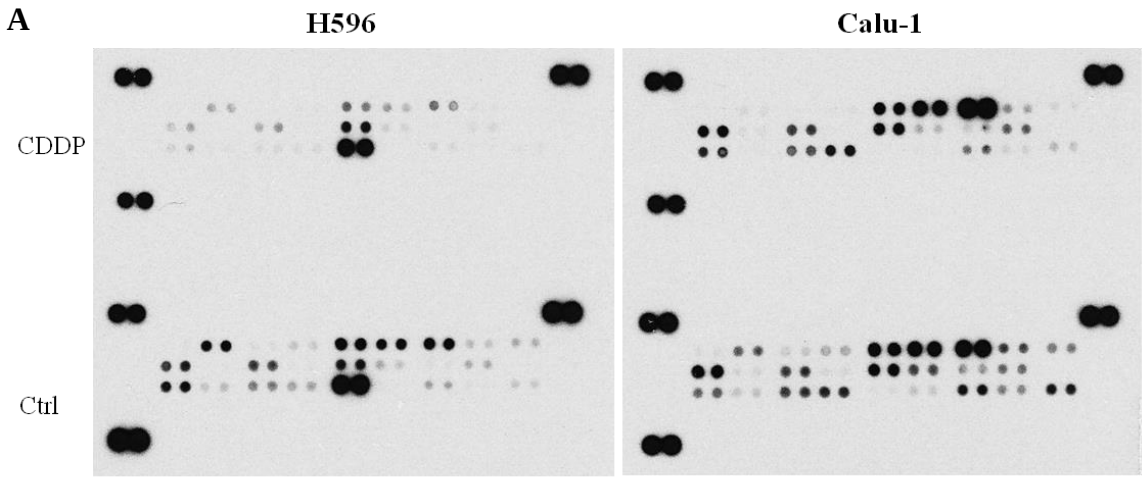
A
H596
Calu-1
CDDP
Ctrl

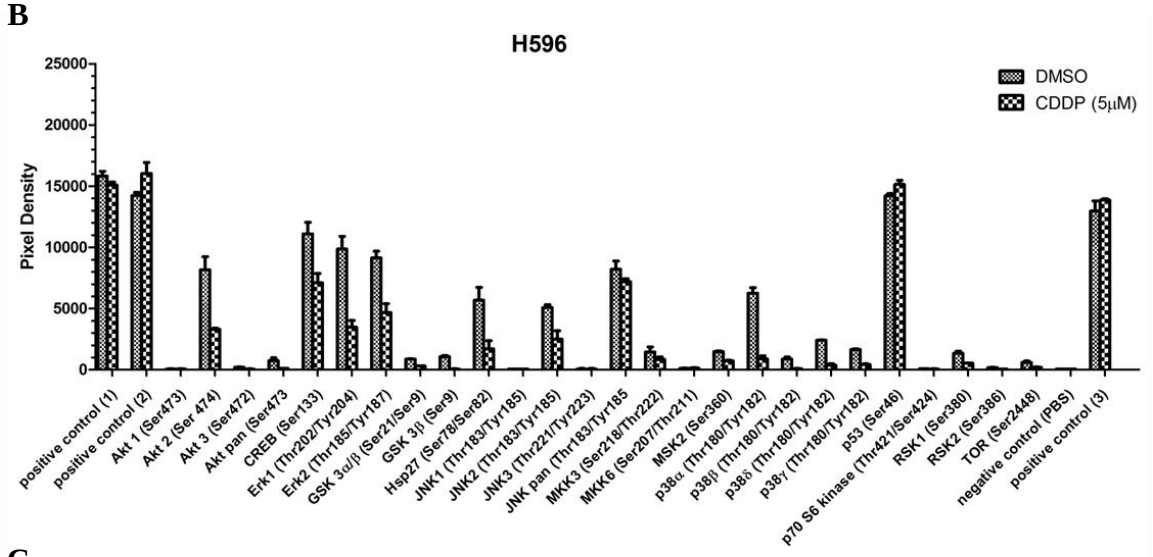
B
H596
DMSO
CDDP (5μM)
Pixel Density
25000
20000
15000
10000
5000
0
positive control (1)
positive control (2)
Akt 1 (Ser473)
Akt 2 (Ser 474)
Akt 3 (Ser472)
Akt pan (Ser473
CREB (Ser133)
Erk1 (Thr202/Tyr204)
Erk2 (Thr185/Tyr187)
GSK 3α/β (Ser21/Ser9)
GSK 3β (Ser9)
Hsp27 (Ser78/Ser82)
JNK1 (Thr183/Tyr185)
JNK2 (Thr183/Tyr185)
JNK3 (Thr221/Tyr223)
JNK pan (Thr183/Tyr185
MKK3 (Ser218/Thr222)
MKK6 (Ser207/Thr211)
MSK2 (Ser360)
p38α (Thr180/Tyr182)
p38β (Thr180/Tyr182)
p38δ (Thr180/Tyr182)
p38γ (Thr180/Tyr182)
p53 (Ser46)
p70 S6 kinase (Thr421/Ser424)
RSK1 (Ser380)
RSK2 (Ser386)
TOR (Ser2448)
negative control (PBS)
positive control (3)

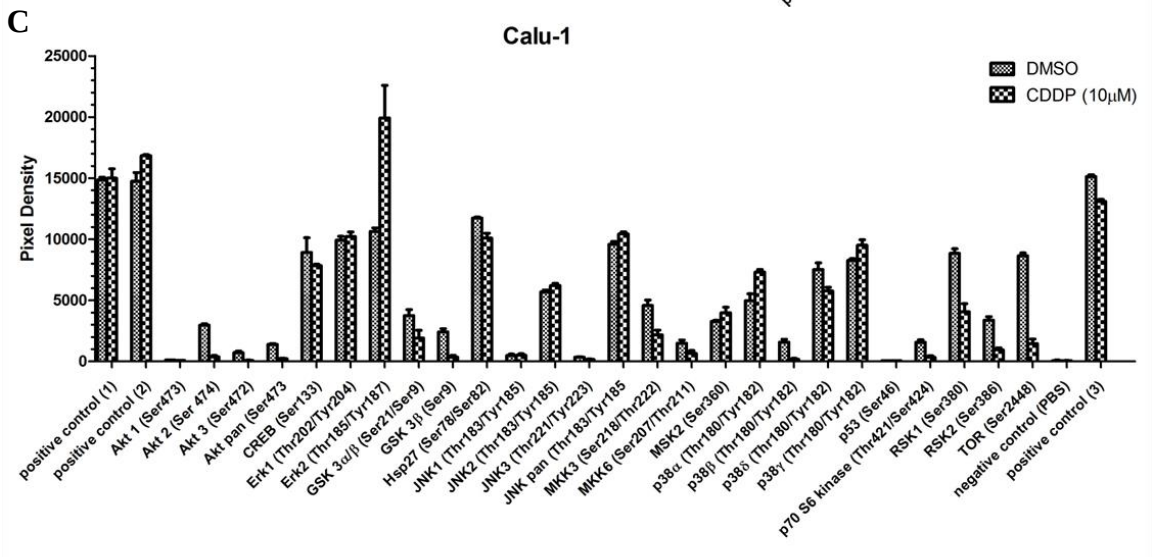
C
Calu-1
DMSO
CDDP (10μM)
Pixel Density
25000
20000
15000
10000
5000
0
positive control (1)
positive control (2)
Akt 1 (Ser473)
Akt 2 (Ser 474)
Akt 3 (Ser472)
Akt pan (Ser473
CREB (Ser133)
Erk1 (Thr202/Tyr204)
Erk2 (Thr185/Tyr187)
GSK 3α/β (Ser21/Ser9)
GSK 3β (Ser9)
Hsp27 (Ser78/Ser82)
JNK1 (Thr183/Tyr185)
JNK2 (Thr183/Tyr185)
JNK3 (Thr221/Tyr223)
JNK pan (Thr183/Tyr185
MKK3 (Ser218/Thr222)
MKK6 (Ser207/Thr211)
MSK2 (Ser360)
p38α (Thr180/Tyr182)
p38β (Thr180/Tyr182)
p38δ (Thr180/Tyr182)
p38γ (Thr180/Tyr182)
p53 (Ser46)
p70 S6 kinase (Thr421/Ser424)
RSK1 (Ser380)
RSK2 (Ser386)
TOR (Ser2448)
negative control (PBS)
positive control (3)

D

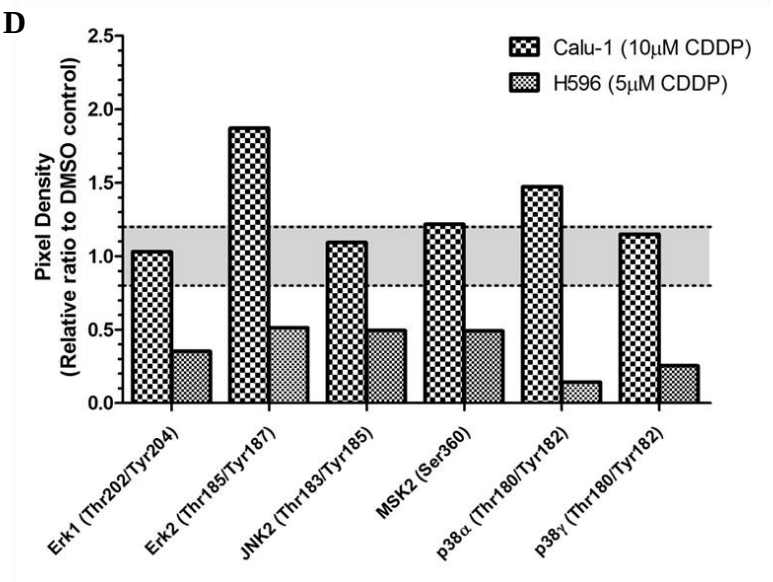

E

	Calu-1		H596	
	Control	CDDP 10μM	Control	CDDP 5μM
Erk1 (Thr202/Tyr204)	1	1.03	1	0.35
Erk2 (Thr185/Tyr187)	1	1.87	1	0.51
JNK2 (Thr183/Tyr185)	1	1.09	1	0.49
MSK2 (Ser360)	1	1.22	1	0.49
p38α (Thr180/Tyr182)	1	1.47	1	0.14
p38γ (Thr180/Tyr182)	1	1.15	1	0.25

Figure 4.2: Calu-1 and H596 have dissimilar regulation of signalling pathways upon cisplatin treatment.

A, H596 (cisplatin-sensitive) and Calu-1 (-resistant) cells were cultured overnight and treated with cisplatin at 5μM and 10μM respectively for 48 hours (*n* = 1). Phospho-kinase array and densitometric analysis were performed as described in Material and Methods. The pixel density of each array spots for H596 (B) and Calu-1 (C) cells were shown. Data are shown as an average of duplicate spots ± SD. The bar chart (D) and the table (E) show the fold change (in relative to untreated control) of indicated phosphoproteins that were expressed differently in Calu-1 and H596 cells in response to cisplatin treatment. Gray-coloured region indicates the defined boundaries for significant changes (< 80%; > 120%). Data are shown as an average of duplicate spots.

4.1.3 Regulation of signal transduction pathways in cisplatin-treated lung SCC cells

Next, the findings of the phospho-kinse arrays were validated using Western blotting analysis on the various signalling proteins. Western blot analyses were performed on independent cell lysates of cisplatin-sensitive (H596, H226 and ChaGo-k-1) and -resistant (Calu-1, H2170 and H520) cell lines. The proteomic analysis had earlier indicated that phosphorylation of Erk1/2, MSK2 and p38α/γ were suppressed in H596 cells, but up-regulated in Calu-1 cells. The expressions of p-Erk1/2 (Thr202/Tyr204), p-MSK1 (Ser360) and p-p38 (Thr180/Tyr182) across the 6 selected lines were verified after exposure to cisplatin. Cleavage of PARP was determined as an indicator of apoptosis.

The range of cisplatin concentrations (0.5 - 10μM) used in this study is well within the achievable concentrations in the plasma of regular doses of cisplatin in patients (van Hennik, van der Vijgh et al. 1987). These data validated that p-Erk1/2, p-MSK1 and p-p38 were suppressed in cisplatin-treated H596 cells dose-dependently (Figure 4.3 A), and were consistent with the phospho-kinase analysis. Among other cisplatin-sensitive cell lines, p-Erk1/2 was down-regulated H226, but unchanged in ChaGo-k-1; p-MSK1 was lowly expressed in H226 and unchanged in ChaGo-k-1; while p-p38 was increased in both H226 and ChaGo-k-1. The down-regulation of p-Erk1/2 in both H596 and H226 corresponded with the cleavage of PARP (Figure 4.3 A).

Western blotting showed that cisplatin treatment induced phosphorylations of Erk1/2 and MSK1 in Calu-1 cells, but did not affect p38 expression. Among other cisplatin-resistant cell lines, p-Erk1/2 was reduced at high dose in H2170 and up-regulated in H520; p-MSK1 was up-regulated in both H2170 and H520; p-p38 was down-regulated in H2170 but unchanged in H520. Cleavage of PARP was observed in Calu-1 and H520 only at high doses of cisplatin (10μM) (Figure 4.3 B).

Collectively, it was shown that exposure to cisplatin generated distinct signalling dynamics among lung SCC cells. In general, p-Erk1/2 and p-MSK1, but not p-p38, were reciprocally regulated in cisplatin-resistant and –sensitive cell lines.

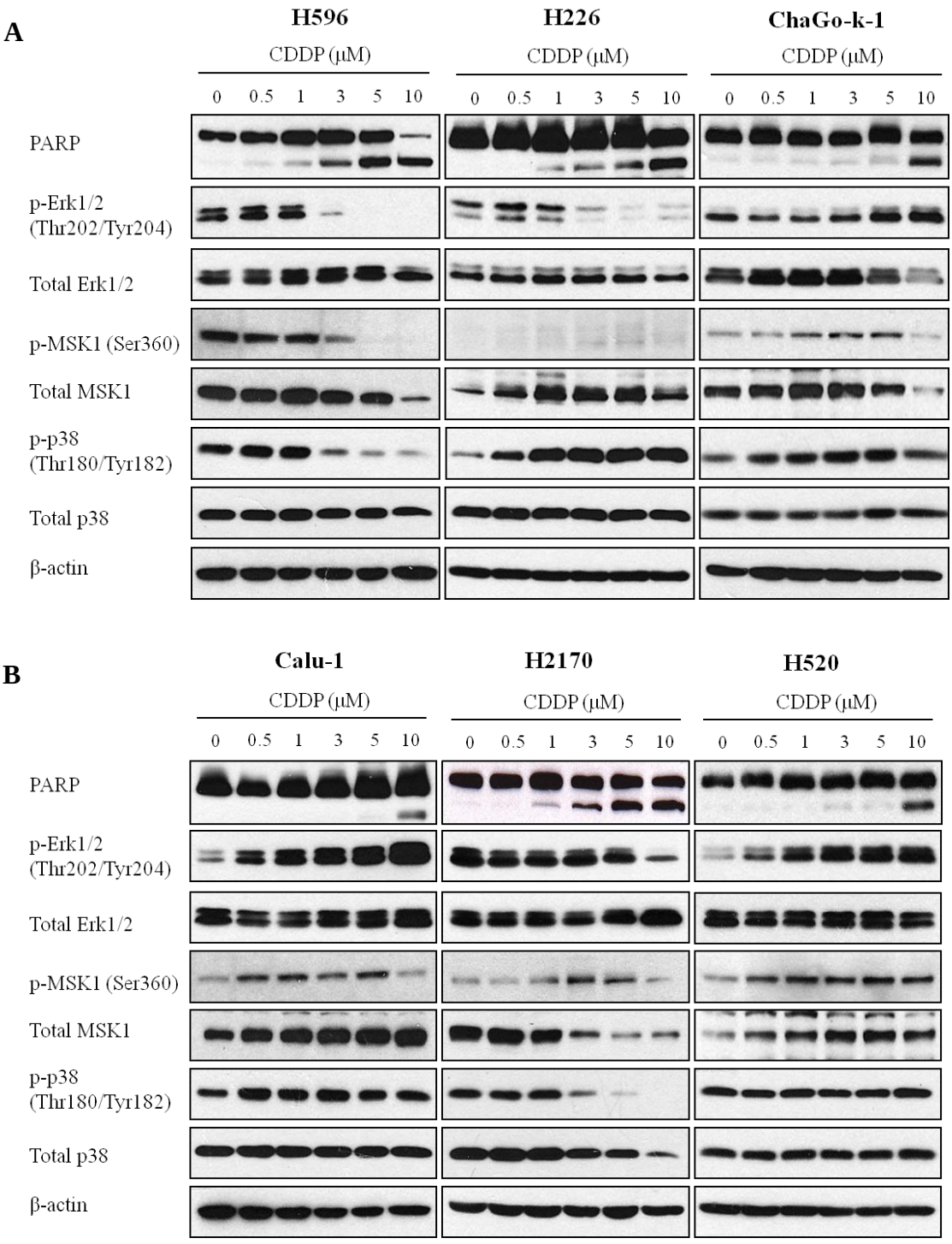

Figure 4.3: Phosphorylation of Erk, MSK1, p38 and cleavage of PARP in lung SCC cells upon cisplatin exposure.

Western blot analyses was performed to investigate the expression of PARP, Erk, MSK and p38 in (A) cisplatin-sensitive (H596, H226, ChaGo-k-1) and (B) cisplatin-resistant (Calu-1, H2170, H520) cells. Cisplatin was given in increasing doses (0.5, 1, 3, 5, and 10μM) for 48 hours. Data shown are representative of three independent experiments for the indicated targets with β-actin as input control.

4.1.4 The signal transduction pathways in belinostat-treated lung SCC cells

In Chapter 3.3.1, it was shown that cisplatin resistant cell lines were more susceptible to belinostat treatment. These selectivity and specificity of belinostat to cisplatin-resistant cells implied for the chemosensitization effects of belinostat in lung SCC cells. Therefore, elucidating the underlying mechanisms of belinostat susceptibility may reveal chemosensitization strategies with significant clinical implications in lung SCC.

Our data demonstrated that belinostat suppressed p-Erk1/2, p-MSK1 and p-p38 dose-dependently in H596 and ChaGo-k-1. In H226, however, Erk1/2 and p38 were phosphorylated at low doses but dephosphorylated in high doses (3μM) of belinostat. Interestingly, cleavage of PARP in these cell lines corresponded with the deactivation of Erk and p38, suggesting that apoptosis is dependent on inhibition of these MAPK pathways (Figure 4.4 A). In all three cisplatin-resistant cell lines (Calu-1, H2170, H520), belinostat abrogated the expression of p-Erk1/2, p-MSK1 and p-p38, while inducing PARP cleavage in a dose-dependent manner (Figure 4.4 B)

These data confirmed that phosphorylation of Erk1/2, MSK1 and p38 were consistently abrogated by belinostat in lung SCC cells, particularly in those with higher tolerability to cisplatin. Accordingly, the role of these signal transduction pathways in mediating cisplatin sensitivity was examined.

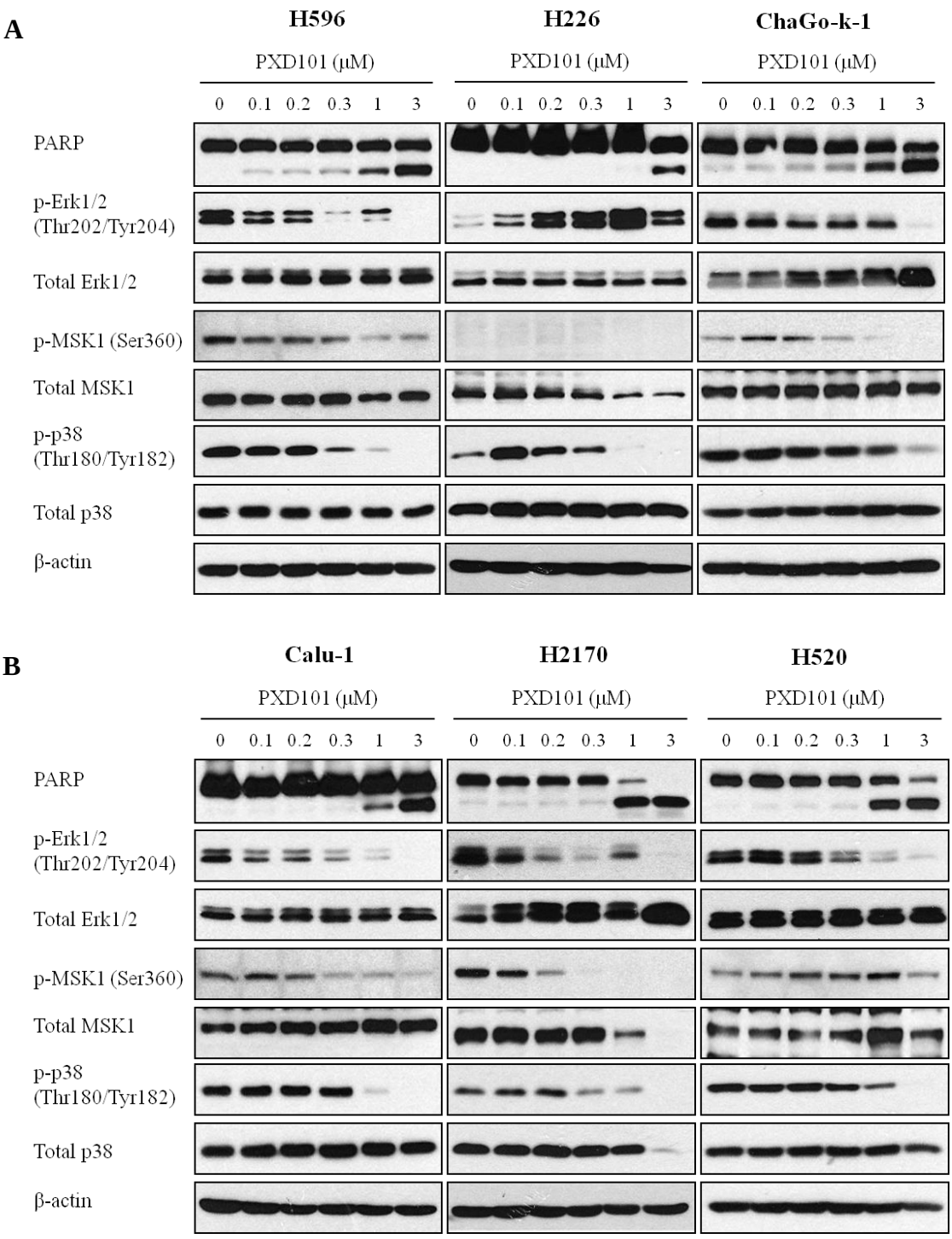

Figure 4.4: Phosphorylation of Erk, MSK1, p38 and cleavage of PARP in lung SCC cells upon belinostat exposure.

Western blot analysis was performed to investigate the expression of PARP, Erk, MSK and p38 in (A) cisplatin-sensitive (H596, H226, ChaGo-k-1) and (B) cisplatin-resistant (Calu-1, H2170, H520) cells. Belinostat (PXD101) was given in increasing doses (0.1, 0.2, 0.3, 1, and 3μM) for 48 hours with DMSO (0.03%) as vehicle control. Data shown are representative of three independent experiments for the indicated targets with β-actin as input control.

Summary of findings in Chapter 4.1:

- Genes related to ErbB pathway, MAPK pathway and phosphatidylinositol pathway were down-regulated in cisplatin-sensitive cells under pressure of cisplatin treatment, but not in cisplatin-resistant cells.
- Phospho-kinase array analysis showed that p-Erk1/2, p-MSK2 and p-p38α/γ were up-regulated in Calu-1 (drug-resistant) cells but suppressed in H596 (drug-sensitive) cells after cisplatin treatment.
- Western blotting analysis showed that Erk1/2 was phosphorylated in cisplatin-resistant cell lines (Calu-1, H520) and dephosphorylated in cisplatin-sensitive cell lines (H596, H226) after cisplatin treatment.
- These data suggested that p44/42 MAPK signalling might mediate cisplatin resistance in lung SCC.
- Belinostat consistently reduced phosphorylation of Erk1/2, MSK2 and p38 in all lung SCC cell lines.
- Belinostat may sensitize cisplatin-resistant lung SCC cells to cisplatin treatment through abrogation of p-Erk1/2.

4.2 Impact of cisplatin and belinostat on p44/42 MAPK signalling in lung SCC cells

4.2.1 Differential regulation of MAPK-B-Raf-MEK signalling axis by cisplatin and belinostat

Our analysis showed the persistent abrogation of Erk and MSK by belinostat; while the reciprocal regulation of Erk and MSK by cisplatin correlated with cisplatin sensitivities. As MSK1 is a down-stream kinase of Erk1/2, these findings suggested that p44/42 MAPK signalling may be important in regulation of cell survival in these cell lines. The expressions of two upstream molecules of Erk1/2, B-Raf and MEK1/2, were investigated.

Among the cisplatin-sensitive cell lines, both p-B-Raf and p-MEK1/2 were not affected by cisplatin treatment in H226 and ChaGo-k-1 cells, but reduced in H596 cells (Figure 4.5 A). Among the cisplatin-resistant cells, p-B-Raf and p-MEK1/2 were found to be up-regulated by cisplatin in Calu-1 and H520, but down-regulated at high dose (10μM) in H2170 cells (Figure 4.5 B). Similar to the trend of Erk1/2, belinostat suppressed the expression of p-B-Raf and p-MEK1/2 amongst the 6 lung SCC cell (Figure 4.6 A, B).

Collectively, a consistent trend in the regulation of B-Raf-MEK-Erk signalling axis by cisplatin and belinostat was observed. These findings suggested that activation of p44/42 MAPK pathway could be associated with cisplatin-resistance in lung SCC cells; while abrogation of p44/42 MAPK signalling by belinostat resulted in strong cytotoxicity in these resistant cells.

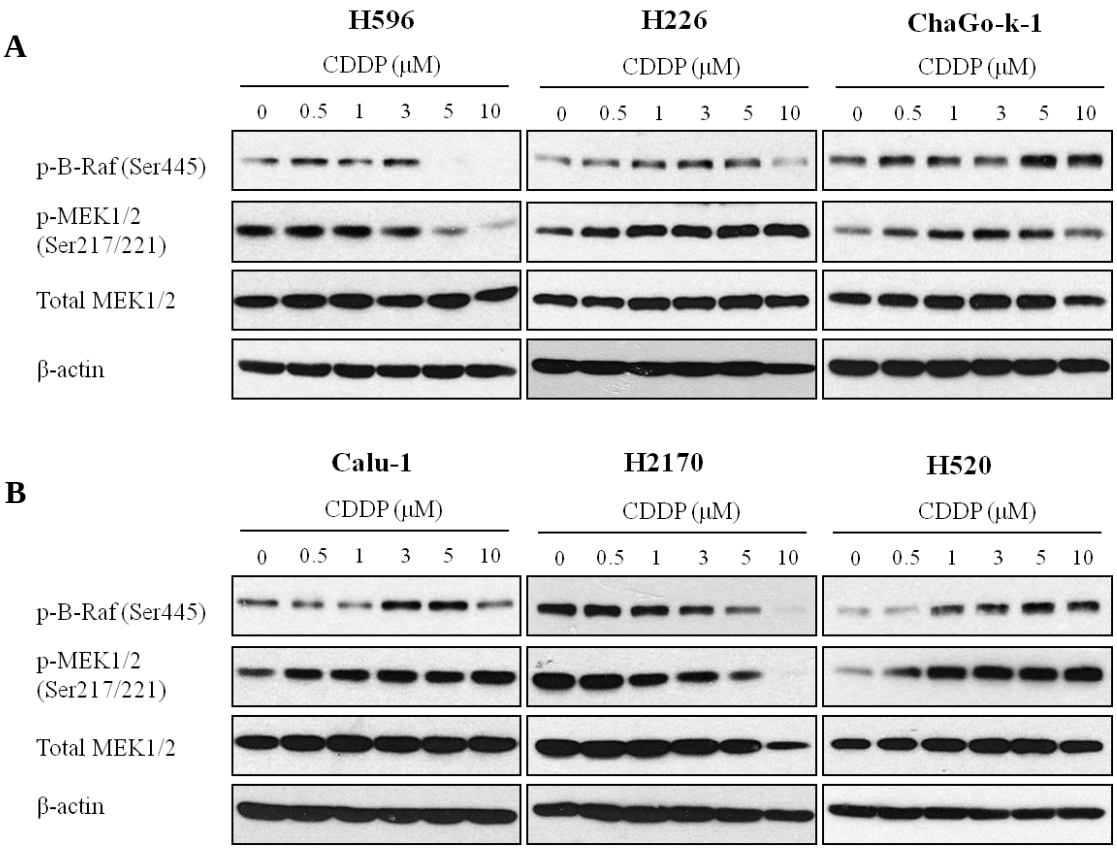

Figure 4.5: Regulation of MEK1/2 and B-Raf in lung SCC cell lines upon cisplatin treatment.

Western blot analyses were performed to study the expression of p-B-Raf and p-MEK1/2 in (A) cisplatin-sensitive (H596, H226 and ChaGo-k-1); and (B) cisplatin-resistant (Calu-1, H2170 and H520) cells after exposure to cisplatin (0.5, 1, 3, 5, and 10μM) for 48 hours. Data shown are representative of two independent experiments for the indicated targets with β-actin as input control.

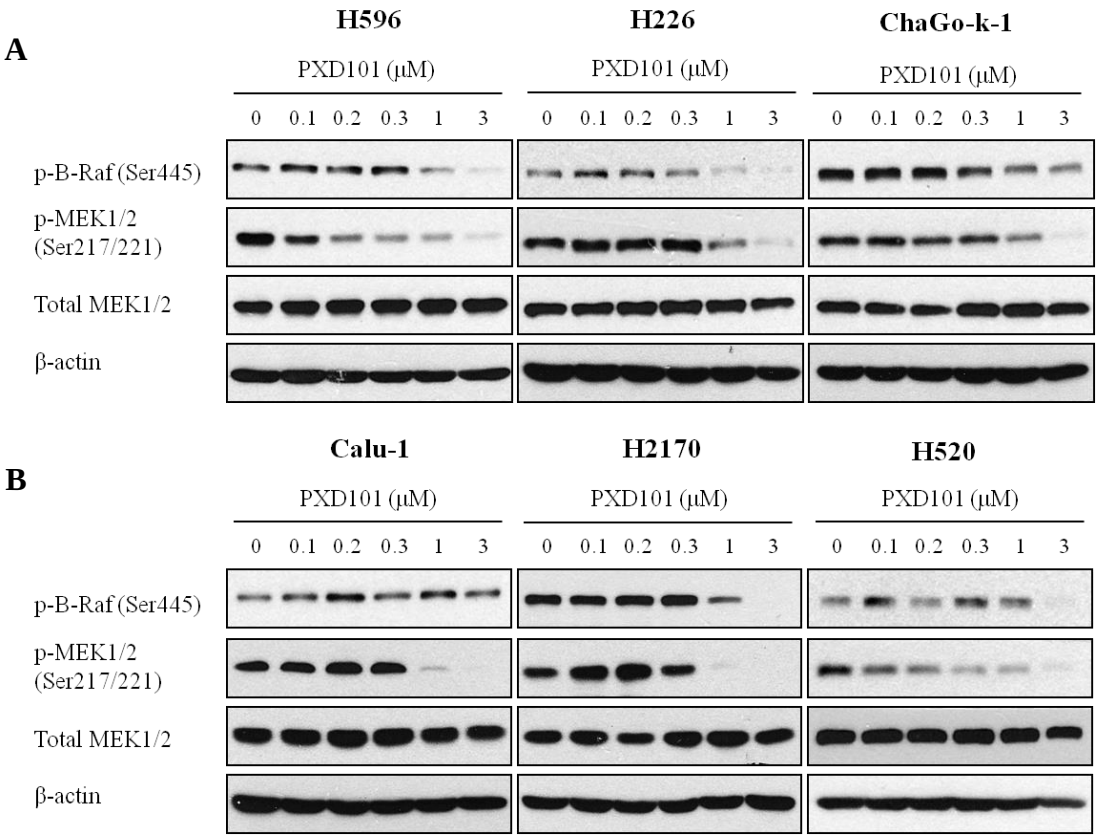

Figure 4.6: Belinostat treatment suppressed p-B-Raf and p-MEK1/2 in lung SCC cell lines.

Western blot analyses were performed to study the expression of p-B-Raf and p-MEK1/2 in (A) cisplatin-sensitive (H596, H226 and ChaGo-k-1); and (B) cisplatin-resistant (Calu-1, H2170 and H520) cells after exposure to belinostat (PXD101) (0.1, 0.2, 0.3, 1 and 3μM) for 48 hours with DMSO (0.03%) as vehicle control. Data shown are representative of two independent experiments for the indicated targets with β-actin as input control.

4.2.2 Synergistic combination of belinostat and cisplatin on p44/42 MAPK signalling in lung SCC cell lines

4.2.2.1 Induction of apoptosis in belinostat/cisplatin-treated Calu-1 and H520 cells

As previously discussed, chemosensitization of HDAC inhibitor was observed in several tumour types, with the induction of apoptosis a common outcome (Bangert, Häcker et al. 2011, Häcker, Karl et al. 2011). The drug combination analysis suggested that cisplatin-belinostat combination was synergistic. Furthermore, p44/42 MAPK was shown to be regulated by the cellular processing of cisplatin and belinostat. Accordingly, it was hypothesized that belinostat-induced abrogation of p-Erk1/2 potentiates cisplatin cytotoxicity in lung SCC cells.

Here, the combinatorial effect of belinostat and cisplatin in Calu-1and H520 cells was investigated, as both of these cell lines showed significant activation of the MAPK-MEK-Erk in response to cisplatin treatment. The expressions of two apoptotic markers, PARP and caspase 3, were determined to monitor drug-mediated apoptosis. The data showed that p-MEK1/2 and p-Erk1/2 were abrogated by 1μM belinostat and activated by 10μM cisplatin. At the indicated doses, belinostat induced mild cleavage of PARP and caspase 3 in H520 cells but not Calu-1; while cisplatin treatment triggered cleavage of these apoptotic markers in both cell lines (Figure 4.7). When both drugs were incubated simultaneously, ciplatin-induced p-Erk1/2 and p-MEK1/2 activation was suppressed. Importantly, in relation to the down-regulation of p-Erk1/2, combination treatment potentiated the cleavage of PARP and caspase 3 in relative to single drug treatment (Figure 4.7).

These data clearly demonstrated that through inhibiting cisplatin-activated p44/42 MAPK signalling, belinostat enhanced the induction of apoptosis in two cisplatin-resistant cell lines (Calu-1 and H520), thus supporting the hypothesis. Such findings revealed a novel therapeutic strategy for intervention of cisplatin resistance in lung SCC cells.

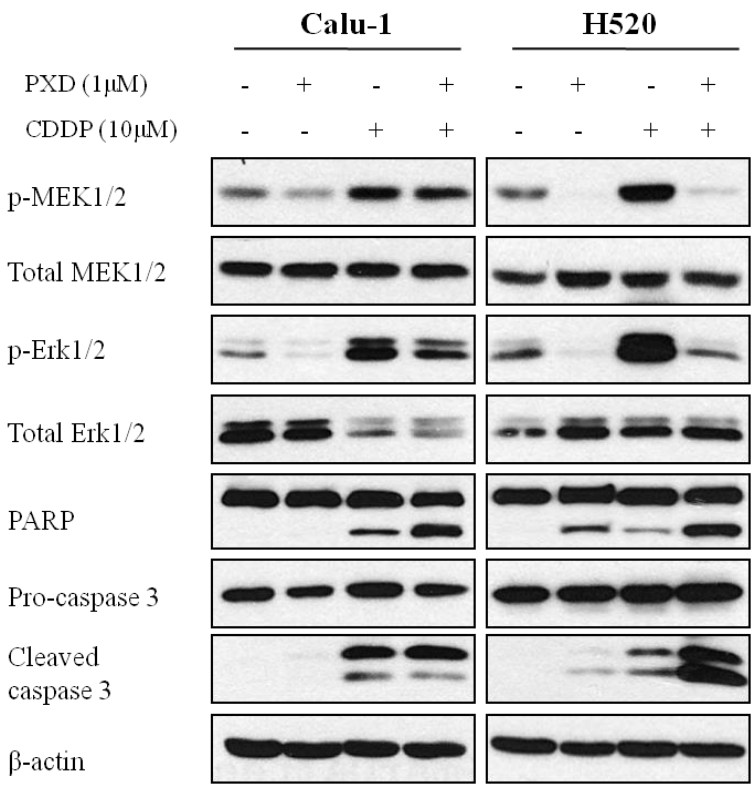

Figure 4.7: Belinostat suppresses phosphorylation of Erk1/2 in cisplatin-treated cells, and triggers cleavage of PARP and caspase 3.

Western blot analyses were performed on cisplatin-resistant Calu-1 and H520 cells after cisplatin (10μM), belinostat (PXD101) (1μM) and combination treatment with DMSO (0.01%) as vehicle control. Western blot data shown are representative of three independent experiments for the indicated targets with β-actin as input control.

4.2.2.2 Nuclear/cytosolic localization of p-Erk1/2 in belinostat- and cisplatin-treated Calu-1 and H596 cells

The Erk phosphorylation cascade plays an important role in the intracellular signalling that controls cell proliferation, differentiation and survival. Erk regulates growth factor-responsive targets in the cytoplasm, as well as translocates to the nucleus for activation of downstream transcription factors (Brunet, Roux et al. 1999, Wada and Penninger 2004). In current chapter, through identifying the translocalization of phosphorylated Erk1/2 in both Calu-1 and H596 cells, the mechanisms involved in cisplatin/belinostat-mediated p44/42 MAPK signalling in lung SCC were examined.

Immunofluorescence staining showed accumulation of p-Erk1/2 in Calu-1 cells after cisplatin treatment and reduction after belinostat treatment (Figure 4.8 A). High content analysis was subsequently performed through segmentation of nuclear and cytoplasmic regions to investigate the localization of p-Erk1/2 in Calu-1 cells. The data showed that the activated Erk1/2 was increased by 2-fold in cytoplasm and 1.5-fold in the nucleus upon cisplatin treatment, while belinostat reduced cytoplasmic and nuclear p-Erk1/2 by about 5-fold (Figure 4.8 B, C). When administered together, belinostat suppressed the cytoplasmic activation and nuclear translocation of p-Erk1/2 (Figure 4.8 B, C). In the H596 cell, however, cisplatin treatment did not induce nuclear or cytoplasmic p-Erk1/2 accumulation. When belinostat was administered singly or in combination, both cytoplasmic and nuclear p-Erk1/2 were reduced (Figure 4.9 A, B, C).

These observation in p-Erk1/2 staining corresponded with the Western blotting analysis. Cisplatin treatment up-regulated p-Erk1/2, and coincided with the increase in cytoplasmic accumulation and nuclear translocation in cisplatin-resistant Calu-1 but not cisplatin-sensitive H596. On the contrary, belinostat suppressed p-Erk1/2 in both cell lines, and notably inhibited cisplatin-induced nuclear translocation of p-Erk1/2 in Calu-1 cells. These suggested that Erk1/2 was differentially regulated in cisplatin-resistant and –sensitive cells, while suppression of Erk1/2 was consistent in lung SCC cells.

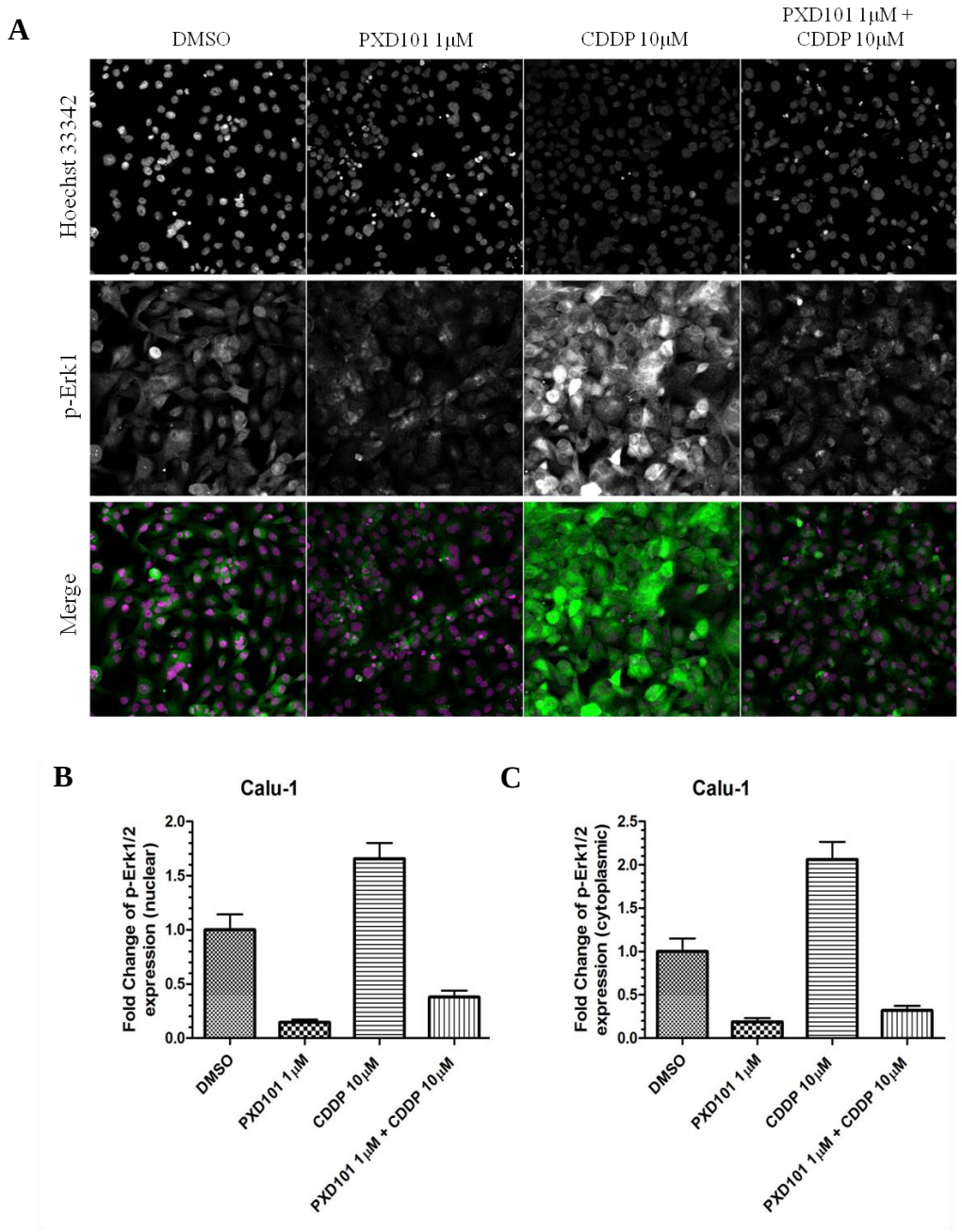

Figure 4.8: Belinostat inhibits nuclear translocation of Erk1/2 in cisplatin-treated Calu-1 cells.

Cisplatin-resistant Calu-1 cells were treated with belinostat (PXD101) (1µM), cisplatin (10µM) and combination treatment with DMSO (0.01%) as vehicle control for 48 hours. Immunofluorescence staining was performed to determine the translocalization of p-Erk1/2 (Alexa Fluor-488) in Calu-1 cells. A, Representative confocal fluorescent images at 400x magnification were shown for three independent experiments. **Grey indicates DAPI and p-Erk1/2 in single channel**; **purple indicates DAPI in merge channel**; **green indicates p-Erk1/2 in merged channel**. High content analyses were performed for p-Erk1/2 signal intensity in cell nucleus (B) and cytoplasm (C). Data are normalized against the number of nuclei and presented as mean ± SD for one representative experiment (n=3).

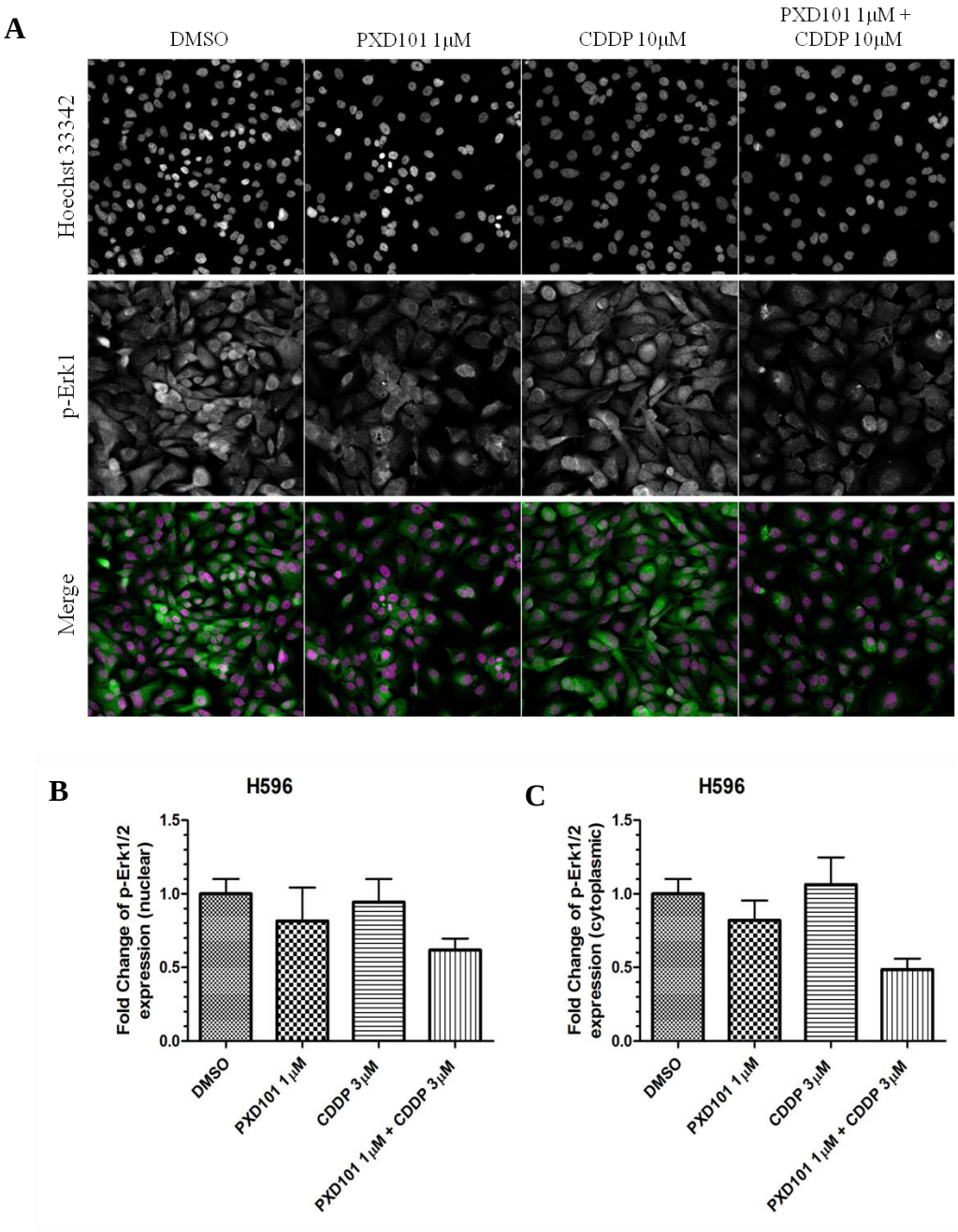

Figure 4.9: Belinostat reduces nuclear translocation of Erk1/2 in cisplatin-treated H596 cells.

Cisplatin-sensitive H596 cells were treated with belinostat (PXD101) (1μM), cisplatin (3μM) and combination treatment with DMSO (0.01%) as vehicle control for 48 hours. Immunofluorescence staining was performed to determine the translocalization of p-Erk1/2 (Alexa Fluor-488) in H596 cells. A, Representative confocal fluorescent images at 400x magnification were shown for three independent experiments. **Grey indicates DAPI and p-Erk1/2 in single channel**; **purple indicates DAPI in merged channel**; **green indicates p-Erk1/2 in merged channel**. High content analyses were performed for p-Erk1/2 signal intensity in cell nucleus (B) and cytoplasm (C). Data are normalized against the number of nuclei and presented as mean ± SD for one representative experiment (n=2).

4.2.3 Upstream regulation of p44/42 MAPK signalling by cisplatin and belinostat in lung SCC cells

4.2.3.1 Regulation of SOS1/SOS2 in cisplatin- and belinostat- treated cells

Thus far, the data have suggested a correlation between ERK and cellular response to cisplatin. However, the factor(s) leading to the differential regulation of p-ERK in relation to cisplatin sensitivity remains unclear. It is important to note that EGFR phosphorylation was not affected by cisplatin across the panel of SCC cells (data not shown), which suggested the involvement of other factor(s) in controlling MAPK/ERK signaling. To identify the factor(s), the suppressed genes in cisplatin-treated H596 cells that were associated with MAPK signalling were re-evaluated (Table 4.1). Interesting, the genes that were profoundly suppressed included Son of Sevenless homolog 2 (SOS2), a key regulator of the MAPK signaling cascade. *SOS* encodes guanine nucleotide exchange protein (GEP). GEP is essential for the activation of GTPases through mediating GDP/GTP exchange (Cherfils and Zeghouf 2013). In MAPK signalling, SOS1 and SOS2 are two major GEP that act as molecular switches that activate Ras (GTPase) (Egan, Giddings et al. 1993). Subsequently, the interaction of SOS and Ras triggers the down-stream activation of p44/42 MAPK signalling (Rogge, Karlovich et al. 1991). Accordingly, it was hypothesized that SOS is essential in modulating p-Erk in cisplatin-resistant lung SCC cells.

As shown in Figure 4.10 A, exposure to cisplatin repressed both SOS1 and SOS2 in H596 cells, but had no effect in H226 and ChaGo-k-1. In contrast, cisplatin induced the up-regulation of SOS in Calu-1 and H520, with unchanged expression of SOS in H2170 (Figure 4.10 B). Importantly, exposure to belinostat resulted in down-regulation of both SOS1 and SOS2 in a dose-dependent manner in all tested lung SCC cells (Figure 4.10 C, D).

Collectively, these data showed the induction of both SOS1 and SOS2 by cisplatin in 2 of the 3 resistant cell lines but repressed in cisplatin-sensitive H596 cells. More importantly, the observed trends of SOS1 and SOS2 coincided with the patterns in which p44/42 MAPK pathway were regulated by cisplatin and belinostat, suggesting that SOS is critical in determining drug sensitivity to cisplatin in lung SCC cells.

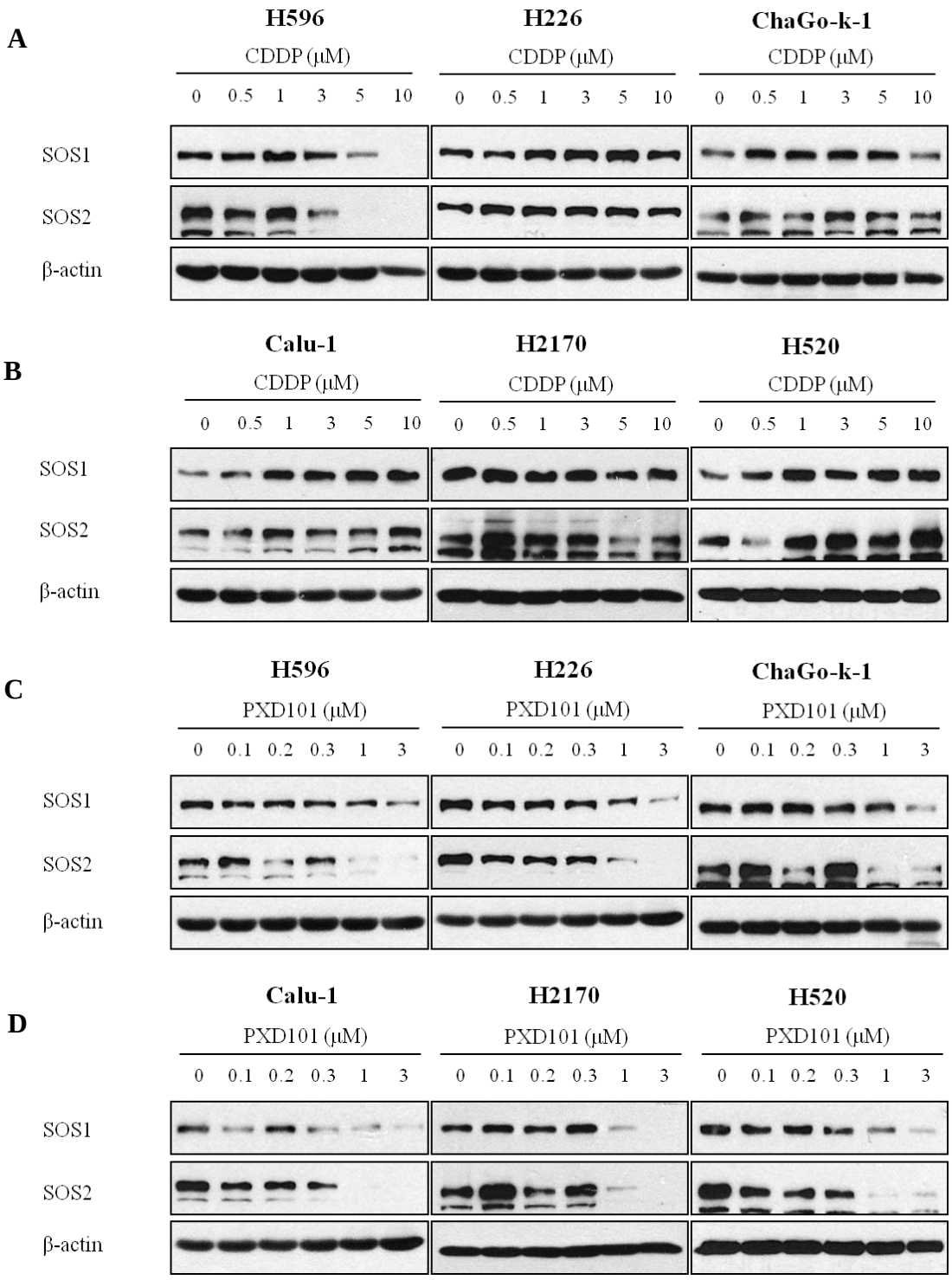

Figure 4.10: Differential regulation of SOS1 and SOS2 by cisplatin and belinostat.

Western blot analyses were performed to investigate the expression of SOS1 and SOS2 in (A) cisplatin-sensitive (H596, H226 and ChaGo-k-1); and (B) cisplatin-resistant (Calu-1, H2170 and H520) cells after cisplatin (0.5, 1, 3, 5, and 10μM) treatment for 48 hours; and in (C) cisplatin-sensitive and (D) –sensitive cell lines after belinostat (PXD101) (0.1, 0.2, 0.3 1 and 3μM) for 48 hours with DMSO (0.03%) as vehicle control. Western blot data shown are representative of three independent experiments for the indicated targets with β-actin as input control.

4.2.3.2 Regulatory effects of SOS1/SOS2 in Erk1/2 signalling

The regulation of SOS1 and SOS2 by co-treatment of cisplatin and belinostat in Calu-1 and H520 cells was next investigated. In both cisplatin-resistant lines, belinostat treatment at 1μM reduced the SOS1 expression while completely abrogated SOS2 expression (Figure 4.11 A). These trends correlated with the reduction in p-Erk1/2 in these cells when belinostat was given singly and in combination (Figure 4.7).

To validate the association between SOS1/2 and p-Erk1/2, siRNA knockdown was performed on both SOS1 and SOS2 in Calu-1 and H520. Mechanistically, individual silencing of SOS1 and SOS2 was associated with decreased Erk1/2 phosphorylation (Figure 4.11 B). Despite achieving complete disruption of SOS1 through siRNA interference, knockdown of SOS2 alone appeared to be ineffective; interestingly, expression of SOS1 was reduced when silencing of SOS2 was conducted (Figure 4.11 B). However, when both siRNA were delivered, SOS1 and SOS2 were successfully abrogated (Figure 4.11 B). This suggested the essential role of SOS1 in maintaining SOS2 stability. Finally, ablation of both SOS1 and SOS2 profoundly suppressed expression of p-Erk1/2 (Figure 4.11 B).

Taken together, SOS1 and SOS2 are shown to be regulatory upstream molecules of Erk1/2 in lung SCC cells. Therefore, induction of SOS1 and SOS2 leading to activation of the MAPK-Erk axis may be an important mechanism of cisplatin resistance, which could be abrogated by belinostat.

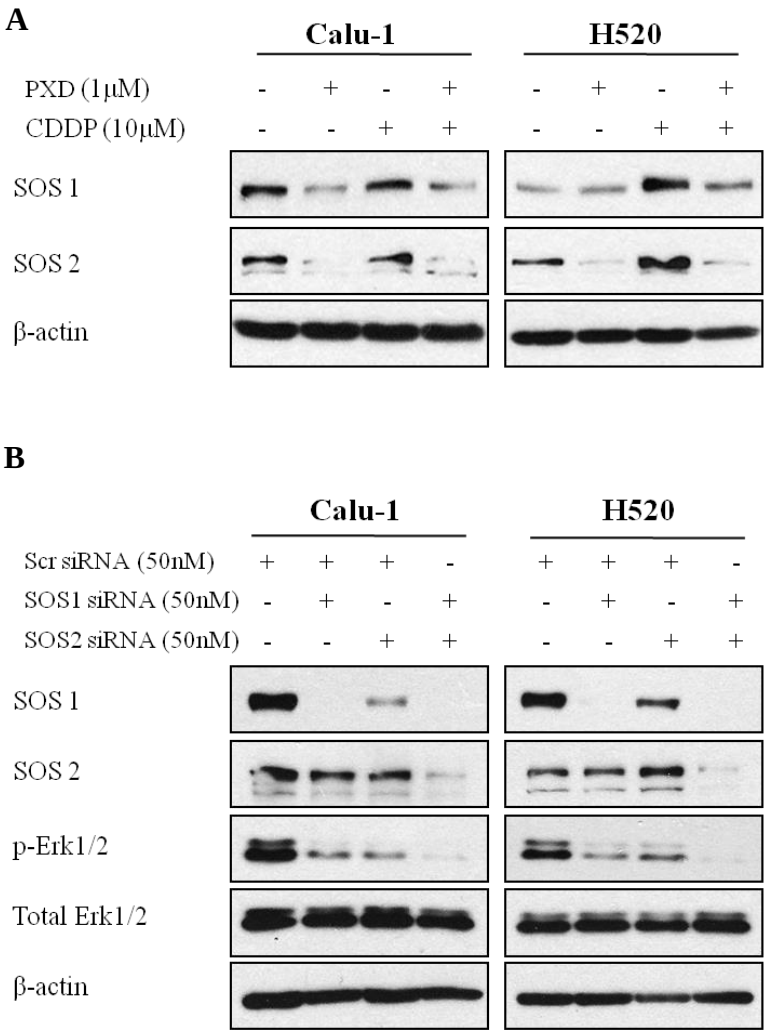

Figure 4.11: Silencing of SOS1 and SOS2 suppresses Erk1/2 phosphorylation.

A, Regulatory effect of belinostat (1μM), cisplatin (10μM) and combination treatment on SOS1 and SOS2 in cisplatin-resistant Calu-1 and H520 cells using western blotting. DMSO (0.01%) was treated as vehicle control. B, Western blot analyses on the regulation of p-Erk1/2 after SOS1 and SOS2 siRNA-silencing in Calu-1 and H520 cells. 50nM of siRNA was used per transfection. Western blot data shown are representative of three independent experiments for the indicated targets with β-actin as input control.

Summary of findings in Chapter 4.2:

- Upstream kinases of Erk (B-Raf, MEK) were phosphorylated in cisplatin-resistant cell lines (Calu-1, H520) and dephosphorylated in cisplatin-sensitive cell lines (H596, H226) after cisplatin treatment.
- Belinostat abrogated both p-B-Raf and p-MEK1/2 in all tested lung SCC cell lines.
- Combination of belinostat and cisplatin suppressed cisplatin-induced p-Erk1/2 and p-MEK1/2 in Calu-1 and H520 cells.
- Combination of belinostat and cisplatin potentiated the induction of apoptosis.
- Cisplatin pressure increased nuclear and cytoplasmic p-Erk1/2 levels in Calu-1 (drug resistant) cells but not H596 (drug sensitive) cells.
- Combination of belinostat and cisplatin suppressed cisplatin-induced cellular accumulation and nuclear translocation of p-Erk1/2 in Calu-1 cells.
- Cisplatin treatment up-regulated SOS1 and SOS2 in Calu-1 and H520 cells, which corresponded with the increase in p-Erk1/2.
- Belinostat treatment consistently down-regulated expressions of SOS1 and SOS2 in all lung SCC cell lines.
- Combination of belinostat and cisplatin suppressed cisplatin-induced SOS1 and SOS2 in Calu-1 and H520 cells.
- siRNA silencing of both SOS1 and SOS2 effectively abrogated p-Erk1/2 in Calu-1 and H520 cells.

4.3 Targeting p44/42 MAPK signalling in cisplatin-resistant lung SCC cells

4.3.1 Silencing of Erk1/2 increases cisplatin cytotoxicity in lung SCC cells

Thus far, Erk1/2 activation is shown to be associated with a lack of cytotoxic response to cisplatin treatment in two cisplatin-resistant lung SCC cell lines. However, a direct connection between p44/42 MAPK pathway and cisplatin cytotoxicity has not been established. In order to evaluate the impact of p44/42 MAPK inhibition in cisplatin cytotoxicity, gene-silencing was performed on Erk1/2 at 24 hours prior to treatment with increasing doses of cisplatin, and cell viability of Calu-1 and H2170 cells was examined 24 and 48 hours after drug treatment. The data suggested that siRNA knockdown of Erk1/2 significantly reduced expression of activated p-Erk1/2 in Calu-1 and H2170 cells at 48 hours (Data not shown) and 72 hours post-transfection (Figure 4.12 C, D). Down-regulation of either Erk1 or Erk2 led to decreased cell viability in Calu-1 and H2170 cells, while combined knockdown further potentiated the growth inhibitory effects of cisplatin in a dose-dependent manner at 48 hours post-treatment (72 hours post-transfection) (Figure 4.12 A, B).

In comparison with scrambled control-transfected cells, ablation of Erk1/2 shifted the dose-response curve to the left and reduced the IC_{50} to cisplatin by more than 2 fold in all 3 cisplatin-resistant cell lines tested (Calu-1, H2170, H520) (Figure 4.13 A, C, D). As Erk signalling is mainly regulated by MEK1/2 in the Ras/Raf/MEK/Erk/MAPK pathway, siRNA silencing of MEK1/2 was conducted in Calu-1 cells. Ablation of MEK1/2 led to abrogation of MEK1/2 and Erk1/2 phosphorylation, and had similar effects as Erk knockdown in reducing cisplatin IC_{50} in Calu-1 cells (Figure 4.13 B).

These data demonstrated the positive contribution of both Erk1 and Erk2 to cell proliferation under drug pressure. Reduced expression of both kinases was essential for effective enhancement of growth inhibition. However, despite showing silencing of Erk1/2 at 48 hours post-transfection, substantial inhibition of cell proliferation was only observed 72 hours post-transfection (48 hours post-treatment). This observation suggests that Erk-dependent downstream regulation, rather that immediate Erk signalling, is essential for cisplatin sensitization. Furthermore, silencing of MEK1/2 and Erk1/2 indicated that inhibition of p44/42 MAPK signalling could sensitize lung SCC cells to cisplatin treatment.

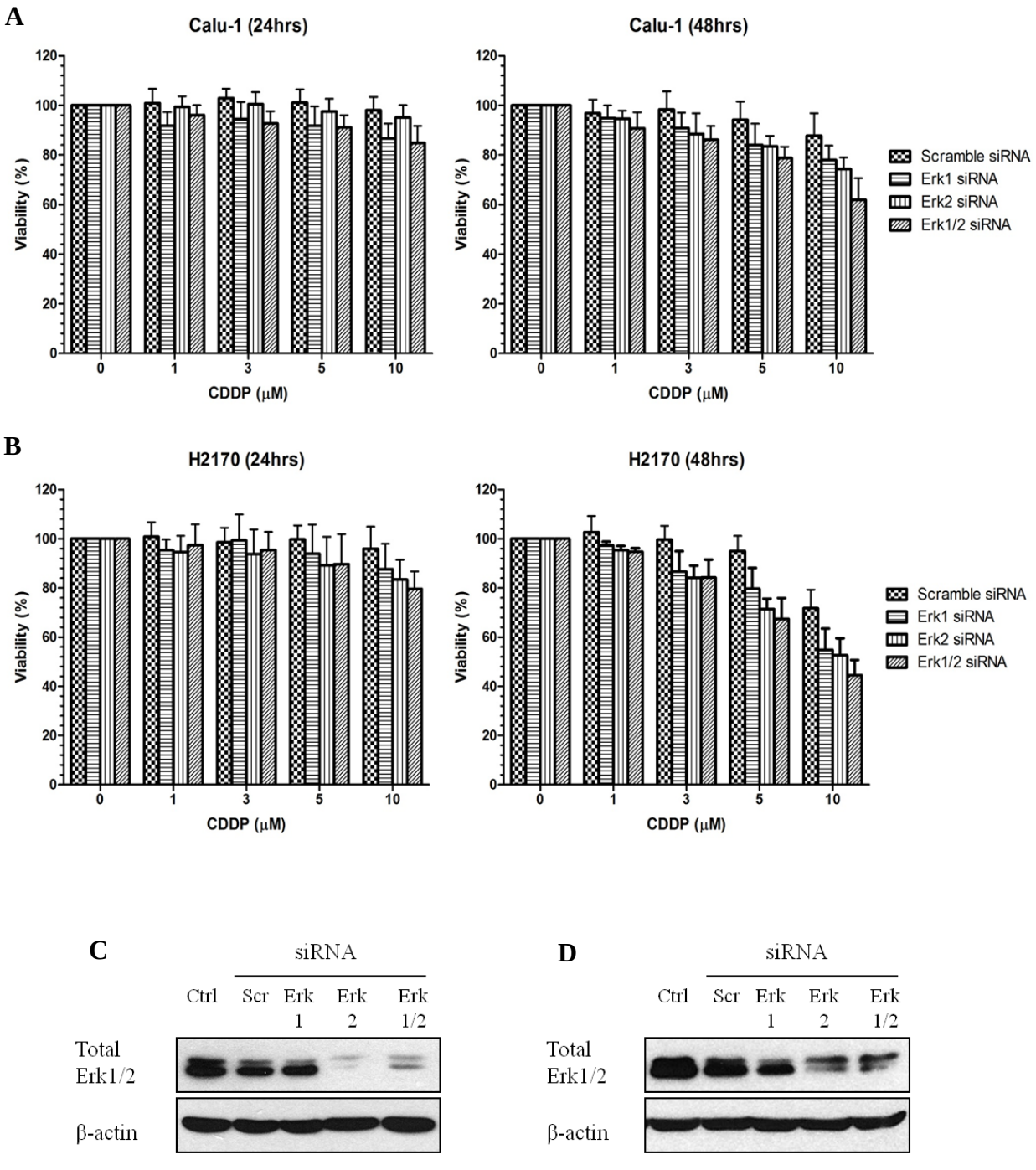

Figure 4.12: Individual and dual silencing of Erk1/2 increases cisplatin sensitivities in cisplatin-resistant cells.

Cell viability of (A) Calu-1 and (B) H2170 cells upon cisplatin treatment (24 hours and 48 hours post-treatment) after Erk1, Erk2 and combined knockdown was measured with MTS assay. Data are presented as mean ± SD (n = 4). Western blotting validation of Erk siRNA silencing in (C) Calu-1 and (D) H2170 cells at 48 hours post-treatment. Western blot data shown are representative of three independent experiments for the indicated targets with β-actin as input control.

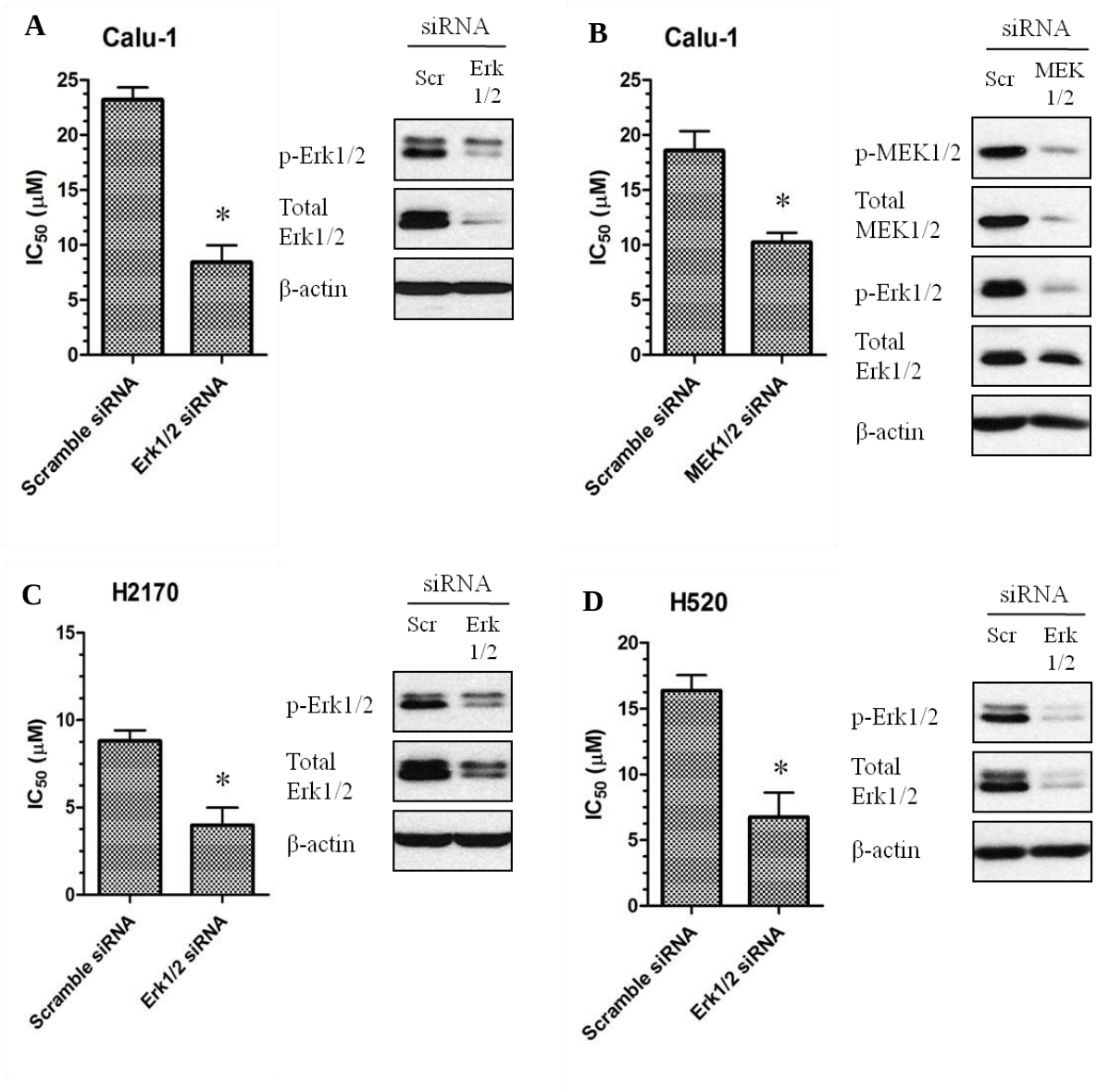

Figure 4.13: Silencing of Erk1/2 enhances cisplatin cytotoxicity in cisplatin-resistant cells.

Cisplatin IC_{50} of Calu-1 cells with respective Western blot validation after (A) Erk1/2 and (B) MEK1/2 siRNA silencing. Cisplatin IC_{50} of (C) H2170 and (D) H520 cells with respective Western blot validation after Erk1/2 siRNA silencing (72 hours post-treatment). 50nM of siRNA was used per transfection. Cisplatin was administered for 72 hours. Data are shown as average ± SD for three independent experiments. Western blot data shown are representative of three independent experiments for the indicated targets with β-actin as input control. Statistical analyses were performed by unpaired t-test. *Significant difference from scramble control, $P < 0.05$.

4.3.2 Pharmacological inhibition of p44/42 MAPK signalling increases cisplatin cytotoxicity in lung SCC cells

Thus far, inhibition of p44/42 MAPK signalling is shown to enhance cell death in the context of cisplatin resistant cell lines. To place clinical relevance to these findings, inhibition MAPK/MEK/Erk pathway was performed in concurrent with cisplatin treatment. Several pharmacological inhibitors of the EGFR/Ras/Raf/MEK/Erk pathway: EGFR antibody (Cetuximab), B-Raf small-molecule inhibitor (GDC0879), and multiple MEK inhibitors (PD0325901, RDEA119 and GSK1120212), were tested on Calu-1 cell line. Calu-1 has wild-type EGFR and B-raf but mutant Kras.

The sub-lethal doses of these inhibitors in Calu-1 cells were determined with cell proliferation assay (Data not shown). Cetuximab (25μg/mL) treatment did not affect downstream signalling of MAPK/Erk; GDC0879 (10μM) treatment reduced p-B-Raf, but up-regulated p-MEK1/2 and p-Erk1/2. On the contrary, MEK inhibitors did not prevent phosphorylation of MEK1/2 by B-raf, but inhibited MEK functions and abrogated p-Erk1.2 (Figure 4.14 D). Cetuximab and GDC0879 did not sensitize Calu-1 cells to cisplatin treatment (Figure 4.14 A). However, co-incubation of cisplatin and MEK inhibitors significantly lowered cisplatin IC_{50} (Figure 4.14 B). Similarly, inhibiting activity of MEK in H520 cells led to substantial abrogation of p-Erk1/2 as well as sensitization towards cisplatin treatment (Figure 4.14 C, E). In addition, co-treatment with MEK inhibitors at 48 hours potentiated cisplatin-induced apoptosis as shown by the cleavages of PARP and caspase 3 in cisplatin-treated Calu-1 cells (Figure 4.15).

The cytotoxicity of cisplatin and GSK1120212 under anchorage-independent condition was next assessed. In Calu-1 cells, GSK1120212 displayed strong inhibitory effects on colony forming ability, with significant reduction in colony counts after treatment with 10nM (Figure 4.16 A). In H520 cells, GSK1120212 has a high IC_{50} of 1.9μM, but was synergised with cisplatin. Reducing its IC_{50} from 193nM to 132nM (Figure 4.16 B, C), with a CI of 0.83 and DRI of 1.32 (in relative to cisplatin) (Figure 4.16 D).

By using 3 different allosteric inhibitors of MEK, it was shown that suppression of Erk1/2 activation by MEK1/2 at sub-lethal doses consistently augmented cisplatin cytotoxicity through induction of apoptosis in lung SCC cells. Moreover, GSK1120212 produces favourable growth inhibition on Calu-1 and H520 cells under anchorage-independent condition. Therefore, inhibition of Erk appeared to be a clinically applicable therapeutic strategy to enhance cisplatin treatment in lung SCC with up-regulation of Erk1/2.

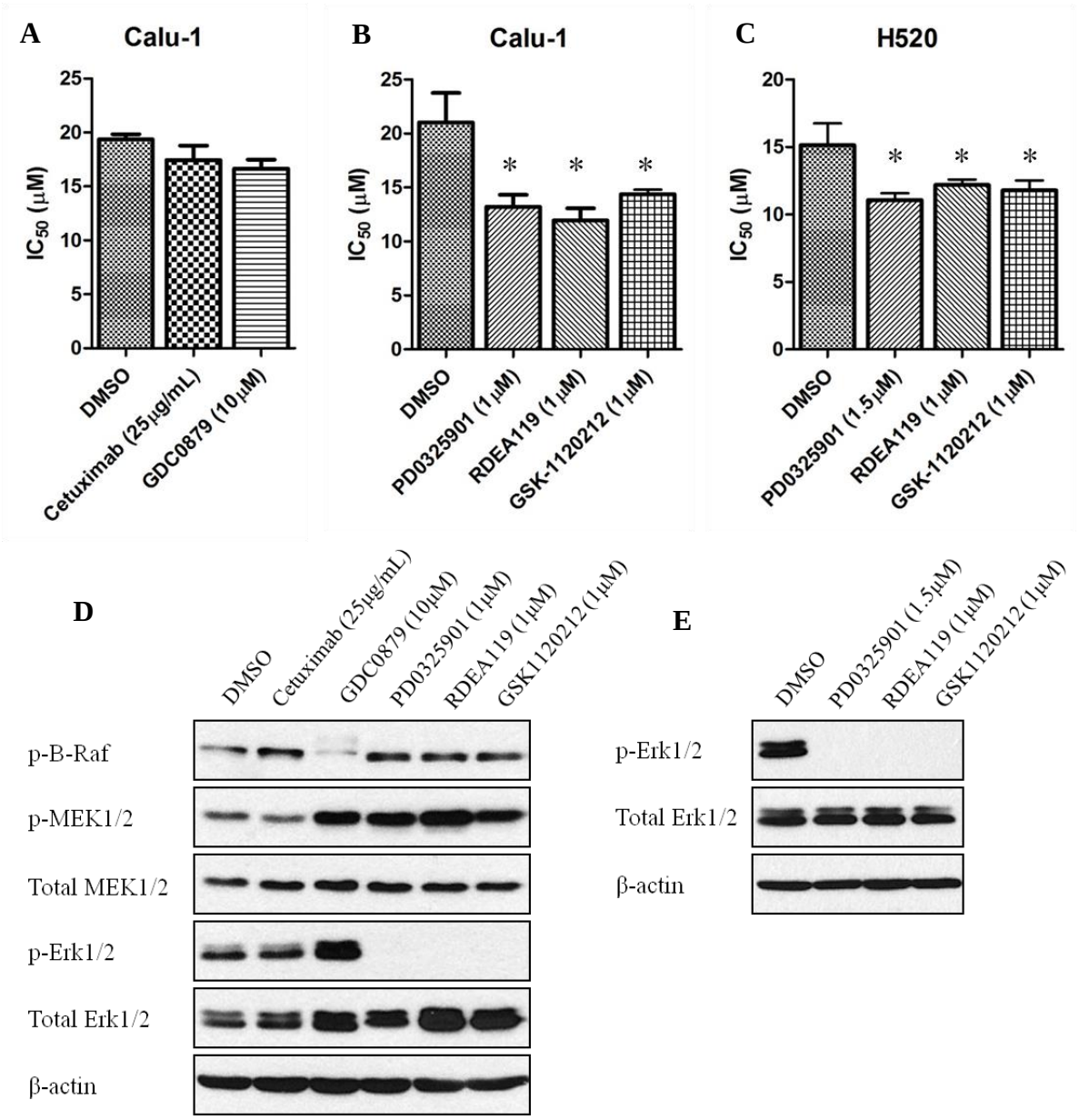

Figure 4.14: MEK inhibitors enhance cisplatin cytotoxicity in cisplatin-resistant cells.

A, Bar charts show cisplatin IC_{50} of Calu-1 cells after co-treatment with DMSO, Cetuximab (25μg/mL) or GDC0879 (10μM). Bar charts show cisplatin IC_{50} of (B) Calu-1 and (C) H520 cells after co-treatment with DMSO or MEK inhibitors (PD0325901, RDEA119 and GSK1120212). Drugs were treated for 72 hours. Data are presented as mean ± SD for three independent experiments. D, western blot analyses were performed on Calu-1 cells treated with DMSO (0.1%), Cetuximab, GDC0879, or MEK inhibitors. E, Western blot analyses were performed on H520 cells treated with DMSO (0.01 or 0.015%) or MEK inhibitors. Western blot data shown are representative of three independent experiments for the indicated targets with β-actin as input control. Statistical analyses were performed by unpaired t-test. *Significant difference from vehicle control, $P < 0.05$.

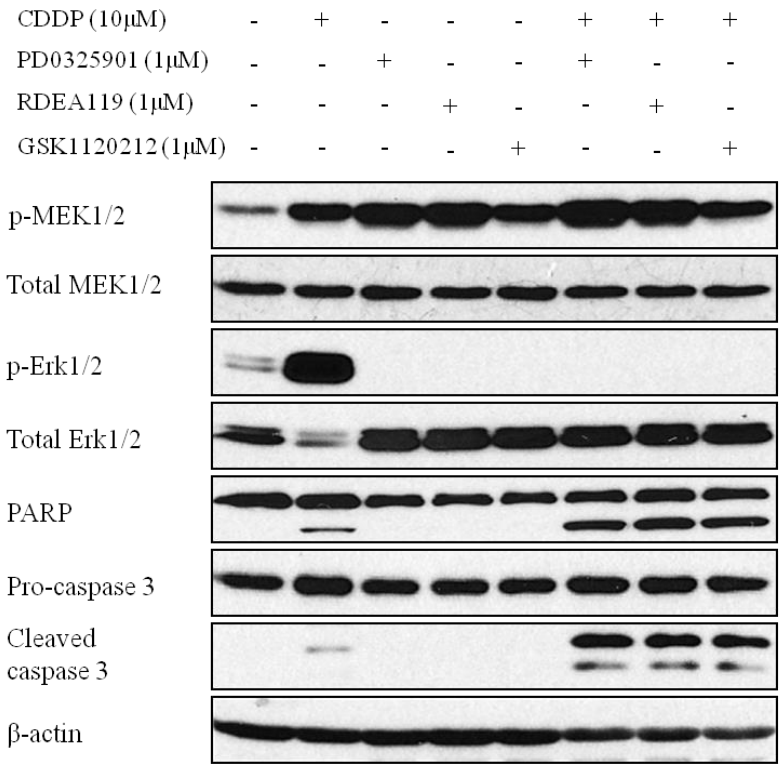

Figure 4.15: MEK inhibitors potentiate apoptosis in cisplatin-treated Calu-1 cells.

Western blot analyses were performed on Calu-1 cells treated with DMSO (0.01%), cisplatin (10μM), MEK inhibitors (1μM of PD0325901, RDEA119 or GSK1120212) or combination treatment for 48 hours. Western blot data shown are representative of three independent experiments for the indicated targets with β-actin as input control.

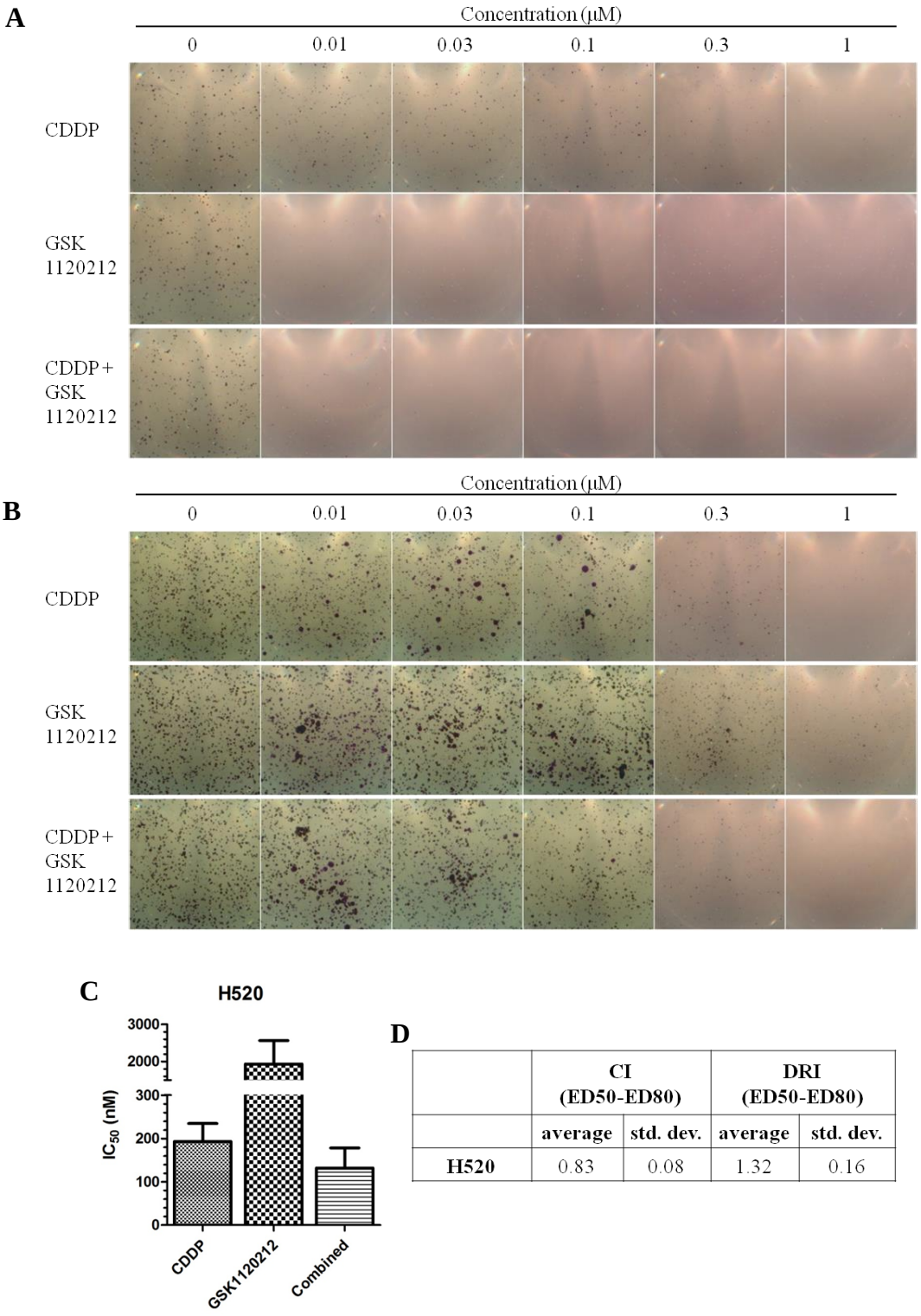

D

	CI (ED50-ED80)		DRI (ED50-ED80)	
	average	std. dev.	average	std. dev.
H520	0.83	0.08	1.32	0.16

Figure 4.16: Cytotoxicity of GSK1120212 and cisplatin in Calu-1 and H520 cells under anchorage-independent condition.

Soft agar colony forming assay was performed to determine the sensitivities of lung SCC cells to cisplatin and GSK1120212 under anchorage-independent condition. Representative images for colony formations and dose-dependent colony inhibitions in Calu-1 (A) and H520 (B) cell lines are presented. C, IC_{50} of cisplatin, GSK1120212 and combined

treatment. Cisplatin and GSK1120212 were combined at 1:1 ratio at the indicated doses. Reduction in colony formation was determined by MTT assay. IC_{50} are shown as mean ± SD (n = 3). D, Combination index (CI) and dose reduction index (DRI) of cisplatin for H520 cells in soft agar assay are assessed. The nature of drug interaction is defined as synergism (CI < 0.8), additive effect (0.8 < CI < 1.2), and antagonism (CI > 1.2). Data are presented as mean ± SD (n = 3).

Summary of findings in Chapter 4.3:

- siRNA silencing of MEK1/2 suppressed phosphorylation of Erk1/2.
- siRNA silencing of Erk1/2 or MEK1/2 sensitized lung SCC cell lines to cisplatin treatment.
- Cetuximab did not affect MAPK signalling in Kras mutant Calu-1 cells.
- B-Raf inhibitor (GDC0879) abrogated phosphorylation of B-Raf but does not affect phosphorylations of MEK and Erk.
- Both Cetuximab and GDC0879 did not sensitize Calu-1cells to cisplatin treatment.
- MEK inhibitors (RDEA119, PD0325901 and GSK1120212) induced cellular accumulation of p-MEK1/2 and effectively abrogated p-Erk1/2 in Calu-1 and H520 cells.
- Sub-lethal doses of MEK inhibitors potentiated cisplatin-induced apoptosis in Calu-1 cells.
- Calu-1 cells were sensitive to GSK1120212 under anchorage-independent condition.
- Synergistic combination of cisplatin and GSK1120212 was observed in H520 cells under anchorage-independent condition.

4.4 High p-Erk1/2 expression correlates with shorter progression-free survival in HNSCC patients after adjuvant chemotherapy

It was hypothesized that Erk1/2 activity correlates with occurrence of cisplatin resistance. To test the hypothesis that strong Erk1/2 activity-induced cisplatin resistance in SCC, clinicopathological analysis was conducted on SCC samples with interval to tumour relapse as assessment endpoint. However, acquisition of post-treatment biopsies was technically difficult for retrospective studies. Therefore, a retrospective study was conducted to analyse the correlation between p-Erk1/2 expression and clinical outcome in SCC. For current study, archival resected SCC specimens were retrieved from the Department of Pathology, NUH. Lung SCC samples selected for NGS analysis in Chapter 3.1 was initially used for this analysis. However, the assessment of clinical data for these lung SCC samples was restricted as most lung SCC patients were not treated with single-agent cisplatin, and the correlation of p-ERK expression and patient survival may be confounded by the addition of a second chemotherapeutic agent. Therefore, clinicopathological analysis was conducted on SCC of the head and neck (HNSCC) instead where concurrent single-agent cisplatin treatment with radiotherapy is the standard first-line regime. It is generally accepted that HNSCC share similar etiology and histopathological characteristics of SCC of the lung. (Kaufmann, Fietze et al. 2001, Day, Davis et al. 2003, Agrawal, Frederick et al. 2011, Stransky, Egloff et al. 2011). The characteristics of this patient population were presented in Figure 4.18 B. Treatment was in the form of a combined modality: surgical resection followed by concurrent chemoradiation or primarily concurrent chemoradiation followed by salvage surgery for persistent disease. In all patients, the chemotherapy regime was the weekly administration of 40 mg/m^2 cisplatin of at least 5 cycles of treatment.

A total of 45 head and neck SCC (HNSCC) paraffin embedded specimens who underwent surgery in 2003 – 2010 were obtained and analysed under protocols (Chapter 2.11) approved by NUHS Institutional Review Board (IRB). The strength and intracellular distribution of p-Erk1/2 expression were evaluated by IHC with anti-p-Erk1/2 antibody (Table 2.22). As described in Chapter 4.2.2, Erk activity could be determined by the nuclear/cytosolic translocalization of the phosphorylated protein. To investigate the Erk level activity in the tissue specimens, whole tissue sections were scored based on staining intensity (0 – 3), stained region (nuclear or cytoplasmic) and intracellular distribution of stained tumour (0 – 100%). Stained tissues showed different expression patterns with 3 specimens having no p-Erk1/2 staining. In HNSCC specimens, 1 tumour showed only cytoplasmic p-Erk1/2 staining (Figure 4.17 A), while others showed different intensities of cytoplasmic and nuclear staining: low intensity (1) (Figure 4.17 B), moderate intensity (2) (Figure 4.17 C) and high intensity (3) (Figure 4.18D). Immunoreactive score (ranging from

0 to 300) was obtained for each specimen as described in Chapter 2.11.6. Data were then grouped into multiple scoring groups (0 – 50; 51 – 100; 101 – 150; 151 – 200; 201 – 250; 251 – 300). The evaluation of proportion of specimens in each scoring group is shown in Figure 4.17 E.

Detailed clinical records of these cases, which include time to tumour progression, were collected from the Computerized Patient Support System (CPSS). Staining data of p-Erk1/2 from HNSCC patients were split into high (immunoreactive score > 50; n = 27) and low (immunoreactive score < 50; n = 18) scoring categories. Patients who died from factors not related to the disease and those who were not followed up during the observation period were excluded in the subsequent analysis (censored) as indicated by vertical ticks in Figure 4.18 A. The disease-free survival (DFS)—defined as the interval between the chemoradiation completion to the first histologically or radiologically confirmed tumor recurrence locally in the head and neck region or distant metastases—was presented using Kaplan–Meier analysis for 45 patients who provided consent for the use of their patient data. Significantly shorter DFS was determined for patients with higher expression of p-ERK (log-rank test, $P = 0.02$) (Figure 4.18 A), suggesting that activation of the MAPK/ERK pathway is predictive of cisplatin efficacy in the treatment of SCC. It is important to note that human papillomavirus (HPV) is a known cause of HNSCC and is associated with better prognosis (Liang, Marsit et al. 2012). Using p16 as a surrogate biomarker for HPV infection, four patients from each of the p-ERK high and low groups were p16 positive (Figure 4.18 B). Therefore, the HPV status is not likely a confounding variable in the association of p-ERK and DFS among the HNSCC cases.

In conclusion, the clinicopathological analyses demonstrated that high p-Erk1/2 in HNSCC contributed to shorter DFS. Interestingly, most positively-stained tumours expressed p-Erk1/2 in both nucleus and cytoplasm, suggesting both nuclear-bound and cytoplasmic p-Erk1/2 as candidate predictive marker indicative of tumour relapse.

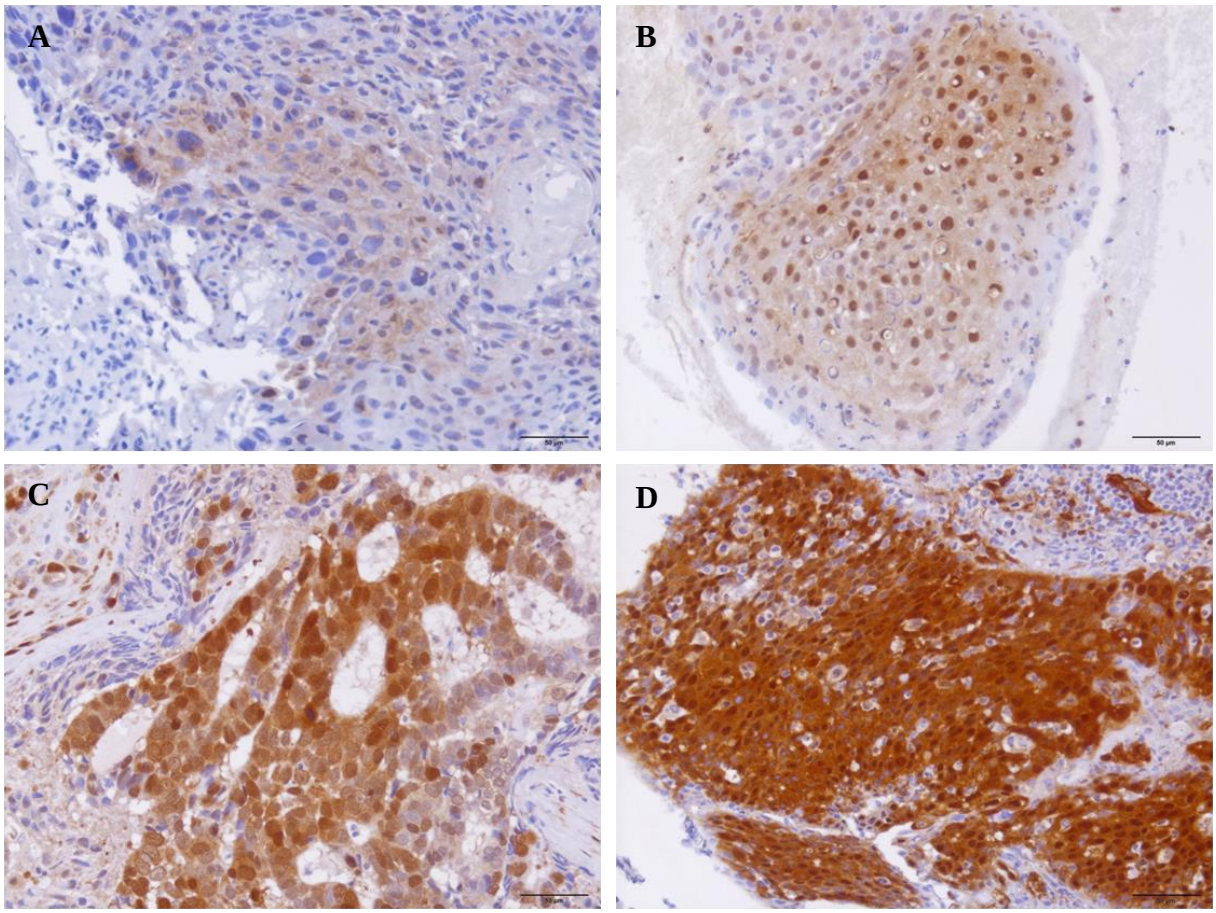

E

Immunoreactive score	No. of specimens
0 – 50	**17**
51 – 100	**3**
101 – 150	**6**
151 – 200	**5**
201 – 250	**9**
251 – 300	**5**

Figure 4.17: p-Erk1/2 staining in human HNSCC tumurs.

A panel of tissue sections derived from 33 HNSCC patients with known case histories was analysed for intracellular distribution of p-Erk1/2 by IHC. Intensities of p-Erk1/2 were scored. A, Photomicrograph revealed tumour with predominantly p-Erk1/2 staining at cytoplasms than that in nuclei. B – D, Photomicrographs revealed tumours with p-Erk1/2 staining at both cytoplasms and nuclei. Representative images for positively stained tumours with intensity of 1 (B), 2 (C) and 3 (D) were shown. E, Distribution of the immunoreactive scores [intensity of p-Erk1/2 (0 – 3) x fraction of stained tumour cells (0 – 100%)] in all HNSCC samples was shown. All photomicrographs where taken in 400x magnification. Scale bars in A – D, 50μm.

A

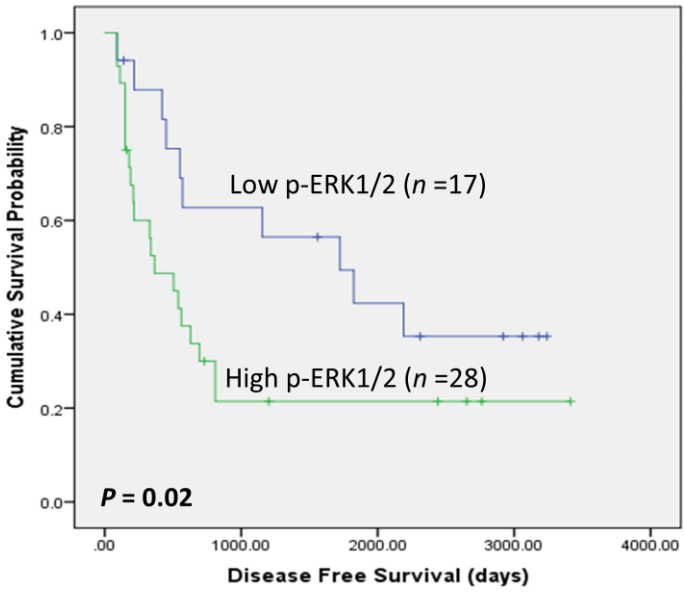

B

Characteristic	Low phospho-ERK (n=17)	High phospho-ERK (n=28)
Age	51 (25 to 68)	57 (29 to 81)
Gender		
Male	12	19
Female	5	9
Stage (%)		
2	2 (12)	1 (4)
3	0	2 (7)
4	15 (88)	25 (89)
Site of disease (%)		
Larynx	4 (24)	9 (32)
Hypopharynx	0 (0)	4 (14)
Oropharynx	5 (29)	7 (25)
Oral cavity	8 (47)	7 (25)
Nasal cavity	0 (0)	1 (4)
HPV status		
p16 positive	4	4

Figure 4.18: High p-Erk1/2 correlates to poor disease-free survival in patients with HNSCC following adjuvant cisplatin therapy.

Intracellular p-Erk1/2 distribution (Figure 4.17) was analysed in all HNSCC samples. A, Kaplan Meier curves for DFS are plotted for the high and low p-ERK1/2 populations. Tick marks indicate patients for whom data was censored (Data cutoff point: June 2014). B, Baseline characteristics of the head and neck squamous cell carcinoma (HNSCC) population, classified according to the p-ERK1/2 scoring.Statistical analysis was performed using Chi-squared test with Gehan-Breslow-Wilcoxon Test. Significant difference between the two expression groups, $P < 0.05$.

Summary of findings in Chapter 4.4:

- Immunoreactive scoring of p-Erk1/2 was performed on 45 HNSCC specimens.
- p44/42 MAPK activity in tumour cells is indicated by nuclear and cytosolic accumulation of p-Erk1/2.
- Patients with higher p-Erk1/2 expression in their tumours had significantly higher 5-year DFS rates that those with low p-Erk1/2 after adjuvant chemotherapy.
- p-Erk1/2 expression is a potential predictive biomarker for adjuvant cisplatin chemotherapy in patients with HNSCC.

4.5 Discussion

4.5.1 The molecular mechanisms of cisplatin resistance in lung SCC

Over the past 30 years, multiple mechanisms have been proposed to describe cisplatin resistance with intensive studies being conducted on clinical settings whereby cisplatin represent the major therapeutic intervention, which include ovarian carcinoma, NSCLC, head and neck cancer and cervical cancer (Muggia 1991, Lebwohl and Canetta 1998). However, despite being the standard-of-care treatment for lung SCC, the underlying cisplatin resistant mechanism(s) have not been exploited in this disease.

In this chapter, the activation of survival signalling that confer cisplatin resistance in lung SCC were discussed. Through comparative analyses on the transcriptomic and phospho-kinetics perturbations (Chapter 4.1), cisplatin treatment was shown to induce differential modulation of p44/42 MAPK signalling between the sensitive and resistant phenotypes. Cisplatin sensitive cells displayed decreased mRNA expression of MAPK signalling pathway-related genes and down-regulation of phospho-MAPK (B-Raf, MEK1/2, Erk1/2 and MSK1). Conversely, activation of MAPK/Erk was a common phenomenon among resistant cell lines. This observation is consistent with previous studies which showed stimulation of Erk signalling in a time- and dose-dependent manner upon exposure to cisplatin (Cui, Yazlovitskaya et al. 2000, Wang, Martindale et al. 2000). Furthermore, the analyses showed that cisplatin treatment reduced the expression of Akt and JNK in both resistant and sensitive cell lines (Chapter 4.1.2), while p38 was regulated in random patterns (Chapter 4.1.3), thus downplaying the relevance of these kinases in cisplatin resistance. The striking differences on cisplatin-induced p44/42 MAPK signalling between resistant and sensitive phenotypes implicate the involvement of this pathway in cisplatin resistance.

Members of the MAPK signalling family (JNK, p38 and Erk) are crucial for the maintenance of cellular processing. Erk has been original shown to be important for cell survival, while JNK and p38 are widely deemed to mediate cell death (Xia, Dickens et al. 1995). However, the role of MAPK/Erk in apoptosis regulation is more complicated that initially thought as there have been conflicting reports on the functions of Erk in cisplatin-induced response (Wada and Penninger 2004). While some studies have demonstrated that Erk activation promotes cellular survival of cisplatin-treated ovarian and melanoma cancer cells (Hayakawa, Ohmichi et al. 1999, Persons, Yazlovitskaya et al. 1999, Wang, Zhou et al. 2007), several other reports have emphasized the involvement of Erk in cisplatin-induced apoptosis (Dent and Grant 2001, Mandic, Viktorsson et al. 2001, Yeh, Chuang et al. 2002). These conflicting reports suggest that the relationship between Erk activation and cisplatin cytotoxicity is cell-context dependent and could vary among different types of cancer.

The role of Erk in determining cellular survival/death in lung SCC cells under cisplatin pressure was investigated in this study. The data suggested that siRNA-mediated depletion of Erk activity could enhance cisplatin cytotoxicity in several lung SCC cells, while the similar observations were seen after silencing of MEK (Chapter 4.3.1). These observations provided compelling evidence that p44/42 MAPK signalling favours cell survival instead of cell death in cisplatin-treated SCC cells. Interestingly, belinostat specifically disrupted p44/42 MAPK signalling in lung SCC lines through suppressing B-Raf, MEK1/2, Erk1/2 and MSK (Chapter 4.1.3, Chapter 4.2.1). Furthermore, cisplatin-induced up-regulation of Erk activity in resistant cells was abrogated in combination with belinostat (Chapter 4.2.2), probably resulted in the synergistic cytotoxicity within lung SCC cells. Some recent studies have reported that belinostat could repress proliferation of thyroid cancer cells and displayed synergistic combinatorial effects with doxorubicin, paclitaxel, pazopanib and dasatinib, partially through suppression of Erk signalling (Chan, Zheng et al. 2013, Lin, Lin et al. 2013). These findings implicate that belinostat possibly sensitizes lung SCC cells to cisplatin through inhibition of p44/42 MAPK signalling,

4.5.2 Regulating p44/42 MAPK signalling in lung SCC

As illustrated in Figure 4.19, the p44/42 MAPK signal transduction pathway is a chain of cellular proteins that forms a signalling network linking extracellular stimuli to transcriptional activities. Key components of p44/42 MAPK signalling include membrane spanning RTK (EGFR), GTPase exchange factors (GEFs) (SOS1, SOS2), GTPase activating proteins (GAPs), GTPase binding protein (Ras), kinase cascade (Raf, MEK, Erk) and downstream effector kinases [MAPK-interacting kinase (MNK), Ribosomal Protein S6 kinse (RSK), and MSK] (Buday and Downward 1993, Huang, Marshall et al. 1993). Briefly, extracellular signal such as EGF activates the tyrosine kinase activity through phosphorylation of the cytoplasmic domain of the receptor, which then recruits Growth Factor Receptor Bound Protein 2 (GRB2) (Schulze, Deng et al. 2005) and subsequently activates SOS constitutively (Rogge, Karlovich et al. 1991, Li, Batzer et al. 1993). Activated SOS molecules facilitate the GDP-GTP exchange of Ras, allowing it to interact with Raf (Avruch, Khokhlatchev et al. 2001). This triggers the activation of Erk kinase cascade, by which Raf phosphorylates MEK1/2 and MEK phosphorylates Erk1/2. Upon its activation, Erk could indirectly regulate transcription by phosphorylating cytosolic RSK and MNK, two transcription factors that regulate cell proliferation through cAMP response-element binding (CREB) signalling (Chen, Sarnecki et al. 1992, Waskiewicz, Flynn et al. 1997); or directly translocates into the nucleus for phosphorylation of target kinases, such as MSK1 that mediates stress-induced activation of CREB (Deak, Clifton et al. 1998).

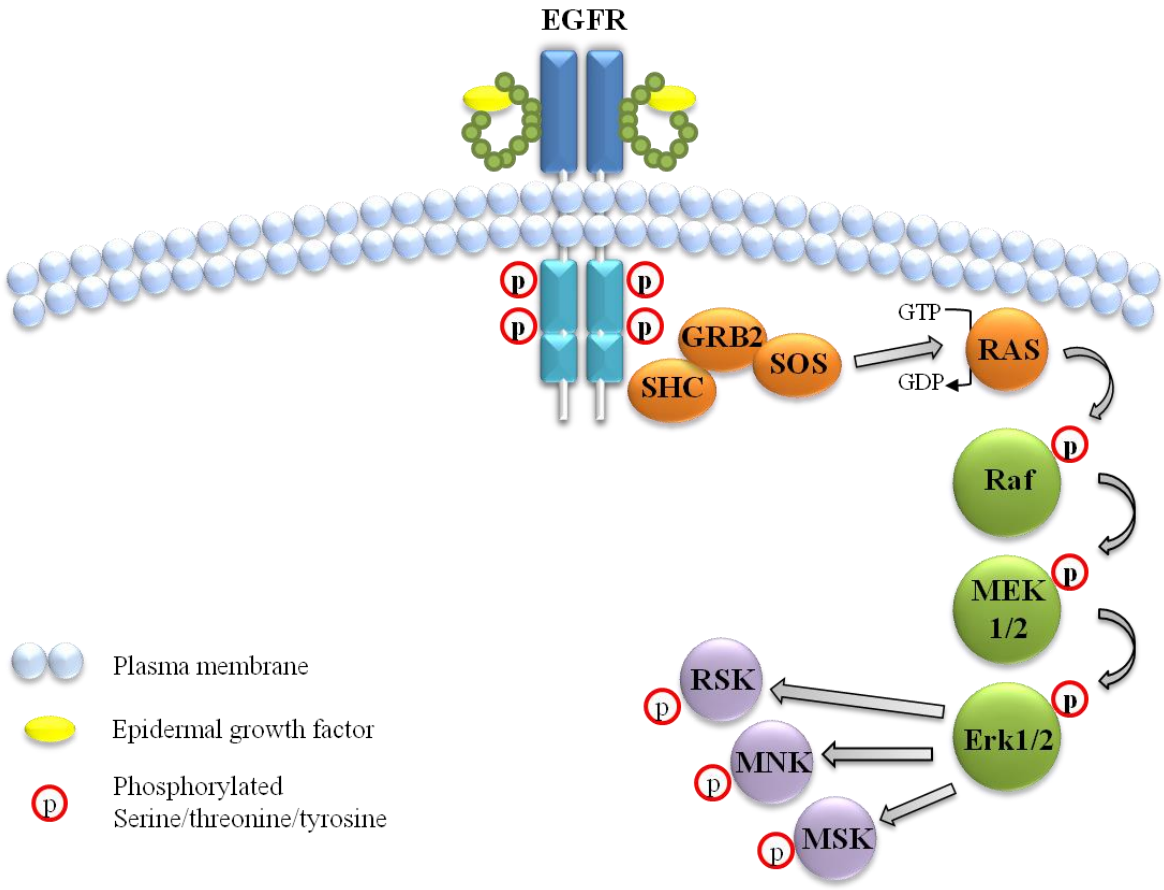

Figure 4.19: Regulation of the p44/42 MAPK signalling pathway.

The MAPK pathway could be triggered by binding of EGF to EGFR and assembly of a signalling complex that include Src-homology and collagen homology (SHC), GRB2 and SOS. This leads to the induction of p44/42 MAPK signalling: SOS activates Ras; Ras activates Raf: Raf activates MEK1/2; MEK1/2 activates Erk1/2; and Erk1/2 activates RSK, MNK and MSK.

Collectively, the p44/42 MAPK pathway functions as a key regulator for cellular proliferation, survival, differentiation and apoptosis. Dysregulations of Erk cascade that lead to its inappropriate activation are common aberrations in tumourigenesis (Blume-Jensen and Hunter 2001). For instant, EGFR mutations are frequently detected in lung cancer (Blume-Jensen and Hunter 2001); while Ras mutations are found in almost one-third of all human cancer (Pylayeva-Gupta, Grabocka et al. 2011). However, in line with the genomic characterization reported by TCGA (Network 2012), the analysis suggested that somatic mutations of EGFR and its family members are lacking among lung SCC and cell lines (Chapter 3.1). Therefore, the sustained activity of Erk signalling was proposed as a cisplatin

resistance mechanism. In this study, up-regulation of SOS (Chapter 4.2.3.1), constitutive activation of Erk1/2 (Chapter 4.1.3), nuclear translocation of activated Erk (Chapter 4.2.2.2), and phosphorylation of MSK1 (Chapter 4.1.3) occurred simultaneously in cell lines that are more tolerable to cisplatin. Taken together, it is likely that in cisplatin-resistant cells, Erk1/2 is activated via regulation of SOS under cisplatin pressure, and eventually promotes cellular survival through downstream activation of MSK and other transcription factors (Deak, Clifton et al. 1998, Brunet, Roux et al. 1999) (Figure 4.20). Therefore, a novel correlation between SOS and B-Raf-MEK-Erk signalling in conferring cisplatin resistance was proposed in lung SCC cells.

In the present study, belinostat was shown to effectively abrogate p44/42 MAPK activity in concurrent with the down-regulation of SOS expressions in all lung SCC cell lines (Chapter 4.2.3.1). It was further demonstrated that gene silencing of SOS1 and SOS2 significantly attenuated Erk phosphorylation in lung SCC cell lines irrespective of the mutational status of Kras (Calu-1), suggesting that belinostat negatively regulated the p44/42 MAPK pathway by suppression of SOS molecules (Chapter 4.2.3.2). However, currently available SOS inhibitors are limited only to research purposes (Patgiri, Yadav et al. 2011, Maurer, Garrenton et al. 2012). Therefore, these findings highlighted the need for strategies that inhibit p44/42 MAPK signalling in lung SCC cells.

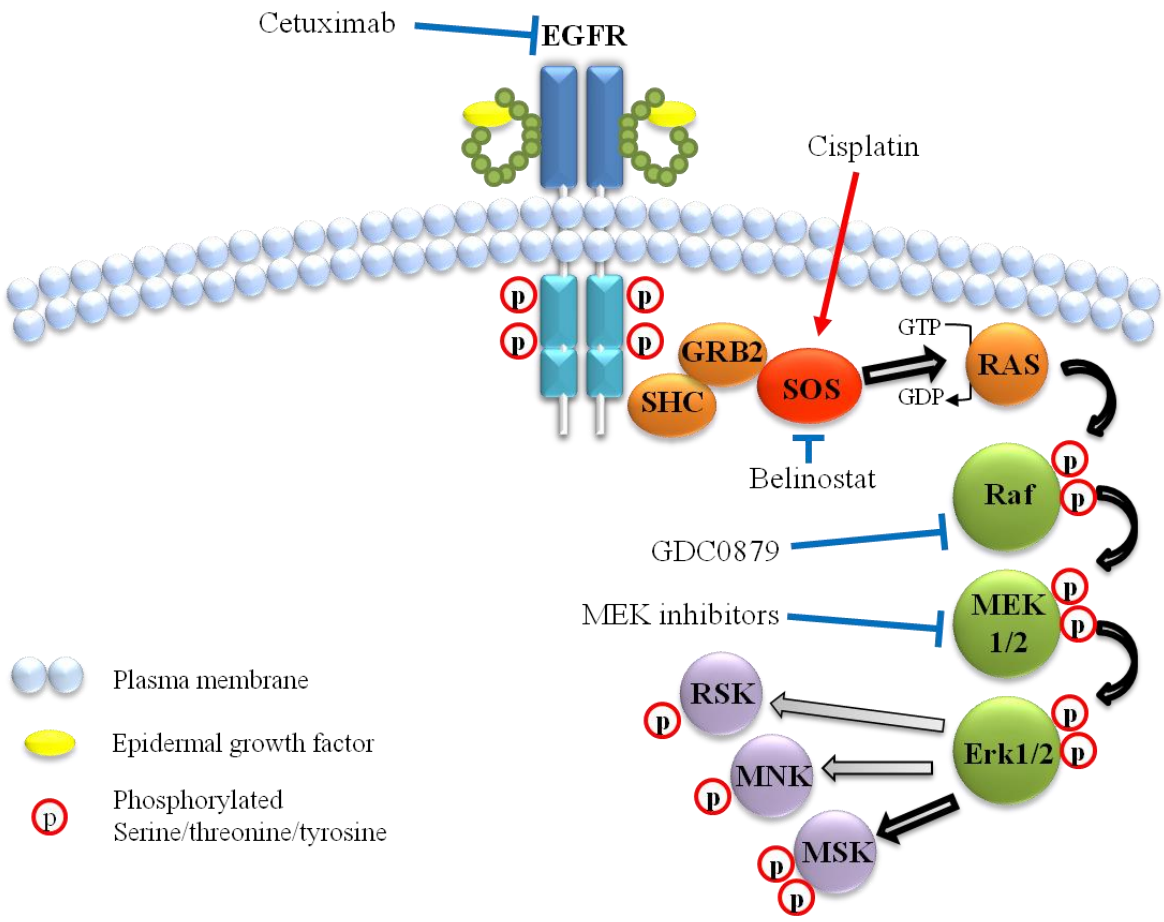

Figure 4.20: Activation of p44/42 MAPK via SOS up-regulation as a mechanism of cisplatin resistance in lung SCC cells and selection of inhibitors for suppression of Erk signalling.

Cisplatin treatment induces activation of Raf/MEK/Erk/MSK in cisplatin-resistant lung SCC cells through up-regulation of SOS1 and SOS2. Belinostat (PXD101) deactivates p44/42 MAPK through inhibition of SOS; Cetuximab turns off EGFR signalling; GDC0879 blocks B-Raf activity; MEK inhibitors (PD0325901, RDEA119 and GSK1120212) block Erk1/2 activity through allosteric inhibition of MEK1/2.

4.5.3 Targeting p44/42 MAPK as a chemosensitization strategy in lung SCC

Our findings suggested Erk suppression as the mechanism behind the synergistic cytotoxicity of cisplatin and belinostat in lung SCC cell lines. However, with the exception of CTCL (Mann, Johnson et al. 2007), clinical trials on HDAC inhibitors have not achieved superior progress in advanced solid malignancies despite the strong *in vitro* anti-neoplastic effects (Bradley, Rathkopf et al. 2009, Ramalingam, Belani et al. 2009, Mackay, Hirte et al. 2010). Thus, the combinatory effects of cisplatin and various MAPK-targeting inhibitors

were explored. For years, inhibition of the EGFR/Ras/Raf/MAPK/Erk pathway has been one of the key focuses in developing anti-cancer agents. For instance, gefitinib and erlotinib have shown improved clinical response in NSCLC patients with EGFR mutation (Paez, Jänne et al. 2004, Tsao, Sakurada et al. 2005); B-Raf inhibitor, vemurafenib, has been proven to inhibit metastatic melanoma with mutated B-Raf (Flaherty, Puzanov et al. 2010, Flaherty, Infante et al. 2012); while several MEK inhibitors have progressed to phase II trials on NSCLC and melanoma patients (Haura, Ricart et al. 2010, Catalanotti, Solit et al. 2013).

For the current study, several MAPK-targeting inhibitors were selected based on their clinical relevance to the disease model. According to COSMIC database, Calu-1 is an EGFR wild-type cell line with Kras mutation. Therefore, Cetuximab was chosen over gefitinib and erlotinib due to its non-selectivity on the mutational status of EGFR (O'Byrne, Gatzemeier et al. 2011, Misale, Yaeger et al. 2012); GDC0879 was selected to inhibit B-Raf; while PD0325901, RDEA119, GSK1120212 were selected for MEK inhibition. Cetuximab did not affect p44/42 MAPK signalling, probably due to the mutant Kras that constitutively activated MEK and Erk (Lièvre, Bachet et al. 2008). Intriguingly, GDC0879 did not affect Erk activity of Calu-1 cells despite inhibiting phosphorylation of B-Raf. However, sub-lethal doses of MEK inhibitors completely abrogated phosphorylation of Erk in Calu-1 cells. Among these inhibitors, only MEK inhibitors sensitized Calu-1 to cisplatin treatment (Chapter 4.3.2). Consistently, blocking Erk activity in H520 increased cisplatin sensitivity as well. Therefore, from a therapeutic perspective, targeting MEK/Erk concurrently with cisplatin could improve survival outcome in treatment of SCCs.

To date, molecularly targeting approaches in lung SCC have achieved limited successes in clinical settings. Unlike lung adenocarcinoma, patients with SCCs often provided with limited therapeutic options. Identification of biomarkers that could predict sensitivity and selection of optimal drug combinations are the two major challenges in designing targeted therapy regimen in this disease. This study suggested that attenuation of MEK/Erk activity enhanced efficacy of cisplatin. Recently, several MEK inhibitors, such as selumetinib (AZD6244) and trametinib (GSK1120212), have progressed to Phase II clinical trial. Despite failing to demonstrate superior clinical outcome as a single drug treatment among NSCLC patients (Haura, Ricart et al. 2010, Jänne, Shaw et al. 2013), combinations of MEK inhibitor with other agents have manifested promising anti-neoplastic activity in several clinical trials, particularly among NSCLC patients harbouring Kras mutant. (Chen and Sweet-Cordero 2013, Huang, Lee et al. 2013, Jänne, Shaw et al. 2013). Consistently, GSK1120212 strongly inhibit colony formation in Kras mutant Calu-1 cells under anchorage-independent growth conditions (Chapter 4.3.2). Currently, several active trials

are exploring the combination of cisplatin and MEK inhibitors in NSCLC (ClinicalTrials.gov Identifier NCT01809210; NCT01192165), but mutation on Kras remains as the key selection criteria for these studies. The findings provided strong indication to assign MEK/Erk activity as predictive biomarker to recruit patients for these studies.

Previously, clinical study on treating NSCLC with PD0325901 had been terminated due to the ocular and neurological toxicity (ClinicalTrials.gov Identifier NCT00174369; A4581001) (Huang, Yang et al. 2009), while serious ocular neuropathy was recognized as common dose-limiting toxicity across all MEK inhibitors (Akinleye, Furqan et al. 2013). Both the *in vitro* assays under anchorage-dependent and –independent conditions suggested that low doses of MEK inhibitors were sufficient to induce synergic combination with csiplatin (Chapter 4.3.2). These findings supported the combination of cisplatin and MEK inhibitor at tolerable doses in patients with relapsed to adjuvant cisplatin therapy.

4.5.4 High p-Erk1/2 expression correlates with shorter progression-free survival in SCC cases

Since high p-Erk1/2 has been linked with cisplatin resistance in lung SCC cell lines, the clinical relevance of Erk expression in SCC was next investigated. However, selection of lung SCC samples was limited due to the lack of appropriate cases that had undergone adjuvant chemotherapy with long-term follow-up. In view of these limitations, HNSCC samples were utilised as an alternative model to test the hypothesis on p-Erk1/2 expression and drug resistance. Interestingly, both lung SCC and HNSCC were often detected in the same patient. For instance, patients with laryngeal carcinoma had an increased risk of lung cancer (Levi, Randimbison et al. 2003), while pulmonary SCC often developed following HNSCC (Geurts, Nederlof et al. 2005). These new lung lesions observed in patients with prior history of HNSCC might represent second primary tumours or metastases from previously treated head and neck tumours (Leong, Rezai et al. 1998, Geurts, Nederlof et al. 2005). Furthermore, both lung SCC and HNSCC shared highly similar characteristics, as site of origin of SCC were often indistinguishable based on traditional histopathological examination. Common SCC markers such as p63 and CK5/6 were positively detected in both lung SCC and HNSCC specimens (Kaufmann, Fietze et al. 2001). Furthermore, both cancers were shown to share common etiological and risk factors such as tobacco smoking (Day, Davis et al. 2003). Moreover, recent studies have demonstrated that HNSCC shared multiple genetic alterations common in lung SCC without evidence of HPV infection and these include aberrations in *TP53*, *CDKN2A*, *PTEN*, *PIK3CA*, *HRAS* and *NOTCH1*

(Agrawal, Frederick et al. 2011, Stransky, Egloff et al. 2011). Taken together, all these findings suggested that these two diseases could share similar tumour biology.

While genetic aberrations in MAPK signalling are not common in lung SCC (Network 2012) (Chapter 3.1), the findings in this study have otherwise suggested Erk as a predictive biomarker triggered by treatment pressure and could account for cisplatin resistance in lung SCC cell lines. Clinically, these findings indicate that Erk activity may facilitate resistance to adjuvant cisplatin treatment in SCC, which commonly results in cancer relapse (Ledermann and Kristeleit 2010, Beck and Blanpain 2013). The correlation between endogenous p-Erk1/2 expression and DFS was examined in the selected HNSCC. Despite the well-characterized differential functions of nuclear and cytosolic Erk, high expressions of Erk were seen in both regions in most positively stained tumours. This result indicates that activation of p44/42 MAPK signalling may involve intracellular accumulation of Erk molecules in nucleus and cytoplasm. In concordant with the hypothesis, high expression of p-Erk1/2 is found correlated with significantly higher 5-year DFS (Figure 4.18 B).

Clinically, the analysis on 45 NSCC specimens suggested that p-Erk1/2 could be utilised as an independent predictive biomarker for cisplatin treatment outcome in SCC with a clear difference in DFS between the high and low scoring categories. Collectively, these findings provide ample evidence on p-Erk1/2 as a predictive indicator for shorter DFS among HNSCC patients treated with adjuvant cisplatin-containing therapy.

4.5.5 Conclusions and future directions

Growing understanding of tumourigenesis has led to the development of a wider range of anti-neoplastic agents targeting specific oncogenic pathways. However, the current understanding of lung SCC suggests a paucity of driver oncogenic mutations (Lynch, Bell et al. 2004, Shukuya, Takahashi et al. 2011, Rekhtman, Paik et al. 2012). Furthermore, despite showing initial response to cisplatin treatment, lung SCC usually relapsed more aggressively by acquiring mechanisms which include pathway redundancy and oncogenic bypass (Holohan, Van Schaeybroeck et al. 2013). In the current study, the observation of synergistic cytotoxicity on SCC cells with belinostat, a HDAC inhibitor, and cisplatin, a standard chemotherapy drug for SCC, has led to an analysis of possible mechanisms to explain this.

In summary, this study describes that up-regulation of MEK/ERK is induced by cisplatin treatment in cisplatin-resistant cells and inhibition of this pathway may improve cisplatin sensitivity. Although there are other known mechanisms of cisplatin resistance including

reduced influx transport via the copper transporter, conjugation by glutathione and methionine, and enhanced DNA repair, the relative importance of each of these pathways is still not defined in SCC. However, given the complexity of drug bioavailability and tumour-stroma interaction, it remains debatable whether cell lines are suitable models for understanding of drug resistance, identification of clinically relevant biomarkers as well as evaluation of drug combination. Cancer cell-derived xenograft models that imitate tumour microenvironment may provide better assessment of the proposed therapeutic approach. For this study, H520-derived xenografts are in progress to evaluate the potency of cisplatin and PD0325901.

Furthermore, the clinicopathological analyses on HNSCC specimens strongly support the role of p-Erk1/2 as a predictive biomarker for adjuvant cisplatin chemotherapy. More crucially, the data suggest a role for the combined use of cisplatin with the MEK inhibitor, or belinostat, for patients with up-regulated MAPK/ERK signaling in SCC of the head and neck and lung. Several MEK inhibitors currently undergoing clinical development have shown promising endpoint results in various trials on NSCLC (Chen and Sweet-Cordero 2013, Huang, Lee et al. 2013, Jänne, Shaw et al. 2013). Furthermore, both MEK inhibitors and belinostat have demonstrated favorable tolerability profiles and side effects. Cisplatin is well established and has a non-overlapping toxicity profile, which lends its potential to be combined with a MEK inhibitor or belinostat. For a proof-of-concept, it will be critical to study the combination of cisplatin and a MEK inhibitor in patients whose tumors demonstrate evidence of ERK phosphorylation. Such studies are currently being planned.

CHAPTER 5 Restoration of p53-mediated apoptosis: A gain-of-function event in mutant p53

There has been a rapid advancement in the understanding on the anti-neoplastic activities of HDAC inhibitors. As a class of epigenetic therapeutic agents, HDAC inhibitors exert a broad spectrum of cellular mechanisms over a range of doses, including cell death, cell senescence, and cell differentiation (Chapter 1.5.4.1). The diverse activities of this class of compounds have offered much therapeutic potential as anti-cancer agents, however, the clinical efficacy of HDAC inhibitors have been limited by the many adverse side effects and poor bioavailability (Bruserud, Stapnes et al. 2007, Elaut, Rogiers et al. 2007) (Chapter 1.5.4.2). It is known that high doses of HDAC inhibitors often favour the induction of cell death over cell differentiation (Marks, Richon et al. 2000). In Chapter 4, belinostat at high dose (1μM) was shown to sensitize SCC cells to cisplatin through abrogation of p44/42 MAPK signalling via inhibition of SOS. However, the capacity of belinostat to interfere with cellular reprogramming in lung SCC remains unclear. Interestingly, exposure to belinostat for 48 hours at a dose as low as 0.1μM was sufficient to acetylate histones (Figure 3.5), whereas cleavage of PARP was observed only at 1μM (Figure 4.4). This observation strongly suggested that at sub-lethal dose, belinostat could mediate alternative cellular responses, rather than the direct induction of apoptosis.

In Chapter 3.1.2 and Chapter 3.2.1, high frequencies of *TP53* mutations were detected in both lung SCC specimens and cell lines that resulted in dysfunctional DNA-binding domains. Furthermore, mutated *TP53* has been correlated to poor treatment response to cisplatin (O'Connor, Jackman et al. 1997). In line with the current knowledge, the transcriptomic analysis (Chapter 3.4.1) revealed that genes related to p53 signalling pathway were down-regulated in cisplatin-resistant cell lines. These observations suggested that therapeutic strategies which reactivate p53 activities could offer a new strategic approach in cancer therapy. Several treatment strategies, including the use of HDAC inhibitors, have been exploited to reinstate p53 functions. Apart from affecting histone hyperacetylation and restructuring (Grunstein 1997, Gregory, Wagner et al. 2001), HDAC inhibitors have also been reported to acetylate and activate a range of non-histone effector molecules which include E2F1, GATA, Hsp90, Ku70, NF-κB, Runx, STAT3, and p53 (Minucci and Pelicci 2006). Importantly, several classes of HDAC inhibitors have shown anti-tumour activities through induction of p53 acetylation (Vaziri, Dessain et al. 2001).

Taken together, it was hypothesized that belinostat sensitize lung SCC cells to cisplatin cytotoxicity via cellular reprogramming that activates p53 signaling. To test this hypothesis, the chemosensitization effects of belinostat at low doses was explored in cisplatin-treated

lung SCC cells. The synergistic cytotoxicity of cisplatin with belinostat (0.1μM) was first determined among a panel of lung SCC cell lines. Next, the molecular mechanisms of this drug combination were elucidated and correlated to the mutational status of *TP53* gene. In this chapter, the loss-of-function mutation in p53, synergistic cytotoxicity of belinostat and cisplatin, as well as the gain-of-function event of mutant p53 in lung SCC cells will be discussed.

5.1 Combinatorial effect of cisplatin with sub-lethal dose of belinostat in lung SCC cell lines

To first investigate the synergistic effects of cisplatin with low dose of belinostat, induction of cell death was analysed in lung SCC cell lines treated with belinostat (0.1μM), cisplatin (3 or 10μM) and combination of both agents. Both H2066 and SW900 cell lines were omitted from this investigation for the same reason as mentioned in Chapter 4.1.2. Regulation of apoptosis was determined by the cleavages of PARP and caspase 3.

Across the 8 cell lines tested, cisplatin treatment induced minimal apoptosis in Calu-1, H520, SK-MES-1 and H226 cells (Figure 5.1 B, C, D, E). Except for H226, all these cell lines were classified as cisplatin-resistant cells. Combination with belinostat potentiated expression of cleaved PARP and caspase 3 in H226 cells (Figure 5.1 E) but not in Calu-1, H520 and SK-MES-1. On the contrary, H2170, H596, H1869 and ChaGo-k-1 were found to be more sensitive to cisplatin treatment (Figure 5.1 A, F, G, H). Combination with belinostat increased induction of apoptosis in H2170 and H1869 cell lines.

The differential response of lung SCC cell lines towards cisplatin and sub-lethal dose of belinostat suggest that the underlying synergistic cisplatin-mediated cytotoxicity may be context-dependent. Cell lines that showed significantly increased apoptosis, especially the cisplatin-resistant H2170 cells, were utilised as study models to elucidate the mechanisms of synergistic cytotoxicity.

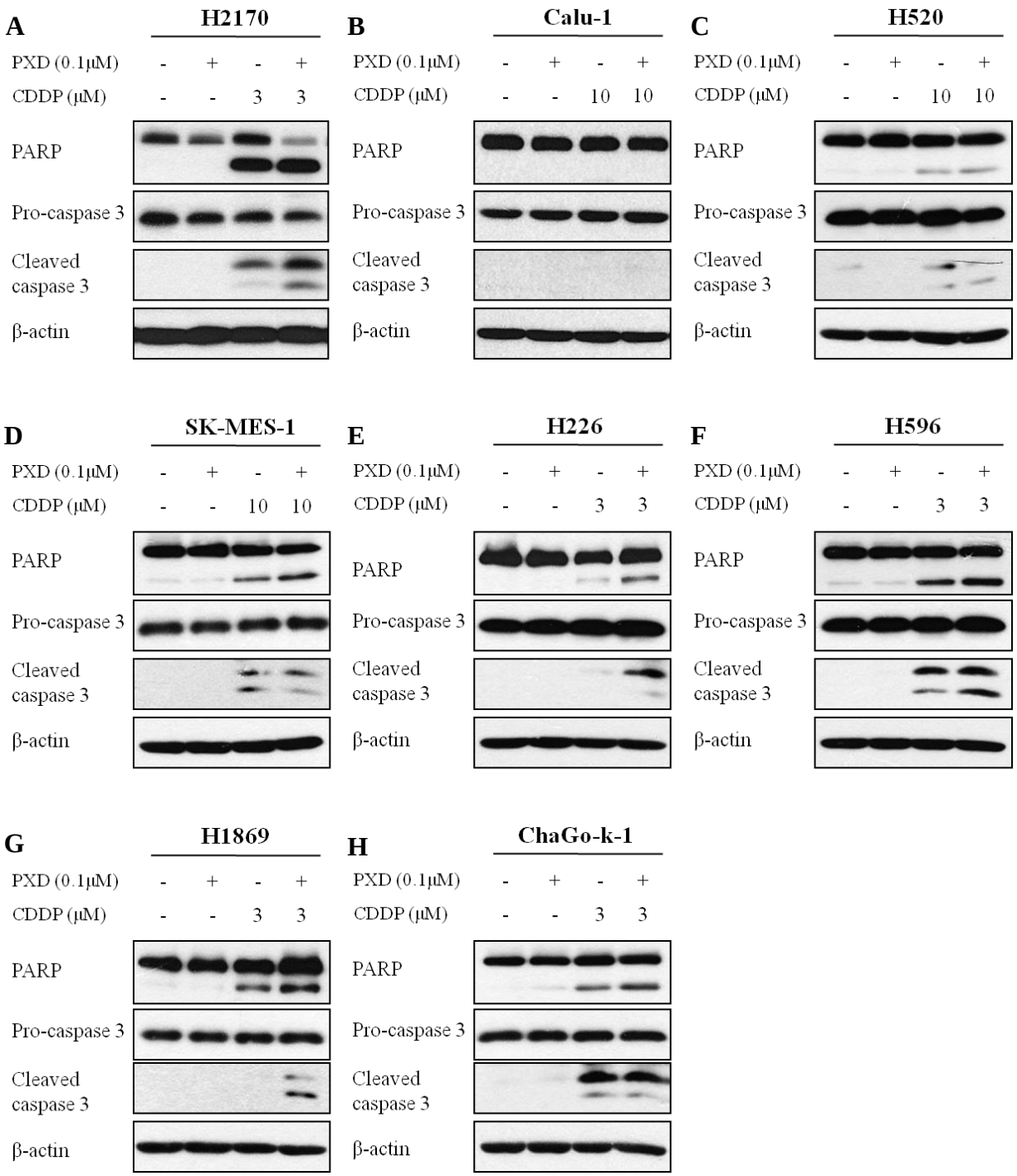

Figure 5.1: Effect of belinostat (at 0.1μM) and cisplatin on cleavage of PARP and caspase 3 in lung SCC cell lines.

H2170 (A), Calu-1 (B), H520 (C), SK-MES-1 (D), H226 (E), H596 (F), H1869 (G) and ChaGo-k-1 (H) cells were exposed to PXD101 (PXD101) (0.1μM), cisplatin (3 or 10μM), or combination treatment for 48 hours. Western blot analysis was performed to investigate the expression of PARP and caspase 3. Data shown are representative of two independent experiments for the indicated targets with β-actin as input control.

5.2 Transcriptional activation of apoptosis by belinostat and cisplatin in lung SCC

5.2.1 Induction of apoptosis in H2170 cells by cisplatin and belinostat

To characterize the cellular apoptotic pathway trigger by cisplatin and belinostat in H2170 cells, the regulation of pro-survival (Bcl-2, Bcl-xl and XIAP) and pro-apoptotic (BAX, caspase 3 and 9) markers was investigated after trug treatment. In Figure 4.3 B and 4.4 B, the cleavage of PARP was shown to be induced by cisplatin and belinostat respectively. The data here further demonstrated that both cisplatin and belinostat triggered dose-dependent cleavage of caspase 9 and 3. Cisplatin down-regulated Bcl-2 and Bcl-xl but had minimal effect on XIAP, while belinostat reduced expression of Bcl-xl and XIAP but not Bcl-2 (Figure 5.2). Expression of BAX was unchanged for both treatments, probably due to the oversaturation of this protein in whole cell lysate.

Taken together, these data suggested differences in apoptotic activation for the two agents. Despite inducing acetylation of H3 and H4 at low doses (0.1μM) (Figure 3.5), belinostat triggered cellular apoptosis only at higher doses. Interestingly, as shown in Figure 5.1, combination of cisplatin with low doses of belinostat remarkably potentiated apoptosis in several lung SCC cell lines. Thus, exploring the mechanisms that lead to the observed synergistic cytotoxicity could reveal window of opportunity for new therapeutic approach.

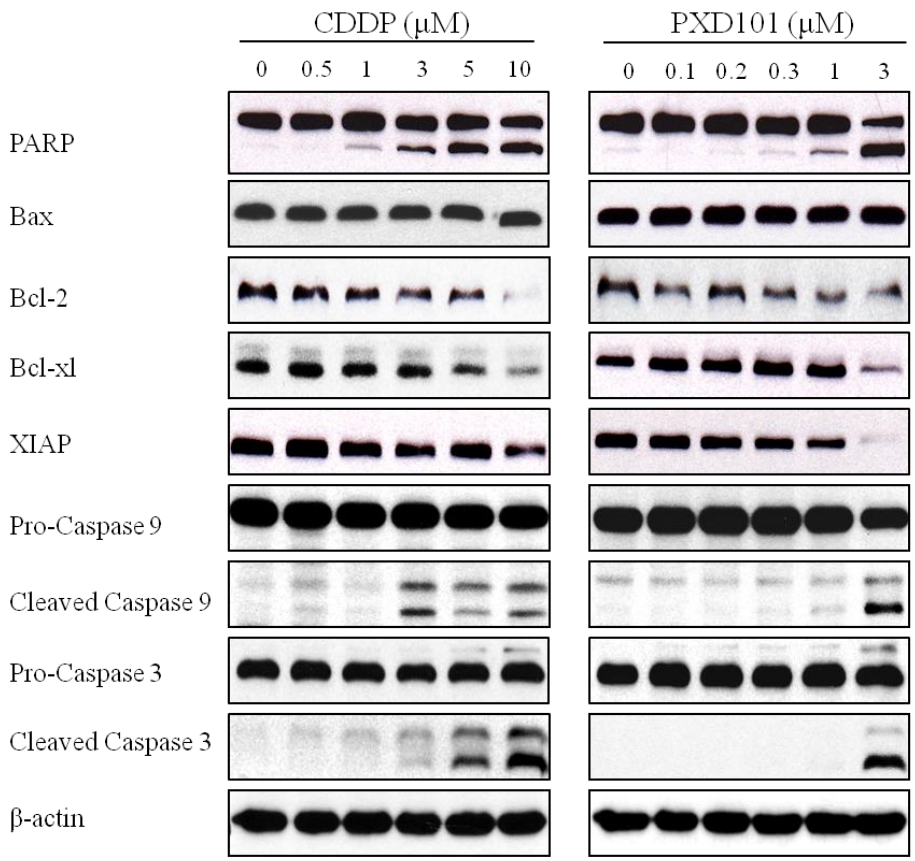

Figure 5.2: Cisplatin and PXD101 initiate apoptosis in H2170 cells in a dose-dependent manner.

H2170 cells were exposed with cisplatin (0.5, 1, 3, 5, 10μM) or PXD101 (PXD101) (0.1, 0.2, 0.3, 0.5, 1μM) for 48 hours. Western blot analysis was performed to investigate the expression of PARP, BAX, Bcl-2, Bcl-xl, XIAP, caspase 9 and caspase 3. Data shown are representative of three independent experiments for the indicated targets with β-actin as input control.

5.2.2 Belinostat induces acetylation of histones and nuclear proteins in cisplatin-treated H2170 cells

Next, the mechanisms by which belinostat enhanced cisplatin cytotoxicity was elucidated. As belinostat was developed as a HDAC inhibitor, the degree of histone acetylation was examined under exposure of belinostat/cisplatin. Experiments were conducted on H2170 cells. While cisplatin alone did not induce acetylation of histones, belinostat consistently induced acetylation of both H3 (Lys23, Lys9/14) and H4 at 0.1μM with and without exposure to cisplatin, confirming its ability to acetylate histone proteins at this low concentration (Figure 5.3 A). As HDAC inhibitors are known to alter the acetylation of non-histone effectors, immunofluorescence staining was conducted to detect the extent of lysine acetylation when exposed to belinostat. The data showed an accumulation of acetyl-lysine in belinostat-treated cells (Figure 5.3 B). As the detected acetylation was mainly nuclear-bound, these data thus support that belinostat mainly modifies acetylation of nuclear proteins, including histones and non-histone transcriptional factors (Glozak and Seto 2007).

Modification of cellular acetylation by belinostat at a sub-lethal dose implies that the observed synergy between cisplatin and belinostat could be accounted for by two possible mechanisms: (1) transcriptional activation of apoptosis-related genes through histone acetylation; and (2) modulation of cellular apoptosis through acetylation of non-histone targets. These mechanisms could potentially lead to the sensitization of H2170 cells to cisplatin. Subsequent chapters will be focusing on elucidating these mechanisms. Furthermore, it was shown in this chapter that several cell lines (H226, H1869 and H2170) showed synergistic cytotoxicity with combination of cisplatin and belinostat (0.1μM). These cell lines could be used as study models to elucidate the underlying mechanisms.

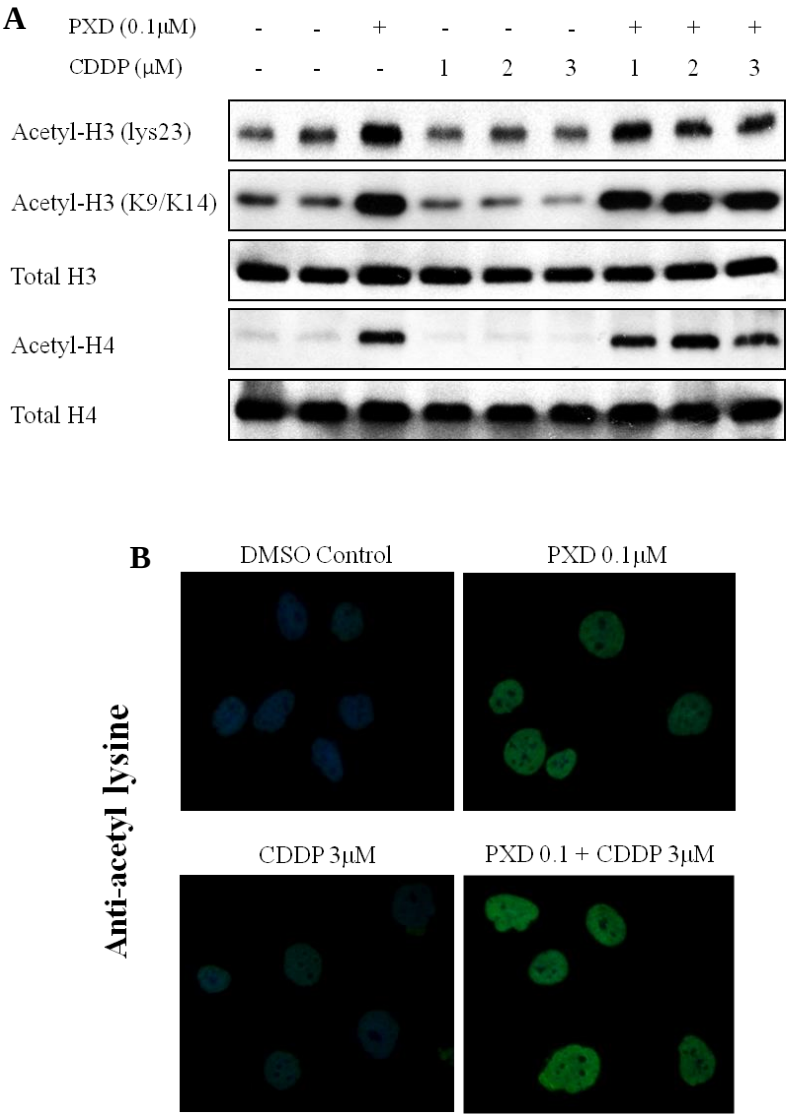

Figure 5.3: Acetylation of histone molecules is mediated by belinostat independently of cisplatin.

A, Western blot analyses were performed on H3 and H4 in H2170 cells after belinostat (PXD101) (0.1μM), cisplatin (1, 2 and 3μM) and combination treatment with DMSO as vehicle control. Histones were purified through acid extraction. Western blot data shown are representative of three independent experiments for the indicated targets with total H3 as input control. B, Representative images for immunofluorescence staining on total acetylated lysine in H2170 cells after cisplatin (3μM), belinostat (0.1μM) or combination treatment (*n* = 3). **Blue indicates DAPI** and **green indicates acetyl-lysine**. Fluorescent images were taken at 1000x magnification.

5.2.3 Belinostat potentiates both intrinsic and extrinsic apoptosis in cisplatin-treated H2170 cells

Prior to elucidate the underlying synergistic mechanisms between belinostat and cisplatin, the extent of apoptosis was first verified with Annexin-V and propidium iodide (PI) staining. Apoptosis is a programmed cell death mechanism that could be distinguished by early and late-stage events. Early-stage apoptosis is characterized by loss of mitochondria potential and the translocation of phosphatidylserine from cytosolic to extracellular portion of the cell membrane (Li, Sarkisian et al. 2003), while late-stage is usually accompanied by increase cell membrane permeability (Krysko, Vanden Berghe et al. 2008). Extent of apoptosis can be quantified by determining the amount of cells that could be stained by Annexin-V, which bind to phosphatidylserine, and PI, which penetrate leaked plasma membrane (Koopman, Reutelingsperger et al. 1994).

In this study, total number of apoptotic cells was quantified after belinostat, cisplatin and combination treatment. These data confirmed that belinostat alone (at a low concentration of 0.1μM) does not induce apoptosis as the number of Annexin-V and PI-stained cells remained unchanged as compared to DMSO treated cells. Cisplatin increased early apoptotic cells (Annexin-V positive, PI negative) from 4.6% to 12%, and late apoptotic cells (Annexin-V positive, PI positive) from 2.6% to 7.8%, implying that cisplatin alone is sufficient to trigger apoptosis. Combination treatment further increased the amount of early apoptotic cells to 21.2% and late apoptotic cells to 15.2% (Figure 5.4 A). Total abundance of apoptotic cells is determined by the amount of cells stained with Annexin-V. These data showed that cisplatin induced dose-dependent increase of Annexin-V stained cells, while combination with belinostat at 0.1μM significantly potentiate apoptosis in H2170 cells (Figure 5. 4 B).

Apoptosis involves a series of biochemical events that lead to changes in cell morphology and cell death. This process can be controlled by a range of intracellular and extracellular cell signals. The results of the analysis indicated that cisplatin induced the cleavages of caspase 3/7, 8 and 9 in conjunction with the degradation of PARP, while concurrent treatment with belinostat (0.1μM) further augmented these cleavages (Figure 5.6 A). By determining the drug-induced effect on the protease activities of caspase 3/7, caspase 8 and caspase 9, these data showed that cisplatin produced a dose-dependent increase in all caspase activities in H2170 cells. In contrast, belinostat at 0.1μM did not affect caspase activity, but significantly increased cisplatin-induced caspase 3/7, caspase 8 and caspase 9 activities (Figure 5.6 B, C, D).

To investigate whether belinostat and cisplatin treatments could affect Bcl-2 family protein levels in H2170 cells, the regulations of Bcl-2 family members were investigated. The expression of two inhibitors of apoptosis, XIAP and survivin, was examined as well. While cisplatin alone has minimal effects on the expression level of Bcl-2, Bcl-xl, Bcl-w, XIAP and survivin, belinostat suppressed Bcl-2, Bcl-w and XIAP when used in combination (Figure 5.6 E). Among the pro-apoptotic Bcl-2 family proteins, BAX was detected in abundance in H2170 cells and may be oversaturated to detect any further increase upon drug treatment. Expressions of BAD and BAK were unaffected by cisplatin alone, but remarkably increased upon combination treatment. Among the three isoforms of BIM, BIM_S and BIM_L were significantly expressed upon combination treatment (Figure 5.6 F). The shortest isoform, BIM_S, is reported to be cytotoxic and only expressed during apoptosis (O'Connor, Strasser et al. 1998). BID is another crucial pro-apoptotic Bcl-2 member that interacts with BAX to form MAC on the outer membrane of mitochondria. BID is a common effector of both intrinsic and extrinsic apoptosis (Wang, Yin et al. 1996), and cleavage of BID to its activated form, tBID, is mediated by caspase-2 and caspase-8 (Li, Zhu et al. 1998, Upton, Austgen et al. 2008). Cisplatin as a single agent induced BID cleavage, while combination with belinostat further increased the release of tBID (Figure 5.6 F). Through siRNA silencing of BAX in H2170 cells, drug-induced PARP cleavage and caspase 3 activation were both reduced in comparison to scrambled siRNA transfected control (Figure 5.7)

While the expressions of most Bcl-2 proteins were unaffected in cisplatin-treated cells, the tested anti-apoptotic and pro-apoptotic markers were remarkably modulated by combination treatment of belinostat and cisplatin. Moreover, knockdown of BAX partially abrogated the drug-induced apoptosis. Figure 5.5 showed a schematic diagram that provides an overview of the regulation of apoptosis by belinostat and cisplatin. These data collectively suggest that belinostat triggers mitochondrial-controlled apoptosis in cisplatin-treated H2170 cells. Furthermore, activation of BID, as well as caspase 8 and 9, were detected upon drug exposure. Taken together, it was postulated that combination of belinostat and cisplatin could trigger the induction of both intrinsic and extrinsic apoptotic pathways through a common pathway.

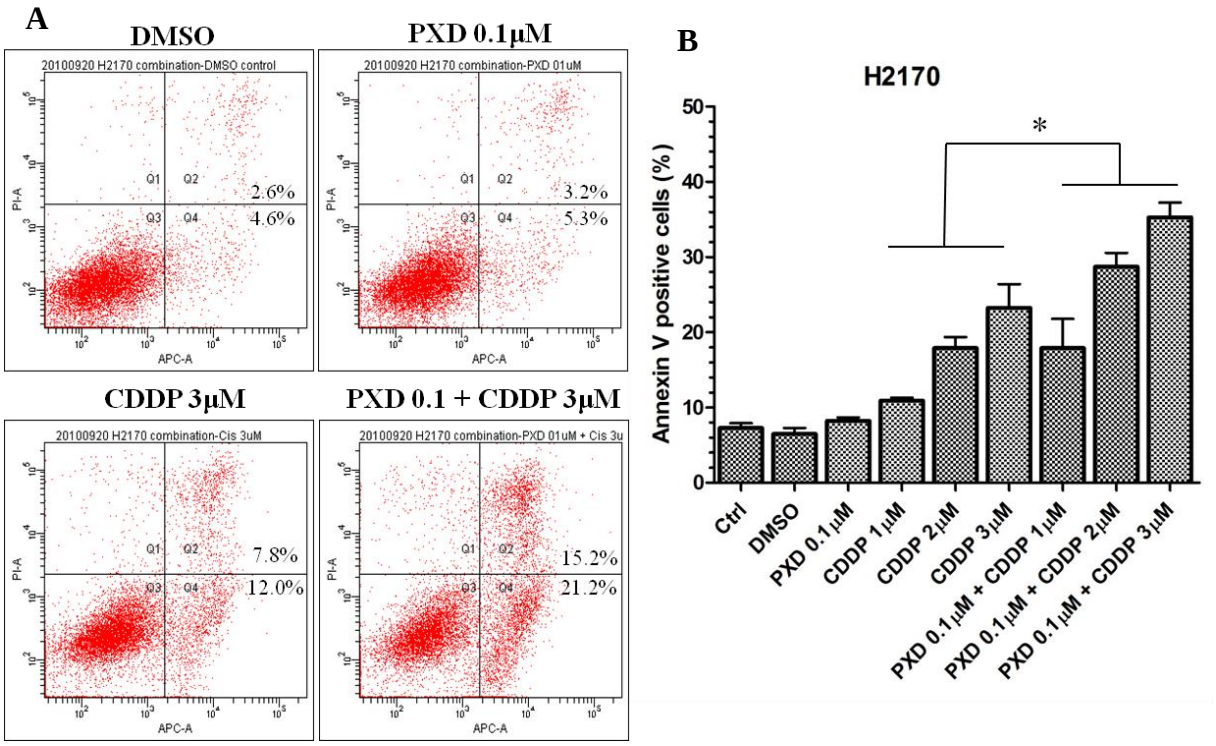

Figure 5.4: Belinostat potentiates cisplatin-induced apoptosis in H2170 cells.

H2170 cells were treated with belinostat (PXD101) (0.1μM), cisplatin (1, 2 and 3μM) and combination treatment with DMSO (0.001%) as vehicle control. Annexin-V and propidium iodide (PI) staining was performed. A, Dot blots on percentage of Annexin-V (+/-) and PI (+/-) cells. B, Bar chart on the percentage of Annexin-V positive cells in H2170. Data are shown as mean ± SD for three independent experiments. Statistical analyses were performed by unpaired t-test. *Significant difference from cisplatin treatment, $P < 0.05$.

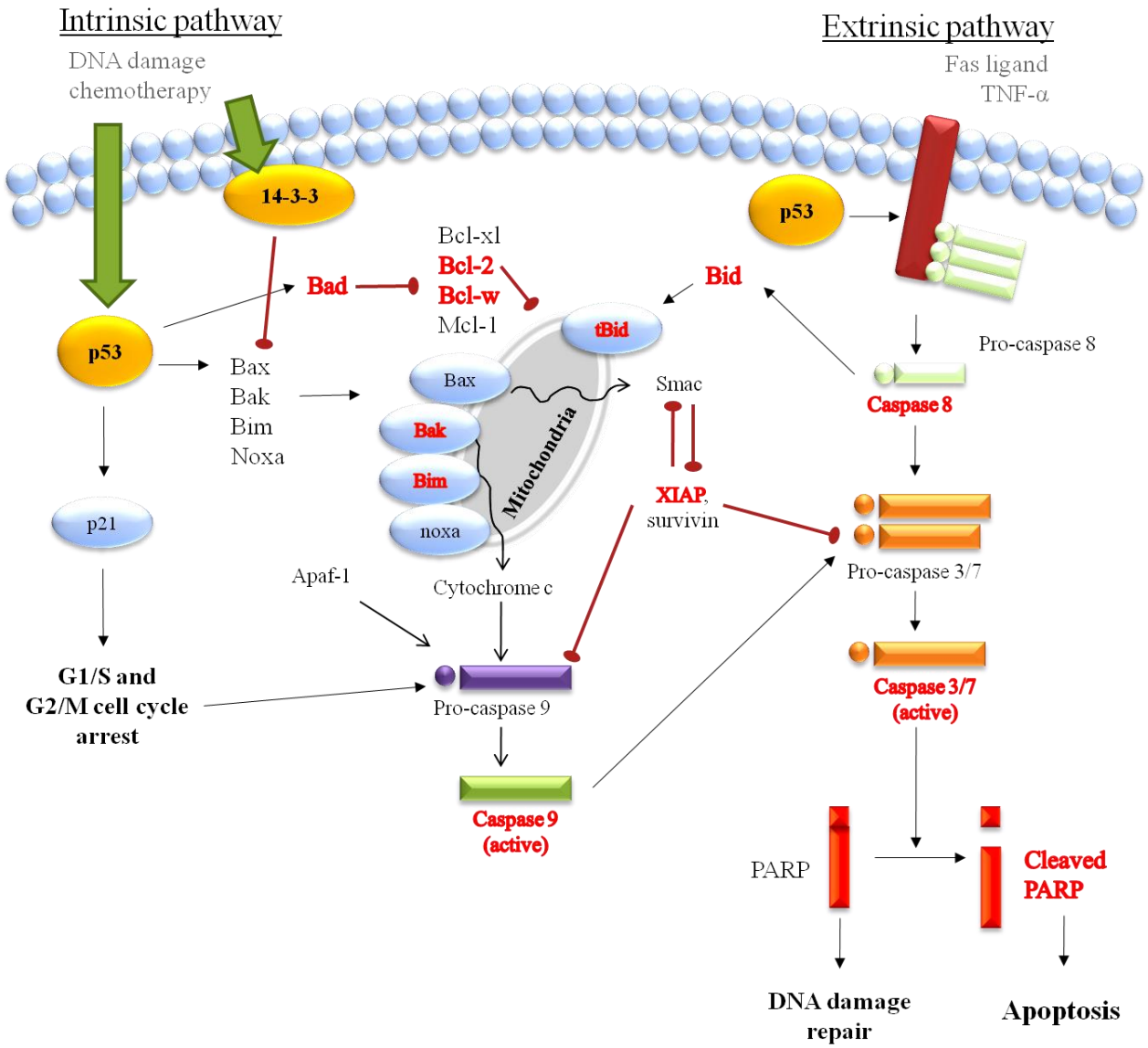

Figure 5.5: Illustrated schema of both intrinsic and extrinsic pathways of apoptosis induced by cisplatin and belinostat treatment.

Texts highlighted in **Red** indicate apoptotic markers that are regulated by combination of cisplatin and belinostat in H2170 cells.

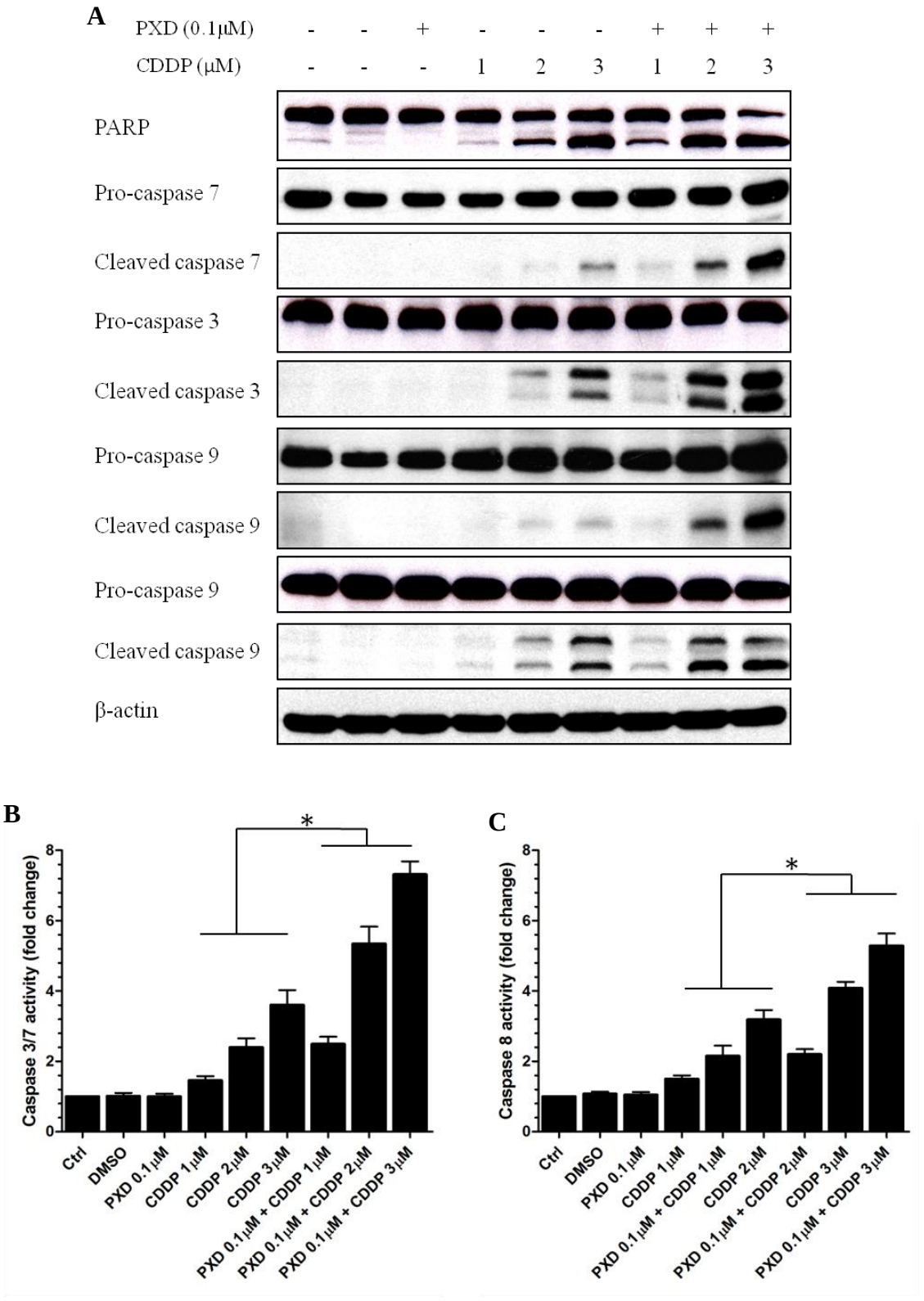
A
PXD (0.1μM) - - + - - - + + +
CDDP (μM) - - - 1 2 3 1 2 3
PARP
Pro-caspase 7
Cleaved caspase 7
Pro-caspase 3
Cleaved caspase 3
Pro-caspase 9
Cleaved caspase 9
Pro-caspase 9
Cleaved caspase 9
β-actin
B
Caspase 3/7 activity (fold change)
0
2
4
6
8
*
Ctrl
DMSO
PXD 0.1μM
CDDP 1μM
CDDP 2μM
CDDP 3μM
PXD 0.1μM + CDDP 1μM
PXD 0.1μM + CDDP 2μM
PXD 0.1μM + CDDP 3μM
C
Caspase 8 activity (fold change)
0
2
4
6
8
*
Ctrl
DMSO
PXD 0.1μM
CDDP 1μM
PXD 0.1μM + CDDP 1μM
CDDP 2μM
PXD 0.1μM + CDDP 2μM
CDDP 3μM
PXD 0.1μM + CDDP 3μM

D

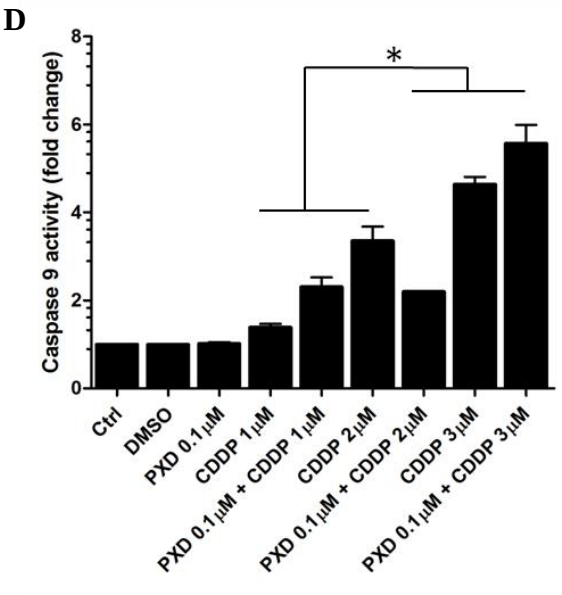
Caspase 9 activity (fold change)
0
2
4
6
8
*
Ctrl
DMSO
PXD 0.1μM
CDDP 1μM
PXD 0.1μM + CDDP 1μM
CDDP 2μM
PXD 0.1μM + CDDP 2μM
CDDP 3μM
PXD 0.1μM + CDDP 3μM

E

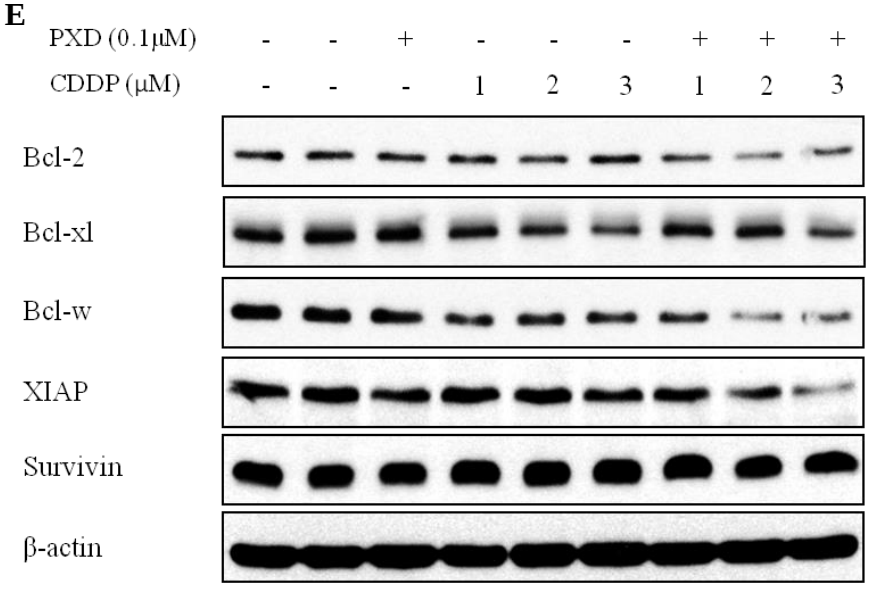
PXD (0.1μM) - - + - - - + + +
CDDP (μM) - - - 1 2 3 1 2 3
Bcl-2
Bcl-xl
Bcl-w
XIAP
Survivin
β-actin

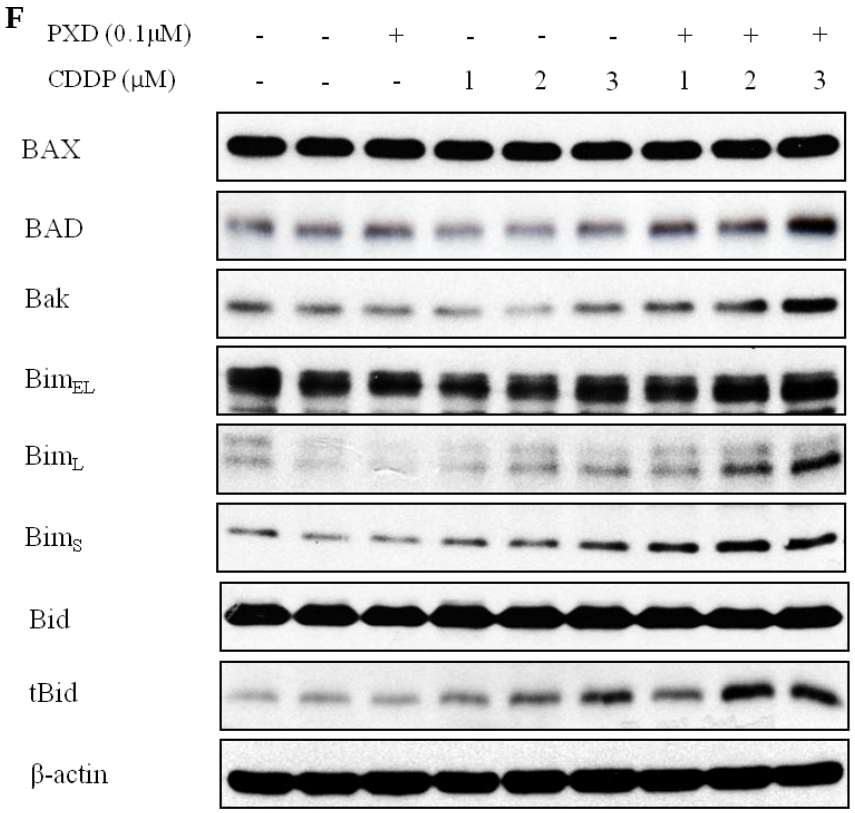

Figure 5.6: Combination of belinostat and cisplatin triggers the intrinsic apoptotic pathways in H2170 cells.

H2170 cells were treated with belinostat (PXD101) (0.1μM), cisplatin (1, 2 and 3μM) and combination treatment with DMSO (0.001%) as vehicle control. A, Western blot analyses was performed to investigate the expression of PARP, caspase 3, 7, 8 and 9. Caspase 3/7 (B), caspase 8 (C) and caspase 9 (D) activities were monitored by cleavage of the DEVD-aminoluciferin as described in Material and Methods. Data are shown as mean ± SD (n = 3). Statistical analyses were performed by unpaired t-test. *Significant difference from cisplatin treatment, $P < 0.05$. E, Western blot analyses was performed to investigate the expression of Bcl-2, Bcl-xl, Bcl-w, XIAP and surviving. F, Western blot analyses was performed to investigate the expression of Bad, Bax, Bak, Bim and Bid. Western blot data shown are representative of three independent experiments for the indicated targets with β-actin as input control. Statistical analyses were performed by unpaired t-test. *Significant difference from cisplatin treatment, $P < 0.05$.

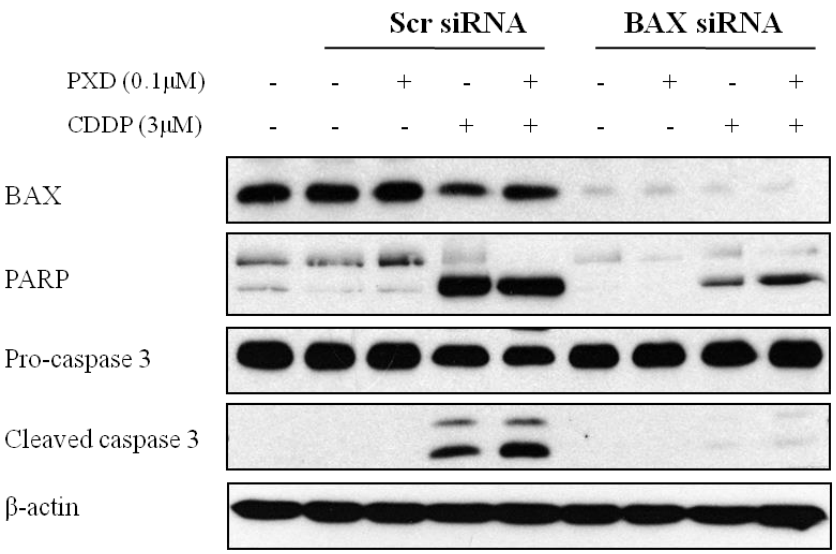

Figure 5.7: Silencing of BAX abrogates apoptosis in cisplatin and belinostat-treated H2170 cells.

BAX siRNA was transfected to H2170 cells. 100nM of siRNA was used per transfection. H2170 cells were treated with belinostat (PXD101) (0.1μM), cisplatin (3μM) and combination treatment with DMSO as vehicle control for 48 hours. Western blot analysis was performed to investigate the expression of BAX, PARP and caspase 3. Western blot data shown are representative of three independent experiments for the indicated targets with β-actin as input control.

5.2.4 Transcriptional activation of apoptosis in H2170 cells

Activation of apoptosis requires induction of several factors including DNA damage, cellular stress, and loss of survival signals (Lessene, Czabotar et al. 2008). In healthy cells, majority of the pro-apoptotic proteins are kept inactivated. For instance, 14-3-3, a cytosolic-bound chaperone, bind to BAX under unstressed condition and inhibit apoptosis (Nomura, Shimizu et al. 2003, Clapp, Portt et al. 2012). Apoptosis is triggered upon DNA damage. Numerous studies have demonstrated the regulation of key components in both the intrinsic (Bcl-2 family) and extrinsic pathways (Fas, DR5) by various transcription factors, such as p53 and STAT (Lane 1993, Battle and Frank 2002). In Chapter 5.2.3, it was clearly demonstrated that several members of the Bcl-2 family were modulated upon combination of cisplatin and belinostat, the transcriptional regulations of these apoptotic markers were determined after drug treatment.

Fas, a cell surface receptor, is an important regulator of the extrinsic apoptosis (Nagata and Golstein 1995). Fas is known to be activated through binding of its ligand, FasL, thus initiates the formation of DISC complex and caspase-8 activation. According to the transcriptomic analysis, *FAS* gene is down-regulated in cisplatin-resistant lung SCC cells (Figure 3.6 C). Importantly, FasL is predominantly expressed by T cells (Muzio 1998). The absence of immune regulatory cells in this study model implies that drug-induced activation of Fas is probably regulated at the mRNA level within H2170 cells. The data showed that mRNA expression of *FAS* was increased by 2.54-fold and 3.36-fold upon cisplatin and combination treatment respectively (Figure 5.8 A). Furthermore, the mRNA expression of several Bcl-2 family members was shown to be significantly modified by exposure to drugs. These data also demonstrated that both cisplatin and combination treatment, but not belinostat alone, down-regulated the expression of *Bcl-2* significantly (Figure 5.8 B). When used singly, both drugs have insignificant regulatory effects on *BAX*, *BAK1*, *BAD* and *BIM*, but combined treatment with belinostat significantly increased the transcription of these pro-apoptotic markers by 2.61, 1.78, 2.11 and 1.71-fold respectively (Figure 5.8 C, D, E, F), suggesting the transcriptional activation of apoptosis.

The combined treatment with cisplatin and belinostat induced efficient induction of intrinsic and extrinsic apoptosis through transcriptional activation of several apoptosis-related genes. Several of these genes are known downstream targets of p53. For instance, induction of *FAS* mRNA expression through p53 transactivation has been reported in several cancer types, including lung (Bouvard, Zaitchouk et al. 2000). In addition, p53-response elements have been identified in the *BAX* gene, *BAD* and *Bcl-2* (Thornborrow, Patel et al. 2002). Therefore, the hypothesis for the observed synergistic cytotoxicity of belinostat and cisplatin may involve p53 signalling pathway.

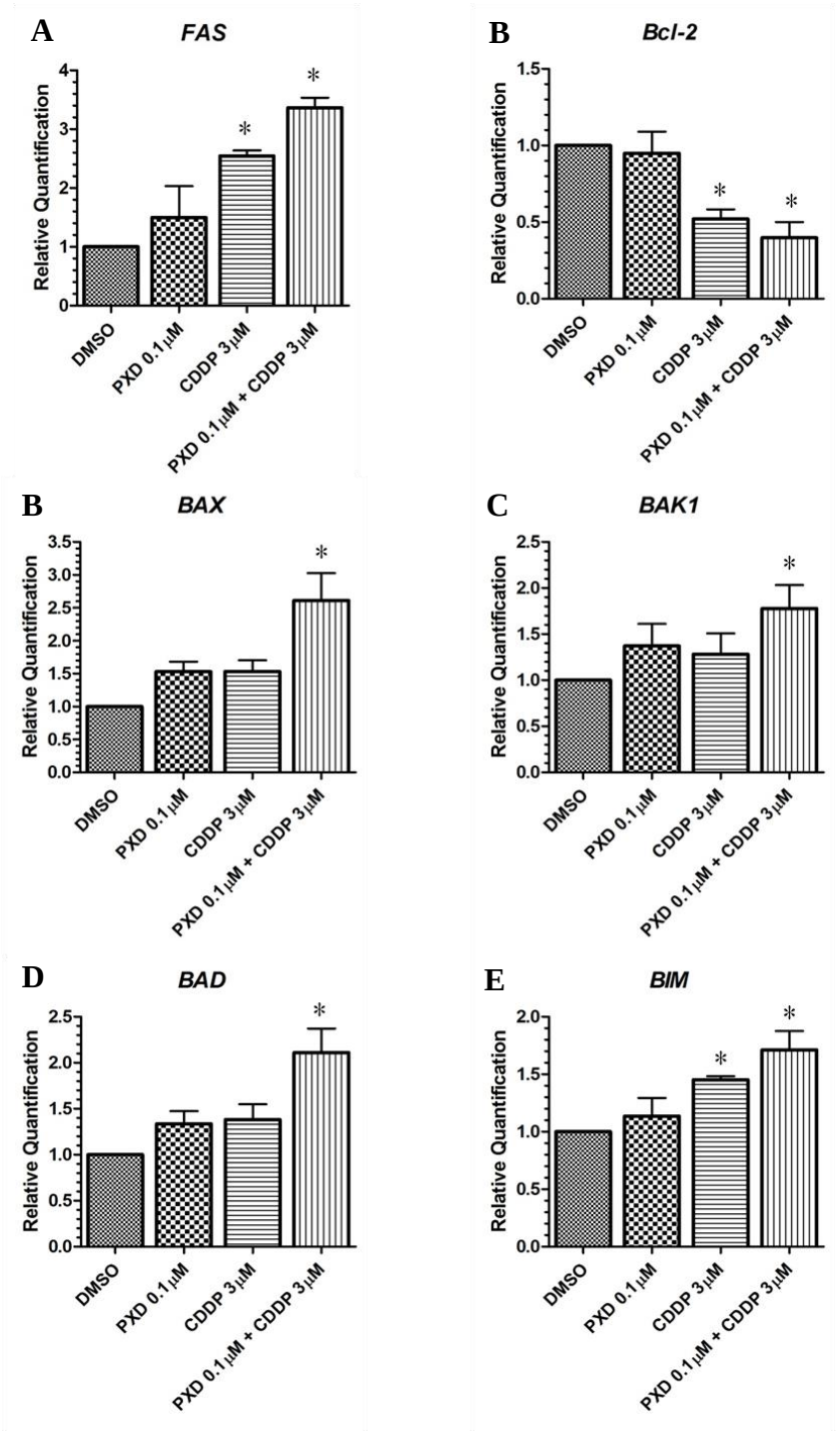

Figure 5.8: Cisplatin and belinostat induce transcriptional activation of apoptosis.

H2170 cells were treated with belinostat (PXD101) (0.1μM), cisplatin (3μM) and combination treatment with DMSO (0.001%) as vehicle control for 48 hours. Total RNA was isolated and reverse transcribed to cDNA. Expressions of (A) *FAS*, (B) *Bcl-2*, (C) *BAX*, (D) *BAK1*, (E) *BAD* and (F) *BIM* were analysed using real-time qPCR. Data are shown as mean ± SD from three independent experiments. Statistical analyses were performed by unpaired t-test. *Significant difference from vehicle control (0.001% DMSO), $P < 0.05$.

Summary of findings in Chapter 5.1 and 5.2:

- At 0.1μM, belinostat potentiated cisplatin-induced apoptosis in H226, H1869 and H2170 cells.
- In H2170 cells, cisplatin alone decreased Bcl-2 and Bcl-xl; while increased cleavage of PARP and caspase 3, 9 in dose-dependent manner.
- In H2170 cells, belinostat alone decreased Bcl-2, Bcl-xl and XIAP; while increased cleavage of PARP and caspase 3, 9 in dose-dependent manner.
- At 0.1μM, belinostat induced histone acetylation independently of cisplatin in H2170 cells.
- Combination of cisplatin at belinostat (at 0.1μM) triggered both intrinsic and extrinsic apoptosis in H2170 cells.
- Combination of cisplatin at belinostat (at 0.1μM) reduced mRNA level of *Bcl-2* gene.
- Combination of cisplatin at belinostat (at 0.1μM) increased transcriptional activation of several apoptosis-related genes (*FAS*, *BAX*, *BAK1*, *BAD*, and *BIM*).
- Apoptotic pathways activated by cisplatin and belinostat is transcriptional-dependent.
- Some of the apoptotic genes affected by this treatment (*FAS*, *BAX*, *BAD* and *Bcl-2*) are downstream targets of p53 signalling.

5.3 Transactivation of mutant p53 is correlated to post-translational modifications

5.3.1 Transcriptional modulation of mutant p53 by cisplatin, belinostat and Nutlin-3a

To assess the relevance of p53 to drug-induced apoptosis in H2170 cells, it was essential to first determine the ability of this p53 mutant cell line to induce a p53-responsive promoter. H2170 cells were transiently transfected with a luciferase reporter plasmid that contains tandem repeat of the p21 promoter as described in Material and Methods. Constructs with constitutively expressing luciferase and non-inducible luciferase were transfected as positive and negative controls. Both these constructs confirmed the validity of the reporter system, with positive control giving a marked activation and negative control showing no response after drug treatment (Data not shown). In H2170 cells transfected with p53-responsive construct, no significant induction of luciferase activity was observed 24 hours post drug treatment. At 48 hours, combination treatment of cisplatin and belinostat showed a profound activation of luciferase activity when compared to vehicle control. At 72 hours, both cisplatin and combined treatment induced marked activation of this promoter activity (Figure 5.9). These findings suggested that the transactivation of p53 proteins in H2170 cells could be induced by cisplatin alone, but combined treatment of belinostat (0.1μM) potentiated this transcriptional activity.

In Chapter 3.2.1, H2170 was verified to be a p53 mutant line with mutation on its DNA-binding domain at residue 158 (R158G) by Sanger sequencing. Such mutant is conventionally considered to lack the DNA-binding capability and therefore its transactivation ability is impaired. Mechanistically, mutant p53 is unable to bind specifically to consensus DNA site and activate p53 downstream genes. However, combination treatment of both belinostat and cisplatin induced transactivation of p53 promoter activity in H2170 cells, therefore suggesting that this combination could restore the transcriptional function of p53. To verify the functionality of this mutated p53, the mRNA levels of *CDKN1A* and *MDM2* were determined upon Nutlin-3a exposure in H2170 cells. Nutlin-3a is a pharmacologic activator of p53 that is known to stabilize p53 through inhibiting the p53-MDM2 interaction (Vassilev, Vu et al. 2004). A dose-dependent up-regulation of *MDM2* and *CDKN1A* was observed in lung normal fibroblast cells (MRC5) but not H2170 cells (Figure 5.10 A, B). This confirms the presence of a loss-of-function mutation in H2170 cells, as blocking MDM2 inhibition on p53 does not induce transcriptional activation as displayed in the p53 wild-type cells.

The results obtained so far suggested that, at least in H2170 cells, p53-mediated transcriptional activation can be restored in p53 carrying the R158G mutation. The next step

was to elucidate the mechanism of this observation. As Nutlin-3a is an antagonist for MDM2, the binding of Nutlin-3a at the p53-binding pocket of MDM2 inhibits p53-MDM2 interaction, thus releasing functional p53 (Vassilev, Vu et al. 2004). Therefore, activation of p53 by Nutlin-3a does not require p53 phosphorylation (Thompson, Tovar et al. 2004). Furthermore, cytotoxic agents are known to induce p53 activity through its post-translational modifications. Therefore, it was believed that activation of p53 by belinostat and cisplatin may involve phosphorylation and/or acetylation of p53.

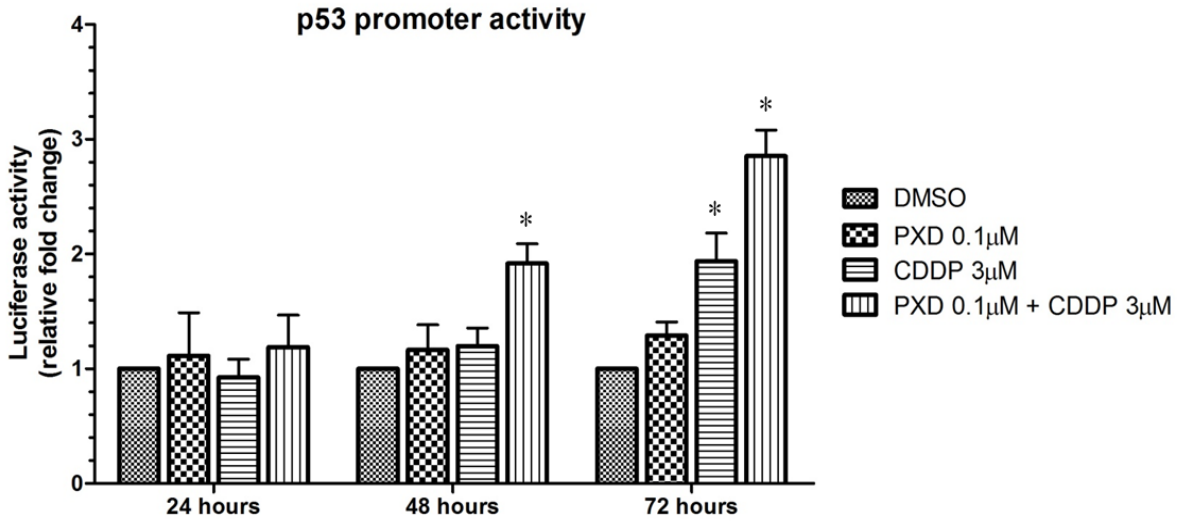

Figure 5.9: Transactivation of a p53-dependent promoter by belinostat and cisplatin.

H2170 cells were transfected with p53 reporter plasmid (p21 promoter). After 24 hours of transfection, H2170 cells were treated with belinostat (PXD101) (0.1μM), cisplatin (3μM) and combination treatment with DMSO as vehicle control (0.001% DMSO) for 24, 48 and 72 hours. Dual luciferase assay was performed as described in Material and Methods. Promoter activities are expressed in fold change in relative to DMSO control at 24 hours post treatment by using a Renilla reporter as internal normalization. Data are shown as mean ± SD from triplicates within one representative experiment (n = 3). Statistical analyses were performed by unpaired t-test. *Significant difference from vehicle control, $P < 0.05$.

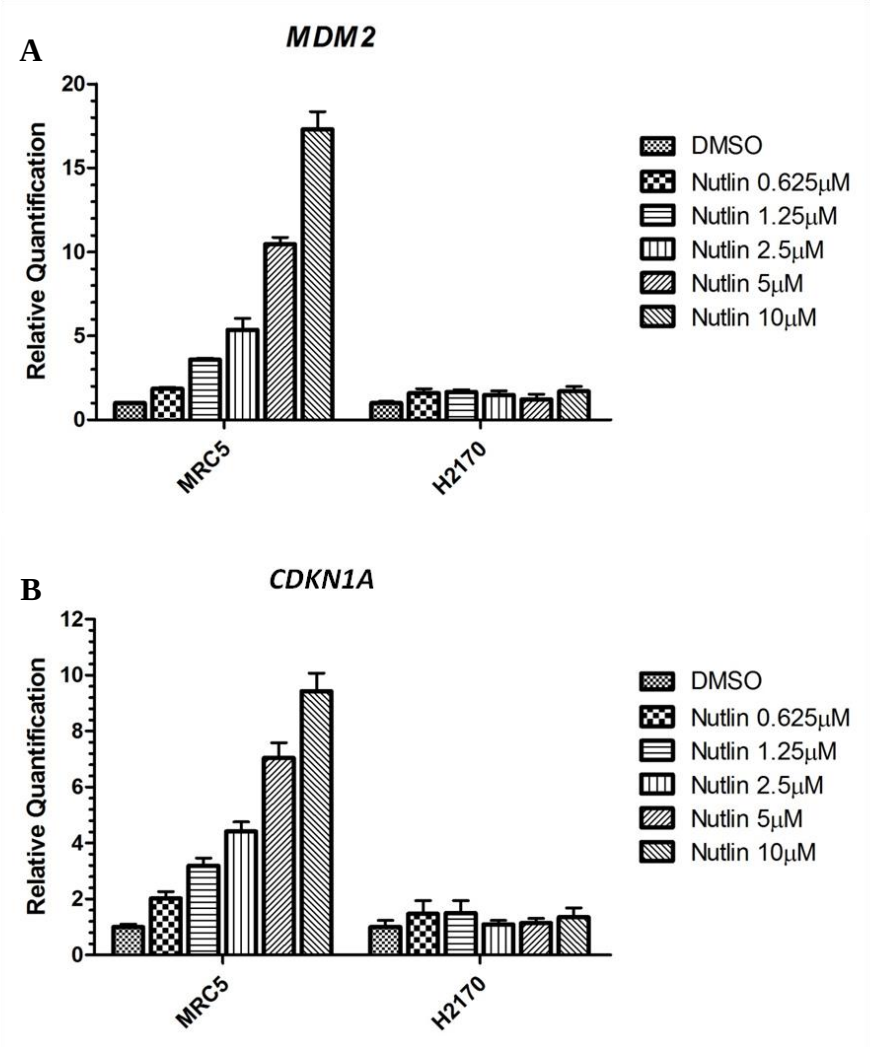

Figure 5.10: Nutlin-3a induces mRNA expression of *CDKN1A* and *MDM2* in MRC5 but not H2170 cells.

MRC5 and H2170 cells were treated with belinostat (PXD101) (0.1μM), cisplatin (1, 2 and 3μM) and combination treatment with DMSO (0.001%) as vehicle control for 48 hours. Total RNA was isolated and reverse transcribed to cDNA. Expression of (A) *MDM2* and (B) *CDKN1A* were analysed using real-time qPCR. Data are shown as mean ± SD for triplicates (n = 1).

5.3.2 Belinostat and cisplatin induce post-translational modifications of p53

Through years of intensive research on the molecule, the transcription-dependent activation of p53 has been comprehensively characterized. In unstressed cells, p53 level is suppressed through continual ubiquitination of p53 (Hock, Vigneron et al. 2011). MDM2, a downstream target as well as negative regulator of p53, binds to and mediates the degradation of p53, thus maintaining a low basal level of p53 in the nucleus. Upon induction by oncogene-activated signalling or genotoxic stress, p53 undergoes post-translational modifications which disrupt p53-MDM2 binding and leads to p53 accumulation with activation of downstream p53 effectors. Thus, tumour suppressor function of p53 is tightly regulated under physiological conditions. DNA damage has been demonstrated to induce p53 phosphorylation at Ser15 and Ser20, which then suppressed interaction of p53 and MDM2 (Shieh, Ikeda et al. 1997, Siliciano, Canman et al. 1997). While phosphorylation at other residues have been reported to influence DNA binding, growth suppression, apoptosis and transactivation, acetylation of lysine residues at position 379 and 382 lead to cellular accumulation of p53 and enhance DNA-binding capacity of p53 (Sakaguchi, Herrera et al. 1998, Ito, Lai et al. 2001).

The role of post-translational modification of mutant p53 was next examined. The data indicated that cisplatin induced dose-dependent increase of p53, p-p53 (Ser15) and acetyl-p53 (Lys379, Lys382). In comparison, belinostat reduced total p53 accumulation in H2170 cells, while not affecting the phosphorylation and acetylation of p53 up to 1μM (Figure 5.11 A). When used in combination with cisplatin, belinostat (0.1μM) did not affect expression of total p53 and p-p53 but significantly potentiated acetylation of p53 at both lysine residues (Figure 5.11 C).

Generally, p53 activation is coupled with its post-translational modifications that promote DNA-binding and inhibit MDM2 interaction. Cisplatin treatment, but not low doses of belinostat, induced phosphorylation and acetylation of p53. This contradicts other reports that HDAC inhibitors could induce acetylation of p53 (Juan, Shia et al. 2000, Luo, Su et al. 2000). Interestingly, while low dose of belinostat does not affect p53, combined treatment increases acetylation of p53 in cisplatin-treated cells. More importantly, increased acetylated p53 correlates with the induction of apoptosis in H2170 cells, further suggesting the modulatory role of acetylation for the apoptotic functions of mutant p53.

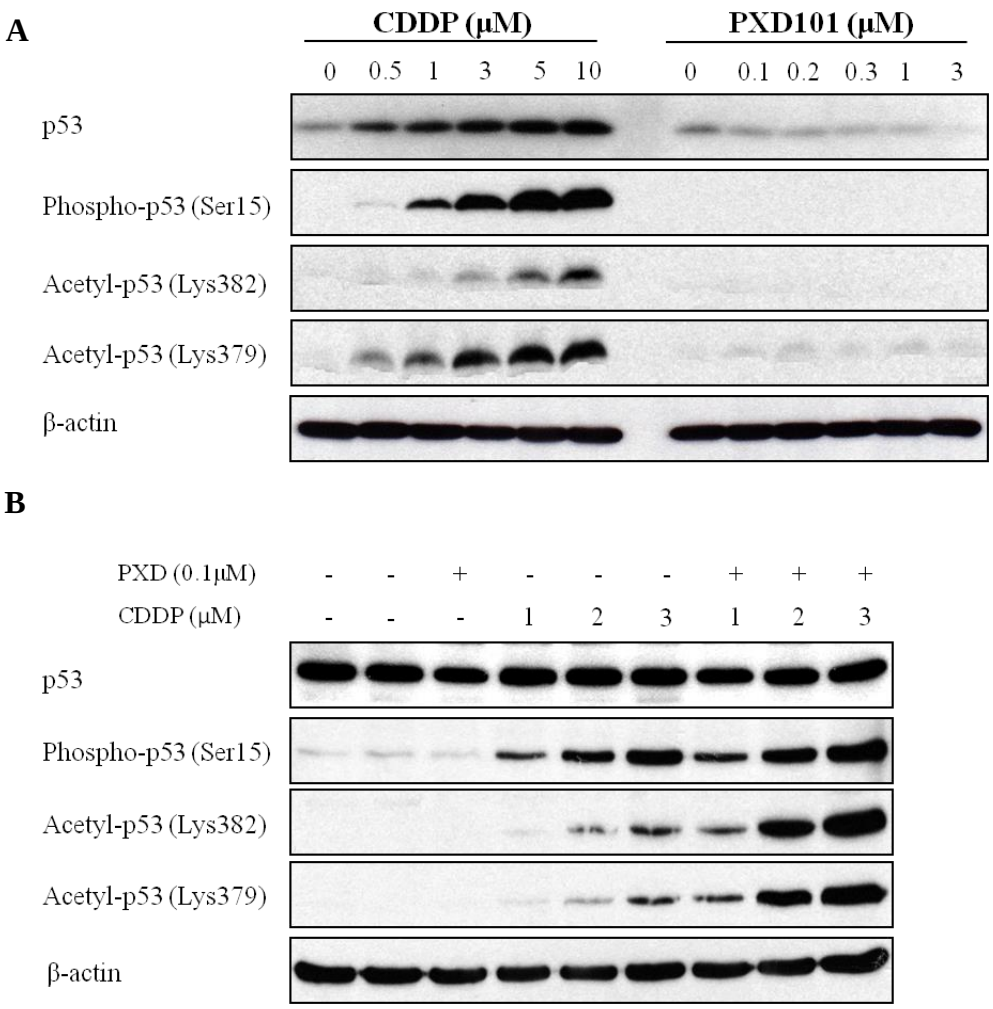

Figure 5.11: Cisplatin and belinostat regulate post-translational modification of p53.

A, H2170 cells were treated with cisplatin (0.5, 1, 2, 3, 5μM) or PXD101 (PXD101) (0.1, 0.2, 0.3, 0.5, 1μM) with DMSO (0.03%) as vehicle control for 48 hours. B, H2170 cells were treated with belinostat (0.1μM), cisplatin (1, 2 and 3μM) and combination treatment with DMSO (0.001%) as vehicle control for 48 hours. Western blot analysis was performed to investigate the expression of p53, p-p53 (Ser15) and acetyl-p53 (Lys379, Lys382). Data shown are representative of three independent experiments for the indicated targets with β-actin as input control.

5.3.3 Nuclear and cytoplasmic localization of p53

The mechanisms by which p53 mediates apoptosis has been a matter of intensive study since this was first demonstrated. As a transcriptional factor, p53 accumulates in the nucleus and transactivates apoptosis-related genes. More recently, cytoplasmic accumulation and mitochondrial localization of p53 have been shown to facilitate the formation of MAC, without affecting the cellular transcriptional activities (Marchenko, Zaika et al. 2000, Chipuk, Kuwana et al. 2004). These findings suggest that p53 functions can be determined by its nuclear and cytoplasmic localization.

Furthermore, p53 molecules were found in both nuclear and cytoplasmic fractions of H2170 cells. The phosphorylated and acetylated p53, however, were highly detected in the nucleus as compared to the cytoplasmic fraction (Figure 5.12 A, B). Confocal images were captured after immunofluorescence staining of p53 in H2170 to verify the localization of p53 molecules. DAPI and Phalloidin were used to counterstain DNA and cytoplasmic actin to allow for better visualization of nuclear and cytoplasmic fractions. These data indicated that p53 was predominantly retained in the nucleus after drug treatment (Figure 5.12 C), thus supporting its role as a transcription factor.

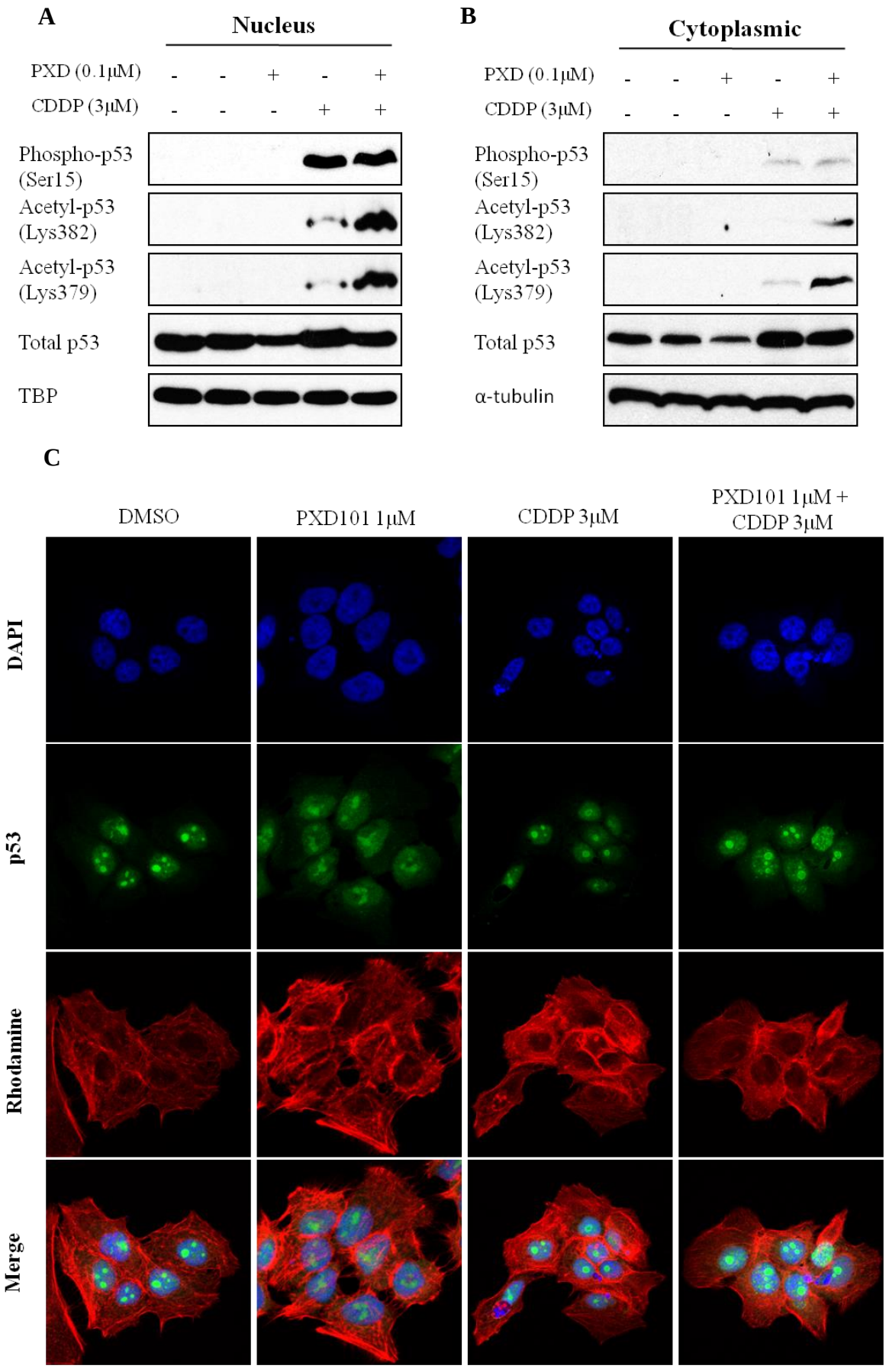
A
Nucleus
PXD (0.1μM) - - + - +
CDDP (3μM) - - - + +
Phospho-p53 (Ser15)
Acetyl-p53 (Lys382)
Acetyl-p53 (Lys379)
Total p53
TBP
B
Cytoplasmic
PXD (0.1μM) - - + - +
CDDP (3μM) - - - + +
Phospho-p53 (Ser15)
Acetyl-p53 (Lys382)
Acetyl-p53 (Lys379)
Total p53
α-tubulin
C
DMSO
PXD101 1μM
CDDP 3μM
PXD101 1μM + CDDP 3μM
DAPI
p53
Rhodamine
Merge

Figure 5.12: Nuclear translocation of p53 after drug treatment.

H2170 cells were treated with belinostat (PXD101) (0.1μM), cisplatin (3μM) and combination treatment with DMSO (0.001%) as vehicle control for 48 hours. Nuclear and cytoplasmic fractions of H2170 cells were separated as described in Material and Methods. Western blot analysis was performed to investigate the expression of p53, p-p53 (Ser15) and acetyl-p53 (Lys379, Lys382) in (A) nuclear and (B) cytoplasmic fraction. Western blot data shown are representative of three independent experiments for the indicated targets with TATA-box binding protein (TBP) and α-tubulin as input control for nuclear and cytoplasmic fraction respectively. C, Immunofluorescence staining of p53 (Alexa Fluor-488) in H2170 cells was conducted. DAPI and Phalloidin were used to counter-stain nucleus and actin respectively. Representative confocal images are shown at 1000x magnification for three independent experiments. **Blue indicates DAPI**, **green indicates p53** and **red indicates Phalloidin**.

Summary of findings in Chapter 5.3:

- H2170 harbours a loss-of-function mutation on the DNA-binding domain of p53.
- Nutlin-3a failed to activate p53-dependent transcriptional activation of *MDM2* and *CDKN1A* in H2170 cells.
- Combination of cisplatin and belinostat (at 0.1μM) induced transactivation of p53 at the *CDKN1A* promoter region.
- The p53 signalling pathway is likely restored in mutant p53 by combined treatment of cisplatin and belinostat (at 0.1μM).
- Cisplatin induced both acetylation and phosphorylation of p53 in H2170 cells in a dose-dependent manner.
- Belinostat (at 0.1μM) did not induce phosphorylation/acetylation of p53 when used as a single agent.
- Belinostat (at 0.1μM) potentiated cisplatin-induced acetylation of p53.
- The p53 protein was predominantly retained in cell nucleus after cisplatin/belinostat treatment.
- Nuclear-bound acetylated p53 was correlated to the induction of cell death and activation of p53 functions in p53 mutant cells.

5.4 The role of mutant p53 in cisplatin/belinostat-induced apoptosis

5.4.1 Synergistic cytotoxicity of belinostat and cisplatin is dependent on p53

Thus far, the observations have demonstrated that transactivation of p53 downstream genes occurred simultaneously with the post-translational modification and nuclear localization of p53. These data collectively raise the possibility that p53 function could be induced in this mutant cell line. To assess the relative contribution of mutated p53 to transcriptional-activated apoptosis in H2170 cells, inhibition of p53 through siRNA transfection and shRNA infection was conducted.

Gene silencing of p53 using siRNA was performed in H2170 cells with a scramble siRNA as negative control. Western blotting verified that p53 was successfully silenced as shown by the ablation of p53 expression (Figure 5.13). Upon drug treatment, induction of apoptosis was suppressed in p53-silenced cells as demonstrated by the decrease in cleaved caspase 3 and cleaved PARP as compared to vehicle control (Figure 5.13). To establish study models for further investigations, two independent lentiviral-based p53 shRNAs and two negative control shRNAs (non-targeting and luciferase-targeting) were infected to H2170 cells and selected with puromycin to obtain stable knockdown clones. Satisfactory inhibitions of both p53 mRNA and protein in H2170 were achieved with both shRNAs, sh56 and sh55. The mRNA expression of p53 was decreased by approximately 80% by sh56 and 60% by sh55 in comparison to a non-targeting shRNA control (shNT) (Figure 5.14 A). Protein expression of p53 was markedly reduced by sh56 and sh55 as well (Figure 5.14 B). When drug treatment was administered, apoptosis was triggered in all three clones. However, cleavages of PARP, caspase 9 and caspase 3 were more robust in shNT than sh56 and sh55, implying that p53 knockdown clones are more resistant to cisplatin and combination treatment (Figure 5.15 A). Quantification of apoptotic cells for each clone was analysed by FACS. Similar to parental H2170 cells, cisplatin induced apoptosis in shNT and shLuc cells in combination with belinostat further increased the percentage of Annexin-V positive cells. In both sh56 and sh55 clones, cisplatin-induced apoptosis was reduced. Unexpectedly, knockdown of p53 significantly reduced the synergistic effect with belinostat, as apoptosis induced by combination treatment was abrogated (Figure 5.15 B).

These data suggest an indispensable role of p53 in regulating the cytotoxicity of belinostat and cisplatin, supporting the claim that mutant p53 regains wild-type function. Despite having minimal effect on cisplatin-induced apoptosis, the synergistic combination of belinostat in H2170 cells was abrogated through silencing of p53.

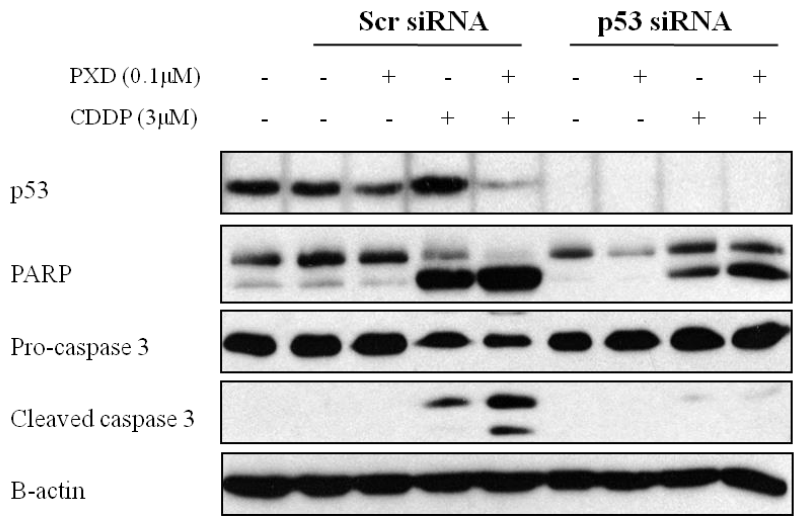

Figure 5.13: Silencing of p53 abrogates apoptosis in cisplatin and belinostat-treated H2170 cells.

p53 siRNA was transfected to H2170 cells. 100nM of siRNA was used per transfection. H2170 cells were treated with belinostat (PXD101) (0.1μM), cisplatin (3μM) and combination treatment with DMSO (0.001%) as vehicle control for 48 hours. Western blot analysis was performed to investigate the expression of p53, PARP and caspase 3. Western blot data shown are representative of three independent experiments for the indicated targets with β-actin as input control.

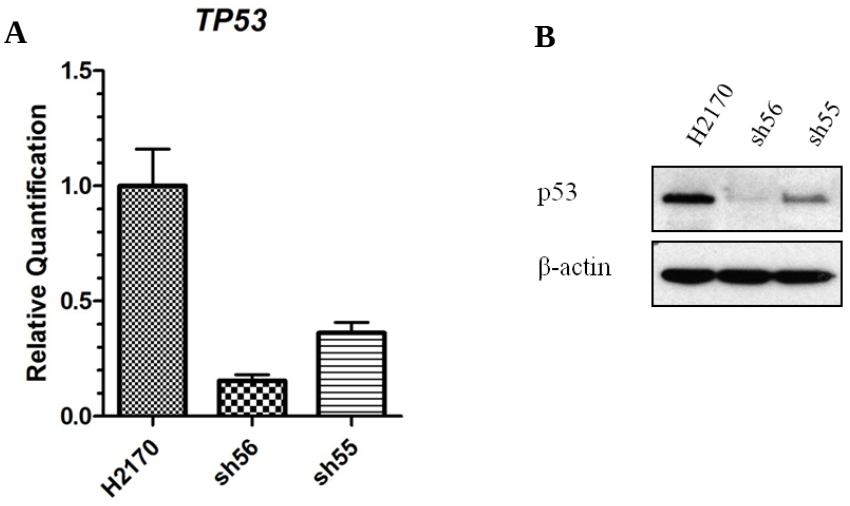

Figure 5.14: Stable shRNA knockdown of *TP53* in H2170 cells.

H2170 was infected with lentivirus packaged with 2 shRNA targeting *TP53* (sh55, sh56). Stable clones were selected by puromycin (5μg/ml) treatment. Efficiency of knockdown was determined by (A) real time qPCR and (B) Western blotting. Real time data are shown as mean ± SD (n = 1). Western blot data shown are representative of two independent experiments for the indicated targets with β-actin as input control.

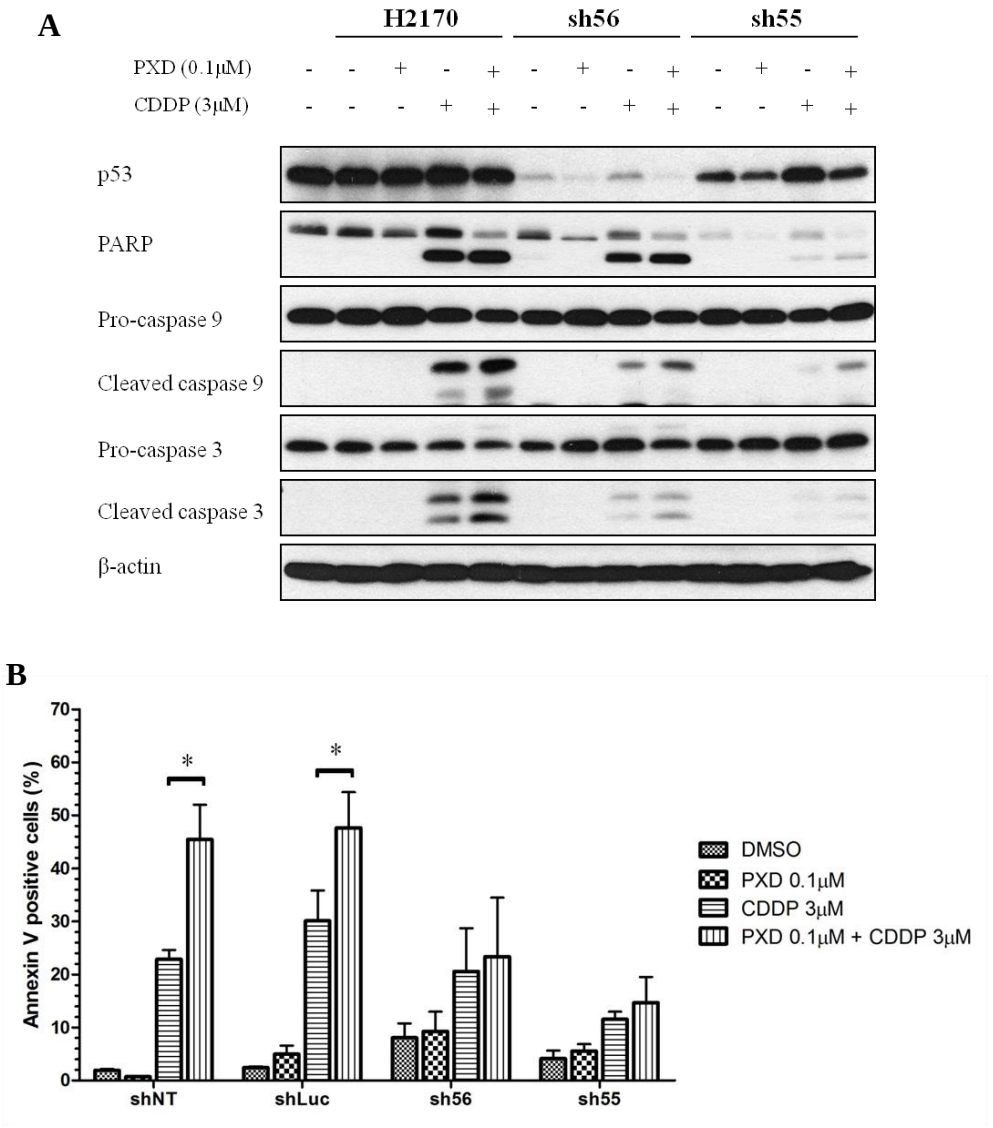

Figure 5.15: Knockdown of p53 attenuates potentiation of apoptosis by belinostat in cisplatin-treated H2170 cells.

Stable p53 knockdown H2170 clones (Sh55, sh56) were generated by lentiviral transfection. All cells were treated with belinostat (PXD101) (0.1μM), cisplatin (3μM) and combination treatment with DMSO (0.001%) as vehicle control for 48 hours. (A) Western blot analysis was performed to investigate the expression of p53, PARP, caspase 9 and caspase 3. Western blot data shown are representative of three independent experiments for the indicated targets with β-actin as input control. (B) Annexin-V and propidium iodide (PI) staining was performed to investigate the proportion of apoptotic cells in each clone upon exposure to belinostat (0.1μM), cisplatin (3μM) and combination treatment with DMSO (0.001%) as vehicle control for 48 hours. Two stable clones expressing non-targeting (shNT) and luciferase-targeting (shLuc) shRNAs were generated as negative control. Percentage of Annexin-V (+/-) and PI (+/-) cells were determined. Bar chart showing the percentage of Annexin-V positive cells in each clone was displayed. Data are shown as mean ± SD for three independent experiments. Statistical analyses were performed by unpaired t-test. *Significant difference from cisplatin-treated group, $P < 0.05$.

5.4.2 *In vitro* overexpression of human p53 cDNA and characterization of p53 signalling in lung SCC cells

5.4.2.1 Belinostat and cisplatin induce transactivation of wild-type p53 in lung fibroblast cells

The p53 molecule mediates cellular processes in response to a variety of stresses by activating different downstream signals. As a tumour suppressor, p53 affects the transcription of genes related to intrinsic mitochondrial apoptotic pathway and cell cycle arrest, thus providing checkpoints to constrain tumourigenesis (Levine, Momand et al. 1991).

Pharmacological activation of p53 was achieved with Nutlin-3a treatment in wild-type p53 MRC5 cells (Vassilev, Vu et al. 2004). The data showed a dose-dependent increase of p53 upon Nutlin-3a treatment. Two main downstream effectors of p53, p-MDM2 and p21, were shown to increase in similar pattern as p53 (Figure 5.16 A). The transcriptional activation of *CDKN1A* and *MDM2* was shown earlier in Nutlin-3a-treated MRC5 cells (Figure 5.10). Despite resulting in a significant accumulation of p53 protein, Nutlin-3a reduced the mRNA expression of *TP53* in MRC5 cells (Figure 5.16 B). In addition, a dose-dependent decline of p73 at the mRNA level was observed (Figure 5.16 C).

Next, the underlying mechanisms in which cisplatin and belinostat trigger p53-dependent apoptosis in wild-type cells were investigated. In MRC5 cells, exposure to cisplatin but not belinostat induced accumulation of p53, increased acetylation of p53, and triggered apoptosis through cleavage of PARP and caspase 3 (Figure 5.17 A). To relate the cytotoxicity with p53 signalling, the activation of downstream target genes was investigated. Cisplatin and combination treatment, but not belinostat, increased mRNA expression of *CDKN1A*, *MDM2*, *PUMA* and *Noxa* (Figure 5.17 B, C, D, E). However, mRNA expression of *TP53* and *TP73* were reduced (Figure 5.17 F, G). Collectively, these data demonstrated the transactivtion of p53 downstream genes upon drug treatment in MRC5. Interestingly, mRNA levels of both *TP53* and *TP73* were reduced, probably due to the auto-regulatory effects of these proteins (Chen, Zheng et al. 2001, Grob, Novak et al. 2001).

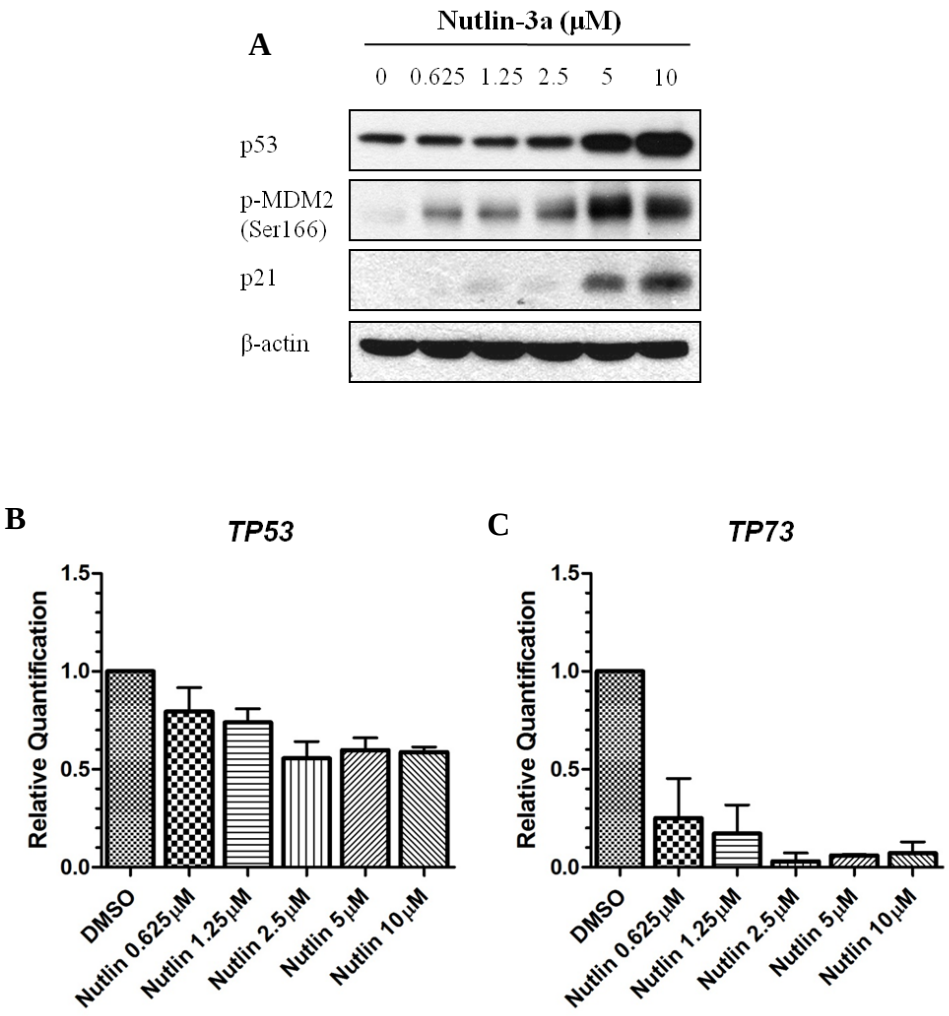

Figure 5.16: Activation of p53 signalling pathway by Nutlin-3a in MRC5 cells.

MRC5 cells were treated with Nutlin-3a (0.625, 1.25, 2.5, 5, 10μM) with DMSO (0.01%) as vehicle control for 48 hours. A, Western blotting analysis was performed to investigate the expression of p53, p-MDM2 (Ser166) and p21. Data shown are representative of three independent experiments for the indicated targets with β-actin as input control. Real-time qPCR was conducted to determine the expression of (A) *TP53* and (B) *TP73*. Data are shown as mean ± SD for two independent experiments.

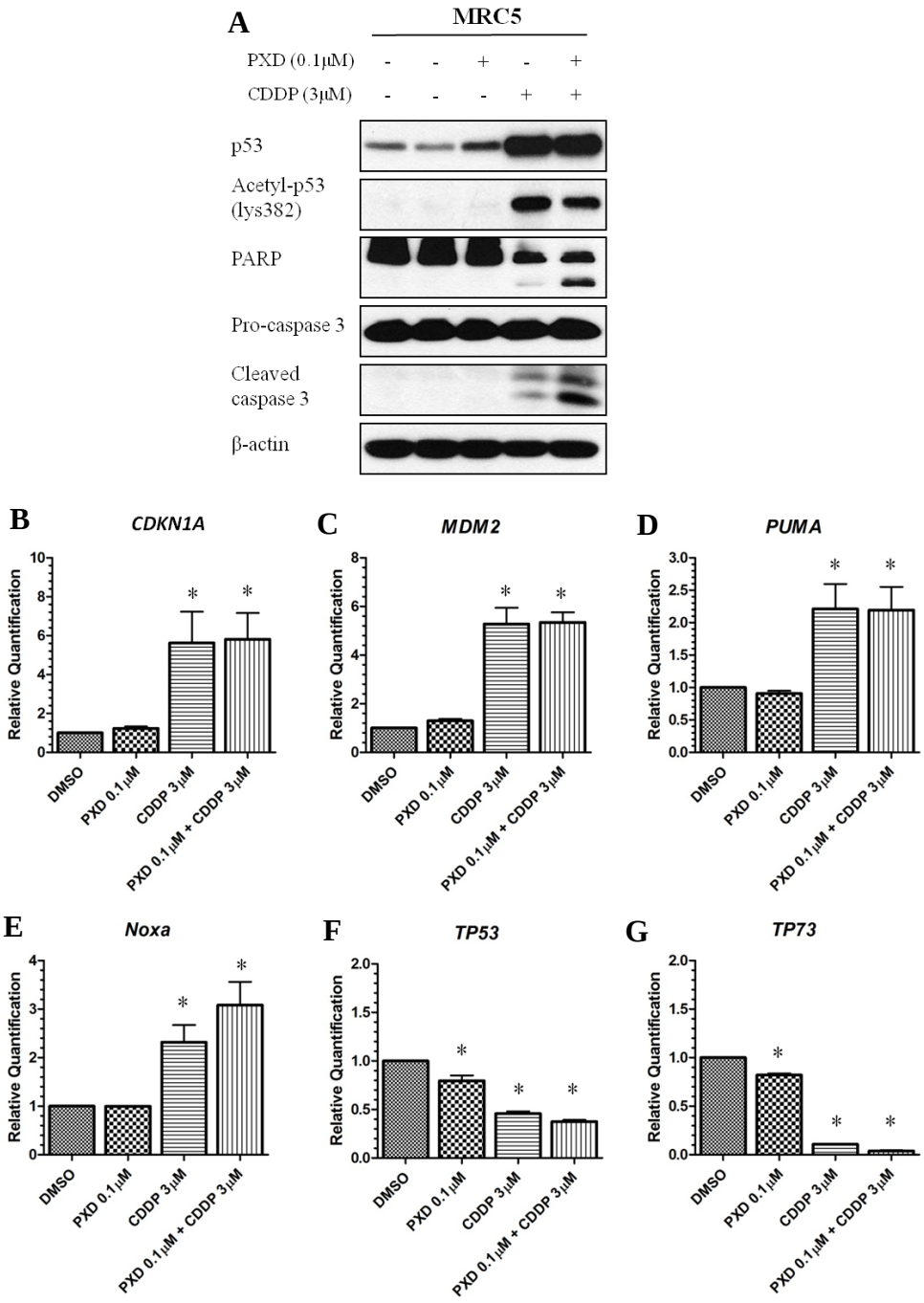

Figure 5.17: Exposure to belinostat and cisplatin activate p53 downstream signalling.

MRC5 cells were treated with belinostat (PXD101) (0.1μM), cisplatin (3μM) and combination treatment with DMSO (0.001%) as vehicle control for 48 hours. A, Western blotting analysis was performed to investigate the expression of p53, acetyl-p53 (Lys382), caspase 9 and caspase 3. Data shown are representative of three independent experiments for the indicated targets with β-actin as input control. Total RNA was isolated and reverse transcribed to cDNA. Expressions of (B) *CDKN1A*, (C) *MDM2*, (D) *PUMA*, (E) *Noxa*, (F) *TP53* and (G) *TP73* were analysed using Real-time qPCR. Data are shown as mean ± SD from three independent experiments. Statistical analyses were performed by unpaired t-test. *Significant difference from vehicle control, $P < 0.05$.

5.4.2.2 Belinostat and cisplatin induce downstream signalling that mimicks p53 transactivation in H2170 cells

Despite verifying the loss-of-function mutation in H2170 cells, but the data have by far demonstrated a contradicting mechanism involving p53 activation that could be trigger by cisplatin and belinostat, possibly via post-translational modification of p53. These observations were reaffirmed in Figure 5.18 A, as shown by the cleavage of PARP and caspase 3. It was earlier discussed in Figure 5.8 that cisplatin and belinostat up-regulated *BAX* and *FAS*. The regulations of other p53 target genes in H2170 cells were discussed here. The data demonstrated increases in *CDKN1A*, *PUMA* and *Noxa* when cisplatin was administered singly and in combination with belinostat (Figure 5.18 B, D, E). In contrary, expression of *MDM2* and *TP53* were unaffected by drug treatment (Figure 5.18 C, F). These findings suggest that p53 signalling may be involved in cytotoxicity of cisplatin. When compared to MRC5 cells, cisplatin and combination treatment induced a similar mRNA expression profiles in H2170 cells that mimic p53 activation to a certain extent, with the exception of *TP53* and *MDM2*. This unique expression pattern of p53 target genes in H2170 cells prompted the query as to which extent the tumour suppression effect is restored in mutant p53.

Up to this point, it was demonstrated that exposure to cisplatin and belinostat activated both intrinsic and extrinsic apoptosis at the transcriptional level (Chapter 5.2.3 and 5.2.4). Unexpectedly, this drug-induced apoptosis was observed in parallel with the increase in p53 promoter activity (Chapter 5.3.1) and up-regulation of nuclear-bound acetylated p53 (Chapter 5.3.2). In addition, knockdown of p53 through siRNA and shRNA significantly abrogated the induction of apoptosis in this p53 mutant line (Chapter 5.4.1). Accordingly, it was hypothesized that a low dose of belinostat (0.1μM) could substantially potentiates the cytotoxicity of cisplatin and increases cisplatin-induced acetylation of p53. To prove this hypothesis, the functions of wild-type and mutant p53 were investigated through ectopic expression of *TP53* genes in a p53 null cell line (Calu-1).

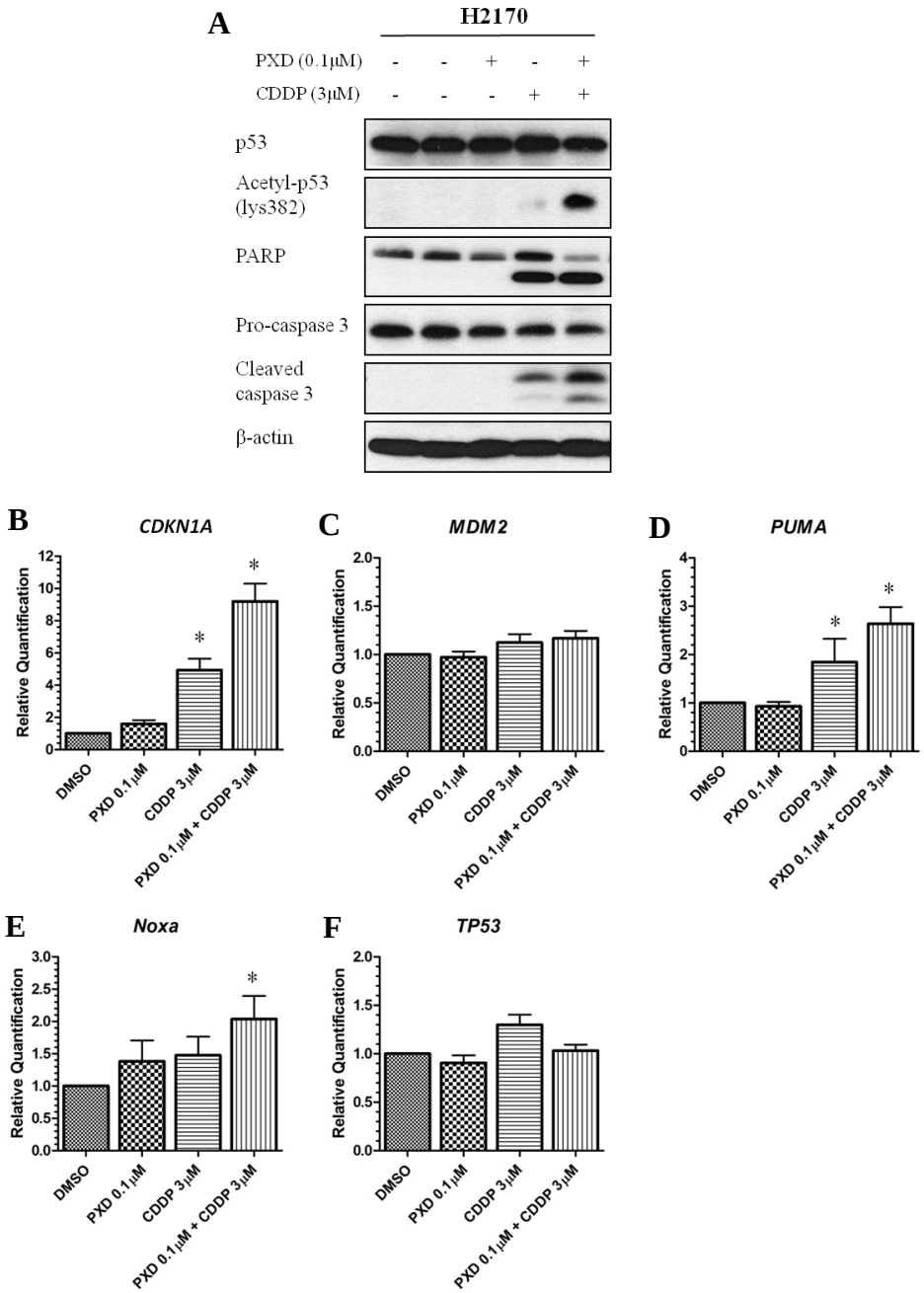

Figure 5.18: Exposure to belinostat and cisplatin induce p53 downstream signalling in H2170 cells that is comparable to wild-type p53 cells.

H2170 cells were treated with belinostat (PXD101) (0.1μM), cisplatin (3μM) and combination treatment with DMSO (0.001%) as vehicle control for 48 hours. A, Western blotting analysis was performed to investigate the expression of p53, acetyl-p53 (Lys382), caspase 9 and caspase 3. Data shown are representative of three independent experiments for the indicated targets with β-actin as input control. Total RNA was isolated and reverse transcribed to cDNA. mRNA expressions of (B) *CDKN1A*, (C) *MDM2*, (D) *PUMA*, (E) *Noxa* and (F) *TP53* were analysed using Real-time qPCR. Data are shown as mean ± SD from three independent experiments. Statistical analyses were performed by unpaired t-test. *Significant difference from vehicle control, $P < 0.05$.

5.4.2.3 Ectopic expression of p53 in Calu-1 (p53-null) cells

The synergistic combination of belinostat and cisplatin in H2170 cells is seemingly dependent on p53 activation. However, it remains unclear of how these events take place. As H2170 cells harbour a dominant negative loss-of-function mutant p53 (R158G), it is possible that the observed pathway activation of p53 may be due to other alternative mechanisms that mimick p53 activity. To address the critical question on the role of mutant p53, mutant p53 constructs were genetically transfected into p53 null Calu-1 cells. cDNA sequences of p53 were obtained from MRC5 (p53 wild-type) and H2170 (p53R158G mutant). A HA-tag was inserted at the 5' end of the amplified p53 cDNA for immunoprecipitation studies. Both sequences were cloned into pCMV vector, expanded in bacteria culture, and purified to obtained pCMV-p53-HA clones as described in Material and Methods. The molecular sequences of both wild-type and mutant clones were verified by Sanger sequencing with two vector sequencing primers.

To establish cellular models with simultaneous presence of p53 molecules, these plasmids (pCMV, pCMV-p53wt-HA and pCMV-p53R158G-HA) were transfected into Calu-1 cells, and selected with Geneticin (250μg/mL) to obtain stable transfectants. To generate homogenous clonal population, single cell cloning was performed on each clone through various rounds of limiting dilution under Geneticin selection as described in Materials and Methods. The expanded clonal cell populations were subjected to further screening based on their morphology and proliferation rates by comparing with the parental cell line. Through this process, 1 Empty vector control (EV), 1 wild-type clone (WT 6) and 5 mutant clones (R158G) were established. Expression of wild-type and mutant form of murine p53 was driven constitutively by the strong CMV immediate-early regulatory element.

Expression levels of p53 in these clones were verified with Real-time qPCR. In relative to WT clone, all 5 mutant clones showed > 40-fold increase in p53 expression, with no expression in EV clone (Figure 5.19 A). Western blotting analysis was further performed to verify the p53 protein expression. Both p53 and p21 were not expressed by EV clone, while WT clone has stable expression of p53 and high expression of p21. In all five mutant clones, p53 protein was found in abundance. Interestingly, these mutant clones expressed p21 as well (Figure 5.19 B). As p53 is a nuclear-bound transcription factor, immunofluorescence staining was conducted to detect the translocalization of the protein. In Figure 5.19 C, both EV and WT 6 clones expressed undetected basal p53 (too low in WT clone for detection), while all 5 mutant clones expressed high amount of p53 that are mainly positioned in the cell nuclei. These data supported the observations through real time qPCR and Western blotting analyses.

Taken together, expressions of p53 molecules in all genetically modified Calu-1 cells were verified. These clones served as study models for investigating whether mutant p53 (R158G) alone is sufficient to mediate the synergistic effect of cisplatin and belinostat in lung SCC cells.

.

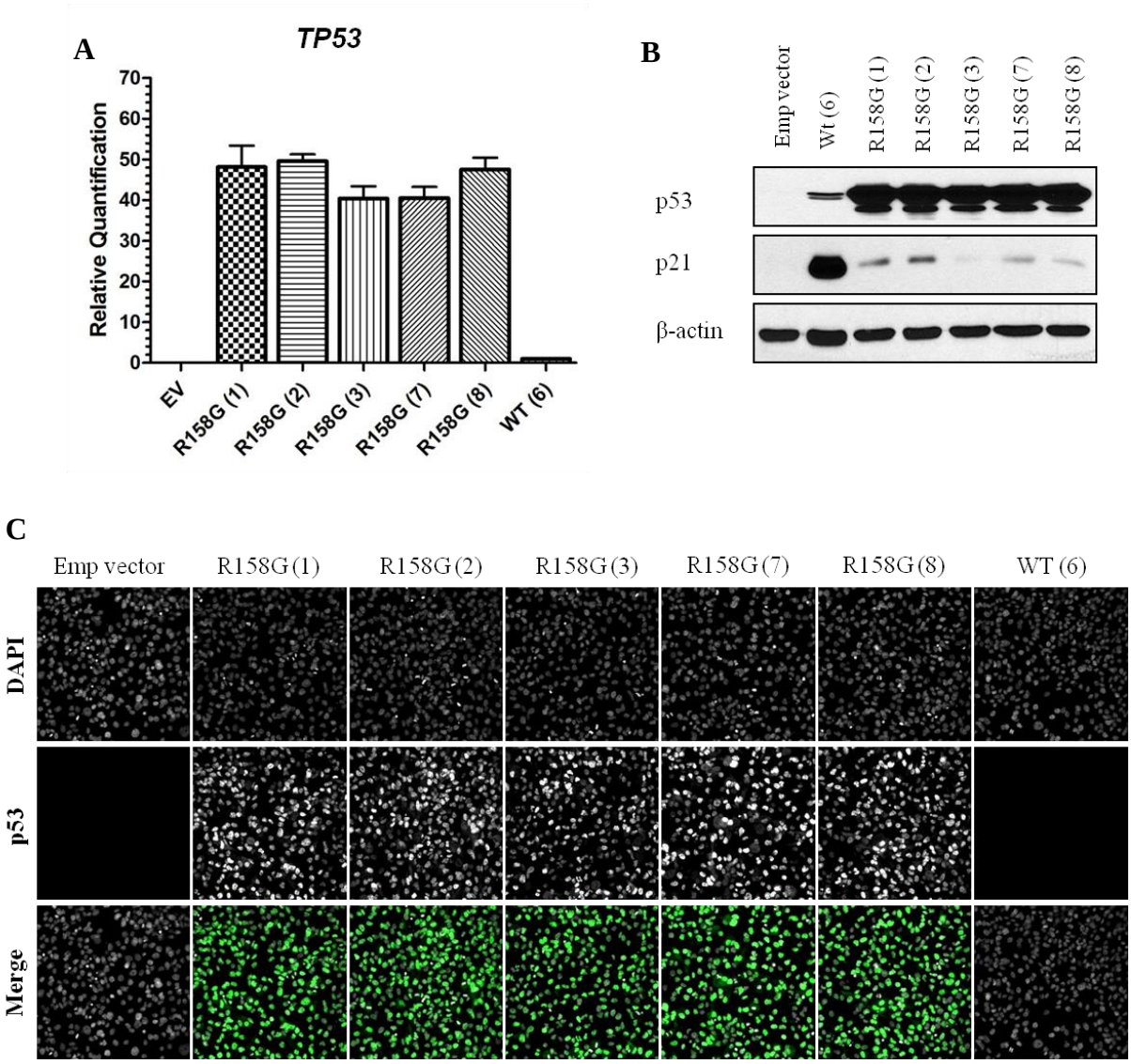

Figure 5.19: Overexpression of mutant and wild-type p53 in p53 null Calu-1 cells.

Calu-1 cells were transfected with p53 (Wild-type), p53 (R158G mutant) and pCMV vector plasmids. Single clones with stable cDNA expression were selected by Geneticin (250µg/ml) treatment. Empty vector control clone (EV), p53wt clone (WT 6) and p53mutant clones (R158G 1, 2, 3, 7, 8) were established. A, Expressions of *TP53* cDNA in all clones were quantified using Real time qPCR by using p53wt clone as the reference group. Data are shown as mean ± SD from three independent experiments. B, Western blotting analysis was performed to investigate the expression of p53 and p21 in each clone. Data shown are representative of three independent experiments for the indicated targets with β-actin as input control. C, Immunofluorescence staining was performed to determine the translocalization of p53 molecules (Alexa Fluor-488) in each clone. Representative images are shown at 400x magnification for two independent experiments. **Grey indicates DAPI and p53 in single channel**; while **green indicates p53 in merged channel**.

5.4.2.4 Sensitivities of p53 overexpressing clones to cisplatin and belinostat

From the earlier analysis, Calu-1 was determined to be a cisplatin-resistant, belinostat-sensitive lung SCC cell line. If p53 indeed plays a major role in induction of apoptosis to cisplatin, the lack of p53 may contribute to this resistance. Using cell proliferation assay, the response of the established p53-overexpressing clones to cisplatin and belinostat treatment was determined.

EV clone was shown to have similar sensitivities to cisplatin and belinostat as compared to parental Calu-1 cells. Expectedly, p53wt overexpressing clone displayed highest sensitivity to cisplatin among the modified clones. All p53R158G clones demonstrated greater sensitivity to cisplatin as compared to EV clone (Figure 5.20 A). When treated with belinostat, EV clone and p53wt clone have similar IC_{50} to parental Calu-1cells. However, all p53R158G clones have significantly higher belinostat IC_{50} (Figure 5.20 B). Based on the earlier data, mutant p53 may be accounted for the synergy between belinostat and cisplatin. Here, the cisplatin IC_{50} of all clones was determined when combined with belinostat at 0.1μM. The data demonstrated that belinostat did not increase cisplatin cytotoxicity in EV and p53wt clones. However, in 4 out of the 5 p53R158G clones, combination with belinostat significantly reduced cisplatin IC_{50} (Figure 5.20 C).

Expectedly, overexpression of wild-type p53 increases sensitivity to cisplatin, but the data here suggested that mutant p53 could affect cellular response to cisplatin as well. More importantly, synergistic combination of belinostat and cisplatin was observed in p53 mutant clones. In addition, p53 mutant clones were shown to be more resistant to belinostat, which corresponded with the earlier observation that lung SCC cell lines have reciprocally inverse sensitivities to both cisplatin and belinostat. These data clearly supported that mutant p53 increased cellular response to cisplatin.

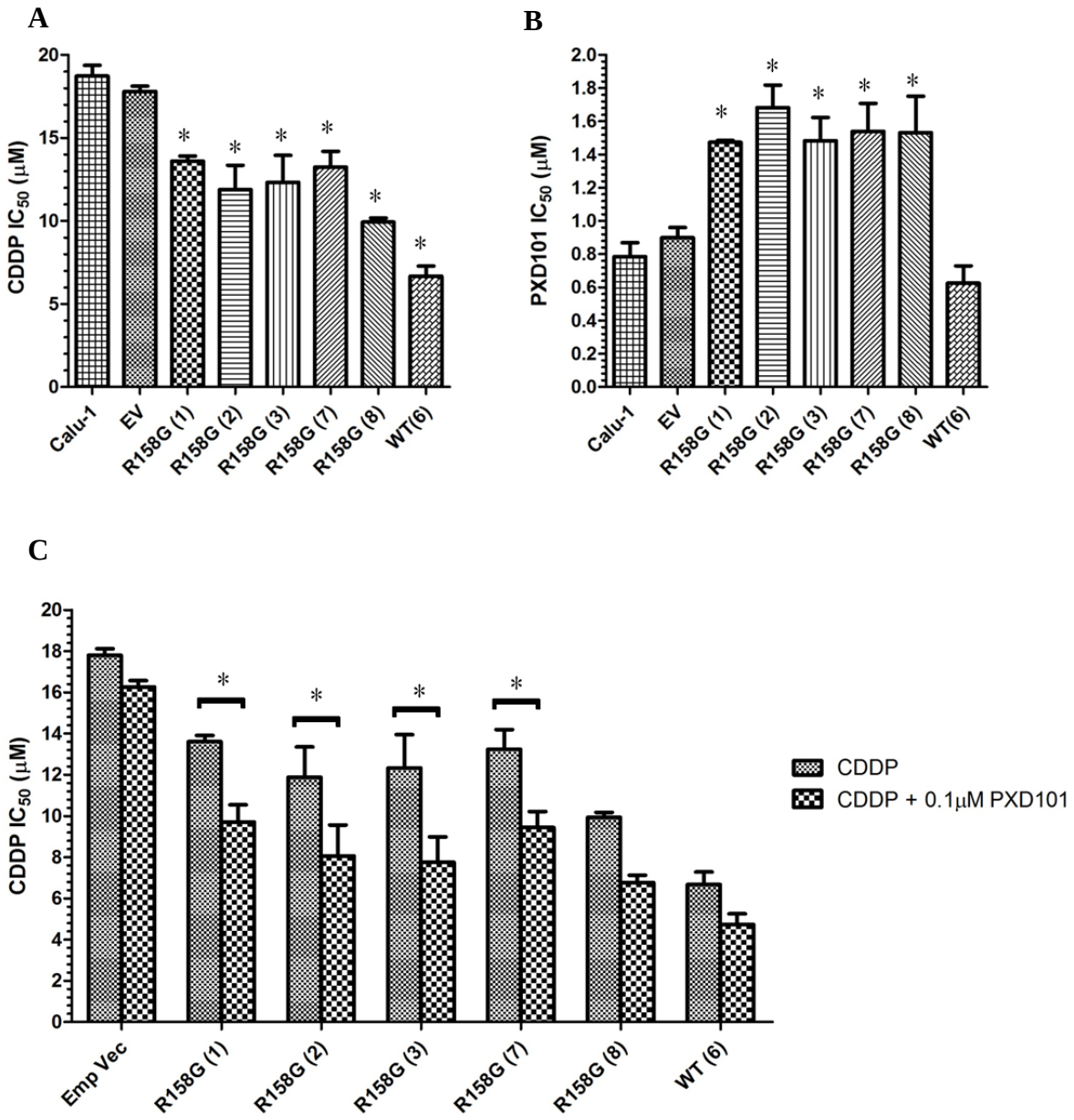

Figure 5.20: p53-expressing Calu-1 clones exhibit differential responses to cisplatin, belinostat and combination treatment.

EV clone, p53wt clone, and p53R158G clones were drug treated for 72 hours and cell viability assay (MTS) was used to determine the IC_{50} of (A) cisplatin and (B) belinostat (PXD101). Data are presented as mean ± SD (n = 3). Statistical analyses were performed by unpaired t-test. *Significant difference from EV clone, $P < 0.05$. C, Cisplatin IC_{50} in combination with 0.1μM belinostat of each clone was shown. Data are presented as mean ± SD (n = 3). Statistical analyses were performed by unpaired t-test. *Significant difference from vehicle control (0.001% DMSO), $P < 0.05$.

5.4.2.5 Modification of mRNA expression of p53 target genes in p53 overexpressing clones

As demonstrated, p53 signalling was transctivated after drug treatment in H2170 cells. The expression levels of several downstream target genes of p53 (*MDM2*, *CDKN1A*, *PUMA*, *Noxa*, *BAX*, and *TP73*) were determined in p53-expressing clones. In line with current knowledge, wild-type p53 clone expressed higher mRNA level of *MDM2*, *CDKN1A*, *PUMA* and *Noxa*. In reference to EV clone, p53 mutant clones have similar expression of *MDM2* and *PUMA* (Figure 5.21 A, C), higher expression of p21 and lower expression of *Noxa* (Figure 5.21 B, D). *BAX* mRNA level was consistent among EV, WT and T158G clones (Figure 5.22 E). Unexpectedly, both wild-type and mutant p53 molecules have reduced *TP73* mRNA expression (Figure 5.22 E).

From these observations, it could be concluded that transcriptome of p53-related genes was modified in the overexpressing clones: a fully functional p53 (WT) consistently activates *MDM2*, *CDKN1A*, *PUMA* and *Noxa*; in mutant cells, *MDM2* expression is not affected (consistent with the lack of transactivation ability of mutant p53 to MDM2), while *CDKN1A* and *Noxa* genes were differentially regulated. *BAX* expression was unaffected in all clones, as it requires external stress signal to be transactivated. In addition, mRNA level of *TP73* is reduced by approximately 80%, as compared to EV clones. Taken together, these data suggested the insertion of mutant p53 partially restored the p53-regulated transcriptomic profiles in Calu-1 cells.

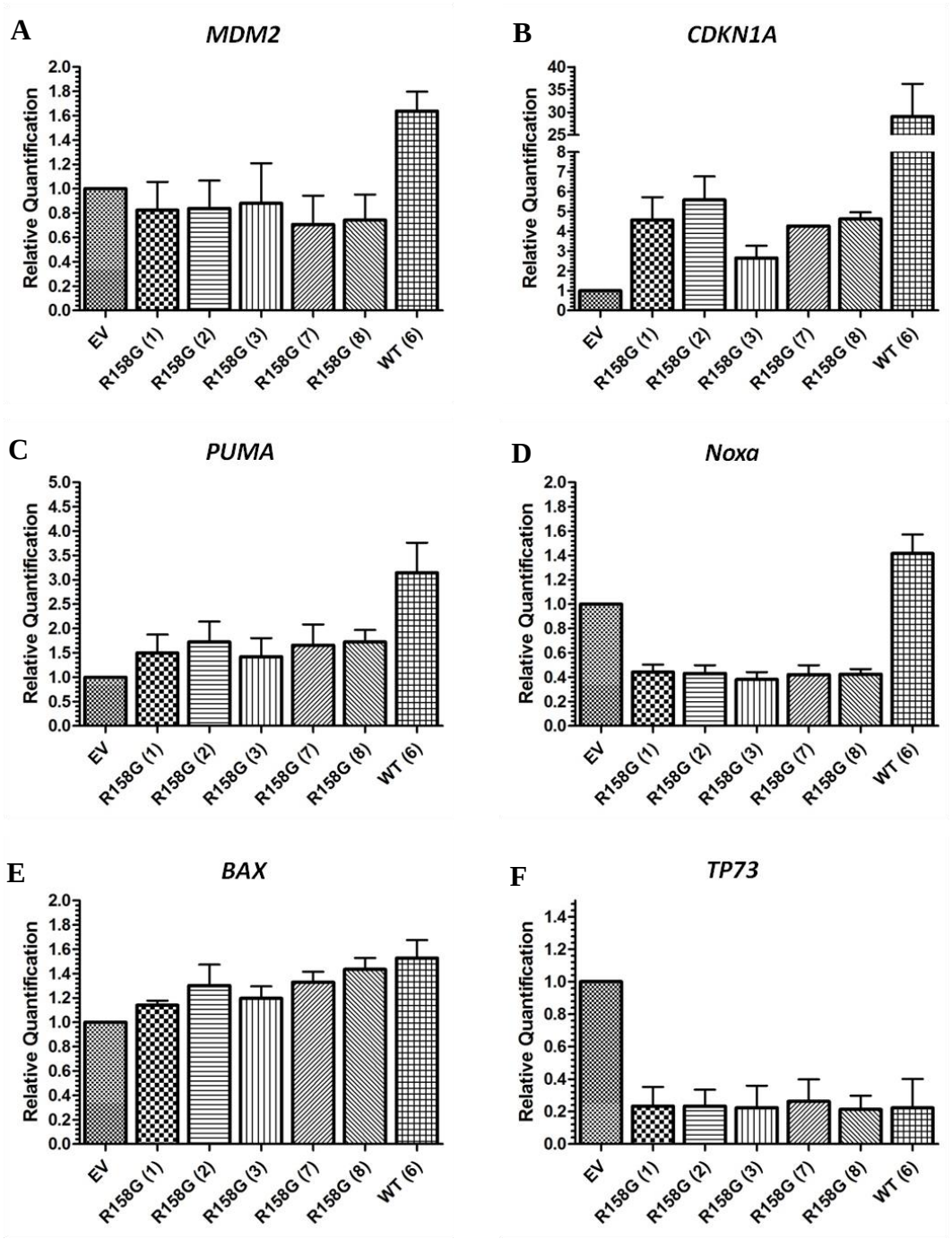

Figure 5.21: p53-expressing Calu-1 clones have dissimilar gene expression profiles for p53 downstream genes.

Total RNA for each clone was isolated and reverse transcribed to cDNA. mRNA expressions of (A) *MDM2*, (B) *CDKN1A*, (C) *PUMA* (D) *Noxa*, (E) *BAX* and (F) *TP73* were analysed using real-time qPCR. Untreated EV clone was applied as reference group. Data are shown as mean ± SD from three independent experiments.

5.4.2.6 Drug-induced modification of p53 target genes in p53 overexpressing clones

In order to ascertain if p53 signalling is triggered in these mutant clones, the mRNA expression of p53 target genes was profiled after belinostat, cisplatin and combination treatment. Analysis on the expression of p53-related genes again displayed diverse transcriptional regulation among EV, WT and R158G mutant clones upon drug treatment.

As demonstrated, a classical pattern of activated p53 signalling was observed in p53 wild-type clone. *MDM2* was significantly up-regulated in WT clone by cisplatin and combination treatment, but no activity was observed in all EV and p53R158G clones Figure 5.22 A). In relative to the untreated EV clones, a substantial increase of *CDKN1A* was observed in drug-treated WT cells. Similar expression pattern of *CDKN1A* level was observed in all mutant clones with a lower magnitude of increase after drug treatment (Figure 5.22 B). Cisplatin and combination treatment induced *PUMA* expression in WT clone and mutant clones (especially R158G clone 3 and 8), but not in EV clone (Figure 5.22 C). Expression level of *Noxa* was inducible by cisplatin and belinostat in EV and WT clones but not in mutant clones (Figure 5.22 D). As illustrated in Figure 5.21 E, all clones expressed similar mRNA level of *BAX*. Cisplatin exposure induced *BAX* expression in all clones, while combination treatment further potentiated the up-regulation of *BAX* gene. In comparison, EV clone demonstrated the lowest induction (~2-fold) of *BAX*, with the highest expression (~5-fold) observed in WT clone (Figure 5.22 E). In EV clone, *TP73* was decreased by both belinostat and cisplatin, while combination treatment further reduced its expression. However, cisplatin alone did not affect *TP73* in all p53 overexpressing clones, while both belinostat and combination treatment substantially suppressed expression of *TP73* (Figure 5.22 F).

MDM2 is commonly described to be mainly mediated by p53 transactivation (Barak, Juven et al. 1993). These analyses have verified that belinostat and cisplatin treatments did not affect *MDM2* expression in EV and p53 mutant clones, strongly indicating the loss-of-function event through missense mutation at the DNA-binding domain. Despite so, concurrent activation of other p53 target genes (*CDKN1A*, *BAX* ad *PUMA*) among mutant clones suggested that mutant p53 may be activated and functional to a certain extent under treatment pressure.

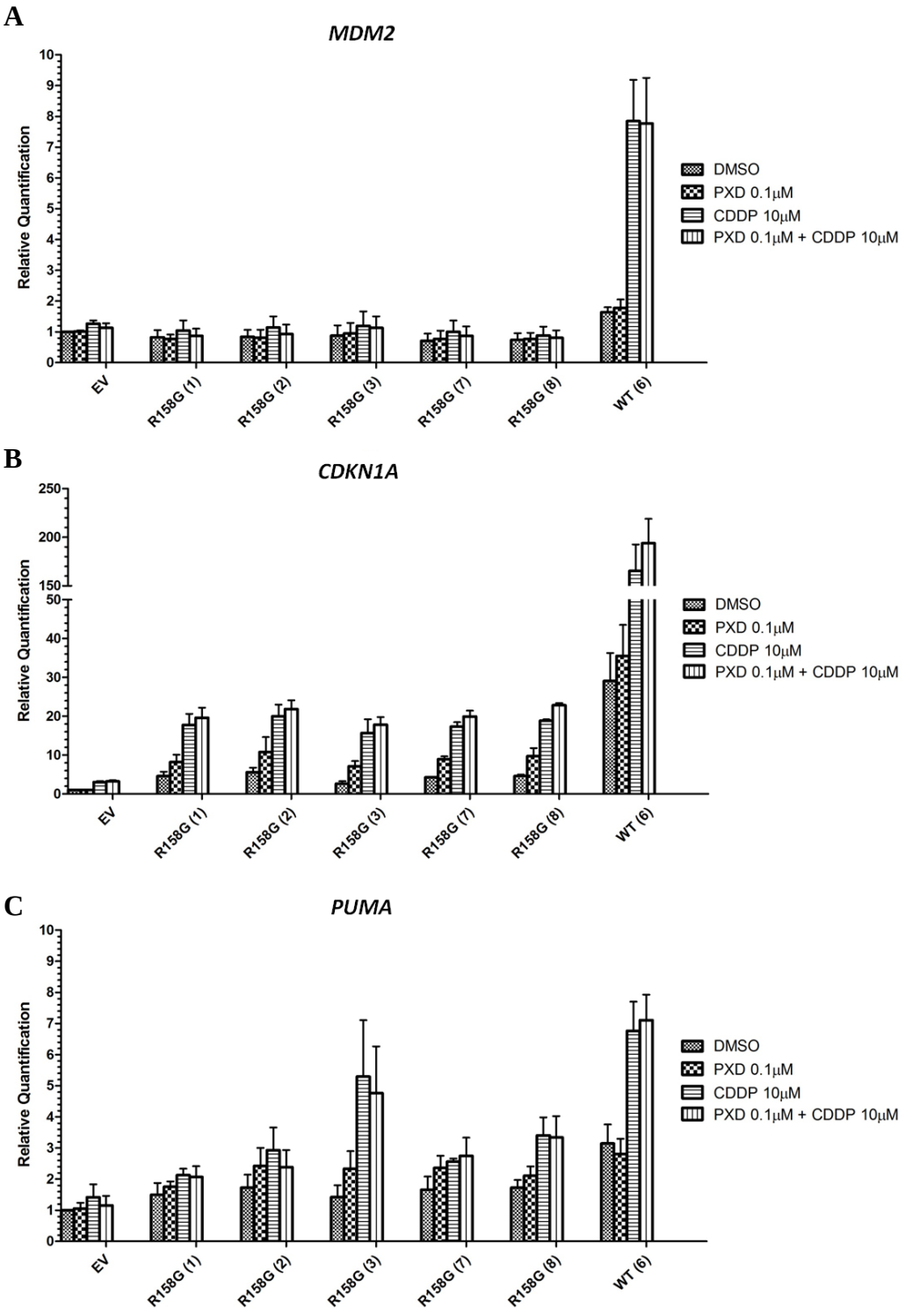
A
MDM2
Relative Quantification
DMSO
PXD 0.1μM
CDDP 10μM
PXD 0.1μM + CDDP 10μM
EV
R158G (1)
R158G (2)
R158G (3)
R158G (7)
R158G (8)
WT (6)
B
CDKN1A
Relative Quantification
DMSO
PXD 0.1μM
CDDP 10μM
PXD 0.1μM + CDDP 10μM
EV
R158G (1)
R158G (2)
R158G (3)
R158G (7)
R158G (8)
WT (6)
C
PUMA
Relative Quantification
DMSO
PXD 0.1μM
CDDP 10μM
PXD 0.1μM + CDDP 10μM
EV
R158G (1)
R158G (2)
R158G (3)
R158G (7)
R158G (8)
WT (6)

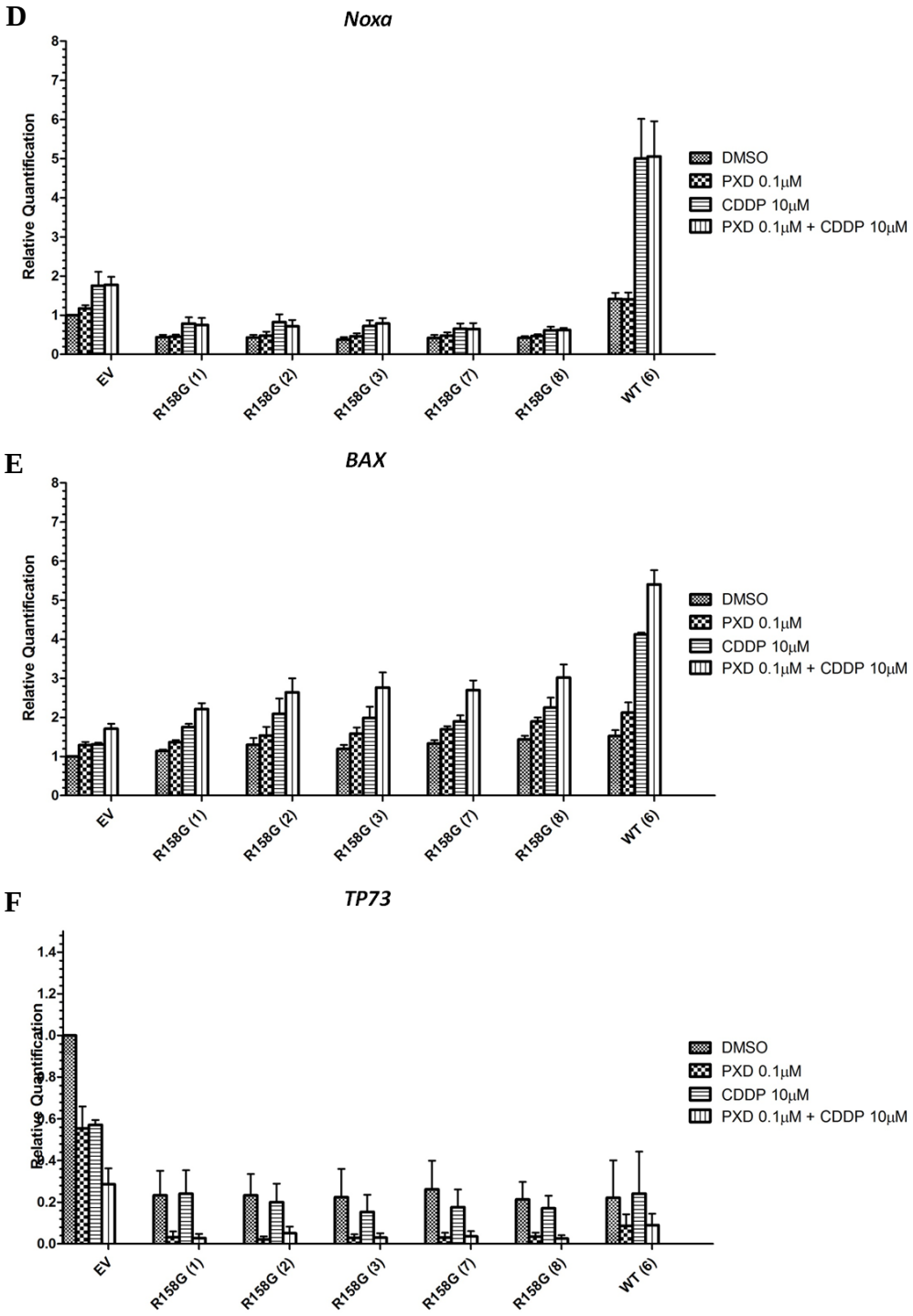

Figure 5.22: Belinostat and cisplatin differentially mediate p53 downstream genes in p53-expressiong Calu-1 clones.

EV clone, p53wt clone, p53R158G clones were treated with belinostat (PXD101) (0.1μM), cisplatin (10μM) and combination treatment with DMSO (0.001%) as vehicle control for 48 hours. Total RNA for each clone was isolated and reverse transcribed to cDNA. mRNA expressions of (A) *MDM2*, (B) *CDKN1A*, (C) *PUMA* (D) *Noxa*, (E) *BAX* and (F) *TP73* were analysed using Real-time qPCR. Untreated EV clone was applied as reference group. Data are shown as mean ± SD from three independent experiments.

5.4.2.7 Induction of apoptosis by cisplatin and belinostat in p53 overexpressing clones

Since transcriptional activation of p53-mediated apoptotic genes was detected in p53 mutant clones upon drug treatment, the post-translational modification of p53 as well as the extent of apoptosis in these clones were next investigated. The activation of p53 signalling in WT clone was determined. Upon cisplatin and combination treatment, expression of HA-tag, p53, p-p53 (Ser15) and acetyl-p53 (Lys279, Lys382) were up-regulated in WT clones, implying that p53 pathway was activated. The downstream targets, p21 and PUMA, were increased in concurrent with the cleavage of PARP and caspase 3 (Figure 5.23).

Expression of p53 and HA tag was undetectable in EV clone, confirming that it is a p53 null cell. As anticipated, low expressions of p21, BAX and PUMA were observed, and were not significantly altered by cisplatin, belinostat and combination treatment. Minimal PARP and caspase 3 cleavage were detected (Figure 5.24 A). Among the 5 p53R158G mutant clones, p53 and HA-tag were expressed in abundance, consistent with the reduced ubiquitination of p53 and tilt of balance to accumulation of mutant p53. Belinostat alone slightly induced p53 acetylation, unlike the lack of change in H2170 cells (Figure 5.11). This is consistent with the mode-of-action of belinostat as a protein acetylation agent. Similar to H2170 cells, cisplatin alone substantially induced p53 acetylation and phosphorylation in all mutant clones, while combination with belinostat further acetylated p53. This modification of mutant p53 up-regulated downstream targets of p53: p21, BAX and PUMA. Importantly, cisplatin-induced apoptosis, as indicated by PARP and caspase 3, was further potentiated by belinostat at a sub-lethal dose (especially R158G clone 2, 3 and 8) (Figure 5.24 A, B).

Despite being regulated by the same CMV promoter, differential expression of p53 was observed among WT and mutant clones. This is probably due to the interaction with MDM2, as MDM2 serves as a negative regulator of p53 molecule and thus inhibit p53 function in healthy cells with wild-type p53 (Kussie, Gorina et al. 1996). In WT clone, activation of p53-mediated apoptosis appeared to be similar to that of MRC5, and was mainly influenced by the cytotoxicity of cisplatin. Consistent with previous analysis on H2170 cells, combination with belinostat potentiated the cisplatin-induced acetylation of p53. Concurrently, drug-induced apoptosis was associated to acetylation of mutant p53. These findings provided compelling evidence that apoptosis could be triggered through p53 signalling in cells harbouring p53 mutation, probably via induction of acetylation.

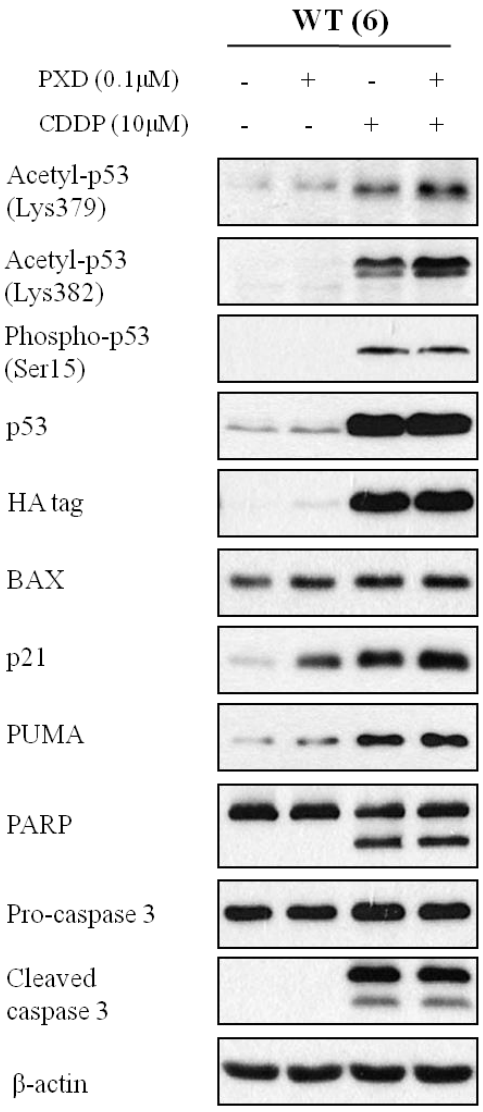

Figure 5.23: Belinostat and cisplatin induce apoptosis in Calu-1 cells expressing wild-type p53.

Calu-1 p53wt clone was treated with belinostat (PXD101) (0.1μM), cisplatin (10μM) and combination treatment with DMSO (0.001%) as vehicle control for 48 hours. Western blotting analysis was performed to investigate the expression of p-p53 (Ser15), acetyl-p53 (Lys279, Lys382), p53, BAX, p21, PUMA, PARP and caspase 3. Data shown are representative of three independent experiments for the indicated targets with β-actin as input control.

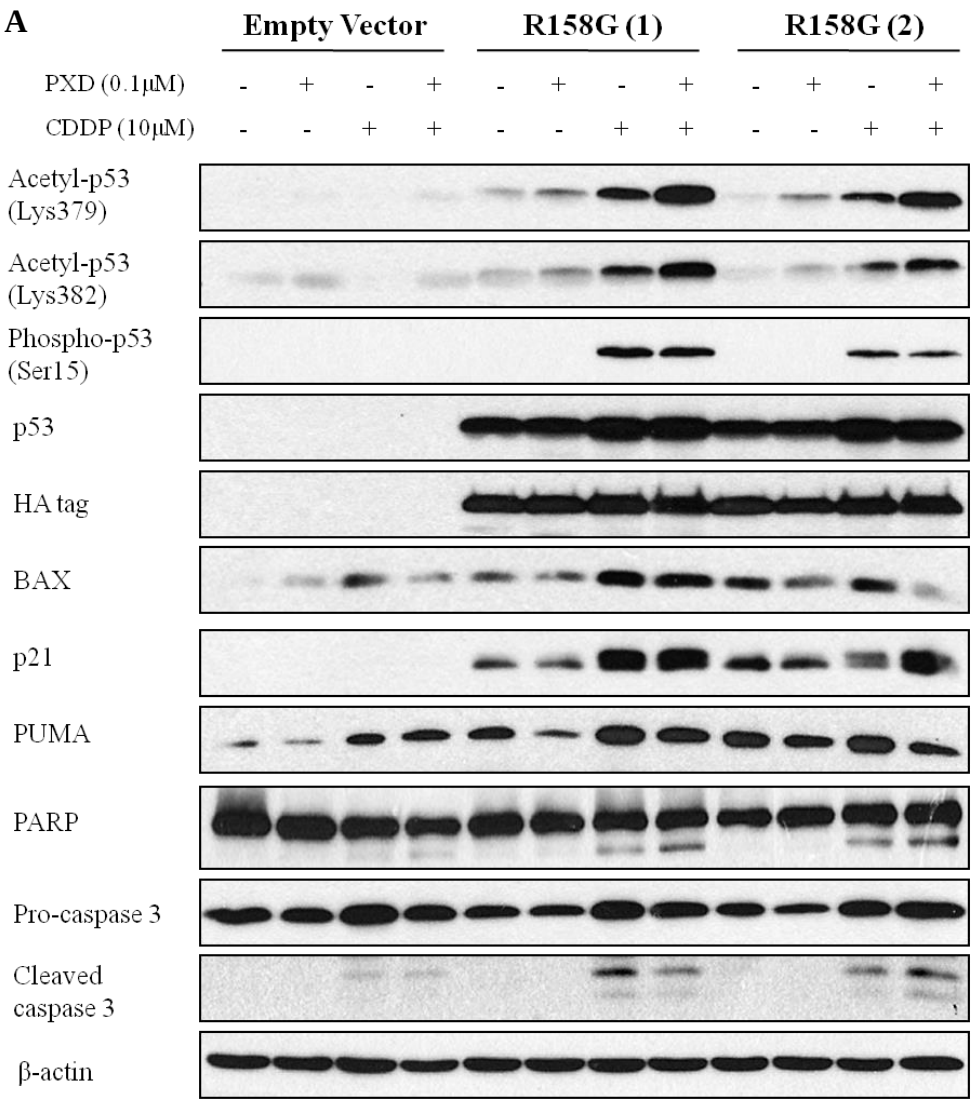
A
Empty Vector
R158G (1)
R158G (2)
PXD (0.1μM)
CDDP (10μM)
Acetyl-p53 (Lys379)
Acetyl-p53 (Lys382)
Phospho-p53 (Ser15)
p53
HA tag
BAX
p21
PUMA
PARP
Pro-caspase 3
Cleaved caspase 3
β-actin

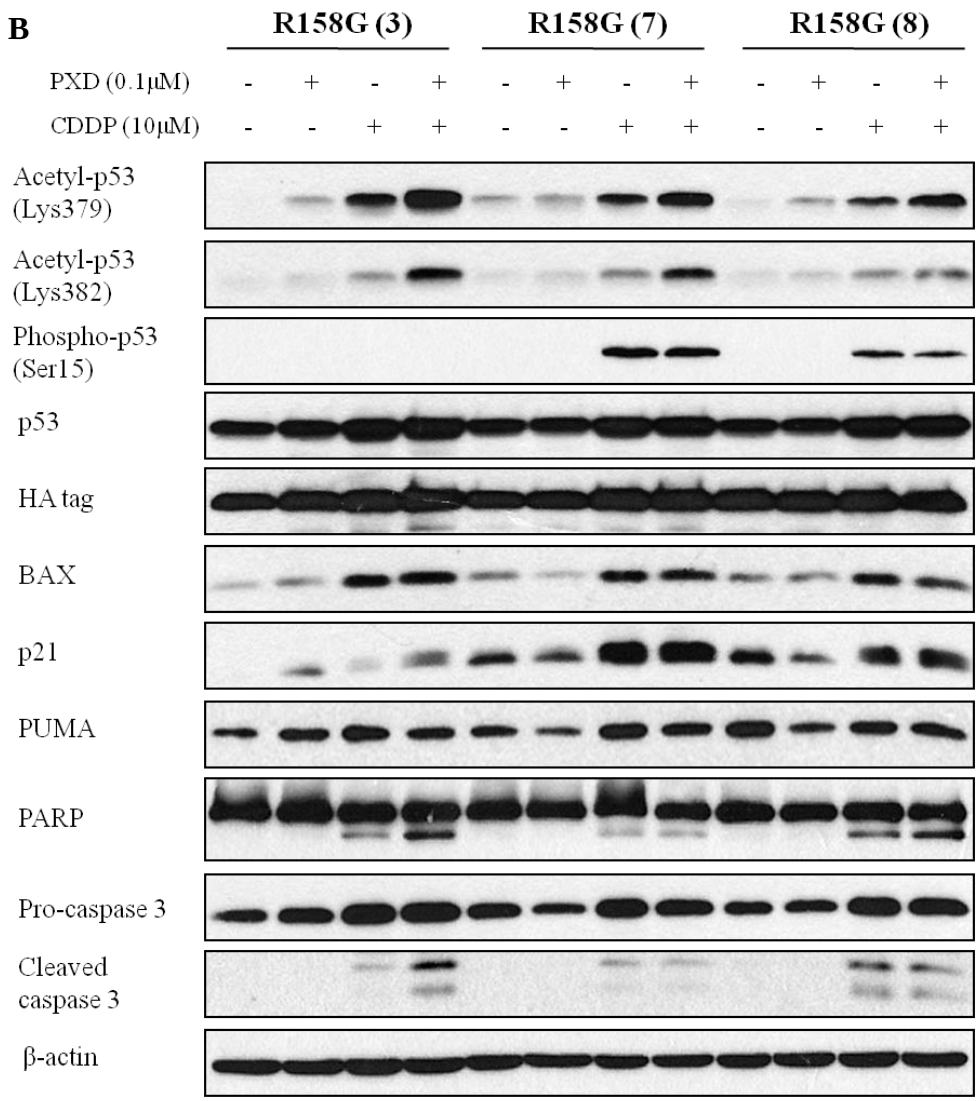

Figure 5.24: Belinostat and cisplatin induce up-regulation of acetylated p53, BAX, p21, PUMA as well as cleavage of PARP and caspase 3 in Calu-1 cells expressing mutant p53.

Calu-1 EV clone and p53R158G clones were treated with belinostat (PXD101) (0.1μM), cisplatin (10μM) and combination treatment with DMSO as vehicle control for 48 hours. Western blotting analysis was performed to investigate the expression of p-p53 (Ser15), acetyl-p53 (Lys279, Lys382), p53, BAX, p21, PUMA, PARP and caspase 3 in (A) EV, R158G (1), R158G (2) and (B) R158G (3), R158G (7), R158G (8). Data shown are representative of three independent experiments for the indicated targets with β-actin as input control.

5.4.2.8 Distribution of acetylated and phosphorylated p53 in p53 overexpressing clones

Next, the distribution of the acetylated/phosphorylated p53 in the established clones after drug treatment was determined with immunofluorescence staining [Acetyl-p53 (Green), p-p53 (Red) and co-localization (yellow)]. Weak signals were detected in WT clone, probably due to the low expression of p53 through negative regulation by MDM2. Among the p53 mutant clones, belinostat induced green signals; cisplatin induced green, red and yellow signals; while combined treatment induced all three colours as well with a larger yellow population (Figure 5.25 A). The expression and localization of the modified p53 was quantified and analysed.

High content analysis was subsequently performed through segmentation of nuclear fraction as described in Material and Methods to determine the expression of acetylated/phosphorylated p53 in WT and p53R158G clones. In Figure 5.25 B, acetylated p53 (Lys382) was shown to be increased upon belinostat (~6-fold for WT; ~4-fold for mutant clones), cisplatin (unchanged for WT; ~4-fold for mutant clones) and combined treatment (~10-fold for all clones). Belinostat, however, had no effect on the phosphorylation of p53. Cisplatin alone and combination treatment induced similar fold increase of p-p53 (50 - 100-fold) for all clones (Figure 5.25 C). Lastly, WT clone expressed low basal signal for both acetyl- and p-p53 in relative to mutant clones.

Image cytometry was next conducted to investigate the distribution and localization of acetyl- and p-p53 under drug exposure in each of the mutant clone. The parameters for each individual nucleus (integrated densities of acetyl- and p-p53) were first determined by high content analyses on the images taken (Figure 5.25 A). Figure 5.26 A and B showed representative scatter plots for R158G (3) and (8) clones. The nuclear intensities of both targets in DMSO treated cells were set as baseline signals for gating purposes. With these gating, nuclei expressing signals higher than that of the vehicle control were identified. Comprehensive breakdown analysis on distribution of nucleus signal in each nucleus was displayed in Figure 5.26 C. These data showed that belinostat treatment right-shifted the cell population, with > 10% increase in acetyl-p53 positive cells; cisplatin shifted the cell population diagonally to the top-right, with substantial increases of p-p53 positive cells (> 30%) and dual-stained positive cells (> 20%). Combination treatment reduced the proportion of p-p53 positive cells (~20%) but increased the proportion of cell population with both acetylated and phosphorylated p53 (> 50%).

Defined roles of p53 modifications, such as ubiquitination, phosphorylation and acetylation, have been well-characterized. The profound roles of these modifications structured the

molecular basis for p53 regulation (Brooks and Gu 2003). Through the analysis on the immunofluorescence images, nuclear accumulations of both acetylated and phosphorylated p53 under drug pressure were confirmed: belinostat induced acetylation but not phosphorylation of p53; while cisplatin induced both acetylation and phosphorylation. In line with the earlier analysis on H2170 cells (Figure 5.11 C), combining belinostat and cisplatin further increased the cell population with acetylated p53. It is important to note that a large population of cell nuclei contained co-localization of both acetyl- and p-p53. These observations suggested that belinostat acetylated a proportion of p53 that was initially phosphorylated (but not acetylated) under cisplatin exposure. Collectively, combination of cisplatin and belinostat concomitantly induced acetylation and phosphorylation of p53 in the cell nucleus. Together with the up-regulation of p53 target genes, these observations strongly suggest the functional activation of acetylated and phosphorylated mutant p53.

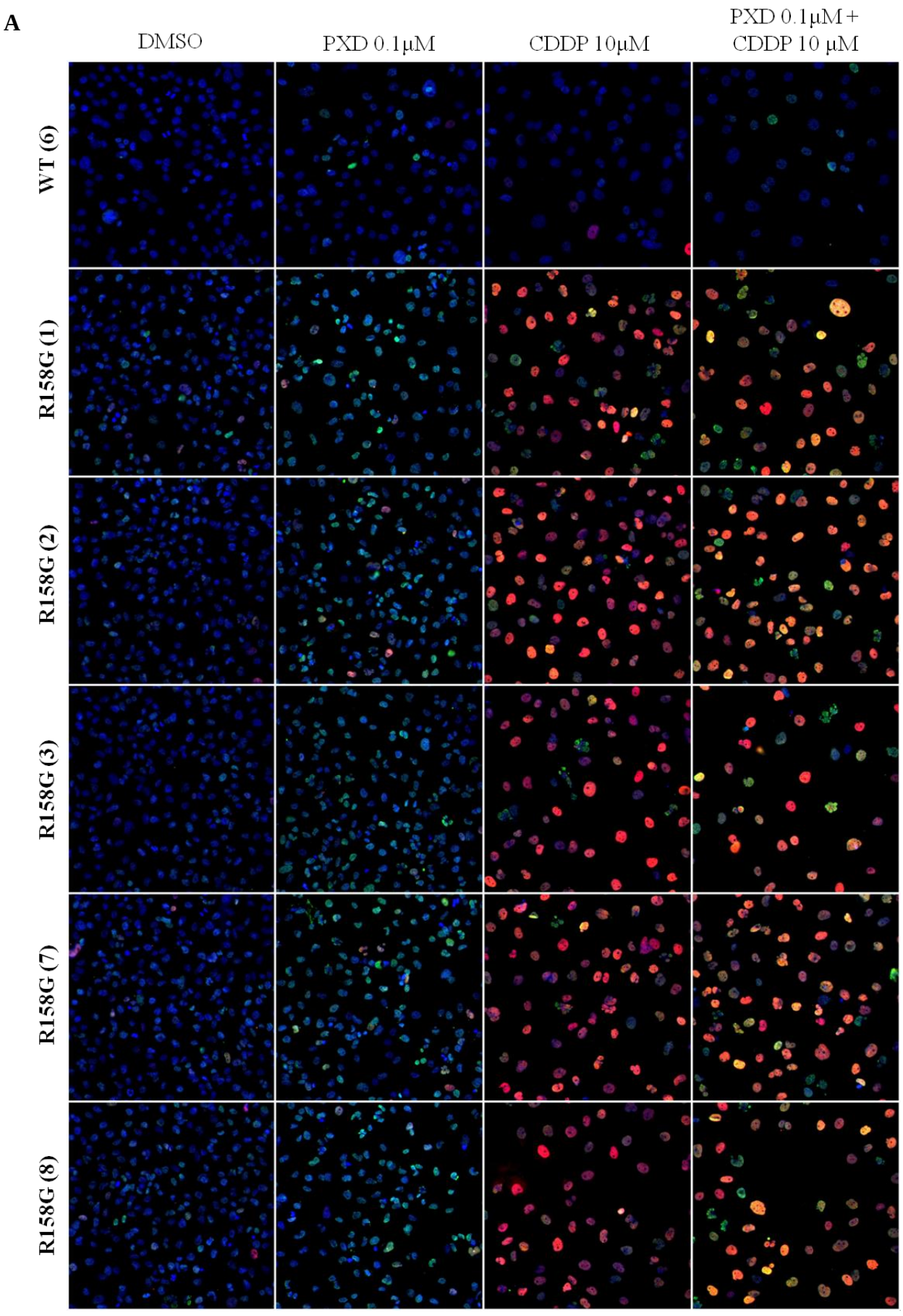
A
DMSO
PXD 0.1μM
CDDP 10μM
PXD 0.1μM+
CDDP 10 μM
WT (6)
R158G (1)
R158G (2)
R158G (3)
R158G (7)
R158G (8)

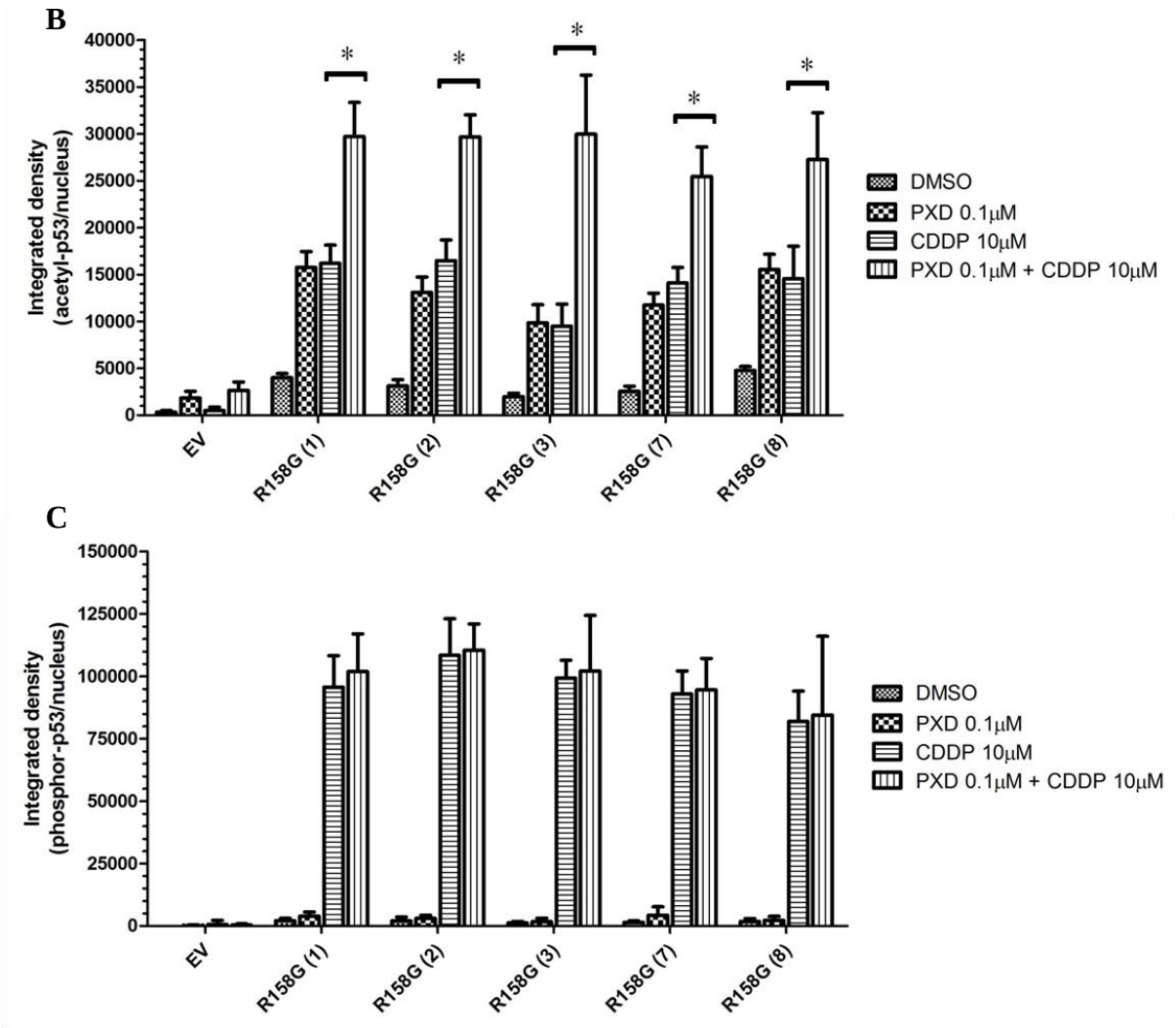

Figure 5.25: Belinostat and cisplatin induce nuclear accumulation of acetyl- and p-p53 in p53 overexpressing cells.

A, Calu-1 WT clone and p53R158G clones were treated with belinostat (PXD101) (0.1μM), cisplatin (10μM) and combination treatment with DMSO (0.001%) as vehicle control for 48 hours. Immunofluorescence staining was performed to determine the co-localization of acetyl-p53 (Lys382) (Alexa Fluor-488) and p-p53 (Ser15) (Alexa Fluor-568) in WT (6), R158G (1), R158G (2), R158G (3), R158G (7) and R158G (8) clones. Eight independent fields were taken for each condition with a minimum of 50 nuclei per field. Representative confocal images are shown at 400x magnification. Merged images are displayed with **blue indicates DAPI**, **green indicates acetyl-p53**, while **red indicates p-p53.** High content analyses were performed for (B) acetyl- and (C) p-p53 signal intensity in cell nucleus. Data are normalized against the number of nuclei and presented as mean ± SD for 8 independent fields within one representative experiment (n=2). Statistical analyses were performed by unpaired t-test. *Significant difference from cisplatin treated group, $P < 0.05$.

A

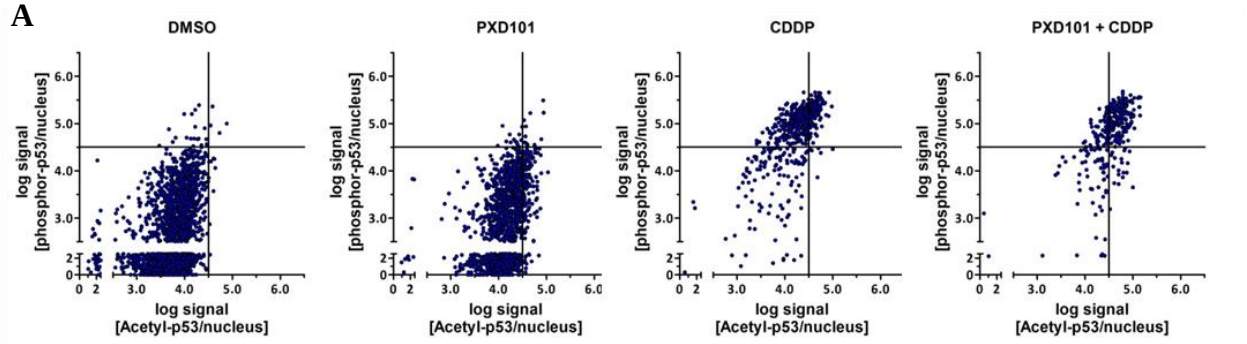

B

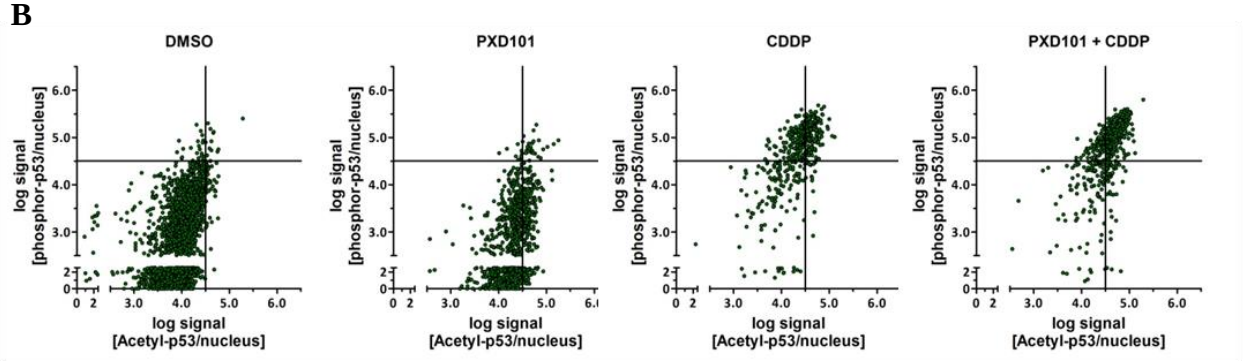

C

		% cell				
		R158G (1)	R158G (2)	R158G (3)	R158G (7)	R158G (8)
DMSO	Q1	95.17	95.99	98.45	96.72	96.30
	Q2	2.17	1.42	0.44	1.36	1.98
	Q3	1.84	2.27	0.92	1.31	1.09
	Q4	0.81	0.33	0.19	0.61	0.64
PXD 0.1μM	Q1	71.51	79.28	88.78	83.42	74.22
	Q2	23.80	17.13	9.56	10.86	22.03
	Q3	0.67	1.17	0.86	2.40	1.18
	Q4	4.02	2.42	0.80	3.32	2.57
CDDP 10μM	Q1	22.79	22.52	22.92	22.94	27.45
	Q2	2.55	0.58	1.14	0.80	3.19
	Q3	34.69	38.51	54.36	42.84	35.53
	Q4	39.97	38.39	21.59	33.42	33.83
PXD 0.1μM CDDP 10μM	Q1	21.36	18.38	19.29	21.49	22.62
	Q2	5.99	4.37	6.11	3.44	11.31
	Q3	13.77	17.48	17.36	21.49	15.74
	Q4	58.88	59.77	57.23	53.58	50.33

Figure 5.26: Distribution of acetyl- and p-p53 in p53 overexpressing clones after belinostat and cisplatin treatment.

Calu-1 p53R158G clones were treated with belinostat (PXD101) (0.1μM), cisplatin (10μM) and combination treatment with DMSO as vehicle control for 48 hours. Immunofluorescence staining was performed to determine the co-localization of acetyl-p53 (Lys382) (Alexa Fluor-488) and p-p53 (Ser15) (Alexa Fluor-568). Integrated density for each nucleus was determined by ImageJ as described in Material and Methods. Scatter plots of individual nuclei for (A) R158G (3) and (B) R158G (8) are shown (X: log signal for acetyl-p53; Y: log signal for p-p53). Each scatter plot consists of > 400 nuclei. Gating was determined from vehicle control. C, Tabulation of percentage of cell distribution for all p53R158G clones within one representative experiment (*n*=2) was displayed. Q1: p-p53 negative, acetyl-p53 negative; Q2: p-p53 negative, acetyl-p53 positive; Q3: p-p53 positive, acetyl-p53 negative; and Q4: p-p53 positive, acetyl-p53 positive.

Summary of findings in Chapter 5.4:

- siRNA silencing of p53 abrogated the apoptosis induced by combination of cisplatin and belinostat.
- Similarly, synergistic cytotoxicity of combination treatment was rescued in stable p53 knockdown clones generated by lentiviral infection.
- In p53wt cells (MRC5), cisplatin and combination treatments induced transcriptional activation of p53 downstream genes (*CDKN1A*, *MDM2*, *PUMA*, and *Noxa*) with reduced mRNA expressions of *TP53* and *TP73*.
- In p53R158G mutant cells (H2170), belinostat (0.1μM) potentiated the cisplatin-induced transcriptional activation of p53 downstream genes (*CDKN1A*, *PUMA*, and *Noxa*) but did not affect the expressions of *MDM2* and *TP53*.
- Wild-type and mutant p53 (R158G) were cloned into p53 null Calu-1 cells.
- Overexpression of wild-type p53 sensitized Calu-1 cells to both cisplatin and belinostat treatments.
- Overexpression of wild-type p53 sensitized Calu-1 cells to cisplatin treatment but increased tolerance to belinostat.
- p53R158G clones were more responsive to combination treatment of belinostat (0.1μM) and cisplatin.
- Overexpression of wild-type p53 increased basal mRNA expression of *MDM2*, *CDKN1A*, *PUMA* and *Noxa* in Calu-1 cells. Cisplatin and combination treatments up-regulated *MDM2*, *CDKN1A*, *PUMA*, *Noxa*, and *BAX* in WT clone.
- Interestingly, overexpression of p53R158G increased basal mRNA expression of *CDKN1A* but not *MDM2* and *PUMA* in Calu-1 cells. Instead, baseline expression of Noxa was reduced in p53R158G clones. Cisplatin and combination treatments up-regulated *CDKN1A*, *PUMA*, and *BAX* but not *MDM2* and *Noxa* in p53R158G clones.
- In WT clone, cisplatin treatment alone induced p53 acetylation and induced apoptosis. Combination with belinostat had little effect on the cisplatin-treated cells.
- In p53R158G clones, cisplatin-induced p53 acetylation and apoptosis could be potentiated by combining with belinostat (0.1μM).
- In p53R158G clones, belinostat induced p53 acetylation; cisplatin induced both acetylation and phosphorylation; combination treatment potentiated p53 acetylation but not phosphorylation.
- Combination treatment of belinostat and cisplatin increased cell population expressing both acetylated and phosphorylated p53.

5.5 Inducing p53 acetylation as potential therapeutic approach

5.5.1 Regulation of p53 acetylation by HDACs and HAT

As Calu-1 clones expressing nuclear-bound mutant p53 are more sensitive to combination treatment of cisplatin and belinostat, this observation correlated with the transactivation of p53 downstream genes as well as the post-translational modification of p53, suggesting that p53 acetylation is responsible for the observed synergy in the lung SCC cells. Next, the mechanisms leading to p53 acetylation were investigated.

The role of HATs and HDACs in determining the balance of acetylated p53 has been discussed in Chapter1.3.2.2. Acetylation of p53 could be induced by HATs: CBP/p300 and PCAF acetylates N-terminus of p53; while Tip60 acetylates Lys120 (Lill, Grossman et al. 1997, Liu, Scolnick et al. 1999, Grossman 2001, Tang, Luo et al. 2006). On the contrary, deacetylation of p53 is controlled by HDACs. Although several class I HDACs have been linked with transactivation of p53 function, only HDAC1 (Luo, Su et al. 2000, Ito, Kawaguchi et al. 2002) and HDAC3 (Zeng, Xiao et al. 2006, Karagianni and Wong 2007) have been reported to directly deacetylate p53. A class III HDAC, Sirtuin 1 (SirT1), is found to suppress p53 activity through p53 deacetylation (Vaziri, Dessain et al. 2001, Haigis and Guarente 2006). Furthermore, negative regulation of p53 through SirT1 promotes cell survival in response to DNA damage and oxidative stress (Luo, Nikolaev et al. 2001).

The role of HATs (CBP/p300) and HDACs (HDAC1, HDAC3, SirT1) in drug-treated H2170 cells was next investigated. The Western blotting analysis showed that cisplatin reduced phosphorylation of HDAC3, but exerted minimal effect on acetyl-CBP/p300, HDAC1, p-SirT1, and SirT1 as a single agent. Belinostat alone marginally reduced p-SirT1 and has no effects on p300 and other HDACs. Combining belinostat and cisplatin reduced p-SirT1, SirT1 and p-HDAC3 (Figure 5.27). While neither cisplatin nor belinostat treatment affected expression of the acetylated CBP/p300, combination treatment dramatically increased acetyl-CBP/p300 (Figure 5.27). These data showed that both cisplatin and combination treatment did not affect the expression of HDAC1 (Figure 5.27).

Cisplatin-induced p53 acetylation is widely believed to be mediated by HATs (Di Stefano, Soddu et al. 2005). However, the observations suggest that HDAC3, but not CBP/p300, is an indirect downstream target of cisplatin in H2170 cells as shown by the de-phosphorylation of HDAC3 at Ser424. Decreased phosphorylation of HDAC3 have been shown to reduce enzymatic activity of HDAC3 (Zhang, Ozawa et al. 2005). Furthermore, acetylation of p53 induced by combined treatment of belinostat and cisplatin correlated with the up-regulation of acetyl-CBP/p300 and reduction of p-HDAC3 and p-SirT1. These observations proposed several potential mechanisms of p53 acetylation in H2170 cells.

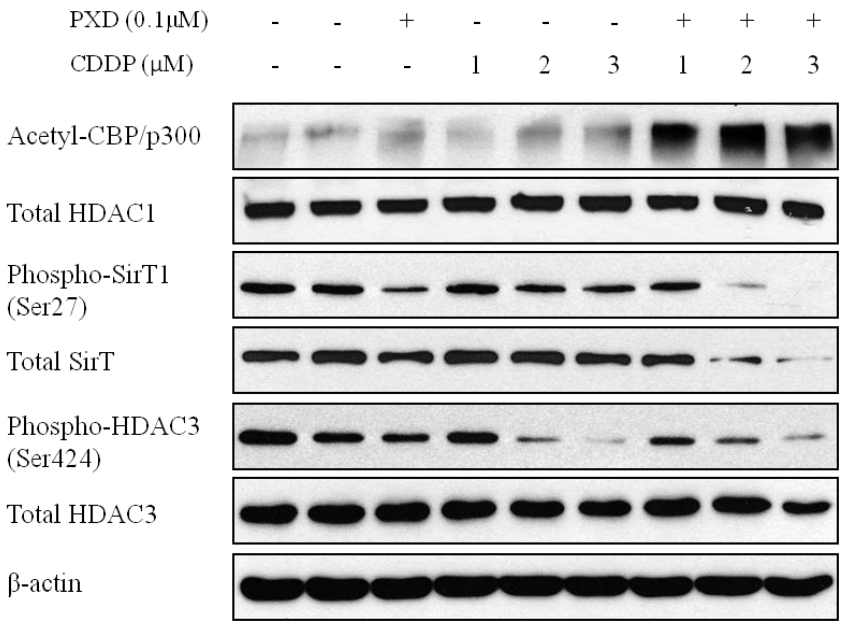

Figure 5.27: Cisplatin and belinostat up-regulate p300 and suppress SirT1 and HDAC 3.

H2170 cells were treated with belinostat (PXD101) (0.1μM), cisplatin (1, 2 and 3μM) and combination treatment with DMSO (0.001%) as vehicle control for 48 hours. Western blot analysis was performed to investigate the expression of acetyl-CBP/p300, HDAC1, p-SirT1 (Ser27), SirT1, p-HDAC3 (Ser424) and HDAC3. Data shown are representative of three independent experiments for the indicated targets with β-actin as input control.

5.5.2 Tenovin-6 triggers apoptosis in p53 mutant cells

Clinically, p53 mutations are commonly detected in most cancers, and accounted for cellular resistance to chemotherapy. These observations strongly suggested that p53 signalling could be partially restored in mutant p53 through molecular acetylation of key lysine residues. This finding may be clinically significant on lung SCC in which majority of the tumour cells harbour mutant p53 with defective DNA-binding ability (Chapter 3.1.2). In Chapter 5.5.1, it was proposed that p53 acetylation induced by belinostat and cisplatin could be regulated by CBP/p300, HDAC3 and SirT-1. A recent finding has described that Trichostatin A (TSA), a HDAC inhibitor, up-regulates expression of *PUMA* through specific inhibition of HDAC3 (Feng, Pan et al. 2013). Furthermore, specific SirT inhibitors have been developed and showed significant pro-apoptotic effects in cancer cells (Lara, Mai et al. 2009, Peck, Chen et al. 2010). Therefore, using a specific acetylator of p53 may improve treatment outcome of lung SCC patients through p53 activation with less off-target adverse effects. In this chapter, the cytotoxicity of tenovin-6, a specific SirT1 inhibitor, was investigated in p53-expressing Calu-1 clones.

Cell proliferation assay was conducted to determine the respective tenovin-6 IC_{50} of each clone. Among the 7 tested clones, EV clone was found to be most resistant (~7μM) to tenovin-6 while WT clone was the most sensitive (~2μM) (Figure 5.28 A). Calu-1 cells overexpressing p53R158G mutant displayed intermediate sensitivity to tenovin-6, with IC_{50} falling in between those of EV and WT clones (~4μM) (Figure 5.28 A). Furthermore, tenovin-6 up-regulated acetyl-p53 (Lys379, Lys382) in both p53R158G clone 3 and 8 without affecting the expression of total p53. However, modification of p53 in WT clone was not observed, probably due to the low expression of p53 in this clone. Interestingly, extensive cleavage of PARP and caspase 3 were observed in both mutant clones at a high tenovin-6 dose (10μM) but not EV clone and WT clone. However, p53 and p21 were substantially up-regulated in WT clone after tenovin-6 treatment (Figure 5.28), indicating the activation of p53 signalling in this clone.

The investigations on tenovin-6 improved the understanding on the activity of p53 signalling, as p53 null, wild-type and mutant cells displayed different responses upon drug exposure. In line with current knowledge, functional wild-type p53 induced cell cycle arrest before apoptosis, as supported by the up-regulation of p21 in WT clone. Conversely, activation of mutant p53 induced apoptosis but not cell cycle arrest. Taken together, these findings here strengthened the hypothesis that p53 acetylation leads to a non-conventional gain-of-function event in mutant p53.

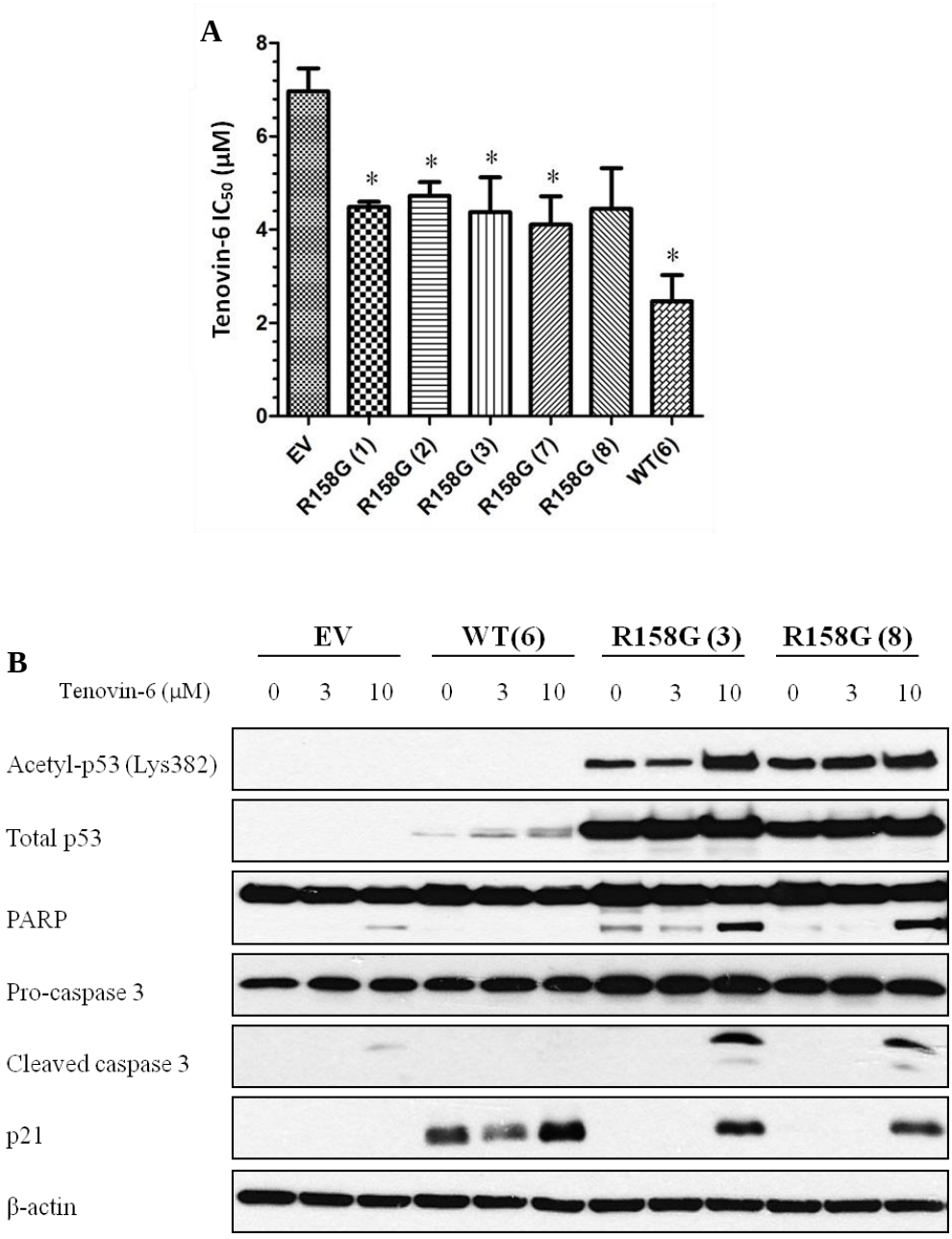

Figure 5.28: Tenovin-6 induces p53 acetylation and triggers apoptosis in p53 overexpressing clones.

EV clone, p53wt clone, and p53R158G clones were treated with increasing doses of tenovin-6. A, Individual clones were drug treated for 72 hours and cell viability assay (MTS) was used to determine the IC_{50} of tenovin-6. Data are presented as mean ± SD (n = 3). B, p53R158G clones were treated with tenovin-6 (3 and 10μM) with DMSO (0.001%) as vehicle control for 48 hours. Western blotting analysis was performed to investigate the expression of p53, acetyl-p53 (Lys279, Lys382), p21, PARP and caspase 3 in EV, WT, R158G (3) and R158G (8) clones. Data shown are representative of three independent experiments for the indicated targets with β-actin as input control. Statistical analyses were performed by unpaired t-test. *Significant difference from EV clone, $P < 0.05$.

5.5.3 The correlation of p53 acetylation and apoptosis in drug-treated lung SCC cells

Among the 8 cell lines tested in Chapter 5.1, H226 was verified as wild-type p53, Calu-1 as p53 null and the remaining 6 as p53 mutant (Figure 3.4). The mutations found in these lines are predominantly point mutation that occurs along the DNA-binding domain, with 2 nonsense mutations (H520 and SK-MES-1) and 4 missense mutations (H2170, H596, H1869 and ChaGo-k-1). Western blotting was performed to verify the p53 expression (Figure 3.2), whereby no p53 protein was detected in H520 and SK-MES-1, while high protein expression was detected in H2170, H596, H1869 and ChaGo-k-1. As it has been hypothesized that induction of p53 acetylation could synergistically enhance cisplatin cytotoxicity, coincidently, cell lines not expressing full length p53 (Calu-1, H520, SK-MES-1) were less responsive to cisplatin and with poorer synergy with belinostat (Chapter 3.3.1). Accordingly, post-translational modifications of p53 among H226, H596, H1869 and ChaGo-k-1 cell lines were investigated.

In H226 (wild-type p53) cells, cisplatin treatment up-regulated p53 and acetyl-p53, while combination treatment further increased p53 acetylation (Figure 5.29 A). Among the remaining cell lines (H596, H1869, ChaGo-k-1), p53 was highly expressed at basal level due to the missense mutations that lead to its loss-of-function. Consistent with the earlier observations on H2170 cells, cisplatin but not belinostat acetylated p53 in these cell lines (Figure 5.29 B, C, D). However, combination treatment with belinostat only increased p53 acetylation in H1869 cells (Figure 5.29 C).

These observations suggested that the induction of p53 acetylation as a result of DNA-damage is universal across cell lines expressing both wild-type and mutant p53. However, the combinatorial effect of belinostat in increasing cisplatin-induced p53 acetylation was only observed in H226, H1869 and the previously characterized H2170 cells. More importantly, when these findings were compared against the cytotoxicity profile (Figure 5.1), cell lines not expressing p53 protein were relatively less responsive to cisplatin and belinostat, while synergistic induction of apoptosis by combination treatment was only detected in H226, H1869 and H2170. These findings supported the hypothesis that acetylation of p53, even in those with mutation within DNA-binding domain, could trigger cell death in lung SCC cell lines.

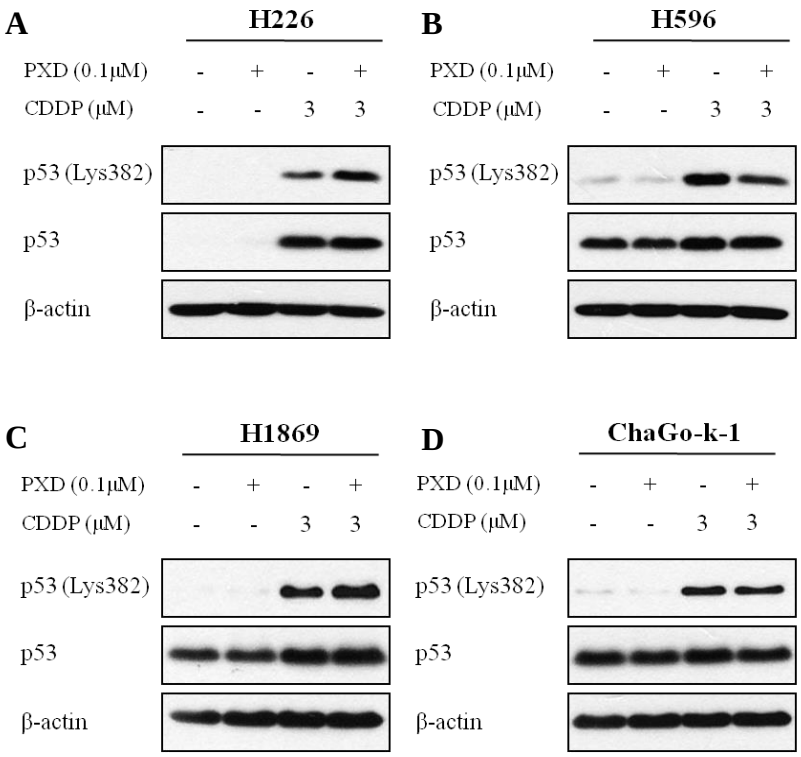

Figure 5.29: Effect of belinostat and cisplatin on p53 acetylation in lung SCC cell lines.

H226 (A), H596 (B), H1869 (D) and ChaGo-k-1 (D) cells were exposed with PXD101 (PXD101) (0.1μM), cisplatin (3μM), or combination treatment with DMSO (0.001%) as vehicle control for 48 hours.. Western blot analysis was performed to investigate the expression of acetyl-p53 (Lys382) and p53. Data shown are representative of two independent experiments for the indicated targets with β-actin as input control.

Summary of findings in Chapter 5.5:

- Up-regulation of acetyl-CBP/p300 as well as down-regulation of p-HDAC3 and p-SirT1 were correlated to the increased in acetylated p53 in H2170 cells.
- Tenovin-6 acetylated p53 molecules in p53R158G clones.
- Calu-1 cells overexpressing wild-type and mutant p53 were more sensitive to tenovin-6 with significantly lower IC_{50}.
- Cisplatin consistently induced p53 acetylation in H226, H596, H1869 and ChaGo-k-1 cells.
- Similar to H2170, belinostat (0.1μM) did not induce acetylation of p53.
- Combination of belinostat (0.1μM) and cisplatin potentiated cisplatin-induced p53 acetylation in H226 and H1869 cells.
- Coincidently, synergistic cytotoxicity of belinostat and cisplatin was observed in H226 and H1869, but not H596 and ChaGo-k-1 cells.

5.6 Discussion

5.6.1 The role of p53 functions in lung SCC cells

Since its discovery in 1979, intensive research has been conducted to characterize the impact and functionality of the p53 protein (Lane and Crawford 1979, Linzer and Levine 1979). Its role as a tumour suppressor gene has since been well-established (Baker, Fearon et al. 1989). As the "guardian of genome", p53 regulates cell proliferation, cell cycle, cell death, DNA damage repair, and aging (Lane 1992). The broad spectrum of tumour-suppressive functions makes it seems unlikely for tumour initiation unless the p53 network is inactivated (Vousden and Lu 2002). The regulation of cellular responses by p53 is dependent on the cell context as well as the nature of the stimuli, which include DNA damage, oncogene activation and hypoxia (Vousden and Lu 2002, Laptenko and Prives 2006).

Under unstressed condition, p53 is expressed as an inert protein and is maintained at low level. The MDM2 oncoprotein is a direct downstream target but also a main negative regulator of p53 (Barak, Juven et al. 1993, Wu, Bayle et al. 1993). Binding of MDM2 to the DNA transactivation domain of p53 first block transcriptional activities (Momand, Zambetti et al. 1992), and subsequently induce p53 nuclear export and degradation through ubiquitination (Wu, Bayle et al. 1993, Haupt, Maya et al. 1997). These justify the low p53 levels detected in H226 and WT 6 clone.

Activation of p53 signalling requires the stabilization of p53 as well as the conversion from inert to active form, which could be achieved through post-translational modifications (Bode and Dong 2004). Upon DNA damage, p53 is phosphorylated by ATM, ATR, Chk1, Chk2 and DNA-PK (Lees-Miller, Sakaguchi et al. 1992, Shieh, Ikeda et al. 1997, Banin, Moyal et al. 1998, Shieh, Taya et al. 1999, Tibbetts, Brumbaugh et al. 1999, Hirao, Kong et al. 2000), and acetylated by HATs (Ito, Lai et al. 2001) (Figure 5.32). Phosphorylation of p53 at amino N-terminus alleviates the inhibition by MDM2 (Kussie, Gorina et al. 1996, Shieh, Ikeda et al. 1997), while acetylation appears to promote the stability of p53 and enhance DNA-binding ability (Ito, Lai et al. 2001). Upon its activation, wild-type p53 usually functions as a nuclear-bound, sequence-specific transcription factor that induces or suppresses the downstream signalling mechanisms such as cell cycle regulation (*CDKN1A*) (el-Deiry, Tokino et al. 1993); apoptosis (*BAX*, *BID*, *FAS*, *PUMA*, *Noxa*) (Miyashita and Reed 1995, Owen-Schaub, Zhang et al. 1995, Oda, Ohki et al. 2000, Nakano and Vousden 2001, Sax, Fei et al. 2002); and auto-regulation of p53 (*MDM2*, *TP73*) (Barak, Juven et al. 1993, Chen, Zheng et al. 2001, Grob, Novak et al. 2001). In line with this knowledge, a similar profile of these direct downstream genes was observed in p53 wild-type clone.

Consistently, *CDKN1A*, *MDM2*, *PUMA*, *BAX*, and *PUMA* were up-regulated upon genetic insertion of wild-type p53, while *TP73* was reduced probably due to the dominant negative feedback loop (Grob, Novak et al. 2001) (Figure 5.21).

Among the panel of lung SCC cell lines, H226 is the only one with wild-type p53. Consistent with current knowledge, this cell line has low level of p53 expression (Figure 3.2) and was shown to be highly sensitive to cisplatin (Figure 3.3 A). Furthermore, H226 was unable to grow under anchorage-independent condition (Data not shown but discussed in Chapter 3.3.2), probably due to the tumour-suppressive effects that prevent malignant transformation in this cell line. Cisplatin treatment up-regulated p53 (Figure 5.29 A) induced apoptosis (Figure 5.1 E) in H226 cells. These observations demonstrated the functions of wild-type p53 in lung SCC cell lines

5.6.2 Mutational spectrum of *TP53* and alterations of p53 functions in lung SCC

Initiation of tumourigenesis usually involved the inactivation of p53 pathway through somatic mutations of p53 or other alternative mechanisms. For instance, amplification or aberrant activation of MDM2 is commonly observed in tumour cells (Leach, Tokino et al. 1993, Manfredi 2010); while p14ARF (encoded by *CDKN2A*), a tumour suppressor that inhibit MDM2 (Bates, Phillips et al. 1998), is frequently inactivated through gene deletion or mutation as well as chromosomal hypermethylation (Liggett and Sidransky 1998, Esteller, Tortola et al. 2000, Esteller, Cordon-Cardo et al. 2001). Despite so, functional inactivation of p53 by somatic mutation is frequently observed in half of all tumours (Olivier, Hollstein et al. 2010). Figure 5.30 shows the spread of p53 mutations across multiple tumour types (Cerami, Gao et al. 2012, Gao, Aksoy et al. 2013). Among these cancer types, mutated p53 is commonly detected in ovarian (~90%), lung SCC (~80%), head and neck and pancreatic carcinoma cases (Cerami, Gao et al. 2012, Gao, Aksoy et al. 2013).

The genetic alterations of p53 pathway in lung SCC were verified by the deep sequencing data as 71.11% of the lung SCC specimens were identified with *TP53* mutations (Chapter 3.1.2). Despite the high mutation frequency, *CDKN2A* gene was found mutated mostly in the intronic region (Table 3.1). These recapitulate *TP53* mutation as the most common phenomenon that alters p53 functions n lung SCC cells. Importantly, missense mutations of p53 frequently occur within the DNA-binding domain (DBD). There are six common "hotspot" amino acids that are commonly detected in all human cancers: residue 282 (2.9%), 249 (2.9%), 245 (3.3%), 175 (5.1%), 273 (6.7%) and 248 (7%) (Freed-Pastor and Prives 2012). However, based on the *TP53* mutation database published by TCGA, these well-documented "hotspots" are uncommon among the lung SCC cases (Figure 5.31) (Cerami,

Gao et al. 2012, Network 2012, Gao, Aksoy et al. 2013). While majority of the *TP53* mutation in lung SCC are found to occur mostly along the region encoding for the DNA-binding domain (DBD), arginine residue at position 158 is found to be the most frequent mutated amino acid among the 178 cases (8/178; 4.5%) (Figure 5.31). In the attempt to verify the mutational status of *TP53* in lung SCC, 6 out of the 45 tumours (13.33%) of the specimens are mutated on residue 248 (Table 3.2). Somatic mutations of *TP53* on the other "hotspots" are rare, with 2 mutations observed on each of residue 249 and 175, as well as 1 on residue 175. Interestingly, 3 tumours are detected with mutation on residue 158 (R158L/P/R) (6.67%) (Table 3.2). Among the SCC cell lines that have substitution mutation on *TP53* gene, only one (H596) has altered amino acid residue on a common "hotspot" (Table 3.4). Coincidently, H2170 cell line has its arginine residue mutated to glycine at position 158 (R158G) (Table 3.4).

Contrary to that observed in H226 cells, p53 protein is found to be accumulated in mutant p53 cells (H2170, H1869, H5796, ChaGo-k-1 and R158G clones), probably due to the lack of negative feedback mechanisms. In H2170 cell, full length p53 was synthesized but was non-responsive to Nutlin-3a. This simple experiment confirmed the loss-of-function mutation in R158G mutant, as inhibition of MDM2 by Nutlin-3a failed to transactivate p53 (*p21* and *MDM2*) (Figure 5.10). In addition, *MDM2* gene was not activated in p53R158G clones after cisplatin treatment (Figure 5.22 A), thus verifying the loss of p53 functions in mutant cells. As missense mutations are common in lung SCC, these data suggest that p53 pathway is likely compromised in p53 mutant cells.

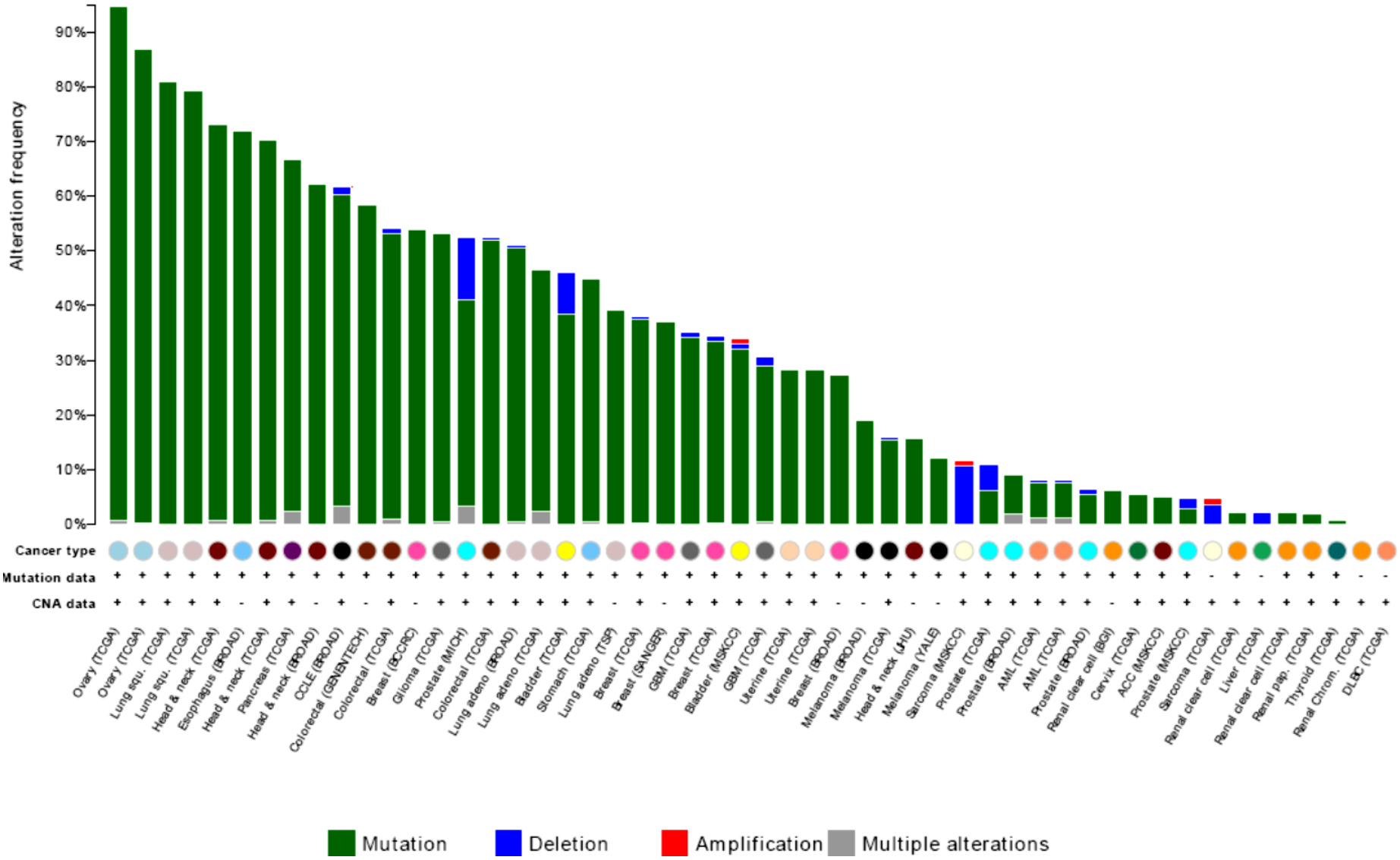

Figure 5.30: Summary of cross-cancer gene alteration in *TP53* from 52 studies (Cited from cBioPortal)

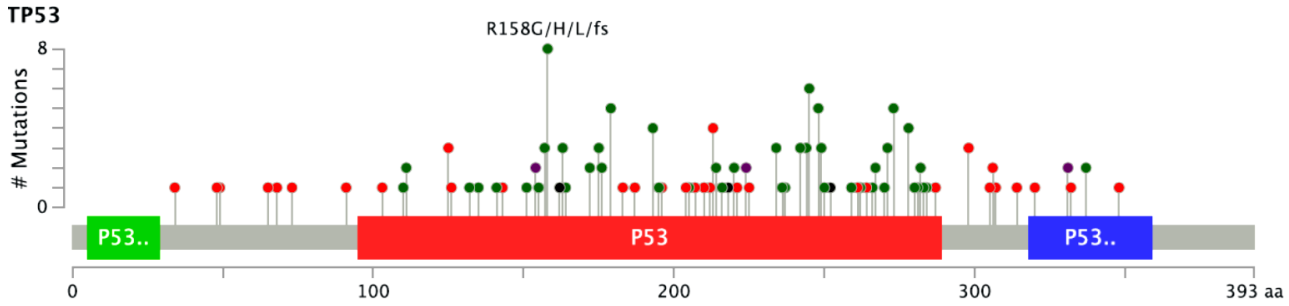

Figure 5.31: Distribution of *TP53* mutations in lung SCC (Cited from cBioPortal).

Somatic mutations of *TP53* genes in 178 patients were reported by TCGA (TCGA 2012). **Green region** is the transcriptional domain; **red region** is the DNA-binding domain; and **blue region** is the tetramerization domain. Corresponding frequency of any mutation at a given residue is shown.

5.6.3 Induction of apoptosis by cisplatin and belinostat in lung SCC cells: A p53-dependent event?

The cellular outcome of p53 has been shown to be crucial for the tumour suppressive functions of wild-type p53 through genetically modified mouse models. Experimentations on mice expressing a p53 mutant (R172P), which has been previously described to retain regulatory effect on cell cycle arrest but not apoptosis (Rowan, Ludwig et al. 1996), demonstrate an overall delay in spontaneous tumour development by maintaining chromosomal stability (Liu, Parant et al. 2004). On the contrary, a mouse model consisting of p53 protein that lacks its proline-rich domain but retains apoptotic function is sufficient to provide cellular protection against spontaneous tumourigenesis (Toledo, Krummel et al. 2006). These findings suggest that all wild-type p53 activities are essential for the tumour suppressive ability, but regulation of programmed cell death may contribute to a bigger role in preventing oncogenesis. It is now certain that p53 is involved in the transcriptional-regulation of both extrinsic and intrinsic apoptosis (Haupt, Berger et al. 2003). However, cytoplasmic-bound p53 has also been reported to induce apoptosis through direct interaction with BAX and caspases (Ding, Lin et al. 2000, Chipuk, Kuwana et al. 2004) (Figure 5.32). Both p53-regulated transcriptional-dependent and –independent apoptotic pathways are described in Chapter 1.3.2.3. Nonetheless, cell death could still be mediated by several other mechanisms that bypass p53, such as the dysregulation of mitochondria pathway through ROS (Kim, Yun et al. 2013), disruption of 14-3-3 (Nomura, Shimizu et al. 2003, Clapp, Portt et al. 2012), and binding of death ligands (Lanni, Lowe et al. 1997, Ossina, Cannas et al. 1997).

In this study, the mechanisms behind synergistic cytotoxicity of belinostat and cisplatin were studied. Among the tested cell lines, the cisplatin-resistant H2170 cells showed promising response towards combination treatment of cisplatin and belinostat (Chapter 5.1). Belinostat and cisplatin have synergistic effects on H2170 cells, which harbours a homozygous R158G mutation in p53 DNA binding domain (Chapter 3.2.1). This mutation renders the inability to activate normal p53 function in the presence of cisplatin treatment. For example, Nutlin-3a treatment did not induce p53 dependent activity. In addition, cisplatin and belinostat did not activate p53 function in the luciferase reporter assay, but the combination of both drugs showed clear induction of p53 activity (Chapter 5.3.1). Silencing of BAX, a pro-apoptotic p53 effector, abrogated the apoptotic activity of cisplatin with belinostat, suggesting that p53 is important for this apoptotic effect (Figure 5.7). Moreover, stable p53 knockdown H2170 clones showed loss of synergistic combinatory effects of cisplatin and belinostat (Figure 5.15). To further support this, several downstream effectors of p53 (*CDKN1A*, *PUMA* and *Noxa*) were up-regulated when cisplatin was administered singly and in combination with belinostat (Figure 5.18). At the same time, acetylation of p53 at residues Lys379 and Lys382 appear to correlate with this synergistic activity (Figure 5.11). The hypothesis is that combination of belinostat and cisplatin acetylates the R158G mutant and, to a certain extent, induces pro-apoptotic functions of this mutant p53.

The hypothesis on p53 reactivation prompted the investigation on the treatment response of lung SCC cell lines to combination of belinostat and cisplatin. Among the cell lines with chromosomal deletion (Calu-1) and nonsense mutation (H520, SK-MES-1), there were no obvious increase in PARP and caspase 3 cleavage upon drug combination (Figure 5.1 B, C, D). Unexpectedly, 2 out of 4 lung SCC cell lines with missense mutation along DBD (H2170, H1869) had higher expression of apoptotic markers that correlated with the increase in acetylated p53 after combination treatment of belinostat and cisplatin (Figure 5.1 A, G). These observations strengthened the hypothesis on the gain-of-function event in mutant p53. Despite so, convincing conclusion could not be drawn as the observed phenomenon could be confounded by the cell-cell variation and signalling complexity of these tumour cells.

The paradigm of p53 in treatment of lung SCC cells was assessed by extopic expression of wild-type p53 and p53R158G mutant into a p53 null cell line (Calu-1). Under treatment pressure, two key observations were made in these clones: firstly, apoptosis was induced together with the transcriptional activation of several p53 apoptotic target genes (*BAX*, *PUMA*, *Noxa*) in WT clone (Figure 5.22 and 5.23); secondly, apoptosis was also triggered in p53R158G clones with an unique transcriptional profile that was similar to the classical

p53 apoptotic pathway (up-regulation of *BAX* and *PUMA*) (Figure 5.22 and 5.24). These observations further implicated the restoration of p53 functions in mutant cells.

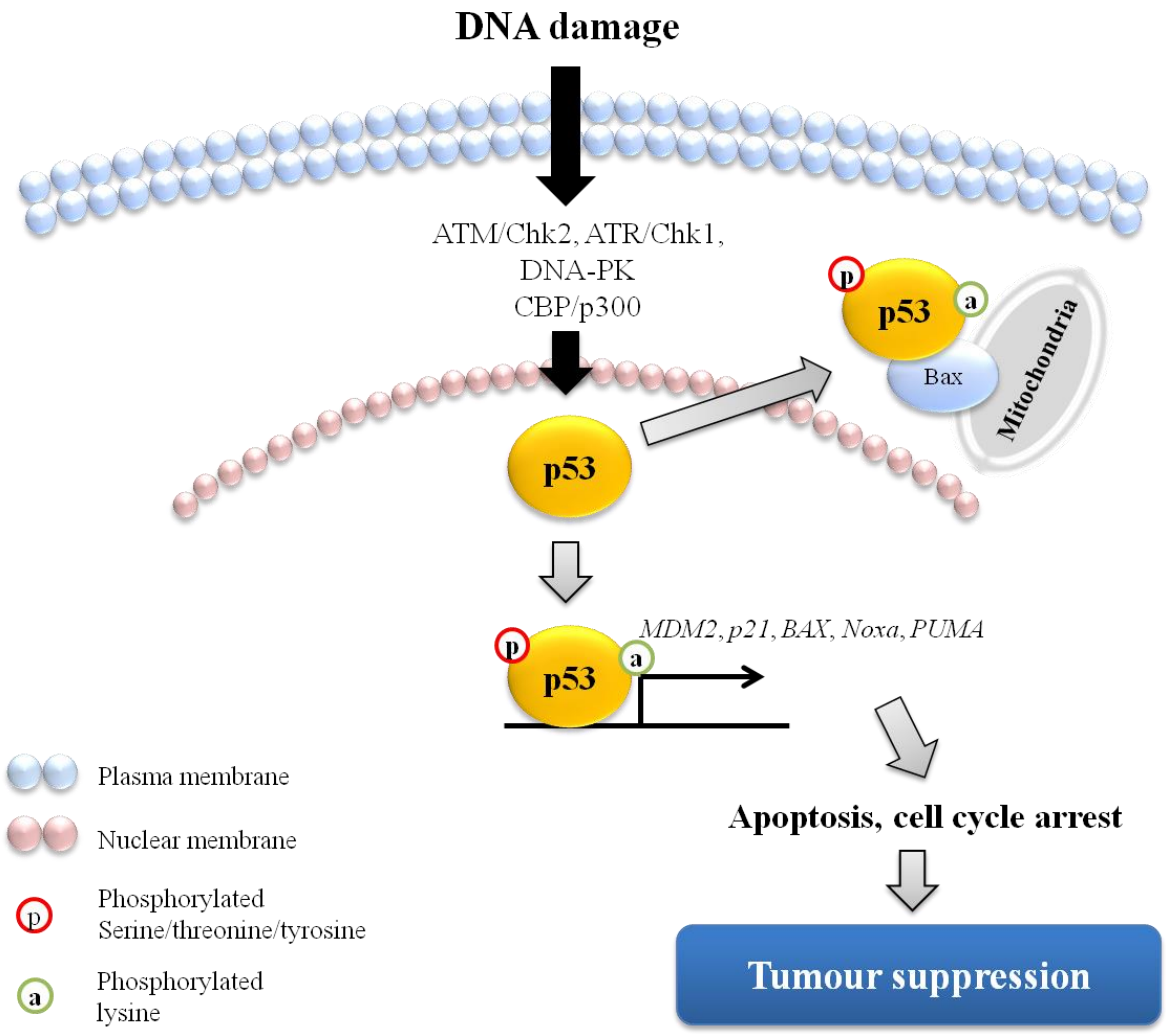

Figure 5.32: Cellular processing of functional wild-type p53.

DNA damage by chemotherapy induces post-translational modifications that stabilize p53 protein, and lead to transcriptional-dependent and -independent regulation of cell cycle arrest and apoptosis.

5.6.4 Non-conventional apoptotic response in mutant p53: Gain-of-function or loss-of-function event?

The first indication that mutated p53 carries specific functions was provided even before the molecule was characterized to be a tumour-suppressor. Initial studies on p53 proteins have demonstrated that overexpressing p53 could transform primary cells (Eliyahu, Raz et al. 1984) as well as promote cellular proliferation (Mercer, Avignolo et al. 1984, Reich and Levine 1984, Shohat, Greenberg et al. 1987, Deppert, Buschhausen-Denker et al. 1990). As the experimented p53 cDNAs was eventually recognized as mutated proteins (Levine and Oren 2009), the transformation of primary cells by p53 and oncogenic Ras probably involved mutated p53 (Hinds, Finlay et al. 1989). Thus, instead of detailing the wild-type p53 functions, these contradictory findings were indeed reporting the role of mutant p53 in tumourigenesis.

More recently, murine models harbouring p53 mutants that mimic common "hotspots" in human p53 revealed that the more metastatic tumours were developed in comparison to p53 knock-out mice (Liu, McDonnell et al. 2000, Lang, Iwakuma et al. 2004, Olive, Tuveson et al. 2004). Several *in vitro* and *in vivo* studies have associated mutant p53 with key factors of tumourigenesis, such as cell proliferation (Bossi, Lapi et al. 2006), chemoresistance (Blandino, Levine et al. 1999, Bristow, Peacock et al. 2003), somatic cell reprogramming (Sarig, Rivlin et al. 2010), metastasis and invasion (Adorno, Cordenonsi et al. 2009, Muller, Caswell et al. 2009, Morton, Timpson et al. 2010). Conclusively, despite losing the transcriptional ability of wild-type p53, it is now widely accepted that mutant p53 is indeed a proto-oncogene. A recent finding by Freed-Pastor *et. al.* demonstrated the direct associate of mutant p53 with mevalonate pathway, and inhibition of this pathway by statins is sufficient to reduce malignancy in breast cancer cells (Freed-Pastor, Mizuno et al. 2012). This finding emphasizes that understanding the oncogenic functions of mutant p53 may provide new insights into strategizing therapeutic approaches.

Despite so, gain of oncogenic mechanisms was not observed within the five mutant R158G clones as they display comparable *in vitro* growth rate and anchorage-independent growth ability to their parental Calu-1 cells (Data not shown). Moreover, these mutant lines have better drug sensitivity towards cisplatin, which contradict the reported chemoresistant property of mutant p53 (Blandino, Levine et al. 1999, Bristow, Peacock et al. 2003). Taken together, mutant p53 does not behave like an oncoprotein in Calu-1 cells as illustrated by others. Instead, a possible activation of p53-mediated apoptosis was observed in these clones. However, drug-induced apoptosis in R158G clones differed from that in WT clone. While *BAX* and *PUMA* were up-regulated, cisplatin and combination treatment did not induce *MDM2* (Figure 5.22), a key target gene of p53 (Wu, Bayle et al. 1993). Furthermore,

the magnitude of *CDKN1A* expression was not comparable to wild-type cells despite increasing in similar pattern. The transactivation of *Noxa*, which was induced in EV and WT clones, was somehow abrogated in all mutant clones (Figure 5.22). Taken together, these data indicate the presence of a p53-dependent, transcriptional-dependent apoptotic mechanism that is different from the classical p53 signalling (Haupt, Berger et al. 2003).

Several mechanisms have been proposed to explain the oncogenic functions of mutant p53. However, no unifying mechanism could be agreeable upon to explain the unique ability of mutant p53 to mediate such a wide range of target genes despite losing its DNA-binding ability. Moreover, a defined DNA response element for mutant p53 has yet to be identified. One common hypothesis is that mutant p53 could interact with other transcription factors, such as NF-Y, PML, Sp1, and VDR (Bargonetti, Chicas et al. 1997, Di Agostino, Strano et al. 2006, Haupt, di Agostino et al. 2009), and enhance the downstream target responses that lead to enhancement in cell proliferation, induction of chemoresistance and alteration of cell metabolism. As various promoters of mutant p53 shared minimal sequence homology, it has been hypothesized that binding of mutant p53 is likely dependent on unique structural changes of DNA motifs instead of sequence specific response elements (Kim and Deppert 2004, Kim and Deppert 2007). Interestingly, Di Agostino *et. al.* reported that both wild-type and mutant p53 have differential preference in recruitment of transcriptional cofactors: while wild-type p53 is commonly bound to HDAC1 (Juan, Shia et al. 2000), mutant p53 forms a complex with p300 (Di Agostino, Strano et al. 2006, Ali, Wang et al. 2013). These suggest that the interaction with different histone-modifying enzymes may signal for opposing transcriptional activity among wild-type and mutant p53. Finally, it has been demonstrated that several mutant p53 proteins are able to interact with p63 and p73 (Di Como, Gaiddon et al. 1999, Gaiddon, Lokshin et al. 2001), two members of the p53 family that exhibit high degree of homology to the DBD of p53 (Irwin and Kaelin 2001). Furthermore, p73 has been further reported to be essential for induction of apoptosis by several chemotherapy (Soussi 2003), it is thus hypothesize that mutant p53 may affect p63/p73-dependent transcriptional activity by inhibiting the interaction with their respective target gene promoter (Gaiddon, Lokshin et al. 2001).

As illustrated in Figure 5.33, these hypotheses on the possible oncogenic mechanisms of mutant p53 provide clues for the gain-of-function event in lung SCC cells with p53R158G mutant. Firstly, the data suggested that co-treatment of a sub-lethal dose of belinostat sufficient to induce histone acetylation synergistically increased cell death in cisplatin-treated cells (Chapter 5.2.3). Next, HDAC inhibitors have been well documented to modify the histone tails, thus resulting in remodelling of chromatin structure en route to mediate gene expression (Gregory, Wagner et al. 2001, Thiagalingam, Cheng et al. 2003).

Concurrently, several p53 downstream target genes were transactivated after drug treatments. Finally, combination treatment substantially acetylates CBP/p300 and p53. By taking all these observations into consideration, it was postulated that low dose of belinostat, despite not inducing cell death, may facilitate mutant p53 transactivation through chromatin restructuring, DNA binding, histone remodelling or post-translational modification.

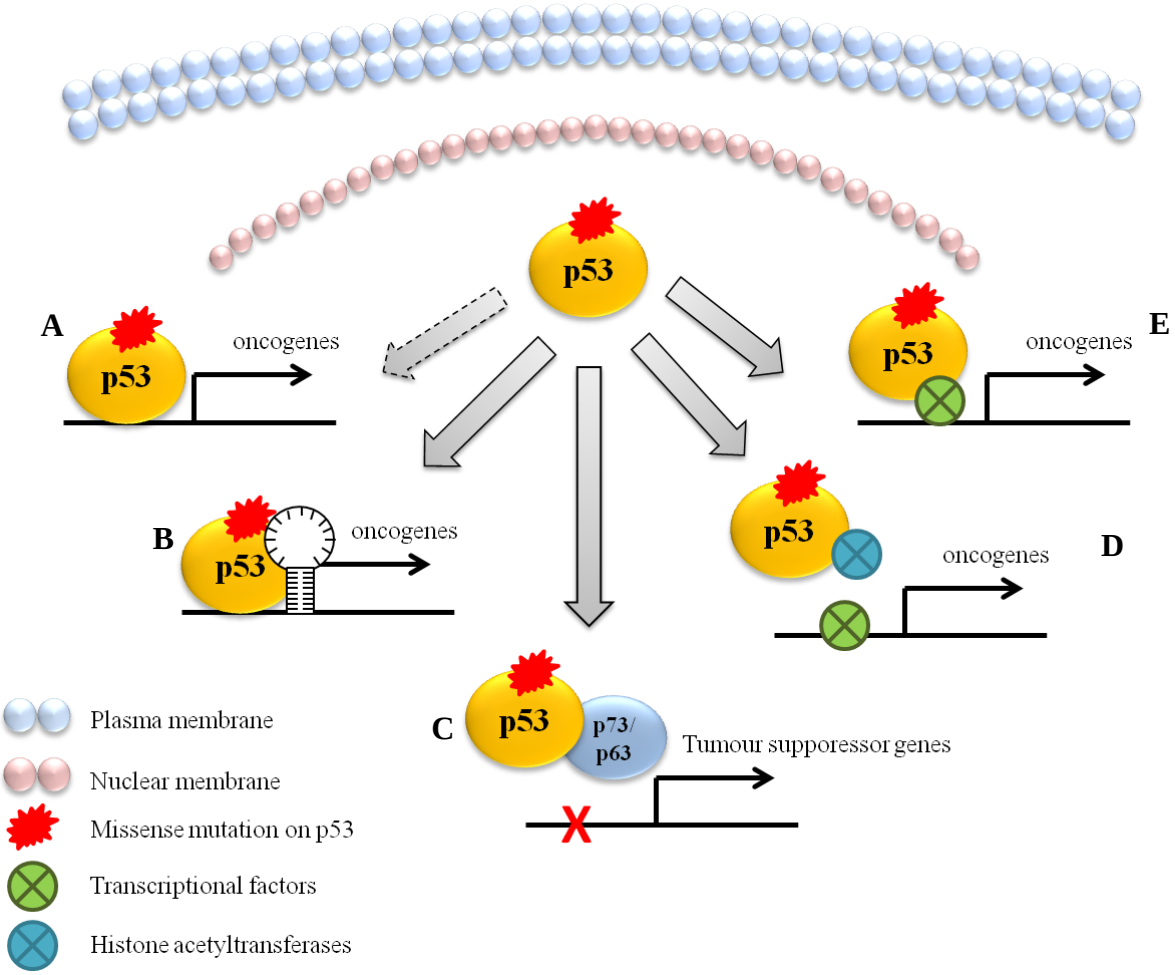

Figure 5.33: Proposed gain-of-function mechanisms of mutant p53.

There are multiple mechanisms that are postulated for the gain-of-function activities of mutant p53 that include both transcriptional-dependent or –independent mechanisms. These include: (A) direct binding to sequence-specific response elements; (B) direct binding to structural specific gene promoters, such as matrix-attachment regions (MARs); (C) inhibition of tumour-suppressive functions of p63 and p73 through protein-protein interaction; (D) direct recruitment of HATs thus leading to histone acetylation and transcriptional activation; and (E) direct interaction with other transcription factors, such as NF-Y, PML, Sp1, and VDR, to induce transactivation of downstream target genes. The dashed arrow indicates the lacking of supportive evidence to support this proposed

mechanism. These interactions resulted in the oncogenic functions of mutant p53, such as inhibition of apoptosis, cell proliferation, chemoresistance, somatic cell reprogramming, metastasis and invasion

5.6.5 Understanding the activation of mutant p53 through post-translational modification

Post-translational modification of p53, especially phosphorylation and acetylation, is a key process by which p53 pathway is activated (Sakaguchi, Herrera et al. 1998). These modulations directly influence p53's stability, nuclear localization and DNA-binding ability. Therefore, belinostat possibly induces p53 reprogramming or modification that subsequently triggers apoptosis in cisplatin-treated cells.

In line with current knowledge, p53 acetylation and phosphorylation occurred concurrently in dose-dependent manner after cisplatin treatment in H2170 cells (Sakaguchi, Herrera et al. 1998) (Chapter 5.3.2). It was further demonstrated that post-translational modifications of mutant p53 were responsible for the synergistic cytotoxicity: firstly, potentiation of apoptosis in the belinostat/cisplatin-treated cells correlated with p53 acetylation but not phosphorylation (Chapter 5.3.2), thus downplaying the significance of phosphorylation in the observed synergy; secondly, image cytometry revealed that combination treatment increased number of nuclei with acetylated p53 (Chapter 5.4.2.7); thirdly, treatment with tenovin-6 induced p53 acetylation and more robust apoptosis in p53R158G clones in comparison to EV and WT clones (Chapter 5.5.2). Taken together, these data suggest that inducing p53 acetylation may be sufficient to trigger cell death in mutant p53.

It was next ask the question of whether acetylation alone is sufficient to recover p53 function. In the p53 overexpressing clones, the extent of post-translational modification in individual nuclei was examined upon cisplatin and belinostat treatment. The sub-populations of nuclei containing acetylated and phosphorylated p53 were assessed upon drug response. Combination treatment of cisplatin and belinostat is associated with the largest cell population of acetylated and phosphorylated p53, but the increase in acetylation is more indicative of the induction of apoptosis. Despite so, these data are insufficient to convincingly exclude the role of p53 phosphorylation in the observed apoptotic phenotype, as concurrent induction of both of these modifications may still be required. A possible approach to study this is to systematically mutate most, if not all, of the lysine residues found on p53 protein to efficiently attenuate acetylation in the study model. Despite being classified previously to be a C-terminal-specific modifications (K357, K370, K372, K373, K381, K382, K386), several acetylation sites have been recently identified along the DNA

binding domain (K120, K164) and oligomerization domain (K305, K319) (Gu and Roeder 1997, Sakaguchi, Herrera et al. 1998, Wang, Tsay et al. 2003, Tang, Luo et al. 2006, Ivanov, Ivanova et al. 2007, Li, Piluso et al. 2007, Kurash, Lei et al. 2008, Tang, Zhao et al. 2008, Joubel, Chalkley et al. 2009). Interestingly, it has been shown that non-acetylated p53 could still mediate the p53-MDM2 feedback loop, but lack of acetylation substantially abolished the p53-dependent cell cycle arrest and apoptosis (Tang, Zhao et al. 2008). Acetylation of p53 at lysine residue 120 (K120) is indispensable for p53-mediated apoptosis but not necessarily crucial for p53-dependent cell cycle arrest (Sykes, Mellert et al. 2006, Tang, Luo et al. 2006). Unlike phosphorylation, the individual function of each acetylated residues has yet to be comprehensively characterized. In the present study, the primary focus was on the acetylated sites along the C-terminus of p53 protein, where lysine residues are most frequently detected. Generation of acetylation-defective p53 could facilitate investigation on the role of acetylation in p53-mediated apoptosis.

More importantly, several reports have illustrated that site-directed mutation of specific phosphorylation sites in p53 could not rescue cells from p53-induced cytotoxicity upon DNA damage (Slingerland, Jenkins et al. 1993, Fiscella, Zambrano et al. 1994, Blattner, Tobiasch et al. 1999). A further attempt to mutate all known phosphorylation sites on the p53 molecule again confirmed that p53 transactivation occurs independently of phosphorylation, as the mutated molecule retained its transcriptional activity (Ashcroft, Kubbutat et al. 1999). It is thus possible that other post-translational modifications, such as acetylation, could sufficiently trigger p53-dependent functions. Furthermore, acetylation of p53 is more associated with its sequence-specific DNA-binding ability (Gu and Roeder 1997, Lill, Grossman et al. 1997, Liu, Scolnick et al. 1999). Therefore, acetylated p53 may bind to sequence-specific response elements that are involved in the observed phenotype. It is also important to note that phosphorylation is generally associated with p53 stability and inhibition of MDM2-mediated degradation (Shieh, Ikeda et al. 1997, Siliciano, Canman et al. 1997), while in the case of mutant p53, the protein is highly expressed. Further investigations are needed to identify the possible mutant p53-interacting DNA sequence.

5.6.6 Restoration of p53-mediated apoptosis in mutant p53

Many chemotherapeutic agents are activator of p53 by causing DNA-damage. However, efficacy of chemotherapy could be hindered in tumours by mechanisms that negatively regulate p53 signalling. Recently, much effort has been dedicated to identify and synthesize small molecules that could reinstate transcriptional activity of p53. As p53 functions could be dysregulated by amplification of MDM2, inhibitors that disrupt the interaction between

p53 and MDM2 are developed, such as Nutlins (Vassilev 2004, Vassilev, Vu et al. 2004). Nutlins have promising p53-dependent anti-tumour effects (Vassilev, Vu et al. 2004), as demonstrated in MRC5 cells with the transactivation of *MDM2* and *CDKN1A* (Figure 5.10). However, Nutlins are selective to tumours that retained wild-type p53. As missense mutation of p53 is commonly detected in lung SCC, inhibitors that disrupt p53-MDM2 interaction may not be effective, as shown in H2170 cells.

A second class of compounds, known as the sirtuin inhibitors, is currently under investigation. Sirtuins, class III NAD+ dependent histone deacetylases, are shown to be aberrantly up-regulated in several cancer types (Bradbury, Khanim et al. 2005, Huffman, Grizzle et al. 2007) and its expression could destabilize p53 through deacetylation at lysine 382 (Vaziri, Dessain et al. 2001). More importantly, knockdown of sirtuin-1 resulted in hyperacetylation of p53 and increased p53-dependent transcriptional activity (Luo, Nikolaev et al. 2001, Ford, Jiang et al. 2005). Till date, multiple inhibitors for sirtuins have been synthesized but, except for sirtinol and tenovins, majority of them do not induce p53 activity as a single agent (Ota, Akishita et al. 2007, Lain, Hollick et al. 2008). In this study, targeting SirT1 in p53 mutant clones using tenovin-6 increased p53 acetylation and induced apoptosis (Figure 5.28 B). Interestingly, although WT 6 were shown to be more sensitive to tenovin-6 (Chapter 5.5.2), expression of p21 but not PARP cleavage was increased upon drug treatment, suggesting that induction of cell cycle arrest preceded cell death in wild-type p53 overexpressing cells. These findings implicate the favourable specificity of the proposed approach in targeting lung SCC, which consist of mostly p53 mutant cells, over normal lung cells with wild-type p53.

In an approach to investigate the molecular mechanisms that explain drug-induced p53 acetylation in the study models, it was observed that both HDAC3 and SirT1 were down-regulated, while acetyl-CBP/p300 was up-regulated (Figure 5.27). Therefore, regulation of specific HDACs and HATs may control p53 acetylation. Intriguingly, although cisplatin is known to induce activity of HATs (Di Stefano, Soddu et al. 2005), the data demonstrted that combination treatment, but not cisplatin alone, substantially activated CBP/p300. Furthermore, belinostat is a hydroxamic acid HDAC inhibitor that is known to inhibit enzymatic activity of class I and II but not class III HDACs (Imai, Armstrong et al. 2000, Johnstone 2002). In this study, however, expressions of both HDAC3 (Class I HDAC) and SirT1 (Class III) were reduced upon combination treatment. Thus, it was believed that the observed inhibition of SirT1 and activation of CBP/p300 may involve the combinatorial effects of both cisplatin and belinostat instead of specific targeting of single agent. While the inhibition of SirT1 using tenovin-6 had demonstrated promising cytotoxicity effect in

p53 mutant cells, the outcome of activating CBP/p300 by HAT activating agents, such as CTPB (Mantelingu, Kishore et al. 2007), has yet to be validated.

In this present study, two potential treatment regimes have been explored: combination of belinostat with cisplatin, and single drug treatment with tenovin-6, that could acetylate p53 in a dose-dependent manner. A study conducted by Solomon *et. al.* had shown that concurrent inhibitions of SirT1 and HDAC dramatically increased p53 acetylation at lysine 382 residue (Solomon, Pasupuleti et al. 2006). However, this author also reported that acetylation of p53 did not affect cell survival after DNA-damage, suggesting that the ability of acetylated p53 to induce apoptosis may be a cell-context dependent mechanism. Among the four lung SCC cell lines with mutated p53, combination with belinostat increased cisplatin-induced acetylation of p53 in H2170 and H1869. In addition, apoptosis was synergistically induced in these two cell lines. However, these regulations of acetylated p53 and cell death were not observed in H596 and ChaGo-k-1 cells. These observations emphasized that cellular response to belinostat in term of p53 acetylation may be cell-context dependent.

5.6.7 Conclusions and future directions

Inactivation of p53 signalling is a common feature in various human tumours. Thirty years of extensive research have provided a comprehensive understanding on the structure, modification and function of p53. The loss of its tumour suppressive function is widely regarded as an almost universal phenomenon in the initiation of tumourigenesis. In this chapter, the role of p53 functions and its aberrant loss-of-function mutation in lung SCC were discussed. More recently, however, multiple reports have suggested that p53 mutants harbour more phenotypic changes than just a loss of its wild-type tumour suppressive functions. The progressive understandings on p53 and its mutant form suggest that there is still much to be explored on a protein that is initially thought to be thoroughly understood.

The p53 overexpressing clones generated from Calu-1 cells are seen as suitable study models for investigating the roles of p53, especially the mutant clones, in tumour biology of lung SCC. Although the gain-of-function events in the mutant clones have been extensively characterized, however, the detailed mechanisms remain elusive. The postulation is that p53 functions can be reinstated in mutant cells either by interaction with transcriptional co-factors, direct binding to DNA through sequence-specific affinity or chromosomal remodelling (Figure 5.34). However, the concept of mutant p53 to regain DNA binding affinity remains highly dubious. Interestingly, though wild-type p53 is unable to interact with p73 and p63, several reports have demonstrated the oligomerization of mutant p53 with

other p53 family members through their DBD (Gaiddon, Lokshin et al. 2001, Strano, Munarriz et al. 2001, Strano, Fontemaggi et al. 2002). These observations suggest that missense mutation occurring at the DNA-binding site may alter the local or global conformation structure of p53 and possibly modulate the binding specificity of mutant p53. This implicates that a single codon mutation is sufficient to disrupt the classical p53-DNA binding while supplement with other non-conventional gain-of-function mechanisms, which may include binding to novel gene promoters. To elucidate the underlying mechanisms, co-immunoprecipitation and chromatin immunoprecipitation could be performed on mutant p53 for identification of binding partners or sequences. In addition, site-directed mutagenesis can be conducted to verify the significance of acetylation in the observed phenotype.

In view of the potential of p53 acetylators as treatment options for lung SCC, the mechanisms to effectively acetylated p53 has emerged as an interesting direction for future study. The findings here suggested that p53 acetylation could be induced by a DNA-damage agent, cisplatin, in combination with belinostat, possibly via inhibition of HDAC3 and sirtuin-1 as well as activation of CBP/p300. However, it is important to note that other molecules, such as Tip60 and sirtuin-2, are known modulators of p53 activity (Frye 2000, Vakhrusheva, Smolka et al. 2008). These molecules were not investigated in the present study. Therefore, the search is on for therapeutic targets that will provide synthetic lethal associations with mutant p53.

In conclusion, despite the increased understanding on p53 pathway and rapid advances in p53-based cancer therapy, many key questions remain unanswered. How does mutant p53 selectively activates cellular apoptosis under drug treatment? Is p53 acetylation sufficient to induce the observed phenotype? What are the key regulators of p53 acetylation in lung SCC? Could these regulator(s) be targeted? How do the modified mutant forms of p53 impose its transcriptional regulation of target genes? What is the role of p73 in this model? Is the observed phenomenon a universal phenotype in all mutant p53, or is it only vital to certain point mutations? The findings in present study emphasize on the functional biology of mutant p53 which lay the groundwork for future discoveries of strategies that are applicable to the large proportion of cancer patients with tumours harbouring mutant p53.

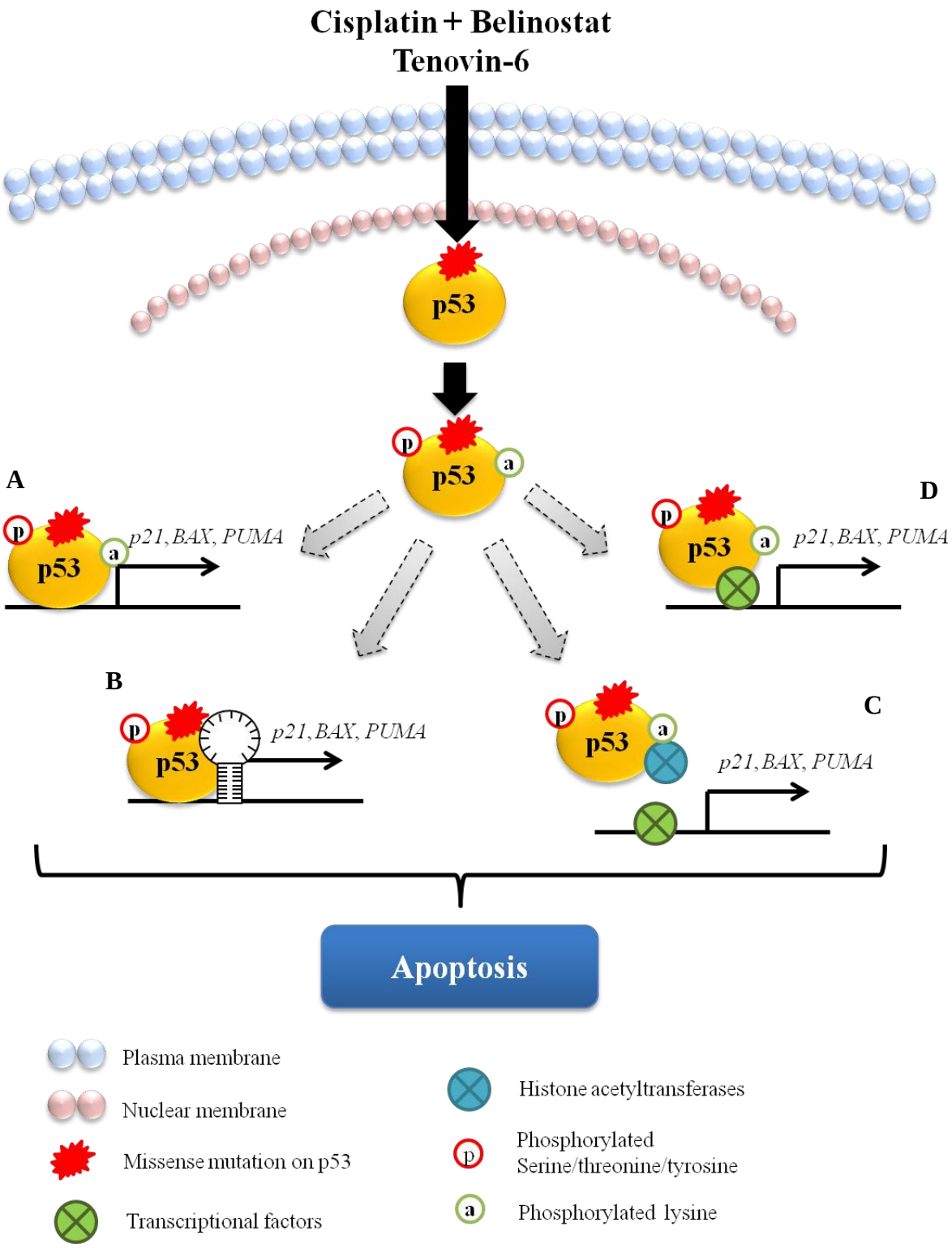
Cisplatin + Belinostat
Tenovin-6
p53
A
p53
p21, BAX, PUMA
D
p53
p21, BAX, PUMA
B
p53
p21, BAX, PUMA
C
p53
p21, BAX, PUMA
Apoptosis
Plasma membrane
Nuclear membrane
Missense mutation on p53
Transcriptional factors
Histone acetyltransferases
Phosphorylated Serine/threonine/tyrosine
Phosphorylated lysine

Figure 5.34: A schematic diagram showing the proposed mechanisms of p53-mediated apoptosis in R158G mutant cells through drug-induced p53 acetylation.

Cytotoxic agents (Tenovin-6; cisplatin and belinostat) that induce p53 acetylation substantially trigger cell death in p53 mutant (R158G) cell lines, probably via transcriptional-dependent p53-mediated apoptosis as shown by the induction of p53 target genes (*CDKN1A*, *BAX*, *PUMA*). This novel observation is postulated to be regulated via: (A) direct recruitment of mutant p53 to unique sequence-specific response elements; (B) direct binding to structural specific DNA motifs; (C) direct recruitment of HATs; and (D) direct interaction with other transcription factors to induce transactivation of downstream target genes. The dashed arrow indicates the lacking of supportive evidence to support these proposed mechanisms.

CHAPTER 6 CONCLUSIONS

Despite a reduction in the incidence rate, the mortality burden of squamous cell carcinoma (SCC) remains high. This could be due to a lack of oncogenic driver lesions that could guide treatment. Historically, the efforts at characterizing the molecular underspinnings of SCC have lagged behind those of adenocarcinoma. Many of the driver oncogenes found in lung adenocarcinoma are rarely detected in SCC. These properties of lung SCC have been verified in SCC tumours of Asian patients by performing deep sequencing after targeted enrinchment. As a consequence, patients with metastatic SCC have fewer options that those with non-squamous NSCLC. For instance, targeting EGFR mutations in the tyrosine kinase domain, ROS1 and EML4-ALK rearrangements have yielded impressive gains in therapeutic efficacy in adenocarcinoma of the lung, as have the use of Bevacizumab and Pemetrexed chemotherapy for non-SCC histologies (Lynch, Bell et al. 2004, Paez, Jänne et al. 2004, Soda, Choi et al. 2007, Patel, Socinski et al. 2013); for SCC histologies, however, Cetuximab remains as the only approved non-cytotoxic agent to date (Lynch, Patel et al. 2010). Therefore, cisplatin remains as the backbone of chemotherapy for SCC of different histotypes either as a single agent or alongside other chemotherapeutic agents of radiotherapy. However, resistance to cisplatin inevitably developed, and the overall survival rates in SCC patients remain low.

Since its approval in 1978, the mechanism-of-action of cisplatin have been well studied, together with the mechanisms that lead to resistance. Understanding these pathways are believed to reveal new therapeutic strategies that could improve clinical outcome. For instance, inactivation of *hMLH1* gene through promoter methylation was known to confer resistance to platinum-containing compounds. A recent clinical study on the combination of decitabine, a demethylating agent, with carboplatin was conducted in ovarian cancer patients based on the hypothesis that reactivation of *hMLH1* promoter through the hypomethylating effect of decitabine could improve the efficacy of carboplatin (Glasspool, Brown et al. 2014). However, this study has failed to achieve good clinical outcome, possibly due to the non-specificity of decitabine (Glasspool, Brown et al. 2014). Therefore in this study, the drug-induced perturbations to gene and protein expression that mediated cisplatin resistance was elucidated; while the strategies that counteract these mechanisms were being explored.

Two main findings have been described in this thesis. The first finding demonstrates a mechanism involving the drug-induced SOS-mediated MAPK/Erk activation that confers resistance to cisplatin. More recent investigations, which are not being included in this

thesis, have shown that activated p-Erk1/2 phosphorylates and induces degradation of pro-apoptic Bim, therefore preventing cisplatin-induced cell death. Clinicopathological analysis on patients with locally advanced SCC treated with concurrent cisplatin and radiotherapy has demonstrated that patients with stronger p-Erk1/2 expression have significantly shorter disease-free survival. Taken together, these observations implicate the potential roles of phosphorylated Erk both as a predictive biomarker and a therapeutic target for SCC patients. Accordingly, pharmacological interventions of MAPK/Erk pathway through MEK inhibitors and belinostat are shown to facilitate induction of apoptosis in SCC cells. For a proof-of-concept, it will be critical to study the combination of cisplatin and a MEK inhibitor or belinostat in patients whose tumors demonstrate evidence of Erk phosphorylation. Such studies are currently being planned.

The second finding in this study describes a gain-of-function events in mutant p53 SCC cells, which facilitates induction and apoptosis and is shown to correlate with the acetylation at the C-terminus. These observations was made while investigating the therapeutic potential of belinostat in combination with cisplatin in SCC cells. When used at 0.1μM, which is achievable in patient's plasma, belinostat enhanced cisplatin-induced apoptosis in H2170 cells that has a loss-of-function mutation along the DNA-binding domain of the p53. Importantly, this observed cell death could be rescued with effective knockdown of p53R158G mutant in H2170 cells; while activated with ectopic expression of p53R158G mutant in p53-null Calu-1 cells. These observations led to the discoveries that drug treatment that induced p53 acetylation, such as belinostat/cisplatin or tenovin-6, could trigger the cell death mechanisms in p53 mutant cells. This is a clinically significant finding as most tumour cells harbour p53 mutation, especially in the case of lung SCC, where there is a lack of oncogenic driver lesions to guide treatment. However, the mechanisms leading to this pro-apoptotic gain-of-function events remain elusive and are currently being investigated.

In conclusion, this thesis has addressed two main hypotheses: one involving Erk activation under treatment pressure that confers cisplatin resistance, and the other demonstrating a restoration of p53-induced apoptosis in p53 mutant cells through acetylation at the C-terminus. The first hypothesis targets SCC patients that have developed refractoriness to cisplatin with tumours that showed Erk up-regulation; the second hypothesis paves way for development of new therapeutic strategies in SCC patients with tumours that have *TP53* mutations. Importantly, the proposed treatment regimens utilize clinically available anti-cancer agents (MEK inhibitors, belinostat and cisplatin) at tolerable doses. The efficacy of these drug combinations is currently being investigated in mouse xenograft models.

CHAPTER 7 REFERENCES

A.D.A.M. Medical Encyclopedia [Internet]. Atlanta (GA): A.D.A.M., Inc.; c1997-2011. Lung cancer - non-small cell; [last reviewed 2011 Aug 24; cited 2013 Dec 30]. Available from: http://www.ncbi.nlm.nih.gov/pubmedhealth/PMH0004462/

Abal, M., J. M. Andreu and I. Barasoain (2003). "Taxanes: microtubule and centrosome targets, and cell cycle dependent mechanisms of action." Curr Cancer Drug Targets **3**(3): 193-203.

Abidin, A. Z., M. C. Garassino, R. Califano, A. Harle and F. Blackhall (2010). "Targeted therapies in small cell lung cancer: a review." Ther Adv Med Oncol **2**(1): 25-37.

Abratt, R. P., W. R. Bezwoda, G. Falkson, L. Goedhals, D. Hacking and T. A. Rugg (1994). "Efficacy and safety profile of gemcitabine in non-small-cell lung cancer: a phase II study." J Clin Oncol **12**(8): 1535-1540.

Abratt, R. P., W. R. Bezwoda, L. Goedhals and D. J. Hacking (1997). "Weekly gemcitabine with monthly cisplatin: effective chemotherapy for advanced non-small-cell lung cancer." J Clin Oncol **15**(2): 744-749.

Adimoolam, S. and J. M. Ford (2002). "p53 and DNA damage-inducible expression of the xeroderma pigmentosum group C gene." Proc Natl Acad Sci U S A **99**(20): 12985-12990.

Adimoolam, S., M. Sirisawad, J. Chen, P. Thiemann, J. M. Ford and J. J. Buggy (2007). "HDAC inhibitor PCI-24781 decreases RAD51 expression and inhibits homologous recombination." Proc Natl Acad Sci U S A **104**(49): 19482-19487.

Adorno, M., M. Cordenonsi, M. Montagner, S. Dupont, C. Wong, B. Hann, A. Solari, S. Bobisse, M. B. Rondina, V. Guzzardo, A. R. Parenti, A. Rosato, S. Bicciato, A. Balmain and S. Piccolo (2009). "A Mutant-p53/Smad complex opposes p63 to empower TGFbeta-induced metastasis." Cell **137**(1): 87-98.

Agarwal, M. L., A. Agarwal, W. R. Taylor and G. R. Stark (1995). "p53 controls both the G2/M and the G1 cell cycle checkpoints and mediates reversible growth arrest in human fibroblasts." Proc Natl Acad Sci U S A **92**(18): 8493-8497.

Agrawal, N., M. J. Frederick, C. R. Pickering, C. Bettegowda, K. Chang, R. J. Li, C. Fakhry, T. X. Xie, J. Zhang, J. Wang, N. Zhang, A. K. El-Naggar, S. A. Jasser, J. N. Weinstein, L. Treviño, J. A. Drummond, D. M. Muzny, Y. Wu, L. D. Wood, R. H. Hruban, W. H. Westra, W. M. Koch, J. A. Califano, R. A. Gibbs, D. Sidransky, B. Vogelstein, V. E. Velculescu, N. Papadopoulos, D. A. Wheeler, K. W. Kinzler and J. N. Myers (2011). "Exome sequencing of head and neck squamous cell carcinoma reveals inactivating mutations in NOTCH1." Science **333**(6046): 1154-1157.

Ahmad, A., A. R. Robinson, A. Duensing, E. van Drunen, H. B. Beverloo, D. B. Weisberg, P. Hasty, J. H. Hoeijmakers and L. J. Niedernhofer (2008). "ERCC1-XPF endonuclease facilitates DNA double-strand break repair." Mol Cell Biol **28**(16): 5082-5092.

Akinleye, A., M. Furqan, N. Mukhi, P. Ravella and D. Liu (2013). "MEK and the inhibitors: from bench to bedside." J Hematol Oncol **6**: 27.

Ali, A., Z. Wang, J. Fu, L. Ji, J. Liu, L. Li, H. Wang, J. Chen, C. Caulin, J. N. Myers, P. Zhang, J. Xiao, B. Zhang and X. Li (2013). "Differential regulation of the REGγ-proteasome pathway by p53/TGF-β signalling and mutant p53 in cancer cells." Nat Commun **4**: 2667.

Alnemri, E. S. (1997). "Mammalian cell death proteases: a family of highly conserved aspartate specific cysteine proteases." J Cell Biochem **64**(1): 33-42.

Alnemri, E. S., D. J. Livingston, D. W. Nicholson, G. Salvesen, N. A. Thornberry, W. W. Wong and J. Yuan (1996). "Human ICE/CED-3 protease nomenclature." Cell **87**(2): 171.

Anderson, H., B. Lund, F. Bach, N. Thatcher, J. Walling and H. H. Hansen (1994). "Single-agent activity of weekly gemcitabine in advanced non-small-cell lung cancer: a phase II study." J Clin Oncol **12**(9): 1821-1826.

Andujar, P., J. Wang, A. Descatha, F. Galateau-Sallé, I. Abd-Alsamad, M. A. Billon-Galland, H. Blons, B. Clin, C. Danel, B. Housset, P. Laurent-Puig, F. Le Pimpec-Barthes, M. Letourneux, I. Monnet, J. F. Régnard, A. Renier, J. Zucman-Rossi, J. C. Pairon and M. C. Jaurand (2010). "p16INK4A inactivation mechanisms in non-small-cell lung cancer patients occupationally exposed to asbestos." Lung Cancer **67**(1): 23-30.

Annunziato, A. T. and J. C. Hansen (2000). "Role of histone acetylation in the assembly and modulation of chromatin structures." Gene Expr **9**(1-2): 37-61.

Arteaga, C. L., A. R. Winnier, M. C. Poirier, D. M. Lopez-Larraza, L. K. Shawver, S. D. Hurd and S. J. Stewart (1994). "p185c-erbB-2 signal enhances cisplatin-induced cytotoxicity in human breast carcinoma cells: association between an oncogenic receptor tyrosine kinase and drug-induced DNA repair." Cancer Res **54**(14): 3758-3765.

Ashcroft, M., M. H. Kubbutat and K. H. Vousden (1999). "Regulation of p53 function and stability by phosphorylation." Mol Cell Biol **19**(3): 1751-1758.

Ashwell, S. and S. Zabludoff (2008). "DNA damage detection and repair pathways--recent advances with inhibitors of checkpoint kinases in cancer therapy." Clin Cancer Res **14**(13): 4032-4037.

Asselin, E., G. B. Mills and B. K. Tsang (2001). "XIAP regulates Akt activity and caspase-3-dependent cleavage during cisplatin-induced apoptosis in human ovarian epithelial cancer cells." Cancer Res **61**(5): 1862-1868.

Avruch, J., A. Khokhlatchev, J. M. Kyriakis, Z. Luo, G. Tzivion, D. Vavvas and X. F. Zhang (2001). "Ras activation of the Raf kinase: tyrosine kinase recruitment of the MAP kinase cascade." Recent Prog Horm Res **56**: 127-155.

Azad, N., C. A. Zahnow, C. M. Rudin and S. B. Baylin (2013). "The future of epigenetic therapy in solid tumours--lessons from the past." Nat Rev Clin Oncol **10**(5): 256-266.

Baker, S. J., E. R. Fearon, J. M. Nigro, S. R. Hamilton, A. C. Preisinger, J. M. Jessup, P. vanTuinen, D. H. Ledbetter, D. F. Barker, Y. Nakamura, R. White and B. Vogelstein (1989). "Chromosome 17 deletions and p53 gene mutations in colorectal carcinomas." Science **244**(4901): 217-221.

Bangert, A., S. Häcker, S. Cristofanon, K. M. Debatin and S. Fulda (2011). "Chemosensitization of glioblastoma cells by the histone deacetylase inhibitor MS275." Anticancer Drugs **22**(6): 494-499.

Banin, S., L. Moyal, S. Shieh, Y. Taya, C. W. Anderson, L. Chessa, N. I. Smorodinsky, C. Prives, Y. Reiss, Y. Shiloh and Y. Ziv (1998). "Enhanced phosphorylation of p53 by ATM in response to DNA damage." Science **281**(5383): 1674-1677.

Barak, Y., T. Juven, R. Haffner and M. Oren (1993). "mdm2 expression is induced by wild type p53 activity." EMBO J **12**(2): 461-468.

Bargmann, C. I., M. C. Hung and R. A. Weinberg (1986). "The neu oncogene encodes an epidermal growth factor receptor-related protein." Nature **319**(6050): 226-230.

Bargonetti, J., A. Chicas, D. White and C. Prives (1997). "p53 represses Sp1 DNA binding and HIV-LTR directed transcription." Cell Mol Biol (Noisy-le-grand) **43**(7): 935-949.

Baritaud, M., L. Cabon, L. Delavallée, P. Galán-Malo, M. E. Gilles, M. N. Brunelle-Navas and S. A. Susin (2012). "AIF-mediated caspase-independent necroptosis requires ATM and DNA-PK-induced histone H2AX Ser139 phosphorylation." Cell Death Dis **3**: e390.

Bartek, J. and J. Lukas (2001). "Mammalian G1- and S-phase checkpoints in response to DNA damage." Curr Opin Cell Biol **13**(6): 738-747.

Bates, S., A. C. Phillips, P. A. Clark, F. Stott, G. Peters, R. L. Ludwig and K. H. Vousden (1998). "p14ARF links the tumour suppressors RB and p53." Nature **395**(6698): 124-125.

Battle, T. E. and D. A. Frank (2002). "The role of STATs in apoptosis." Curr Mol Med **2**(4): 381-392.

Beale, P. J., P. Rogers, F. Boxall, S. Y. Sharp and L. R. Kelland (2000). "BCL-2 family protein expression and platinum drug resistance in ovarian carcinoma." Br J Cancer **82**(2): 436-440.

Beck, B. and C. Blanpain (2013). "Unravelling cancer stem cell potential." Nat Rev Cancer **13**(10): 727-738.

Belani, C., S. Ramalingam, G. Kalemkerian, T. Mok, R. Rosell, M. Ahn, L. Sun, M. Gates, G. Lubiniecki and R. Govindan (2009). "9007 Randomized, double-blind phase II/III study of first-line paclitaxel (P) plus carboplatin (C) in combination with vorinostat or placebo in patients with advanced non-small-cell lung cancer (NSCLC)." European Journal of Cancer Supplements **7**(2): 507.

Bellmunt, J., L. Paz-Ares, M. Cuello, F. L. Cecere, S. Albiol, V. Guillem, E. Gallardo, J. Carles, P. Mendez, J. J. de la Cruz, M. Taron, R. Rosell, J. Baselga and S. O. G. Group (2007). "Gene expression of ERCC1 as a novel prognostic marker in advanced bladder cancer patients receiving cisplatin-based chemotherapy." Ann Oncol **18**(3): 522-528.

Ben David, Y., A. Chetrit, G. Hirsh-Yechezkel, E. Friedman, B. D. Beck, U. Beller, G. Ben-Baruch, A. Fishman, H. Levavi, F. Lubin, J. Menczer, B. Piura, J. P. Struewing, B. Modan and N. I. S. o. O. Cancer (2002). "Effect of BRCA mutations on the length of survival in epithelial ovarian tumors." J Clin Oncol **20**(2): 463-466.

Bennett, M., K. Macdonald, S. W. Chan, J. P. Luzio, R. Simari and P. Weissberg (1998). "Cell surface trafficking of Fas: a rapid mechanism of p53-mediated apoptosis." Science **282**(5387): 290-293.

Binks, S. P. and M. Dobrota (1990). "Kinetics and mechanism of uptake of platinum-based pharmaceuticals by the rat small intestine." Biochem Pharmacol **40**(6): 1329-1336.

Bissett, D., K. J. O'Byrne, J. von Pawel, U. Gatzemeier, A. Price, M. Nicolson, R. Mercier, E. Mazabel, C. Penning, M. H. Zhang, M. A. Collier and F. A. Shepherd (2005). "Phase III study of matrix metalloproteinase inhibitor prinomastat in non-small-cell lung cancer." J Clin Oncol **23**(4): 842-849.

Blanc, C., Q. L. Deveraux, S. Krajewski, R. U. Jänicke, A. G. Porter, J. C. Reed, R. Jaggi and A. Marti (2000). "Caspase-3 is essential for procaspase-9 processing and cisplatin-induced apoptosis of MCF-7 breast cancer cells." Cancer Res **60**(16): 4386-4390.

Blander, G. and L. Guarente (2004). "The Sir2 family of protein deacetylases." Annu Rev Biochem **73**: 417-435.

Blandino, G., A. J. Levine and M. Oren (1999). "Mutant p53 gain of function: differential effects of different p53 mutants on resistance of cultured cells to chemotherapy." Oncogene **18**(2): 477-485.

Blattner, C., E. Tobiasch, M. Litfen, H. J. Rahmsdorf and P. Herrlich (1999). "DNA damage induced p53 stabilization: no indication for an involvement of p53 phosphorylation." Oncogene **18**(9): 1723-1732.

Blaydes, J. P. and T. R. Hupp (1998). "DNA damage triggers DRB-resistant phosphorylation of human p53 at the CK2 site." Oncogene **17**(8): 1045-1052.

Blume-Jensen, P. and T. Hunter (2001). "Oncogenic kinase signalling." Nature **411**(6835): 355-365.

Bode, A. M. and Z. Dong (2004). "Post-translational modification of p53 in tumorigenesis." Nat Rev Cancer **4**(10): 793-805.

Boland, J. M., S. Erdogan, G. Vasmatzis, P. Yang, L. S. Tillmans, M. R. Johnson, X. Wang, L. M. Peterson, K. C. Halling, A. M. Oliveira, M. C. Aubry and E. S. Yi (2009). "Anaplastic lymphoma kinase immunoreactivity correlates with ALK gene rearrangement and transcriptional up-regulation in non-small cell lung carcinomas." Hum Pathol **40**(8): 1152-1158.

Borst, P., R. Evers, M. Kool and J. Wijnholds (2000). "A family of drug transporters: the multidrug resistance-associated proteins." J Natl Cancer Inst **92**(16): 1295-1302.

Bos, J. L. (1989). "ras oncogenes in human cancer: a review." Cancer Res **49**(17): 4682-4689.

Bos, J. L. (1995). "A target for phosphoinositide 3-kinase: Akt/PKB." Trends Biochem Sci **20**(11): 441-442.

Bossi, G., E. Lapi, S. Strano, C. Rinaldo, G. Blandino and A. Sacchi (2006). "Mutant p53 gain of function: reduction of tumor malignancy of human cancer cell lines through abrogation of mutant p53 expression." Oncogene **25**(2): 304-309.

Bouvard, V., T. Zaitchouk, M. Vacher, A. Duthu, M. Canivet, C. Choisy-Rossi, M. Nieruchalski and E. May (2000). "Tissue and cell-specific expression of the p53-target genes: bax, fas, mdm2 and waf1/p21, before and following ionising irradiation in mice." Oncogene **19**(5): 649-660.

Boyes, J., P. Byfield, Y. Nakatani and V. Ogryzko (1998). "Regulation of activity of the transcription factor GATA-1 by acetylation." Nature **396**(6711): 594-598.

Bradbury, C. A., F. L. Khanim, R. Hayden, C. M. Bunce, D. A. White, M. T. Drayson, C. Craddock and B. M. Turner (2005). "Histone deacetylases in acute myeloid leukaemia show a distinctive pattern of expression that changes selectively in response to deacetylase inhibitors." Leukemia **19**(10): 1751-1759.

Bradley, D., D. Rathkopf, R. Dunn, W. M. Stadler, G. Liu, D. C. Smith, R. Pili, J. Zwiebel, H. Scher and M. Hussain (2009). "Vorinostat in advanced prostate cancer patients progressing on prior chemotherapy (National Cancer Institute Trial 6862): trial results and interleukin-6 analysis: a study by the Department of Defense Prostate Cancer Clinical Trial Consortium and University of Chicago Phase 2 Consortium." Cancer **115**(23): 5541-5549.

Branch, P., M. Masson, G. Aquilina, M. Bignami and P. Karran (2000). "Spontaneous development of drug resistance: mismatch repair and p53 defects in resistance to cisplatin in human tumor cells." Oncogene **19**(28): 3138-3145.

Bristow, R. G., J. Peacock, A. Jang, J. Kim, R. P. Hill and S. Benchimol (2003). "Resistance to DNA-damaging agents is discordant from experimental metastatic capacity in MEF ras-transformants-expressing gain of function MTp53." Oncogene **22**(19): 2960-2966.

Brooks, C. L. and W. Gu (2003). "Ubiquitination, phosphorylation and acetylation: the molecular basis for p53 regulation." Curr Opin Cell Biol **15**(2): 164-171.

Brose, M. S., P. Volpe, M. Feldman, M. Kumar, I. Rishi, R. Gerrero, E. Einhorn, M. Herlyn, J. Minna, A. Nicholson, J. A. Roth, S. M. Albelda, H. Davies, C. Cox, G. Brignell, P. Stephens, P. A. Futreal, R. Wooster, M. R. Stratton and B. L. Weber (2002). "BRAF and RAS mutations in human lung cancer and melanoma." Cancer Res **62**(23): 6997-7000.

Brozovic, A., G. Fritz, M. Christmann, J. Zisowsky, U. Jaehde, M. Osmak and B. Kaina (2004). "Long-term activation of SAPK/JNK, p38 kinase and fas-L expression by cisplatin is attenuated in human carcinoma cells that acquired drug resistance." Int J Cancer **112**(6): 974-985.

Brozovic, A. and M. Osmak (2007). "Activation of mitogen-activated protein kinases by cisplatin and their role in cisplatin-resistance." Cancer Lett **251**(1): 1-16.

Brunet, A., D. Roux, P. Lenormand, S. Dowd, S. Keyse and J. Pouysségur (1999). "Nuclear translocation of p42/p44 mitogen-activated protein kinase is required for growth factor-induced gene expression and cell cycle entry." EMBO J **18**(3): 664-674.

Bruserud, Ø., C. Stapnes, E. Ersvaer, B. T. Gjertsen and A. Ryningen (2007). "Histone deacetylase inhibitors in cancer treatment: a review of the clinical toxicity and the modulation of gene expression in cancer cell." Curr Pharm Biotechnol **8**(6): 388-400.

Buckley, M. T., J. Yoon, H. Yee, L. Chiriboga, L. Liebes, G. Ara, X. Qian, D. F. Bajorin, T. T. Sun, X. R. Wu and I. Osman (2007). "The histone deacetylase inhibitor belinostat (PXD101) suppresses bladder cancer cell growth in vitro and in vivo." J Transl Med **5**: 49.

Buday, L. and J. Downward (1993). "Epidermal growth factor regulates p21ras through the formation of a complex of receptor, Grb2 adapter protein, and Sos nucleotide exchange factor." Cell **73**(3): 611-620.

Burgess, A. W., H. S. Cho, C. Eigenbrot, K. M. Ferguson, T. P. Garrett, D. J. Leahy, M. A. Lemmon, M. X. Sliwkowski, C. W. Ward and S. Yokoyama (2003). "An open-and-shut case? Recent insights into the activation of EGF/ErbB receptors." Mol Cell **12**(3): 541-552.

Butler, L. M., X. Zhou, W. S. Xu, H. I. Scher, R. A. Rifkind, P. A. Marks and V. M. Richon (2002). "The histone deacetylase inhibitor SAHA arrests cancer cell growth, up-regulates thioredoxin-binding protein-2, and down-regulates thioredoxin." Proc Natl Acad Sci U S A **99**(18): 11700-11705.

Caelles, C., A. Helmberg and M. Karin (1994). "p53-dependent apoptosis in the absence of transcriptional activation of p53-target genes." Nature **370**(6486): 220-223.

Cameron, E. E., K. E. Bachman, S. Myöhänen, J. G. Herman and S. B. Baylin (1999). "Synergy of demethylation and histone deacetylase inhibition in the re-expression of genes silenced in cancer." Nat Genet **21**(1): 103-107.

Camidge, D. R., F. R. Hirsch, M. Varella-Garcia and W. A. Franklin (2011). "Finding ALK-positive lung cancer: what are we really looking for?" J Thorac Oncol **6**(3): 411-413.

Campisi, J. and F. d'Adda di Fagagna (2007). "Cellular senescence: when bad things happen to good cells." Nat Rev Mol Cell Biol **8**(9): 729-740.

Cappuzzo, F., L. Bemis and M. Varella-Garcia (2006). "HER2 mutation and response to trastuzumab therapy in non-small-cell lung cancer." N Engl J Med **354**(24): 2619-2621.

Carrier, F., P. T. Georgel, P. Pourquier, M. Blake, H. U. Kontny, M. J. Antinore, M. Gariboldi, T. G. Myers, J. N. Weinstein, Y. Pommier and A. J. Fornace (1999). "Gadd45, a p53-responsive stress protein, modifies DNA accessibility on damaged chromatin." Mol Cell Biol **19**(3): 1673-1685.

Carrozza, M. J., R. T. Utley, J. L. Workman and J. Côté (2003). "The diverse functions of histone acetyltransferase complexes." Trends Genet **19**(6): 321-329.

Casas-Delucchi, C. S., J. G. van Bemmel, S. Haase, H. D. Herce, D. Nowak, D. Meilinger, J. H. Stear, H. Leonhardt and M. C. Cardoso (2012). "Histone hypoacetylation is required to maintain late replication timing of constitutive heterochromatin." Nucleic Acids Res **40**(1): 159-169.

Catalanotti, F., D. B. Solit, M. P. Pulitzer, M. F. Berger, S. N. Scott, T. Iyriboz, M. E. Lacouture, K. S. Panageas, J. D. Wolchok, R. D. Carvajal, G. K. Schwartz, N. Rosen and P. B. Chapman (2013). "Phase II trial of MEK inhibitor selumetinib (AZD6244, ARRY-142886) in patients with BRAFV600E/K-mutated melanoma." Clin Cancer Res **19**(8): 2257-2264.

Cerami, E., J. Gao, U. Dogrusoz, B. E. Gross, S. O. Sumer, B. A. Aksoy, A. Jacobsen, C. J. Byrne, M. L. Heuer, E. Larsson, Y. Antipin, B. Reva, A. P. Goldberg, C. Sander and N. Schultz (2012). "The cBio cancer genomics portal: an open platform for exploring multidimensional cancer genomics data." Cancer Discov **2**(5): 401-404.

Cerqueira, N. M., P. A. Fernandes and M. J. Ramos (2007). "Understanding ribonucleotide reductase inactivation by gemcitabine." Chemistry **13**(30): 8507-8515.

Chan, D., Y. Zheng, J. W. Tyner, W. J. Chng, W. W. Chien, S. Gery, G. Leong, G. D. Braunstein and H. P. Koeffler (2013). "Belinostat and panobinostat (HDACI): in vitro and in vivo studies in thyroid cancer." J Cancer Res Clin Oncol **139**(9): 1507-1514.

Chang, L. and M. Karin (2001). "Mammalian MAP kinase signalling cascades." Nature **410**(6824): 37-40.

Chen, C. S., Y. C. Wang, H. C. Yang, P. H. Huang, S. K. Kulp, C. C. Yang, Y. S. Lu, S. Matsuyama and C. Y. Chen (2007). "Histone deacetylase inhibitors sensitize prostate cancer cells to agents that produce DNA double-strand breaks by targeting Ku70 acetylation." Cancer Res **67**(11): 5318-5327.

Chen Lf, W. Fischle, E. Verdin and W. C. Greene (2001). "Duration of nuclear NF-kappaB action regulated by reversible acetylation." Science **293**(5535): 1653-1657.

Chen, M. C., C. H. Chen, J. C. Wang, A. C. Tsai, J. P. Liou, S. L. Pan and C. M. Teng (2013). "The HDAC inhibitor, MPT0E028, enhances erlotinib-induced cell death in EGFR-TKI-resistant NSCLC cells." Cell Death Dis **4**: e810.

Chen, R. and E. A. Sweet-Cordero (2013). "Two is better than one: combining IGF1R and MEK blockade as a promising novel treatment strategy against KRAS-mutant lung cancer." Cancer Discov **3**(5): 491-493.

Chen, R. H., C. Sarnecki and J. Blenis (1992). "Nuclear localization and regulation of erk- and rsk-encoded protein kinases." Mol Cell Biol **12**(3): 915-927.

Chen, X., Y. Zheng, J. Zhu, J. Jiang and J. Wang (2001). "p73 is transcriptionally regulated by DNA damage, p53, and p73." Oncogene **20**(6): 769-774.

Chen, Z., S. Clark, M. Birkeland, C. M. Sung, A. Lago, R. Liu, R. Kirkpatrick, K. Johanson, J. D. Winkler and E. Hu (2002). "Induction and superinduction of growth arrest and DNA damage gene 45 (GADD45) alpha and beta messenger RNAs by histone deacetylase inhibitors trichostatin A (TSA) and butyrate in SW620 human colon carcinoma cells." Cancer Lett **188**(1-2): 127-140.

Cheng, L., R. E. Alexander, G. T. Maclennan, O. W. Cummings, R. Montironi, A. Lopez-Beltran, H. M. Cramer, D. D. Davidson and S. Zhang (2012). "Molecular pathology of lung cancer: key to personalized medicine." Mod Pathol **25**(3): 347-369.

Cheng, Y. W., M. F. Wu, J. Wang, K. T. Yeh, Y. G. Goan, H. L. Chiou, C. Y. Chen and H. Lee (2007). "Human papillomavirus 16/18 E6 oncoprotein is expressed in lung cancer and related with p53 inactivation." Cancer Res **67**(22): 10686-10693.

Cherfils, J. and M. Zeghouf (2013). "Regulation of small GTPases by GEFs, GAPs, and GDIs." Physiol Rev **93**(1): 269-309.

Chetrit, A., G. Hirsh-Yechezkel, Y. Ben-David, F. Lubin, E. Friedman and S. Sadetzki (2008). "Effect of BRCA1/2 mutations on long-term survival of patients with invasive ovarian cancer: the national Israeli study of ovarian cancer." J Clin Oncol **26**(1): 20-25.

Chiao, C., A. M. Carothers, D. Grunberger, G. Solomon, G. A. Preston and J. C. Barrett (1995). "Apoptosis and altered redox state induced by caffeic acid phenethyl ester (CAPE) in transformed rat fibroblast cells." Cancer Res **55**(16): 3576-3583.

Chien, W., D. H. Lee, Y. Zheng, P. Wuensche, R. Alvarez, D. L. Wen, A. M. Aribi, S. M. Thean, N. B. Doan, J. W. Said and H. P. Koeffler (2013). "Growth inhibition of pancreatic cancer cells by Histone Deacetylase inhibitor belinostat through suppression of multiple pathways including HIF, NFkB, and mTOR signaling in vitro and in vivo." Mol Carcinog.

Chin, L., A. Tam, J. Pomerantz, M. Wong, J. Holash, N. Bardeesy, Q. Shen, R. O'Hagan, J. Pantginis, H. Zhou, J. W. Horner, C. Cordon-Cardo, G. D. Yancopoulos and R. A. DePinho

(1999). "Essential role for oncogenic Ras in tumour maintenance." Nature **400**(6743): 468-472.

Chipuk, J. E. and D. R. Green (2008). "How do BCL-2 proteins induce mitochondrial outer membrane permeabilization?" Trends Cell Biol **18**(4): 157-164.

Chipuk, J. E., T. Kuwana, L. Bouchier-Hayes, N. M. Droin, D. D. Newmeyer, M. Schuler and D. R. Green (2004). "Direct activation of Bax by p53 mediates mitochondrial membrane permeabilization and apoptosis." Science **303**(5660): 1010-1014.

Choi, Y. L., M. Soda, Y. Yamashita, T. Ueno, J. Takashima, T. Nakajima, Y. Yatabe, K. Takeuchi, T. Hamada, H. Haruta, Y. Ishikawa, H. Kimura, T. Mitsudomi, Y. Tanio, H. Mano and A. L. C. S. Group (2010). "EML4-ALK mutations in lung cancer that confer resistance to ALK inhibitors." N Engl J Med **363**(18): 1734-1739.

Choi, Y. L., K. Takeuchi, M. Soda, K. Inamura, Y. Togashi, S. Hatano, M. Enomoto, T. Hamada, H. Haruta, H. Watanabe, K. Kurashina, H. Hatanaka, T. Ueno, S. Takada, Y. Yamashita, Y. Sugiyama, Y. Ishikawa and H. Mano (2008). "Identification of novel isoforms of the EML4-ALK transforming gene in non-small cell lung cancer." Cancer Res **68**(13): 4971-4976.

Chou, T. C. (2010). "Drug combination studies and their synergy quantification using the Chou-Talalay method." Cancer Res **70**(2): 440-446.

Chou, T. C. and P. Talalay (1984). "Quantitative analysis of dose-effect relationships: the combined effects of multiple drugs or enzyme inhibitors." Adv Enzyme Regul **22**: 27-55.

Chu, G. (1994). "Cellular responses to cisplatin. The roles of DNA-binding proteins and DNA repair." J Biol Chem **269**(2): 787-790.

Chua, K. N., W. J. Sim, V. Racine, S. Y. Lee, B. C. Goh and J. P. Thiery (2012). "A cell-based small molecule screening method for identifying inhibitors of epithelial-mesenchymal transition in carcinoma." PLoS One **7**(3): e33183.

Chène, P. (2001). "The role of tetramerization in p53 function." Oncogene **20**(21): 2611-2617.

Citri, A. and Y. Yarden (2006). "EGF-ERBB signalling: towards the systems level." Nat Rev Mol Cell Biol **7**(7): 505-516.

Clapp, C., L. Portt, C. Khoury, S. Sheibani, G. Norman, P. Ebner, R. Eid, H. Vali, C. A. Mandato, F. Madeo and M. T. Greenwood (2012). "14-3-3 protects against stress-induced apoptosis." Cell Death Dis **3**: e348.

Colburn, N. H., W. F. Bruegge, J. R. Bates, R. H. Gray, J. D. Rossen, W. H. Kelsey and T. Shimada (1978). "Correlation of anchorage-independent growth with tumorigenicity of chemically transformed mouse epidermal cells." Cancer Res **38**(3): 624-634.

Colomer, R., R. Lupu, S. S. Bacus and E. P. Gelmann (1994). "erbB-2 antisense oligonucleotides inhibit the proliferation of breast carcinoma cells with erbB-2 oncogene amplification." Br J Cancer **70**(5): 819-825.

Crawford, L. V., D. C. Pim and R. D. Bulbrook (1982). "Detection of antibodies against the cellular protein p53 in sera from patients with breast cancer." Int J Cancer **30**(4): 403-408.

Crinò, L., G. Scagliotti, M. Marangolo, F. Figoli, M. Clerici, F. De Marinis, F. Salvati, G. Cruciani, L. Dogliotti, F. Pucci, A. Paccagnella, V. Adamo, G. Altavilla, P. Incoronato, M. Trippetti, A. M. Mosconi, A. Santucci, S. Sorbolini, C. Oliva and M. Tonato (1997). "Cisplatin-gemcitabine combination in advanced non-small-cell lung cancer: a phase II study." J Clin Oncol **15**(1): 297-303.

Cui, W., E. M. Yazlovitskaya, M. S. Mayo, J. C. Pelling and D. L. Persons (2000). "Cisplatin-induced response of c-jun N-terminal kinase 1 and extracellular signal--regulated protein kinases 1 and 2 in a series of cisplatin-resistant ovarian carcinoma cell lines." Mol Carcinog **29**(4): 219-228.

Cui, Y., J. König, J. K. Buchholz, H. Spring, I. Leier and D. Keppler (1999). "Drug resistance and ATP-dependent conjugate transport mediated by the apical multidrug resistance protein, MRP2, permanently expressed in human and canine cells." Mol Pharmacol **55**(5): 929-937.

Cullen, K. J., K. A. Newkirk, L. M. Schumaker, N. Aldosari, J. D. Rone and B. R. Haddad (2003). "Glutathione S-transferase pi amplification is associated with cisplatin resistance in head and neck squamous cell carcinoma cell lines and primary tumors." Cancer Res **63**(23): 8097-8102.

Cummings, B. S. and R. G. Schnellmann (2002). "Cisplatin-induced renal cell apoptosis: caspase 3-dependent and -independent pathways." J Pharmacol Exp Ther **302**(1): 8-17.

Côté, S., A. Rosenauer, A. Bianchini, K. Seiter, J. Vandewiele, C. Nervi and W. H. Miller (2002). "Response to histone deacetylase inhibition of novel PML/RARalpha mutants detected in retinoic acid-resistant APL cells." Blood **100**(7): 2586-2596.

D'Addario, G., M. Pintilie, N. B. Leighl, R. Feld, T. Cerny and F. A. Shepherd (2005). "Platinum-based versus non-platinum-based chemotherapy in advanced non-small-cell lung cancer: a meta-analysis of the published literature." J Clin Oncol **23**(13): 2926-2936.

Dai, Y., S. Chen, L. B. Kramer, V. L. Funk, P. Dent and S. Grant (2008). "Interactions between bortezomib and romidepsin and belinostat in chronic lymphocytic leukemia cells." Clin Cancer Res **14**(2): 549-558.

Dan, H. C., M. Sun, S. Kaneko, R. I. Feldman, S. V. Nicosia, H. G. Wang, B. K. Tsang and J. Q. Cheng (2004). "Akt phosphorylation and stabilization of X-linked inhibitor of apoptosis protein (XIAP)." J Biol Chem **279**(7): 5405-5412.

Dasika, G. K., S. C. Lin, S. Zhao, P. Sung, A. Tomkinson and E. Y. Lee (1999). "DNA damage-induced cell cycle checkpoints and DNA strand break repair in development and tumorigenesis." Oncogene **18**(55): 7883-7899.

Datta, S. R., A. Brunet and M. E. Greenberg (1999). "Cellular survival: a play in three Akts." Genes Dev **13**(22): 2905-2927.

Davies, A. M., P. N. Lara, P. C. Mack and D. R. Gandara (2007). "Incorporating bortezomib into the treatment of lung cancer." Clin Cancer Res **13**(15 Pt 2): s4647-4651.

Davies, H., G. R. Bignell, C. Cox, P. Stephens, S. Edkins, S. Clegg, J. Teague, H. Woffendin, M. J. Garnett, W. Bottomley, N. Davis, E. Dicks, R. Ewing, Y. Floyd, K. Gray, S. Hall, R. Hawes, J. Hughes, V. Kosmidou, A. Menzies, C. Mould, A. Parker, C. Stevens, S. Watt, S. Hooper, R. Wilson, H. Jayatilake, B. A. Gusterson, C. Cooper, J. Shipley, D. Hargrave, K. Pritchard-Jones, N. Maitland, G. Chenevix-Trench, G. J. Riggins, D. D.

Bigner, G. Palmieri, A. Cossu, A. Flanagan, A. Nicholson, J. W. Ho, S. Y. Leung, S. T. Yuen, B. L. Weber, H. F. Seigler, T. L. Darrow, H. Paterson, R. Marais, C. J. Marshall, R. Wooster, M. R. Stratton and P. A. Futreal (2002). "Mutations of the BRAF gene in human cancer." Nature **417**(6892): 949-954.

Dawson, M. A. and T. Kouzarides (2012). "Cancer epigenetics: from mechanism to therapy." Cell **150**(1): 12-27.

Day, T. A., B. K. Davis, M. B. Gillespie, J. K. Joe, M. Kibbey, B. Martin-Harris, B. Neville, M. S. Richardson, S. Rosenzweig, A. K. Sharma, M. M. Smith, S. Stewart and R. K. Stuart (2003). "Oral cancer treatment." Curr Treat Options Oncol **4**(1): 27-41.

de Ruijter, A. J., A. H. van Gennip, H. N. Caron, S. Kemp and A. B. van Kuilenburg (2003). "Histone deacetylases (HDACs): characterization of the classical HDAC family." Biochem J **370**(Pt 3): 737-749.

Deak, M., A. D. Clifton, L. M. Lucocq and D. R. Alessi (1998). "Mitogen- and stress-activated protein kinase-1 (MSK1) is directly activated by MAPK and SAPK2/p38, and may mediate activation of CREB." EMBO J **17**(15): 4426-4441.

Dejean, L. M., S. Martinez-Caballero and K. W. Kinnally (2006). "Is MAC the knife that cuts cytochrome c from mitochondria during apoptosis?" Cell Death Differ **13**(8): 1387-1395.

Dejean, L. M., S. Martinez-Caballero, S. Manon and K. W. Kinnally (2006). "Regulation of the mitochondrial apoptosis-induced channel, MAC, by BCL-2 family proteins." Biochim Biophys Acta **1762**(2): 191-201.

DeLeo, A. B., G. Jay, E. Appella, G. C. Dubois, L. W. Law and L. J. Old (1979). "Detection of a transformation-related antigen in chemically induced sarcomas and other transformed cells of the mouse." Proc Natl Acad Sci U S A **76**(5): 2420-2424.

Dempke, W., W. Voigt, A. Grothey, B. T. Hill and H. J. Schmoll (2000). "Cisplatin resistance and oncogenes--a review." Anticancer Drugs **11**(4): 225-236.

Deng, T. and M. Karin (1994). "c-Fos transcriptional activity stimulated by H-Ras-activated protein kinase distinct from JNK and ERK." Nature **371**(6493): 171-175.

Dent, P. and S. Grant (2001). "Pharmacologic interruption of the mitogen-activated extracellular-regulated kinase/mitogen-activated protein kinase signal transduction pathway: potential role in promoting cytotoxic drug action." Clin Cancer Res **7**(4): 775-783.

Deppert, W., G. Buschhausen-Denker, T. Patschinsky and K. Steinmeyer (1990). "Cell cycle control of p53 in normal (3T3) and chemically transformed (Meth A) mouse cells. II. Requirement for cell cycle progression." Oncogene **5**(11): 1701-1706.

Deroanne, C. F., K. Bonjean, S. Servotte, L. Devy, A. Colige, N. Clausse, S. Blacher, E. Verdin, J. M. Foidart, B. V. Nusgens and V. Castronovo (2002). "Histone deacetylases inhibitors as anti-angiogenic agents altering vascular endothelial growth factor signaling." Oncogene **21**(3): 427-436.

Detterbeck, F. C., D. J. Boffa and L. T. Tanoue (2009). "The new lung cancer staging system." Chest **136**(1): 260-271.

Deubzer, H. E., M. C. Schier, I. Oehme, M. Lodrini, B. Haendler, A. Sommer and O. Witt (2013). "HDAC11 is a novel drug target in carcinomas." Int J Cancer **132**(9): 2200-2208.

Dexter, D. L. and J. T. Leith (1986). "Tumor heterogeneity and drug resistance." J Clin Oncol **4**(2): 244-257.

Dhillon, K. K., E. M. Swisher and T. Taniguchi (2011). "Secondary mutations of BRCA1/2 and drug resistance." Cancer Sci **102**(4): 663-669.

Di Agostino, S., S. Strano, V. Emiliozzi, V. Zerbini, M. Mottolese, A. Sacchi, G. Blandino and G. Piaggio (2006). "Gain of function of mutant p53: the mutant p53/NF-Y protein complex reveals an aberrant transcriptional mechanism of cell cycle regulation." Cancer Cell **10**(3): 191-202.

Di Como, C. J., C. Gaiddon and C. Prives (1999). "p73 function is inhibited by tumor-derived p53 mutants in mammalian cells." Mol Cell Biol **19**(2): 1438-1449.

Di Leonardo, A., S. P. Linke, K. Clarkin and G. M. Wahl (1994). "DNA damage triggers a prolonged p53-dependent G1 arrest and long-term induction of Cip1 in normal human fibroblasts." Genes Dev **8**(21): 2540-2551.

Di Stefano, V., S. Soddu, A. Sacchi and G. D'Orazi (2005). "HIPK2 contributes to PCAF-mediated p53 acetylation and selective transactivation of p21Waf1 after nonapoptotic DNA damage." Oncogene **24**(35): 5431-5442.

Ding, H. F., Y. L. Lin, G. McGill, P. Juo, H. Zhu, J. Blenis, J. Yuan and D. E. Fisher (2000). "Essential role for caspase-8 in transcription-independent apoptosis triggered by p53." J Biol Chem **275**(49): 38905-38911.

Donehower, L. A., M. Harvey, B. L. Slagle, M. J. McArthur, C. A. Montgomery, J. S. Butel and A. Bradley (1992). "Mice deficient for p53 are developmentally normal but susceptible to spontaneous tumours." Nature **356**(6366): 215-221.

Donmez, G. and L. Guarente (2010). "Aging and disease: connections to sirtuins." Aging Cell **9**(2): 285-290.

Downward, J. (2003). "Targeting RAS signalling pathways in cancer therapy." Nat Rev Cancer **3**(1): 11-22.

Driessens, G., B. Beck, A. Caauwe, B. D. Simons and C. Blanpain (2012). "Defining the mode of tumour growth by clonal analysis." Nature **488**(7412): 527-530.

Duan, J., J. Friedman, L. Nottingham, Z. Chen, G. Ara and C. Van Waes (2007). "Nuclear factor-kappaB p65 small interfering RNA or proteasome inhibitor bortezomib sensitizes head and neck squamous cell carcinomas to classic histone deacetylase inhibitors and novel histone deacetylase inhibitor PXD101." Mol Cancer Ther **6**(1): 37-50.

Dudás, A. and M. Chovanec (2004). "DNA double-strand break repair by homologous recombination." Mutat Res **566**(2): 131-167.

Dutt, A., A. H. Ramos, P. S. Hammerman, C. Mermel, J. Cho, T. Sharifnia, A. Chande, K. E. Tanaka, N. Stransky, H. Greulich, N. S. Gray and M. Meyerson (2011). "Inhibitor-sensitive FGFR1 amplification in human non-small cell lung cancer." PLoS One **6**(6): e20351.

Earnshaw, W. C., L. M. Martins and S. H. Kaufmann (1999). "Mammalian caspases: structure, activation, substrates, and functions during apoptosis." Annu Rev Biochem **68**: 383-424.

Eastman, A. (1987). "Cross-linking of glutathione to DNA by cancer chemotherapeutic platinum coordination complexes." Chem Biol Interact **61**(3): 241-248.

Eastman, A. (1987). "The formation, isolation and characterization of DNA adducts produced by anticancer platinum complexes." Pharmacol Ther **34**(2): 155-166.

Eastman, A. (1990). "Activation of programmed cell death by anticancer agents: cisplatin as a model system." Cancer Cells **2**(8-9): 275-280.

Eckardt, J. R., D. L. Bentsion, O. N. Lipatov, I. S. Polyakov, F. R. Mackintosh, D. A. Karlin, G. S. Baker and H. B. Breitz (2009). "Phase II study of picoplatin as second-line therapy for patients with small-cell lung cancer." J Clin Oncol **27**(12): 2046-2051.

Eckelman, B. P., G. S. Salvesen and F. L. Scott (2006). "Human inhibitor of apoptosis proteins: why XIAP is the black sheep of the family." EMBO Rep **7**(10): 988-994.

Egan, S. E., B. W. Giddings, M. W. Brooks, L. Buday, A. M. Sizeland and R. A. Weinberg (1993). "Association of Sos Ras exchange protein with Grb2 is implicated in tyrosine kinase signal transduction and transformation." Nature **363**(6424): 45-51.

el-Deiry, W. S., T. Tokino, V. E. Velculescu, D. B. Levy, R. Parsons, J. M. Trent, D. Lin, W. E. Mercer, K. W. Kinzler and B. Vogelstein (1993). "WAF1, a potential mediator of p53 tumor suppression." Cell **75**(4): 817-825.

el-Khateeb, M., T. G. Appleton, L. R. Gahan, B. G. Charles, S. J. Berners-Price and A. M. Bolton (1999). "Reactions of cisplatin hydrolytes with methionine, cysteine, and plasma ultrafiltrate studied by a combination of HPLC and NMR techniques." J Inorg Biochem **77**(1-2): 13-21.

Elaut, G., V. Rogiers and T. Vanhaecke (2007). "The pharmaceutical potential of histone deacetylase inhibitors." Curr Pharm Des **13**(25): 2584-2620.

Elias, D. J., L. Hirschowitz, L. E. Kline, J. F. Kroener, R. O. Dillman, L. E. Walker, J. A. Robb and R. M. Timms (1990). "Phase I clinical comparative study of monoclonal antibody KS1/4 and KS1/4-methotrexate immunconjugate in patients with non-small cell lung carcinoma." Cancer Res **50**(13): 4154-4159.

ELION, G. B., G. H. HITCHINGS and H. VANDERWERFF (1951). "Antagonists of nucleic acid derivatives. VI. Purines." J Biol Chem **192**(2): 505-518.

Eliyahu, D., D. Michalovitz, S. Eliyahu, O. Pinhasi-Kimhi and M. Oren (1989). "Wild-type p53 can inhibit oncogene-mediated focus formation." Proc Natl Acad Sci U S A **86**(22): 8763-8767.

Eliyahu, D., A. Raz, P. Gruss, D. Givol and M. Oren (1984). "Participation of p53 cellular tumour antigen in transformation of normal embryonic cells." Nature **312**(5995): 646-649.

Ellis, H. M. and H. R. Horvitz (1986). "Genetic control of programmed cell death in the nematode C. elegans." Cell **44**(6): 817-829.

Ellis, L., Y. Pan, G. K. Smyth, D. J. George, C. McCormack, R. Williams-Truax, M. Mita, J. Beck, H. Burris, G. Ryan, P. Atadja, D. Butterfoss, M. Dugan, K. Culver, R. W. Johnstone and H. M. Prince (2008). "Histone deacetylase inhibitor panobinostat induces clinical responses with associated alterations in gene expression profiles in cutaneous T-cell lymphoma." Clin Cancer Res **14**(14): 4500-4510.

Esteller, M., C. Cordon-Cardo, P. G. Corn, S. J. Meltzer, K. S. Pohar, D. N. Watkins, G. Capella, M. A. Peinado, X. Matias-Guiu, J. Prat, S. B. Baylin and J. G. Herman (2001). "p14ARF silencing by promoter hypermethylation mediates abnormal intracellular localization of MDM2." Cancer Res **61**(7): 2816-2821.

Esteller, M., S. Tortola, M. Toyota, G. Capella, M. A. Peinado, S. B. Baylin and J. G. Herman (2000). "Hypermethylation-associated inactivation of p14(ARF) is independent of p16(INK4a) methylation and p53 mutational status." Cancer Res **60**(1): 129-133.

Evers, B. and J. Jonkers (2006). "Mouse models of BRCA1 and BRCA2 deficiency: past lessons, current understanding and future prospects." Oncogene **25**(43): 5885-5897.

Fan, J., D. Banerjee, P. J. Stambrook and J. R. Bertino (1997). "Modulation of cytotoxicity of chemotherapeutic drugs by activated H-ras." Biochem Pharmacol **53**(8): 1203-1209.

Fan, S., W. S. el-Deiry, I. Bae, J. Freeman, D. Jondle, K. Bhatia, A. J. Fornace, I. Magrath, K. W. Kohn and P. M. O'Connor (1994). "p53 gene mutations are associated with decreased sensitivity of human lymphoma cells to DNA damaging agents." Cancer Res **54**(22): 5824-5830.

Fanucchi, M. P., F. V. Fossella, R. Belt, R. Natale, P. Fidias, D. P. Carbone, R. Govindan, L. E. Raez, F. Robert, M. Ribeiro, W. Akerley, K. Kelly, S. A. Limentani, J. Crawford, H. J. Reimers, R. Axelrod, O. Kashala, S. Sheng and J. H. Schiller (2006). "Randomized phase II study of bortezomib alone and bortezomib in combination with docetaxel in previously treated advanced non-small-cell lung cancer." J Clin Oncol **24**(31): 5025-5033.

Farid, R. S., M. E. Bianchi, L. Falciola, B. N. Engelsberg and P. C. Billings (1996). "Differential binding of HMG1, HMG2, and a single HMG box to cisplatin-damaged DNA." Toxicol Appl Pharmacol **141**(2): 532-539.

Farmer, H., N. McCabe, C. J. Lord, A. N. Tutt, D. A. Johnson, T. B. Richardson, M. Santarosa, K. J. Dillon, I. Hickson, C. Knights, N. M. Martin, S. P. Jackson, G. C. Smith and A. Ashworth (2005). "Targeting the DNA repair defect in BRCA mutant cells as a therapeutic strategy." Nature **434**(7035): 917-921.

Fazzone, W., P. M. Wilson, M. J. Labonte, H. J. Lenz and R. D. Ladner (2009). "Histone deacetylase inhibitors suppress thymidylate synthase gene expression and synergize with the fluoropyrimidines in colon cancer cells." Int J Cancer **125**(2): 463-473.

Feng, L., M. Pan, J. Sun, H. Lu, Q. Shen, S. Zhang, T. Jiang, L. Liu, W. Jin, Y. Chen, X. Wang and H. Jin (2013). "Histone deacetylase 3 inhibits expression of PUMA in gastric cancer cells." J Mol Med (Berl) **91**(1): 49-58.

Ferry, K. V., T. C. Hamilton and S. W. Johnson (2000). "Increased nucleotide excision repair in cisplatin-resistant ovarian cancer cells: role of ERCC1-XPF." Biochem Pharmacol **60**(9): 1305-1313.

Fesik, S. W. (2000). "Insights into programmed cell death through structural biology." Cell **103**(2): 273-282.

Finlay, C. A., P. W. Hinds and A. J. Levine (1989). "The p53 proto-oncogene can act as a suppressor of transformation." Cell **57**(7): 1083-1093.

Finnin, M. S., J. R. Donigian, A. Cohen, V. M. Richon, R. A. Rifkind, P. A. Marks, R. Breslow and N. P. Pavletich (1999). "Structures of a histone deacetylase homologue bound to the TSA and SAHA inhibitors." Nature **401**(6749): 188-193.

Fiscella, M., N. Zambrano, S. J. Ullrich, T. Unger, D. Lin, B. Cho, W. E. Mercer, C. W. Anderson and E. Appella (1994). "The carboxy-terminal serine 392 phosphorylation site of human p53 is not required for wild-type activities." Oncogene **9**(11): 3249-3257.

Flaherty, K. T., J. R. Infante, A. Daud, R. Gonzalez, R. F. Kefford, J. Sosman, O. Hamid, L. Schuchter, J. Cebon, N. Ibrahim, R. Kudchadkar, H. A. Burris, G. Falchook, A. Algazi, K. Lewis, G. V. Long, I. Puzanov, P. Lebowitz, A. Singh, S. Little, P. Sun, A. Allred, D. Ouellet, K. B. Kim, K. Patel and J. Weber (2012). "Combined BRAF and MEK inhibition in melanoma with BRAF V600 mutations." N Engl J Med **367**(18): 1694-1703.

Flaherty, K. T., I. Puzanov, K. B. Kim, A. Ribas, G. A. McArthur, J. A. Sosman, P. J. O'Dwyer, R. J. Lee, J. F. Grippo, K. Nolop and P. B. Chapman (2010). "Inhibition of mutated, activated BRAF in metastatic melanoma." N Engl J Med **363**(9): 809-819.

Ford, D., D. F. Easton, M. Stratton, S. Narod, D. Goldgar, P. Devilee, D. T. Bishop, B. Weber, G. Lenoir, J. Chang-Claude, H. Sobol, M. D. Teare, J. Struewing, A. Arason, S. Scherneck, J. Peto, T. R. Rebbeck, P. Tonin, S. Neuhausen, R. Barkardottir, J. Eyfjord, H. Lynch, B. A. Ponder, S. A. Gayther and M. Zelada-Hedman (1998). "Genetic heterogeneity and penetrance analysis of the BRCA1 and BRCA2 genes in breast cancer families. The Breast Cancer Linkage Consortium." Am J Hum Genet **62**(3): 676-689.

Ford, J., M. Jiang and J. Milner (2005). "Cancer-specific functions of SIRT1 enable human epithelial cancer cell growth and survival." Cancer Res **65**(22): 10457-10463.

Ford, J. M. and P. C. Hanawalt (1997). "Expression of wild-type p53 is required for efficient global genomic nucleotide excision repair in UV-irradiated human fibroblasts." J Biol Chem **272**(44): 28073-28080.

Fraser, M., B. M. Leung, X. Yan, H. C. Dan, J. Q. Cheng and B. K. Tsang (2003). "p53 is a determinant of X-linked inhibitor of apoptosis protein/Akt-mediated chemoresistance in human ovarian cancer cells." Cancer Res **63**(21): 7081-7088.

Freed-Pastor, W. A., H. Mizuno, X. Zhao, A. Langerød, S. H. Moon, R. Rodriguez-Barrueco, A. Barsotti, A. Chicas, W. Li, A. Polotskaia, M. J. Bissell, T. F. Osborne, B. Tian, S. W. Lowe, J. M. Silva, A. L. Børresen-Dale, A. J. Levine, J. Bargonetti and C. Prives (2012). "Mutant p53 disrupts mammary tissue architecture via the mevalonate pathway." Cell **148**(1-2): 244-258.

Freed-Pastor, W. A. and C. Prives (2012). "Mutant p53: one name, many proteins." Genes Dev **26**(12): 1268-1286.

Freedman, V. H. and S. I. Shin (1974). "Cellular tumorigenicity in nude mice: correlation with cell growth in semi-solid medium." Cell **3**(4): 355-359.

Frey, R. R., C. K. Wada, R. B. Garland, M. L. Curtin, M. R. Michaelides, J. Li, L. J. Pease, K. B. Glaser, P. A. Marcotte, J. J. Bouska, S. S. Murphy and S. K. Davidsen (2002). "Trifluoromethyl ketones as inhibitors of histone deacetylase." Bioorg Med Chem Lett **12**(23): 3443-3447.

Frye, R. A. (2000). "Phylogenetic classification of prokaryotic and eukaryotic Sir2-like proteins." Biochem Biophys Res Commun **273**(2): 793-798.

Fuchs, S. Y., V. Adler, M. R. Pincus and Z. Ronai (1998). "MEKK1/JNK signaling stabilizes and activates p53." Proc Natl Acad Sci U S A **95**(18): 10541-10546.

Fuchs, Y. and H. Steller (2011). "Programmed cell death in animal development and disease." Cell **147**(4): 742-758.

Fuks, F., W. A. Burgers, A. Brehm, L. Hughes-Davies and T. Kouzarides (2000). "DNA methyltransferase Dnmt1 associates with histone deacetylase activity." Nat Genet **24**(1): 88-91.

Fulda, S., M. Los, C. Friesen and K. M. Debatin (1998). "Chemosensitivity of solid tumor cells in vitro is related to activation of the CD95 system." Int J Cancer **76**(1): 105-114.

Furumai, R., A. Matsuyama, N. Kobashi, K. H. Lee, M. Nishiyama, H. Nakajima, A. Tanaka, Y. Komatsu, N. Nishino, M. Yoshida and S. Horinouchi (2002). "FK228 (depsipeptide) as a natural prodrug that inhibits class I histone deacetylases." Cancer Res **62**(17): 4916-4921.

Gadducci, A., S. Cosio, S. Muraca and A. R. Genazzani (2002). "Molecular mechanisms of apoptosis and chemosensitivity to platinum and paclitaxel in ovarian cancer: biological data and clinical implications." Eur J Gynaecol Oncol **23**(5): 390-396.

Gaiddon, C., M. Lokshin, J. Ahn, T. Zhang and C. Prives (2001). "A subset of tumor-derived mutant forms of p53 down-regulate p63 and p73 through a direct interaction with the p53 core domain." Mol Cell Biol **21**(5): 1874-1887.

Galluzzi, L., I. Vitale, J. M. Abrams, E. S. Alnemri, E. H. Baehrecke, M. V. Blagosklonny, T. M. Dawson, V. L. Dawson, W. S. El-Deiry, S. Fulda, E. Gottlieb, D. R. Green, M. O. Hengartner, O. Kepp, R. A. Knight, S. Kumar, S. A. Lipton, X. Lu, F. Madeo, W. Malorni, P. Mehlen, G. Nuñez, M. E. Peter, M. Piacentini, D. C. Rubinsztein, Y. Shi, H. U. Simon, P. Vandenabeele, E. White, J. Yuan, B. Zhivotovsky, G. Melino and G. Kroemer (2012). "Molecular definitions of cell death subroutines: recommendations of the Nomenclature Committee on Cell Death 2012." Cell Death Differ **19**(1): 107-120.

Gao, J., B. A. Aksoy, U. Dogrusoz, G. Dresdner, B. Gross, S. O. Sumer, Y. Sun, A. Jacobsen, R. Sinha, E. Larsson, E. Cerami, C. Sander and N. Schultz (2013). "Integrative analysis of complex cancer genomics and clinical profiles using the cBioPortal." Sci Signal **6**(269): pl1.

Garcia-Manero, G., S. Assouline, J. Cortes, Z. Estrov, H. Kantarjian, H. Yang, W. M. Newsome, W. H. Miller, C. Rousseau, A. Kalita, C. Bonfils, M. Dubay, T. A. Patterson, Z. Li, J. M. Besterman, G. Reid, E. Laille, R. E. Martell and M. Minden (2008). "Phase 1 study of the oral isotype specific histone deacetylase inhibitor MGCD0103 in leukemia." Blood **112**(4): 981-989.

Garcia-Manero, G., H. M. Kantarjian, B. Sanchez-Gonzalez, H. Yang, G. Rosner, S. Verstovsek, M. Rytting, W. G. Wierda, F. Ravandi, C. Koller, L. Xiao, S. Faderl, Z. Estrov, J. Cortes, S. O'brien, E. Estey, C. Bueso-Ramos, J. Fiorentino, E. Jabbour and J. P. Issa (2006). "Phase 1/2 study of the combination of 5-aza-2'-deoxycytidine with valproic acid in patients with leukemia." Blood **108**(10): 3271-3279.

Garcia-Manero, G., H. Yang, C. Bueso-Ramos, A. Ferrajoli, J. Cortes, W. G. Wierda, S. Faderl, C. Koller, G. Morris, G. Rosner, A. Loboda, V. R. Fantin, S. S. Randolph, J. S. Hardwick, J. F. Reilly, C. Chen, J. L. Ricker, J. P. Secrist, V. M. Richon, S. R. Frankel and H. M. Kantarjian (2008). "Phase 1 study of the histone deacetylase inhibitor vorinostat (suberoylanilide hydroxamic acid [SAHA]) in patients with advanced leukemias and myelodysplastic syndromes." Blood **111**(3): 1060-1066.

Garner, E. and K. Raj (2008). "Protective mechanisms of p53-p21-pRb proteins against DNA damage-induced cell death." Cell Cycle **7**(3): 277-282.

Garrett, T. P., N. M. McKern, M. Lou, T. C. Elleman, T. E. Adams, G. O. Lovrecz, M. Kofler, R. N. Jorissen, E. C. Nice, A. W. Burgess and C. W. Ward (2003). "The crystal structure of a truncated ErbB2 ectodomain reveals an active conformation, poised to interact with other ErbB receptors." Mol Cell **11**(2): 495-505.

Gebauer, G., B. Mirakhur, Q. Nguyen, S. K. Shore, H. Simpkins and N. Dhanasekaran (2000). "Cisplatin-resistance involves the defective processing of MEKK1 in human ovarian adenocarcinoma 2008/C13 cells." Int J Oncol **16**(2): 321-325.

Geurts, T. W., P. M. Nederlof, M. W. van den Brekel, L. J. van't Veer, D. de Jong, A. A. Hart, N. van Zandwijk, H. Klomp, A. J. Balm and M. L. van Velthuysen (2005). "Pulmonary squamous cell carcinoma following head and neck squamous cell carcinoma: metastasis or second primary?" Clin Cancer Res **11**(18): 6608-6614.

Giaccone, G. (2000). "Clinical perspectives on platinum resistance." Drugs **59 Suppl 4**: 9-17; discussion 37-18.

Giaccone, G., A. Rajan, A. Berman, R. J. Kelly, E. Szabo, A. Lopez-Chavez, J. Trepel, M. J. Lee, L. Cao, I. Espinoza-Delgado, J. Spittler and P. J. Loehrer (2011). "Phase II study of belinostat in patients with recurrent or refractory advanced thymic epithelial tumors." J Clin Oncol **29**(15): 2052-2059.

Giles, F., T. Fischer, J. Cortes, G. Garcia-Manero, J. Beck, F. Ravandi, E. Masson, P. Rae, G. Laird, S. Sharma, H. Kantarjian, M. Dugan, M. Albitar and K. Bhalla (2006). "A phase I study of intravenous LBH589, a novel cinnamic hydroxamic acid analogue histone deacetylase inhibitor, in patients with refractory hematologic malignancies." Clin Cancer Res **12**(15): 4628-4635.

Gillet, L. C. and O. D. Schärer (2006). "Molecular mechanisms of mammalian global genome nucleotide excision repair." Chem Rev **106**(2): 253-276.

Gimsing, P., M. Hansen, L. M. Knudsen, P. Knoblauch, I. J. Christensen, C. E. Ooi and P. Buhl-Jensen (2008). "A phase I clinical trial of the histone deacetylase inhibitor belinostat in patients with advanced hematological neoplasia." Eur J Haematol **81**(3): 170-176.

Glaser, K. B. (2007). "HDAC inhibitors: clinical update and mechanism-based potential." Biochem Pharmacol **74**(5): 659-671.

Glasspool, R. M., R. Brown, M. E. Gore, G. J. Rustin, I. A. McNeish, R. H. Wilson, S. Pledge, J. Paul, M. Mackean, G. D. Hall, H. Gabra, S. E. Halford, J. Walker, K. Appleton, R. Ullah, S. Kaye and S. G. T. Group (2014). "A randomised, phase II trial of the DNA-hypomethylating agent 5-aza-2'-deoxycytidine (decitabine) in combination with carboplatin vs carboplatin alone in patients with recurrent, partially platinum-sensitive ovarian cancer." Br J Cancer **110**(8): 1923-1929.

Glozak, M. A., N. Sengupta, X. Zhang and E. Seto (2005). "Acetylation and deacetylation of non-histone proteins." Gene **363**: 15-23.

Glozak, M. A. and E. Seto (2007). "Histone deacetylases and cancer." Oncogene **26**(37): 5420-5432.

Go, R. S. and A. A. Adjei (1999). "Review of the comparative pharmacology and clinical activity of cisplatin and carboplatin." J Clin Oncol **17**(1): 409-422.

Goldstraw, P., J. Crowley, K. Chansky, D. J. Giroux, P. A. Groome, R. Rami-Porta, P. E. Postmus, V. Rusch, L. Sobin, I. A. f. t. S. o. L. C. I. S. Committee and P. Institutions (2007). "The IASLC Lung Cancer Staging Project: proposals for the revision of the TNM stage groupings in the forthcoming (seventh) edition of the TNM Classification of malignant tumours." J Thorac Oncol **2**(8): 706-714.

Gonzalez, V. M., M. A. Fuertes, C. Alonso and J. M. Perez (2001). "Is cisplatin-induced cell death always produced by apoptosis?" Mol Pharmacol **59**(4): 657-663.

Goodman, G. E., I. Hellström, L. Brodzinsky, C. Nicaise, B. Kulander, D. Hummel and K. E. Hellström (1990). "Phase I trial of murine monoclonal antibody L6 in breast, colon, ovarian, and lung cancer." J Clin Oncol **8**(6): 1083-1092.

Gore, S. D., S. Baylin, E. Sugar, H. Carraway, C. B. Miller, M. Carducci, M. Grever, O. Galm, T. Dauses, J. E. Karp, M. A. Rudek, M. Zhao, B. D. Smith, J. Manning, A. Jiemjit, G. Dover, A. Mays, J. Zwiebel, A. Murgo, L. J. Weng and J. G. Herman (2006). "Combined DNA methyltransferase and histone deacetylase inhibition in the treatment of myeloid neoplasms." Cancer Res **66**(12): 6361-6369.

Govindan, R., L. Ding, M. Griffith, J. Subramanian, N. D. Dees, K. L. Kanchi, C. A. Maher, R. Fulton, L. Fulton, J. Wallis, K. Chen, J. Walker, S. McDonald, R. Bose, D. Ornitz, D. Xiong, M. You, D. J. Dooling, M. Watson, E. R. Mardis and R. K. Wilson (2012). "Genomic landscape of non-small cell lung cancer in smokers and never-smokers." Cell **150**(6): 1121-1134.

Gray, S. G. and T. J. Ekström (2001). "The human histone deacetylase family." Exp Cell Res **262**(2): 75-83.

Gregory, P. D., K. Wagner and W. Hörz (2001). "Histone acetylation and chromatin remodeling." Exp Cell Res **265**(2): 195-202.

Grilli, R., A. D. Oxman and J. A. Julian (1993). "Chemotherapy for advanced non-small-cell lung cancer: how much benefit is enough?" J Clin Oncol **11**(10): 1866-1872.

Grob, T. J., U. Novak, C. Maisse, D. Barcaroli, A. U. Lüthi, F. Pirnia, B. Hügli, H. U. Graber, V. De Laurenzi, M. F. Fey, G. Melino and A. Tobler (2001). "Human delta Np73 regulates a dominant negative feedback loop for TAp73 and p53." Cell Death Differ **8**(12): 1213-1223.

Grossman, S. R. (2001). "p300/CBP/p53 interaction and regulation of the p53 response." Eur J Biochem **268**(10): 2773-2778.

Group, N. M.-A. C. (2008). "Chemotherapy in addition to supportive care improves survival in advanced non-small-cell lung cancer: a systematic review and meta-analysis of individual patient data from 16 randomized controlled trials." J Clin Oncol **26**(28): 4617-4625.

Grozinger, C. M., E. D. Chao, H. E. Blackwell, D. Moazed and S. L. Schreiber (2001). "Identification of a class of small molecule inhibitors of the sirtuin family of NAD-dependent deacetylases by phenotypic screening." J Biol Chem **276**(42): 38837-38843.

Grunstein, M. (1997). "Histone acetylation in chromatin structure and transcription." Nature **389**(6649): 349-352.

Gu, W. and R. G. Roeder (1997). "Activation of p53 sequence-specific DNA binding by acetylation of the p53 C-terminal domain." Cell **90**(4): 595-606.

Guadamillas, M. C., A. Cerezo and M. A. Del Pozo (2011). "Overcoming anoikis--pathways to anchorage-independent growth in cancer." J Cell Sci **124**(Pt 19): 3189-3197.

Guenther, M. G., O. Barak and M. A. Lazar (2001). "The SMRT and N-CoR corepressors are activating cofactors for histone deacetylase 3." Mol Cell Biol **21**(18): 6091-6101.

Gui, C. Y., L. Ngo, W. S. Xu, V. M. Richon and P. A. Marks (2004). "Histone deacetylase (HDAC) inhibitor activation of p21WAF1 involves changes in promoter-associated proteins, including HDAC1." Proc Natl Acad Sci U S A **101**(5): 1241-1246.

Guinea Viniegra, J., J. Hernández Losa, V. J. Sánchez-Arévalo, C. Parada Cobo, V. M. Fernández Soria, S. Ramón y Cajal and R. Sánchez-Prieto (2002). "Modulation of PI3K/Akt pathway by E1a mediates sensitivity to cisplatin." Oncogene **21**(46): 7131-7136.

Hackel, P. O., E. Zwick, N. Prenzel and A. Ullrich (1999). "Epidermal growth factor receptors: critical mediators of multiple receptor pathways." Curr Opin Cell Biol **11**(2): 184-189.

Haigis, M. C. and L. P. Guarente (2006). "Mammalian sirtuins--emerging roles in physiology, aging, and calorie restriction." Genes Dev **20**(21): 2913-2921.

Halder, S. K., Y. J. Cho, A. Datta, G. Anumanthan, A. J. Ham, D. P. Carbone and P. K. Datta (2011). "Elucidating the mechanism of regulation of transforming growth factor β Type II receptor expression in human lung cancer cell lines." Neoplasia **13**(10): 912-922.

Hall, S. R., L. E. Campbell and D. W. Meek (1996). "Phosphorylation of p53 at the casein kinase II site selectively regulates p53-dependent transcriptional repression but not transactivation." Nucleic Acids Res **24**(6): 1119-1126.

Hamilton, T. C., M. A. Winker, K. G. Louie, G. Batist, B. C. Behrens, T. Tsuruo, K. R. Grotzinger, W. M. McKoy, R. C. Young and R. F. Ozols (1985). "Augmentation of adriamycin, melphalan, and cisplatin cytotoxicity in drug-resistant and -sensitive human ovarian carcinoma cell lines by buthionine sulfoximine mediated glutathione depletion." Biochem Pharmacol **34**(14): 2583-2586.

Hammerman, P. S., M. L. Sos, A. H. Ramos, C. Xu, A. Dutt, W. Zhou, L. E. Brace, B. A. Woods, W. Lin, J. Zhang, X. Deng, S. M. Lim, S. Heynck, M. Peifer, J. R. Simard, M. S. Lawrence, R. C. Onofrio, H. B. Salvesen, D. Seidel, T. Zander, J. M. Heuckmann, A. Soltermann, H. Moch, M. Koker, F. Leenders, F. Gabler, S. Querings, S. Ansén, E. Brambilla, C. Brambilla, P. Lorimier, O. T. Brustugun, A. Helland, I. Petersen, J. H. Clement, H. Groen, W. Timens, H. Sietsma, E. Stoelben, J. Wolf, D. G. Beer, M. S. Tsao, M. Hanna, C. Hatton, M. J. Eck, P. A. Janne, B. E. Johnson, W. Winckler, H. Greulich, A. J. Bass, J. Cho, D. Rauh, N. S. Gray, K. K. Wong, E. B. Haura, R. K. Thomas and M. Meyerson (2011). "Mutations in the DDR2 kinase gene identify a novel therapeutic target in squamous cell lung cancer." Cancer Discov **1**(1): 78-89.

Hanahan, D. and R. A. Weinberg (2000). "The hallmarks of cancer." Cell **100**(1): 57-70.

Hanahan, D. and R. A. Weinberg (2011). "Hallmarks of cancer: the next generation." Cell **144**(5): 646-674.

Hanawalt, P. C. (2002). "Subpathways of nucleotide excision repair and their regulation." Oncogene **21**(58): 8949-8956.

Handra-Luca, A., J. Hernandez, G. Mountzios, E. Taranchon, J. Lacau-St-Guily, J. C. Soria and P. Fouret (2007). "Excision repair cross complementation group 1 immunohistochemical expression predicts objective response and cancer-specific survival in patients treated by Cisplatin-based induction chemotherapy for locally advanced head and neck squamous cell carcinoma." Clin Cancer Res **13**(13): 3855-3859.

Harper, J. W., G. R. Adami, N. Wei, K. Keyomarsi and S. J. Elledge (1993). "The p21 Cdk-interacting protein Cip1 is a potent inhibitor of G1 cyclin-dependent kinases." Cell **75**(4): 805-816.

Harper, J. W. and S. J. Elledge (2007). "The DNA damage response: ten years after." Mol Cell **28**(5): 739-745.

Harvey, M., M. J. McArthur, C. A. Montgomery, A. Bradley and L. A. Donehower (1993). "Genetic background alters the spectrum of tumors that develop in p53-deficient mice." FASEB J **7**(10): 938-943.

Haupt, S., M. Berger, Z. Goldberg and Y. Haupt (2003). "Apoptosis - the p53 network." J Cell Sci **116**(Pt 20): 4077-4085.

Haupt, S., S. di Agostino, I. Mizrahi, O. Alsheich-Bartok, M. Voorhoeve, A. Damalas, G. Blandino and Y. Haupt (2009). "Promyelocytic leukemia protein is required for gain of function by mutant p53." Cancer Res **69**(11): 4818-4826.

Haupt, Y., R. Maya, A. Kazaz and M. Oren (1997). "Mdm2 promotes the rapid degradation of p53." Nature **387**(6630): 296-299.

Haura, E. B., A. D. Ricart, T. G. Larson, P. J. Stella, L. Bazhenova, V. A. Miller, R. B. Cohen, P. D. Eisenberg, P. Selaru, K. D. Wilner and S. M. Gadgeel (2010). "A phase II study of PD-0325901, an oral MEK inhibitor, in previously treated patients with advanced non-small cell lung cancer." Clin Cancer Res **16**(8): 2450-2457.

Hayakawa, J., M. Ohmichi, H. Kurachi, H. Ikegami, A. Kimura, T. Matsuoka, H. Jikihara, D. Mercola and Y. Murata (1999). "Inhibition of extracellular signal-regulated protein kinase or c-Jun N-terminal protein kinase cascade, differentially activated by cisplatin, sensitizes human ovarian cancer cell line." J Biol Chem **274**(44): 31648-31654.

Hayakawa, J., M. Ohmichi, H. Kurachi, Y. Kanda, K. Hisamoto, Y. Nishio, K. Adachi, K. Tasaka, T. Kanzaki and Y. Murata (2000). "Inhibition of BAD phosphorylation either at serine 112 via extracellular signal-regulated protein kinase cascade or at serine 136 via Akt cascade sensitizes human ovarian cancer cells to cisplatin." Cancer Res **60**(21): 5988-5994.

Hengstler, J. G., J. Lange, A. Kett, N. Dornhöfer, R. Meinert, M. Arand, P. G. Knapstein, R. Becker, F. Oesch and B. Tanner (1999). "Contribution of c-erbB-2 and topoisomerase IIalpha to chemoresistance in ovarian cancer." Cancer Res **59**(13): 3206-3214.

Henkels, K. M. and J. J. Turchi (1999). "Cisplatin-induced apoptosis proceeds by caspase-3-dependent and -independent pathways in cisplatin-resistant and -sensitive human ovarian cancer cell lines." Cancer Res **59**(13): 3077-3083.

Hennessy, B. T., D. L. Smith, P. T. Ram, Y. Lu and G. B. Mills (2005). "Exploiting the PI3K/AKT pathway for cancer drug discovery." Nat Rev Drug Discov **4**(12): 988-1004.

Henson, E. S. and S. B. Gibson (2006). "Surviving cell death through epidermal growth factor (EGF) signal transduction pathways: implications for cancer therapy." Cell Signal **18**(12): 2089-2097.

Herceg, Z. and Z. Q. Wang (2001). "Functions of poly(ADP-ribose) polymerase (PARP) in DNA repair, genomic integrity and cell death." Mutat Res **477**(1-2): 97-110.

Hernández Losa, J., C. Parada Cobo, J. Guinea Viniegra, V. J. Sánchez-Arevalo Lobo, S. Ramón y Cajal and R. Sánchez-Prieto (2003). "Role of the p38 MAPK pathway in cisplatin-based therapy." Oncogene **22**(26): 3998-4006.

Hertel, L. W., G. B. Boder, J. S. Kroin, S. M. Rinzel, G. A. Poore, G. C. Todd and G. B. Grindey (1990). "Evaluation of the antitumor activity of gemcitabine (2',2'-difluoro-2'-deoxycytidine)." Cancer Res **50**(14): 4417-4422.

Hess-Stumpp, H. (2005). "Histone deacetylase inhibitors and cancer: from cell biology to the clinic." Eur J Cell Biol **84**(2-3): 109-121.

Heymach, J. V., M. Nilsson, G. Blumenschein, V. Papadimitrakopoulou and R. Herbst (2006). "Epidermal growth factor receptor inhibitors in development for the treatment of non-small cell lung cancer." Clin Cancer Res **12**(14 Pt 2): 4441s-4445s.

Hinds, P., C. Finlay and A. J. Levine (1989). "Mutation is required to activate the p53 gene for cooperation with the ras oncogene and transformation." J Virol **63**(2): 739-746.

Hirao, A., Y. Y. Kong, S. Matsuoka, A. Wakeham, J. Ruland, H. Yoshida, D. Liu, S. J. Elledge and T. W. Mak (2000). "DNA damage-induced activation of p53 by the checkpoint kinase Chk2." Science **287**(5459): 1824-1827.

Hock, A. K., A. M. Vigneron, S. Carter, R. L. Ludwig and K. H. Vousden (2011). "Regulation of p53 stability and function by the deubiquitinating enzyme USP42." EMBO J **30**(24): 4921-4930.

Hockenbery, D. M., Z. N. Oltvai, X. M. Yin, C. L. Milliman and S. J. Korsmeyer (1993). "Bcl-2 functions in an antioxidant pathway to prevent apoptosis." Cell **75**(2): 241-251.

Hodi, F. S., R. J. Soiffer, J. Clark, D. M. Finkelstein and F. G. Haluska (2002). "Phase II study of paclitaxel and carboplatin for malignant melanoma." Am J Clin Oncol **25**(3): 283-286.

Holohan, C., S. Van Schaeybroeck, D. B. Longley and P. G. Johnston (2013). "Cancer drug resistance: an evolving paradigm." Nat Rev Cancer **13**(10): 714-726.

Holzer, A. K. and S. B. Howell (2006). "The internalization and degradation of human copper transporter 1 following cisplatin exposure." Cancer Res **66**(22): 10944-10952.

Holzer, A. K., G. Samimi, K. Katano, W. Naerdemann, X. Lin, R. Safaei and S. B. Howell (2004). "The copper influx transporter human copper transport protein 1 regulates the uptake of cisplatin in human ovarian carcinoma cells." Mol Pharmacol **66**(4): 817-823.

Horowitz, J. M., S. H. Park, E. Bogenmann, J. C. Cheng, D. W. Yandell, F. J. Kaye, J. D. Minna, T. P. Dryja and R. A. Weinberg (1990). "Frequent inactivation of the retinoblastoma anti-oncogene is restricted to a subset of human tumor cells." Proc Natl Acad Sci U S A **87**(7): 2775-2779.

Horvitz, H. R. (1999). "Genetic control of programmed cell death in the nematode Caenorhabditis elegans." Cancer Res **59**(7 Suppl): 1701s-1706s.

Hotta, K., K. Matsuo, H. Ueoka, K. Kiura, M. Tabata and M. Tanimoto (2004). "Meta-analysis of randomized clinical trials comparing Cisplatin to Carboplatin in patients with advanced non-small-cell lung cancer." J Clin Oncol **22**(19): 3852-3859.

Hotta, K., K. Matsuo, H. Ueoka, K. Kiura, M. Tabata and M. Tanimoto (2004). "Role of adjuvant chemotherapy in patients with resected non-small-cell lung cancer: reappraisal with a meta-analysis of randomized controlled trials." J Clin Oncol **22**(19): 3860-3867.

Hromas, R. A., J. A. North and C. P. Burns (1987). "Decreased cisplatin uptake by resistant L1210 leukemia cells." Cancer Lett **36**(2): 197-201.

Huang, D. C., C. J. Marshall and J. F. Hancock (1993). "Plasma membrane-targeted ras GTPase-activating protein is a potent suppressor of p21ras function." Mol Cell Biol **13**(4): 2420-2431.

Huang, d. W., B. T. Sherman and R. A. Lempicki (2009). "Systematic and integrative analysis of large gene lists using DAVID bioinformatics resources." Nat Protoc **4**(1): 44-57.

Huang, H., L. Zhu, B. R. Reid, G. P. Drobny and P. B. Hopkins (1995). "Solution structure of a cisplatin-induced DNA interstrand cross-link." Science **270**(5243): 1842-1845.

Huang, J. C., D. B. Zamble, J. T. Reardon, S. J. Lippard and A. Sancar (1994). "HMG-domain proteins specifically inhibit the repair of the major DNA adduct of the anticancer drug cisplatin by human excision nuclease." Proc Natl Acad Sci U S A **91**(22): 10394-10398.

Huang, M. H., J. H. Lee, Y. J. Chang, H. H. Tsai, Y. L. Lin, A. M. Lin and J. C. Yang (2013). "MEK inhibitors reverse resistance in epidermal growth factor receptor mutation lung cancer cells with acquired resistance to gefitinib." Mol Oncol **7**(1): 112-120.

Huang, S. K., A. M. Scruggs, J. Donaghy, J. C. Horowitz, Z. Zaslona, S. Przybranowski, E. S. White and M. Peters-Golden (2013). "Histone modifications are responsible for decreased Fas expression and apoptosis resistance in fibrotic lung fibroblasts." Cell Death Dis **4**: e621.

Huang, W., A. H. Yang, D. Matsumoto, W. Collette, L. Marroquin, M. Ko, S. Aguirre and H. S. Younis (2009). "PD0325901, a mitogen-activated protein kinase kinase inhibitor, produces ocular toxicity in a rabbit animal model of retinal vein occlusion." J Ocul Pharmacol Ther **25**(6): 519-530.

Hubbert, C., A. Guardiola, R. Shao, Y. Kawaguchi, A. Ito, A. Nixon, M. Yoshida, X. F. Wang and T. P. Yao (2002). "HDAC6 is a microtubule-associated deacetylase." Nature **417**(6887): 455-458.

Huffman, D. M., W. E. Grizzle, M. M. Bamman, J. S. Kim, I. A. Eltoum, A. Elgavish and T. R. Nagy (2007). "SIRT1 is significantly elevated in mouse and human prostate cancer." Cancer Res **67**(14): 6612-6618.

Hung, M. C. and Y. K. Lau (1999). "Basic science of HER-2/neu: a review." Semin Oncol **26**(4 Suppl 12): 51-59.

Hwang, B. J., J. M. Ford, P. C. Hanawalt and G. Chu (1999). "Expression of the p48 xeroderma pigmentosum gene is p53-dependent and is involved in global genomic repair." Proc Natl Acad Sci U S A **96**(2): 424-428.

Häcker, S., S. Karl, I. Mader, S. Cristofanon, T. Schweitzer, J. Krauss, S. Rutkowski, K. M. Debatin and S. Fulda (2011). "Histone deacetylase inhibitors prime medulloblastoma cells for chemotherapy-induced apoptosis by enhancing p53-dependent Bax activation." Oncogene **30**(19): 2275-2281.

Imai, S., C. M. Armstrong, M. Kaeberlein and L. Guarente (2000). "Transcriptional silencing and longevity protein Sir2 is an NAD-dependent histone deacetylase." Nature **403**(6771): 795-800.

Imai, T., S. Adachi, K. Nishijo, M. Ohgushi, M. Okada, T. Yasumi, K. Watanabe, R. Nishikomori, T. Nakayama, S. Yonehara, J. Toguchida and T. Nakahata (2003). "FR901228 induces tumor regression associated with induction of Fas ligand and activation of Fas signaling in human osteosarcoma cells." Oncogene **22**(58): 9231-9242.

Imamura, T., H. Izumi, G. Nagatani, T. Ise, M. Nomoto, Y. Iwamoto and K. Kohno (2001). "Interaction with p53 enhances binding of cisplatin-modified DNA by high mobility group 1 protein." J Biol Chem **276**(10): 7534-7540.

Irmer, D., J. O. Funk and A. Blaukat (2007). "EGFR kinase domain mutations - functional impact and relevance for lung cancer therapy." Oncogene **26**(39): 5693-5701.

Irwin, M. S. and W. G. Kaelin (2001). "Role of the newer p53 family proteins in malignancy." Apoptosis **6**(1-2): 17-29.

Ishida, S., J. Lee, D. J. Thiele and I. Herskowitz (2002). "Uptake of the anticancer drug cisplatin mediated by the copper transporter Ctr1 in yeast and mammals." Proc Natl Acad Sci U S A **99**(22): 14298-14302.

Ishida, S., F. McCormick, K. Smith-McCune and D. Hanahan (2010). "Enhancing tumor-specific uptake of the anticancer drug cisplatin with a copper chelator." Cancer Cell **17**(6): 574-583.

Ishikawa, T. (1992). "The ATP-dependent glutathione S-conjugate export pump." Trends Biochem Sci **17**(11): 463-468.

Ito, A., Y. Kawaguchi, C. H. Lai, J. J. Kovacs, Y. Higashimoto, E. Appella and T. P. Yao (2002). "MDM2-HDAC1-mediated deacetylation of p53 is required for its degradation." EMBO J **21**(22): 6236-6245.

Ito, A., C. H. Lai, X. Zhao, S. Saito, M. H. Hamilton, E. Appella and T. P. Yao (2001). "p300/CBP-mediated p53 acetylation is commonly induced by p53-activating agents and inhibited by MDM2." EMBO J **20**(6): 1331-1340.

Ivanov, G. S., T. Ivanova, J. Kurash, A. Ivanov, S. Chuikov, F. Gizatullin, E. M. Herrera-Medina, F. Rauscher, D. Reinberg and N. A. Barlev (2007). "Methylation-acetylation interplay activates p53 in response to DNA damage." Mol Cell Biol **27**(19): 6756-6769.

Jackson, E. L., N. Willis, K. Mercer, R. T. Bronson, D. Crowley, R. Montoya, T. Jacks and D. A. Tuveson (2001). "Analysis of lung tumor initiation and progression using conditional expression of oncogenic K-ras." Genes Dev **15**(24): 3243-3248.

Jacobson, S. and L. Pillus (1999). "Modifying chromatin and concepts of cancer." Curr Opin Genet Dev **9**(2): 175-184.

Jain, S., J. Zain and O. O'Connor (2012). "Novel therapeutic agents for cutaneous T-Cell lymphoma." J Hematol Oncol **5**: 24.

Jamieson, E. R. and S. J. Lippard (1999). "Structure, Recognition, and Processing of Cisplatin-DNA Adducts." Chem Rev **99**(9): 2467-2498.

Janku, F., J. J. Wheler, S. N. Westin, S. L. Moulder, A. Naing, A. M. Tsimberidou, S. Fu, G. S. Falchook, D. S. Hong, I. Garrido-Laguna, R. Luthra, J. J. Lee, K. H. Lu and R. Kurzrock (2012). "PI3K/AKT/mTOR inhibitors in patients with breast and gynecologic malignancies harboring PIK3CA mutations." J Clin Oncol **30**(8): 777-782.

Jayaraman, J. and C. Prives (1995). "Activation of p53 sequence-specific DNA binding by short single strands of DNA requires the p53 C-terminus." Cell **81**(7): 1021-1029.

Jayaraman, L., N. C. Moorthy, K. G. Murthy, J. L. Manley, M. Bustin and C. Prives (1998). "High mobility group protein-1 (HMG-1) is a unique activator of p53." Genes Dev **12**(4): 462-472.

Jenuwein, T. and C. D. Allis (2001). "Translating the histone code." Science **293**(5532): 1074-1080.

Jiang, J., X. Liang, X. Zhou, R. Huang and Z. Chu (2007). "A meta-analysis of randomized controlled trials comparing carboplatin-based to cisplatin-based chemotherapy in advanced non-small cell lung cancer." Lung Cancer **57**(3): 348-358.

Jiang, X. and X. Wang (2000). "Cytochrome c promotes caspase-9 activation by inducing nucleotide binding to Apaf-1." J Biol Chem **275**(40): 31199-31203.

Jin, S., T. Tong, W. Fan, F. Fan, M. J. Antinore, X. Zhu, L. Mazzacurati, X. Li, K. L. Petrik, B. Rajasekaran, M. Wu and Q. Zhan (2002). "GADD45-induced cell cycle G2-M arrest associates with altered subcellular distribution of cyclin B1 and is independent of p38 kinase activity." Oncogene **21**(57): 8696-8704.

Jing, X. B., X. B. Cai, H. Hu, S. Z. Chen, B. M. Chen and J. Y. Cai (2007). "Reactive oxygen species and mitochondrial membrane potential are modulated during CDDP-induced apoptosis in EC-109 cells." Biochem Cell Biol **85**(2): 265-271.

Joerger, A. C. and A. R. Fersht (2008). "Structural biology of the tumor suppressor p53." Annu Rev Biochem **77**: 557-582.

Joerger, A. C. and A. R. Fersht (2010). "The tumor suppressor p53: from structures to drug discovery." Cold Spring Harb Perspect Biol **2**(6): a000919.

Johnson, D. H. (2000). "Evolution of cisplatin-based chemotherapy in non-small cell lung cancer: a historical perspective and the eastern cooperative oncology group experience." Chest **117**(4 Suppl 1): 133S-137S.

Johnson, G. L. and R. Lapadat (2002). "Mitogen-activated protein kinase pathways mediated by ERK, JNK, and p38 protein kinases." Science **298**(5600): 1911-1912.

Johnson, S. W., P. B. Laub, J. S. Beesley, R. F. Ozols and T. C. Hamilton (1997). "Increased platinum-DNA damage tolerance is associated with cisplatin resistance and cross-resistance to various chemotherapeutic agents in unrelated human ovarian cancer cell lines." Cancer Res **57**(5): 850-856.

Johnstone, R. W. (2002). "Histone-deacetylase inhibitors: novel drugs for the treatment of cancer." Nat Rev Drug Discov **1**(4): 287-299.

Joubel, A., R. J. Chalkley, K. F. Medzihradszky, H. Hondermarck and A. L. Burlingame (2009). "Identification of new p53 acetylation sites in COS-1 cells." Mol Cell Proteomics **8**(6): 1167-1173.

Ju, R. and M. T. Muller (2003). "Histone deacetylase inhibitors activate p21(WAF1) expression via ATM." Cancer Res **63**(11): 2891-2897.

Juan, L. J., W. J. Shia, M. H. Chen, W. M. Yang, E. Seto, Y. S. Lin and C. W. Wu (2000). "Histone deacetylases specifically down-regulate p53-dependent gene activation." J Biol Chem **275**(27): 20436-20443.

Jänne, P. A., A. T. Shaw, J. R. Pereira, G. Jeannin, J. Vansteenkiste, C. Barrios, F. A. Franke, L. Grinsted, V. Zazulina, P. Smith, I. Smith and L. Crinò (2013). "Selumetinib plus docetaxel for KRAS-mutant advanced non-small-cell lung cancer: a randomised, multicentre, placebo-controlled, phase 2 study." Lancet Oncol **14**(1): 38-47.

Kachhap, S. K., N. Rosmus, S. J. Collis, M. S. Kortenhorst, M. D. Wissing, M. Hedayati, S. Shabbeer, J. Mendonca, J. Deangelis, L. Marchionni, J. Lin, N. Höti, J. W. Nortier, T. L. DeWeese, H. Hammers and M. A. Carducci (2010). "Downregulation of homologous recombination DNA repair genes by HDAC inhibition in prostate cancer is mediated through the E2F1 transcription factor." PLoS One **5**(6): e11208.

Kanzawa, T., Y. Kondo, H. Ito, S. Kondo and I. Germano (2003). "Induction of autophagic cell death in malignant glioma cells by arsenic trioxide." Cancer Res **63**(9): 2103-2108.

Karagianni, P. and J. Wong (2007). "HDAC3: taking the SMRT-N-CoRrect road to repression." Oncogene **26**(37): 5439-5449.

Karagiannis, T. C., K. N. Harikrishnan, H. Kn and A. El-Osta (2007). "Disparity of histone deacetylase inhibition on repair of radiation-induced DNA damage on euchromatin and constitutive heterochromatin compartments." Oncogene **26**(27): 3963-3971.

Kartalou, M. and J. M. Essigmann (2001). "Recognition of cisplatin adducts by cellular proteins." Mutat Res **478**(1-2): 1-21.

Kasahara, K., Y. Fujiwara, K. Nishio, T. Ohmori, Y. Sugimoto, K. Komiya, T. Matsuda and N. Saijo (1991). "Metallothionein content correlates with the sensitivity of human small cell lung cancer cell lines to cisplatin." Cancer Res **51**(12): 3237-3242.

Katano, K., A. Kondo, R. Safaei, A. Holzer, G. Samimi, M. Mishima, Y. M. Kuo, M. Rochdi and S. B. Howell (2002). "Acquisition of resistance to cisplatin is accompanied by changes in the cellular pharmacology of copper." Cancer Res **62**(22): 6559-6565.

Katayama, R., A. T. Shaw, T. M. Khan, M. Mino-Kenudson, B. J. Solomon, B. Halmos, N. A. Jessop, J. C. Wain, A. T. Yeo, C. Benes, L. Drew, J. C. Saeh, K. Crosby, L. V. Sequist, A. J. Iafrate and J. A. Engelman (2012). "Mechanisms of acquired crizotinib resistance in ALK-rearranged lung Cancers." Sci Transl Med **4**(120): 120ra117.

Kaufmann, O., E. Fietze, J. Mengs and M. Dietel (2001). "Value of p63 and cytokeratin 5/6 as immunohistochemical markers for the differential diagnosis of poorly differentiated and undifferentiated carcinomas." Am J Clin Pathol **116**(6): 823-830.

Kawano, O., H. Sasaki, K. Endo, E. Suzuki, H. Haneda, H. Yukiue, Y. Kobayashi, M. Yano and Y. Fujii (2006). "PIK3CA mutation status in Japanese lung cancer patients." Lung Cancer **54**(2): 209-215.

Kedar, A., M. E. Cohen and A. I. Freeman (1978). "Peripheral neuropathy as a complication of cis-dichlorodiammineplatinum(II) treatment: a case report." Cancer Treat Rep **62**(5): 819-821.

Kelland, L. (2007). "The resurgence of platinum-based cancer chemotherapy." Nat Rev Cancer **7**(8): 573-584.

Kelley, S. L., A. Basu, B. A. Teicher, M. P. Hacker, D. H. Hamer and J. S. Lazo (1988). "Overexpression of metallothionein confers resistance to anticancer drugs." Science **241**(4874): 1813-1815.

Kelly, R. J., C. A. Carter and G. Giaccone (2012). "HER2 mutations in non-small-cell lung cancer can be continually targeted." J Clin Oncol **30**(26): 3318-3319.

Kelly, W. K. and P. A. Marks (2005). "Drug insight: Histone deacetylase inhibitors--development of the new targeted anticancer agent suberoylanilide hydroxamic acid." Nat Clin Pract Oncol **2**(3): 150-157.

Kelly, W. K., O. A. O'Connor and P. A. Marks (2002). "Histone deacetylase inhibitors: from target to clinical trials." Expert Opin Investig Drugs **11**(12): 1695-1713.

Kerr, J. F., A. H. Wyllie and A. R. Currie (1972). "Apoptosis: a basic biological phenomenon with wide-ranging implications in tissue kinetics." Br J Cancer **26**(4): 239-257.

Kessis, T. D., R. J. Slebos, W. G. Nelson, M. B. Kastan, B. S. Plunkett, S. M. Han, A. T. Lorincz, L. Hedrick and K. R. Cho (1993). "Human papillomavirus 16 E6 expression disrupts the p53-mediated cellular response to DNA damage." Proc Natl Acad Sci U S A **90**(9): 3988-3992.

Khochbin, S., A. Verdel, C. Lemercier and D. Seigneurin-Berny (2001). "Functional significance of histone deacetylase diversity." Curr Opin Genet Dev **11**(2): 162-166.

Kiernan, R., V. Brès, R. W. Ng, M. P. Coudart, S. El Messaoudi, C. Sardet, D. Y. Jin, S. Emiliani and M. Benkirane (2003). "Post-activation turn-off of NF-kappa B-dependent transcription is regulated by acetylation of p65." J Biol Chem **278**(4): 2758-2766.

Kigawa, J., Y. Minagawa, X. Cheng and N. Terakawa (1998). "Gamma-glutamyl cysteine synthetase up-regulates glutathione and multidrug resistance-associated protein in patients with chemoresistant epithelial ovarian cancer." Clin Cancer Res **4**(7): 1737-1741.

Kim, E. and W. Deppert (2004). "Transcriptional activities of mutant p53: when mutations are more than a loss." J Cell Biochem **93**(5): 878-886.

Kim, E. and W. Deppert (2007). "Interactions of mutant p53 with DNA: guilt by association." Oncogene **26**(15): 2185-2190.

Kim, H., H. C. Tu, D. Ren, O. Takeuchi, J. R. Jeffers, G. P. Zambetti, J. J. Hsieh and E. H. Cheng (2009). "Stepwise activation of BAX and BAK by tBID, BIM, and PUMA initiates mitochondrial apoptosis." Mol Cell **36**(3): 487-499.

Kim, I. A., I. H. Kim, H. J. Kim, E. K. Chie and J. S. Kim (2010). "HDAC inhibitor-mediated radiosensitization in human carcinoma cells: a general phenomenon?" J Radiat Res **51**(3): 257-263.

Kim, M. J., H. S. Yun, E. H. Hong, S. J. Lee, J. H. Baek, C. W. Lee, J. H. Yim, J. S. Kim, J. K. Park, H. D. Um and S. G. Hwang (2013). "Depletion of end-binding protein 1 (EB1) promotes apoptosis of human non-small-cell lung cancer cells via reactive oxygen species and Bax-mediated mitochondrial dysfunction." Cancer Lett **339**(1): 15-24.

Kim, S. H., S. Ahn, J. W. Han, H. W. Lee, H. Y. Lee, Y. W. Lee, M. R. Kim, K. W. Kim, W. B. Kim and S. Hong (2004). "Apicidin is a histone deacetylase inhibitor with anti-invasive and anti-angiogenic potentials." Biochem Biophys Res Commun **315**(4): 964-970.

Kohno, T., H. Ichikawa, Y. Totoki, K. Yasuda, M. Hiramoto, T. Nammo, H. Sakamoto, K. Tsuta, K. Furuta, Y. Shimada, R. Iwakawa, H. Ogiwara, T. Oike, M. Enari, A. J. Schetter, H. Okayama, A. Haugen, V. Skaug, S. Chiku, I. Yamanaka, Y. Arai, S. Watanabe, I. Sekine, S. Ogawa, C. C. Harris, H. Tsuda, T. Yoshida, J. Yokota and T. Shibata (2012). "KIF5B-RET fusions in lung adenocarcinoma." Nat Med **18**(3): 375-377.

Koike, K., T. Kawabe, T. Tanaka, S. Toh, T. Uchiumi, M. Wada, S. Akiyama, M. Ono and M. Kuwano (1997). "A canalicular multispecific organic anion transporter (cMOAT) antisense cDNA enhances drug sensitivity in human hepatic cancer cells." Cancer Res **57**(24): 5475-5479.

Kojima, H., K. Endo, H. Moriyama, Y. Tanaka, E. S. Alnemri, C. A. Slapak, B. Teicher, D. Kufe and R. Datta (1998). "Abrogation of mitochondrial cytochrome c release and caspase-3 activation in acquired multidrug resistance." J Biol Chem **273**(27): 16647-16650.

Komatsu, N., N. Kawamata, S. Takeuchi, D. Yin, W. Chien, C. W. Miller and H. P. Koeffler (2006). "SAHA, a HDAC inhibitor, has profound anti-growth activity against non-small cell lung cancer cells." Oncol Rep **15**(1): 187-191.

Koo, C. L., L. F. Kok, M. Y. Lee, T. S. Wu, Y. W. Cheng, J. D. Hsu, A. Ruan, K. C. Chao and C. P. Han (2009). "Scoring mechanisms of p16INK4a immunohistochemistry based on either independent nucleic stain or mixed cytoplasmic with nucleic expression can significantly signal to distinguish between endocervical and endometrial adenocarcinomas in a tissue microarray study." J Transl Med **7**: 25.

Koopman, G., C. P. Reutelingsperger, G. A. Kuijten, R. M. Keehnen, S. T. Pals and M. H. van Oers (1994). "Annexin V for flow cytometric detection of phosphatidylserine expression on B cells undergoing apoptosis." Blood **84**(5): 1415-1420.

Korita, P. V., T. Wakai, Y. Shirai, Y. Matsuda, J. Sakata, M. Takamura, M. Yano, A. Sanpei, Y. Aoyagi, K. Hatakeyama and Y. Ajioka (2010). "Multidrug resistance-associated protein 2 determines the efficacy of cisplatin in patients with hepatocellular carcinoma." Oncol Rep **23**(4): 965-972.

Kornberg, R. D. and Y. Lorch (1999). "Twenty-five years of the nucleosome, fundamental particle of the eukaryote chromosome." Cell **98**(3): 285-294.

Kovacs, J. J., P. J. Murphy, S. Gaillard, X. Zhao, J. T. Wu, C. V. Nicchitta, M. Yoshida, D. O. Toft, W. B. Pratt and T. P. Yao (2005). "HDAC6 regulates Hsp90 acetylation and chaperone-dependent activation of glucocorticoid receptor." Mol Cell **18**(5): 601-607.

Kozak, M. (1987). "An analysis of 5'-noncoding sequences from 699 vertebrate messenger RNAs." Nucleic Acids Res **15**(20): 8125-8148.

Kraker, A. J., C. A. Mizzen, B. G. Hartl, J. Miin, C. D. Allis and R. L. Merriman (2003). "Modulation of histone acetylation by [4-(acetylamino)-N-(2-amino-phenyl) benzamide] in HCT-8 colon carcinoma." Mol Cancer Ther **2**(4): 401-408.

Kress, M., E. May, R. Cassingena and P. May (1979). "Simian virus 40-transformed cells express new species of proteins precipitable by anti-simian virus 40 tumor serum." J Virol **31**(2): 472-483.

Krysko, D. V., T. Vanden Berghe, E. Parthoens, K. D'Herde and P. Vandenabeele (2008). "Methods for distinguishing apoptotic from necrotic cells and measuring their clearance." Methods Enzymol **442**: 307-341.

Kuerbitz, S. J., B. S. Plunkett, W. V. Walsh and M. B. Kastan (1992). "Wild-type p53 is a cell cycle checkpoint determinant following irradiation." Proc Natl Acad Sci U S A **89**(16): 7491-7495.

Kummar, S., M. Gutierrez, E. R. Gardner, E. Donovan, K. Hwang, E. J. Chung, M. J. Lee, K. Maynard, M. Kalnitskiy, A. Chen, G. Melillo, Q. C. Ryan, B. Conley, W. D. Figg, J. B. Trepel, J. Zwiebel, J. H. Doroshow and A. J. Murgo (2007). "Phase I trial of MS-275, a histone deacetylase inhibitor, administered weekly in refractory solid tumors and lymphoid malignancies." Clin Cancer Res **13**(18 Pt 1): 5411-5417.

Kundu, T. K., V. B. Palhan, Z. Wang, W. An, P. A. Cole and R. G. Roeder (2000). "Activator-dependent transcription from chromatin in vitro involving targeted histone acetylation by p300." Mol Cell **6**(3): 551-561.

Kurash, J. K., H. Lei, Q. Shen, W. L. Marston, B. W. Granda, H. Fan, D. Wall, E. Li and F. Gaudet (2008). "Methylation of p53 by Set7/9 mediates p53 acetylation and activity in vivo." Mol Cell **29**(3): 392-400.

Kussie, P. H., S. Gorina, V. Marechal, B. Elenbaas, J. Moreau, A. J. Levine and N. P. Pavletich (1996). "Structure of the MDM2 oncoprotein bound to the p53 tumor suppressor transactivation domain." Science **274**(5289): 948-953.

Kwak, E. L., Y. J. Bang, D. R. Camidge, A. T. Shaw, B. Solomon, R. G. Maki, S. H. Ou, B. J. Dezube, P. A. Jänne, D. B. Costa, M. Varella-Garcia, W. H. Kim, T. J. Lynch, P. Fidias, H. Stubbs, J. A. Engelman, L. V. Sequist, W. Tan, L. Gandhi, M. Mino-Kenudson, G. C. Wei, S. M. Shreeve, M. J. Ratain, J. Settleman, J. G. Christensen, D. A. Haber, K. Wilner, R. Salgia, G. I. Shapiro, J. W. Clark and A. J. Iafrate (2010). "Anaplastic lymphoma kinase inhibition in non-small-cell lung cancer." N Engl J Med **363**(18): 1693-1703.

Köberle, B., M. T. Tomicic, S. Usanova and B. Kaina (2010). "Cisplatin resistance: preclinical findings and clinical implications." Biochim Biophys Acta **1806**(2): 172-182.

LaBaer, J., M. D. Garrett, L. F. Stevenson, J. M. Slingerland, C. Sandhu, H. S. Chou, A. Fattaey and E. Harlow (1997). "New functional activities for the p21 family of CDK inhibitors." Genes Dev **11**(7): 847-862.

Lachner, M., D. O'Carroll, S. Rea, K. Mechtler and T. Jenuwein (2001). "Methylation of histone H3 lysine 9 creates a binding site for HP1 proteins." Nature **410**(6824): 116-120.

Lain, S., J. J. Hollick, J. Campbell, O. D. Staples, M. Higgins, M. Aoubala, A. McCarthy, V. Appleyard, K. E. Murray, L. Baker, A. Thompson, J. Mathers, S. J. Holland, M. J. Stark, G. Pass, J. Woods, D. P. Lane and N. J. Westwood (2008). "Discovery, in vivo activity, and mechanism of action of a small-molecule p53 activator." Cancer Cell **13**(5): 454-463.

Lakin, N. D., B. C. Hann and S. P. Jackson (1999). "The ataxia-telangiectasia related protein ATR mediates DNA-dependent phosphorylation of p53." Oncogene **18**(27): 3989-3995.

Lakin, N. D. and S. P. Jackson (1999). "Regulation of p53 in response to DNA damage." Oncogene **18**(53): 7644-7655.

Lane, D. P. (1992). "Cancer. p53, guardian of the genome." Nature **358**(6381): 15-16.

Lane, D. P. (1993). "Cancer. A death in the life of p53." Nature **362**(6423): 786-787.

Lane, D. P. and L. V. Crawford (1979). "T antigen is bound to a host protein in SV40-transformed cells." Nature **278**(5701): 261-263.

Lang, G. A., T. Iwakuma, Y. A. Suh, G. Liu, V. A. Rao, J. M. Parant, Y. A. Valentin-Vega, T. Terzian, L. C. Caldwell, L. C. Strong, A. K. El-Naggar and G. Lozano (2004). "Gain of function of a p53 hot spot mutation in a mouse model of Li-Fraumeni syndrome." Cell **119**(6): 861-872.

Lanni, J. S., S. W. Lowe, E. J. Licitra, J. O. Liu and T. Jacks (1997). "p53-independent apoptosis induced by paclitaxel through an indirect mechanism." Proc Natl Acad Sci U S A **94**(18): 9679-9683.

Laptenko, O. and C. Prives (2006). "Transcriptional regulation by p53: one protein, many possibilities." Cell Death Differ **13**(6): 951-961.

Lara, E., A. Mai, V. Calvanese, L. Altucci, P. Lopez-Nieva, M. L. Martinez-Chantar, M. Varela-Rey, D. Rotili, A. Nebbioso, S. Ropero, G. Montoya, J. Oyarzabal, S. Velasco, M. Serrano, M. Witt, A. Villar-Garea, A. Imhof, A. Inhof, J. M. Mato, M. Esteller and M. F. Fraga (2009). "Salermide, a Sirtuin inhibitor with a strong cancer-specific proapoptotic effect." Oncogene **28**(6): 781-791.

Lau, O. D., T. K. Kundu, R. E. Soccio, S. Ait-Si-Ali, E. M. Khalil, A. Vassilev, A. P. Wolffe, Y. Nakatani, R. G. Roeder and P. A. Cole (2000). "HATs off: selective synthetic inhibitors of the histone acetyltransferases p300 and PCAF." Mol Cell **5**(3): 589-595.

Leach, F. S., T. Tokino, P. Meltzer, M. Burrell, J. D. Oliner, S. Smith, D. E. Hill, D. Sidransky, K. W. Kinzler and B. Vogelstein (1993). "p53 Mutation and MDM2 amplification in human soft tissue sarcomas." Cancer Res **53**(10 Suppl): 2231-2234.

Lebwohl, D. and R. Canetta (1998). "Clinical development of platinum complexes in cancer therapy: an historical perspective and an update." Eur J Cancer **34**(10): 1522-1534.

Ledermann, J. A. and R. S. Kristeleit (2010). "Optimal treatment for relapsing ovarian cancer." Ann Oncol **21 Suppl 7**: vii218-222.

Lee, H., N. Sengupta, A. Villagra, N. Rezai-Zadeh and E. Seto (2006). "Histone deacetylase 8 safeguards the human ever-shorter telomeres 1B (hEST1B) protein from ubiquitin-mediated degradation." Mol Cell Biol **26**(14): 5259-5269.

Lee, J. H., M. L. Choy, L. Ngo, S. S. Foster and P. A. Marks (2010). "Histone deacetylase inhibitor induces DNA damage, which normal but not transformed cells can repair." Proc Natl Acad Sci U S A **107**(33): 14639-14644.

Lee, J. H., M. L. Choy, L. Ngo, G. Venta-Perez and P. A. Marks (2011). "Role of checkpoint kinase 1 (Chk1) in the mechanisms of resistance to histone deacetylase inhibitors." Proc Natl Acad Sci U S A **108**(49): 19629-19634.

Lee, Y. Y., C. H. Choi, I. G. Do, S. Y. Song, W. Lee, H. S. Park, T. J. Song, M. K. Kim, T. J. Kim, J. W. Lee, D. S. Bae and B. G. Kim (2011). "Prognostic value of the copper transporters, CTR1 and CTR2, in patients with ovarian carcinoma receiving platinum-based chemotherapy." Gynecol Oncol **122**(2): 361-365.

Lees-Miller, S. P., K. Sakaguchi, S. J. Ullrich, E. Appella and C. W. Anderson (1992). "Human DNA-activated protein kinase phosphorylates serines 15 and 37 in the amino-terminal transactivation domain of human p53." Mol Cell Biol **12**(11): 5041-5049.

Leighl, N. B., L. Paz-Ares, J. Y. Douillard, C. Peschel, A. Arnold, A. Depierre, A. Santoro, D. C. Betticher, U. Gatzemeier, J. Jassem, J. Crawford, D. Tu, A. Bezjak, J. S. Humphrey, M. Voi, S. Galbraith, K. Hann, L. Seymour and F. A. Shepherd (2005). "Randomized phase III study of matrix metalloproteinase inhibitor BMS-275291 in combination with paclitaxel and carboplatin in advanced non-small-cell lung cancer: National Cancer Institute of Canada-Clinical Trials Group Study BR.18." J Clin Oncol **23**(12): 2831-2839.

Leong, P. P., B. Rezai, W. M. Koch, A. Reed, D. Eisele, D. J. Lee, D. Sidransky, J. Jen and W. H. Westra (1998). "Distinguishing second primary tumors from lung metastases in patients with head and neck squamous cell carcinoma." J Natl Cancer Inst **90**(13): 972-977.

Lessene, G., P. E. Czabotar and P. M. Colman (2008). "BCL-2 family antagonists for cancer therapy." Nat Rev Drug Discov **7**(12): 989-1000.

Levi, F., L. Randimbison, V. C. Te and C. La Vecchia (2003). "Second primary cancers in laryngeal cancer patients." Eur J Cancer **39**(2): 265-267.

Levine, A. J. (1997). "p53, the cellular gatekeeper for growth and division." Cell **88**(3): 323-331.

Levine, A. J., J. Momand and C. A. Finlay (1991). "The p53 tumour suppressor gene." Nature **351**(6326): 453-456.

Levine, A. J. and M. Oren (2009). "The first 30 years of p53: growing ever more complex." Nat Rev Cancer **9**(10): 749-758.

Levine, B. and D. J. Klionsky (2004). "Development by self-digestion: molecular mechanisms and biological functions of autophagy." Dev Cell **6**(4): 463-477.

Levine, B. and J. Yuan (2005). "Autophagy in cell death: an innocent convict?" J Clin Invest **115**(10): 2679-2688.

Levresse, V., L. Marek, D. Blumberg and L. E. Heasley (2002). "Regulation of platinum-compound cytotoxicity by the c-Jun N-terminal kinase and c-Jun signaling pathway in small-cell lung cancer cells." Mol Pharmacol **62**(3): 689-697.

Lewis, A. D., J. D. Hayes and C. R. Wolf (1988). "Glutathione and glutathione-dependent enzymes in ovarian adenocarcinoma cell lines derived from a patient before and after the onset of drug resistance: intrinsic differences and cell cycle effects." Carcinogenesis **9**(7): 1283-1287.

Li, A. G., L. G. Piluso, X. Cai, B. J. Gadd, A. G. Ladurner and X. Liu (2007). "An acetylation switch in p53 mediates holo-TFIID recruitment." Mol Cell **28**(3): 408-421.

Li, H., H. Zhu, C. J. Xu and J. Yuan (1998). "Cleavage of BID by caspase 8 mediates the mitochondrial damage in the Fas pathway of apoptosis." Cell **94**(4): 491-501.

Li, J., J. Wang, Z. Nawaz, J. M. Liu, J. Qin and J. Wong (2000). "Both corepressor proteins SMRT and N-CoR exist in large protein complexes containing HDAC3." EMBO J **19**(16): 4342-4350.

Li, M. O., M. R. Sarkisian, W. Z. Mehal, P. Rakic and R. A. Flavell (2003). "Phosphatidylserine receptor is required for clearance of apoptotic cells." Science **302**(5650): 1560-1563.

Li, N., A. Batzer, R. Daly, V. Yajnik, E. Skolnik, P. Chardin, D. Bar-Sagi, B. Margolis and J. Schlessinger (1993). "Guanine-nucleotide-releasing factor hSos1 binds to Grb2 and links receptor tyrosine kinases to Ras signalling." Nature **363**(6424): 85-88.

Li, P., D. Nijhawan and X. Wang (2004). "Mitochondrial activation of apoptosis." Cell **116**(2 Suppl): S57-59, 52 p following S59.

Li, Q., K. Gardner, L. Zhang, B. Tsang, F. Bostick-Bruton and E. Reed (1998). "Cisplatin induction of ERCC-1 mRNA expression in A2780/CP70 human ovarian cancer cells." J Biol Chem **273**(36): 23419-23425.

Li, Q., J. J. Yu, C. Mu, M. K. Yunmbam, D. Slavsky, C. L. Cross, F. Bostick-Bruton and E. Reed (2000). "Association between the level of ERCC-1 expression and the repair of cisplatin-induced DNA damage in human ovarian cancer cells." Anticancer Res **20**(2A): 645-652.

Li, Q., L. Zhang, B. Tsang, K. Gardner, F. Bostick-Bruton and E. Reed (1999). "Phorbol ester exposure activates an AP-1-mediated increase in ERCC-1 messenger RNA expression in human ovarian tumor cells." Cell Mol Life Sci **55**(3): 456-466.

Li, W. and D. W. Melton (2012). "Cisplatin regulates the MAPK kinase pathway to induce increased expression of DNA repair gene ERCC1 and increase melanoma chemoresistance." Oncogene **31**(19): 2412-2422.

Liang, C., C. J. Marsit, M. D. McClean, H. H. Nelson, B. C. Christensen, R. I. Haddad, J. R. Clark, R. O. Wein, G. A. Grillone, E. A. Houseman, G. Halec, T. Waterboer, M. Pawlita, J. F. Krane and K. T. Kelsey (2012). "Biomarkers of HPV in head and neck squamous cell carcinoma." Cancer Res **72**(19): 5004-5013.

Liang, S. H. and M. F. Clarke (1999). "A bipartite nuclear localization signal is required for p53 nuclear import regulated by a carboxyl-terminal domain." J Biol Chem **274**(46): 32699-32703.

Lieberthal, W., V. Triaca and J. Levine (1996). "Mechanisms of death induced by cisplatin in proximal tubular epithelial cells: apoptosis vs. necrosis." Am J Physiol **270**(4 Pt 2): F700-708.

Liggett, W. H. and D. Sidransky (1998). "Role of the p16 tumor suppressor gene in cancer." J Clin Oncol **16**(3): 1197-1206.

Lill, N. L., S. R. Grossman, D. Ginsberg, J. DeCaprio and D. M. Livingston (1997). "Binding and modulation of p53 by p300/CBP coactivators." Nature **387**(6635): 823-827.

Lin, S. F., J. D. Lin, T. C. Chou, Y. Y. Huang and R. J. Wong (2013). "Utility of a Histone Deacetylase Inhibitor (PXD101) for Thyroid Cancer Treatment." PLoS One **8**(10): e77684.

Lin, X. and S. B. Howell (2006). "DNA mismatch repair and p53 function are major determinants of the rate of development of cisplatin resistance." Mol Cancer Ther **5**(5): 1239-1247.

Linzer, D. I. and A. J. Levine (1979). "Characterization of a 54K dalton cellular SV40 tumor antigen present in SV40-transformed cells and uninfected embryonal carcinoma cells." Cell **17**(1): 43-52.

Little, J. B. (1968). "Delayed initiation of DNA synthesis in irradiated human diploid cells." Nature **218**(5146): 1064-1065.

Liu, G., T. J. McDonnell, R. Montes de Oca Luna, M. Kapoor, B. Mims, A. K. El-Naggar and G. Lozano (2000). "High metastatic potential in mice inheriting a targeted p53 missense mutation." Proc Natl Acad Sci U S A **97**(8): 4174-4179.

Liu, G., J. M. Parant, G. Lang, P. Chau, A. Chavez-Reyes, A. K. El-Naggar, A. Multani, S. Chang and G. Lozano (2004). "Chromosome stability, in the absence of apoptosis, is critical for suppression of tumorigenesis in Trp53 mutant mice." Nat Genet **36**(1): 63-68.

Liu, L., D. M. Scolnick, R. C. Trievel, H. B. Zhang, R. Marmorstein, T. D. Halazonetis and S. L. Berger (1999). "p53 sites acetylated in vitro by PCAF and p300 are acetylated in vivo in response to DNA damage." Mol Cell Biol **19**(2): 1202-1209.

Lièvre, A., J. B. Bachet, V. Boige, A. Cayre, D. Le Corre, E. Buc, M. Ychou, O. Bouché, B. Landi, C. Louvet, T. André, F. Bibeau, M. D. Diebold, P. Rougier, M. Ducreux, G. Tomasic, J. F. Emile, F. Penault-Llorca and P. Laurent-Puig (2008). "KRAS mutations as an independent prognostic factor in patients with advanced colorectal cancer treated with cetuximab." J Clin Oncol **26**(3): 374-379.

Lockshin, R. A. and J. Beaulaton (1974). "Programmed cell death." Life Sci **15**(9): 1549-1565.

Lowe, S. W. and A. W. Lin (2000). "Apoptosis in cancer." Carcinogenesis **21**(3): 485-495.

Lu, J., T. A. McKinsey, R. L. Nicol and E. N. Olson (2000). "Signal-dependent activation of the MEF2 transcription factor by dissociation from histone deacetylases." Proc Natl Acad Sci U S A **97**(8): 4070-4075.

Lu, J., T. A. McKinsey, C. L. Zhang and E. N. Olson (2000). "Regulation of skeletal myogenesis by association of the MEF2 transcription factor with class II histone deacetylases." Mol Cell **6**(2): 233-244.

Luger, K., A. W. Mäder, R. K. Richmond, D. F. Sargent and T. J. Richmond (1997). "Crystal structure of the nucleosome core particle at 2.8 A resolution." Nature **389**(6648): 251-260.

Lum, J. J., R. J. DeBerardinis and C. B. Thompson (2005). "Autophagy in metazoans: cell survival in the land of plenty." Nat Rev Mol Cell Biol **6**(6): 439-448.

Lund, B., P. E. Kristjansen and H. H. Hansen (1993). "Clinical and preclinical activity of 2',2'-difluorodeoxycytidine (gemcitabine)." Cancer Treat Rev **19**(1): 45-55.

Luo, J., A. Y. Nikolaev, S. Imai, D. Chen, F. Su, A. Shiloh, L. Guarente and W. Gu (2001). "Negative control of p53 by Sir2alpha promotes cell survival under stress." Cell **107**(2): 137-148.

Luo, J., F. Su, D. Chen, A. Shiloh and W. Gu (2000). "Deacetylation of p53 modulates its effect on cell growth and apoptosis." Nature **408**(6810): 377-381.

Luo, X., I. Budihardjo, H. Zou, C. Slaughter and X. Wang (1998). "Bid, a Bcl2 interacting protein, mediates cytochrome c release from mitochondria in response to activation of cell surface death receptors." Cell **94**(4): 481-490.

Lynch, T. J., D. W. Bell, R. Sordella, S. Gurubhagavatula, R. A. Okimoto, B. W. Brannigan, P. L. Harris, S. M. Haserlat, J. G. Supko, F. G. Haluska, D. N. Louis, D. C. Christiani, J. Settleman and D. A. Haber (2004). "Activating mutations in the epidermal growth factor receptor underlying responsiveness of non-small-cell lung cancer to gefitinib." N Engl J Med **350**(21): 2129-2139.

Lynch, T. J., T. Patel, L. Dreisbach, M. McCleod, W. J. Heim, R. C. Hermann, E. Paschold, N. O. Iannotti, S. Dakhil, S. Gorton, V. Pautret, M. R. Weber and D. Woytowitz (2010). "Cetuximab and first-line taxane/carboplatin chemotherapy in advanced non-small-cell lung cancer: results of the randomized multicenter phase III trial BMS099." J Clin Oncol **28**(6): 911-917.

Léveillard, T., L. Andera, N. Bissonnette, L. Schaeffer, L. Bracco, J. M. Egly and B. Wasylyk (1996). "Functional interactions between p53 and the TFIIH complex are affected by tumour-associated mutations." EMBO J **15**(7): 1615-1624.

Ma, B. B., F. Sung, Q. Tao, F. F. Poon, V. W. Lui, W. Yeo, S. L. Chan and A. T. Chan (2010). "The preclinical activity of the histone deacetylase inhibitor PXD101 (belinostat) in hepatocellular carcinoma cell lines." Invest New Drugs **28**(2): 107-114.

Mabuchi, S., M. Ohmichi, Y. Nishio, T. Hayasaka, A. Kimura, T. Ohta, M. Saito, J. Kawagoe, K. Takahashi, N. Yada-Hashimoto, M. Sakata, T. Motoyama, H. Kurachi, K. Tasaka and Y. Murata (2004). "Inhibition of NFkappaB increases the efficacy of cisplatin in in vitro and in vivo ovarian cancer models." J Biol Chem **279**(22): 23477-23485.

Macciò, A. and C. Madeddu (2013). "Cisplatin : an old drug with a newfound efficacy -- from mechanisms of action to cytotoxicity." Expert Opin Pharmacother **14**(13): 1839-1857.

Mackay, H. J., H. Hirte, T. Colgan, A. Covens, K. MacAlpine, P. Grenci, L. Wang, J. Mason, P. A. Pham, M. S. Tsao, J. Pan, J. Zwiebel and A. M. Oza (2010). "Phase II trial of

the histone deacetylase inhibitor belinostat in women with platinum resistant epithelial ovarian cancer and micropapillary (LMP) ovarian tumours." Eur J Cancer **46**(9): 1573-1579.

Majno, G. and I. Joris (1995). "Apoptosis, oncosis, and necrosis. An overview of cell death." Am J Pathol **146**(1): 3-15.

Mandic, A., K. Viktorsson, T. Heiden, J. Hansson and M. C. Shoshan (2001). "The MEK1 inhibitor PD98059 sensitizes C8161 melanoma cells to cisplatin-induced apoptosis." Melanoma Res **11**(1): 11-19.

Manfredi, J. J. (2010). "The Mdm2-p53 relationship evolves: Mdm2 swings both ways as an oncogene and a tumor suppressor." Genes Dev **24**(15): 1580-1589.

Mann, B. S., J. R. Johnson, M. H. Cohen, R. Justice and R. Pazdur (2007). "FDA approval summary: vorinostat for treatment of advanced primary cutaneous T-cell lymphoma." Oncologist **12**(10): 1247-1252.

Mansouri, A., L. D. Ridgway, A. L. Korapati, Q. Zhang, L. Tian, Y. Wang, Z. H. Siddik, G. B. Mills and F. X. Claret (2003). "Sustained activation of JNK/p38 MAPK pathways in response to cisplatin leads to Fas ligand induction and cell death in ovarian carcinoma cells." J Biol Chem **278**(21): 19245-19256.

Mansouri, A., Q. Zhang, L. D. Ridgway, L. Tian and F. X. Claret (2003). "Cisplatin resistance in an ovarian carcinoma is associated with a defect in programmed cell death control through XIAP regulation." Oncol Res **13**(6-10): 399-404.

Mantelingu, K., A. H. Kishore, K. Balasubramanyam, G. V. Kumar, M. Altaf, S. N. Swamy, R. Selvi, C. Das, C. Narayana, K. S. Rangappa and T. K. Kundu (2007). "Activation of p300 histone acetyltransferase by small molecules altering enzyme structure: probed by surface-enhanced Raman spectroscopy." J Phys Chem B **111**(17): 4527-4534.

Marchenko, N. D., A. Zaika and U. M. Moll (2000). "Death signal-induced localization of p53 protein to mitochondria. A potential role in apoptotic signaling." J Biol Chem **275**(21): 16202-16212.

Mariadason, J. M., G. A. Corner and L. H. Augenlicht (2000). "Genetic reprogramming in pathways of colonic cell maturation induced by short chain fatty acids: comparison with trichostatin A, sulindac, and curcumin and implications for chemoprevention of colon cancer." Cancer Res **60**(16): 4561-4572.

Marino, P., S. Pampallona, A. Preatoni, A. Cantoni and F. Invernizzi (1994). "Chemotherapy vs supportive care in advanced non-small-cell lung cancer. Results of a meta-analysis of the literature." Chest **106**(3): 861-865.

Marks, P. A. (2006). "Thioredoxin in cancer--role of histone deacetylase inhibitors." Semin Cancer Biol **16**(6): 436-443.

Marks, P. A., V. M. Richon and R. A. Rifkind (2000). "Histone deacetylase inhibitors: inducers of differentiation or apoptosis of transformed cells." J Natl Cancer Inst **92**(15): 1210-1216.

Marmorstein, R. and S. Y. Roth (2001). "Histone acetyltransferases: function, structure, and catalysis." Curr Opin Genet Dev **11**(2): 155-161.

Marsit, C. J., S. Zheng, K. Aldape, P. W. Hinds, H. H. Nelson, J. K. Wiencke and K. T. Kelsey (2005). "PTEN expression in non-small-cell lung cancer: evaluating its relation to tumor characteristics, allelic loss, and epigenetic alteration." Hum Pathol **36**(7): 768-776.

Martin, C. and Y. Zhang (2005). "The diverse functions of histone lysine methylation." Nat Rev Mol Cell Biol **6**(11): 838-849.

Matsuoka, S., M. Huang and S. J. Elledge (1998). "Linkage of ATM to cell cycle regulation by the Chk2 protein kinase." Science **282**(5395): 1893-1897.

Maurer, T., L. S. Garrenton, A. Oh, K. Pitts, D. J. Anderson, N. J. Skelton, B. P. Fauber, B. Pan, S. Malek, D. Stokoe, M. J. Ludlam, K. K. Bowman, J. Wu, A. M. Giannetti, M. A. Starovasnik, I. Mellman, P. K. Jackson, J. Rudolph, W. Wang and G. Fang (2012). "Small-molecule ligands bind to a distinct pocket in Ras and inhibit SOS-mediated nucleotide exchange activity." Proc Natl Acad Sci U S A **109**(14): 5299-5304.

Maya, R., M. Balass, S. T. Kim, D. Shkedy, J. F. Leal, O. Shifman, M. Moas, T. Buschmann, Z. Ronai, Y. Shiloh, M. B. Kastan, E. Katzir and M. Oren (2001). "ATM-dependent phosphorylation of Mdm2 on serine 395: role in p53 activation by DNA damage." Genes Dev **15**(9): 1067-1077.

Mayo, L. D. and D. B. Donner (2001). "A phosphatidylinositol 3-kinase/Akt pathway promotes translocation of Mdm2 from the cytoplasm to the nucleus." Proc Natl Acad Sci U S A **98**(20): 11598-11603.

Mayo, L. D. and D. B. Donner (2002). "The PTEN, Mdm2, p53 tumor suppressor-oncoprotein network." Trends Biochem Sci **27**(9): 462-467.

McGuire, W. P., E. K. Rowinsky, N. B. Rosenshein, F. C. Grumbine, D. S. Ettinger, D. K. Armstrong and R. C. Donehower (1989). "Taxol: a unique antineoplastic agent with significant activity in advanced ovarian epithelial neoplasms." Ann Intern Med **111**(4): 273-279.

McKinsey, T. A., C. L. Zhang and E. N. Olson (2000). "Activation of the myocyte enhancer factor-2 transcription factor by calcium/calmodulin-dependent protein kinase-stimulated binding of 14-3-3 to histone deacetylase 5." Proc Natl Acad Sci U S A **97**(26): 14400-14405.

Mercer, W. E., C. Avignolo and R. Baserga (1984). "Role of the p53 protein in cell proliferation as studied by microinjection of monoclonal antibodies." Mol Cell Biol **4**(2): 276-281.

Metzger, R., C. G. Leichman, K. D. Danenberg, P. V. Danenberg, H. J. Lenz, K. Hayashi, S. Groshen, D. Salonga, H. Cohen, L. Laine, P. Crookes, H. Silberman, J. Baranda, B. Konda and L. Leichman (1998). "ERCC1 mRNA levels complement thymidylate synthase mRNA levels in predicting response and survival for gastric cancer patients receiving combination cisplatin and fluorouracil chemotherapy." J Clin Oncol **16**(1): 309-316.

Milosavljevic, N., C. Duranton, N. Djerbi, P. H. Puech, P. Gounon, D. Lagadic-Gossmann, M. T. Dimanche-Boitrel, C. Rauch, M. Tauc, L. Counillon and M. Poët (2010). "Nongenomic effects of cisplatin: acute inhibition of mechanosensitive transporters and channels without actin remodeling." Cancer Res **70**(19): 7514-7522.

Minamiya, Y., T. Ono, H. Saito, N. Takahashi, M. Ito, M. Mitsui, S. Motoyama and J. Ogawa (2011). "Expression of histone deacetylase 1 correlates with a poor prognosis in patients with adenocarcinoma of the lung." Lung Cancer **74**(2): 300-304.

Minn, A. J., C. M. Rudin, L. H. Boise and C. B. Thompson (1995). "Expression of bcl-xL can confer a multidrug resistance phenotype." Blood **86**(5): 1903-1910.

Minucci, S. and P. G. Pelicci (2006). "Histone deacetylase inhibitors and the promise of epigenetic (and more) treatments for cancer." Nat Rev Cancer **6**(1): 38-51.

Misale, S., R. Yaeger, S. Hobor, E. Scala, M. Janakiraman, D. Liska, E. Valtorta, R. Schiavo, M. Buscarino, G. Siravegna, K. Bencardino, A. Cercek, C. T. Chen, S. Veronese, C. Zanon, A. Sartore-Bianchi, M. Gambacorta, M. Gallicchio, E. Vakiani, V. Boscaro, E. Medico, M. Weiser, S. Siena, F. Di Nicolantonio, D. Solit and A. Bardelli (2012). "Emergence of KRAS mutations and acquired resistance to anti-EGFR therapy in colorectal cancer." Nature **486**(7404): 532-536.

Miyashita, H., Y. Nitta, S. Mori, A. Kanzaki, K. Nakayama, K. Terada, T. Sugiyama, H. Kawamura, A. Sato, H. Morikawa, K. Motegi and Y. Takebayashi (2003). "Expression of copper-transporting P-type adenosine triphosphatase (ATP7B) as a chemoresistance marker in human oral squamous cell carcinoma treated with cisplatin." Oral Oncol **39**(2): 157-162.

Miyashita, T. and J. C. Reed (1995). "Tumor suppressor p53 is a direct transcriptional activator of the human bax gene." Cell **80**(2): 293-299.

Mizzen, C. A. and C. D. Allis (1998). "Linking histone acetylation to transcriptional regulation." Cell Mol Life Sci **54**(1): 6-20.

Molina, J. R., P. Yang, S. D. Cassivi, S. E. Schild and A. A. Adjei (2008). "Non-small cell lung cancer: epidemiology, risk factors, treatment, and survivorship." Mayo Clin Proc **83**(5): 584-594.

Mollinedo, F. and C. Gajate (2003). "Microtubules, microtubule-interfering agents and apoptosis." Apoptosis **8**(5): 413-450.

Momand, J., G. P. Zambetti, D. C. Olson, D. George and A. J. Levine (1992). "The mdm-2 oncogene product forms a complex with the p53 protein and inhibits p53-mediated transactivation." Cell **69**(7): 1237-1245.

Montgomery, J. A., R. D. Elliott, P. W. Allan, L. M. Rose and L. L. Bennett (1978). "Metabolism and mechanism of action of some new purine antimetabolites." Adv Enzyme Regul **17**: 419-435.

Moody, S. E., D. Perez, T. C. Pan, C. J. Sarkisian, C. P. Portocarrero, C. J. Sterner, K. L. Notorfrancesco, R. D. Cardiff and L. A. Chodosh (2005). "The transcriptional repressor Snail promotes mammary tumor recurrence." Cancer Cell **8**(3): 197-209.

Moody, S. E., C. J. Sarkisian, K. T. Hahn, E. J. Gunther, S. Pickup, K. D. Dugan, N. Innocent, R. D. Cardiff, M. D. Schnall and L. A. Chodosh (2002). "Conditional activation of Neu in the mammary epithelium of transgenic mice results in reversible pulmonary metastasis." Cancer Cell **2**(6): 451-461.

Moore, P. S., S. Barbi, M. Donadelli, C. Costanzo, C. Bassi, M. Palmieri and A. Scarpa (2004). "Gene expression profiling after treatment with the histone deacetylase inhibitor trichostatin A reveals altered expression of both pro- and anti-apoptotic genes in pancreatic adenocarcinoma cells." Biochim Biophys Acta **1693**(3): 167-176.

More, S. S., O. Akil, A. G. Ianculescu, E. G. Geier, L. R. Lustig and K. M. Giacomini (2010). "Role of the copper transporter, CTR1, in platinum-induced ototoxicity." J Neurosci **30**(28): 9500-9509.

Mori, S., J. T. Chang, E. R. Andrechek, N. Matsumura, T. Baba, G. Yao, J. W. Kim, M. Gatza, S. Murphy and J. R. Nevins (2009). "Anchorage-independent cell growth signature identifies tumors with metastatic potential." Oncogene **28**(31): 2796-2805.

Morton, J. P., P. Timpson, S. A. Karim, R. A. Ridgway, D. Athineos, B. Doyle, N. B. Jamieson, K. A. Oien, A. M. Lowy, V. G. Brunton, M. C. Frame, T. R. Evans and O. J. Sansom (2010). "Mutant p53 drives metastasis and overcomes growth arrest/senescence in pancreatic cancer." Proc Natl Acad Sci U S A **107**(1): 246-251.

Mowat, M., A. Cheng, N. Kimura, A. Bernstein and S. Benchimol (1985). "Rearrangements of the cellular p53 gene in erythroleukaemic cells transformed by Friend virus." Nature **314**(6012): 633-636.

Muggia, F. M. (1991). "Cisplatin update." Semin Oncol **18**(1 Suppl 3): 1-4.

Mukhopadhyay, N. K., E. Weisberg, D. Gilchrist, R. Bueno, D. J. Sugarbaker and M. T. Jaklitsch (2006). "Effectiveness of trichostatin A as a potential candidate for anticancer therapy in non-small-cell lung cancer." Ann Thorac Surg **81**(3): 1034-1042.

Muller, P. A., P. T. Caswell, B. Doyle, M. P. Iwanicki, E. H. Tan, S. Karim, N. Lukashchuk, D. A. Gillespie, R. L. Ludwig, P. Gosselin, A. Cromer, J. S. Brugge, O. J. Sansom, J. C. Norman and K. H. Vousden (2009). "Mutant p53 drives invasion by promoting integrin recycling." Cell **139**(7): 1327-1341.

Munroe, D. G., B. Rovinski, A. Bernstein and S. Benchimol (1988). "Loss of a highly conserved domain on p53 as a result of gene deletion during Friend virus-induced erythroleukemia." Oncogene **2**(6): 621-624.

Munshi, A., J. F. Kurland, T. Nishikawa, T. Tanaka, M. L. Hobbs, S. L. Tucker, S. Ismail, C. Stevens and R. E. Meyn (2005). "Histone deacetylase inhibitors radiosensitize human melanoma cells by suppressing DNA repair activity." Clin Cancer Res **11**(13): 4912-4922.

Munshi, N., M. Merika, J. Yie, K. Senger, G. Chen and D. Thanos (1998). "Acetylation of HMG I(Y) by CBP turns off IFN beta expression by disrupting the enhanceosome." Mol Cell **2**(4): 457-467.

Murphree, A. L. and W. F. Benedict (1984). "Retinoblastoma: clues to human oncogenesis." Science **223**(4640): 1028-1033.

Muzio, M. (1998). "Signalling by proteolysis: death receptors induce apoptosis." Int J Clin Lab Res **28**(3): 141-147.

Muzio, M., B. R. Stockwell, H. R. Stennicke, G. S. Salvesen and V. M. Dixit (1998). "An induced proximity model for caspase-8 activation." J Biol Chem **273**(5): 2926-2930.

Müller, M., S. Strand, H. Hug, E. M. Heinemann, H. Walczak, W. J. Hofmann, W. Stremmel, P. H. Krammer and P. R. Galle (1997). "Drug-induced apoptosis in hepatoma cells is mediated by the CD95 (APO-1/Fas) receptor/ligand system and involves activation of wild-type p53." J Clin Invest **99**(3): 403-413.

Nagata, S. (1997). "Apoptosis by death factor." Cell **88**(3): 355-365.

Nagata, S. and P. Golstein (1995). "The Fas death factor." Science **267**(5203): 1449-1456.

Nakano, K. and K. H. Vousden (2001). "PUMA, a novel proapoptotic gene, is induced by p53." Mol Cell **7**(3): 683-694.

Nakayama, J., J. C. Rice, B. D. Strahl, C. D. Allis and S. I. Grewal (2001). "Role of histone H3 lysine 9 methylation in epigenetic control of heterochromatin assembly." Science **292**(5514): 110-113.

Naoki, K., T. H. Chen, W. G. Richards, D. J. Sugarbaker and M. Meyerson (2002). "Missense mutations of the BRAF gene in human lung adenocarcinoma." Cancer Res **62**(23): 7001-7003.

Narita, M., S. Nũnez, E. Heard, A. W. Lin, S. A. Hearn, D. L. Spector, G. J. Hannon and S. W. Lowe (2003). "Rb-mediated heterochromatin formation and silencing of E2F target genes during cellular senescence." Cell **113**(6): 703-716.

Nasu, Y., K. Nishida, S. Miyazawa, T. Komiyama, Y. Kadota, N. Abe, A. Yoshida, S. Hirohata, A. Ohtsuka and T. Ozaki (2008). "Trichostatin A, a histone deacetylase inhibitor, suppresses synovial inflammation and subsequent cartilage destruction in a collagen antibody-induced arthritis mouse model." Osteoarthritis Cartilage **16**(6): 723-732.

Neal, J. W. and L. V. Sequist (2012). "Complex role of histone deacetylase inhibitors in the treatment of non-small-cell lung cancer." J Clin Oncol **30**(18): 2280-2282.

Nebbioso, A., N. Clarke, E. Voltz, E. Germain, C. Ambrosino, P. Bontempo, R. Alvarez, E. M. Schiavone, F. Ferrara, F. Bresciani, A. Weisz, A. R. de Lera, H. Gronemeyer and L. Altucci (2005). "Tumor-selective action of HDAC inhibitors involves TRAIL induction in acute myeloid leukemia cells." Nat Med **11**(1): 77-84.

Network, C. G. A. R. (2012). "Comprehensive genomic characterization of squamous cell lung cancers." Nature **489**(7417): 519-525.

Nishioka, M., T. Kohno, M. Tani, N. Yanaihara, Y. Tomizawa, A. Otsuka, S. Sasaki, K. Kobayashi, T. Niki, A. Maeshima, Y. Sekido, J. D. Minna, S. Sone and J. Yokota (2002). "MYO18B, a candidate tumor suppressor gene at chromosome 22q12.1, deleted, mutated, and methylated in human lung cancer." Proc Natl Acad Sci U S A **99**(19): 12269-12274.

Nomura, M., S. Shimizu, T. Sugiyama, M. Narita, T. Ito, H. Matsuda and Y. Tsujimoto (2003). "14-3-3 Interacts directly with and negatively regulates pro-apoptotic Bax." J Biol Chem **278**(3): 2058-2065.

North, B. J. and E. Verdin (2004). "Sirtuins: Sir2-related NAD-dependent protein deacetylases." Genome Biol **5**(5): 224.

Notte, A., L. Leclere and C. Michiels (2011). "Autophagy as a mediator of chemotherapy-induced cell death in cancer." Biochem Pharmacol **82**(5): 427-434.

Novogrodsky, A., A. Dvir, A. Ravid, T. Shkolnik, K. H. Stenzel, A. L. Rubin and R. Zaizov (1983). "Effect of polar organic compounds on leukemic cells. Butyrate-induced partial remission of acute myelogenous leukemia in a child." Cancer **51**(1): 9-14.

O'Byrne, K. J., U. Gatzemeier, I. Bondarenko, C. Barrios, C. Eschbach, U. M. Martens, Y. Hotko, C. Kortsik, L. Paz-Ares, J. R. Pereira, J. von Pawel, R. Ramlau, J. K. Roh, C. T. Yu, C. Stroh, I. Celik, A. Schueler and R. Pirker (2011). "Molecular biomarkers in non-small-

cell lung cancer: a retrospective analysis of data from the phase 3 FLEX study." Lancet Oncol **12**(8): 795-805.

O'Connor, L., A. Strasser, L. A. O'Reilly, G. Hausmann, J. M. Adams, S. Cory and D. C. Huang (1998). "Bim: a novel member of the Bcl-2 family that promotes apoptosis." EMBO J **17**(2): 384-395.

O'Connor, P. M., D. K. Ferris, G. A. White, J. Pines, T. Hunter, D. L. Longo and K. W. Kohn (1992). "Relationships between cdc2 kinase, DNA cross-linking, and cell cycle perturbations induced by nitrogen mustard." Cell Growth Differ **3**(1): 43-52.

O'Connor, P. M., J. Jackman, I. Bae, T. G. Myers, S. Fan, M. Mutoh, D. A. Scudiero, A. Monks, E. A. Sausville, J. N. Weinstein, S. Friend, A. J. Fornace and K. W. Kohn (1997). "Characterization of the p53 tumor suppressor pathway in cell lines of the National Cancer Institute anticancer drug screen and correlations with the growth-inhibitory potency of 123 anticancer agents." Cancer Res **57**(19): 4285-4300.

Obasaju, C. and G. R. Hudes (2001). "Paclitaxel and docetaxel in prostate cancer." Hematol Oncol Clin North Am **15**(3): 525-545.

Oda, E., R. Ohki, H. Murasawa, J. Nemoto, T. Shibue, T. Yamashita, T. Tokino, T. Taniguchi and N. Tanaka (2000). "Noxa, a BH3-only member of the Bcl-2 family and candidate mediator of p53-induced apoptosis." Science **288**(5468): 1053-1058.

Ogawara, Y., S. Kishishita, T. Obata, Y. Isazawa, T. Suzuki, K. Tanaka, N. Masuyama and Y. Gotoh (2002). "Akt enhances Mdm2-mediated ubiquitination and degradation of p53." J Biol Chem **277**(24): 21843-21850.

Ohashi, K., L. V. Sequist, M. E. Arcila, C. M. Lovly, X. Chen, C. M. Rudin, T. Moran, D. R. Camidge, C. L. Vnencak-Jones, L. Berry, Y. Pan, H. Sasaki, J. A. Engelman, E. B. Garon, S. M. Dubinett, W. A. Franklin, G. J. Riely, M. L. Sos, M. G. Kris, D. Dias-Santagata, M. Ladanyi, P. A. Bunn and W. Pao (2013). "Characteristics of lung cancers harboring NRAS mutations." Clin Cancer Res **19**(9): 2584-2591.

Olaussen, K. A. (2009). "A new step ahead for the consideration of ERCC1 as a candidate biomarker to select NSCLC patients for the treatment of cetuximab in combination with cisplatin." Cancer Biol Ther **8**(20): 1922-1923.

Olaussen, K. A., A. Dunant, P. Fouret, E. Brambilla, F. André, V. Haddad, E. Taranchon, M. Filipits, R. Pirker, H. H. Popper, R. Stahel, L. Sabatier, J. P. Pignon, T. Tursz, T. Le Chevalier, J. C. Soria and I. B. Investigators (2006). "DNA repair by ERCC1 in non-small-cell lung cancer and cisplatin-based adjuvant chemotherapy." N Engl J Med **355**(10): 983-991.

Oliva, R., D. P. Bazett-Jones, L. Locklear and G. H. Dixon (1990). "Histone hyperacetylation can induce unfolding of the nucleosome core particle." Nucleic Acids Res **18**(9): 2739-2747.

Olive, K. P., D. A. Tuveson, Z. C. Ruhe, B. Yin, N. A. Willis, R. T. Bronson, D. Crowley and T. Jacks (2004). "Mutant p53 gain of function in two mouse models of Li-Fraumeni syndrome." Cell **119**(6): 847-860.

Olivier, M., M. Hollstein and P. Hainaut (2010). "TP53 mutations in human cancers: origins, consequences, and clinical use." Cold Spring Harb Perspect Biol **2**(1): a001008.

Olson, J. M. and A. R. Hallahan (2004). "p38 MAP kinase: a convergence point in cancer therapy." Trends Mol Med **10**(3): 125-129.

Osada, H., Y. Tatematsu, H. Saito, Y. Yatabe, T. Mitsudomi and T. Takahashi (2004). "Reduced expression of class II histone deacetylase genes is associated with poor prognosis in lung cancer patients." Int J Cancer **112**(1): 26-32.

Ossina, N. K., A. Cannas, V. C. Powers, P. A. Fitzpatrick, J. D. Knight, J. R. Gilbert, E. M. Shekhtman, L. D. Tomei, S. R. Umansky and M. C. Kiefer (1997). "Interferon-gamma modulates a p53-independent apoptotic pathway and apoptosis-related gene expression." J Biol Chem **272**(26): 16351-16357.

Ostrem, J. M., U. Peters, M. L. Sos, J. A. Wells and K. M. Shokat (2013). "K-Ras(G12C) inhibitors allosterically control GTP affinity and effector interactions." Nature **503**(7477): 548-551.

Ota, H., M. Akishita, M. Eto, K. Iijima, M. Kaneki and Y. Ouchi (2007). "Sirt1 modulates premature senescence-like phenotype in human endothelial cells." J Mol Cell Cardiol **43**(5): 571-579.

Owen-Schaub, L. B., W. Zhang, J. C. Cusack, L. S. Angelo, S. M. Santee, T. Fujiwara, J. A. Roth, A. B. Deisseroth, W. W. Zhang and E. Kruzel (1995). "Wild-type human p53 and a temperature-sensitive mutant induce Fas/APO-1 expression." Mol Cell Biol **15**(6): 3032-3040.

Owonikoko, T. K., S. S. Ramalingam, B. Kanterewicz, T. E. Balius, C. P. Belani and P. A. Hershberger (2010). "Vorinostat increases carboplatin and paclitaxel activity in non-small-cell lung cancer cells." Int J Cancer **126**(3): 743-755.

Ozawa, Y., M. Towatari, S. Tsuzuki, F. Hayakawa, T. Maeda, Y. Miyata, M. Tanimoto and H. Saito (2001). "Histone deacetylase 3 associates with and represses the transcription factor GATA-2." Blood **98**(7): 2116-2123.

Pabla, N. and Z. Dong (2008). "Cisplatin nephrotoxicity: mechanisms and renoprotective strategies." Kidney Int **73**(9): 994-1007.

Pace, A., D. Giannarelli, E. Galiè, A. Savarese, S. Carpano, M. Della Giulia, A. Pozzi, A. Silvani, P. Gaviani, V. Scaioli, B. Jandolo, L. Bove and F. Cognetti (2010). "Vitamin E neuroprotection for cisplatin neuropathy: a randomized, placebo-controlled trial." Neurology **74**(9): 762-766.

Pacifico, A. and G. Leone (2007). "Role of p53 and CDKN2A inactivation in human squamous cell carcinomas." J Biomed Biotechnol **2007**(3): 43418.

Paez, J. G., P. A. Jänne, J. C. Lee, S. Tracy, H. Greulich, S. Gabriel, P. Herman, F. J. Kaye, N. Lindeman, T. J. Boggon, K. Naoki, H. Sasaki, Y. Fujii, M. J. Eck, W. R. Sellers, B. E. Johnson and M. Meyerson (2004). "EGFR mutations in lung cancer: correlation with clinical response to gefitinib therapy." Science **304**(5676): 1497-1500.

Paik, J. H., G. Choe, H. Kim, J. Y. Choe, H. J. Lee, C. T. Lee, J. S. Lee, S. Jheon and J. H. Chung (2011). "Screening of anaplastic lymphoma kinase rearrangement by immunohistochemistry in non-small cell lung cancer: correlation with fluorescence in situ hybridization." J Thorac Oncol **6**(3): 466-472.

Paik, P. K., M. E. Arcila, M. Fara, C. S. Sima, V. A. Miller, M. G. Kris, M. Ladanyi and G. J. Riely (2011). "Clinical characteristics of patients with lung adenocarcinomas harboring BRAF mutations." J Clin Oncol **29**(15): 2046-2051.

Pan, B., K. S. Yao, B. P. Monia, N. M. Dean, R. A. McKay, T. C. Hamilton and P. J. O'Dwyer (2002). "Reversal of cisplatin resistance in human ovarian cancer cell lines by a c-jun antisense oligodeoxynucleotide (ISIS 10582): evidence for the role of transcription factor overexpression in determining resistant phenotype." Biochem Pharmacol **63**(9): 1699-1707.

Pao, W. and K. E. Hutchinson (2012). "Chipping away at the lung cancer genome." Nat Med **18**(3): 349-351.

Pao, W., V. Miller, M. Zakowski, J. Doherty, K. Politi, I. Sarkaria, B. Singh, R. Heelan, V. Rusch, L. Fulton, E. Mardis, D. Kupfer, R. Wilson, M. Kris and H. Varmus (2004). "EGF receptor gene mutations are common in lung cancers from "never smokers" and are associated with sensitivity of tumors to gefitinib and erlotinib." Proc Natl Acad Sci U S A **101**(36): 13306-13311.

Pasello, M., F. Michelacci, I. Scionti, C. M. Hattinger, M. Zuntini, A. M. Caccuri, K. Scotlandi, P. Picci and M. Serra (2008). "Overcoming glutathione S-transferase P1-related cisplatin resistance in osteosarcoma." Cancer Res **68**(16): 6661-6668.

Patel, J. D., M. A. Socinski, E. B. Garon, C. H. Reynolds, D. R. Spigel, M. R. Olsen, R. C. Hermann, R. M. Jotte, T. Beck, D. A. Richards, S. C. Guba, J. Liu, B. Frimodt-Moller, W. J. John, C. K. Obasaju, E. J. Pennella, P. Bonomi and R. Govindan (2013). "PointBreak: a randomized phase III study of pemetrexed plus carboplatin and bevacizumab followed by maintenance pemetrexed and bevacizumab versus paclitaxel plus carboplatin and bevacizumab followed by maintenance bevacizumab in patients with stage IIIB or IV nonsquamous non-small-cell lung cancer." J Clin Oncol **31**(34): 4349-4357.

Patel, J. H., Y. Du, P. G. Ard, C. Phillips, B. Carella, C. J. Chen, C. Rakowski, C. Chatterjee, P. M. Lieberman, W. S. Lane, G. A. Blobel and S. B. McMahon (2004). "The c-MYC oncoprotein is a substrate of the acetyltransferases hGCN5/PCAF and TIP60." Mol Cell Biol **24**(24): 10826-10834.

Paterson, A. R., N. Kolassa and C. E. Cass (1981). "Transport of nucleoside drugs in animal cells." Pharmacol Ther **12**(3): 515-536.

Patgiri, A., K. K. Yadav, P. S. Arora and D. Bar-Sagi (2011). "An orthosteric inhibitor of the Ras-Sos interaction." Nat Chem Biol **7**(9): 585-587.

Pavletich, N. P., K. A. Chambers and C. O. Pabo (1993). "The DNA-binding domain of p53 contains the four conserved regions and the major mutation hot spots." Genes Dev **7**(12B): 2556-2564.

Payen, L., L. Sparfel, A. Courtois, L. Vernhet, A. Guillouzo and O. Fardel (2002). "The drug efflux pump MRP2: regulation of expression in physiopathological situations and by endogenous and exogenous compounds." Cell Biol Toxicol **18**(4): 221-233.

Peart, M. J., G. K. Smyth, R. K. van Laar, D. D. Bowtell, V. M. Richon, P. A. Marks, A. J. Holloway and R. W. Johnstone (2005). "Identification and functional significance of genes regulated by structurally different histone deacetylase inhibitors." Proc Natl Acad Sci U S A **102**(10): 3697-3702.

Peart, M. J., K. M. Tainton, A. A. Ruefli, A. E. Dear, K. A. Sedelies, L. A. O'Reilly, N. J. Waterhouse, J. A. Trapani and R. W. Johnstone (2003). "Novel mechanisms of apoptosis induced by histone deacetylase inhibitors." Cancer Res **63**(15): 4460-4471.

Peck, B., C. Y. Chen, K. K. Ho, P. Di Fruscia, S. S. Myatt, R. C. Coombes, M. J. Fuchter, C. D. Hsiao and E. W. Lam (2010). "SIRT inhibitors induce cell death and p53 acetylation through targeting both SIRT1 and SIRT2." Mol Cancer Ther **9**(4): 844-855.

Peng, C. Y., P. R. Graves, R. S. Thoma, Z. Wu, A. S. Shaw and H. Piwnica-Worms (1997). "Mitotic and G2 checkpoint control: regulation of 14-3-3 protein binding by phosphorylation of Cdc25C on serine-216." Science **277**(5331): 1501-1505.

Peng, H. Q., D. Hogg, D. Malkin, D. Bailey, B. L. Gallie, M. Bulbul, M. Jewett, J. Buchanan and P. E. Goss (1993). "Mutations of the p53 gene do not occur in testis cancer." Cancer Res **53**(15): 3574-3578.

Perego, P., M. Giarola, S. C. Righetti, R. Supino, C. Caserini, D. Delia, M. A. Pierotti, T. Miyashita, J. C. Reed and F. Zunino (1996). "Association between cisplatin resistance and mutation of p53 gene and reduced bax expression in ovarian carcinoma cell systems." Cancer Res **56**(3): 556-562.

Perez, E. A. (1998). "Paclitaxel in Breast Cancer." Oncologist **3**(6): 373-389.

Perrone, F., P. Bossi, B. Cortelazzi, L. Locati, P. Quattrone, M. A. Pierotti, S. Pilotti and L. Licitra (2010). "TP53 mutations and pathologic complete response to neoadjuvant cisplatin and fluorouracil chemotherapy in resected oral cavity squamous cell carcinoma." J Clin Oncol **28**(5): 761-766.

Persons, D. L., E. M. Yazlovitskaya, W. Cui and J. C. Pelling (1999). "Cisplatin-induced activation of mitogen-activated protein kinases in ovarian carcinoma cells: inhibition of extracellular signal-regulated kinase activity increases sensitivity to cisplatin." Clin Cancer Res **5**(5): 1007-1014.

Peters, B. G. (1994). "An overview of chemotherapy toxicities." Top Hosp Pharm Manage **14**(2): 59-88.

Peters, S., O. Michielin and S. Zimmermann (2013). "Dramatic response induced by vemurafenib in a BRAF V600E-mutated lung adenocarcinoma." J Clin Oncol **31**(20): e341-344.

Phiel, C. J., F. Zhang, E. Y. Huang, M. G. Guenther, M. A. Lazar and P. S. Klein (2001). "Histone deacetylase is a direct target of valproic acid, a potent anticonvulsant, mood stabilizer, and teratogen." J Biol Chem **276**(39): 36734-36741.

Piekarz, R. L., R. Frye, H. M. Prince, M. H. Kirschbaum, J. Zain, S. L. Allen, E. S. Jaffe, A. Ling, M. Turner, C. J. Peer, W. D. Figg, S. M. Steinberg, S. Smith, D. Joske, I. Lewis, L. Hutchins, M. Craig, A. T. Fojo, J. J. Wright and S. E. Bates (2011). "Phase 2 trial of romidepsin in patients with peripheral T-cell lymphoma." Blood **117**(22): 5827-5834.

Piekarz, R. L., R. Frye, M. Turner, J. J. Wright, S. L. Allen, M. H. Kirschbaum, J. Zain, H. M. Prince, J. P. Leonard, L. J. Geskin, C. Reeder, D. Joske, W. D. Figg, E. R. Gardner, S. M. Steinberg, E. S. Jaffe, M. Stetler-Stevenson, S. Lade, A. T. Fojo and S. E. Bates (2009). "Phase II multi-institutional trial of the histone deacetylase inhibitor romidepsin as monotherapy for patients with cutaneous T-cell lymphoma." J Clin Oncol **27**(32): 5410-5417.

Pietras, R. J., B. M. Fendly, V. R. Chazin, M. D. Pegram, S. B. Howell and D. J. Slamon (1994). "Antibody to HER-2/neu receptor blocks DNA repair after cisplatin in human breast and ovarian cancer cells." Oncogene **9**(7): 1829-1838.

Pignon, J. P., H. Tribodet, G. V. Scagliotti, J. Y. Douillard, F. A. Shepherd, R. J. Stephens, A. Dunant, V. Torri, R. Rosell, L. Seymour, S. G. Spiro, E. Rolland, R. Fossati, D. Aubert, K. Ding, D. Waller, T. Le Chevalier and L. C. Group (2008). "Lung adjuvant cisplatin evaluation: a pooled analysis by the LACE Collaborative Group." J Clin Oncol **26**(21): 3552-3559.

Pil, P. M. and S. J. Lippard (1992). "Specific binding of chromosomal protein HMG1 to DNA damaged by the anticancer drug cisplatin." Science **256**(5054): 234-237.

Pirker, R., J. R. Pereira, A. Szczesna, J. von Pawel, M. Krzakowski, R. Ramlau, I. Vynnychenko, K. Park, C. T. Yu, V. Ganul, J. K. Roh, E. Bajetta, K. O'Byrne, F. de Marinis, W. Eberhardt, T. Goddemeier, M. Emig, U. Gatzemeier and F. S. Team (2009). "Cetuximab plus chemotherapy in patients with advanced non-small-cell lung cancer (FLEX): an open-label randomised phase III trial." Lancet **373**(9674): 1525-1531.

Plumb, J. A., P. W. Finn, R. J. Williams, M. J. Bandara, M. R. Romero, C. J. Watkins, N. B. La Thangue and R. Brown (2003). "Pharmacodynamic response and inhibition of growth of human tumor xenografts by the novel histone deacetylase inhibitor PXD101." Mol Cancer Ther **2**(8): 721-728.

Plunkett, W., P. Huang, Y. Z. Xu, V. Heinemann, R. Grunewald and V. Gandhi (1995). "Gemcitabine: metabolism, mechanisms of action, and self-potentiation." Semin Oncol **22**(4 Suppl 11): 3-10.

Pommier, Y., O. Sordet, S. Antony, R. L. Hayward and K. W. Kohn (2004). "Apoptosis defects and chemotherapy resistance: molecular interaction maps and networks." Oncogene **23**(16): 2934-2949.

Porter, A. G. and R. U. Jänicke (1999). "Emerging roles of caspase-3 in apoptosis." Cell Death Differ **6**(2): 99-104.

Pospísilová, S., V. Brázda, K. Kucharíková, M. G. Luciani, T. R. Hupp, P. Skládal, E. Palecek and B. Vojtesek (2004). "Activation of the DNA-binding ability of latent p53 protein by protein kinase C is abolished by protein kinase CK2." Biochem J **378**(Pt 3): 939-947.

Potapova, O., A. Haghighi, F. Bost, C. Liu, M. J. Birrer, R. Gjerset and D. Mercola (1997). "The Jun kinase/stress-activated protein kinase pathway functions to regulate DNA repair and inhibition of the pathway sensitizes tumor cells to cisplatin." J Biol Chem **272**(22): 14041-14044.

Price, B. D., L. Hughes-Davies and S. J. Park (1995). "Cdk2 kinase phosphorylates serine 315 of human p53 in vitro." Oncogene **11**(1): 73-80.

Pruss, D., B. Bartholomew, J. Persinger, J. Hayes, G. Arents, E. N. Moudrianakis and A. P. Wolffe (1996). "An asymmetric model for the nucleosome: a binding site for linker histones inside the DNA gyres." Science **274**(5287): 614-617.

Purdie, C. A., D. J. Harrison, A. Peter, L. Dobbie, S. White, S. E. Howie, D. M. Salter, C. C. Bird, A. H. Wyllie and M. L. Hooper (1994). "Tumour incidence, spectrum and ploidy in mice with a large deletion in the p53 gene." Oncogene **9**(2): 603-609.

Pylayeva-Gupta, Y., E. Grabocka and D. Bar-Sagi (2011). "RAS oncogenes: weaving a tumorigenic web." Nat Rev Cancer **11**(11): 761-774.

Qian, X., W. J. LaRochelle, G. Ara, F. Wu, K. D. Petersen, A. Thougaard, M. Sehested, H. S. Lichenstein and M. Jeffers (2006). "Activity of PXD101, a histone deacetylase inhibitor, in preclinical ovarian cancer studies." Mol Cancer Ther **5**(8): 2086-2095.

Raghavan, D. (2003). "Testicular cancer: maintaining the high cure rate." Oncology (Williston Park) **17**(2): 218-228; discussion 228-219, 234-215, passim.

Rajeswaran, A., A. Trojan, B. Burnand and M. Giannelli (2008). "Efficacy and side effects of cisplatin- and carboplatin-based doublet chemotherapeutic regimens versus non-platinum-based doublet chemotherapeutic regimens as first line treatment of metastatic non-small cell lung carcinoma: a systematic review of randomized controlled trials." Lung Cancer **59**(1): 1-11.

Ramalingam, S. and C. P. Belani (2004). "Paclitaxel for non-small cell lung cancer." Expert Opin Pharmacother **5**(8): 1771-1780.

Ramalingam, S. S., C. P. Belani, C. Ruel, P. Frankel, B. Gitlitz, M. Koczywas, I. Espinoza-Delgado and D. Gandara (2009). "Phase II study of belinostat (PXD101), a histone deacetylase inhibitor, for second line therapy of advanced malignant pleural mesothelioma." J Thorac Oncol **4**(1): 97-101.

Ramalingam, S. S., M. L. Maitland, P. Frankel, A. E. Argiris, M. Koczywas, B. Gitlitz, S. Thomas, I. Espinoza-Delgado, E. E. Vokes, D. R. Gandara and C. P. Belani (2010). "Carboplatin and Paclitaxel in combination with either vorinostat or placebo for first-line therapy of advanced non-small-cell lung cancer." J Clin Oncol **28**(1): 56-62.

Ramalingam, S. S., R. A. Parise, R. K. Ramanathan, R. K. Ramananthan, T. F. Lagattuta, L. A. Musguire, R. G. Stoller, D. M. Potter, A. E. Argiris, J. A. Zwiebel, M. J. Egorin and C. P. Belani (2007). "Phase I and pharmacokinetic study of vorinostat, a histone deacetylase inhibitor, in combination with carboplatin and paclitaxel for advanced solid malignancies." Clin Cancer Res **13**(12): 3605-3610.

Raymond, E., S. Faivre, S. Chaney, J. Woynarowski and E. Cvitkovic (2002). "Cellular and molecular pharmacology of oxaliplatin." Mol Cancer Ther **1**(3): 227-235.

Reed, J. C. (1995). "Regulation of apoptosis by bcl-2 family proteins and its role in cancer and chemoresistance." Curr Opin Oncol **7**(6): 541-546.

Reich, N. C. and A. J. Levine (1984). "Growth regulation of a cellular tumour antigen, p53, in nontransformed cells." Nature **308**(5955): 199-201.

Reimer, P. and S. Chawla (2013). "Long-term complete remission with belinostat in a patient with chemotherapy refractory peripheral t-cell lymphoma." J Hematol Oncol **6**(1): 69.

Rekhtman, N., P. K. Paik, M. E. Arcila, L. J. Tafe, G. R. Oxnard, A. L. Moreira, W. D. Travis, M. F. Zakowski, M. G. Kris and M. Ladanyi (2012). "Clarifying the spectrum of driver oncogene mutations in biomarker-verified squamous carcinoma of lung: lack of EGFR/KRAS and presence of PIK3CA/AKT1 mutations." Clin Cancer Res **18**(4): 1167-1176.

Richon, V. M., T. W. Sandhoff, R. A. Rifkind and P. A. Marks (2000). "Histone deacetylase inhibitor selectively induces p21WAF1 expression and gene-associated histone acetylation." Proc Natl Acad Sci U S A **97**(18): 10014-10019.

Richon, V. M., Y. Webb, R. Merger, T. Sheppard, B. Jursic, L. Ngo, F. Civoli, R. Breslow, R. A. Rifkind and P. A. Marks (1996). "Second generation hybrid polar compounds are potent inducers of transformed cell differentiation." Proc Natl Acad Sci U S A **93**(12): 5705-5708.

Riggs, M. G., R. G. Whittaker, J. R. Neumann and V. M. Ingram (1977). "n-Butyrate causes histone modification in HeLa and Friend erythroleukaemia cells." Nature **268**(5619): 462-464.

Righetti, S. C., G. Della Torre, S. Pilotti, S. Ménard, F. Ottone, M. I. Colnaghi, M. A. Pierotti, C. Lavarino, M. Cornarotti, S. Oriana, S. Böhm, G. L. Bresciani, G. Spatti and F. Zunino (1996). "A comparative study of p53 gene mutations, protein accumulation, and response to cisplatin-based chemotherapy in advanced ovarian carcinoma." Cancer Res **56**(4): 689-693.

Rixe, O., W. Ortuzar, M. Alvarez, R. Parker, E. Reed, K. Paull and T. Fojo (1996). "Oxaliplatin, tetraplatin, cisplatin, and carboplatin: spectrum of activity in drug-resistant cell lines and in the cell lines of the National Cancer Institute's Anticancer Drug Screen panel." Biochem Pharmacol **52**(12): 1855-1865.

Robey, R. W., Z. Zhan, R. L. Piekarz, G. L. Kayastha, T. Fojo and S. E. Bates (2006). "Increased MDR1 expression in normal and malignant peripheral blood mononuclear cells obtained from patients receiving depsipeptide (FR901228, FK228, NSC630176)." Clin Cancer Res **12**(5): 1547-1555.

Robinson, M. J. and M. H. Cobb (1997). "Mitogen-activated protein kinase pathways." Curr Opin Cell Biol **9**(2): 180-186.

Rogge, R. D., C. A. Karlovich and U. Banerjee (1991). "Genetic dissection of a neurodevelopmental pathway: Son of sevenless functions downstream of the sevenless and EGF receptor tyrosine kinases." Cell **64**(1): 39-48.

Rosato, R. R., J. A. Almenara and S. Grant (2003). "The histone deacetylase inhibitor MS-275 promotes differentiation or apoptosis in human leukemia cells through a process regulated by generation of reactive oxygen species and induction of p21CIP1/WAF1 1." Cancer Res **63**(13): 3637-3645.

Rosato, R. R., S. C. Maggio, J. A. Almenara, S. G. Payne, P. Atadja, S. Spiegel, P. Dent and S. Grant (2006). "The histone deacetylase inhibitor LAQ824 induces human leukemia cell death through a process involving XIAP down-regulation, oxidative injury, and the acid sphingomyelinase-dependent generation of ceramide." Mol Pharmacol **69**(1): 216-225.

Rosenberg, B., L. Van Camp, E. B. Grimley and A. J. Thomson (1967). "The inhibition of growth or cell division in Escherichia coli by different ionic species of platinum(IV) complexes." J Biol Chem **242**(6): 1347-1352.

Ross, H. J., G. R. Blumenschein, J. Aisner, N. Damjanov, A. Dowlati, J. Garst, J. R. Rigas, M. Smylie, H. Hassani, K. E. Allen, L. Leopold, T. Z. Zaks and F. A. Shepherd (2010). "Randomized phase II multicenter trial of two schedules of lapatinib as first- or second-line monotherapy in patients with advanced or metastatic non-small cell lung cancer." Clin Cancer Res **16**(6): 1938-1949.

Ross, H. J., L. L. Hart, P. M. Swanson, M. U. Rarick, R. A. Figlin, A. D. Jacobs, D. E. McCune, A. H. Rosenberg, A. D. Baron, L. E. Grove, M. D. Thorn, D. M. Miller, J. G. Drachman and C. M. Rudin (2006). "A randomized, multicenter study to determine the safety and efficacy of the immunoconjugate SGN-15 plus docetaxel for the treatment of non-small cell lung carcinoma." Lung Cancer **54**(1): 69-77.

Roth, M. and W. Y. Chen (2013). "Sorting out functions of sirtuins in cancer." Oncogene.

Rotter, V. (1983). "p53, a transformation-related cellular-encoded protein, can be used as a biochemical marker for the detection of primary mouse tumor cells." Proc Natl Acad Sci U S A **80**(9): 2613-2617.

Rowan, S., R. L. Ludwig, Y. Haupt, S. Bates, X. Lu, M. Oren and K. H. Vousden (1996). "Specific loss of apoptotic but not cell-cycle arrest function in a human tumor derived p53 mutant." EMBO J **15**(4): 827-838.

Ruefli, A. A., M. J. Ausserlechner, D. Bernhard, V. R. Sutton, K. M. Tainton, R. Kofler, M. J. Smyth and R. W. Johnstone (2001). "The histone deacetylase inhibitor and chemotherapeutic agent suberoylanilide hydroxamic acid (SAHA) induces a cell-death pathway characterized by cleavage of Bid and production of reactive oxygen species." Proc Natl Acad Sci U S A **98**(19): 10833-10838.

Ryan, Q. C., D. Headlee, M. Acharya, A. Sparreboom, J. B. Trepel, J. Ye, W. D. Figg, K. Hwang, E. J. Chung, A. Murgo, G. Melillo, Y. Elsayed, M. Monga, M. Kalnitskiy, J. Zwiebel and E. A. Sausville (2005). "Phase I and pharmacokinetic study of MS-275, a histone deacetylase inhibitor, in patients with advanced and refractory solid tumors or lymphoma." J Clin Oncol **23**(17): 3912-3922.

Saccomanno, G., V. E. Archer, O. Auerbach, R. P. Saunders and L. M. Brennan (1974). "Development of carcinoma of the lung as reflected in exfoliated cells." Cancer **33**(1): 256-270.

Safaei, R., A. K. Holzer, K. Katano, G. Samimi and S. B. Howell (2004). "The role of copper transporters in the development of resistance to Pt drugs." J Inorg Biochem **98**(10): 1607-1613.

Sakaguchi, K., J. E. Herrera, S. Saito, T. Miki, M. Bustin, A. Vassilev, C. W. Anderson and E. Appella (1998). "DNA damage activates p53 through a phosphorylation-acetylation cascade." Genes Dev **12**(18): 2831-2841.

Sakai, W., E. M. Swisher, B. Y. Karlan, M. K. Agarwal, J. Higgins, C. Friedman, E. Villegas, C. Jacquemont, D. J. Farrugia, F. J. Couch, N. Urban and T. Taniguchi (2008). "Secondary mutations as a mechanism of cisplatin resistance in BRCA2-mutated cancers." Nature **451**(7182): 1116-1120.

Samuels, Y., Z. Wang, A. Bardelli, N. Silliman, J. Ptak, S. Szabo, H. Yan, A. Gazdar, S. M. Powell, G. J. Riggins, J. K. Willson, S. Markowitz, K. W. Kinzler, B. Vogelstein and V. E. Velculescu (2004). "High frequency of mutations of the PIK3CA gene in human cancers." Science **304**(5670): 554.

Sandler, A., R. Gray, M. C. Perry, J. Brahmer, J. H. Schiller, A. Dowlati, R. Lilenbaum and D. H. Johnson (2006). "Paclitaxel-carboplatin alone or with bevacizumab for non-small-cell lung cancer." N Engl J Med **355**(24): 2542-2550.

Sandler, A. B., J. Nemunaitis, C. Denham, J. von Pawel, Y. Cormier, U. Gatzemeier, K. Mattson, C. Manegold, M. C. Palmer, A. Gregor, B. Nguyen, C. Niyikiza and L. H. Einhorn (2000). "Phase III trial of gemcitabine plus cisplatin versus cisplatin alone in patients with locally advanced or metastatic non-small-cell lung cancer." J Clin Oncol **18**(1): 122-130.

Sandor, V., S. Bakke, R. W. Robey, M. H. Kang, M. V. Blagosklonny, J. Bender, R. Brooks, R. L. Piekarz, E. Tucker, W. D. Figg, K. K. Chan, B. Goldspiel, A. T. Fojo, S. P. Balcerzak and S. E. Bates (2002). "Phase I trial of the histone deacetylase inhibitor, depsipeptide (FR901228, NSC 630176), in patients with refractory neoplasms." Clin Cancer Res **8**(3): 718-728.

Sarig, R., N. Rivlin, R. Brosh, C. Bornstein, I. Kamer, O. Ezra, A. Molchadsky, N. Goldfinger, O. Brenner and V. Rotter (2010). "Mutant p53 facilitates somatic cell reprogramming and augments the malignant potential of reprogrammed cells." J Exp Med **207**(10): 2127-2140.

Sasakawa, Y., Y. Naoe, T. Noto, T. Inoue, T. Sasakawa, M. Matsuo, T. Manda and S. Mutoh (2003). "Antitumor efficacy of FK228, a novel histone deacetylase inhibitor, depends on the effect on expression of angiogenesis factors." Biochem Pharmacol **66**(6): 897-906.

Sasaki, T., J. Koivunen, A. Ogino, M. Yanagita, S. Nikiforow, W. Zheng, C. Lathan, J. P. Marcoux, J. Du, K. Okuda, M. Capelletti, T. Shimamura, D. Ercan, M. Stumpfova, Y. Xiao, S. Weremowicz, M. Butaney, S. Heon, K. Wilner, J. G. Christensen, M. J. Eck, K. K. Wong, N. Lindeman, N. S. Gray, S. J. Rodig and P. A. Jänne (2011). "A novel ALK secondary mutation and EGFR signaling cause resistance to ALK kinase inhibitors." Cancer Res **71**(18): 6051-6060.

Sato, M., D. S. Shames, A. F. Gazdar and J. D. Minna (2007). "A translational view of the molecular pathogenesis of lung cancer." J Thorac Oncol **2**(4): 327-343.

Sax, J. K., P. Fei, M. E. Murphy, E. Bernhard, S. J. Korsmeyer and W. S. El-Deiry (2002). "BID regulation by p53 contributes to chemosensitivity." Nat Cell Biol **4**(11): 842-849.

Schiller, J. H. (2001). "Current standards of care in small-cell and non-small-cell lung cancer." Oncology **61 Suppl 1**: 3-13.

Schiller, J. H., D. Harrington, C. P. Belani, C. Langer, A. Sandler, J. Krook, J. Zhu, D. H. Johnson and E. C. O. Group (2002). "Comparison of four chemotherapy regimens for advanced non-small-cell lung cancer." N Engl J Med **346**(2): 92-98.

Schiltz, R. L., C. A. Mizzen, A. Vassilev, R. G. Cook, C. D. Allis and Y. Nakatani (1999). "Overlapping but distinct patterns of histone acetylation by the human coactivators p300 and PCAF within nucleosomal substrates." J Biol Chem **274**(3): 1189-1192.

Schmelzle, T. and M. N. Hall (2000). "TOR, a central controller of cell growth." Cell **103**(2): 253-262.

Schrump, D. S. (2009). "Cytotoxicity mediated by histone deacetylase inhibitors in cancer cells: mechanisms and potential clinical implications." Clin Cancer Res **15**(12): 3947-3957.

Schulze, W. X., L. Deng and M. Mann (2005). "Phosphotyrosine interactome of the ErbB-receptor kinase family." Mol Syst Biol **1**: 2005.0008.

Seki, K., H. Yoshikawa, K. Shiiki, Y. Hamada, N. Akamatsu and K. Tasaka (2000). "Cisplatin (CDDP) specifically induces apoptosis via sequential activation of caspase-8, -3 and -6 in osteosarcoma." Cancer Chemother Pharmacol **45**(3): 199-206.

Seshadri, T. and J. Campisi (1990). "Repression of c-fos transcription and an altered genetic program in senescent human fibroblasts." Science **247**(4939): 205-209.

Shao, W., J. D. Growney, Y. Feng, G. O'Connor, M. Pu, W. Zhu, Y. M. Yao, P. Kwon, S. Fawell and P. Atadja (2010). "Activity of deacetylase inhibitor panobinostat (LBH589) in cutaneous T-cell lymphoma models: Defining molecular mechanisms of resistance." Int J Cancer **127**(9): 2199-2208.

Sharma, S. V., D. Y. Lee, B. Li, M. P. Quinlan, F. Takahashi, S. Maheswaran, U. McDermott, N. Azizian, L. Zou, M. A. Fischbach, K. K. Wong, K. Brandstetter, B. Wittner, S. Ramaswamy, M. Classon and J. Settleman (2010). "A chromatin-mediated reversible drug-tolerant state in cancer cell subpopulations." Cell **141**(1): 69-80.

Sharp, D. J., G. C. Rogers and J. M. Scholey (2000). "Microtubule motors in mitosis." Nature **407**(6800): 41-47.

Shaw, A. T., B. Y. Yeap, B. J. Solomon, G. J. Riely, J. Gainor, J. A. Engelman, G. I. Shapiro, D. B. Costa, S. H. Ou, M. Butaney, R. Salgia, R. G. Maki, M. Varella-Garcia, R. C. Doebele, Y. J. Bang, K. Kulig, P. Selaru, Y. Tang, K. D. Wilner, E. L. Kwak, J. W. Clark, A. J. Iafrate and D. R. Camidge (2011). "Effect of crizotinib on overall survival in patients with advanced non-small-cell lung cancer harbouring ALK gene rearrangement: a retrospective analysis." Lancet Oncol **12**(11): 1004-1012.

Sherr, C. J. (1993). "Mammalian G1 cyclins." Cell **73**(6): 1059-1065.

Shi, J. and H. M. Shen (2008). "Critical role of Bid and Bax in indirubin-3'-monoxime-induced apoptosis in human cancer cells." Biochem Pharmacol **75**(9): 1729-1742.

Shi, Y. (2001). "A structural view of mitochondria-mediated apoptosis." Nat Struct Biol **8**(5): 394-401.

Shieh, S. Y., M. Ikeda, Y. Taya and C. Prives (1997). "DNA damage-induced phosphorylation of p53 alleviates inhibition by MDM2." Cell **91**(3): 325-334.

Shieh, S. Y., Y. Taya and C. Prives (1999). "DNA damage-inducible phosphorylation of p53 at N-terminal sites including a novel site, Ser20, requires tetramerization." EMBO J **18**(7): 1815-1823.

Shiga, H., E. I. Heath, A. A. Rasmussen, B. Trock, P. G. Johnston, A. A. Forastiere, M. Langmacher, A. Baylor, M. Lee and K. J. Cullen (1999). "Prognostic value of p53, glutathione S-transferase pi, and thymidylate synthase for neoadjuvant cisplatin-based chemotherapy in head and neck cancer." Clin Cancer Res **5**(12): 4097-4104.

Shimmyo, T., T. Hashimoto, Y. Kobayashi, Y. Miyagi, Y. Ishikawa, K. Nakagawa, H. Osada and E. Tsuchiya (2006). "p53 mutation spectra for squamous cell carcinomas at different levels of human bronchial branches." Int J Cancer **119**(3): 501-507.

Shiseki, M., T. Kohno, J. Adachi, T. Okazaki, T. Otsuka, H. Mizoguchi, M. Noguchi, S. Hirohashi and J. Yokota (1996). "Comparative allelotype of early and advanced stage non-small cell lung carcinomas." Genes Chromosomes Cancer **17**(2): 71-77.

Shiseki, M., T. Kohno, R. Nishikawa, Y. Sameshima, H. Mizoguchi and J. Yokota (1994). "Frequent allelic losses on chromosomes 2q, 18q, and 22q in advanced non-small cell lung carcinoma." Cancer Res **54**(21): 5643-5648.

Shohat, O., M. Greenberg, D. Reisman, M. Oren and V. Rotter (1987). "Inhibition of cell growth mediated by plasmids encoding p53 anti-sense." Oncogene **1**(3): 277-283.

Shukuya, T., T. Takahashi, R. Kaira, A. Ono, Y. Nakamura, A. Tsuya, H. Kenmotsu, T. Naito, K. Kaira, H. Murakami, M. Endo, K. Takahashi and N. Yamamoto (2011). "Efficacy of gefitinib for non-adenocarcinoma non-small-cell lung cancer patients harboring epidermal growth factor receptor mutations: a pooled analysis of published reports." Cancer Sci **102**(5): 1032-1037.

Siddik, Z. H. (2003). "Cisplatin: mode of cytotoxic action and molecular basis of resistance." Oncogene **22**(47): 7265-7279.

Siliciano, J. D., C. E. Canman, Y. Taya, K. Sakaguchi, E. Appella and M. B. Kastan (1997). "DNA damage induces phosphorylation of the amino terminus of p53." Genes Dev **11**(24): 3471-3481.

Slamon, D. J., W. Godolphin, L. A. Jones, J. A. Holt, S. G. Wong, D. E. Keith, W. J. Levin, S. G. Stuart, J. Udove and A. Ullrich (1989). "Studies of the HER-2/neu proto-oncogene in human breast and ovarian cancer." Science **244**(4905): 707-712.

Slebos, R. J., M. H. Lee, B. S. Plunkett, T. D. Kessis, B. O. Williams, T. Jacks, L. Hedrick, M. B. Kastan and K. R. Cho (1994). "p53-dependent G1 arrest involves pRB-related proteins and is disrupted by the human papillomavirus 16 E7 oncoprotein." Proc Natl Acad Sci U S A **91**(12): 5320-5324.

Slingerland, J. M., J. R. Jenkins and S. Benchimol (1993). "The transforming and suppressor functions of p53 alleles: effects of mutations that disrupt phosphorylation, oligomerization and nuclear translocation." EMBO J **12**(3): 1029-1037.

Smith, J., L. M. Tho, N. Xu and D. A. Gillespie (2010). "The ATM-Chk2 and ATR-Chk1 pathways in DNA damage signaling and cancer." Adv Cancer Res **108**: 73-112.

Smith, M. L., I. T. Chen, Q. Zhan, P. M. O'Connor and A. J. Fornace (1995). "Involvement of the p53 tumor suppressor in repair of u.v.-type DNA damage." Oncogene **10**(6): 1053-1059.

Smith, M. L. and Y. R. Seo (2002). "p53 regulation of DNA excision repair pathways." Mutagenesis **17**(2): 149-156.

Soda, M., Y. L. Choi, M. Enomoto, S. Takada, Y. Yamashita, S. Ishikawa, S. Fujiwara, H. Watanabe, K. Kurashina, H. Hatanaka, M. Bando, S. Ohno, Y. Ishikawa, H. Aburatani, T. Niki, Y. Sohara, Y. Sugiyama and H. Mano (2007). "Identification of the transforming EML4-ALK fusion gene in non-small-cell lung cancer." Nature **448**(7153): 561-566.

Solomon, J. M., R. Pasupuleti, L. Xu, T. McDonagh, R. Curtis, P. S. DiStefano and L. J. Huber (2006). "Inhibition of SIRT1 catalytic activity increases p53 acetylation but does not alter cell survival following DNA damage." Mol Cell Biol **26**(1): 28-38.

Song, M. S., L. Salmena and P. P. Pandolfi (2012). "The functions and regulation of the PTEN tumour suppressor." Nat Rev Mol Cell Biol **13**(5): 283-296.

Soriano, A. O., H. Yang, S. Faderl, Z. Estrov, F. Giles, F. Ravandi, J. Cortes, W. G. Wierda, S. Ouzounian, A. Quezada, S. Pierce, E. H. Estey, J. P. Issa, H. M. Kantarjian and G. Garcia-Manero (2007). "Safety and clinical activity of the combination of 5-azacytidine, valproic acid, and all-trans retinoic acid in acute myeloid leukemia and myelodysplastic syndrome." Blood **110**(7): 2302-2308.

Souquet, P. J., F. Chauvin, J. P. Boissel, R. Cellerino, Y. Cormier, P. A. Ganz, S. Kaasa, J. L. Pater, E. Quoix and E. Rapp (1993). "Polychemotherapy in advanced non small cell lung cancer: a meta-analysis." Lancet **342**(8862): 19-21.

Soussi, T. (2003). "p53 mutations and resistance to chemotherapy: A stab in the back for p73." Cancer Cell **3**(4): 303-305.

Soussi, T., C. Caron de Fromentel and P. May (1990). "Structural aspects of the p53 protein in relation to gene evolution." Oncogene **5**(7): 945-952.

Soussi, T., C. Caron de Fromentel, M. Méchali, P. May and M. Kress (1987). "Cloning and characterization of a cDNA from Xenopus laevis coding for a protein homologous to human and murine p53." Oncogene **1**(1): 71-78.

Srinivasula, S. M., M. Ahmad, T. Fernandes-Alnemri and E. S. Alnemri (1998). "Autoactivation of procaspase-9 by Apaf-1-mediated oligomerization." Mol Cell **1**(7): 949-957.

Steele, N. L., J. A. Plumb, L. Vidal, J. Tjørnelund, P. Knoblauch, A. Rasmussen, C. E. Ooi, P. Buhl-Jensen, R. Brown, T. R. Evans and J. S. DeBono (2008). "A phase 1 pharmacokinetic and pharmacodynamic study of the histone deacetylase inhibitor belinostat in patients with advanced solid tumors." Clin Cancer Res **14**(3): 804-810.

Stein, G. H., L. F. Drullinger, R. S. Robetorye, O. M. Pereira-Smith and J. R. Smith (1991). "Senescent cells fail to express cdc2, cycA, and cycB in response to mitogen stimulation." Proc Natl Acad Sci U S A **88**(24): 11012-11016.

Stephens, P., C. Hunter, G. Bignell, S. Edkins, H. Davies, J. Teague, C. Stevens, S. O'Meara, R. Smith, A. Parker, A. Barthorpe, M. Blow, L. Brackenbury, A. Butler, O. Clarke, J. Cole, E. Dicks, A. Dike, A. Drozd, K. Edwards, S. Forbes, R. Foster, K. Gray, C. Greenman, K. Halliday, K. Hills, V. Kosmidou, R. Lugg, A. Menzies, J. Perry, R. Petty, K. Raine, L. Ratford, R. Shepherd, A. Small, Y. Stephens, C. Tofts, J. Varian, S. West, S. Widaa, A. Yates, F. Brasseur, C. S. Cooper, A. M. Flanagan, M. Knowles, S. Y. Leung, D. N. Louis, L. H. Looijenga, B. Malkowicz, M. A. Pierotti, B. Teh, G. Chenevix-Trench, B. L. Weber, S. T. Yuen, G. Harris, P. Goldstraw, A. G. Nicholson, P. A. Futreal, R. Wooster and M. R. Stratton (2004). "Lung cancer: intragenic ERBB2 kinase mutations in tumours." Nature **431**(7008): 525-526.

Stommel, J. M., N. D. Marchenko, G. S. Jimenez, U. M. Moll, T. J. Hope and G. M. Wahl (1999). "A leucine-rich nuclear export signal in the p53 tetramerization domain: regulation of subcellular localization and p53 activity by NES masking." EMBO J **18**(6): 1660-1672.

Strahl, B. D. and C. D. Allis (2000). "The language of covalent histone modifications." Nature **403**(6765): 41-45.

Strano, S., G. Fontemaggi, A. Costanzo, M. G. Rizzo, O. Monti, A. Baccarini, G. Del Sal, M. Levrero, A. Sacchi, M. Oren and G. Blandino (2002). "Physical interaction with human tumor-derived p53 mutants inhibits p63 activities." J Biol Chem **277**(21): 18817-18826.

Strano, S., E. Munarriz, M. Rossi, L. Castagnoli, Y. Shaul, A. Sacchi, M. Oren, M. Sudol, G. Cesareni and G. Blandino (2001). "Physical interaction with Yes-associated protein enhances p73 transcriptional activity." J Biol Chem **276**(18): 15164-15173.

Stransky, N., A. M. Egloff, A. D. Tward, A. D. Kostic, K. Cibulskis, A. Sivachenko, G. V. Kryukov, M. S. Lawrence, C. Sougnez, A. McKenna, E. Shefler, A. H. Ramos, P. Stojanov, S. L. Carter, D. Voet, M. L. Cortés, D. Auclair, M. F. Berger, G. Saksena, C. Guiducci, R. C. Onofrio, M. Parkin, M. Romkes, J. L. Weissfeld, R. R. Seethala, L. Wang, C. Rangel-Escareño, J. C. Fernandez-Lopez, A. Hidalgo-Miranda, J. Melendez-Zajgla, W. Winckler, K. Ardlie, S. B. Gabriel, M. Meyerson, E. S. Lander, G. Getz, T. R. Golub, L. A. Garraway and J. R. Grandis (2011). "The mutational landscape of head and neck squamous cell carcinoma." Science **333**(6046): 1157-1160.

Strevel, E. L., D. J. Ing and L. L. Siu (2007). "Molecularly targeted oncology therapeutics and prolongation of the QT interval." J Clin Oncol **25**(22): 3362-3371.

Stros, M. (1998). "DNA bending by the chromosomal protein HMG1 and its high mobility group box domains. Effect of flanking sequences." J Biol Chem **273**(17): 10355-10361.

Struhl, K. (1998). "Histone acetylation and transcriptional regulatory mechanisms." Genes Dev **12**(5): 599-606.

Subramanian, J. and R. Govindan (2007). "Lung cancer in never smokers: a review." J Clin Oncol **25**(5): 561-570.

Sutheesophon, K., N. Nishimura, Y. Kobayashi, Y. Furukawa, M. Kawano, K. Itoh, Y. Kano and H. Ishii (2005). "Involvement of the tumor necrosis factor (TNF)/TNF receptor system in leukemic cell apoptosis induced by histone deacetylase inhibitor depsipeptide (FK228)." J Cell Physiol **203**(2): 387-397.

Svechnikova, I., P. M. Almqvist and T. J. Ekström (2008). "HDAC inhibitors effectively induce cell type-specific differentiation in human glioblastoma cell lines of different origin." Int J Oncol **32**(4): 821-827.

Sykes, S. M., H. S. Mellert, M. A. Holbert, K. Li, R. Marmorstein, W. S. Lane and S. B. McMahon (2006). "Acetylation of the p53 DNA-binding domain regulates apoptosis induction." Mol Cell **24**(6): 841-851.

Sánchez-Perez, I., J. R. Murguía and R. Perona (1998). "Cisplatin induces a persistent activation of JNK that is related to cell death." Oncogene **16**(4): 533-540.

Takenaka, I., F. Morin, B. R. Seizinger and N. Kley (1995). "Regulation of the sequence-specific DNA binding function of p53 by protein kinase C and protein phosphatases." J Biol Chem **270**(10): 5405-5411.

Takeuchi, K., M. Soda, Y. Togashi, R. Suzuki, S. Sakata, S. Hatano, R. Asaka, W. Hamanaka, H. Ninomiya, H. Uehara, Y. Lim Choi, Y. Satoh, S. Okumura, K. Nakagawa, H. Mano and Y. Ishikawa (2012). "RET, ROS1 and ALK fusions in lung cancer." Nat Med **18**(3): 378-381.

Tang, C. H., C. Parham, E. Shocron, G. McMahon and N. Patel (2011). "Picoplatin overcomes resistance to cell toxicity in small-cell lung cancer cells previously treated with cisplatin and carboplatin." Cancer Chemother Pharmacol **67**(6): 1389-1400.

Tang, Y., J. Luo, W. Zhang and W. Gu (2006). "Tip60-dependent acetylation of p53 modulates the decision between cell-cycle arrest and apoptosis." Mol Cell **24**(6): 827-839.

Tang, Y., W. Zhao, Y. Chen, Y. Zhao and W. Gu (2008). "Acetylation is indispensable for p53 activation." Cell **133**(4): 612-626.

Taylor, W. R. and G. R. Stark (2001). "Regulation of the G2/M transition by p53." Oncogene **20**(15): 1803-1815.

Teo, M. C. and K. C. Soo (2013). "Cancer trends and incidences in Singapore." Jpn J Clin Oncol **43**(3): 219-224.

Thelen, P., S. Schweyer, B. Hemmerlein, W. Wuttke, F. Seseke and R. H. Ringert (2004). "Expressional changes after histone deacetylase inhibition by valproic acid in LNCaP human prostate cancer cells." Int J Oncol **24**(1): 25-31.

Thiagalingam, S., K. H. Cheng, H. J. Lee, N. Mineva, A. Thiagalingam and J. F. Ponte (2003). "Histone deacetylases: unique players in shaping the epigenetic histone code." Ann N Y Acad Sci **983**: 84-100.

Thompson, T., C. Tovar, H. Yang, D. Carvajal, B. T. Vu, Q. Xu, G. M. Wahl, D. C. Heimbrook and L. T. Vassilev (2004). "Phosphorylation of p53 on key serines is dispensable for transcriptional activation and apoptosis." J Biol Chem **279**(51): 53015-53022.

Thornborrow, E. C., S. Patel, A. E. Mastropietro, E. M. Schwartzfarb and J. J. Manfredi (2002). "A conserved intronic response element mediates direct p53-dependent transcriptional activation of both the human and murine bax genes." Oncogene **21**(7): 990-999.

Tibbetts, R. S., K. M. Brumbaugh, J. M. Williams, J. N. Sarkaria, W. A. Cliby, S. Y. Shieh, Y. Taya, C. Prives and R. T. Abraham (1999). "A role for ATR in the DNA damage-induced phosphorylation of p53." Genes Dev **13**(2): 152-157.

Toledo, F., K. A. Krummel, C. J. Lee, C. W. Liu, L. W. Rodewald, M. Tang and G. M. Wahl (2006). "A mouse p53 mutant lacking the proline-rich domain rescues Mdm4 deficiency and provides insight into the Mdm2-Mdm4-p53 regulatory network." Cancer Cell **9**(4): 273-285.

Tsai, C. M., D. Yu, K. T. Chang, L. H. Wu, R. P. Perng, N. K. Ibrahim and M. C. Hung (1995). "Enhanced chemoresistance by elevation of p185neu levels in HER-2/neu-transfected human lung cancer cells." J Natl Cancer Inst **87**(9): 682-684.

Tsao, M. S., A. Sakurada, J. C. Cutz, C. Q. Zhu, S. Kamel-Reid, J. Squire, I. Lorimer, T. Zhang, N. Liu, M. Daneshmand, P. Marrano, G. da Cunha Santos, A. Lagarde, F. Richardson, L. Seymour, M. Whitehead, K. Ding, J. Pater and F. A. Shepherd (2005). "Erlotinib in lung cancer - molecular and clinical predictors of outcome." N Engl J Med **353**(2): 133-144.

Turner, N. C. and J. S. Reis-Filho (2012). "Genetic heterogeneity and cancer drug resistance." Lancet Oncol **13**(4): e178-185.

Upton, J. P., K. Austgen, M. Nishino, K. M. Coakley, A. Hagen, D. Han, F. R. Papa and S. A. Oakes (2008). "Caspase-2 cleavage of BID is a critical apoptotic signal downstream of endoplasmic reticulum stress." Mol Cell Biol **28**(12): 3943-3951.

Ura, K., J. J. Hayes and A. P. Wolffe (1995). "A positive role for nucleosome mobility in the transcriptional activity of chromatin templates: restriction by linker histones." EMBO J **14**(15): 3752-3765.

Ura, K., H. Kurumizaka, S. Dimitrov, G. Almouzni and A. P. Wolffe (1997). "Histone acetylation: influence on transcription, nucleosome mobility and positioning, and linker histone-dependent transcriptional repression." EMBO J **16**(8): 2096-2107.

Vaisman, A., S. E. Lim, S. M. Patrick, W. C. Copeland, D. C. Hinkle, J. J. Turchi and S. G. Chaney (1999). "Effect of DNA polymerases and high mobility group protein 1 on the carrier ligand specificity for translesion synthesis past platinum-DNA adducts." Biochemistry **38**(34): 11026-11039.

Vaisman, A., M. Varchenko, A. Umar, T. A. Kunkel, J. I. Risinger, J. C. Barrett, T. C. Hamilton and S. G. Chaney (1998). "The role of hMLH1, hMSH3, and hMSH6 defects in cisplatin and oxaliplatin resistance: correlation with replicative bypass of platinum-DNA adducts." Cancer Res **58**(16): 3579-3585.

Vakhrusheva, O., C. Smolka, P. Gajawada, S. Kostin, T. Boettger, T. Kubin, T. Braun and E. Bober (2008). "Sirt7 increases stress resistance of cardiomyocytes and prevents apoptosis and inflammatory cardiomyopathy in mice." Circ Res **102**(6): 703-710.

van 't Veer, L. J., R. Hermens, L. A. van den Berg-Bakker, N. C. Cheng, G. J. Fleuren, J. L. Bos, F. J. Cleton and P. I. Schrier (1988). "ras oncogene activation in human ovarian carcinoma." Oncogene **2**(2): 157-165.

van Hennik, M. B., W. J. van der Vijgh, I. Klein, F. Elferink, J. B. Vermorken, B. Winograd and H. M. Pinedo (1987). "Comparative pharmacokinetics of cisplatin and three analogues in mice and humans." Cancer Res **47**(23): 6297-6301.

Van Lint, C., S. Emiliani and E. Verdin (1996). "The expression of a small fraction of cellular genes is changed in response to histone hyperacetylation." Gene Expr **5**(4-5): 245-253.

Vandenabeele, P., L. Galluzzi, T. Vanden Berghe and G. Kroemer (2010). "Molecular mechanisms of necroptosis: an ordered cellular explosion." Nat Rev Mol Cell Biol **11**(10): 700-714.

Vassilev, L. T. (2004). "Small-molecule antagonists of p53-MDM2 binding: research tools and potential therapeutics." Cell Cycle **3**(4): 419-421.

Vassilev, L. T., B. T. Vu, B. Graves, D. Carvajal, F. Podlaski, Z. Filipovic, N. Kong, U. Kammlott, C. Lukacs, C. Klein, N. Fotouhi and E. A. Liu (2004). "In vivo activation of the p53 pathway by small-molecule antagonists of MDM2." Science **303**(5659): 844-848.

Vaziri, H., S. K. Dessain, E. Ng Eaton, S. I. Imai, R. A. Frye, T. K. Pandita, L. Guarente and R. A. Weinberg (2001). "hSIR2(SIRT1) functions as an NAD-dependent p53 deacetylase." Cell **107**(2): 149-159.

Vekris, A., D. Meynard, M. C. Haaz, M. Bayssas, J. Bonnet and J. Robert (2004). "Molecular determinants of the cytotoxicity of platinum compounds: the contribution of in silico research." Cancer Res **64**(1): 356-362.

Venkitaraman, A. R. (2002). "Cancer susceptibility and the functions of BRCA1 and BRCA2." Cell **108**(2): 171-182.

Venot, C., M. Maratrat, C. Dureuil, E. Conseiller, L. Bracco and L. Debussche (1998). "The requirement for the p53 proline-rich functional domain for mediation of apoptosis is correlated with specific PIG3 gene transactivation and with transcriptional repression." EMBO J **17**(16): 4668-4679.

Veprintsev, D. B., S. M. Freund, A. Andreeva, S. E. Rutledge, H. Tidow, J. M. Cañadillas, C. M. Blair and A. R. Fersht (2006). "Core domain interactions in full-length p53 in solution." Proc Natl Acad Sci U S A **103**(7): 2115-2119.

Vigushin, D. M., S. Ali, P. E. Pace, N. Mirsaidi, K. Ito, I. Adcock and R. C. Coombes (2001). "Trichostatin A is a histone deacetylase inhibitor with potent antitumor activity against breast cancer in vivo." Clin Cancer Res **7**(4): 971-976.

Villalba, J. M. and F. J. Alcaín (2012). "Sirtuin activators and inhibitors." Biofactors **38**(5): 349-359.

Vousden, K. H. and D. P. Lane (2007). "p53 in health and disease." Nat Rev Mol Cell Biol **8**(4): 275-283.

Vousden, K. H. and X. Lu (2002). "Live or let die: the cell's response to p53." Nat Rev Cancer **2**(8): 594-604.

Vucic, D., K. Deshayes, H. Ackerly, M. T. Pisabarro, S. Kadkhodayan, W. J. Fairbrother and V. M. Dixit (2002). "SMAC negatively regulates the anti-apoptotic activity of melanoma inhibitor of apoptosis (ML-IAP)." J Biol Chem **277**(14): 12275-12279.

Wada, C. K., R. R. Frey, Z. Ji, M. L. Curtin, R. B. Garland, J. H. Holms, J. Li, L. J. Pease, J. Guo, K. B. Glaser, P. A. Marcotte, P. L. Richardson, S. S. Murphy, J. J. Bouska, P. Tapang, T. J. Magoc, D. H. Albert, S. K. Davidsen and M. R. Michaelides (2003). "Alpha-keto amides as inhibitors of histone deacetylase." Bioorg Med Chem Lett **13**(19): 3331-3335.

Wada, T. and J. M. Penninger (2004). "Mitogen-activated protein kinases in apoptosis regulation." Oncogene **23**(16): 2838-2849.

Wajant, H. (2002). "The Fas signaling pathway: more than a paradigm." Science **296**(5573): 1635-1636.

Waldman, T., K. W. Kinzler and B. Vogelstein (1995). "p21 is necessary for the p53-mediated G1 arrest in human cancer cells." Cancer Res **55**(22): 5187-5190.

Wang, D., R. Hara, G. Singh, A. Sancar and S. J. Lippard (2003). "Nucleotide excision repair from site-specifically platinum-modified nucleosomes." Biochemistry **42**(22): 6747-6753.

Wang, D. and S. J. Lippard (2005). "Cellular processing of platinum anticancer drugs." Nat Rev Drug Discov **4**(4): 307-320.

Wang, J., J. Y. Zhou and G. S. Wu (2007). "ERK-dependent MKP-1-mediated cisplatin resistance in human ovarian cancer cells." Cancer Res **67**(24): 11933-11941.

Wang, K., X. M. Yin, D. T. Chao, C. L. Milliman and S. J. Korsmeyer (1996). "BID: a novel BH3 domain-only death agonist." Genes Dev **10**(22): 2859-2869.

Wang, L. C., L. Wang, S. Kwauk, J. A. Woo, L. Q. Wu, H. Zhu, L. Z. Zhan, N. L. Sun and L. Zhang (2011). "Analysis on the clinical features of 22 basaloid squamous cell carcinoma of the lung." J Cardiothorac Surg **6**: 10.

Wang, R., P. Cherukuri and J. Luo (2005). "Activation of Stat3 sequence-specific DNA binding and transcription by p300/CREB-binding protein-mediated acetylation." J Biol Chem **280**(12): 11528-11534.

Wang, W. and W. D. Figg (2008). "Secondary BRCA1 and BRCA2 alterations and acquired chemoresistance." Cancer Biol Ther **7**(7): 1004-1005.

Wang, W. D., R. Li, Z. T. Chen, D. Z. Li, Y. Z. Duan and Z. H. Cao (2005). "Cisplatin-controlled p53 gene therapy for human non-small cell lung cancer xenografts in athymic nude mice via the CArG elements." Cancer Sci **96**(10): 706-712.

Wang, X., J. L. Martindale and N. J. Holbrook (2000). "Requirement for ERK activation in cisplatin-induced apoptosis." J Biol Chem **275**(50): 39435-39443.

Wang, X. W., Q. Zhan, J. D. Coursen, M. A. Khan, H. U. Kontny, L. Yu, M. C. Hollander, P. M. O'Connor, A. J. Fornace and C. C. Harris (1999). "GADD45 induction of a G2/M cell cycle checkpoint." Proc Natl Acad Sci U S A **96**(7): 3706-3711.

Wang, Y. and C. Prives (1995). "Increased and altered DNA binding of human p53 by S and G2/M but not G1 cyclin-dependent kinases." Nature **376**(6535): 88-91.

Wang, Y., J. F. Schwedes, D. Parks, K. Mann and P. Tegtmeyer (1995). "Interaction of p53 with its consensus DNA-binding site." Mol Cell Biol **15**(4): 2157-2165.

Wang, Y. H., Y. G. Tsay, B. C. Tan, W. Y. Lo and S. C. Lee (2003). "Identification and characterization of a novel p300-mediated p53 acetylation site, lysine 305." J Biol Chem **278**(28): 25568-25576.

Wani, M. C., H. L. Taylor, M. E. Wall, P. Coggon and A. T. McPhail (1971). "Plant antitumor agents. VI. The isolation and structure of taxol, a novel antileukemic and antitumor agent from Taxus brevifolia." J Am Chem Soc **93**(9): 2325-2327.

Waskiewicz, A. J., A. Flynn, C. G. Proud and J. A. Cooper (1997). "Mitogen-activated protein kinases activate the serine/threonine kinases Mnk1 and Mnk2." EMBO J **16**(8): 1909-1920.

Watamoto, K., M. Towatari, Y. Ozawa, Y. Miyata, M. Okamoto, A. Abe, T. Naoe and H. Saito (2003). "Altered interaction of HDAC5 with GATA-1 during MEL cell differentiation." Oncogene **22**(57): 9176-9184.

Watanabe, M., A. Nobuta, J. Tanaka and M. Asaka (1996). "An effect of K-ras gene mutation on epidermal growth factor receptor signal transduction in PANC-1 pancreatic carcinoma cells." Int J Cancer **67**(2): 264-268.

Wei, M. C., T. Lindsten, V. K. Mootha, S. Weiler, A. Gross, M. Ashiya, C. B. Thompson and S. J. Korsmeyer (2000). "tBID, a membrane-targeted death ligand, oligomerizes BAK to release cytochrome c." Genes Dev **14**(16): 2060-2071.

Weinstein, I. B. (2002). "Cancer. Addiction to oncogenes--the Achilles heal of cancer." Science **297**(5578): 63-64.

Weiss, J., M. L. Sos, D. Seidel, M. Peifer, T. Zander, J. M. Heuckmann, R. T. Ullrich, R. Menon, S. Maier, A. Soltermann, H. Moch, P. Wagener, F. Fischer, S. Heynck, M. Koker, J. Schöttle, F. Leenders, F. Gabler, I. Dabow, S. Querings, L. C. Heukamp, H. Balke-Want, S. Ansén, D. Rauh, I. Baessmann, J. Altmüller, Z. Wainer, M. Conron, G. Wright, P. Russell, B. Solomon, E. Brambilla, C. Brambilla, P. Lorimier, S. Sollberg, O. T. Brustugun, W. Engel-Riedel, C. Ludwig, I. Petersen, J. Sänger, J. Clement, H. Groen, W. Timens, H. Sietsma, E. Thunnissen, E. Smit, D. Heideman, F. Cappuzzo, C. Ligorio, S. Damiani, M. Hallek, R. Beroukhim, W. Pao, B. Klebl, M. Baumann, R. Buettner, K. Ernestus, E. Stoelben, J. Wolf, P. Nürnberg, S. Perner and R. K. Thomas (2010). "Frequent and focal FGFR1 amplification associates with therapeutically tractable FGFR1 dependency in squamous cell lung cancer." Sci Transl Med **2**(62): 62ra93.

Welcsh, P. L. and M. C. King (2001). "BRCA1 and BRCA2 and the genetics of breast and ovarian cancer." Hum Mol Genet **10**(7): 705-713.

Werling, U., S. Siehler, M. Litfin, H. Nau and M. Göttlicher (2001). "Induction of differentiation in F9 cells and activation of peroxisome proliferator-activated receptor delta by valproic acid and its teratogenic derivatives." Mol Pharmacol **59**(5): 1269-1276.

World Health Organization (2013). "Cancer Fact Sheet no. 297." Retrieved August, 2013, from http://www.who.int/mediacentre/factsheets/fs297/en/.

Wiernik, P. H. and A. I. Einzig (1993). "Taxol in malignant melanoma." J Natl Cancer Inst Monogr(15): 185-187.

Wilkerson, M. D., X. Yin, K. A. Hoadley, Y. Liu, M. C. Hayward, C. R. Cabanski, K. Muldrew, C. R. Miller, S. H. Randell, M. A. Socinski, A. M. Parsons, W. K. Funkhouser, C. B. Lee, P. J. Roberts, L. Thorne, P. S. Bernard, C. M. Perou and D. N. Hayes (2010). "Lung squamous cell carcinoma mRNA expression subtypes are reproducible, clinically important, and correspond to normal cell types." Clin Cancer Res **16**(19): 4864-4875.

Wilson, A. J., E. Holson, F. Wagner, Y. L. Zhang, D. M. Fass, S. J. Haggarty, S. Bhaskara, S. W. Hiebert, S. L. Schreiber and D. Khabele (2011). "The DNA damage mark pH2AX differentiates the cytotoxic effects of small molecule HDAC inhibitors in ovarian cancer cells." Cancer Biol Ther **12**(6): 484-493.

Wilson, A. J., A. S. Lalani, E. Wass, J. Saskowski and D. Khabele (2012). "Romidepsin (FK228) combined with cisplatin stimulates DNA damage-induced cell death in ovarian cancer." Gynecol Oncol **127**(3): 579-586.

Wistuba, I. I., C. Behrens, S. Milchgrub, D. Bryant, J. Hung, J. D. Minna and A. F. Gazdar (1999). "Sequential molecular abnormalities are involved in the multistage development of squamous cell lung carcinoma." Oncogene **18**(3): 643-650.

Witta, S. E., R. M. Gemmill, F. R. Hirsch, C. D. Coldren, K. Hedman, L. Ravdel, B. Helfrich, R. Dziadziuszko, D. C. Chan, M. Sugita, Z. Chan, A. Baron, W. Franklin, H. A. Drabkin, L. Girard, A. F. Gazdar, J. D. Minna and P. A. Bunn (2006). "Restoring E-cadherin expression increases sensitivity to epidermal growth factor receptor inhibitors in lung cancer cell lines." Cancer Res **66**(2): 944-950.

Witta, S. E., R. M. Jotte, K. Konduri, M. A. Neubauer, A. I. Spira, R. L. Ruxer, M. Varella-Garcia, P. A. Bunn and F. R. Hirsch (2012). "Randomized phase II trial of erlotinib with and without entinostat in patients with advanced non-small-cell lung cancer who progressed on prior chemotherapy." J Clin Oncol **30**(18): 2248-2255.

Wong, D. W., E. L. Leung, K. K. So, I. Y. Tam, A. D. Sihoe, L. C. Cheng, K. K. Ho, J. S. Au, L. P. Chung, M. Pik Wong and U. o. H. K. L. C. S. Group (2009). "The EML4-ALK fusion gene is involved in various histologic types of lung cancers from nonsmokers with wild-type EGFR and KRAS." Cancer **115**(8): 1723-1733.

Wong, E. and C. M. Giandomenico (1999). "Current status of platinum-based antitumor drugs." Chem Rev **99**(9): 2451-2466.

Wu, D., Y. Pang, M. D. Wilkerson, D. Wang, P. S. Hammerman and J. S. Liu (2013). "Gene-expression data integration to squamous cell lung cancer subtypes reveals drug sensitivity." Br J Cancer **109**(6): 1599-1608.

Wu, W., H. D. Wang, W. Guo, K. Yang, Y. P. Zhao, Y. G. Jiang and P. He (2010). "Up-regulation of Fas reverses cisplatin resistance of human small cell lung cancer cells." J Exp Clin Cancer Res **29**: 49.

Wu, X., J. H. Bayle, D. Olson and A. J. Levine (1993). "The p53-mdm-2 autoregulatory feedback loop." Genes Dev **7**(7A): 1126-1132.

Xia, Z., M. Dickens, J. Raingeaud, R. J. Davis and M. E. Greenberg (1995). "Opposing effects of ERK and JNK-p38 MAP kinases on apoptosis." Science **270**(5240): 1326-1331.

Xiong, Y., H. Zhang and D. Beach (1992). "D type cyclins associate with multiple protein kinases and the DNA replication and repair factor PCNA." Cell **71**(3): 505-514.

Xiong, Y., H. Zhang and D. Beach (1993). "Subunit rearrangement of the cyclin-dependent kinases is associated with cellular transformation." Genes Dev **7**(8): 1572-1583.

Yamamoto, T., S. Ikawa, T. Akiyama, K. Semba, N. Nomura, N. Miyajima, T. Saito and K. Toyoshima (1986). "Similarity of protein encoded by the human c-erb-B-2 gene to epidermal growth factor receptor." Nature **319**(6050): 230-234.

Yamasaki, M., T. Makino, T. Masuzawa, Y. Kurokawa, H. Miyata, S. Takiguchi, K. Nakajima, Y. Fujiwara, N. Matsuura, M. Mori and Y. Doki (2011). "Role of multidrug resistance protein 2 (MRP2) in chemoresistance and clinical outcome in oesophageal squamous cell carcinoma." Br J Cancer **104**(4): 707-713.

Yaneva, J. N., E. G. Paneva, S. I. Zacharieva and J. Zlatanova (2007). "Histone H1 interacts preferentially with DNA fragments containing a cisplatin-induced 1,2-intrastrand cross-link." Z Naturforsch C **62**(11-12): 905-908.

Yang, J., K. Winkler, M. Yoshida and S. Kornbluth (1999). "Maintenance of G2 arrest in the Xenopus oocyte: a role for 14-3-3-mediated inhibition of Cdc25 nuclear import." EMBO J **18**(8): 2174-2183.

Yang, X. J. and E. Seto (2003). "Collaborative spirit of histone deacetylases in regulating chromatin structure and gene expression." Curr Opin Genet Dev **13**(2): 143-153.

Yarden, Y. and M. X. Sliwkowski (2001). "Untangling the ErbB signalling network." Nat Rev Mol Cell Biol **2**(2): 127-137.

Yeh, P. Y., S. E. Chuang, K. H. Yeh, Y. C. Song, C. K. Ea and A. L. Cheng (2002). "Increase of the resistance of human cervical carcinoma cells to cisplatin by inhibition of the MEK to ERK signaling pathway partly via enhancement of anticancer drug-induced NF kappa B activation." Biochem Pharmacol **63**(8): 1423-1430.

Yeo, W., H. C. Chung, S. L. Chan, L. Z. Wang, R. Lim, J. Picus, M. Boyer, F. K. Mo, J. Koh, S. Y. Rha, E. P. Hui, H. C. Jeung, J. K. Roh, S. C. Yu, K. F. To, Q. Tao, B. B. Ma, A. W. Chan, J. H. Tong, C. Erlichman, A. T. Chan and B. C. Goh (2012). "Epigenetic therapy using belinostat for patients with unresectable hepatocellular carcinoma: a multicenter phase I/II study with biomarker and pharmacokinetic analysis of tumors from patients in the Mayo Phase II Consortium and the Cancer Therapeutics Research Group." J Clin Oncol **30**(27): 3361-3367.

Yi, E. S., J. M. Boland, J. J. Maleszewski, A. C. Roden, A. M. Oliveira, M. C. Aubry, M. R. Erickson-Johnson, B. L. Caron, Y. Li, H. Tang, S. Stoddard, J. Wampfler, K. Kulig and P. Yang (2011). "Correlation of IHC and FISH for ALK gene rearrangement in non-small cell lung carcinoma: IHC score algorithm for FISH." J Thorac Oncol **6**(3): 459-465.

Yokota, J. and T. Kohno (2004). "Molecular footprints of human lung cancer progression." Cancer Sci **95**(3): 197-204.

Yoshida, K. and Y. Miki (2004). "Role of BRCA1 and BRCA2 as regulators of DNA repair, transcription, and cell cycle in response to DNA damage." Cancer Sci **95**(11): 866-871.

Yoshida, M., M. Kijima, M. Akita and T. Beppu (1990). "Potent and specific inhibition of mammalian histone deacetylase both in vivo and in vitro by trichostatin A." J Biol Chem **265**(28): 17174-17179.

Yuan, J., S. Shaham, S. Ledoux, H. M. Ellis and H. R. Horvitz (1993). "The C. elegans cell death gene ced-3 encodes a protein similar to mammalian interleukin-1 beta-converting enzyme." Cell **75**(4): 641-652.

Zabarovsky, E. R., M. I. Lerman and J. D. Minna (2002). "Tumor suppressor genes on chromosome 3p involved in the pathogenesis of lung and other cancers." Oncogene **21**(45): 6915-6935.

Zakut-Houri, R., B. Bienz-Tadmor, D. Givol and M. Oren (1985). "Human p53 cellular tumor antigen: cDNA sequence and expression in COS cells." EMBO J **4**(5): 1251-1255.

Zamble, D. B., T. Jacks and S. J. Lippard (1998). "p53-Dependent and -independent responses to cisplatin in mouse testicular teratocarcinoma cells." Proc Natl Acad Sci U S A **95**(11): 6163-6168.

Zamble, D. B., Y. Mikata, C. H. Eng, K. E. Sandman and S. J. Lippard (2002). "Testis-specific HMG-domain protein alters the responses of cells to cisplatin." J Inorg Biochem **91**(3): 451-462.

Zamble, D. B., D. Mu, J. T. Reardon, A. Sancar and S. J. Lippard (1996). "Repair of cisplatin--DNA adducts by the mammalian excision nuclease." Biochemistry **35**(31): 10004-10013.

Zanke, B. W., K. Boudreau, E. Rubie, E. Winnett, L. A. Tibbles, L. Zon, J. Kyriakis, F. F. Liu and J. R. Woodgett (1996). "The stress-activated protein kinase pathway mediates cell death following injury induced by cis-platinum, UV irradiation or heat." Curr Biol **6**(5): 606-613.

Zdraveski, Z. Z., J. A. Mello, C. K. Farinelli, J. M. Essigmann and M. G. Marinus (2002). "MutS preferentially recognizes cisplatin- over oxaliplatin-modified DNA." J Biol Chem **277**(2): 1255-1260.

Zeng, L., Q. Xiao, A. Margariti, Z. Zhang, A. Zampetaki, S. Patel, M. C. Capogrossi, Y. Hu and Q. Xu (2006). "HDAC3 is crucial in shear- and VEGF-induced stem cell differentiation toward endothelial cells." J Cell Biol **174**(7): 1059-1069.

Zhan, Q., M. J. Antinore, X. W. Wang, F. Carrier, M. L. Smith, C. C. Harris and A. J. Fornace (1999). "Association with Cdc2 and inhibition of Cdc2/Cyclin B1 kinase activity by the p53-regulated protein Gadd45." Oncogene **18**(18): 2892-2900.

Zhang, C. L., T. A. McKinsey, S. Chang, C. L. Antos, J. A. Hill and E. N. Olson (2002). "Class II histone deacetylases act as signal-responsive repressors of cardiac hypertrophy." Cell **110**(4): 479-488.

Zhang, X., Y. Ozawa, H. Lee, Y. D. Wen, T. H. Tan, B. E. Wadzinski and E. Seto (2005). "Histone deacetylase 3 (HDAC3) activity is regulated by interaction with protein serine/threonine phosphatase 4." Genes Dev **19**(7): 827-839.

Zhang, X. D., S. K. Gillespie, J. M. Borrow and P. Hersey (2004). "The histone deacetylase inhibitor suberic bishydroxamate regulates the expression of multiple apoptotic mediators and induces mitochondria-dependent apoptosis of melanoma cells." Mol Cancer Ther **3**(4): 425-435.

Zhou, B. P., Y. Liao, W. Xia, Y. Zou, B. Spohn and M. C. Hung (2001). "HER-2/neu induces p53 ubiquitination via Akt-mediated MDM2 phosphorylation." Nat Cell Biol **3**(11): 973-982.

Zhou, L. L., L. Y. Zhou, K. Q. Luo and D. C. Chang (2005). "Smac/DIABLO and cytochrome c are released from mitochondria through a similar mechanism during UV-induced apoptosis." Apoptosis **10**(2): 289-299.

Zhu, Q., M. A. Wani, M. El-Mahdy and A. A. Wani (2000). "Decreased DNA repair efficiency by loss or disruption of p53 function preferentially affects removal of cyclobutane pyrimidine dimers from non-transcribed strand and slow repair sites in transcribed strand." J Biol Chem **275**(15): 11492-11497.

Zotchev, S. B., M. Protopopova and G. Selivanova (2000). "p53 C-terminal interaction with DNA ends and gaps has opposing effect on specific DNA binding by the core." Nucleic Acids Res **28**(20): 4005-4012.

APPENDICES

Up-regulated														
C1orf201	LSM1	BPNT1	C14orf135	GAGE1	KBTBD8	CDKN3	UCHL1	PEX5L	FRMD3	MOSC2	BCAT1	SNORD13	RRAGD	INA	SNORD116-3
C11orf54	KPNA5	GLIPR1	COQ3	PLAC8	DNALI1	CMTM7	PROS1	C5	HMGA2	DCAF16	FAM171B	F5	CNIH3	CABYR	PAR5
GBE1	WASF1	LOC401397	PTGR2	UBE2T	KLHDC2	TKTL1	LRFN5	TMOD2	FZD5	RALGAPA1	GNG4	CHD1L	FLG	PMP22	ETV1
C6orf35	FGFR1OP2	RFXAP	HIST1H2BC	APOD	ERBB2	ANGEL2	NEGR1	LOC654342	KIAA0586	ZNF717	RNU1-1	KHDRBS3	ACAA2	PRKAA2	SNORD116-17
GAFA3	C1orf97	SPAG1	C20orf30	C2orf43	SPIN2A	CTGF	HIST1H4B	KIAA1383	WDR19	SEC23A	ETNK1	SNORD13	LPXN	PHKA1	FN1
SPATS2L	TMEM176B	FUCA1	HIST2H2BE	SDC2	C11orf67	PHACTR2	CCNJ	KIAA1715	CCDC68	MXRA7	KIF16B	WDSUB1	HEBP2	GSPT2	KIAA1324L
KCNS3	MTMR7	GABBR2	BRMS1L	LONRF3	GCLM	DCP1B	OSGEPL1	SNORA5A	FAM175A	C12orf72	CTPS2	ZNF253	PRCP	PTGR1	
ZNF570	KATNA1	METTL4	PAK3	ANKRD36B	AP3M2	ZNF91	RPAIN	HOXB6	POLE2	UGDH	KIAA1244	C3orf57	CMTM8	TBC1D4	
HLA-DRA	EIF2B2	TWSG1	MCFD2	PGM5	ZNF32	KLHL23	ACVR1C	CDH7	HLTF	LRRCC1	GEM	C18orf54	TUSC3	RAB3B	
FUNDC2	SERTAD2	BRP44L	PKIA	TP53INP1	GSTA4	HIST1H2AC	MT1A	GSTM3	RAP2A	PYGO1	NRN1	STEAP1	C11orf92	BMPR1B	
BBS10	POLR3F	RCOR3	CCNB1IP1	FAM169A	ZNF585B	GPD1L	SMPDL3A	HIST1H1D	RNF157	ZNF253	SPRY2	ACP6	NR0B1	AFAP1	
C14orf126	KITLG	OVOS2	SCAMP5	PPAPDC1A	ATG4C	SNX16	GPC6	TMEM38B	FKBP1A	HIST2H2BF	TBC1D19	ST8SIA4	AGR2	F2RL2	
TMEM133	C7orf41	SIKE1	ADORA2B	GNA13	PRKRA	SERF1A	RASSF6	SSPN	LCA5	PHYHIPL	HSN2	CD109	DDHD1	VCAN	
LEPROTL1	RFX3	LIAS	TXNDC16	SPA17|SIAE	MTERFD2	LMCD1	TFF1	GLT25D2	C12orf60	MKKS	AMN1	ZNF724P	HECW2	CMBL	
ATIC	SNRPD1	PAIP2B	NRP2	IRAK1BP1	LOC171220	LSP1	TEC	C12orf47	C14orf167	G6PD	ANTXR2	CENPV	RGS4	AP1S2	
C10orf58	CHIC1	VIM	FAM27E3	PLAG1	C9orf123	INTS7	KIAA1797	SNORD116-4	RNU1-1	C11orf74	FAM55C	KDELC1	ANKRD1	HNMT	
YIPF1	RGS2	SMYD3	EIF2C4	SUPT3H	DOCK8	TRIM24	CDKN1B	ZNF30	LGALS8	ADAMTS6	TTC21B	PRTFDC1	MEGF9	CSAG2	
TBC1D1	ZNF260	SHPRH	ANKS4B	PTHLH	CTAGE5	ARMCX3	TCP11L2	PRPSAP2	SYTL2	SLC16A14	AKR1C3	TRAPPC6B	AP1S2	SNORD115-11	
GPR155	GGH	CDC14A	STAMBPL1	CTNNAL1	DERA	SAMHD1	RNFT2	KLF12	SVIP	C1orf51	ANK2	ZNF706	ADD3	PLEKHA5	
ERO1LB	GLUL	LOC100132167	ARL17A	DUSP10	PLS1	RBPJ	GABRB3	MRPS28	HIST2H2BF	CA8	GLCCI1	NEUROD1	EXPH5	TFPI	
ALS2CR4	SLC2A13	TRPC1	CMAS	RERG	LOC100132167	C16orf62	BMP6	STK17B	FAM47E	C20orf7	STC2	CFL2	TNFRSF11B	ALDH1A1	
TPK1	EBF3	ERGIC2	ENPEP	CDH18	EXOC6B	GSR	PELI2	PRDM5	RPSAP58	EML5	DKFZp434H1419	CYP2R1	CHN1	NRCAM	
EFHA2	CCNDBP1	REP15	BMF	CYP4F3	RASGRP3	NARS2	DENND5B	RB1	FKBP1A	SGTB	PSD3	CPPED1	SLAIN1	UGT8	
NEK3	TBC1D8B	PRKG2	MPHOSPH9	MCM8	RGS5	C7orf23	MAP1A	SYT4	KCNJ8	FRK	DOCK4	GSTP1	CCDC88A	SLC40A1	
AIG1	FBXL20	STK38L	ZFP28	FNIP2	PLEKHH2	SOX2	HTATIP2	GTF2E2	CROT	ZNF804A	TSPAN12	HPGD	CAPRIN2	ZNF730	
PRDX4	HOXB7	GAGE1	MAML3	TBPL1|SLC2A12	C18orf8	THYN1	FITM2	CD68	SGCB	GULP1	LY75	CXorf57	FKBP7	SCRN1	
WDR48	MTERFD1	PGM5	G2E3	C9orf72	HS6ST2	OVOS	REPS1	ABHD3	SPANXA2	UNC13B	RGL1	TMEM176A	SH3BGRL2	GPX2	
SPANXB1	GSTO1	SNRPB	CISD1	AGTPBP1	SNTB1	GAGE1	PBK	SNORD33	EPHA7	MMP1	KCNK2	AGPAT9	PRRG1	PDK4	
PECR	MBIP	TCF12	GPR98	PDK3	C17orf75	ZADH2	ZNF559	C20orf114	CCDC28A	CCDC77	CHGB	NCF2	CSAG2	PM20D2	
SPIN4	RGNEF	FBXL4	HIST1H2BG	SPRED1	PLCH1	CCNB3	DHRS7	C17orf51	TUBA1A	DECR1	HRSP12	CABLES1	SDR42E1	ME1	
ANKRD46	C16orf63	NARF	MED21	ORC3L	THSD7A	MTR	EYA1	ATP11C	ZNF608	RNU1-1	STRADB	WDR35	SEMA3A	LCP1	
DPY19L2P2	ARHGAP18	MRPS33	SORBS2	FUT8	WNK1	C17orf37	CDC42EP3	F2R	KCNQ5	ZBTB25	B3GALT1	ASCL1	SCCPDH	RBP1	
CDK19	FOXG1	ZNF430	CAPS2	LBR	SLC38A3	LRP12	GYG2	FBXO43	PGAP1	PKIB	KIAA0528	LSP1	DNAJC12	MIPOL1	
UBR7	CYB5R4	NPC1	NDUFAF4	PELO	EXOSC8	E2F5	GSTM2	PMAIP1	ANUBL1	STX1A	TXNIP	AOX1	PRKD1	GCNT1	
LOC147727	SLC35A1	PNMA1	WDR76	COCH	JAM3	ANG	SNORD3A	HIST1H3B	NNT	TMEM55A	ZNF253	FTL	PAX9	HAS2	
SNRPB2	EFHA1	PHEX	HIST1H4C	KRAS	BARD1	PPFIA2	ASF1A	SRXN1	GPRIN3	HIST1H2BH	FOXN3	SYT1	SCML1	TSPAN8	
C13orf38	SPATA6	LOC440957	CCDC34	GLRX5	FAM60A	LPPR1	NELL2	QDPR	GDAP1	FAR2	MAP9	PRKAR2B	SRPX	EDIL3	
GUCY1A2	E2F7	GAGE1	IGF2BP1	FZD3	C15orf41	SUSD1	LANCL1	ALDH7A1	C6orf192	ZNF300	FAM161A	ACADSB	SATB2	LY75	
RNF128	GZF1	C1D	MLPH	MRPS28	SLC4A4	SIP1	C20orf94	SPIN2B	CYP39A1	RTKN2	A1CF	SNORD116-6	SNORD116-2	CYB5A	
NAA20	MAGED1	CENPJ	DTNA	GMFB	PEX3	NDUFC2	NT5E	CHML	EPS8	HIST1H3F	SERPINI1	EPCAM	QPCT	SCG5	
SKA1	SLC4A7	NEFM	PAK6	C4orf34	ZNF506	ZNF280C	MIR1977	TBC1D5	SPANXA2	ST3GAL6	CHMP4C	SNAI2	ENPP2	LDHB	
ALS2	GPHN	PPFIBP1	CENPW	C14orf109	PLK1S1	EPB41L5	ACYP1	SAT2	ZNF681	ZNF486	CNTN1	SCG2	SLC7A2	HSD17B11	
MAP2	C14orf156	RUNX2	SESN3	TSGA14	TLR6	MMD	PDE1C	FBXO33	SMAD9	RBBP9	TSPAN5	PLAGL1	C3orf14	SPP1	
PHF6	PLCE1	C14orf128	LRIG3	PDE6D	C4orf52	NDUFB6	SEMA6A	FMN1	CTSC	C20orf72	HNF4G	C6orf162	GABRA3	TEX15	
RHOBTB3	SEPSECS	ATP8B2	C11orf1	ORC2L	PLCB1	WIPF1	PPP2R3C	COG2	TGFB2	AK3	ZNF738	ICK	FZD7	C12orf75	
ZNF675	ZNF519	HACL1	EGR2	JPH1	FUNDC1	OSBPL6	PRKAB2	ZC3HAV1L	ZNF711	RAB38	PPARGC1A	SEMA3E	AKR1C2	CLGN	
LOC151009	CENPF	SPATA7	MATN3	LOC728819	SCML2	GRIN3A	ASAH1	TCF4	ENPP1	GALC	C4BPB	LGR4	SATB1	TMEM156	
ACAT1	BHLHB9	THEM4	GSTA1	SLC2A12	ARL3	LYPLAL1	BNIP3	GSTM1	HOXB9	GPR116	NRP1	FST	NCAM1	SNRPN	
NSMCE4A	TRAF5	MIR103-2	MARK1	ZNF141	PTCH1	BUB1B	MRPS35	DDX43	NAP1L5	BVES	SNAP25	RCAN3	TMEFF2	MGST1	
KIAA0391	RPS6KA5	AASS	CD24	RASA4	MNAT1	TTC39C	IPO8	TMEM75	CCDC91	PSAT1	FAM164A	LOC100128816	MPP1	POPDC3	

Appendix 1: Genes that were enriched in cisplatin resistant lung SCC cell lines (fold change > 1.5; *P* < 0.1).

Down-regulated															
TIMP3	OTUD1	SEMA3C	HLA-H	FAM38B	SPRR2A	NMI	FAM188B	PLEKHM2	ZNF814	HSPB1	ZYX	TRIM21	SNORD38B	FRMD4B	DHDDS	OBFC2A
SLPI	RARRES1	CFB|C2	SFN	CD9	EPHA3	RBMS3	BTN3A2	FBP1	PSG4	LAMC1	DSE	ACOT7	FBLN1	QTRTD1	VATIL	S100A16
RPS4Y1	ALDH1A3	CXorf61	FER	SULF2	KYNU	SAMD9L	FBXO2	BDNF	HDAC3	GSTT1	GABRE	HIVEP1	RAB15	ARHGAP10	TRIM58	PDCD4
FAM83B	ANTXR1	GBP2	EREG	LAMP3	F11R	SNORA31	SGK269	NCAM2	TNFRSF10B	FNTA	CDH1	LMAN2	LIPA	KIAA1191	HEXIM1	PAX6
C1S	EPB41L4A	UPK1B	ABCA12	ATP11A	TAPBP	ZNF544	TUFT1	ANKRD22	PPP2R2B	RAB13	UBE2E2	OR2W3	IREB2	GLS	MINA	
FGFBP1	KRT5	OAS1	LRRC16A	TM4SF1	PLXDC2	C3orf58	ITPR3	IGSF3	SHC1	NRIP1	BTG3	ADCY6	DHRS3	IGFBP7	ERGIC1	
CLDN1	CXCL16	SLCO3A1	STARD4	IFI16	TP63	SERPINH1	KAL1	CLDN22	RAB31	FLRT3	DDX58	SLC16A1	RAB5C	HINT3	WDR61	
DRAM1	PHLDB2	SP110	C15orf48	SP100	DDR2	SLC7A7	BACE2	ACE2	LOC648987	IQCK	CAST	EPHA4	CCDC18	BCL2L1	RAI14	
MPZL2	CPA4	CA2	PLD1	RASGRP1	TMEM217	OAS2	TMEM184B	ERC1	NF1	LRCH1	TACSTD2	MCTP2	IGF2BP2	RBPMS2	SLC39A6	
GPR87	SQRDL	LITAF	ICAM1	KRT6C	TRIM5	OPTN	PSG7	AP2M1	GPR137B	DNER	CADM1	C22orf46	ERAP2	GRHL2	CARD16	
MX1	IFIT1	PDZD2	DDX60	PYGL	TMEM63B	MOV10	SASH1	TREM1	DKK1	SLFN5	DCLK1	LONRF2	AN06	KIAA0922	MED15	
FGF9	AP0L1	SNX10	KIRREL	ACTBL2	SH3RF2	MST1R	LIFR	RNASEL	ADAMTS9	ISL1	GALNT10	SEMA5A	IFNAR2	ENPP3	MAN2A1	
C3	PARP14	DUSP1	DOK5	NMNAT2	IL1R1	FYN	ERAP1	HCLS1	CXCL2	BARX2	SLC9A8	WNT2B	CTSO	SYT10	NIT2	
TFPI2	MSN	IL6	C1R	ZFPM2	EPHA2	PSG7	SCGB3A2	SLC16A2	SPPL2A	TMSB10	P4HA2	NFAT5	HMG20A	SLIT3	LACTB	
FAS	SPRR1B	PTPRF	SLC39A8	FGD6	ARF3	CREB5	KRT6B	CD83	RASA2	STAT1	SLC44A2	TNFRSF12A	CES1	EIF2C3	PDPN	
MUC1	TNS4	EFNB2	BNC1	SLC22A4	LCN2	LGALS1	DSG3	SIK2	ZNF654	SNORD24	TNFRSF1A	THSD1	RCC2	ALDH1L2	LY6E	
CCL20	BDKRB1	MYOF	CFB	INADL	NCEH1	LOC100131726	SLC30A4	FLNB	SGPP2	PLAUR	BNIP2	C1orf54	RNF180	BMPR1A	PLOD1	
OSMR	TRIM29	MME	NEDD4	PB	GCH1	RPL39L	C21orf63	ASB8	KIAA0090	SERINC5	ANXA11	DDI2	MOCOS	KDR	BST1	
COL12A1	CXADR	BHLHE40	SDC4	STAT3	CD47	PDZK1IP1	CALB2	IVL	ARHGAP1	NEK11	KDELR3	BCL2A1	DGKH	PTPRE	PTPLA	
LEPREL1	LAMC2	FAM134B	HLA-J	TRIM38	C5orf32	PRRG4	PSTPIP2	CASP1	CTSL1	TMLHE	CXCL1	SFTA2	TTC27	PDE8B	DIRC2	
FSTL1	IFIH1	INHBA	ODZ2	ITGA3	CD200	NCOA7	IL20RB	LY6G5B	CCDC3	TNFRSF9	TMEM163	ABCA5	TLE1	ZNF814	SRPRB	
CCDC80	TFAP2A	IFITM1	CLMN	CRISPLD1	IFITM2	HLA-E	AREG	SCD	GLB	IL8	FSCN1	VTCN1	STK17A	PTENP1	ITSN1	
ITGB8	PTGFRN	CAV1	IFIT2	SPRR1A	MAL2	DGKA	ACTA2	DAG1	RBAK|LOC389458	C7orf70	ATAD1	IGF1R	HSD17B4	TBX18	AHNAK	
TLE4	MIR622	AP0L6	FGFR2	FKBP11	MIR205	LPAR3	TEX9	ELOVL7	SLC41A2	HIBADH	ACSL4	IFI6	CTTNBP2NL	GRINA	MYST3	
IGFBP3	DAPP1	DIO2	PBX1	BST2	RIMKLB	NFIX	THBS3	GJC1	ZNF256	SULT1A3	ARHGAP28	PRLR	CACNB3	PAQR7	RNF111	
GBP1	DAPK1	SRGN	PTGIS	LHFP	ADAMTS1	B4GALT1	TPD52L1	ZNF609	MARVELD2	CD55	ANKRD50	TMTC2	C12orf59	NSUN4	NT5C3	
FBN2	DDX60L	GPRC5B	BTN3A3	SERPINB8	KRT8	STOM	NTN4	PDIA5	DHRS1	ARHGEF5	CCL5	DMGDH	FLJ38109	QRICH1	ANKRD57	
CDH3	LAMA4	IFIT3	LPHN2	SOD2	TNIP1	MUC16	ARHGAP29	STARD5	MOSPD2	USP18	RALB	SLC35F2	CLSTN1	VIPR1	TMEM87A	
EGFR	CRIM1	SLIT2	MSX2	PLXNB2	LYN	GALNT1	STK32A	S100A2	COL4A1	GNPTAB	SH2D4A	HERPUD1	CCL2	C1GALT1	LPHN1	
FAT1	FNDC3B	GPR50	EMP2	FABP3	SNX24	SPRR2A|SPRR2B	NOB1	L1CAM	MTF1	SLC10A7	GABPB2	MFSD2A	MICB	HIPK3	TMEM39A	
CTSH	PAPPA	CACHD1	ALDH1A2	HLA-F	ERCC6	MYO1E	ATP2B4	MAPK4	CYB5R1	C12orf41	AAGAB	TMEM208	S100A9	PIK3C2B	PSMC3	
PAPSS2	XAF1	LIMA1	XAGE1A	KIAA1217	FAM84B	B4GALT4	IFI35	MAP3K13	OR2A4	CCL22	S100A10	KIAA1199	ATP6V0D1	TAGLN2	KLK5	
ASS1	VGLL3	GPNMB	PSMB8	ITGB4	CMIP	GFPT2	WWTR1	TNS3	ZNF134	SYT16	LOC402778	IFT57	SULT1A3	LGALS3BP	SLC2A3	
IL18	CGA	IL1RAP	MFAP5	KCNK1	C5orf22	CMAH	TBC1D2B	WDR73	ADPGK	ZNF814	MEST	CSF2RA	LPCAT1	PARVA	SERPINE1	
GPRC5A	HLA-B	ZFHX4	FGF2	TNFAIP3	ZNF83	ESD	FEZ1	MTAP	PARP12	OR2A4	DUSP7	TBC1D23	PMEPA1	CASP8	HOXA2	
CASP4	SLC1A3	SGK1	IFIT5	CELF2	TANC1	CLU	DOCK11	ELOVL1	NUAK2	MPZL3	TBC1D9	ARHGEF35	SLC9A7	FAT2	LMBRD2	
NNMT	SAMD9	HBEGF	RAB25	MST4	COTL1	JAK1	SNORD45B	CDRT1	C3orf37	FEM1C	FXYD3	FAM189A2	ZNF592	PMS2	HMOX1	
DPP4	IFI44	SLC7A5	AKAP13	CSRP1	FAM38B	CXCL5	GPX8	PSG4	BMP7	CYR61	POLH	SNORD12C	IRF6	TBC1D2B	SNUPN	
RARRES3	DSP	THBS2	C3orf59	HMGCS1	SLC22A5	PTPRJ	PSG8	PDE4B	TP53	HYOU1	AMOTL1	KIAA0895	PTK2B	ADRM1	MLKL	
GBP1	EPAS1	CRABP2	NPNT	TNFRSF21	ASAM	XDH	RCN1	COPG	SLC16A6	MXRA5	FLOT2	MOBKL2B	FHL2	APLP2	JOSD1	
BIRC3	FAM129A	NAALADL2	NFKB1	FAM38B	TRPS1	WWC1	TSPAN3	ABCF3	AQP3	AP4E1	C10orf28	EHD2	ATXN7	GNA14	VCL	
HLA-A	CCND2	BMP5	GPR126	SPRR3	CPVL	CNN3	THSD4	ENTPD7	IFFO2	HERC6	CD59	DNAJC16	ZNF583	GRHL1	ZIC1	
TMEM154	MUC21	TFAP2C	WDR69	IFITM3	ARPC1B	BCAR3	BHMT2	ESRP1	SH3BP5	PHC3	FADS2	DHCR7	RCAN1	CEACAM1	CTAGE6	
APP	CSTA	KRT7	PDLIM1	VAMP8	TFAP2A	RHOU	SLC9A1	DSEL	MGAT4A	IQGAP1	NPR3	ESRP2	CRTC3	CCNT1	KCNB1	
ANXA8	EDN1	TPM2	MYADM	COBLL1	ZNF841	TNNT1	ODZ3	ETS1	SERPINA1	ITGA6	OGDH	PTGER4	SCAMP2	NDST1	VPS33B	
ITGB6	NEDD9	KLK6	ANXA3	TLR3	RNF19B	HOOK1	TRIM2	EDA2R	OXTR	SLC34A2	RHBDL2	PTPRM	COL17A1	CHD9	ADARB1	
TLL1	TAP1	BCO2	OAS3	KRT6A	FAM13B	UBE2L6	FBXW10	TNIP3	TST	SMARCA1	CPM	CRYBB2P1	DDX23	DAXX	CCL28	
PARP9	PDGFA	HGSNAT	IFI30	FAM111A	SGK196	NOX1	CDC42SE2	TRPM7	CYBRD1	TRANK1|LBA1	C1orf144	SCN9A	HFE	KRT13	OSBPL2	
PSMB9	KRT18	LRRC1	AZGP1	TNFAIP8	IFI44L	FAM63B	XPO6	BASP1	NCRNA00152	BNC2	FAM107B	C7orf70	CDC23	S100A7	ZNF776	
GCNT4	CYP4X1	ZFY	MICAL2	BTN3A1	TMEM40	IGFBP4	MYPN	PLBD1	SGMS2	COBL	MAPK13	BAIAP2L1	TMEM194B	NECAP2	NAPSA	

Appendix 2: Genes that were suppressed in cisplatin resistant lung SCC cell lines (fold change > 1.5; *P* < 0.1).

Down-regulated						Up-regulated	
Sensitive					Resistant	Sensitive	Resistant
CSPP1	RTN4IP1	SLCO3A1	LYST	FIGN	SNORD116-2	COQ10A	PPP1R3C
AKT3	FAM160A1	RSRC1	TRIO	LRRC16A	HIST1H3B	ATG12	KBTBD8
HIST1H2BF	SDCCAG8	SH3D19	FAM172A	INADL	ARHGAP24	RHBDD2	AMY1A
HOMER1	FGD6	ARHGEF3	BMPER	DIP2B	PHF20	ZNF468	PRPF39
SVIL	POLR3B	ZFAND3	NBEAL1	LRCH1	HECW2	TUBA4A	SNORD24
ARFGEF1	TTC27	SNX29	MAP2K5	BNC2	IRF2	SLFN5	PTGS2
WDFY3	TULP4	PTPN4	TYW1	DIAPH3	RBMS1	C14orf28	C3orf58
CCDC18	TEC	KIAA0922	INPP4B	SGK269	FRMD3	ARRDC3	KLRA1
NEK1	ZFYVE9	NEK11	ST7	BMPR1A	NRG1	E2F7	SNORD22
RTTN	MSH3+E55	ODZ3	PRKCH	PRIM2	RGL1	BRD2	IL12A
KIF18A	ZNF277	NAV3	KIF13A	CMIP	HIST1H4B	SLC41A1	SNORD59B
SOS2	MYO1E	CHD6	ATAD2B	OPHN1	HIST1H2AC	DCLRE1B	HHEX
PTPRM	BTBD9	RABGAP1L	TRPS1	RALGPS2	SYT1	C17orf71	
DPYD	ZSWIM6	ITPR2	C14orf145	N4BP2	TMEM133	TP53INP1	
ARNTL	LRBA	MAP4K3	C3orf26	FGD4	B3GALT1	ASF1B	
UBR1	TSPAN5	ELP4	PLD1	MAGI3		PLAC8L1	
ZMYND8	SPIRE1	TPST1	ARHGAP10	SLIT2		ZKSCAN1	
LGR4	TRMT61B	PITPNC1	PDZD2	MNAT1		LY6G5B	
POT1	USP32	PDE10A	RAPGEF6	RPS6KC1		POLR2A	
NF1	KIF15	DYM	STK3	GULP1		LOC643837	
CDK19+B82	ARHGAP19	IFT81	EPB41L4A	RAPGEF2		CTSK	
PPP2R3A	TEAD1	ZEB1	VAV2	TOX		ZRSR1	
THSD4	CWF19L2	FTO	MED27	FAF1		BTG2	
PHLPP1	SRGAP2	CWC27	SCLT1	ARHGAP18			
FCHO2	TGFBR3	CDC42BPA	PRKCA	NCOA1			
SLC38A9	ELOVL6	PLCL2	KIAA0391	ANKS1A			
RAB28	OSBPL10	MBNL2	PPP1R9A	SBF2			
MEIS2	ATG10	CEP170	DAPK1	VPS13B			
RPGRIP1L	KIF14	HERC3	G2E3	RFWD2			
SMAD3	ATG7	CDK6	EYA4	DENND5B			
UBR3	PARP8	ARHGAP12	CACHD1	ZNF609			
KIAA0586	NUP35	SEMA3A	C20orf94	EXOC6			
CNKSR2	IPO11	PIP4K2A	DIAPH2	SPATA5			
ARHGAP32	DOCK7	DAAM1	SNX25	WDR7			
RPTOR	SRPK2	SRBD1	FRYL	DENND1B			
C15orf41	KIF20B	PAPPA	CBLB	ZNF407			
DEPDC1B	TMCC1	FBXL20	UBE2E2	C7orf60			
CNOT6L	EXOC2	BBX	GTDC1	ENOX2			
DENND4C	BCAR3	SLC25A12	SSH2	ENOX1			
ARID4B	EPHA4	SASH1	MED27	MYO9A			
FNBP1L	ASH1L+B118	NBAS	AGAP1	SENP7			
ACBD6	SUPT3H	GHR	PDS5B	CDKAL1			
ZCCHC11	LPP	TBC1D12	MCTP1	TMTC2			
CABLES1	TMCO7	MID1	GREB1L+B234	RBMS3			
MRPS28+B29	GSK3B	DMXL1	CCDC91				
COMMD1	ZFPM2	DTWD2	MCTP2				
CREB5	UTRN	PHF21A	GLI3				
OSBPL3	PTPN13	SLC25A13	THADA				

Appendix 3: Genes that were differentially regulated in both cisplatin-resistant and –sensitive phenotypes after cisplatin treatment.

The table showed the cluster of genes that were significantly up or down-regulated at 1.5 fold after cisplatin treatment in either cisplatin-sensitive or cisplatin-resistant phenotypes. Genes that were commonly altered in both phenotypes were not shown.

Contributions	Name	Instutute
Illumina Hi-Seq on gDNA harvested from SCC tumours.	-	Macrogen, Korea
Preparation for SCC tissue specimens.	E.Y. Foo, Y.H. Pang	Department of Pathology, National University Health System (NUHS) , Singapore
Scoring of IHC slides.	M.E. Nga	Department of Pathology, National University Health System (NUHS) , Singapore
Clinocopathological analyses	J. Ho	Department of Haematology-Oncology, National University Health System (NUHS) , Singapore
STR analysis and cell line authentication	-	Centre for Translational Research and Diagnostics (CTRAD), Cancer Science Institute, Singapore
Gene expression profiling analysis	C. Bi	Cancer Science Institute, Singapore

Appendix 4: Contributions of collaborators in the completion of this thesis.